Downloaded from orbit.dtu.dk on: Apr 25, 2024

DTU Library

Market-based Approaches for the Coordinated Operation of Electricity and Natural Gas Systems

Ordoudis, Christos

Publication date:
2018

Document Version
Publisher's PDF, also known as Version of record

Link back to DTU Orbit

Citation (APA):
Ordoudis, C. (2018). *Market-based Approaches for the Coordinated Operation of Electricity and Natural Gas Systems*. Technical University of Denmark.

General rights
Copyright and moral rights for the publications made accessible in the public portal are retained by the authors and/or other copyright owners and it is a condition of accessing publications that users recognise and abide by the legal requirements associated with these rights.

- Users may download and print one copy of any publication from the public portal for the purpose of private study or research.
- You may not further distribute the material or use it for any profit-making activity or commercial gain
- You may freely distribute the URL identifying the publication in the public portal

If you believe that this document breaches copyright please contact us providing details, and we will remove access to the work immediately and investigate your claim.

Technical University of Denmark

Market-based Approaches for the Coordinated Operation of Electricity and Natural Gas Systems

Christos Ordoudis

Ph.D. Thesis

Kgs. Lyngby, Denmark 2018

DTU Center for Electric Power and Energy
Department of Electrical Engineering

Uncertainty is an uncomfortable position.
But certainty is an absurd one.

— Voltaire

To my grandfather

Preface

This thesis was prepared at the Department of Electrical Engineering of the Technical University of Denmark (DTU) in partial fulfillment of the requirements for acquiring a Ph.D degree.

The Ph.D. studies were funded by the Danish research project CITIES (Center for IT-Intelligent Energy Systems in cities, No. 1305-00027B/DSF). This dissertation covers the work carried out by the author during his Ph.D. project, which started on 1st July 2015 and was completed on 30th September 2018.

The thesis consists of a summary report and six attached scientific papers, three of which have been peer-reviewed and published, whereas one of them is currently under review. The last two are working papers to be submitted for journal publication.

Christos Ordoudis
30 September 2018

Acknowledgements

This thesis sums up the work of the last 3 years carried out at the Center for Electric Power and Energy (CEE) of DTU Elektro. First and foremost, I wish to thank my Ph.D. supervisor Prof. Pierre Pinson. Since the days I began my Master in Sustainable Energy, Pierre was very encouraging regarding my research and professional career and became a good mentor to me. I would like to express my sincere gratitude to him for the inspiration, guidance and support he has provided to me during all these years.

Special thanks to my co-supervisor Assist. Prof. Jalal Kazempour. Working with Jalal has been a great pleasure. I appreciate the time he has devoted to advising me and his valuable insights into my research.

I would also like to thank Assoc. Prof. Juan Miguel Morales, who has been my co-supervisor. His valuable knowledge and enthusiasm for research that he has shared with me are highly appreciated. I have also particularly enjoyed all our fruitful discussions.

I am also thankful to my advisor Prof. Daniel Kuhn for hosting me during my external stay at École Polytechnique Fédérale de Lausanne and for embracing me into his research group. I also thank him for the great inspiration of scientific research he has given to me. I would also like to thank Viet Anh Nguyen for the very good collaboration and beneficial discussions we had.

Current and former colleagues and friends at the ELMA group have made the efforts towards my degree infinitely more pleasant. I particularly thank Stefanos and Thanasis for the good time we spent together, as well as the excellent collaboration we had. In addition, I would like to thank Lejla, Lesia and Guillaume for the common path we shared since the beginning of our Ph.D. studies. Thank you, Tue, Tiago, Nicolo, Emil, Lazare, Emil, Vladimir, Fabio, Andrea, Jakob, Morten, Andreas, Giorgo, Anna, Spyro, Vassili, Tiago, Nicola, and Corey, for being great colleagues.

Last but not least, I would like to thank my close friends in Denmark and those in Greece for all the pleasant moments and experiences. I would like to thank Panagiota for her understanding, help and support and for being by my side. I am indebted to my family and especially to my parents, Thalia and Triantafyllos, and my sister Katerina for their unconditional love and encouragement. I could not have made it without all of them!

Christos Ordoudis

Kgs. Lyngby, Denmark, 2018

Table of Contents

List of Figures

List of Tables

Abstract

Numerous unprecedented changes have taken place in the whole energy system over the last years, such as the transformation of the power generation mix and the increased interactions among different energy systems, which have introduced both opportunities and challenges. The electricity system is transitioning towards a renewable-based system mainly due to worldwide environmental concerns and natural gas is expected to play an important role in the future development of the electricity system. This is due to the fact that Gas-fired Power Plants (GFPPs) are one of the least polluting conventional technologies, as well as efficient and flexible. The co-existence of these two types of power production technologies serves as a promising combination for a smooth transition to a sustainable energy system that is flexible enough to accommodate high shares of renewables. As a consequence, the interactions between the electricity and natural gas systems will be strengthened, while the uncertainty and variability of renewables will eventually affect the operation of both systems. Moreover, electricity and natural gas are traded in markets, which eventually need to adapt to these recent and forthcoming changes. In this context, the objective of this thesis is to propose market-based coordination frameworks to support the operation of electricity and natural gas systems under the uncertainty introduced by the power production from renewable energy sources, such as wind and solar.

An increasing need for flexibility has occurred due to the inherent characteristics, i.e. uncertainty and variability, of renewable energy sources that can be covered by various sources, such as electricity storage, demand response and GFPPs. On top of the ability of GFPPs to provide operational flexibility, these plants are the link between the two energy systems and thus give the opportunity to exploit the flexibility in the natural gas system. More specifically, the natural gas system can act as a storage buffer thanks to the ability of storing natural gas in the pipelines and in the seasonal storage facilities. A special focus in this thesis is placed on developing operational models for the optimal use of the different assets and components of the whole energy system, while simultaneously integrating them in the market operations.

Currently, the electricity and natural gas markets are operated in a decoupled manned without taking into account each system's complexities and limitations. In addition, a common practice is to adopt a deterministic view of uncertainties when operating the systems and markets, since these were fairly limited when the operational models were first developed. Seeking for new operational models, we analyze different levels of coordination in terms of coupling the systems, as well as consider various approaches to obtain an uncertainty-aware scheduling of the system in view of stochastic power production from renewables. We introduce a model that co-optimizes the electricity and natural gas systems under uncertainty by using stochastic programming, while also considering the flexibility of the natural gas system. Under this proposed approach, the importance of proper natural gas system modeling in short-term operations is highlighted to reveal flexibility and increase security of supply. Therefore, adopting a fully coupled view of the two systems and

having a probabilistic description of uncertainty can provide ideal solutions for the system and market operators.

Such stochastic dispatch models optimally use the available flexibility to provide an ideal dispatch with the minimum expected cost. However, these models are usually incompatible with the current market designs. System and market operators are highly challenged by the increasing penetration of renewables, since the traditional market designs are based on a sequential clearing of trading floors with deterministic view of uncertainties. As a result, these models become highly inefficient and experience high operational costs as the penetration of stochastic power production increases. Acknowledging the advantages of adopting a coupled view of the electricity and natural gas systems, we propose two dispatch models that exploit the physical and economic links established between the electricity and natural gas systems by GFPPs to improve the current sequential clearing of trading floors. The proposed improved dispatch models anticipate the real-time flexibility needs and optimally set flexibility volume and price signals to provide the system dispatch that approximates the ideal stochastic solution in terms of expected cost, while still clearing the day-ahead and real-time trading floors sequentially.

Taking advantage of the continuously increasing availability of renewable power production data, recent developments on data-driven optimization can be employed to deal with uncertain renewables. Two data-driven models are proposed for the operation of the electricity and natural gas systems, which are able to efficiently capture the true characteristics of renewable power production directly from the available data. That way, the proposed data-driven models inherently incorporate valuable information regarding the spatial and temporal correlations. In the first data-driven model, we solve the energy and reserve dispatch model with fuel constraints for GFPPs in view of a strong interdependence between electricity and natural gas systems. The focus is placed on developing approaches to solve distributionally robust joint chance constrained programs, in which the sample data are directly utilized for the uncertainty characterization and a systematic tuning of robustness allows to attain cost-effective solutions. The second data-driven model is developed based on the estimation of the first- and second-order moments from the historical data and provides an independent, yet coordinated dispatch of electricity and natural gas systems in view of uncertain power supply. This distributed approach permits to share only a limited amount of information between the two system or market operators and is performed in a transparent manner.

Resumé

I de seneste år har energisystemet gennemgået en del bemærkelsesværdige forandringer, så som ændringer i sammensætningen af el-produktionen og den øgede interaktion mellem forskellige energisystemer. Dette har skabt både interessante muligheder og store udfordringer. El-systemet er ved at overgå til et system baseret på vedvarende energi som hovedsageligt skyldes globale bekymringer for miljøet. Naturgas forventes at spille en vigtig rolle i den fremtidige udvikling af el systemet. Dette er fordi gasfyrede kraftværker (GFKV'er) er én af de mindst forurenende konventionelle teknologier, og de er desuden meget effektive og fleksible. Koordinering af gasfyrede- og vedvarende el-produktion er en lovende kombination for at overgå til et bæredygtigt energisystem der er fleksibelt nok til at rumme en høj andel af vedvarende energi. Interaktionerne mellem el- og naturgassystemerne vil derfor styrkes, mens usikkerhed og variabilitet af den vedvarende energi i sidste ende vil påvirke driften af begge systemer. Derudover handles el og naturgas på markeder som også bliver nød til at tilpasse sig til kommende ændringer. Denne Afhandling foreslår markedsbaserede koordinering der kan understøtte driften af el- og naturgassystemerne, ved samtidigt at tage højde for den usikkerhed som el-produktionen fra vedvarende energikilder som vind og sol fører med sig.

Der er et stigende behov for fleksibilitet, på grund af de medfødte karakteristika ved vedvarende energi (dvs. usikkerhed og variabilitet). Denne fleksibilitet kan dækkes af forskellige kilder, såsom lagring af elektrisk energi, demand-response og GFKV'er. Ud over GFKV'ers evne til at yde operationel fleksibilitet er disse kraftværker bindeled mellem de to energisystemer og åbner således op for at udnytte fleksibiliteten i naturgassystemet. Mere konkret kan naturgassystemet agere som energi-lager takket være muligheden for at lagre naturgas i rørledninger og sæsonlagre. Et specielt fokus i denne afhandling lægges på at udvikle operationelle modeller til brug for optimal udnyttelse af de forskellige aktiver og komponenter i hele energisystemet, samtidig med at disse integreres i et marked.

I dag opereres el- og naturgasmarkeder afkoblet af hinanden, uden hensynstagen til de enkelte systemers kompleksiteter eller begrænsninger. Desuden er det gængs praksis at anlægge et deterministisk syn på usikkerheder i systemernes drift, fordi usikkerhederne var ret begrænsede da de operationelle modeller oprindeligt blev udviklet. I søgen efter nye operationelle modeller undersøger vi forskellige niveauer af koordination med henblik på at sammenkoble el- og gas-systemer, og benytter forskellige måder for at planlægge driften, ved at tage usikkerheden af systemerne med henblik på stokastisk el-produktion fra den vedvarende energi i betragtning. Vi introducerer en model der co-optimerer el- og naturgassystemerne under usikkerhed ved at benytte stokastisk programmering, mens vi tager hensyn til naturgassystemets fleksibilitet. Med denne metode fremhæves vigtigheden af korrekt modellering af naturgassystemet for at synliggøre fleksibilitet og øge forsyningssikkerheden. Således kan vi, ved at indføre et fuldt koblet syn på de to systemer og have en probabilistisk beskrivelse af usikkerheden, tilbyde ideelle løsninger til både systemet og markedsoperatørerne.

Sådanne stokastiske dispatch modeller kan på optimal vis udnytte den tilgængelige fleksibilitet og opnå en ideel dispatch med minimale forventede omkostninger. Men disse modeller er normalt inkompatible med det nuværende markeds designs. Desuden har system- og markedsoperatører store udfordringer som følge af den forøgede penetration af vedvarende energi, idet de traditionelle markeds designs er baseret på en sekventiel clearing af markederne med deterministisk beskrivelse af usikkerhederne. Som et resultat af dette bliver disse modeller meget ineffektive og oplever høje operationelle omkostninger når andelen af stokastisk el-produktion stiger. Idet vi anerkender fordelene ved at anlægge et koblet syn på el- og naturgassystemerne, foreslår vi to dispatch modeller der udnytter de fysiske og økonomiske bånd mellem el og naturgassystemerne, som GFKV'er tilvejebringer, til at forbedre det nuværende markeder med sekventiel clearing. De foreslåede forbedrede modeller forudser real-tids fleksibilitetsbehovet og sætter på optimal vis fleksibilitetsmængde og prissignaler ved at tilbyde et system dispatch der tilnærmer den stokastiske løsnings ideele forventede omkostninger, imens day-ahead- og real-tidsmarkederne stadig cleares sekventielt.

Ved at drage fordel af den stødt stigende tilgængelighed af data fra vedvarende el-produktions kilder, kan den seneste tids fremskridt indenfor datadrevet optimering anvendes til at håndtere usikkerheden ved vedvarende energikilder. Der foreslås to datadrevne modeller til driften af el-og naturgassystemerne, som effektivt fanger den vedvarende el-produktions sande egenskaber direkte fra observationerne af de tilgængelige data. På den måde inkorporerer de foreslåede datadrevne modeller selv de fulde oplysninger om rum- og tids korrelationer. I den første datadrevne model løser vi energi- og reserve dispatch modellen med brændstof bi-betingelser for GFKV'er med antagelsen af stærke indbyrdes afhængigheder mellem el-og naturgassystemerne. Fokus er at udvikle metoder til at løse distribuerede robuste "joint chance constrained" programmer, hvor det tilgængelige data direkte udnyttes til at karakterisere usikkerhed og hvor en systematisk tuning af robusthed gør det muligt at opnå omkostningseffektive løsninger. Den anden datadrevne model er udviklet på grundlag af en estimering af første- og andenordensmomenter fra de observerede data og giver en uafhængig, men koordineret dispatch af el-og naturgassystemerne under hensyntagen til en usikker elforsyning. Denne distribuerede metode tillader at kun en begrænset mængde oplysninger deles mellem de to systemer eller markedsoperatører og metoden udføres på en gennemsigtig måde.

Acronyms

GFPP Gas-Fired Power Plant

BRPs Balance Responsible Parties

TSO Transmission System Operator

FERC Federal Energy Regulatory Commission

CHP Combined Heat and Power

EEX European Energy Exchange

PDE Partial Differential Equation

GTF Gas Transfer Facility

ETF Exchange Transfer Facility

MPEC Mathematical Program with Equilibrium Constraints

ADMM Alternating Direction Method of Multipliers

LNG Liquefied Natural Gas

CAISO California Independent System Operator

ISO Independent System Operator

KKT Karush-Kuhn-Tucker

MILP Mixed-Integer Linear Program

LP Linear Program

i.i.d. Independent and Identically Distributed

SOCP Second-Order Cone Program

List of publications

The relevant publications which are the core of this thesis are listed as follows:

[Paper A] Pierre Pinson, Lesia Mitridati, Christos Ordoudis and Jacob Østergaard (2017). "Towards Fully Renewable Energy Systems: Experience and Trends in Denmark," *CSEE Journal of Power and Energy Systems.*

[Paper B] Christos Ordoudis, Pierre Pinson and Juan Miguel Morales (2018). "An Integrated Market for Electricity and Natural Gas Systems with Stochastic Producers," *European Journal of Operational Research.*

[Paper C] Christos Ordoudis, Stefanos Delikaraoglou, Pierre Pinson and Jalal Kazempour (2017). "Exploiting Flexibility of Coupled Electricity and Natural Gas Systems: A Price-Based Approach," in the *Proceedings of IEEE PowerTech Conference 2017*, Manchester, UK.

[Paper D] Christos Ordoudis, Stefanos Delikaraoglou, Jalal Kazempour and Pierre Pinson (2018). "Market-based Coordination for Integrated Electricity and Natural Gas Systems Under Uncertain Supply," Submitted to *IEEE Transactions on Control of Network Systems.*

[Paper E] Christos Ordoudis, Viet Anh Nguyen, Daniel Kuhn and Pierre Pinson[1] (2018). "Energy and Reserve Dispatch with Distributionally Robust Joint Chance Constraints," working paper to be submitted to *IEEE Transactions on Power Systems.*

[Paper F] Christos Ordoudis and Viet Anh Nguyen[2] (2018). "Data-driven Distributed Operation of Electricity and Natural Gas Systems," *Working paper.*

The following publications have also been prepared during the course of the Ph.D. study, but have been omitted from the thesis because they are not directly related to the primary objective, or they are partially covered by other presented papers.

[Paper G] Stefanos Delikaraoglou, Athanasios Papakonstantinou, Christos Ordoudis and Pierre Pinson (2015). "Price-maker Wind Power Producer Participating in a Joint Day-ahead and Real-time Market", in the *Proceedings of 12th International Conference on the European Energy Market*, Lisbon, Portugal.

[Paper H] Christos Ordoudis and Pierre Pinson (2016). "Impact of Renewable Energy Forecast Imperfections on Market-Clearing Outcomes," in the *Proceedings of IEEE Energycon Conference 2016*, Leuven, Belgium.

[Paper I] Anna Schwele, Christos Ordoudis, Jalal Kazempour and Pierre Pinson (2018). "Arbitrage Options Enhancing the Coordination of Electricity and Natural Gas Markets," *Working paper*.

[1] The list of authors may be subject to changes.
[2] The list of authors may be subject to changes.

CHAPTER 1

Introduction

1.1 Background and motivation

Over the last two decades, the previously independent *electricity* and *natural gas* sectors have experienced a substantial transformation that has led to a gradual convergence of their operations. This trend has been manifested in various ways highlighting the increased interdependencies between the two industries [1, 2]. Firstly, both the electricity and natural gas sectors have been liberalized, which resulted in the unbundling of vertically-integrated utilities and created the conditions for the corresponding commodity markets to develop. Secondly, the increased deployment of Gas-Fired Power Plants (GFPPs) has created tighter links between the electricity and natural gas systems, both from an economic and a technical viewpoint. At the same time, the presence of various utilities involved in the trading of both commodities has created the need for developing decision-making tools that take into account the characteristics and limitations in both energy systems.

In addition to the aforementioned reforms, the increased integration of renewables in the energy systems has introduced significant challenges to be faced in terms of systems and markets operations. This is due to the fact that electricity markets have been designed based on a generation mix that was dominated by fully controllable thermal power plants, while the electricity and natural gas systems had been initially developed and operated in a decoupled manner because of the limited interactions between them. Nevertheless, the power production of renewables is *stochastic*, i.e. it is weather-driven and thus hard to predict, and *non-dispatchable*, i.e. it can only be partly controlled by their operators. The increased stochasticity and variability introduced in the power system impacts also the natural gas system's operations because the links between the two energy systems are expected to be continuously strengthened.

Therefore, challenges can be identified in two dimensions; one with regards to the accommodation of high shares of stochastic renewables in the whole energy system and another relative to the interplay between the electricity and natural gas systems. In this context, there is an increasing need to explore the *redesign* of the respective markets as well. Aiming to have an efficient and cost-effective operation of the whole energy system under these rapid transformations, makes the use of advanced decision-making tools that take *uncertainty* into account more and more essential nowadays.

1.2 Research objectives

The objective of this thesis is to propose novel market-based coordination frameworks to facilitate the operation of electricity and natural gas systems under high shares of stochastic power production from renewables. The development of these tools is based on mathematical optimization with a special focus on incorporating uncertainty in various modeling approaches.

Owing to the extensive deployment of renewable energy sources, and to their special aforementioned characteristics, a significant impact on short-term operations is expected. Hence, the proposed models are developed focusing on short-term markets and particularly from the day-ahead stage up to the real-time operation, where the physical delivery takes place. The system/market operator viewpoint is taken in all studies presented in this thesis and the various players are assumed to participate in the markets under perfect competition. It should be also noticed that wind power is used as the uncertain power in-feed; however, the developed models can be similarly extended to deal with uncertainties stemming from other renewable energy sources with similar characteristics, such as solar power. Wind power is chosen since it has currently the greatest installed capacity in Europe among all renewables, as well as has been widely developed in Denmark [3]. In addition, wind power producers are the first to participate in the electricity market, while having a stochastic and non-dispatchable nature.

The overall quest of this thesis can be summarized by the following three main research questions that lead to the development of the respective research works:

I. How can the coordination of electricity and natural gas systems be enhanced in short-term operations while accounting for uncertainties?

Among others, authors in [4–7] have dealt with the presence of uncertain power production in coordinated electricity and natural gas systems highlighting the need for further elaborating on this topic to facilitate the integration of renewables in a cost-effective manner. The benefits of improving the coordination between the two energy systems under high intraday variability of GFPPs are also indicated in [8]. Therefore, different coordination setups that aim to overcome the aforementioned challenges are studied in this thesis to address this research question. As an initial step, the inefficiencies stemming from the current independent operation between electricity and natural gas systems that takes place under a deterministic view of uncertainties are identified. Then, various operational models are developed to examine how different levels of coordination both between the two systems and between the trading floors (i.e. day-ahead and real-time stages) can enhance the current organizational setup.

II. Which are the benefits of modeling the energy networks in a market-compatible way with regards to revealing flexibility and mitigating uncertain power supply?

Several works in the literature, such as [8–13], included natural gas network constraints in the system modeling to reveal its inherent flexibility and ensure reliability in short-term operations. Revealing additional flexibility plays an important role to facilitate the integration of renewables in the whole energy system, while taking into account network constraints in the market-clearing procedure not only increases the security of supply but also allows for a more efficient utilization of the existing resources. This thesis seeks to develop models that efficiently incorporate system components and network constraints in the market-clearing models to have a more realistic view of the underlying physical characteristics of the systems. Accomplishing this goal can reveal various benefits; for instance, the operation of GFPPs can be optimized and the inherent flexibility of the natural gas system can be exploited resulting in a reduced operational cost of the integrated energy system. Moreover, incorporating the network models in a market-compatible way allows to derive meaningful prices for the traded commodities that can support the participation of various actors in the markets. Similarly, the interplay with the heating sector can increase the overall system's flexibility [14, 15].

III. How can the available data of renewable energy production be utilized efficiently to characterize uncertainties in operational models?

Moving towards an era with an increased availability of data, it is becoming highly important to use data analytics and develop data-driven models to deal with uncertainties. The utilization of analytics can provide valuable insights to facilitate the process of making predictions and characterize uncertainties. Two example approaches for the representation of uncertainties in operational models are presented in [16] and [17], where probabilistic wind power forecasting and definition of dynamic uncertainty sets are proposed respectively. Then, the acquired high quality uncertainty characterizations can be combined with proper decision-making tools to develop advanced operational models. Another approach that can be followed is to develop directly data-driven models, as in [18, 19], which effectively extract valuable information from the available data. The aforementioned approaches facilitate the handling of uncertainties from renewables and are utilized in this thesis.

1.3 Scientific contributions

As an inspiration to this thesis, the current status and future trends in Denmark in the energy transition period are studied in [Paper A]. Denmark, which is considered a pioneer in the development of wind energy, has successfully integrated high shares of renewable power production and has ambitious goals to cover fully the energy supply by renewables by 2050 [20]. Another interesting characteristic is the existence of the three main energy carriers in the Danish energy system (i.e. electricity, natural gas and heat), which presents a great potential to study the coordination among them in order to reveal additional existing flexibility. More importantly, the electricity and natural gas systems are operated by a common system operator (i.e. Energinet.dk), which promotes the establishment of efficient coordination mechanisms. These mechanisms are considered attractive and inexpensive as opposed to solutions, such as building new interconnections or investing in electrical energy storage options. Therefore, the case of Denmark provides valuable insights and motivates a holistic view of the energy system to support renewable energy integration.

Sufficient levels of flexibility are of utmost importance as we move towards a renewable-based power system and GFPPs are considered one of the most suitable conventional technologies to accommodate the uncertainty and variability of stochastic power production. Due to their favorable operational capabilities, such as high efficiency and flexibility along with reduced carbon emissions, these units usually compensate for the variability caused by intermittent renewables. Therefore, GFPPs are strengthening the link between electricity and natural gas systems, which causes though higher variability in the natural gas system [8]. Accounting for the natural gas network properties during decision making can be considered an effective approach to increase the levels of security of supply and to reveal additional flexibility. The reason for that is the inherent flexibility of the natural gas network, in which the pipelines can be used for short-term storage of gas, the so called *linepack* flexibility, and the large storage facilities that can be utilized either as a back-up option for short-term needs or as a seasonal storage option [13].

The benefits of incorporating a natural gas system model with linepack flexibility and storage facilities in the dispatch procedure of the whole energy system are presented in [Paper B] under three setups with various degrees of coordination both system-wise and between the trading floors. In this work, a dispatch model for a coupled electricity and natural gas system is proposed, which is formulated as a two-stage stochastic program [21]. The proposed model utilizes the flexibility of

the natural gas system in a way that the minimum expected cost of the coupled energy system is attained and increases security of supply. Moreover, the two deterministic models that are developed, one of an integrated energy system and one that treats the two systems independently, clear the subsequent trading floors in a sequential manner and demonstrate an inferior performance than the proposed model. The *coordination parameters*, here considered to be the natural gas price and volume availability for power production from GFPPs, are identified and their impact on the dispatch of both energy systems is assessed.

Following an approach based on two-stage stochastic programming allows for an advanced setup to dispatch the electricity and natural gas systems by accounting for uncertainties and anticipating future balancing needs. The dispatch provided by this approach yields the minimum expected cost but it is usually not compatible with the current market designs and regulations. In practice, market participants and system/market operators may hesitate to adopt radical changes and prefer to face only slight adjustments that guarantee a sufficient level of efficiency to handle uncertainties. Following this rationale, two systematic approaches to optimally define the aforementioned coordination parameters in a coupled electricity and natural gas system are given in [Paper C] and [Paper D], while maintaining the sequential arrangement between the trading floors. In particular, [Paper C] presents a *price-based* model to generate proper flexibility price signals that adjust the natural gas price perceived by GFPPs, while [Paper D] proposes a *volume-based* model to determine the optimal value of natural gas availability for power production. Both models improve the temporal coordination between day-ahead and real-time stages by communicating the currently missing information regarding the stochastic power production at the day-ahead stage. The price-based and volume-based models are formulated as stochastic bilevel programs and then reformulated to Mathematical Programs with Equilibrium Constraints (MPECs) [22]. The two-stage stochastic programming approach serves as an ideal benchmark to quantify the efficiency improvement in terms of expected cost obtained by the proposed models with regards to the deterministic and sequential approach. Therefore, [Paper C] and [Paper D] develop models that enhance the temporal coordination between the trading floors via accounting for uncertainties in power production, while taking advantage of a fully coordinated setup between the two energy systems to exploit operational flexibility.

The development of well-designed decision-making tools that describe with the highest possible detail the problem in question is an important aspect to accomplish an efficient and secure operation of energy systems. These tools are formally formulated as mathematical programs and their solutions highly depend on the input data. More specifically, the quality and accuracy of the input data to characterize uncertainties play an important role and may significantly alter the decisions in a suboptimal way. The proper representation of uncertain power production from renewables is essential and highly challenging. A usual approach to describe the stochastic processes related to wind power is the utilization of modern forecasting techniques to generate scenarios that capture the spatial and temporal dependencies [23]. This approach has been widely used in relation to stochastic programming and has demonstrated attractive results by using high quality inputs. In an attempt to sidestep potential low quality inputs and inaccurate estimates in the decision-making process, various data-driven optimization techniques can be employed. We address this task in [Paper E] and [Paper F] by developing *data-driven* models that utilize the available data from stochastic power production to provide knowledgeable decisions for the problem in question.

In a data-driven framework, the mathematical models utilized by the system/market operator are fed with the available data without involving any additional processes, such as scenario

or uncertainty set generation. The input data can then directly provide valuable information regarding the spatial and temporal correlations in the models. In this respect, [Paper E] and [Paper F] consider such data-driven approaches based on distributionally robust optimization [18, 19]. More specifically, in [Paper E], the co-optimization of energy and reserve dispatch with fuel constraints for GFPPs is studied in view of the increased interdependencies between the two systems and high reliance on GFPPs for operational flexibility. In this case, the data samples are used to approximate the true probability distribution of renewable power production by an empirical distribution. Then, we are able to optimize over a family of distributions that contains the distributions close to the empirical one based on a probability metric selected. In this work, we choose the Wasserstein metric [24] to build the family of distributions and we are able to systematically tune the robustness of the model to attain cost-effective solutions. An important characteristic of the proposed model is that it provides solutions to distributionally robust joint chance constrained programs. Thus, we make no assumption for the probability distribution of the uncertain parameter and handle multiple constraints simultaneously, as opposed to individual chance constrained programs. Furthermore, in [Paper F], an independent but coordinated dispatch of the electricity and natural gas systems is considered, motivated by the fact that the two systems are commonly operated by different entities that may not wish to share their private information, such as system topology and market participant's data. Aiming to have the minimum information exchange between them, a distributed approach based on the Alternating Direction Method of Multipliers (ADMM) [25] is developed. In a similar vein, a data-driven approach is followed for the description of uncertainties through estimated quantitative measures that summarize the sample data from the true probability distribution. In particular, the first- and second-order moments (i.e. mean and covariance) are used to build the corresponding family of distributions that we take into account. This approach is in agreement with the requirement of having a minimum amount of information to be shared between the electricity and natural gas systems operators as well as is performed in a transparent manner since it is based on publicly available historical data of stochastic production.

1.4 Thesis outline

This thesis is structured as follows. Part I is a report introducing the fundamental concepts that comprise the focus of this thesis and summarizing the contributions of the papers that have been developed during this Ph.D. project. Within this part, Chapter 2 presents a brief introduction of the electricity and natural gas markets along with the position of Denmark in the energy transition period. Chapter 3 provides an overview of the electricity and natural gas network modeling methods and the coordination framework between them under the uncertainty introduced by renewables. The main methodologies that have been developed and a summary of the results obtained in the papers are given in Chapters 4-6. More specifically, Chapter 4 outlines the basic coordination frameworks and presents an advanced model for the natural gas system that approximates efficiently the dynamics involved and reveal its inherent flexibility. A fine-tuning of the key coordination parameters (i.e. natural gas price and volume availability for power production) to improve the coordination between the trading floors in short-term scheduling is presented in Chapter 5. Chapter 6 focuses on the two data-driven optimization methods, as well as on the distributed approach to dispatch electricity and natural gas systems independently but in a coordinated manner. Finally, conclusions and suggestions for future work are given in Chapter 7.

Part II contains all the publications that contribute to this thesis:

- **[Paper A]** is a journal article published in the *CSEE Journal of Power and Energy Systems*. This paper provides a review of the recent and current trends in Denmark towards a fully renewable energy system. A holistic view of the energy system, which includes the interplay of power, natural gas and heat systems is discussed.
- **[Paper B]** is a journal article published in the *European Journal of Operational Research*. This paper introduces an integrated operational model for electricity and natural gas systems under uncertain power supply, where a tractable model that approximates the dynamics of the natural gas system is proposed to reveal its inherent flexibility. The proposed model is developed in a market-compatible way.
- **[Paper C]** is peer-reviewed article published in the *Proceedings of the IEEE PowerTech Conference* (2017). The topic of this paper is the optimal adjustment of the natural gas price that is perceived by GFPPs in order to increase the efficiency of current sequential clearing of day-ahead and real-time markets in terms of expected system cost. The corresponding appendix, which includes some mathematical extensions and additional results, is provided just after the manuscript.
- **[Paper D]** is a journal article submitted to *IEEE Transactions on Control of Network Systems*. This paper deals with the optimal definition of the available natural gas volume for power production scheduling at the day-ahead stage, anticipating the flexibility needs in the real-time stage. Results of [Paper C] are included in [Paper D] for an extended comparison, since both papers share the goal of enhancing the temporal coordination of day-ahead and real-time stages via the optimal definition of specified coordination parameters (i.e. natural gas price and volume availability). The corresponding appendix, which includes some mathematical extensions, proofs, a detailed nomenclature and additional results, is provided just after the manuscript.
- **[Paper E]** is a working paper (to be submitted to *IEEE Transactions on Power Systems*). This paper proposes a novel approach to conservatively approximate distributionally robust joint chance constraints, where the ambiguity set is defined as a Wasserstein ball in the space of probability distributions. This approach is applied to the energy and reserve dispatch problem with fuel constraints for GFPPs to examine its performance under stochastic power supply. The corresponding appendix, which includes the mathematical proofs, system data, a detailed nomenclature and additional results, is provided just after the manuscript.
- **[Paper F]** is a working paper (to be submitted for a journal publication). This paper presents a distributed algorithm based on ADMM to optimally dispatch the electricity and natural gas systems in an independent, yet coordinated manner with the minimum amount of information shared between the two system operators. A distributionally robust chance constrained approach is followed to deal with uncertainty, where the ambiguity set is defined by the first- and second-order moments of the underlying probability distribution. In particular, the mean and covariance are estimated from the available historical data, which promotes transparency, and the operators can be more easily persuaded to treat them as common knowledge.

CHAPTER 2

Electricity and Natural Gas Markets

Over the last decades, the electricity and natural gas sectors have been undergoing substantial changes especially through their liberalization and the establishment of energy markets. Although the two markets have been operated in an independent manner for decades, a tighter economical and physical coordination is currently needed to maximize the efficiency of the entire energy system. This necessary coordination improvement can be attained by well-functioning market mechanisms.

We outline the transition towards a renewable-based energy system with increased interactions between the electricity and natural gas systems in Section 2.1 by presenting facts and examples from countries around the world. Moreover, we provide an overview of the electricity and natural gas market organizations along with the foreseen challenges stemming from the increased penetration of renewable power production and the potential necessary reforms on their designs. In particular, Section 2.2 presents the current structure of electricity markets and discusses the corresponding emerging challenges, while an analogous presentation for the natural gas markets is given in Section 2.3.

The interested reader is referred to [26], [27] and [28] for a detailed overview of electricity markets and power system economics, while a comprehensive overview of natural gas markets can be found in [29] and [30].

2.1 Transitioning towards higher interdependencies between electricity and natural gas sectors

Most of the countries around the world are experiencing a transition in their energy sector nowadays. This stems from the fact that the generation mix is changing gradually. Renewables have been the fastest growing energy source with the fossil fuels demonstrating a decreasing trend. However, natural gas consumption is expected to have an increase due to the large reserves and its robust production. A special focus has been placed over the last years on the coordination between the energy systems with the goal of transforming the whole energy system to a more sustainable one in Europe, as well as in the United States [31]. Among other European countries, Denmark has been a pioneer in investing and developing wind power. Denmark has also set ambitious goals towards a green energy system and is at the right path to accomplish them. Thus, mainly paradigms and facts from Denmark are presented in the remaining part.

More specifically, Denmark's energy strategy aims at achieving a complete independence of fossil fuels by 2050, while reaching 100% electricity production from renewables by putting a great focus on wind energy together with biogas and biomass [20]. Figure 2.1 illustrates the steady course

towards the accomplishment of strategic goals since one can observe the continuous increase of both installed capacities and share of wind production in the total electricity supply, which was equal to 43.4% in 2017.

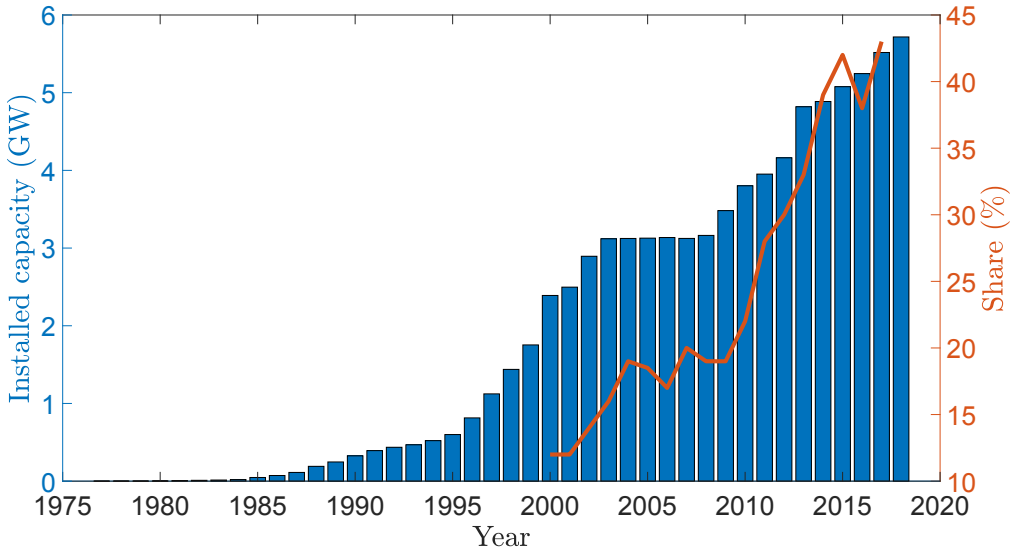

Figure 2.1: Evolution of installed wind power capacities and wind power penetration in Denmark (Figure from [32]).

Integrating high shares of renewables in energy systems, such as wind and solar power, results in significant challenges that have to be faced mainly due to their variable and stochastic power production that highly depends on meteorological factors. The penetration of renewable and green power production in the total energy system will be mainly realized via the electricity sector. However, there is a high potential for interaction among the electricity, natural gas and district heating systems in Denmark that can facilitate the integration of renewables. These three energy systems interact through various actors, such as Combined Heat and Power (CHP) plants, Gas-Fired Power Plants (GFPPs) and heat pumps, but in an uncoordinated manner until recently. It has been only lately that an increased awareness for potential possibilities has been noticed.

Denmark serves as an ideal case, where electricity, natural gas and heating networks are well interconnected. The coordination of energy services is considered an inexpensive solution to increase system's flexibility compared to other approaches, such as grid reinforcement, further interconnections and investing in electricity storage options. Additionally, an important characteristic of the Danish case is the existence of a single operator for the electricity and natural gas systems, i.e. Energinet.dk, that readily permits a coordinated and cost-effective operation of the two energy systems, while a similar setup can be also found in other European countries, e.g. Estonia, Luxembourg and Portugal. Moreover, Energinet.dk [33] owns two storage facilities with a capacity of 11 TWh and additionally 15-20 GWh in the network in the form of linepack, which may be seen as additional seasonal or short-term storage capability for the whole energy system.

On the market side, the day-ahead electricity market in Denmark is operated by Nord Pool [34], which is the single market operator for the whole Scandinavia; also covering other countries, such as the Baltic countries and United Kingdom. Electricity markets around the world have been extensively developed over the years of deregulation by taking into account the impact

of renewable energy sources. However, natural gas markets are only recently moving towards short-term trading mainly due to the increased interaction with the electricity sector. A similar trend has been observed also in Denmark, where substantial changes have been taking place over the last years. Initially, the Danish natural gas exchange, Gaspoint Nordic [35], was established in 2007 and became increasingly important every year. More specifically, a significant shift of the traded volume from the bilateral trades to Gaspoint Nordic has been noticed, since the traded volume in Gaspoint Nordic was 8.3% of the total volume in 2010, while in 2016, this number increased to 70%, showing a transformation towards a more competitive market model [36]. Gaspoint Nordic was owned until 2016 by Energinet.dk and European Energy Exchange (EEX) [37], when EEX took over full ownership through its subsidiary company Powernext [38]. All the natural gas products of Gaspoint Nordic are now available at the European trading platform PEGAS [39].

Denmark is also putting a lot of focus on the transformation of natural gas system to a greener one by investing to biogas. This can be accomplished by producing biogas from renewable energy sources, such as from biomass by thermal gasification or wind power by electrolysis. Biogas production is expected to reach 15 PJ in 2020, which is more than triple of the total annual production in 2012. In order to inject biogas in the natural gas network, it has first to be upgraded to biomethane. Then, it can be directly consumed and traded in the market. The historical and expected production of biogas and its use in Denmark from 2012 to 2020 is illustrated in Figure 2.2.

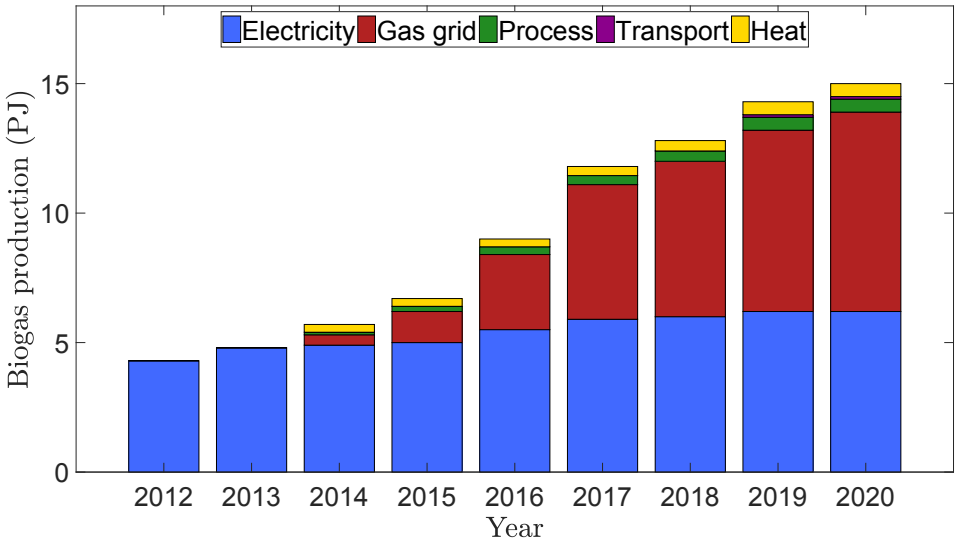

Figure 2.2: Historical and expected future biogas production and its use in Denmark 2012-2020 (Figure reproduced from [40]).

A detailed overview of the Danish transition towards a fully renewable energy system is provided in [Paper A], along with more insights of the interactions with the heat sector. In the following, we focus on the electricity and natural gas markets organization.

2.2 Electricity markets

Electricity is considered a vital commodity for the everyday life of consumers and plays an important role in the economical evolution in most of the countries around the world, since the

operation of many sectors relies on the sufficient and continuous electrical power supply. The interface of the physical and economical aspects of electricity is organized via electricity markets that provide proper trading mechanisms to ensure security of supply and competitiveness.

Until 35 years ago, the operation of power systems was organized in a centralized manner by vertically-integrated utilities, which were usually owned by states. In other words, the whole chain from production to retail was operated and managed by monopolies. However, such a centralized and monopolistic organization was not able to transmit proper incentives for new investments, as well as to promote innovation and competition that would eventually reduce costs and electricity prices. In 1982, the first separation of generation, transmission and distribution took place in Chile that introduced the liberalization of electricity markets. Then, many countries in Europe and America, as well as Australia and New Zealand, moved towards this direction in 1990s [41].

The liberalization process has not been implemented under the same rules in all countries, the basic characteristics, though, are common due to the unique features of electricity. Firstly, the electricity demand is highly inelastic because there is no other commodity able to substitute it equivalently. In addition, electricity is a homogeneous product since consumers do not distinguish its characteristics with respect to the source of production. The fact that electricity cannot be stored economically as of today in large scales results in the requirement for a continuous balance between its production and consumption. Therefore, the market designs have to take into account all these special characteristics and respect the physical network that electricity is transfered, which is imposing constraints relative to the power flow and capacity of the system.

2.2.1 Basic structures of electricity markets

In modern electricity markets that operate after the liberalization, the trading between different participants takes place in various time spans, ranging from long-term financial contracts to the real-time operation of the power system. The long-term financial products are traded in forward and futures markets allowing market participants to hedge against uncertainties and volatile prices. The focus of the thesis is on short-term electricity markets and thus the description of long-term financial markets is disregarded.

In short-term markets, it does not exist a single organizational model for electricity trading; however, two main structures are identified by analyzing various electricity markets around the world, namely *power pools* and *power exchanges*. More specifically, a power pool represents a centrally organized market, where all producers and consumers submit their offers/bids to the market operator. A centralized market-clearing algorithm is utilized to schedule the power producers that take into account all the techno-economical characteristics of the power plants, such as start-up and no-load costs, ramping capabilities, minimum capacity limits and minimum up/down times. Moreover, various services are simultaneously optimized like energy and reserves. The marginal clearing price resulting from the market-clearing algorithm is the same for all participants and is utilized for all settlements and payments. However, if the transmission network constraints are considered, a locational marginal price is calculated for each node of the electricity network. In power pools, there exists also make-whole side payments to producers in case they are not able to recover their total operating cost by the resulting market price. On the other hand, power exchanges are trading platforms that clear the market based on the merit-order principle that ranks the energy sources based on an ascending order of prices, without an explicit description of either technical characteristic of power plants or transmission constraints. In power exchanges,

the market participants are able to submit simple hourly price-quantity bids but also and more complex bids (e.g. block orders) that mimic some of the power plants' technical characteristics, such as minimum capacity limits. The market price is derived by the matching of the aggregated supply and demand curves for each trading period in the case that transmission constraints are not binding. In the presence of transmission congestions, a zonal pricing scheme is used where different market prices are calculated for the areas linked by the congested line [34].

One would notice that the market designs in United States are closer to a centralized organization with unit commitment and transmission constraints that result in the calculation of nodal prices, as in power pools. On the other hand, most of the European countries have followed an approach that is based on power exchanges with zonal pricing. Short-term trading in electricity markets takes place from 36 hours to several minutes before the actual delivery in three main trading floors, i.e. day-ahead, intra-day and real-time markets, in a sequential order. Figure 2.3 illustrates the main trading floors according to the European market structure.

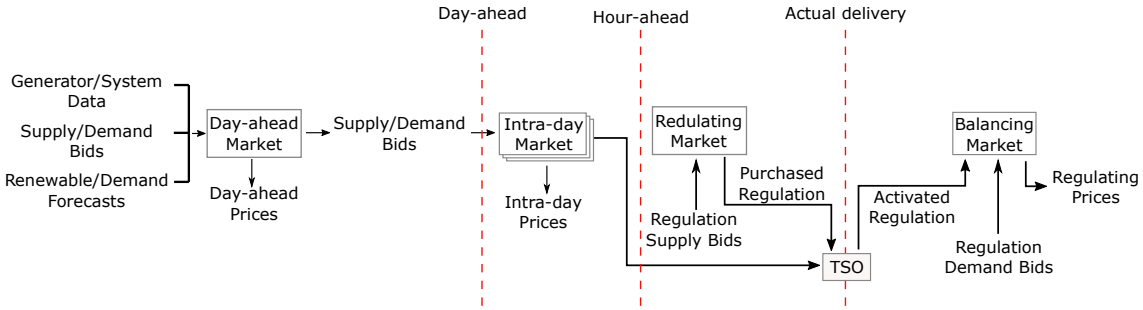

Figure 2.3: Main trading floors in the European market design.

Day-ahead market

The day-ahead markets are cleared 12-36 before the physical delivery of electricity. They are usually referred to as *spot market* in Europe and *forward market* in United States. The market is organized as a two-sided auction, where producers, retailers and large consumers are able to submit their bids. Each participant submits an offer/bid for each trading period (typically, one hour) that consists of a price-quantity pair. On the one hand, producers are submitting selling offers, while consumers are submitting purchasing bids of buying energy. More inputs may be required before clearing the market based on the specific market design, such as technical characteristics of power plants, unit commitment decisions and transmission constraints.

Intra-day market

After the day-ahead market is cleared, market participants are able to adjust their day-ahead schedules until one hour before delivery. This trading floor permits the participants to deal with possible deviations in production or consumption and modify their position based on updated information (e.g. forecast of renewable energy production). Intra-day markets can be efficiently utilized by participants to reduce their exposure to potential penalties and risks stemming from a mismatch of production and consumption in real-time. The liquidity of intra-day markets varies among different countries in Europe, while it highly depends on the organization of trading in this specific floor and the prices of the subsequent markets [42]. For example, the intra-day market

of Nord Pool [34], namely Elbas, has relatively low liquidity, while Iberian MIBEL market [43] is characterized as highly liquid.

Real-time market

The real-time market permits the compensation of any possible deviation resulting after the day-ahead and intra-day markets in order to ensure the simultaneous balancing of production and consumption at any time period and region of the power system.

In the European context, two different settlements comprise the real-time markets, for the regulating and balancing power. Bids for the regulating power are submitted by the Balance Responsible Parties (BRPs) either for up-regulation or down-regulation and are activated by the system operator in case they are needed. Then, unwanted deviations are settled ex-post in the balancing market according to the actual production of each market participant. Real-time markets are also organized in United States to cover potential imbalances from the initial schedules. Similarly to the day-ahead trading floor, a centralized algorithm is utilized to optimally re-dispatch the power system that takes into account technical characteristics of power plants and transmission constraints.

Reserve capacity market

Apart from the energy markets, i.e. day-ahead, intra-day and real-time markets, there exist also reserve capacity markets to guarantee the availability of sufficient regulation services. Energy markets are related to the transactions for the energy that is injected to or withdrawn from the system, while reserve capacity markets refer to the capacity that can be reserved to be utilized in real-time in order to provide the required balancing and are managed by the Transmission System Operator (TSO). Reserve capacity markets are organized either as an independent market or via a simultaneous auction that co-optimizes the procurement of energy and reserves. The first approach is commonly used in the European context, while the latter is usually employed in the United States.

2.2.2 Challenges in electricity market designs

Electricity markets have always been an organizational framework with continuously reshaping rules. Recently, electricity markets have been mainly challenged by the high integration of variable renewable power supply. This calls for a revision of current market structures that have been developed on a power system operating with a limited level of uncertainties, in which the majority of the generation capacity has being controllable. In the current paradigm, the generators are scheduled based on a deterministic view of all uncertain parameters at the day-ahead stage, while the deviations from forecast errors are balanced in real time. Such a *sequential* clearing of the trading floors is thus performed with a point forecast describing the uncertainties and is myopic to balancing costs stemming from forecast errors. For example, Figure 2.4 illustrates the effect of renewable power production on the shape of aggregated supply and demand curves that affects the market-clearing price.

Acknowledging the need to schedule the systems with more information regarding uncertain parameters, various approaches have been proposed in the literature to provide an *uncertainty-aware* schedule at the day-ahead stage. For instance, a two-stage stochastic programming approach is proposed in [44, 45], while robust optimization [46, 47] has been also utilized extensively. Recently,

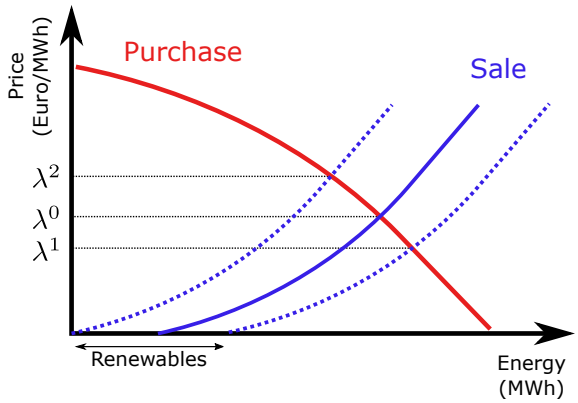

Figure 2.4: Aggregated supply and demand curves in an electricity exchange along with the impact of renewables on the market-clearing price.

chance constrained programming [48, 49] and distributionally robust optimization [50, 51] have also come into play. Market participants' payments are similarly affected by the increased penetration of renewables, which results in higher financial risks to be faced.

Moreover, distribution grids, which have traditionally represented a large portion of the total demand, are changing over the last years. Distributed energy sources are largely deployed transforming consumers to prosumers, who may also have a stochastic nature (e.g. solar panels). In this case, the main question to be answered is how the new markets can better exploit the services provided by the distribution level that will play a more active role in the future power system. Another challenge is related to the non-convexities that may arise in the optimization problems used to clear the market. For example, non-convexities are introduced from the unit commitment decisions in the United States, while the incorporation of AC power flow constraints raises similar issues. The issues raised by unit commitment decisions have been well-known and various ways such as uplift payments have been used to deal with them [52]. Similar ways to deal with non-convexities coming from AC power flow constraints can be adopted. Finally, an interesting topic is the development of tools to analyze strategic behavior of market participants to inform regulators and update market design. An extensive analysis of the aforementioned challenges is given in [53] and references therein.

2.3 Natural gas markets

Natural gas is a commodity that is widely used in various sectors, with the main ones being the power generation, transportation and domestic use for heating and cooking. In contrast to other fossil fuels, such as coal and oil, but similarly to electricity it is transfered via a physical network, which does not allow for a fully open trade. More specifically, the transport is performed mainly through the natural gas network consisting of pipelines, while in the operation of natural gas markets both the physical and economical aspects are considered. An alternative solution of natural gas transport in between regions where pipelines do not exist is in form of Liquefied Natural Gas (LNG) that has highly developed over the last two decades [29].

Prior to the natural gas market liberalization, there were only a few companies that were involved in the business sectors of the natural gas value chain comprising exploitation, imports, exports, transport, storage and trading. Thus, the most common organizational structure was characterized

by a vertically-integrated national utility controlling the whole chain. The liberalization started firstly in United States, where important steps are considered the issue of Orders 436, 500 and 636 by the Federal Energy Regulatory Commission (FERC) [54]. FERC Order 436 was issued in 1985 and unbundled natural gas commodity from transport sales, which gave the opportunity to producers and consumers to trade gas and only pay the pipeline operator the required fees. Then, FERC Order 500 basically revised some rules related to the long-term contracts and allowed pipeline operators to charge specific fees to the customers in order to support the already signed contracts. Finally, FERC Order 636, issued in 1992, was able to finalize the unbundling process by requiring the pipeline operators to separate transportation and sales giving to the customers the opportunity to select the gas provider, transportation and storage services. The liberalization came at a later stage in Europe, starting in 1990s [29]. The starting point is considered the First Gas Derivative, which opened the market and allowed network access to many participants. In order to speed up the process of liberalization, a Second Gas Derivative was issued in 2003 enabling non-household buyers to acquire natural gas from a supplier of their choice. Finally, stricter rules for unbundling were introduced by the Third Energy Package in 2009, which required the implementation of the entry-exit market model and decoupled the physical system from the market.

2.3.1 Basic structures of natural gas markets

Natural gas markets are undergoing a continuous development, since the sector has only recently been liberalized; especially, in Europe. Even though the natural gas market was mainly based on long-term contracts, an increase of short-term trading is observed lately [54].

There exist four basic market players in the natural gas market, namely the natural gas suppliers and consumers, as well as the TSO and flexibility providers [55]. The natural gas supplier acquires gas from either foreign or domestic producers through long-term contracts or the spot market and sells it to natural gas consumers. Natural gas consumers are retail suppliers that provide natural gas to residential customers and large natural gas consumers like GFPPs or industries. The TSO operates the network, guarantees security of supply and provides the transportation services. Finally, providers of flexibility own storage facilities and participate in the market to help keeping the system in balance.

At this point, the definition of the *shipper* is provided since it constitutes an important entity in the natural gas market. More specifically, the shipper refers to any player that has signed a contract with the TSO to transport natural gas in the network resulting in having both supply and sales contracts, as well as access to flexibility services [30]. Thus, the shipper possesses a variety of contracts along the whole value chain. On the supply side, the shippers have long-term bilateral contracts with the producers but they can also rely on short-term options, such as the spot market or shorter-term contracts. On the demand side, the shippers have to sign selling contracts with the customers, which vary depending on the load profile of each one. Moreover, the shipper has two options for flexibility services; one that can be bought ex-ante, such as access to storage, interruptible customers and flexibility from the suppliers and one that is related to the balancing mechanism provided by the TSO.

In Europe, the TSOs typically operate the natural gas transportation services under variants of the *entry-exit model*, which gives the ability to shippers to book capacity contracts for injection and withdrawal rights in the network within certain limits [29]. Most of the contracts are booked on a

long-term basis (i.e. weeks to years) before the actual delivery. On the day before delivery, the shippers have to nominate the amount of the booked capacity that they would like to transport so that the TSO is able to schedule the system flows. A renomination process also exists that permits adjustments of nominations up to 2 hours before the actual delivery. Moreover, the capacities that are not nominated are released to be auctioned as day-ahead capacities. There are two types of capacity, namely *firm* and *interruptible*, which are made available [30]. For the firm capacity, the TSO has to ensure that the nominated natural gas flows will be always transported if the network is at a well-functioning state. Firm capacities may not be interrupted except in severe cases that failures, which cannot be anticipated, affect the operation of the network. Regarding interruptible capacity, the TSO is obliged to transport only partially or not at all, if needed for technical feasibility, the nominated natural gas flows.

In the entry-exit model, the trading of the natural gas takes place by ignoring the network and the transportation path. The shippers are allowed to inject natural gas at every entry point and withdraw at every exit point of the network. Moreover, the entry and exit capacities can be booked independently in different quantities and durations. The entry-exit model that realizes in a specific geographical area defines a *market area* in which a *virtual trading point* belongs to [30]. Then, in the specific market area an entry contract allows for transport from the entry point to the virtual trading point, while the exit contract from the virtual trading point to the exit point that may be a consumer, an interconnection to another market area or a storage facility. It is very important to highlight that the amount of natural gas injected in the network has to be equal to the amount withdrawn at least in the long run in order to ensure the secure operation of the system. The shippers are gathered in balancing groups and each of these groups has to be maintained in balance. In the balancing process, there are hourly and daily imbalance tolerances and in case of exceeding them fees have to be paid.

Figure 2.5 illustrates the entry-exit model in Denmark, where shippers are commercially moving natural gas in and out of the Danish gas transmission system. Natural gas enters and exits Denmark from three points, namely Nybro, Ellund and Dragør. Additionally, one entry point for biogas (BNG) exists, where the shippers can inject biomethane in the system. The Exit Zone Denmark allows the natural gas suppliers to provide gas to all Danish customers via the distribution networks but also feeds natural gas to the three GFPPs that are directly connected to the transmission system. Moreover, the storage points are depicted at which the corresponding customers can inject or withdraw natural gas. The virtual transfer point offers two different options to shippers to acquire or sell natural gas; the Exchange Transfer Facility (ETF) for trades at the Danish exchange (Gaspoint Nordic) and the Gas Transfer Facility (GTF) which is related to the bilateral trades.

The firm and interruptible capacities are determined by the TSO based on natural gas flow simulations, as well as by taking into account historical and forecast demand profiles and flows. Then, the capacities are sold by auctioning in standardized forms for various durations, including yearly to daily products. In the process of calculating the capacities, the TSO needs to consider the ability of the shippers to transfer natural gas from an entry point to any exit point and reserve the necessary capacities along the various network paths. Consequently, there might exist combinations of injection and withdrawal rights that create the so called *contractual congestion*, where the TSO cannot offer more firm capacity to the shipper even though the system is not actually congested. A direct consequence of contractual congestion is the inefficient utilization of natural gas system's capacity due to the simplified view of the network in the marketplace. Note

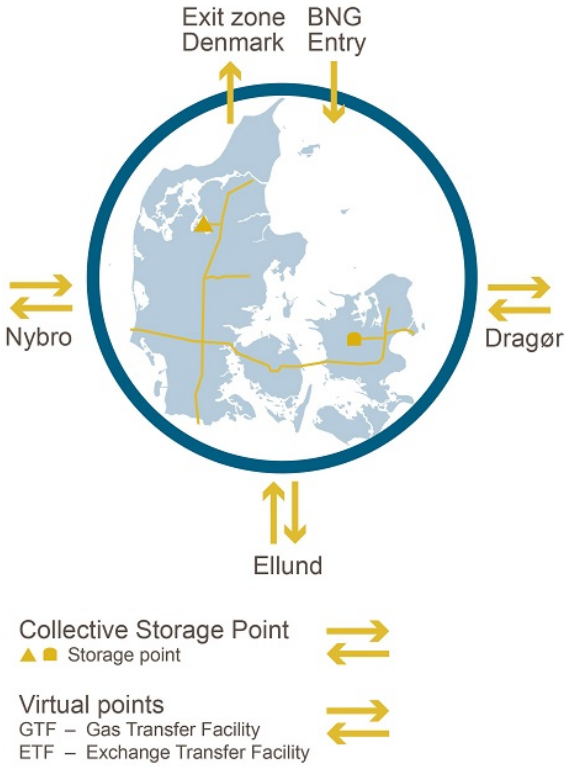

Figure 2.5: Natural gas entry-exit model in Denmark (Figure from [56]).

that based on the Third Energy Package, contractual congestion is defined as a situation where the level of firm capacity demand exceeds the technical capacity, while the physical congestion as a situation where the level of demand for actual deliveries exceeds the technical capacity at some point in time [29].

A different organization of the network services exists in the United States and in some Australian markets that is based on a *point-to-point* definition of the entry and exit rights [29]. In this setup, the shipper specifies the points of injection and withdrawal and thus a specific path in the network is defined. Compared to the European approach, the point-to-point trades comprise more characteristics of the physical network representation and the markets are organized for independent pipelines.

2.3.2 Challenges in natural gas market designs

Choosing either the entry-exit or point-to-point model results in different implications in the temporal and spatial flexibility [57]. The entry-exit model allows for a high spatial flexibility since the shippers are able to inject and withdraw natural gas from any point of the network, while the point-to-point model is a less simplified version since the actual path assigned with the trade needs to be defined. Regarding time flexibility, most of the natural gas markets around the world rely on up to a specific level of time flexibility, since the storage ability is not as limited as the electricity system. For example, daily products are traded in some natural gas markets, which implies that the injections and withdrawals have the same price throughout the day.

Ensuring security of supply involves a tighter coordination between network services and commodity trading [57]. On the other hand, network simplification increases liquidity but at

the same time implies that some of the services related to the network use are not priced. More specifically, an important consequence of following the entry-exit model is that the cost associated with the network is not allocated based on the actual use of the network, as it would be if a nodal price model similar to the context of electricity markets in United States, was utilized. Hence, the entry-exit model requires some additional elements to transform the market decisions to feasible physical network flows. Usually these elements come via the balancing services that result in the relevant costs to be socialized among the network users.

Furthermore, the lack of a detailed network representation in the majority of natural gas markets does not promote the definition of additional network services, such the allocation of linepack, to fully exploit natural gas network's flexibility [55]. Linepack is the ability of utilizing the natural gas network as a storage facility by adjusting the pressure differences between the various nodes. Moreover, the pressure differentials impact the flow in the pipelines and affect their transport capacity. Therefore, linepack and transport capacities are substitute services and both of them important in short-term operations to have an efficient communication between the network services and commodity trading. A fully decoupled approach of gas trading and transportation services results in solutions with a reduced welfare because of the suboptimal utilization of the actual available capacities. A tighter coupling with the electricity system increases the need for using the natural gas network services efficiently because of the variability and uncertainty introduced to the withdrawals from GFPPs. Similarly to the electricity system, various non-convexities may arise in the market-clearing optimization problems for the natural gas market if network constraints are considered. To overcome such an issue either market-compatible network models that allow the development of pricing schemes would need to be incorporated in the market-clearing algorithms or similar approaches to uplift payments would have to be adopted.

These issues are addressed in [Paper B] of this thesis, where the benefits of utilizing the actual value of natural gas both in the temporal and spatial dimension to dispatch the coupled electricity and natural gas systems are discussed, along with the flexibility provided by linepack in the transportation services.

CHAPTER 3

Electricity and Natural Gas Systems Coordination

The worldwide environmental concerns, the increased availability of natural gas supply and the prominent role of Gas-Fired Power Plants (GFPPs) as one of the main flexible and efficient generation technologies in the whole energy system are increasing the interdependence between the electricity and natural gas systems. Therefore, the design and coordination of the electricity and natural gas markets needs to be reconsidered by taking into account the interactions between the energy systems, in order to reveal the full operational flexibility and facilitate the integration of more variable and uncertain renewable energy sources. Several studies, such as [1, 10, 13, 54], exist in the literature indicating the need for further elaborating on this topic.

This chapter reviews the market-based interactions between the electricity and natural gas systems highlighting the need for an increased coordination, which can be enabled via proper modeling of the energy networks and system components. The interactions between the energy sectors are presented in Section 3.1. In Section 3.2, we present the modeling approaches to incorporate network constraints in the market-clearing mechanisms. Finally, the developed coordination frameworks in short-term operations are presented in Section 3.3.

3.1 Interactions between electricity and natural gas systems in a market environment

Historically, the withdrawals from the natural gas network were characterized by limited variability and uncertainty as the majority of consumers had relatively stable and predictable demands profiles. For this reason, the transactions of natural gas were mainly based on fixed delivery contracts at the day-ahead stage that required the portfolio of the shippers to be balanced at the end of the day. However, fundamental changes have been observed lately by the increasing share of demand related to power production by the GFPPs [29].

The increased natural gas demand of GFPPs results in a tighter interaction between the electricity and natural gas systems and eventually of the corresponding markets. Moreover, the deployment of intermittent renewable energy sources, such as solar and wind power, is highly increasing in the power system. The GFPPs are characterized by high efficiency and flexibility, which makes them one of the main conventional technologies to provide power and guarantee the security of supply as a controllable generating unit. Therefore, the uncertainty and variability of renewables is transfered to the natural gas systems via the fuel demand of GFPPs, which brings numerous challenges on the operation of both systems [54].

In the electricity sector, both the market's and system's operations are faster than in the natural gas sector. Moreover, more and more uncertainties are introduced in the natural gas system operation.

These changes on the operation of the natural gas system increase the uncertainty of natural gas availability and prices, which in turn affects the power system dispatch via the GFPPs. In order to address these challenges, a better synchronization and harmonization of the markets is needed to improve intra-day market coordination and communication. Currently the two markets are operated under different designs as explained in the Chapter 2, where on the electricity side the production and consumption have to be in continuous balance because of the limited storage capability, while on the natural gas side there is a higher flexibility regarding the matching of supply and demand.

The electricity and natural gas systems interact via physical and economic links established by GFPPs. From a physical perspective, these two systems interact through the natural gas consumption of GFPPs, while from an economic viewpoint they are implicitly coordinated through the natural gas price the GFPPs buy their fuel. Figure 3.1 illustrates the interdependency of electricity and natural gas markets via such coordination parameters, i.e. the price of natural gas and the consumption of GFPPs, as well as the available quantity of natural gas for power production.

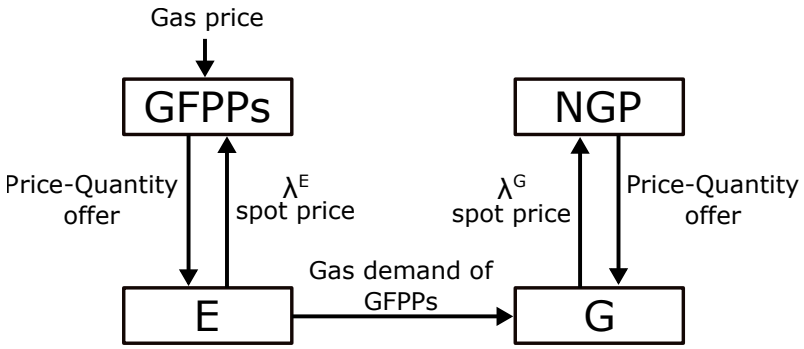

Figure 3.1: Electricity and natural gas markets coordination (GFPPs: gas-fired power plants, NGP: natural gas producers or shippers with natural gas sales contracts, E: electricity market, G: natural gas market).

In the natural gas market, GFPPs act as buyers to acquire their fuel for power production and mainly purchase natural gas via short-term interruptible contracts or in the gas spot market. The natural gas supply contracts are signed at a predefined price, while in the gas spot market the GFPPs buy their fuel at the spot price. The natural gas spot price usually remains the same throughout the gas day and may be unknown for a period of the following day at the time of bidding in the electricity market due to the asynchronous setup between the two markets. The asynchronous timing of electricity and natural gas markets is considered an additional source of inefficiency on their operation, which becomes highly essential under the increased system interaction with fluctuating renewables in place [1, 2]. Figure 3.2 shows the time shift of the electricity market with the corresponding natural gas market in the European context, where it can be observed that the GFPPs acquire their fuel from two different natural gas trading days in order to participate in an electricity trading day. More specifically, the GFPPs are bidding for electricity day "D" at 12 PM of electricity day "D-1" by knowing only their fuel nominations of natural gas day "D-1" and by having to make their decisions for natural gas day "D" after the outcomes for electricity day "D". Therefore, GFPPs have to use an estimation of the natural gas price and in turn face uncertainty about the price and natural gas availability, when participating in both markets. In such an independent setup, the fuel price utilized by GFPPs to bid in the electricity market is

considered fixed, regardless of the procurement procedure (i.e. supply contract or spot market) and may not reflect the *actual price* of natural gas at the specific region of the system and point in time.

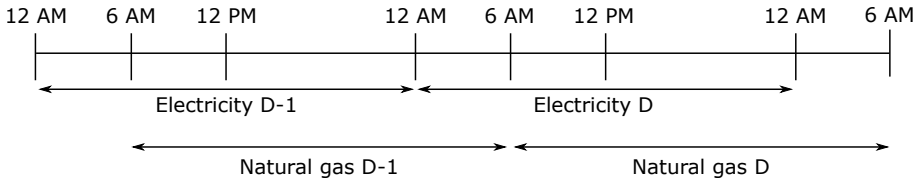

Figure 3.2: Electricity and natural gas trading days.

The price-quantity offers in the electricity market are placed depending on the natural gas price, fuel the availability and the technical characteristics of GFPPs. Then, the electricity market is cleared and the natural gas demand of GFPPs is given as a fixed input to the natural gas market. In a similar fashion, the natural gas market is cleared based on the price-quantity offers of the natural gas producers or the respective shippers to meet the demand of natural gas consumers, such as industrial and residential customers as well as GFPPs. Note that the fuel demand of GFPPs is usually assigned with a lower priority than industrial and residential gas loads, which may constrain the operation of GFPPs in systems where natural gas is widely used both for power production and heating.

Furthermore, a technology that can transform the interaction of the electricity and natural gas systems to be bi-directional is the power-to-gas facilities that consume electricity to produce hydrogen or synthetic natural gas. This technology has a considerable potential to facilitate the integration of renewables in the energy system, as excess production is converted in compatible natural gas to be stored or utilized in the natural gas infrastructure. This technology is not in the scope of this thesis and the reader is referred to [58] and [59] for a detailed description of its characteristics. Moreover, since the interdependence between electricity and natural gas systems is expected to tighten in the future, coordinated decisions also for planning problems need to be taken, as discussed in [60, 61].

Advanced modeling and optimization techniques with modern market designs can increase the efficiency of operating the whole energy system under high shares of renewables in a cost-effective manner and decrease the need for costly investments to ensure security of supply. However, regulatory changes are still needed and market designs have to be improved. It has only been recently that some regulatory changes have promoted the coordination between the energy sectors and markets. For instance, the Federal Energy Regulatory Commission (FERC) Order 787 that was finalized in November 2013 endorsed the voluntary sharing of information between the electricity and natural gas operators to promote reliable service and operation. Finally, FERC Order 809 that was issued in April 2015 aimed at synchronizing the electricity and natural gas markets.

3.2 Modeling framework of energy networks to enable coordination

The transportation of electricity and natural gas from the production to consumption points takes place through complex networks and is characterized by specific physics laws. In short-term clearing of the energy markets and operation of the energy systems, the flows in the networks need to be taken into account to guarantee that production always meets demand. Moreover, additional inherent flexibility of the natural gas network can be exploited by an advanced modeling of its physical characteristics.

3.2.1 Electricity system

The power flow in the electricity network is characterized by a set of the so-called AC power flow equations that determine the active and reactive power, the losses on each line and the voltages at the nodes of the network. These equations are non-convex and non-linear resulting in computational and optimality challenges in an optimization framework. Recent developments in the area of convex optimization, see [62–64], have provided tight convex relaxations of these equations. However, a linearized lossless DC approximation is utilized in this thesis that has been widely used in the literature [65], since the focus is placed on the natural gas system modeling and the integration of electricity and natural gas systems under uncertainty. We provide briefly the basic assumptions and formulas, while we refer the reader to [66] and [67] for an extensive analysis on power flows studies.

The linearized lossless DC approximation of AC power flow considers only the active power flows and neglects reactive power flows. The AC representation of the active power flow f in a transmission line is expressed by

$$f_{n,r} = |V_n|^2 \mathcal{G}_{n,r} - |V_n||V_r|\mathcal{G}_{n,r}\cos(\theta_n - \theta_r) - |V_n||V_r|B_{n,r}\sin(\theta_n - \theta_r), \tag{3.1}$$

where $B_{n,r}$ is the susceptance matrix and $\mathcal{G}_{n,r}$ is the conductance matrix. Moreover, V is the voltage amplitude and θ the voltage angle at each node n.

The formulation of the DC power flow is based on three assumptions:

1. The line resistances R are negligible compared to line reactances $\mathcal{X}$ and thus the line parameters are simplified and losses are neglected (i.e. $R_{n,r} \ll \mathcal{X}_{n,r}$ for all lines; thus, we have $\mathcal{G}_{n,r} = \frac{R_{n,r}}{R_{n,r}^2+\mathcal{X}_{n,r}^2} \approx 0$ and $B_{n,r} = \frac{-\mathcal{X}_{n,r}}{R_{n,r}^2+\mathcal{X}_{n,r}^2} \approx -\frac{1}{\mathcal{X}_{n,r}}$).

2. All nodes have the same voltage amplitude (i.e. $|V_n| \approx 1\ p.u.$).

3. Voltage angle differences between adjacent nodes are small, which allows for the linearization of sinusoidal terms (i.e. $\sin(\theta_n - \theta_r) \approx \theta_n - \theta_r$ and $\cos(\theta_n - \theta_r) \approx 1$).

Following these assumptions, the active power flow equation between nodes n and r simplifies to

$$f_{n,r} = B_{n,r}(\theta_n - \theta_r). \tag{3.2}$$

An alternative representation of the DC power flow is given via the PTDF matrix $Q_{l,n}$ [65], which describes in a linear manner the relationships between power injections and active power flows through the transmission lines l, as in

$$f_l = Q_{l,n}P_n, \tag{3.3}$$

where P_n is the nodal injections at node n. The DC power flow model can be formulated as a set of linear constraints and thus results in a Linear Program (LP).

3.2.2 Natural gas system

The dynamics of the natural gas flow in the pipelines are modeled by a set of non-linear Partial Differential Equations (PDEs) that are able to describe the actual temporal and spatial dimensions of the flow [68, 69]. This approach provides the most accurate modeling but it involves a high computational burden and may lead to possible market design issues related to natural gas pricing. An application of such model to the power and natural gas coordination problem can be found in [8], while its incorporation in a market framework is discussed in [54]. In this thesis, some simplifying assumptions are made in order to partly, but yet efficiently, capture the dynamics of the natural gas flow and take them into account in the market-clearing procedure and optimal dispatch of the systems. More specifically, a stationary model, i.e. the natural gas is in steady state, with an isothermal gas flow in horizontal pipelines is assumed that allows the utilization of the *Weymouth* equation [30], which has been widely used in the literature as in [70–73]. The natural gas flow from node m to node u is described by

$$q_{m,u} = K^f_{m,u}\sqrt{pr^2_m - pr^2_u}, \tag{3.4}$$

where $K^f_{m,u}$ is the Weymouth constant that depends on the characteristics of the pipeline and pr_m is the pressure of node m. Figure 3.3 illustrates the natural gas flow from node m to node u as a function of the pressures of the adjacent nodes.

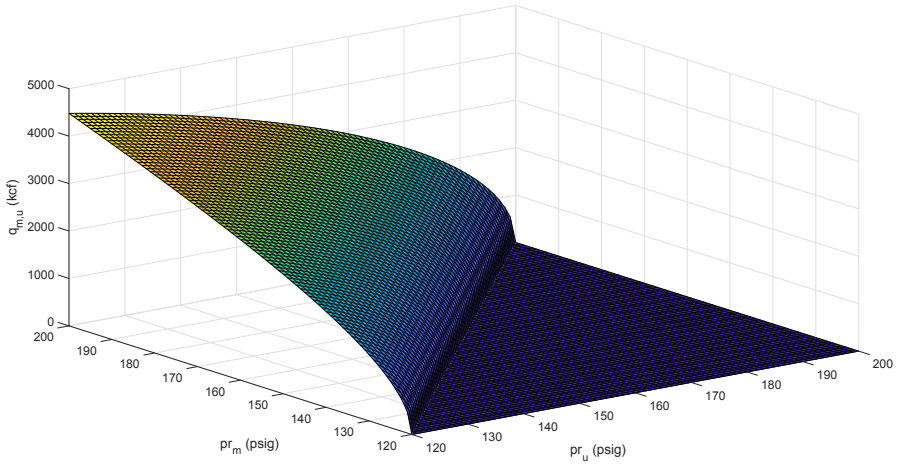

Figure 3.3: Three dimensional illustration of Weymouth equation showing the flow as a function of pressures at inlet and outlet nodes.

The sign function that needs to be modeled for the bi-directional flows along with the quadratic terms makes the Weymouth equation non-linear and non-convex. In this thesis, the natural gas system is taken into account by the three following models that utilize the Weymouth equation in different ways.

Contract and fuel capacity constraints

In this approach, the natural gas system is simplified to a linear model that neglects the physical characteristics of the flow and provides capacity constraints to one or a set of GFPPs in an area of

the system by

$$0 \leq D_t^{\mathrm{p}} \leq \overline{G}_t \tag{3.5}$$

for each time period t, where D^{p} is the natural gas consumption of a specific GFPP or a set of GFPPs and $\overline{G}$ the hourly natural gas available capacity of the system. Moreover, contract capacity constraints can be used as

$$0 \leq \sum_{t \in T} D_t^{\mathrm{p}} \leq \overline{G}^{\mathrm{D}}, \tag{3.6}$$

where $\overline{G}$ is daily natural gas available capacity of the system. The capacities $\overline{G}$ and $\overline{G}^{\mathrm{D}}$ can be estimated via an ex-ante calculation from the Weymouth equation along with the natural gas injections and withdrawals in the system. More specifically, $\overline{G}$ is calculated by subtracting the natural gas demand of residential/industrial loads from the maximum transportation capacity of the network to the specific area and $\overline{G}^{\mathrm{D}}$ as the total injected natural gas minus the total residential/industrial demand throughout the whole day. The total maximum transportation capacity is equal to the maximum capacity of the pipelines transporting gas in the specific area. The Weymouth equation is utilized to compute the maximum capacity by using the maximum pressure difference for the adjacent nodes of each pipeline. This set of linear constraints is utilized in [Paper C], [Paper D] and [Paper E]. The final model is an LP.

Controllable flow model

In this model, there is a representation of the natural gas network with its nodes and pipelines. The natural gas flow is fully controllable up to a maximum flow limit that is calculated ex-ante via the Weymouth equation by taking the maximum pressure difference of the adjacent nodes. The nodal natural gas balance is enforced, while the injections and withdrawals are also controllable variables. The model is formulated as an LP and utilized in [Paper F].

Flow model with approximated dynamics

The introduction of nodal pressures as control variables permits the definition of the natural gas flow by the Weymouth equation. The nodal pressures are constrained by

$$PR_m^{min} \leq pr_m \leq PR_m^{max} \tag{3.7}$$

for each node m by the minimum PR_m^{min} and maximum PR_m^{max} pressure limits. In order to overcome the non-linear and non-convex nature of the Weymouth equation, an outer approximation based on Taylor series expansion around fixed pressured points is used to linearize it. Therefore, the Weymouth equation can be replaced by a set of linear inequalities

$$q_{m,u} \leq K_{m,u}^f \left(\frac{PR_{m,v}}{\sqrt{PR_{m,v}^2 - PR_{u,v}^2}} pr_m - \frac{PR_{u,v}}{\sqrt{PR_{m,v}^2 - PR_{u,v}^2}} pr_u \right), \tag{3.8}$$

where $v \in \mathcal{V}$ is the set of fixed pressure points $(PR_{m,v}, PR_{u,v})$. Using a significant number of fixed points (e.g. around 20 pairs as stated in [71]) ensures a sufficient approximation of the Weymouth equation. The outer approximation is given by a number of tangent planes to the cone defined by the Weymouth equation. Figure 3.4 depicts in two dimensions the outer approximation of the Weymouth equation.

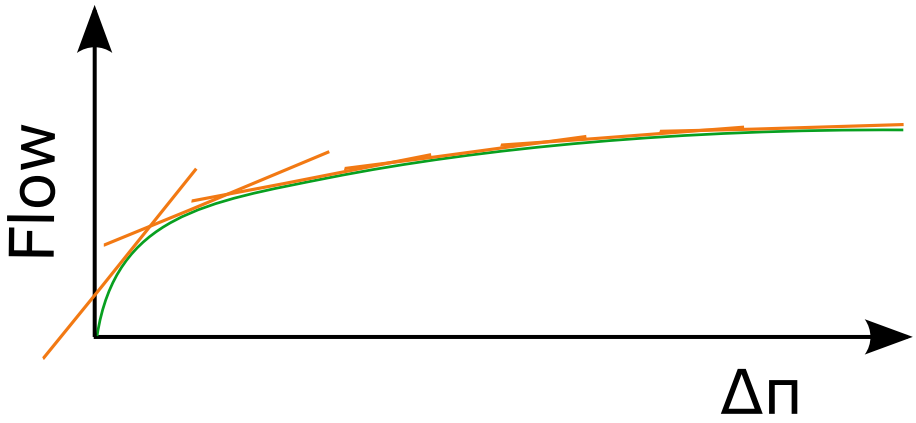

Figure 3.4: Outer approximation based on Taylor series expansion ($\Delta\pi = pr_m^2 - pr_u^2$, green line: Weymouth equation, orange lines: tangent planes).

The natural gas flow in each pipeline is approximated by the linear constraint to be binding [74]. These linear constraints are calculated based on fixed pressure points generated by choosing multiple pressure values of the adjacent nodes between the pressure limits. The acquired fixed pressure points are used to describe the flow for one direction in the pipeline and may differ from the ones used to describe the opposite direction, since the pressure limits of the adjacent nodes are not the same. Therefore, the set of linear inequalities may be different in the opposite direction and a binary variable needs to be introduced in order to pick the proper set of inequalities to formulate the model with bi-directional flows. A detailed description of the equations is given in [Paper B].

The dynamics of the natural gas system are incorporated by allowing each pipeline to act as a storage facility providing an economic way of storing energy, which is referred to as *linepack*. Linepack $\tilde{h}_{m,u,t}$ in the pipeline between nodes m and u in time t is modeled by

$$\tilde{h}_{m,u,t} = K^h_{m,u} \frac{pr_{m,t} + pr_{u,t}}{2} \tag{3.9}$$

$$\tilde{h}_{m,u,t} = \tilde{h}_{m,u,t-1} + q^{in}_{m,u,t} - q^{out}_{m,u,t}, \tag{3.10}$$

where $K^h_{m,u}$ is a constant describing the pipeline characteristics. The average mass of natural gas in the pipeline is proportional to the average pressure of adjacent nodes and the mass conservation in time is calculated by the inflow $q^{in}_{m,u,t}$ and outflow $q^{out}_{m,u,t}$ of the pipeline. Figure 3.5 illustrates the dependence of linepack and natural gas flow in a pipeline, where the linepack acts as a buffer absorbing the differences between the inflow and outflow.

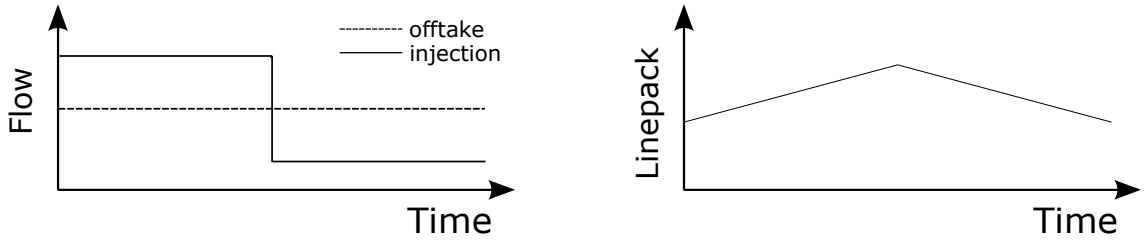

Figure 3.5: Natural gas flow and linepack interdependence in a pipeline.

Finally, the branches of the network with compressors are modeled via a simplified approach that uses a compressor factor Γ_z for branch z to define the relation of pressure at the two adjacent nodes

as follows

$$pr_u \leq \Gamma_z pr_m. \tag{3.11}$$

The natural gas flow model with approximated dynamics that yields a Mixed-Integer Linear Program (MILP) is described in detail in [Paper B] and utilized in [Paper D].

3.3 Coordination framework for electricity and natural gas systems

Based on the presentation of the two systems interplay in Section 3.1, one can formulate two different approaches for the coordination of electricity and natural gas systems, namely the *decoupled* and the *coupled* one. In the decoupled operation of the two energy systems, the system dispatch takes place independently and only a limited amount of information is shared between the operators. More specifically, the natural gas consumption of GFPPs needs to be shared and the GFPPs have to use an estimation of their fuel price when participating in the electricity market. In the coupled operation, the electricity and natural gas systems are dispatched and operated in a centralized manner, where the power production cost of GFPPs is defined endogenously and emerges from the actual value of natural gas. Moreover, the fuel demand of GFPPs can be altered in view of a cost-effective operation of both energy systems. The decoupled approach models a setup that is closer to the current practice, while the coupled one yields the optimal solution for the whole integrated energy system and can give relevant insights towards the future tighter coordination of electricity and natural gas systems.

Focusing on the temporal dimension, the different market floors are currently cleared in a *sequential* and deterministic fashion. Therefore, any uncertain parameter is characterized by a point forecast (e.g. expected value of wind power) that is utilized as input to the operational model. Before the extensive introduction of renewables, such approaches were considered adequate since the uncertainties related to electricity and natural gas systems operations were relatively limited. However, the conditions under which systems are operated today are becoming increasingly challenging due to the stochasticity introduced by renewables. This effect is more profound under high shares of wind and solar power production, which is characterized by limited predictability and high variability due to its dependency on the weather conditions. Hence, current market designs need to be coupled with modern optimization techniques and advanced modeling of uncertainties to facilitate the accommodation of renewables and the coordination of electricity and natural gas systems. In view of the stochastic nature of renewables, an *uncertainty-aware* schedule at the day-ahead stage that adopts a probabilistic characterization of uncertainties would ensure sufficient operational flexibility close to real-time operation and reduce the operating cost of the systems. Figure 3.6 sketches the sequential and uncertainty-aware scheduling, where all future uncertainties are either characterized in a single-valued forecast or a greater range of potential outcomes is considered.

Towards an uncertainty-aware energy system dispatch, one can utilize various approaches proposed in the literature to deal with uncertainties, such as stochastic programming, robust optimization, chance constraints and distributionally robust optimization. In stochastic programming [21], it is common to make assumptions regarding the probability distribution of the random parameter within the process of generating scenarios in order to obtain a discrete distribution of the random parameter. In the stochastic programming framework, the focus is placed on optimizing for the

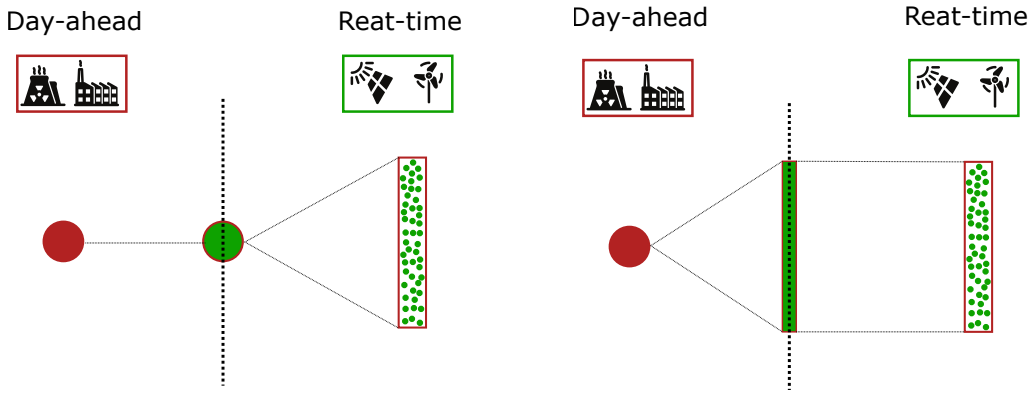

Figure 3.6: Temporal dimension of scheduling the systems under the sequential (left) and uncertainty-aware (right) approaches.

expectation of potential outcomes (e.g. expected operational cost), while in robust optimization the decisions are optimized for the worst-case realization in the uncertainty set [75]. Therefore, robust optimization may yield overly conservative solutions; this conservativeness though can be controlled by a proper definition of the uncertainty (e.g. by considering some spatial dependence for the random parameters). Alternatively, chance constrained programming [21] can be utilized to obtain less conservative solutions by ensuring that constraints including random parameters are only satisfied for a predefined probability. Analytical reformulations can be attained by assuming the distribution of the uncertain parameter (e.g. Gaussian distribution) or by sampling a finite number of constraints, where the number of samples depends on the predefined probability and structure of the problem, in order to create an approximate problem to be solved. Finally, novel data-driven approaches that fill the gap between stochastic programming and robust optimization can be employed. More specifically, distributionally robust optimization that optimizes over a family of distributions (i.e. ambiguity set) without requiring the exact knowledge of the underlying distribution has been utilized recently. Two types of ambiguity sets are more commonly used in the literature: the moment-based [18] and the metric-based ones [19]. Moment-based ambiguity sets are defined by the distributions satisfying moment constraints (e.g. having the same mean and covariance matrix), while in the latter approach the ambiguity set contains the distributions that are close to the empirical one based on the probability metric selected. In this context, the worst-case expected value over the ambiguity set is optimized, while chance constraints are reformulated to ambiguous chance constraints that are defined over the ambiguity set. Following each of the aforementioned approaches, the decision maker has an uncertainty-aware attitude, as opposed to a deterministic one.

Depending on the level of coordination between the electricity and natural gas systems and the temporal coordination of various trading floors, four different approaches can be followed to study all potential setups as illustrated in Figure 3.7. The sequential and decoupled arrangement resembles current markets designs that only have limited coordination, while the fully coordinated approach of uncertainty-aware coupled scheduling treats the system in with holistic view that accounts for future uncertainties. The two models in between gradually enhance the coordination and allow to identify inefficiencies that arise when following a sequential or decoupled approach.

Except for presenting the detailed modeling of the natural gas flow with approximated dynamics, [Paper B] studies *Seq-Dec*, *Seq-Coup* and *UA-Coup* models by utilizing two-stage stochastic

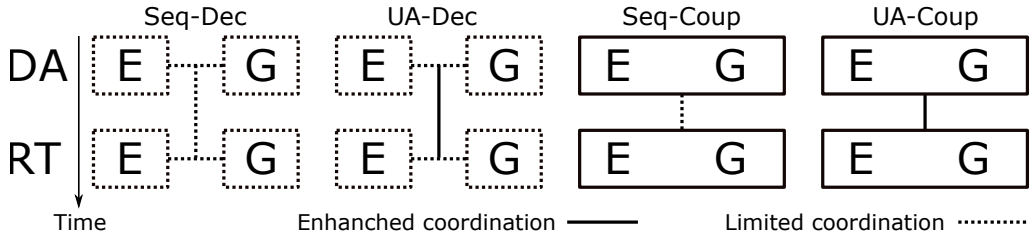

Figure 3.7: Coordination of electricity and natural gas markets in short-term operations (DA: day-ahead stage, RT: real-time stage, E: electricity, G: natural gas, Seq: sequential, UA: uncertainty aware, Dec: decoupled, Coup: coupled).

programming to account for stochastic power production from renewables. The importance of proper natural gas system modeling in short-term operations to reveal the inherent flexibility of the natural gas system is demonstrated, along with the effectiveness of accommodating high shares of renewables. Moreover, the coordination parameters between electricity and natural gas system are identified, as also discussed in Section 3.1, and their impact on the operation of the systems and on the dispatch is presented.

Having identified the natural gas price perceived by GFPPs and the natural gas volume availability for power production made available to GFPPs as the coordination parameters, their optimal control by the operator in view of future balancing needs due to forecast errors from uncertain power supply allows to bridge the efficiency gap in terms of expected system cost between *Seq-Coup* and *UA-Coup*. [Paper C] and [Paper D] propose a price-based and a volume-based approach to achieve a better temporal coordination in coupled electricity and natural gas systems, while keeping the sequential clearing of day-ahead and real-time stages, respectively. These approaches can be highly attractive in cases that electricity and natural gas systems are operated by the same entity, as Energinet.dk in Denmark.

On the other hand, various challenges may arise in cases where the systems are operated independently and the system operators are not willing to follow a fully coupled setup due to different strategies or privacy issues with regards to the system and market data. To overcome such issues, distributed algorithms that optimally dispatch each system independently with the minimum information sharing can be employed. This is the topic of [Paper F], which proposes a systematic data-driven distributed algorithm to solve *UA-Dec* by utilizing distributionally robust optimization with a moment-based ambiguity set to deal with uncertainty in an efficient and transparent way. An important element of this approach is that the ambiguity set is built based on the first- and second-order moments of the random parameter that are inferred from historical data. Moreover, the algorithm converges to the same solution of *UA-Coup* model that accomplishes an enhanced coordination both system-wise and in the temporal dimension. The proposed approach is additionally compared with *Seq-Dec* and with a case that utilizes chance constrained programming under the assumption of Gaussian uncertainty resulting in an improved performance.

Moving towards a renewable-based power system, the system dispatch needs to take place via advanced models that account for the variability and uncertainty of renewable generation. Stochastic production from renewables does not follow any specific distribution in reality. Therefore, assuming the existence of the true probability distribution in any parametric family or approximating it by a discrete empirical distribution may yield to poor performance of the system dispatch when the actual stochastic power production realizes. This effect is more profound in cases when only a

limited number of samples is available. A distributionally robust approach based on a metric-based ambiguity set permits to mitigate the inaccurate estimates of the true underlying distribution via tuning the size of ambiguity set depending on the number of available samples. Additionally, a problem reformulation with joint chance constraints gives the freedom to the decision-maker to impose system-wide risk parameters regarding the violation of the corresponding constraints instead of imposing specific risk parameters for individual ones. These topics are presented in [Paper E], which proposes a novel approach to conservatively approximate distributionally robust joint chance constraints on the *UA-Coup* model.

The terms *scheduling* and *dispatch* refer to the outcome of a market design, that resembles the centralized operation of vertically integrated structures, in which all assets are owned and operated by a single entity that aims to minimize the system cost, while ensuring technical feasibility. On the other hand, the term *market-clearing* refers to the equilibrium of several market participants seeking to maximize their profits, usually internalizing their technical constraints and their degrees of risk aversion. In this thesis, the aim is to define models that can serve as benchmarks in terms of minimum system cost and contribute towards the design of efficient market architectures. Therefore, these terms are often used interchangeably in the context of this thesis.

CHAPTER 4

Market Design Alternatives for Electricity and Natural Gas Systems

In this chapter, we present three market-clearing models with various degrees of coordination between the electricity and natural gas systems, as well as between the trading floors. We identify the key coordination parameters, which are the natural gas price and fuel availability for Gas-Fired Power Plants (GFPPs), and demonstrate their effect on the dispatch of the whole energy system. The proposed models incorporate the description of the natural gas system into the market-clearing models in a market-compatible way, which provides the opportunity to study the benefits of the natural gas system's inherent flexibility. Further insights with regards to improving the coordination between the two trading floors via a fine-tuning of the two key coordination parameters are provided in Chapter 5.

The methodologies developed in this chapter focus on short-term operations of electricity and natural gas markets with the stochastic power supply being wind power. The uncertainty-aware dispatch is built by utilizing two-stage stochastic programming, while the natural gas flow model with approximated dynamics (see Section 3.2.2) is used to highlight the benefits of network modeling in facilitating the integration of renewables. This natural gas flow model permits to explore the benefits of linepack flexibility. The models and results outlined in this chapter are presented in [Paper B] in detail. A series of recent studies has dealt with the presence of uncertain power production in electricity and natural gas systems as in [4, 76]. Moreover, the importance of taking into account the natural gas system for flexibility and reliability is highlighted in [13, 54]. For a more detailed literature survey, see the introduction of [Paper B].

In Section 4.1, we provide an overview of the market-clearing models and highlight the impact of the coordination parameters on the operation of electricity and natural gas systems. The mathematical formulation of the market-clearing models is presented in Section 4.2. A comparison among the proposed models is performed in Section 4.3, where the impact of coordination parameters is further investigated. Finally, the benefits of incorporating the natural gas network constraints in a market-compatible way are demonstrated in Section 4.4.

4.1 Description of market-clearing models for electricity and natural gas systems

This section presents and describes the market-clearing models for electricity and natural gas systems with a focus on the key coordination parameters (i.e. natural gas price and fuel availability

for power production from GFPPs). The interactions between electricity and natural gas markets are mainly based on the communication interface provided by GFPPs via the coordination parameters, such as the fuel consumption, which depends on the dispatch in the electricity market, and the natural gas price [77]. Under an imperfect and limited coordination between the two systems, these parameters are defined in a *static* way that does not permit an efficient coordination of the two systems. However, several schemes to improve the coordination and define the parameters in a more sophisticated manner have been considered in practice in various regions around the world which are highly dependent on GFPPs for electricity production. For instance, ISO New England has faced a lot of challenges to ensure adequate fuel supply for GFPPs during winter periods when the heating demand is high, which made it necessary to consider an increased coordination with the natural gas sector to reduce the fuel-security risk and guarantee a secure operation of the power system [78]. In particular, hourly natural gas consumptions of GFPPs are calculated and it is verified whether they can be accommodated by the corresponding pipelines that the GFPPs are connected to. Then, it may be chosen to revise the next-day operating plan in case needed. Following these observations, we consider different levels of coordination between the electricity and natural gas systems through a static or *endogenous* definition of these parameters.

In the temporal dimension, we focus on short-term markets to study the effect of stochastic power production from renewables. Electricity has been widely traded in short-term markets, while natural gas markets have been historically based on long-term contracts with limited short-term variability. However, recent trends show a transition towards short-term trading, which is further strengthened by the needs of GFPPs that have an increased intraday fuel variability. This is due to the fact that they serve as a back-up technology to compensate for the fluctuating renewable power production [8]. Participation in the natural gas spot market, even when supplemented with some natural gas forward purchases for hedging, is also preferred by GFPPs as discussed in [79].

The main focus is placed on two trading floors, namely the day-ahead and real-time stages. Depending on the level of coordination between the two energy systems and between the trading floors, the following three market-clearing models are considered.

4.1.1 Sequential dispatch of decoupled electricity and natural gas systems

This model aims to mimic the existing setup where the two energy systems are operated in a decoupled manner with a deterministic view of uncertain power supply, as shown in Figure 4.1. Initially, the electricity system is scheduled by having as an input a single-valued forecast of the stochastic power production, which results in determining the fuel consumption of GFPPs. Then, the fuel consumption of GFPPs is submitted as a fixed demand to the natural gas market. In the electricity market, the GFPPs submit the price-quantity offers based on an estimation of the natural gas price or on the price of the natural gas supply contract. Thus, both the natural gas price and fuel demand of GFPPs are treated as predefined parameters and may not be the optimal values that would yield the most cost-effective system dispatch. In the natural gas system, the residential and industrial natural gas loads are assigned with a higher priority than the demand of GFPPs, which results in GFPPs being the first to be curtailed in case it is not feasible to cover the total natural gas demand needs. An iterative approach to dispatch the two energy systems is followed that identifies possible infeasible fuel consumption schedules of GFPPs and generate proper fuel constrains for the GFPPs [76]. This approach does not guarantee an optimal operation of the two energy systems compared to an approach that co-optimizes them simultaneously. Getting closer

to the actual operation, when the realization of stochastic power production ω' is known, the balancing actions to compensate potential forecast errors are optimized by following the same iterative approach.

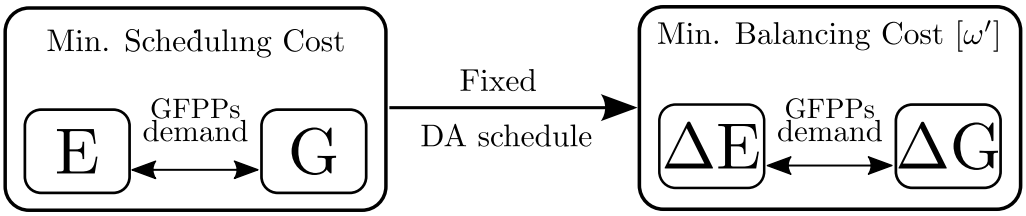

Figure 4.1: Sequential dispatch of decoupled electricity and natural gas systems (GFPPs: gas-fired power plants, DA: day-ahead, E: electricity, G: natural gas, ΔE: electricity adjustment, ΔG: natural gas adjustment).

4.1.2 Sequential dispatch of coupled electricity and natural gas systems

To improve the coordination between the two energy systems, a coupled operational model is constructed. In this case, we model a perfect inter-systems coordination, while a deterministic view of stochastic power production is used that results in clearing the day-ahead and real-time trading floors independently, as illustrated in Figure 4.2. The coupled dispatch of the two systems via a single optimization model allows for a non-static (i.e. endogenous) definition of the coordination parameters. That way the demand of GFPPs is treated as a variable and the power production cost of GFPPs is endogenously defined based on the *actual value* of natural gas at the specific time period and location. This model allows to identify potential inefficiencies that arise by following a decoupled dispatch of electricity and natural gas systems, as well as to assess the value of temporal coordination between the day-ahead and balancing markets by providing a basis for comparison with the following stochastic dispatch model.

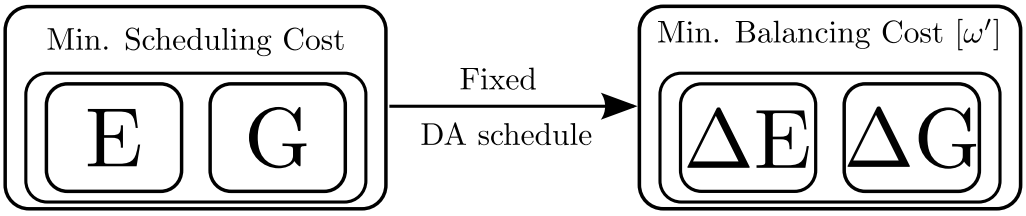

Figure 4.2: Sequential dispatch of coupled electricity and natural gas systems (E: electricity, G: natural gas, ΔE: electricity adjustment, ΔG: natural gas adjustment).

4.1.3 Stochastic dispatch of coupled electricity and natural gas systems

An uncertainty-aware dispatch is followed in this case, where the dispatch of the coupled energy system is co-optimized based on a probabilistic description of uncertain supply. More specifically, we develop a two-stage stochastic programming model that accounts for future balancing costs in real-time operation and minimizes the total expected system cost, as presented schematically in Figure 4.3. Such probabilistic description is based on the available forecast at the day-ahead stage and may not cover the exact realization in real-time. However, given that the uncertainty modeling adequately captures the true characteristics of the stochastic processes involved, the potential realizations will be represented via a set of scenarios Ω. This model achieves an enhanced inter-systems and inter-temporal coordination, assuming that a realistic range and probability distribution of scenarios is considered.

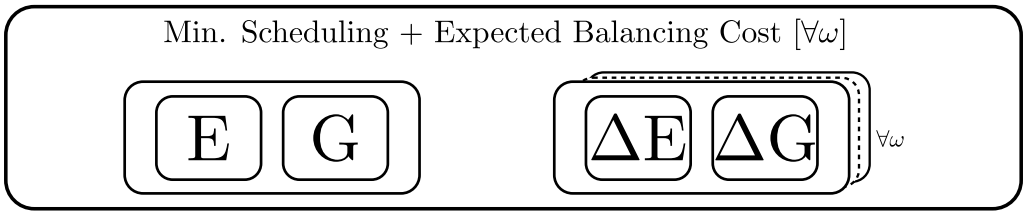

Figure 4.3: Stochastic dispatch of coupled electricity and natural gas systems (E: electricity, G: natural gas, ΔE: electricity adjustment, ΔG: natural gas adjustment).

4.2 Mathematical formulation of market-clearing models

In this section, the three aforementioned market-clearing models are formulated as compact mathematical programs to demonstrate the underlying interactions between the systems and markets. The link between the two systems is provided by GFPPs, which consume natural gas as fuel and produce electrical power. Assuming inelastic electricity and natural gas demands, we equivalently write the social welfare maximization problem as a cost minimization problem for the system operation. In the electricity system, we adopt a DC power flow model. In the natural gas system, the natural gas flow model with approximated dynamics is used, as presented in Section 3.2.2. Considering that the natural gas flow direction in the pipelines is controlled by a set of binary variables, this natural gas flow problem is formulated as a Mixed-Integer Linear Program (MILP). Following the common practice, we derive the electricity and natural gas prices as the dual variables of the corresponding balance constraints of the Linear Program (LP) obtained by fixing the binary variables of the initial MILP to their optimal values. A potential caveat of this approach, due to the non-convexity of the original MILP, is that the resulting prices may not adequately support the economic dispatch. In that case, corrective out-of-market payments may be considered, e.g. similar to uplift payments in the unit commitment problem, to provide the right incentives to follow the dispatch instructions. In all three market-clearing models, we consider a network representation for electricity and natural gas systems both at the day-ahead and real-time stages. More specifically, we consider a combined electricity and natural gas system with $\mathcal{N}$ electricity nodes, G conventional power plants, W stochastic producers, $\mathcal{D}$ electricity demands, M natural gas nodes, $\mathcal{E}$ pipelines, $\mathcal{U}$ natural gas producers, $\mathcal{S}$ natural gas storage facilities and $\mathcal{H}$ natural gas demands. The following mathematical programs are suited for multi-period problems, we omit though the time dimension T from the variables and parameters for clarity. A full formulation of the market-clearing models is given in [Paper B].

4.2.1 Sequential dispatch of decoupled electricity and natural gas systems

The sequential dispatch of decoupled electricity and natural gas systems consists of the following four individual mathematical programs. Let $p^{\mathrm{D}} \in \mathbb{R}_{+}^{G}$ and $w^{\mathrm{D}} \in \mathbb{R}_{+}^{W}$ be the day-ahead schedule of conventional and stochastic producers. The optimal schedule $\left(p^{\mathrm{D}^*}, w^{\mathrm{D}^*}\right)$ that minimizes the day-ahead electricity cost $\mathcal{C}_{\mathrm{E}}^{\mathrm{D}}(p^{\mathrm{D}})$ is determined by model (4.1) as follows:

$$\min_{p^{\mathrm{D}}, w^{\mathrm{D}}, \theta^{\mathrm{D}}} \quad \mathcal{C}_{\mathrm{E}}^{\mathrm{D}}(p^{\mathrm{D}}) \tag{4.1a}$$

$$\text{s. t.} \quad h_{\mathrm{E}}^{\mathrm{D}}(p^{\mathrm{D}}, w^{\mathrm{D}}, \theta^{\mathrm{D}}) - A^{\mathrm{e}} D^{\mathrm{e}} = 0 : \lambda_{\mathrm{E}}^{\mathrm{D}} \tag{4.1b}$$

$$f_{\mathrm{E}}^{\mathrm{D}}(p^{\mathrm{D}}, \theta^{\mathrm{D}}) \leq 0 \tag{4.1c}$$

$$0 \leq w^{\mathrm{D}} \leq \widehat{W}, \tag{4.1d}$$

where $\widehat{W} \in \mathbb{R}_{+}^{W}$ is the forecast of stochastic power production. The objective function in (4.1a) reflects the operating cost of the electricity system where an estimation of the natural gas spot price or of the price of the natural gas contract is used to calculate the marginal cost of GFPPs. Equality constraints (4.1b) enforce the power balance for each node of the power system by stating that the power production plus the net power flow is equal to the demand $D^{\mathrm{e}} \in \mathbb{R}_{+}^{\mathcal{D}}$ at each node. The electricity demand D^{e} is mapped to the nodes of the electricity network by the incidence matrix $A^{\mathrm{e}} \in \mathbb{R}_{+}^{\mathcal{N}\times D}$. Note that the power flows are determined by the nodal voltage angles $\theta^{\mathrm{D}} \in \mathbb{R}^{\mathcal{N}}$. The day-ahead locational marginal prices are defined as the dual variables of (4.1b) by $\lambda_{\mathrm{E}}^{\mathrm{D}} \in \mathbb{R}^{\mathcal{N}}$. The inequalities (4.1c) include all the constraints relative to upper and lower bounds of power production and power flows. The day-ahead schedule of stochastic producers is constrained by (4.1d). Model (4.2) minimizes the day-ahead natural gas cost $\mathcal{C}_{\mathrm{G}}^{\mathrm{D}}(g^{\mathrm{D}}, s^{\mathrm{D}})$ as follows:

$$\min_{g^{\mathrm{D}}, s^{\mathrm{D}}, pr^{\mathrm{D}}, q^{\mathrm{D}}, y^{\mathrm{D}}} \quad \mathcal{C}_{\mathrm{G}}^{\mathrm{D}}(g^{\mathrm{D}}, s^{\mathrm{D}}) \tag{4.2a}$$

$$\text{s. t.} \quad h_{\mathrm{G}}^{\mathrm{D}}(g^{\mathrm{D}}, s^{\mathrm{D}}, q^{\mathrm{D}}) - A^{\mathrm{g}} D^{\mathrm{g}} - A^{\mathrm{p}} D^{\mathrm{p}} = 0 : \lambda_{\mathrm{G}}^{\mathrm{D}} \tag{4.2b}$$

$$f_{\mathrm{G}}^{\mathrm{D}}(g^{\mathrm{D}}, s^{\mathrm{D}}, pr^{\mathrm{D}}, q^{\mathrm{D}}, y^{\mathrm{D}}) \leq 0 \tag{4.2c}$$

$$y^{\mathrm{D}} \in \{0, 1\}, \tag{4.2d}$$

where $D^{\mathrm{p}} \in \mathbb{R}_{+}^{G}$ is the fuel consumption of GFPPs and is calculated by multiplying the power conversion factor $\Phi \in \mathbb{R}_{+}^{G\times G}$ with the schedule p^{D^*} of GFPPs. Diagonal matrix Φ contains the power conversion factor of GFPPs, while the entries for non-GFPPs are zero. In model (4.2), D^{p} is treated as a fixed parameter. The operating cost of the natural gas system is represented by the objective function (4.2a) as the cost of natural gas injected in the network by producers $g^{\mathrm{D}} \in \mathbb{R}_{+}^{\mathcal{U}}$ and storage facilities $s^{\mathrm{D}} \in \mathbb{R}^{\mathcal{S}}$. We denote by s^{D} the inflow and outflow of the natural gas storage facilities. The natural gas balance at each node of the natural gas system is determined by equality (4.2b) where the natural gas injections plus the net natural gas flows $q^{\mathrm{D}} \in \mathbb{R}^{\mathcal{E}}$ and the net inflow/outflow from the storage facilities are equal to the residential/industrial demand $D^{\mathrm{g}} \in \mathbb{R}_{+}^{\mathcal{H}}$ and fuel demand D^{p} of GFPPs. The natural gas demand D^{g} and fuel consumption of GFPPs D^{p} are mapped to the nodes of the natural gas network by the incidence matrices $A^{\mathrm{g}} \in \mathbb{R}_{+}^{M\times\mathcal{H}}$ and $A^{\mathrm{p}} \in \mathbb{R}_{+}^{M\times G}$, respectively. The inequalities (4.2c) describe the natural gas capacity, natural gas flow, linepack and system operational constraints. Notice that the natural gas flows are determined by the nodal pressures $pr^{\mathrm{D}} \in \mathbb{R}_{+}^{M}$. The direction of natural gas flow is determined by binary variable y^{D} that is defined in (4.2d). The dual variables $\lambda_{\mathrm{G}}^{\mathrm{D}} \in \mathbb{R}^{M}$ of the balancing constraints define the day-ahead natural gas locational marginal prices when fixing the natural gas flow direction. In real-time operation, wind power production $W_{\omega'} \in \mathbb{R}_{+}^{W}$ is realized and the respective balancing markets are cleared. The day-ahead decisions $\left(p^{\mathrm{D}^*}, w^{\mathrm{D}^*}, \theta^{\mathrm{D}^*}\right)$ are treated as parameters in the electricity balancing market (4.3) that deals with the energy imbalance caused by stochastic production as follows:

$$\min_{p_{\omega'}^{\mathrm{R}}, pl_{\omega'}^{\mathrm{R}}, w_{\omega'}^{\mathrm{R}}, \theta_{\omega'}^{\mathrm{R}}} \quad \mathcal{C}_{\mathrm{E}}^{\mathrm{R}}(p_{\omega'}^{\mathrm{R}}, pl_{\omega'}^{\mathrm{R}}) \tag{4.3a}$$

$$\text{s. t.} \quad h_{\mathrm{E}}^{\mathrm{D}}(p_{\omega'}^{\mathrm{R}}, pl_{\omega'}^{\mathrm{R}}, w_{\omega'}^{\mathrm{R}}, \theta_{\omega'}^{\mathrm{R}}, \theta^{\mathrm{D}^*}) + A^{\mathrm{w}}(W_{\omega'} - w^{\mathrm{D}^*}) = 0 : \lambda_{\mathrm{E}(\omega')}^{\mathrm{R}} \tag{4.3b}$$

$$f_{\mathrm{E}}^{\mathrm{D}}(p_{\omega'}^{\mathrm{R}}, pl_{\omega'}^{\mathrm{R}}, w_{\omega'}^{\mathrm{R}}, \theta_{\omega'}^{\mathrm{R}}, p^{\mathrm{D}^*}; W_{\omega'}) \leq 0, \tag{4.3c}$$

where $p_{\omega'}^{\mathrm{R}} \in \mathbb{R}^{G}$ denotes the power adjustments of power plants. Moreover, $pl_{\omega'}^{\mathrm{R}} \in \mathbb{R}_{+}^{D}$ and $w_{\omega'}^{\mathrm{R}} \in \mathbb{R}_{+}^{W}$ are the load shedding and wind spilling actions, respectively. The cost of balancing actions $\mathcal{C}_{\mathrm{E}}^{\mathrm{R}}(p_{\omega'}^{\mathrm{R}}, pl_{\omega'}^{\mathrm{R}})$ is minimized in (4.3a). Equality constraints (4.3b) ensure that the power system

is re-dispatched to keep the system balanced. Incidence matrix $A^{\mathrm{w}} \in \mathbb{R}_{+}^{\mathcal{N}\times W}$ maps the stochastic producers to the electricity network. The dual variables $\lambda^{\mathrm{R}}_{\mathrm{E}(\omega')} \in \mathbb{R}^{\mathcal{N}}$ define the locational marginal prices in the electricity balancing market. Inequalities (4.3c) consist of the upper and lower bounds of power adjustments, load shedding, wind spillage and power flows. The real-time power flow is defined by voltage angles $\theta^{\mathrm{R}}_{\omega'} \in \mathbb{R}^{\mathcal{N}}$. Similarly to the day-ahead stage, the fuel consumption deviation $\Delta D^{\mathrm{p}} \in \mathbb{R}^{G}$ of GFPPs can be calculated by the multiplication of power conversion factor Φ and power adjustments $p^{\mathrm{R}}_{\omega'}$. The natural gas balancing market (4.4) is formulated as follows:

$$\min_{\substack{g^{\mathrm{R}}_{\omega'}, s^{\mathrm{R}}_{\omega'}, pr^{\mathrm{R}}_{\omega'}, q^{\mathrm{R}}_{\omega'},\\ gl^{\mathrm{R}}_{\omega'}, y^{\mathrm{R}}_{\omega'}}} \quad \mathcal{C}^{\mathrm{R}}_{\mathrm{G}}(g^{\mathrm{R}}_{\omega'}, s^{\mathrm{R}}_{\omega'}, gl^{\mathrm{R}}_{\omega'}) \tag{4.4a}$$

$$\text{s. t.} \quad h^{\mathrm{R}}_{\mathrm{G}}(g^{\mathrm{R}}_{\omega'}, s^{\mathrm{R}}_{\omega'}, q^{\mathrm{R}}_{\omega'}, gl^{\mathrm{R}}_{\omega'}, q^{\mathrm{D}^*}) - A^{\mathrm{p}}\Delta D^{\mathrm{P}} = 0 : \lambda^{\mathrm{R}}_{\mathrm{G}(\omega')} \tag{4.4b}$$

$$f^{\mathrm{R}}_{\mathrm{G}}(g^{\mathrm{R}}_{\omega'}, s^{\mathrm{R}}_{\omega'}, pr^{\mathrm{R}}_{\omega'}, q^{\mathrm{R}}_{\omega'}, gl^{\mathrm{R}}_{\omega'}, y^{\mathrm{R}}_{\omega'}, g^{\mathrm{D}^*}) \leq 0 \tag{4.4c}$$

$$y^{\mathrm{R}}_{\omega'} \in \{0, 1\}, \tag{4.4d}$$

where ΔD^{P} and the day-ahead decisions are treated as fixed parameters. The balancing actions to be activated comprise adjustments by natural gas producers $g^{\mathrm{R}}_{\omega'} \in \mathbb{R}^{\mathcal{U}}$ and natural gas storage facilities $s^{\mathrm{R}}_{\omega'} \in \mathbb{R}^{\mathcal{S}}$, as well as load shedding $gl^{\mathrm{R}}_{\omega'} \in \mathbb{R}^{\mathcal{H}}_{+}$. The cost of these actions are captured in the objective function (4.4a) to be minimized by $\mathcal{C}^{\mathrm{R}}_{\mathrm{G}}(g^{\mathrm{R}}_{\omega'}, s^{\mathrm{R}}_{\omega'}, gl^{\mathrm{R}}_{\omega'})$. Equality constraints (4.4b) guarantee the nodal natural gas balance of the system where the real-time natural gas net flows are given in $q^{\mathrm{R}}_{\omega'} \in \mathbb{R}^{\mathcal{E}}$ and defined by pressures $pr^{\mathrm{R}}_{\omega'} \in \mathbb{R}^{M}_{+}$. The dual variables $\lambda^{\mathrm{R}}_{\mathrm{G}(\omega')} \in \mathbb{R}^{M}$ define the locational marginal prices in the natural gas balancing market. Similarly to (4.2c), inequalities (4.4c) capture the constraints of natural system operation in real-time. Binary variable $y^{\mathrm{R}}_{\omega'}$, which is defined in (4.4d), determines the direction of the real-time natural gas flows.

4.2.2 Sequential dispatch of coupled electricity and natural gas systems

The sequential dispatch of coupled electricity and natural gas systems is formulated by two independent mathematical programs, one for the day-ahead and one for the balancing stage. The optimal schedule $\left(p^{\mathrm{D}^*}, w^{\mathrm{D}^*}, g^{\mathrm{D}^*}, s^{\mathrm{D}^*}\right)$ that minimizes the day-ahead cost $\mathcal{C}^{\mathrm{D}}_{\mathrm{E}}(p^{\mathrm{D}}) + \mathcal{C}^{\mathrm{D}}_{\mathrm{G}}(g^{\mathrm{D}}, s^{\mathrm{D}})$ of the coupled energy system is determined by model (4.5) as follows:

$$\min_{\substack{p^{\mathrm{D}}, w^{\mathrm{D}}, \theta^{\mathrm{D}}, g^{\mathrm{D}},\\ s^{\mathrm{D}}, pr^{\mathrm{D}}, q^{\mathrm{D}}, y^{\mathrm{D}}}} \quad \mathcal{C}^{\mathrm{D}}_{\mathrm{E}}(p^{\mathrm{D}}) + \mathcal{C}^{\mathrm{D}}_{\mathrm{G}}(g^{\mathrm{D}}, s^{\mathrm{D}}) \tag{4.5a}$$

$$\text{s. t.} \quad h^{\mathrm{D}}_{\mathrm{E}}(p^{\mathrm{D}}, w^{\mathrm{D}}, \theta^{\mathrm{D}}) - A^{\mathrm{e}} D^{\mathrm{e}} = 0 : \lambda^{\mathrm{D}}_{\mathrm{E}} \tag{4.5b}$$

$$f^{\mathrm{D}}_{\mathrm{E}}(p^{\mathrm{D}}, \theta^{\mathrm{D}}) \leq 0 \tag{4.5c}$$

$$0 \leq w^{\mathrm{D}} \leq \widehat{W} \tag{4.5d}$$

$$h^{\mathrm{D}}_{\mathrm{G}}(g^{\mathrm{D}}, s^{\mathrm{D}}, q^{\mathrm{D}}, \Phi p^{\mathrm{D}}) - A^{\mathrm{g}} D^{\mathrm{g}} = 0 : \lambda^{\mathrm{D}}_{\mathrm{G}} \tag{4.5e}$$

$$f^{\mathrm{D}}_{\mathrm{G}}(g^{\mathrm{D}}, s^{\mathrm{D}}, pr^{\mathrm{D}}, q^{\mathrm{D}}, y^{\mathrm{D}}) \leq 0 \tag{4.5f}$$

$$y^{\mathrm{D}} \in \{0, 1\}, \tag{4.5g}$$

where $\widehat{W}$ is the forecast of stochastic power production. In the objective function (4.5a), the *total* day-ahead cost of electricity and natural gas systems is minimized. In this case, the system cost stems from the power production cost of non-GFPPs and the natural gas system cost. Note that the power production cost of GFPPs is not included because it would result in double counting it. The cost of GFPPs is explicitly associated with the natural gas system cost via equality (4.5e),

which enforces the natural gas balancing for each node of the system. The fuel consumption Φp^{D} of GFPPs is treated as a variable under the coupled optimization of the two energy systems. Constraints (4.5b)-(4.5d) and (4.5f)-(4.5g) are the same as those described in Section 4.2.1. The day-ahead decisions are determined by model (4.5) and passed as fixed parameters to the balancing model (4.6). Model (4.6) is solved for each wind power realization $W_{\omega'}$ and writes as follows:

$$\min_{\substack{p^{\mathrm{R}}_{\omega'},pl^{\mathrm{R}}_{\omega'},w^{\mathrm{R}}_{\omega'},\theta^{\mathrm{R}}_{\omega'},g^{\mathrm{R}}_{\omega'},\\ s^{\mathrm{R}}_{\omega'},pr^{\mathrm{R}}_{\omega'},q^{\mathrm{R}}_{\omega'},gl^{\mathrm{R}}_{\omega'},y^{\mathrm{R}}_{\omega'}}} \quad \mathcal{C}^{\mathrm{R}}_{\mathrm{E}}(p^{\mathrm{R}}_{\omega'},pl^{\mathrm{R}}_{\omega'})+\mathcal{C}^{\mathrm{R}}_{\mathrm{G}}(g^{\mathrm{R}}_{\omega'},s^{\mathrm{R}}_{\omega'},gl^{\mathrm{R}}_{\omega'}) \tag{4.6a}$$

$$\text{s. t.} \quad h^{\mathrm{D}}_{\mathrm{E}}(p^{\mathrm{R}}_{\omega'},pl^{\mathrm{R}}_{\omega'},w^{\mathrm{R}}_{\omega'},\theta^{\mathrm{R}}_{\omega'},\theta^{\mathrm{D}*})+A^{\mathrm{w}}(W_{\omega'}-w^{\mathrm{D}*})=0:\lambda^{\mathrm{R}}_{\mathrm{E}(\omega')} \tag{4.6b}$$

$$f^{\mathrm{D}}_{\mathrm{E}}(p^{\mathrm{R}}_{\omega'},pl^{\mathrm{R}}_{\omega'},w^{\mathrm{R}}_{\omega'},\theta^{\mathrm{R}}_{\omega'},p^{\mathrm{D}*};W_{\omega'})\leq 0 \tag{4.6c}$$

$$h^{\mathrm{R}}_{\mathrm{G}}(g^{\mathrm{R}}_{\omega'},s^{\mathrm{R}}_{\omega'},q^{\mathrm{R}}_{\omega'},gl^{\mathrm{R}}_{\omega'},\Phi p^{\mathrm{R}}_{\omega'},q^{\mathrm{D}*})=0:\lambda^{\mathrm{R}}_{\mathrm{G}(\omega')} \tag{4.6d}$$

$$f^{\mathrm{R}}_{\mathrm{G}}(g^{\mathrm{R}}_{\omega'},s^{\mathrm{R}}_{\omega'},pr^{\mathrm{R}}_{\omega'},q^{\mathrm{R}}_{\omega'},gl^{\mathrm{R}}_{\omega'},y^{\mathrm{R}}_{\omega'},g^{\mathrm{D}*})\leq 0 \tag{4.6e}$$

$$y^{\mathrm{R}}_{\omega'}\in\{0,1\}, \tag{4.6f}$$

where $\Phi p^{\mathrm{R}}_{\omega'}$ determines the fuel consumption of GFPPs and treated as variable in the natural gas balancing equality (4.6d). Similarly, the power production cost of GFPPs is not included since it stems from the natural gas system. Constraints (4.6b)-(4.6c) and (4.6e)-(4.6f) are the same as those described in Section 4.2.1.

4.2.3 Stochastic dispatch of coupled electricity and natural gas systems

The stochastic dispatch of coupled electricity and natural gas systems is formulated by a single optimization problem. Model (4.7) is formulated as a two-stage stochastic program as follows:

$$\min_{\substack{p^{\mathrm{D}},w^{\mathrm{D}},\theta^{\mathrm{D}},g^{\mathrm{D}},s^{\mathrm{D}},pr^{\mathrm{D}},q^{\mathrm{D}},p^{\mathrm{R}}_{\omega},pl^{\mathrm{R}}_{\omega},\\ w^{\mathrm{R}}_{\omega},\theta^{\mathrm{R}}_{\omega},g^{\mathrm{R}}_{\omega},s^{\mathrm{R}}_{\omega},pr^{\mathrm{R}}_{\omega},q^{\mathrm{R}}_{\omega},gl^{\mathrm{R}}_{\omega},y^{\mathrm{D}},y^{\mathrm{R}}_{\omega}}} \quad \mathcal{C}^{\mathrm{D}}_{\mathrm{E}}(p^{\mathrm{D}})+\mathcal{C}^{\mathrm{D}}_{\mathrm{G}}(g^{\mathrm{D}},s^{\mathrm{D}})+\mathbb{E}_{\omega}\left[\mathcal{C}^{\mathrm{R}}_{\mathrm{E}}(p^{\mathrm{R}}_{\omega},pl^{\mathrm{R}}_{\omega})+\mathcal{C}^{\mathrm{R}}_{\mathrm{G}}(g^{\mathrm{R}}_{\omega},s^{\mathrm{R}}_{\omega},gl^{\mathrm{R}}_{\omega})\right] \tag{4.7a}$$

$$\text{s. t.} \quad h^{\mathrm{D}}_{\mathrm{E}}(p^{\mathrm{D}},w^{\mathrm{D}},\theta^{\mathrm{D}})-A^{\mathrm{e}}D^{\mathrm{e}}=0:\lambda^{\mathrm{D}}_{\mathrm{E}} \tag{4.7b}$$

$$f^{\mathrm{D}}_{\mathrm{E}}(p^{\mathrm{D}},\theta^{\mathrm{D}})\leq 0 \tag{4.7c}$$

$$0\leq w^{\mathrm{D}}\leq \overline{W} \tag{4.7d}$$

$$h^{\mathrm{D}}_{\mathrm{G}}(g^{\mathrm{D}},s^{\mathrm{D}},pr^{\mathrm{D}},q^{\mathrm{D}},\Phi p^{\mathrm{D}})-A^{\mathrm{g}}D^{\mathrm{g}}=0:\lambda^{\mathrm{D}}_{\mathrm{G}} \tag{4.7e}$$

$$f^{\mathrm{D}}_{\mathrm{E}}(g^{\mathrm{D}},s^{\mathrm{D}},pr^{\mathrm{D}},q^{\mathrm{D}},y^{\mathrm{D}})\leq 0 \tag{4.7f}$$

$$y^{\mathrm{D}}\in\{0,1\} \tag{4.7g}$$

$$h^{\mathrm{D}}_{\mathrm{E}}(p^{\mathrm{R}}_{\omega},pl^{\mathrm{R}}_{\omega},w^{\mathrm{R}}_{\omega},\theta^{\mathrm{R}}_{\omega},\theta^{\mathrm{D}})+A^{\mathrm{w}}(W_{\omega}-w^{\mathrm{D}})=0:\lambda^{\mathrm{R}}_{\mathrm{E}(\omega)},\ \ \forall\omega\in\Omega \tag{4.7h}$$

$$f^{\mathrm{D}}_{\mathrm{E}}(p^{\mathrm{R}}_{\omega},pl^{\mathrm{R}}_{\omega},w^{\mathrm{R}}_{\omega},\theta^{\mathrm{R}}_{\omega},p^{\mathrm{D}};W_{\omega})\leq 0,\ \ \forall\omega\in\Omega \tag{4.7i}$$

$$h^{\mathrm{R}}_{\mathrm{G}}(g^{\mathrm{R}}_{\omega},s^{\mathrm{R}}_{\omega},q^{\mathrm{R}}_{\omega},gl^{\mathrm{R}}_{\omega},\Phi p^{\mathrm{R}}_{\omega},q^{\mathrm{D}})=0:\lambda^{\mathrm{R}}_{\mathrm{G}(\omega)},\ \ \forall\omega\in\Omega \tag{4.7j}$$

$$f^{\mathrm{R}}_{\mathrm{G}}(g^{\mathrm{R}}_{\omega},s^{\mathrm{R}}_{\omega},pr^{\mathrm{R}}_{\omega},q^{\mathrm{R}}_{\omega},gl^{\mathrm{R}}_{\omega},y^{\mathrm{R}}_{\omega},g^{\mathrm{D}})\leq 0,\ \ \forall\omega\in\Omega \tag{4.7k}$$

$$y^{\mathrm{R}}_{\omega}\in\{0,1\},\ \ \forall\omega\in\Omega, \tag{4.7l}$$

where $\overline{W}\in\mathbb{R}^{W}_{+}$ is the capacity of stochastic producers. The total expected system cost is minimized in (4.7a). Model (4.7) permits an implicit temporal coordination of the day-ahead and real-time stages by anticipating balancing costs in (4.7a) and writing constraints (4.7h)-(4.7l) for all scenarios $\omega\in\Omega$. Note that day-ahead decisions are treated as variables and that stochastic power schedule w^{D} is constrained by the capacity $\overline{W}$ in (4.7d). Constraints (4.7b)-(4.7c) and (4.7e)-(4.7l) are the same as those described in Section 4.2.2.

4.2.4 Characteristics of the market-clearing models

Before presenting a comparison among the market-clearing models and the effect of coordination parameters on systems operation, we provide an overview of the features of the models in Table 4.1. The sequential model of decoupled (*Seq-Dec*) electricity and natural gas systems results in an imperfect coordination between the energy systems and trading floors, where the definition of coordination parameters is accomplished in a static manner. The sequential model of coupled (*Seq-Coup*) electricity and natural gas systems attains a perfect inter-systems coordination, while clearing the day-ahead and balancing markets sequentially. Following a coupled approach for the systems coordination allows for an endogenous definition of the coordination parameters since they are treated as variables in the optimization problems. The stochastic dispatch model of coupled (*Stoch-Coup*) electricity and natural gas systems achieves a perfect coordination both regarding the energy systems and trading floors. The inter-temporal coordination is assumed to be perfect in a sense that uncertainty modeling captures the true characteristics of the stochastic processes involved and the potential realizations are represented by scenario set Ω. The three examined market-clearing models are also illustrated in Figure 3.7, which provides a general overview of the different models examined in this thesis. Note that *UA-Coup* in Figure 3.7 is referred to as *Stoch-Coup* in this chapter due to the use of two-stage stochastic programming to have an uncertainty-aware approach.

Table 4.1: Characteristics of market-clearing models.

Model	*Seq-Dec*	*Seq-Coup*	*Stoch-Coup*
Temporal coordination	Imperfect	Imperfect	Perfect
Systems coordination	Imperfect	Perfect	Perfect
Definition of coordination parameters	Static	Endogenous	Endogenous

4.3 Comparison of market-clearing models and the effect of coordination parameters on the operation of electricity and natural gas systems

In this section, the three market-clearing models are compared in terms of expected system cost and the share of the total power production scheduled at the day-ahead stage that is allocated between GFPPs and non-GFPPs. Moreover, the effect of coordination parameters on the dispatch of the two energy systems is analyzed. That way, potential inefficiencies that may arise in the decoupled approach along with the benefits of having a probabilistic description of uncertainties are highlighted. A modified case study is built upon the IEEE 24-bus Reliability Test System (RTS) [80] and a 12-node natural gas system based on [81]. Wind power production is described via 25 equiprobable scenarios [82]. The scheduling horizon is 24 hours. The data and network topology are provided in the online appendix, which is available in [83].

4.3.1 Degrees of coordination and their effect on a cost-effective operation

In coupled operation of electricity and natural gas systems, the power production cost of GFPPs is defined endogenously by the actual value of natural gas, which is defined as the locational marginal price λ_G^D for each time period of the day. In the decoupled approach, the GFPPs have to utilize fixed natural gas prices that represent an estimation of the spot price or the price of fuel supply contracts. We solve *Seq-Coup* to estimate this fixed price. Then in *Seq-Dec*, the day-ahead

offer price of GFPPs in the electricity market can be calculated as the multiplication of the natural gas price λ_G^D obtained by *Seq-Coup* with the power conversion factor of each GFPP. At the balancing stage, the upward and downward regulation offer prices are equal to 1.1 and 0.91 of the day-ahead offer price.

Tables 4.2 and 4.3 present the total expected system cost, as the sum of the day-ahead and balancing costs, along with the share of day-ahead power production scheduling of GFPPs and non-GFPPs for 40% and 50% wind power penetration levels. The expected system cost is calculated based on scenario set Ω and the wind power penetration level is defined as the share of installed wind capacity on total system's electricity demand. Model *Stoch-Coup* attains the solution with the lowest expected system cost in both cases, since it manages to efficiently dispatch the coupled energy system in view of uncertain power supply. Comparing the two sequential models, it can be observed that *Seq-Coup* has a better performance than *Seq-Dec* in terms of expected system cost, highlighting the benefit of co-optimizing the energy systems instead of following a decoupled approach. Utilizing a probabilistic description of uncertainties at the day-ahead stage to schedule the system permits the anticipation of balancing costs. This results in *Stoch-Coup* having an increased day-ahead cost compared to *Seq-Coup* and *Seq-Dec*, as the power plants are scheduled out of the merit order, which is then offset by the highly reduced balancing costs. Moreover, GFPPs, which are considered flexible power producers, are having a higher share of power production under *Stoch-Coup*. The coupled optimization of electricity and natural gas systems schedules the GFPPs based on the actual value of natural gas, as well as optimizes the natural gas flows, linepack flexibility and natural gas levels at storage facilities in view of uncertain power supply. The spatial and temporal allocation of natural gas in the system plays an important role for short-term adequacy and available operational flexibility due to the limitations in the speed of transporting natural gas. For these reasons, *Seq-Dec* results in a higher expected system cost than *Seq-Coup*.

Table 4.2: Expected system cost and share of the total power production scheduled at the day-ahead stage allocated between GFPPs and non-GFPPs when the wind power penetration is 40%.

	Total (M$)	Day-ahead (M$)	Balancing (M$)	GFPPs (%)	non-GFPPs (%)
Stoch-Coup	1.747	1.755	-0.008	10.8	89.2
Seq-Coup	1.817	1.731	0.086	9.1	90.9
Seq-Dec	1.819	1.731	0.088	9.2	90.8
Seq-Dec $\uparrow$	1.821	1.732	0.089	6.8	93.2
Seq-Dec $\downarrow$	1.866	1.741	0.125	14.5	85.5

Table 4.3: Expected system cost and share of the total power production scheduled at the day-ahead stage allocated between GFPPs and non-GFPPs when the wind power penetration is 50%.

	Total (M$)	Day-ahead (M$)	Balancing (M$)	GFPPs (%)	non-GFPPs (%)
Stoch-Coup	1.684	1.686	-0.002	11.7	88.3
Seq-Coup	1.812	1.663	0.149	7.4	92.6
Seq-Dec	1.814	1.664	0.150	7.2	92.8
Seq-Dec $\uparrow$	1.813	1.665	0.148	6.1	93.9
Seq-Dec $\downarrow$	1.874	1.674	0.200	14.3	85.7

Therefore, a decrease in expected system cost, can be noticed as we move from the deterministic and decoupled approach to the stochastic and coupled one. This happens due to the enhanced coordination between the two trading floors as well as between the systems.

4.3.2 The effect of coordination parameters on the operation of electricity and natural gas systems

To simulate the case that GFPPs are mis-estimating the actual natural gas price, a 10% overestimation and underestimation is used. Such deviation is considered adequate due to the relative stable natural gas prices in short-term operations. This case is examined by introducing two additional models for the overestimation and underestimation, which are *Seq-Dec* ↑ and *Seq-Dec* ↓, respectively. The impact of coordination parameters on the dispatch of both energy systems are analyzed by comparing the solutions of *Seq-Dec* ↑ and *Seq-Dec* ↓ with *Seq-Dec*. Model *Seq-Dec* utilizes the actual natural gas price stemming from *Seq-Coup*, while the *Seq-Dec* ↑ and *Seq-Dec* ↓ overestimate or underestimate this price. A fuel price mis-estimation affects the price-quantity bids of GFPPs, which in turn results in building a different aggregated supply curve than *Seq-Dec* to clear the market. For instance, an overestimation of the natural gas price would result in placing the GFPPs higher in the merit-order ranking and thus having less of them scheduled at the day-ahead stage. On the contrary, more GFPPs would be scheduled at the day-ahead stage when the natural gas price is underestimated since they bid in the market with a lower marginal cost than the one related to the actual natural gas value. As shown in Table 4.3 for the case of 50% wind power penetration, model *Seq-Dec* ↑ obtains a reduced total expected system cost compared to *Seq-Dec* because flexible GFPPs are scheduled less at the day-ahead stage which makes them available to provide upward regulation services in real-time operation. In the underestimation case both in Tables 4.2 and 4.3, the GFPPs are scheduled more at the day-ahead stage, which results in the opposite effect and yields an increased total expected system cost. Therefore, an adjustment of the natural gas price perceived by GFPPs is possible to affect the total expected system cost in both a positive and a negative manner.

Apart from the natural gas price, the available quantity of natural gas for power production also affects the scheduling of the GFPPs. This is examined by simulating a case with 30% increased residential/industrial natural gas demand. Table 4.4 presents the total expected system costs and the share of the total power production scheduled at the day-ahead stage allocated between the different technologies. The share of power production from GFPPs is reduced from 9.1% to 6.6% and 9.2% to 6.7% for *Seq-Coup* and *Seq-Dec*, respectively. Therefore, a higher portion of the electricity demand is covered by non-GFPPs. Additionally, the expected unsatisfied natural gas demand of a specific GFPP (i.e. GFPP 11) is illustrated in Figure 4.4. This undesired event takes place during the hours of peak residential/industrial natural gas demand and is more severe when the natural gas price is underestimated because GFPPs are scheduled with a comparatively higher share at the day-ahead stage. This phenomenon does not occur when the systems are simultaneously operated under *Seq-Coup*, which also yields a lower expected system cost compared to *Seq-Dec*. The importance of co-optimizing the energy systems along with the natural gas flows and allocation of linepack is highlighted in this case due to the effect of natural gas volume availability for power production on the operation of the systems.

It has been identified that both coordination parameters have an impact on the operation of both energy systems and the total expected system cost. This paves the way for exploring how a sophisticated definition of these parameters can enhance the coordination between the two energy systems and between the two trading floors in view of high shares of stochastic power production. This topic is further discussed in Chapter 5.

Table 4.4: Expected system cost and share of the total power production scheduled at the day-ahead stage allocated between GFPPs and non-GFPPs when the natural gas demand is increased by 30% and the wind power penetration is 40%.

	Total (M$)	GFPPs (%)	non-GFPPs (%)
Seq-Coup	1.949	6.6	93.4
Seq-Dec	2.018	6.7	93.3

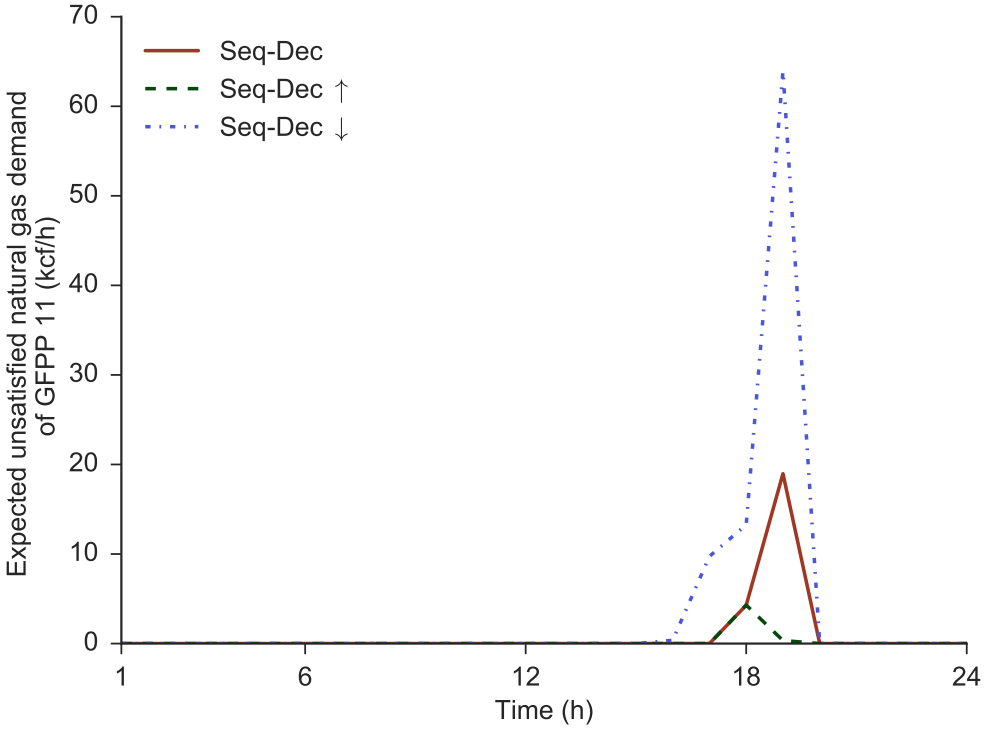

Figure 4.4: Expected unsatisfied demand of GFPP 11 under *Seq-Dec*.

4.4 Benefits of linepack flexibility and its effect on the operation of electricity and natural gas systems

An essential flexible component included in the market-clearing models is the natural gas network with approximated dynamics of the natural gas flow, which allows to store natural gas in the pipelines (i.e. linepack). In this section, the effects of modeling linepack are identified by comparing with a steady-state operation of the natural gas system where no linepack is considered. In the steady-state operation, the same equations of the natural gas network modeling with approximate dynamics are used but the inflow and outflow of each pipeline are set to be equal for each time period ($q^{in}_{m,u,t} = q^{out}_{m,u,t}, \forall (m,u) \in Z, t \in T$). Hence, there is no storage ability in the natural gas network. In the steady-state operation, linepack is neglected both at the day-ahead and at the real-time stages. A performance ratio is utilized to quantify the flexibility revealed by modeling linepack flexibility. To compare on a fair basis, the level of natural gas stored in the network and in the storage facilities between the beginning and the end of the 24-hour scheduling horizon is assumed to be the same. The analysis is performed using the same case study as in Section 4.3.

To examine the effects of linepack flexibility on the operation of electricity and natural gas systems, the total expected system cost is compared for the cases that linepack is considered or neglected under *Seq-Coup* and *Seq-Dec*. The results are presented in Table 4.5. In the steady-state models, the natural gas demand has to be instantly covered at each time period by the producers as it is not possible to store natural gas in the network for utilization in subsequent time periods. For this reason, the most expensive natural gas supplier needs to be scheduled to meet the demand, which results in an increased day-ahead cost for the steady-state models. The deployment of the expensive natural gas supplier increases the natural gas price but makes available more cost-effective capacity for down-regulation in the natural gas system. This increased availability of cheaper down-regulation resources is also reflected in the electricity market via the GFPPs and eventually results in a lower expected balancing cost. On the other hand, only the two cheaper natural gas suppliers are scheduled when linepack is considered since there is a possibility to store natural gas in the network and use it during the hours of the peak demand. This results in a lower day-ahead cost; however, a higher total expected system cost is attained due to the more expensive balancing actions required. This effect depends on the structure of scenarios in set Ω and type of regulation needed in the real-time operation. Nevertheless, it indicates possible inefficiencies that may arise when a flexible component of the system, such as linepack, is myopically operated with regards to future balancing needs.

Table 4.5: Effect of linepack on expected system cost under *Seq-Coup* and *Seq-Dec* when the wind power penetration is 50%.

	Total (M$)	Day-ahead (M$)	Balancing (M$)
Seq-Coup	1.812	1.663	0.149
Steady-state *Seq-Coup*	1.809	1.669	0.140
Seq-Dec	1.814	1.664	0.150
Steady-state *Seq-Dec*	1.813	1.671	0.142

To overcome the aforementioned drawback of deterministic approaches that are myopic to future uncertainties, the *Stoch-Coup* is examined and the results are given in Table 4.6. The steady-state model results in a higher expected system cost and schedules GFPPs less than *Stoch-Coup*, since it cannot take advantage of the natural gas network's storage capability. *Stoch-Coup* exploits the inherent flexibility of the natural gas network by taking into account the balancing needs due to stochastic power production from renewables. Additionally, the effect of utilizing different levels of linepack at the beginning of the scheduling horizon on total expected system cost is examined by considering 5% more or less linepack in relation to the value at the end of the day. In all cases, the same target value for the last time period of the scheduling horizon is required. The total expected system cost is lower when there is a higher level of linepack at the beginning of the scheduling horizon. Moreover, GFPPs are scheduled more by taking advantage of the free energy stored in the network. The opposite observations are noticed for the case of having a 5% less linepack level at the beginning of the scheduling horizon.

Figure 4.5 depicts the total level of linepack in the system and the total level at the storage facilities. It can be observed that the linepack level decreases throughout the scheduling horizon and the storage facilities are not utilized in the case of having a 5% higher initial linepack level. On the contrary, the linepack level increases when its initial value is 5% lower at the beginning of the scheduling horizon. In addition, the storage facilities are utilized to support the operation of the system during the first hour of the day. In both cases, the linepack level is decreased below the final

Table 4.6: Effect of linepack on expected system cost and share of the total power production scheduled at the day-ahead stage allocated between GFPPs and non-GFPPs under *Stoch-Coup* when the wind power penetration is 50%.

	Total (M$)	GFPPs (%)	non-GFPPs (%)
Steady-state *Stoch-Coup*	1.692	9.9	90.1
Stoch-Coup	1.684	11.7	88.3
Stoch-Coup (+5% initial linepack)	1.631	12	88
Stoch-Coup (-5% initial linepack)	1.739	10.8	89.2

hour threshold during the evening hours, where there is a peak of residential/industrial natural gas demand.

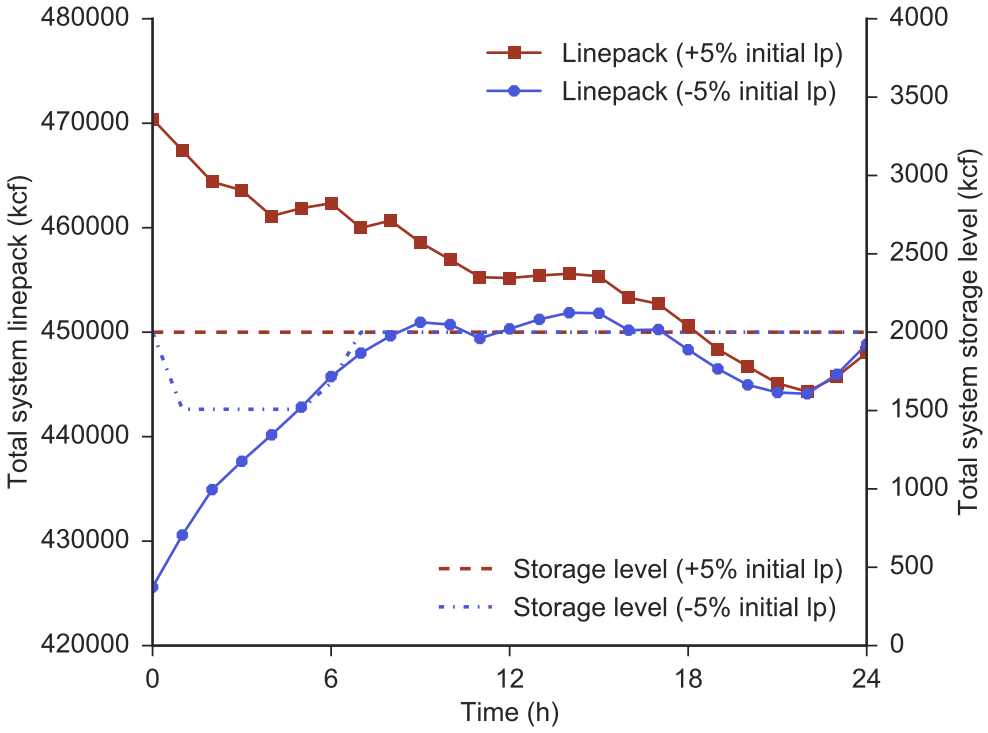

Figure 4.5: Total system linepack and storage level (lp: linepack).

The benefits of incorporating a flexible component that is capable to provide energy storage in the system stem from its ability to flatten the demand profile by filling the "valleys" and shaving the "peaks" in order to utilize cheap energy production, as sketched in Figure 4.6. Linepack is also considered a storage option for the coupled energy system that is offered by the pipelines of the natural gas network.

The flexibility revealed by modeling linepack in *Stoch-Coup* can be quantified by a performance ratio that takes into account two extreme cases and the case where linepack is modeled. The steady-state model, which does not have the ability to store natural gas in the network, provides the solution (EC^{ss}) with the highest expected system cost. The lowest expected system cost (EC^{ideal}) is attained in the case where an ideal storage facility with infinite capacity and charging/discharging rates at each node of the system is introduced. Even though this approach is able to shift the

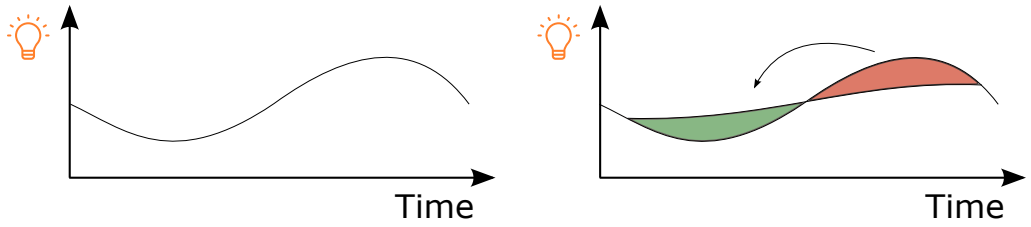

Figure 4.6: Peak-shaving and load-shifting from an ideal storage facility.

demand in every possible way to reduce the expected system cost, it cannot be considered in practice and is only used to provide a lower bound for the performance ratio, which is equal to M$1.629. The performance ratio is calculated as follows:

$$\frac{EC^{ss} - EC}{EC^{ss} - EC^{ideal}} = \frac{1.692 - 1.684}{1.692 - 1.629} \approx 12.4\%,$$

showing that modeling the natural gas network with linepack flexibility reveals 12.4% of an ideal storage facility in terms of expected system cost. This result indicates the benefit of modeling the natural gas network with approximated dynamics in a market-compatible way to exploit the available operational flexibility. For brevity, the M$ units have been used for the expected system cost in this chapter, which results in a slightly different value for the performance ratio than the one presented in [Paper C] where results are presented in $. Hence the "approximately equal" symbol (≈) is used in the equation.

Figure 4.7 shows the total natural gas supply and fuel demand of GFPPs. The natural gas production is significantly higher when there is a 5% lower level of linepack at the beginning of the scheduling horizon since the natural gas network needs to be charged for the subsequent time periods to meet the requirement of the final hour. On the contrary, the utilization of the free energy in the natural gas network in the case of having a 5% higher initial level of linepack results in a reduced natural gas production over the first half of the day. The GFPPs are scheduled more in this case due to the excess of natural gas in the system. It can be observed that GFPPs are scheduled according to the natural gas availability in the system when following a coupled operation of both systems. Therefore, the GFPPs can be utilized as flexible demand components for the natural gas system by either increasing or decreasing their fuel consumption in favor of a cost-effective operation of the integrated energy system.

A fully coupled model with a probabilistic description of uncertain power supply manages to exploit linepack flexibility in a cost-effective manner as opposed to deterministic models. Moreover, introducing an additional source of flexibility requires proper models to efficiently operate it and integrate it in the market-clearing process in view of high shares of stochastic renewables. Finally, the coupled operation of electricity and natural gas systems increases security of supply and allows to fully exploit the system components towards an efficient operation of the whole energy system.

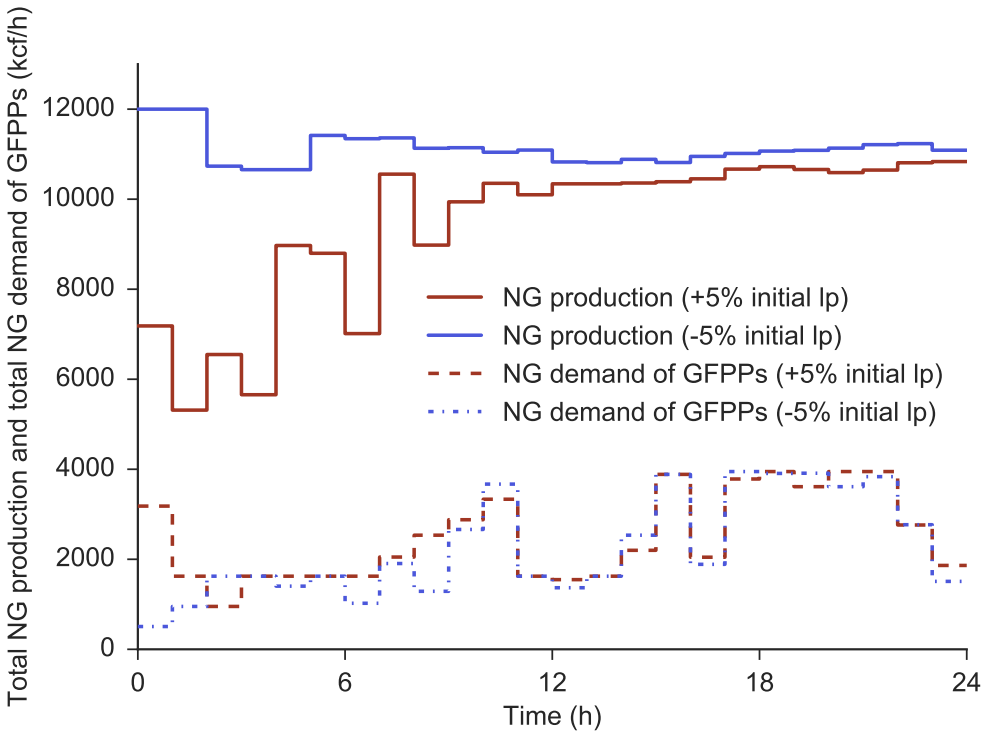

Figure 4.7: Total natural gas production and total natural gas demand of GFPPs (NG: natural gas, lp: linepack).

CHAPTER 5

Market-based Coordination of Electricity and Natural Gas Systems

The benefits of dispatching the energy system with a fully coupled approach by taking into account the stochasticity and variability of renewables are highlighted in Chapter 4. Building upon this observation, this chapter studies the electricity and natural gas systems in a coupled manner that allows to optimally define the coordination parameters, identified in Chapter 4, for a cost-effective operation of both energy systems.

Current market designs that are based on a sequential clearing of successive market floors are highly challenged as the penetration of renewables increases. Recently proposed stochastic market-clearing approaches attain an enhanced temporal coupling between the market floors and minimize the total expected system cost. However, these stochastic models are incompatible with current sequential market designs. In this chapter, we propose two stochastic bilevel programs that improve the temporal coordination of the scheduling and balancing operations, while remaining compatible with the sequential clearing of day-ahead and balancing markets. This is achieved by the optimal definition of two *flexibility signals* in view of future balancing needs due to forecast errors from uncertain power supply. These flexibility signals are determined by controlling the two key coordination parameters. More specifically, a *volume-based* and a *price-based* model are developed. In the volume-based model, the volume of natural gas made available for power production at the day-ahead stage is considered as a control parameter that can be optimally tuned in the favor of minimizing expected system cost. Similarly, the price-based model is able to adjust the natural gas price perceived by Gas-Fired Power Plants (GFPPs). Both models improve the inter-temporal coordination between the day-ahead and real-time stages by communicating missing information with regards to uncertain renewable production at the day-ahead stage. The improved temporal coordination between the trading floors is achieved in an analogous manner as in [84, 85], whereas we further develop the approach to account for both electricity and natural gas systems as well as different control parameters. For a more detailed literature survey, see the introductions of [Paper C] and [Paper D].

In this chapter, we follow a holistic view of the energy systems, where the short-term operation of electricity and natural gas systems is organized in a coupled market setup associated with the day-ahead and balancing stages. Two-stage stochastic programming is used to build the uncertainty-aware dispatch. Initially, the natural gas system is modeled with the contract and fuel capacity constraints (see Section 3.2.2) that permits a comparison between the volume-based and price-based models. Then, the natural gas flow model with approximated dynamics (see

Section 3.2.2) is utilized to examine the performance of the volume-based approach with network constraints. The latter model approximates the dynamics of the natural gas flow and reveals the benefits of linepack flexibility for the whole energy system. A detailed description of the formulation of the proposed models is provided in [Paper C] and [Paper D].

In Section 5.1, we outline the characteristics of the dispatch models for the coupled energy system, as well as comment on their advantages and limitations. Moreover, the effect of controlling the coordination parameters on the day-ahead scheduling is schematically illustrated also in Section 5.1. The mathematical formulation of the dispatch models is presented in Section 5.2 to provide additional insights into their characteristics. A comparison between the volume-based and price-based approaches is performed in Section 5.3. Finally, Section 5.4 elaborates on the performance of different variants of the volume-based model in terms of expected system cost, presents the benefits of linepack flexibility and discusses the cost recovery of flexible producers.

5.1 Description of dispatch models

This section provides a description of the proposed volume-based and price-based models to improve the sequential dispatch of coupled electricity and natural gas system by approximating the solution of the stochastic dispatch model.

In the current sequential arrangement of the day-ahead and balancing stages, the day-ahead market is cleared 12-36 hours ahead of the actual system operation and the necessary adjustments to keep the system balanced are determined in the balancing market. A deterministic view of uncertain power production is used to clear the day-ahead market in this setup, which may become highly inefficient in accommodating high shares of renewable power production by yielding a high expected system cost. The sequential dispatch model is presented in Section 5.1.1. In an attempt to improve the temporal coordination between the two trading floors, two-stage stochastic programming with probabilistic description of uncertain power supply has been extensively utilized as in [44, 45]. This approach attains the lowest expected cost but is incompatible with the current market design and suffers from some design flaws related to the violation of the least-cost merit-order principle [84, 86]. The solution obtained by the stochastic dispatch model, presented in Section 5.1.2, serves as an ideal benchmark in terms of expected system cost. The proposed models manage to provide an improved dispatch which minimizes the total expected cost and simultaneously respects the merit-order principle. The improved dispatch models are presented in Sections 5.1.3 and 5.1.4, where the two ways of improving the sequential dispatch model to anticipate future balancing needs stemming from stochastic renewables are discussed. Section 5.1.5 provides additional insights for the improved dispatch models via illustrating schematically the effect of control parameters on the day-ahead scheduling.

The sequential and stochastic dispatch models follow the same setups with the ones presented in Sections 4.1.2 and 4.1.3, respectively. However, these two models serve as benchmarks in this chapter and the focus is placed on their economic properties. The four dispatch models presented in this chapter attain different levels of temporal coordination between the trading floors for the coupled electricity and natural gas system.

5.1.1 Sequential dispatch of coupled electricity and natural gas systems

The sequential dispatch of the coupled electricity and natural gas systems achieves a perfect coordination between the two energy systems for the day-ahead and balancing stages, as shown in Figure 5.1. The electricity and natural gas systems are co-optimized under a single market setup and the coordination parameters are endogenously defined. The successive trading floors are cleared in a sequential manner with a singe-valued forecast of stochastic power production as an input at the day-ahead stage. After the realization ω' of stochastic production, the necessary re-dispatch actions to cover potential imbalances are determined in the balancing market. Such a deterministic approach may be highly inefficient to describe the highly uncertain and variable power production from renewables nowadays. However, this setup preserves an important economic property: it is guaranteed that the revenue of flexible producers is greater or equal to their operating cost (i.e. cost recovery) for any realization of stochastic power production [84].

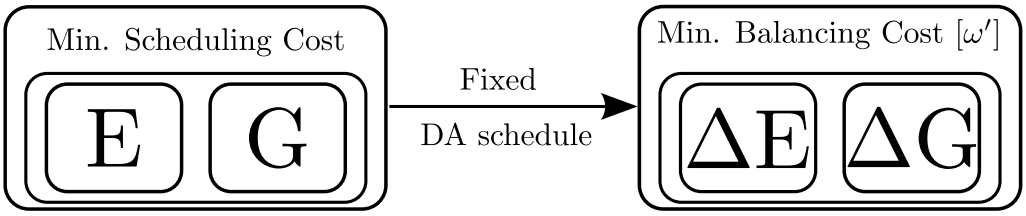

Figure 5.1: Sequential dispatch of coupled electricity and natural gas systems (DA: day-ahead, E: electricity, G: natural gas, ΔE: electricity adjustment, ΔG: natural gas adjustment).

5.1.2 Stochastic dispatch of coupled electricity and natural gas systems

An enhanced temporal coordination between the two trading floors is accomplished via utilizing a probabilistic description of uncertainties at the day-ahead stage. A two-stage stochastic program is developed to schedule the coupled energy system at the day-ahead stage, while anticipating future balancing costs, as shown in Figure 5.2. The uncertainty modeling is performed via a set of scenarios Ω that will cover potential realizations if the true characteristics of the stochastic process are sufficiently captured. The practical implementation of this approach is prevented because cost recovery for flexible producers and revenue adequacy for the system/market operator hold only in expectation and not for any realization in scenario set Ω [45]. Revenue adequacy indicates that the payments made to and received from market participants do not incur financial deficit to the operator. The reason is that some producers may be scheduled out of the merit order at the day-ahead stage and the resulting prices will not be sufficient to ensure these two properties [84].

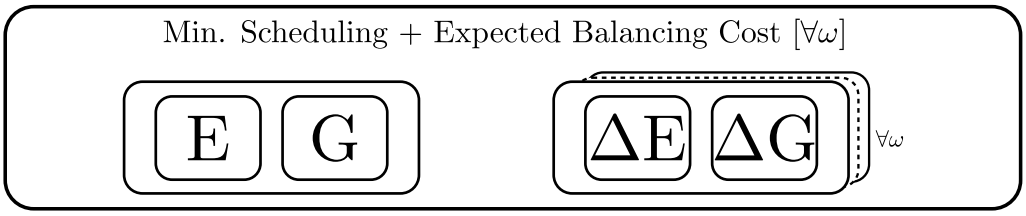

Figure 5.2: Stochastic dispatch of coupled electricity and natural gas systems (E: electricity, G: natural gas, ΔE: electricity adjustment, ΔG: natural gas adjustment).

5.1.3 Volume-based coordination in sequential dispatch of coupled electricity and natural gas systems

The sequential dispatch of the coupled electricity and natural gas system can be improved by the development of a systematic method to determine the available natural gas volume for power production at the day-ahead stage. Through this process, an implicit coordination of the day-ahead and balancing stages is accomplished, yielding a solution in between the sequential and stochastic ones in terms of expected system cost. The systematic definition of the amount χ^v of natural gas volume that is made available to GFPPs at the day-ahead stage is mathematically formulated as a stochastic bilevel model illustrated in Figure 5.3. Volume χ^v affects only the fuel demand of GFPPs at the day-ahead stage, while the full capacity of the natural gas network is released during the real-time stage. Moreover, the residential/industrial natural gas loads are not affected.

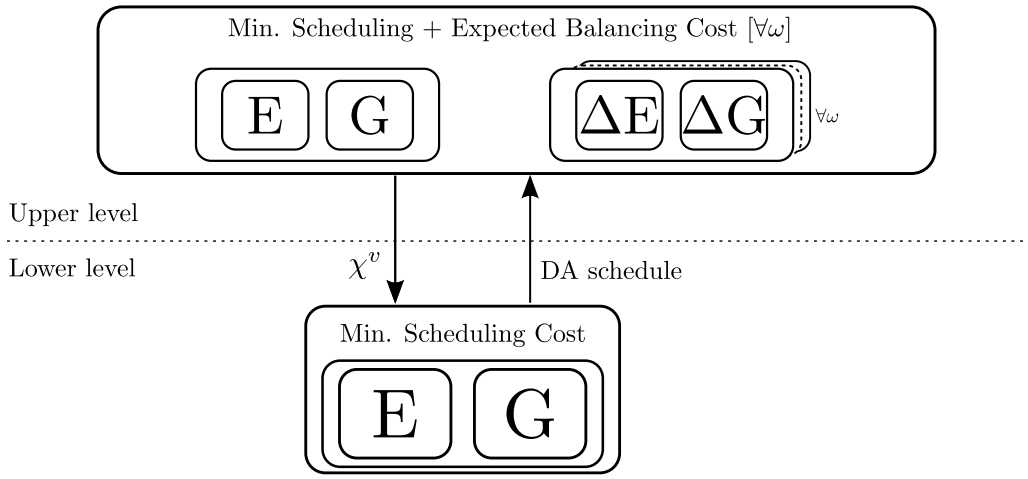

Figure 5.3: Volume-based coordination in sequential dispatch of coupled electricity and natural gas systems (DA: day-ahead, E: electricity, G: natural gas, ΔE: electricity adjustment, ΔG: natural gas adjustment).

The upper-level problem minimizes the total expected cost of operating the integrated energy system by deciding the optimal value of non-negative variable χ^v. The lower-level problem reproduces the day-ahead coupled electricity and natural gas market for a given value of χ^v that is treated as a parameter in the lower level. This framework practically emulates the sequential clearing of the day-ahead and balancing stages, since the day-ahead schedule that is enforced by the lower-level problem has the exact same properties as its counterpart in the sequential dispatch model presented in Figure 5.1. The re-dispatch actions are optimized for each realization in the upper-level problem. Consequently, the value χ^v is determined at the day-ahead market by anticipating future balancing costs.

This coordination framework resembles the "maximum gas burn" constraint recently introduced by the California Independent System Operator (CAISO) to provide a better communication between the electricity and natural gas systems due to the limited operability of the Aliso Canyon natural gas storage facility [87]. This constraint is able to limit the fuel consumption of GFPPs in a specific area to address reliability risks. Similarly, the coordination signal χ^v can be determined for the whole control zone or a tailored group of GFPPs. The proposed mechanism extends CAISO's approach to consider primarily issues pertaining to forecast errors of stochastic power producers.

5.1.4 Price-based coordination in sequential dispatch of coupled electricity and natural gas systems

A model that exploits the economic link between the electricity and natural gas systems through the natural gas price perceived by GFPPs is analogously developed in the price-based approach. The coordination signal χ^p is defined by a stochastic bilevel optimization model depicted schematically in Figure 5.4. Similarly to the volume-based model, the sequential clearing of day-ahead and real-time stages which results in enforcing the merit-order principle is also preserved by the structure of this model.

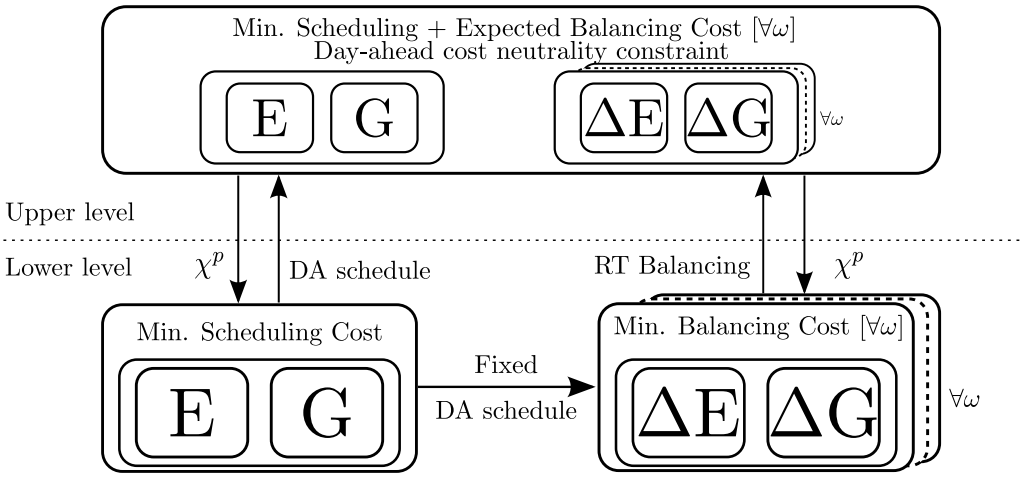

Figure 5.4: Price-based coordination in sequential dispatch of coupled electricity and natural gas systems (DA: day-ahead, RT: real-time, E: electricity, G: natural gas, ΔE: electricity adjustment, ΔG: natural gas adjustment).

This price-based approach allows the system/market operator to optimally adjust the natural gas price perceived by the GFPPs via the free variable χ^p. Such an operation is performed by either increasing (χ^p is positive) or decreasing (χ^p is negative) the short-term marginal costs of GFPPs and consequently their price offered on the electricity side of the integrated energy market in both trading floors. This action can be interpreted as "rewarding" or "penalizing" the power production of GFPPs for specific time periods. However, fairness for all counter-parties is ensured over the scheduling horizon since this mechanisms is designed on a cost-neutral basis by keeping the system/market operator financially balanced at the day-ahead stage. Potential real-time financial imbalance can be compensated by out-of-the-market payments to support flexibility providers similarly to the capacity renumeration mechanisms discussed in the European electricity market context [88].

5.1.5 Redefining the merit order of the day-ahead market via the dispatch models: a schematic representation

The day-ahead scheduling that can be obtained by the four different dispatch models presented in Sections 5.1.1-5.1.4 is illustrated in Figures 5.5-5.7. More specifically, the merit-order curve is presented in a simple setup with one stochastic producer, two non-GFPPs and two GFPPs for a single time period. The aim is to illustrate the way that the volume-based and price-based

models approximate the stochastic dispatch solution. The different effects are also presented in the comparison performed in Section 5.3.

Figure 5.5 presents the merit-order curve under the sequential dispatch and the stochastic dispatch models. The stochastic producer (e.g. wind power) is dispatched first due to the very low or zero marginal cost. It can be observed the power plants are scheduled based on an ascending order of marginal costs (i.e. merit-order principle) until the demand is covered in the sequential model. On the other hand, the stochastic dispatch model may schedule some power plants out of merit order. This decision depends on the structure of scenario set Ω that is available at the day-ahead stage. The power plants are scheduled in a way that cost-effective capacity is revealed for the real-time operation. However, the resulting prices guarantee cost recovery for flexible producers and revenue adequacy for the system/market operator only in expectation as discussed in Section 5.1.2.

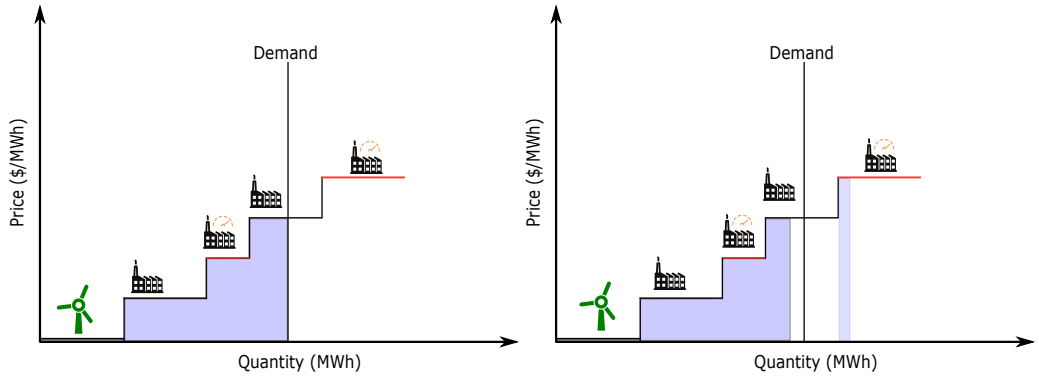

Figure 5.5: Merit-order curve when scheduling the day-ahead stage via the sequential dispatch model (left) and via the stochastic dispatch model (right), where GFPPs are indicated with the red line.

The effect of χ^v, which is defined by two variants of the volume-based dispatch model, on the merit order is depicted in Figure 5.6. When natural gas volume availability χ^v is defined for the whole natural gas system, a decrease of χ^v affects the most expensive GFPP. In this example, it can be noticed that the single GFPP is scheduled less and the marginal power producer is scheduled more by still respecting the merit-order principle. Defining χ^v individually for each GFPP permits to alter the schedule of both GFPPs by decreasing the volume made available for the cheap GFPP and in turn increasing the availability for the expensive GFPP. In both cases, the volume-based models are able to reveal cost-effective flexibility for balancing but simultaneously follow the merit-order principle that guarantees cost recovery for each scenario in Ω.

A similar effect is noticed in Figure 5.7, where the solution of the stochastic model is approximated by the price-based dispatch model that schedules the power plants based on the ascending order of marginal costs. In this case, the system/market operator decreases the natural gas price perceived by GFPPs which results in decreasing their marginal cost and scheduling the most expensive GFPP. Note that natural gas price adjustment is the same for all GFPPs; we illustrate though the effect only for the most expensive GFPP for clarity. A similar outcome may be accomplished by increasing the natural gas perceived by GFPPs. In this case, the schedule of the cheap GFPP would be affected.

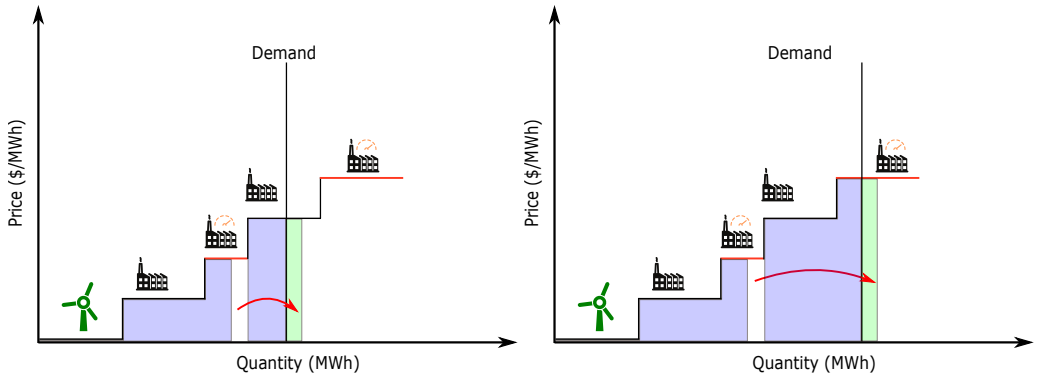

Figure 5.6: Merit-order curve when scheduling the day-ahead stage via the volume-based dispatch model (left) and via the plant-specific volume-based dispatch model (right), where GFPPs are indicated with the red line.

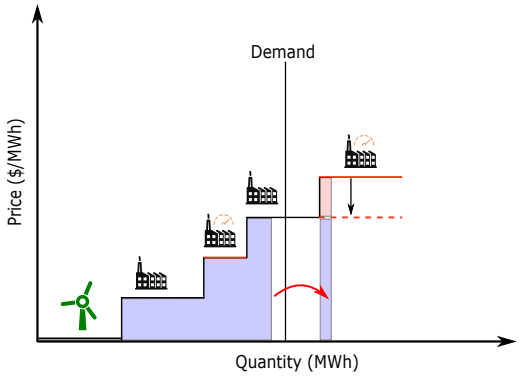

Figure 5.7: Merit-order curve when scheduling the day-ahead stage via the price-based dispatch model, where GFPPs are indicated with the red line.

5.2 Mathematical formulation of dispatch models

In this section, the dispatch models are formulated as compact mathematical optimization problems to demonstrate the effect of coordination parameters χ^v and χ^p. The physical and economical link is provided by GFPPs to couple the electricity and natural gas systems. In all dispatch models, the perspective of the system/market operator is taken to minimize the total system cost. The day-ahead market is cleared with a pool-based approach, i.e. without network capacity constraints, while the balancing market is formulated under two different variants. The first setup is formulated as a Linear Program (LP) under the assumption that the balancing market is cleared as a pool with additional contact and fuel constraints for GFPPs. These constraints are calculated based on an ex-ante analysis as presented in Section 3.2.2. In the second setup, network constraints are introduced for both energy systems. In the electricity system, we adopt a DC power flow model and the natural gas flow model with approximated dynamics is utilized for the natural gas system as introduced in Section 3.2.2. Under the first setup, the balancing market is formulated as an LP which allows the comparison of volume-based and price-based models. For this reason, the mathematical formulation is provided under the first setup in this chapter. The extension to the second setup with network constraints for the volume-based model is similar to the one provided in Section 4.2. In the second setup, the natural gas flow problem is formulated as a Mixed-Integer Linear Program (MILP). As described in Section 4.2, electricity and natural gas prices are derived

from the LP obtained by fixing the binary variables of the initial MILP to their optimal values. More specifically, we consider a combined electricity and natural gas system with G conventional power plants, W stochastic producers, $\mathcal{D}$ electricity demands, $\mathcal{E}$ pipelines, $\mathcal{U}$ natural gas producers and $\mathcal{H}$ natural gas demands. The following mathematical programs are suited for multi-period problems, we omit though the time dimension T from the variables and parameters for clarity. A detailed mathematical description of the models is provided in [Paper C] and [Paper D].

5.2.1 Sequential dispatch of coupled electricity and natural gas systems

The sequential dispatch of coupled electricity and natural gas systems clears independently the day-ahead and balancing stages. Denoting by $p^{\mathrm{D}} \in \mathbb{R}_+^G$ and $w^{\mathrm{D}} \in \mathbb{R}_+^W$ the day-ahead scheduling of conventional and stochastic power producers, as well as by $g^{\mathrm{D}} \in \mathbb{R}_+^{\mathcal{U}}$ the natural gas production, the optimal day-ahead schedule $\left(p^{\mathrm{D}*}, w^{\mathrm{D}*}, g^{\mathrm{D}*}\right)$ minimizes the day-ahead cost $\mathcal{C}_{\mathrm{E}}^{\mathrm{D}}(p^{\mathrm{D}}) + \mathcal{C}_{\mathrm{G}}^{\mathrm{D}}(g^{\mathrm{D}})$ of the coupled energy system by solving model (5.1) which writes as follows:

$$\min_{p^{\mathrm{D}}, w^{\mathrm{D}}, g^{\mathrm{D}}} \quad \mathcal{C}_{\mathrm{E}}^{\mathrm{D}}(p^{\mathrm{D}}) + \mathcal{C}_{\mathrm{G}}^{\mathrm{D}}(g^{\mathrm{D}}) \tag{5.1a}$$

$$\text{s.t.} \quad h_{\mathrm{E}}^{\mathrm{D}}(p^{\mathrm{D}}, w^{\mathrm{D}}) - e^\top D^{\mathrm{e}} = 0 : \lambda_{\mathrm{E}}^{\mathrm{D}} \tag{5.1b}$$

$$f_{\mathrm{E}}^{\mathrm{D}}(p^{\mathrm{D}}) \leq 0 \tag{5.1c}$$

$$0 \leq w^{\mathrm{D}} \leq \widehat{W} \tag{5.1d}$$

$$h_{\mathrm{G}}^{\mathrm{D}}(g^{\mathrm{D}}, \Phi p^{\mathrm{D}}) - e^\top D^{\mathrm{g}} = 0 : \lambda_{\mathrm{G}}^{\mathrm{D}} \tag{5.1e}$$

$$f_{\mathrm{G1}}^{\mathrm{D}}(g^{\mathrm{D}}) \leq 0 \tag{5.1f}$$

$$0 \leq f_{\mathrm{G2}}^{\mathrm{D}}(\Phi p^{\mathrm{D}}) \leq \overline{G}^{\mathrm{D}}, \tag{5.1g}$$

where $\widehat{W} \in \mathbb{R}_+^W$ is the forecast of stochastic power production. The objective function minimized in (5.1a) determines the electricity and natural gas cost, where we have excluded the electricity cost of GFPPs since this is already taken into account through the cost of natural gas consumption. The balance in the electricity system is enforced by equality (5.1b) by stating that the power production is equal to the total electricity demand $D^{\mathrm{e}} \in \mathbb{R}_+^{\mathcal{D}}$. We denote with e a vector of ones with appropriate dimensions. Upper and lower bounds of power production are included in inequalities (5.1c), while stochastic production is constrained by (5.1d). The natural gas system is balanced via equality (5.1e), which enforces the natural gas production to be equal to the total natural gas demand $D^{\mathrm{g}} \in \mathbb{R}_+^{\mathcal{H}}$ and fuel consumption Φp^{D} of GFPPs. The fuel consumption Φp^{D} is treated as a variable in the coupled optimization of energy systems. The natural gas consumption of GFPPs is calculated as the multiplication of power production p^{D} with the power conversion factor $\Phi \in \mathbb{R}_+^{G \times G}$. Diagonal matrix Φ contains the power conversion factor of GFPPs, while the entries for non-GFPPs are zero. Similarly to (5.1c), inequalities (5.1f) describe the upper and lower bounds for natural gas producers. Inequalities (5.1g) limit natural gas fuel consumption of GFPPs by the quantity $\overline{G}^{\mathrm{D}} \in \mathbb{R}_+^{\mathcal{F}}$ made available at the day-ahead stage. This quantity $\overline{G}^{\mathrm{D}}$ can be defined for different groups $\mathcal{F}$ of GFPPs, which may comprise GFPPs in a specific area of the natural gas system or even a single GFPP. The dual variables $\lambda_{\mathrm{E}}^{\mathrm{D}} \in \mathbb{R}$ and $\lambda_{\mathrm{G}}^{\mathrm{D}} \in \mathbb{R}$ of balancing constraints (5.1b) and (5.1e) reflect the market price for electricity and natural gas, respectively. The optimal day-ahead schedule $\left(p^{\mathrm{D}*}, w^{\mathrm{D}*}, g^{\mathrm{D}*}\right)$ is given as a fixed input to the balancing market. The balancing market is represented by model (5.2) and compensates for potential imbalances due

to the stochastic power realization $W_{\omega'} \in \mathbb{R}_+^W$:

$$\min_{p^{\mathrm{R}}_{\omega'}, pl^{\mathrm{R}}_{\omega'}, w^{\mathrm{R}}_{\omega'}, g^{\mathrm{R}}_{\omega'}, gl^{\mathrm{R}}_{\omega'}} \quad \mathcal{C}^{\mathrm{R}}_{\mathrm{E}}(p^{\mathrm{R}}_{\omega'}, pl^{\mathrm{R}}_{\omega'}) + \mathcal{C}^{\mathrm{R}}_{\mathrm{G}}(g^{\mathrm{R}}_{\omega'}, gl^{\mathrm{R}}_{\omega'}) \tag{5.2a}$$

$$\text{s. t.} \quad h^{\mathrm{R}}_{\mathrm{E}}(p^{\mathrm{R}}_{\omega'}, pl^{\mathrm{R}}_{\omega'}, w^{\mathrm{R}}_{\omega'}) + e^{\top}(W_{\omega'} - w^{\mathrm{D}^*}) = 0 : \lambda^{\mathrm{R}}_{\mathrm{E}(\omega')} \tag{5.2b}$$

$$f^{\mathrm{R}}_{\mathrm{E}}(p^{\mathrm{R}}_{\omega'}, pl^{\mathrm{R}}_{\omega'}, w^{\mathrm{R}}_{\omega'}, p^{\mathrm{D}^*}; W_{\omega'}) \leq 0 \tag{5.2c}$$

$$h^{\mathrm{R}}_{\mathrm{G}}(g^{\mathrm{R}}_{\omega'}, gl^{\mathrm{R}}_{\omega'}, \Phi p^{\mathrm{R}}_{\omega'}) = 0 : \lambda^{\mathrm{R}}_{\mathrm{G}(\omega')} \tag{5.2d}$$

$$f^{\mathrm{R}}_{\mathrm{G1}}(g^{\mathrm{R}}_{\omega'}, gl^{\mathrm{R}}_{\omega'}, g^{\mathrm{D}^*}) \leq 0 \tag{5.2e}$$

$$0 \leq f^{\mathrm{R}}_{\mathrm{G2}}(\Phi p^{\mathrm{R}}_{\omega'}, \Phi p^{\mathrm{D}^*}) \leq \overline{G}^{\mathrm{R}}, \tag{5.2f}$$

where $p^{\mathrm{R}}_{\omega'} \in \mathbb{R}^G$ and $g^{\mathrm{R}}_{\omega'} \in \mathbb{R}^{\mathcal{U}}$ denote the power and natural gas adjustments, respectively. Moreover, $pl^{\mathrm{R}}_{\omega'} \in \mathbb{R}_+^D$ and $gl^{\mathrm{R}}_{\omega'} \in \mathbb{R}_+^{\mathcal{H}}$ are the electricity and natural gas load shedding, while wind spilling is denoted by $w^{\mathrm{R}}_{\omega'} \in \mathbb{R}_+^W$. The cost of balancing actions is minimized in (5.2a) to deal with the energy imbalance caused by stochastic production. Equality constraints (5.2b) enforce the power system balancing in real-time operation. Inequalities (5.2c) collect all the constraints relative to the upper and lower bounds of power adjustments, load shedding and wind spillage. The natural gas system is balanced via (5.2d). Dual variables $\lambda^{\mathrm{R}}_{\mathrm{E}(\omega')} \in \mathbb{R}$ and $\lambda^{\mathrm{R}}_{\mathrm{G}(\omega')} \in \mathbb{R}$ reflect the respective market prices prices at the balancing stage. Capacity constraints for natural gas production adjustments and load shedding are enforced by inequalities (5.2e). The real-time physical capacity $\overline{G}^{\mathrm{R}} \in \mathbb{R}_+^{\mathcal{E}}$ made available to GFPPs is imposed by (5.2f). The value of $\overline{G}^{\mathrm{R}}$ is calculated by an ex-ante analysis, where the residential/industrial natural gas demand is subtracted by the maximum physical capacity of the pipeline.

5.2.2 Stochastic dispatch of coupled electricity and natural gas systems

The stochastic dispatch model of coupled electricity and natural gas systems is formulated as a single mathematical program. In model (5.3), the day-ahead and balancing stages are jointly optimized for the coupled energy system via a two-stage stochastic program that writes as follows:

$$\min_{\substack{p^{\mathrm{D}}, w^{\mathrm{D}}, g^{\mathrm{D}}, p^{\mathrm{R}}_{\omega}, \\ pl^{\mathrm{R}}_{\omega}, w^{\mathrm{R}}_{\omega}, g^{\mathrm{R}}_{\omega}, gl^{\mathrm{R}}_{\omega}}} \quad \mathcal{C}^{\mathrm{D}}_{\mathrm{E}}(p^{\mathrm{D}}) + \mathcal{C}^{\mathrm{D}}_{\mathrm{G}}(g^{\mathrm{D}}) + \mathbb{E}_{\omega}\left[\mathcal{C}^{\mathrm{R}}_{\mathrm{E}}(p^{\mathrm{R}}_{\omega}, pl^{\mathrm{R}}_{\omega}) + \mathcal{C}^{\mathrm{R}}_{\mathrm{G}}(g^{\mathrm{R}}_{\omega}, gl^{\mathrm{R}}_{\omega})\right] \tag{5.3a}$$

$$\text{s. t.} \quad h^{\mathrm{D}}_{\mathrm{E}}(p^{\mathrm{D}}, w^{\mathrm{D}}) - e^{\top} D^{\mathrm{e}} = 0 : \lambda^{\mathrm{D}}_{\mathrm{E}} \tag{5.3b}$$

$$f^{\mathrm{D}}_{\mathrm{E}}(p^{\mathrm{D}}) \leq 0 \tag{5.3c}$$

$$0 \leq w^{\mathrm{D}} \leq \overline{W} \tag{5.3d}$$

$$h^{\mathrm{D}}_{\mathrm{G}}(g^{\mathrm{D}}, \Phi p^{\mathrm{D}}) - e^{\top} D^{\mathrm{g}} = 0 : \lambda^{\mathrm{D}}_{\mathrm{G}} \tag{5.3e}$$

$$f^{\mathrm{D}}_{\mathrm{G1}}(g^{\mathrm{D}}) \leq 0 \tag{5.3f}$$

$$0 \leq f^{\mathrm{D}}_{\mathrm{G2}}(\Phi p^{\mathrm{D}}) \leq \overline{G}^{\mathrm{D}} \tag{5.3g}$$

$$h^{\mathrm{R}}_{\mathrm{E}}(p^{\mathrm{R}}_{\omega}, pl^{\mathrm{R}}_{\omega}, w^{\mathrm{R}}_{\omega}) + A^{\mathrm{w}}(W_{\omega} - w^{\mathrm{D}}) = 0 : \lambda^{\mathrm{R}}_{\mathrm{E}(\omega)}, \ \ \forall \omega \in \Omega \tag{5.3h}$$

$$f^{\mathrm{R}}_{\mathrm{E}}(p^{\mathrm{R}}_{\omega}, pl^{\mathrm{R}}_{\omega}, w^{\mathrm{R}}_{\omega}, p^{\mathrm{D}}; W_{\omega}) \leq 0, \ \ \forall \omega \in \Omega \tag{5.3i}$$

$$h^{\mathrm{R}}_{\mathrm{G}}(g^{\mathrm{R}}_{\omega}, gl^{\mathrm{R}}_{\omega}, \Phi p^{\mathrm{R}}_{\omega}) = 0 : \lambda^{\mathrm{R}}_{\mathrm{G}(\omega)}, \ \ \forall \omega \in \Omega \tag{5.3j}$$

$$f^{\mathrm{R}}_{\mathrm{G1}}(g^{\mathrm{R}}_{\omega}, gl^{\mathrm{R}}_{\omega}, g^{\mathrm{D}}) \leq 0, \ \ \forall \omega \in \Omega \tag{5.3k}$$

$$0 \leq f^{\mathrm{R}}_{\mathrm{G2}}(\Phi p^{\mathrm{R}}_{\omega}, \Phi p^{\mathrm{D}}) \leq \overline{G}^{\mathrm{R}}, \ \ \forall \omega \in \Omega, \tag{5.3l}$$

where $\overline{W} \in \mathbb{R}^{W}_{+}$ is the capacity of stochastic producers. The aim is to minimize the total expected cost in (5.3a), where future balancing costs are anticipated via the scenarios $\omega \in \Omega$. Moreover, the temporal coordination in enhanced via writing constraints (5.3h)-(5.3l) for all scenarios $\omega \in \Omega$. Note that the day-ahead schedule of stochastic producers is restricted by the installed capacity $\overline{W}$, according to (5.3d), instead of the forecast value $\widehat{W}$ and day-ahead decisions are treated as variables. Constraints (5.3b)-(5.3c) and (5.3e)-(5.3l) are the same as ones described in Section 5.2.1.

5.2.3 Volume-based coordination in sequential dispatch of coupled electricity and natural gas systems

The volume-based model minimizes the total expected cost of the coupled energy system and defines the optimal natural gas volume availability for power production $\chi^{v} \in \mathbb{R}^{\mathcal{F}}_{+}$ is formulated as a stochastic bilevel program. Model (5.4) writes as follows:

$$\min_{\substack{\chi^{v},p^{\mathrm{D}},w^{\mathrm{D}},g^{\mathrm{D}},\\ p^{\mathrm{R}}_{\omega},pl^{\mathrm{R}}_{\omega},w^{\mathrm{R}}_{\omega},g^{\mathrm{R}}_{\omega},gl^{\mathrm{R}}_{\omega}}} \quad \mathcal{C}^{\mathrm{D}}_{\mathrm{E}}(p^{\mathrm{D}}) + \mathcal{C}^{\mathrm{D}}_{\mathrm{G}}(g^{\mathrm{D}}) + \mathbb{E}_{\omega}\left[\mathcal{C}^{\mathrm{R}}_{\mathrm{E}}(p^{\mathrm{R}}_{\omega}, pl^{\mathrm{R}}_{\omega}) + \mathcal{C}^{\mathrm{R}}_{\mathrm{G}}(g^{\mathrm{R}}_{\omega}, gl^{\mathrm{R}}_{\omega})\right] \tag{5.4a}$$

$$\text{s.t.} \quad h^{\mathrm{R}}_{\mathrm{E}}(p^{\mathrm{R}}_{\omega}, pl^{\mathrm{R}}_{\omega}, w^{\mathrm{R}}_{\omega}) + e^{\top}(W_{\omega} - w^{\mathrm{D}}) = 0 : \lambda^{\mathrm{R}}_{\mathrm{E}(\omega)}, \ \ \forall \omega \in \Omega \tag{5.4b}$$

$$f^{\mathrm{R}}_{\mathrm{E}}(p^{\mathrm{R}}_{\omega}, pl^{\mathrm{R}}_{\omega}, w^{\mathrm{R}}_{\omega}, p^{\mathrm{D}}; W_{\omega}) \leq 0, \ \ \forall \omega \in \Omega \tag{5.4c}$$

$$h^{\mathrm{R}}_{\mathrm{G}}(g^{\mathrm{R}}_{\omega}, gl^{\mathrm{R}}_{\omega}, \Phi p^{\mathrm{R}}_{\omega}) = 0 : \lambda^{\mathrm{R}}_{\mathrm{G}(\omega)}, \ \ \forall \omega \in \Omega \tag{5.4d}$$

$$f^{\mathrm{R}}_{\mathrm{G1}}(g^{\mathrm{R}}_{\omega}, gl^{\mathrm{R}}_{\omega}, g^{\mathrm{D}}) \leq 0, \ \ \forall \omega \in \Omega \tag{5.4e}$$

$$0 \leq f^{\mathrm{R}}_{\mathrm{G2}}(\Phi p^{\mathrm{R}}_{\omega}, \Phi p^{\mathrm{D}}) \leq \overline{G}^{\mathrm{R}}, \ \ \forall \omega \in \Omega \tag{5.4f}$$

$$0 \leq \chi^{v} \leq \overline{G}^{\mathrm{D}} \tag{5.4g}$$

$$(p^{\mathrm{D}}, w^{\mathrm{D}}, g^{\mathrm{D}}) \in \arg\Big\{$$

$$\min_{p^{\mathrm{D}},w^{\mathrm{D}},g^{\mathrm{D}}} \mathcal{C}^{\mathrm{D}}_{\mathrm{E}}(p^{\mathrm{D}}) + \mathcal{C}^{\mathrm{D}}_{\mathrm{G}}(g^{\mathrm{D}}) \tag{5.4h}$$

$$\text{s.t.} \ \ h^{\mathrm{D}}_{\mathrm{E}}(p^{\mathrm{D}}, w^{\mathrm{D}}) - e^{\top} D^{\mathrm{e}} = 0 : \lambda^{\mathrm{D}}_{\mathrm{E}} \tag{5.4i}$$

$$f^{\mathrm{D}}_{\mathrm{E}}(p^{\mathrm{D}}) \leq 0 \tag{5.4j}$$

$$0 \leq w^{\mathrm{D}} \leq \widehat{W} \tag{5.4k}$$

$$h^{\mathrm{D}}_{\mathrm{G}}(g^{\mathrm{D}}, \Phi p^{\mathrm{D}}) - e^{\top} D^{\mathrm{g}} = 0 : \lambda^{\mathrm{D}}_{\mathrm{G}} \tag{5.4l}$$

$$f^{\mathrm{D}}_{\mathrm{G1}}(g^{\mathrm{D}}) \leq 0 \tag{5.4m}$$

$$0 \leq f^{\mathrm{D}}_{\mathrm{G2}}(\Phi p^{\mathrm{D}}) \leq \chi^{v} \Big\}, \tag{5.4n}$$

where the objective function (5.4a) is the same as (5.3a). The upper-level minimizes the total expected cost and defines the optimal value of χ^{v} which is constrained by inequality (5.4g). The upper bound in (5.4g) is equal to the natural gas quantity $\overline{G}^{\mathrm{D}}$ made available for power production at the day-ahead stage. Variable χ^{v} limits the scheduled natural gas consumption of GFPPs at the day-ahead in (5.4n). The lower-level problem reproduces the day-ahead coupled electricity and natural gas market. Under this setup the sequential clearing of day-ahead and balancing markets is practically simulated since the day-ahead decisions are fixed to the sequential dispatch through (5.4h)-(5.4n) and the balancing market is simulated for each independent scenario by imposing constraints (5.4b)-(5.4f) for all $\omega \in \Omega$. Notice that the upper-level variable χ^{v} has an impact on the lower-level decision variables as the total fuel availability for GFPPs affect the day-ahead schedule of the integrated energy system. The lower-level variables are also affecting the total expected cost of operating the system. Consequently, the structure of model (5.4) permits the minimization

of expected system cost by revealing the flexibility of GFPPs and ensures that the merit-order principle is respected, as in the model presented in Section 5.2.1.

5.2.4 Price-based coordination in sequential dispatch of coupled electricity and natural gas systems

The price-based model minimizes the total expected cost of the coupled energy system and defines the optimal natural gas price adjustment $\chi^p \in \mathbb{R}$. Model (5.5) is formulated as a stochastic bilevel program and writes as follows:

$$\min_{\substack{\chi^p, p^{\mathrm{D}}, w^{\mathrm{D}}, g^{\mathrm{D}}, \\ p^{\mathrm{R}}_\omega, pl^{\mathrm{R}}_\omega, w^{\mathrm{R}}_\omega, g^{\mathrm{R}}_\omega, gl^{\mathrm{R}}_\omega}} \quad \mathcal{C}^{\mathrm{D}}_{\mathrm{E}}(p^{\mathrm{D}}) + \mathcal{C}^{\mathrm{D}}_{\mathrm{G}}(g^{\mathrm{D}}) + \mathbb{E}_\omega \left[\mathcal{C}^{\mathrm{R}}_{\mathrm{E}}(p^{\mathrm{R}}_\omega, pl^{\mathrm{R}}_\omega) + \mathcal{C}^{\mathrm{R}}_{\mathrm{G}}(g^{\mathrm{R}}_\omega, gl^{\mathrm{R}}_\omega)\right] \tag{5.5a}$$

$$\text{s.t.} \quad -\overline{X} \leq \chi^p \leq \overline{X} \tag{5.5b}$$

$$h^{\mathrm{D}}_{\mathrm{G2}}(e^\top \chi^p \Phi p^{\mathrm{D}}) = 0 \tag{5.5c}$$

$$(p^{\mathrm{D}}, w^{\mathrm{D}}, g^{\mathrm{D}}) \in \arg\Big\{$$

$$\min_{p^{\mathrm{D}}, w^{\mathrm{D}}, g^{\mathrm{D}}} \mathcal{C}^{\mathrm{D}}_{\mathrm{E}}(p^{\mathrm{D}}, \chi^p) + \mathcal{C}^{\mathrm{D}}_{\mathrm{G}}(g^{\mathrm{D}}) \tag{5.5d}$$

$$\text{s.t.} \quad h^{\mathrm{D}}_{\mathrm{E}}(p^{\mathrm{D}}, w^{\mathrm{D}}) - e^\top D^{\mathrm{e}} = 0 : \lambda^{\mathrm{D}}_{\mathrm{E}} \tag{5.5e}$$

$$f^{\mathrm{D}}_{\mathrm{E}}(p^{\mathrm{D}}) \leq 0 \tag{5.5f}$$

$$0 \leq w^{\mathrm{D}} \leq \widehat{W} \tag{5.5g}$$

$$h^{\mathrm{D}}_{\mathrm{G1}}(g^{\mathrm{D}}, \Phi p^{\mathrm{D}}) - e^\top D^{\mathrm{g}} = 0 : \lambda^{\mathrm{D}}_{\mathrm{G}} \tag{5.5h}$$

$$f^{\mathrm{D}}_{\mathrm{G1}}(g^{\mathrm{D}}) \leq 0 \tag{5.5i}$$

$$0 \leq f^{\mathrm{D}}_{\mathrm{G2}}(\Phi p^{\mathrm{D}}) \leq \overline{G}^{\mathrm{D}} \Big\} \tag{5.5j}$$

$$(p^{\mathrm{R}}_\omega, pl^{\mathrm{R}}_\omega, w^{\mathrm{R}}_\omega, g^{\mathrm{R}}_\omega, gl^{\mathrm{R}}_\omega) \in \arg\Big\{$$

$$\min_{p^{\mathrm{R}}_\omega, pl^{\mathrm{R}}_\omega, w^{\mathrm{R}}_\omega, g^{\mathrm{R}}_\omega, gl^{\mathrm{R}}_\omega} \mathcal{C}^{\mathrm{R}}_{\mathrm{E}}(p^{\mathrm{R}}_\omega, pl^{\mathrm{R}}_\omega, \chi^p) + \mathcal{C}^{\mathrm{R}}_{\mathrm{G}}(g^{\mathrm{R}}_\omega, gl^{\mathrm{R}}_\omega) \tag{5.5k}$$

$$\text{s.t.} \quad h^{\mathrm{R}}_{\mathrm{E}}(p^{\mathrm{R}}_\omega, pl^{\mathrm{R}}_\omega, w^{\mathrm{R}}_\omega) + e^\top (W_\omega - w^{\mathrm{D}}) = 0 : \lambda^{\mathrm{R}}_{\mathrm{E}(\omega)} \tag{5.5l}$$

$$f^{\mathrm{R}}_{\mathrm{E}}(p^{\mathrm{R}}_\omega, pl^{\mathrm{R}}_\omega, w^{\mathrm{R}}_\omega, p^{\mathrm{D}}; W_\omega) \leq 0 \tag{5.5m}$$

$$h^{\mathrm{R}}_{\mathrm{G}}(g^{\mathrm{R}}_\omega, gl^{\mathrm{R}}_\omega, \Phi p^{\mathrm{R}}_\omega) = 0 : \lambda^{\mathrm{R}}_{\mathrm{G}(\omega)} \tag{5.5n}$$

$$0 \leq f^{\mathrm{R}}_{\mathrm{G2}}(\Phi p^{\mathrm{R}}_\omega, \Phi p^{\mathrm{D}}) \leq \overline{G}^{\mathrm{R}} \Big\}, \ \ \forall \omega \in \Omega, \tag{5.5o}$$

where the objective function (5.5a) is the same as (5.3a). Similarly to model (5.4), the upper-level problem minimizes the total expected cost and optimally decides the value of natural gas price adjustment χ^p. The lower-level problems practically simulate the sequential dispatch of day-ahead and balancing stages, since the day-ahead decisions are fixed to the sequential dispatch via (5.5d)-(5.5j) and the balancing stage is simulated for each scenario by imposing (5.5k)-(5.5o) for all $\omega \in \Omega$. Variable χ^p is bounded by constraint (5.5b) indicating the limits $\overline{X} \in \mathbb{R}_+$ that the operator may vary the natural gas price perceived by GFPPs. Equality (5.5c) enforces cost-neutrality at the day-ahead stage guaranteeing that there is no financial deficit or surplus to the system/market operator throughout the scheduling horizon (i.e. one day). This property is enforced by stating that the sum of quantity $e^\top \chi^p \Phi p^{\mathrm{D}}$ over the time periods is equal to zero. Potential deficit or surplus at the balancing stage is expected to be fairly limited and can be addressed via proper regulation. The upper-level variable χ^p affects the decisions of lower-level problems by the day-ahead and

balancing offer prices of GFPPs, which in turn influences the objective functions (5.5d) and (5.5k) in the lower-level problems. The dispatch of GFPPs affects the lower-level decision variables which have an impact on the total expected cost of the coupled energy system. Hence, model (5.5) provides the optimal system schedule that anticipates future balancing costs and simultaneously respects the merit-order principle, as the model presented in Section 5.2.1.

5.2.5 On the features of volume-based and price-based models towards tractable reformulations

Formulating the volume-based and price-based models as stochastic bilevel programs permits to maintain the actual sequential structure of the day-ahead and balancing markets, which at the same time guarantees cost recovery for flexible producers for each realization of stochastic production in scenario set Ω. In the volume-based model, the lower level problem contains only the day-ahead stage because the natural gas volume availability χ^v affects the day-ahead fuel consumption of GFPPs and then the physical capacity of the natural gas network is made available in the balancing stage. On the other hand, the price-based model exploits the economic link between the two systems and requires both day-ahead and balancing stages to be included in the lower-level problem. The reason is that χ^p has to adjust the natural gas price perceived by GFPPs in both trading floors in a consistent manner. This price adjustment χ^p affects the marginal cost of GFPPs at the day-ahead stage and the real-time price offers have to be altered accordingly to preserve the incentive of provisioning balancing services.

The stochastic bilevel programs can admit a single-level reformulation if the lower-level problems are convex [22]. In this case, the bilevel problems can be reformulated as a Mathematical Program with Equilibrium Constraints (MPEC) by replacing the convex lower-level problems by their Karush-Kuhn-Tucker (KKT) conditions and eventually recast a tractable MILP. These reformulations are given in detain in [Paper C] and [Paper D]. The balancing market is modeled under two setups. In the first one, the balancing market is formulated as an LP which allows the comparison of the volume-based and price-based models. The second variant approximates the dynamics of the natural gas flows in the real-time stage, which requires the introduction of binary variables that make the problem non-convex. Therefore, we are able to apply the second variant only to the volume-based model. As far as computational tractability is concerned, the volume-based model results in fewer binary variables than the price-based one since the balancing market is not included in the lower level. Sidestepping the inclusion of the balancing market in the lower-level problem of the volume-based model results in having independent binary variables from the number of scenarios and thus in a formulation that is less computationally expensive.

5.2.6 Characteristics of the dispatch models

Before proceeding to the experimental comparison of dispatch models, we provide an overview of their features in Table 5.1. In this chapter, all dispatch models are related to the coupled electricity and natural gas system so we have dropped "-*Coup*" from the names presented in Figure 3.7 for clarity. Moreover, the uncertainty-aware dispatch is performed via two-stage stochastic programming in this chapter and referred to as *Stoch*. The models with network constraints in the balancing market are indicated with "*N*", while the price-based model does not have this variant as aforementioned. The sequential (*Seq*) dispatch of coupled electricity and natural gas systems achieves an imperfect temporal coordination via a single-valued forecast. On the other hand, an

ideal benchmark solution for the integrated energy system is attained by the stochastic (*Stoch*) dispatch model when utilizing a proper probabilistic description of uncertainties (i.e. scenario set Ω adequately represents potential realizations), which provides the dispatch with the minimum total expected cost. The volume-based (*V-B*) and price-based (*P-B*) models provide a partial temporal coordination implicitly via the fine-tuning of the corresponding control parameters. Hence, these two improved dispatch models bridge the gap between the *Seq* and *Stoch*.

Table 5.1: Characteristics of dispatch models.

Fuel / Network constraints	*Seq* / *Seq-N*	*Stoch* / *Stoch-N*	*V-B* / *V-B-N*	*P-B* / –
Temporal coordination	Imperfect	Perfect	Partial	Partial
Coordination mechanism	Non-existing	Explicit	Implicit via χ^v *	Implicit via χ^p

* The value of χ^v can be defined for the whole market, specific areas or GFPPs.

5.3 Improving the sequential market arrangement with optimal flexibility signals

The sequential dispatch of coupled electricity and natural gas systems is improved by the optimal definition of the flexibility volume and price signals. In this section, we study the impact of controlling parameters χ^v and χ^p on the dispatch of the coupled energy system. A detailed analysis is provided via an illustrative 1-hour example, while a more thorough comparison is provided for the dispatch models over a 24-hour period based on a tailored case study.

A system which comprises three thermal power plants (G_1, G_2 and G_5), two GFPPs (G_3 and G_4) that acquire their fuel from the natural gas market, one wind farm (WP) and two natural gas producers ($\mathcal{U}_1$ and $\mathcal{U}_2$) is utilized in this section as presented in Table 5.2. Wind power production is characterized via a set of 2 equiprobable scenarios ω_1 (166 MW) and ω_2 (86 MW). The offer prices in the balancing market are calculated as 1.1 and 0.9 of the day-ahead offer prices for upward and downward regulation, respectively. The natural gas price adjustment is limited to \$1.35/kcf. The peak electricity and natural gas demand for residential/industrial loads are equal to 430 MW and 3,600 kcf/h, respectively. The two GFPPs are connected to a single pipeline with a capacity of 6,000 kcf.

Table 5.2: Electricity and natural gas system data for the tailored case study.

Unit G	G_1	G_2	G_3	G_4	G_5	Unit $\mathcal{U}$	$\mathcal{U}_1$	$\mathcal{U}_2$
Maximum capacity (MW)	80	110	50	100	100	Maximum capacity (kcf)	10,000	6,000
Maximum up regulation (MW)	10	0	30	25	20	Maximum up regulation (kcf)	2,500	1,000
Maximum down regulation (MW)	10	0	30	25	20	Maximum down regulation (kcf)	2,500	1,000
Day-ahead offer price (\$/MWh)	30	10	-	-	60	Day-ahead offer price (\$/kcf)	2	3
Power conversion factor (kcf/MWh)	-	-	12	18	-			

The detailed results are given for a specific time period after solving all dispatch models for 24-hours. Two variants of the volume-based model, where natural gas volume availability is determined for the whole market (*V-B*) and for each individual GFPP (*V-B gen*), are studied. In this instance, natural gas is produced only by unit $\mathcal{U}_1$, hence the natural gas price is \$2/kcf and the marginal costs of GFPPs G_3 and G_4 are \$24/MWh and \$36/MWh. The marginal costs are calculated by multiplying the power conversion factor with the natural gas price.

Initially, the performance of all dispatch models is quantified in terms of expected system cost, which is illustrated with its breakdown in Table 5.3. Model *Stoch* returns the solution with the minimum expected system cost, while *Seq* the solution with the highest one. Models *P-B*, *V-B* and *V-B gen* yield an expected system cost in between the ideal solution of *Stoch* and the one of *Seq*.

Table 5.3: Expected system cost and its breakdown when total electricity load is 387 MW.

	Total	Day-ahead ($)	Balancing ($)	Up regulation ($)	Down regulation ($)
Seq	10,400	9,982	418	990	-572
Stoch	10,234	10,222	12	660	-648
P-B	10,273	10,042	231	825	-594
V-B	10,400	9,982	418	990	-572
V-B gen	10,261	10,162	99	693	-594

Table 5.4 provides the detailed system dispatch to demonstrate the effect of the operator-defined parameters χ^v and χ^p. Model *Seq* dispatches the system based on an ascending order of marginal costs where the wind power is dispatched to its expected value which is equal to 126 MW. Then, the power plants need to adjust their production to meet the demand in each wind power scenario ω_1 and ω_2. Having wind power dispatched with its expected value, models *P-B*, *V-B* and *V-B gen* provide alternative solutions. In *P-B*, the price adjustment signal is $\chi^p = -\$0.333$/kcf, which results in decreasing the natural gas price to \$1.666/kcf. This price decrease affects the marginal cost of GFPP G_4 and makes it equal to \$30/MWh, which is the same as the one of unit G_1. For this specific time period, the operator is able to dispatch unit G_1 to 70 MW and GFPP G_4 to 31 MW without breaking the merit order. This action increases the day-ahead cost compared to model *Seq* but reveals more cost-effective capacity in real-time that results in a lower total expected system cost. In the case of *V-B*, the same dispatch as *Seq* is acquired because a change in the total natural gas volume would not decrease the total expected cost. On the contrary, model *V-B gen* has a better performance due to its ability to influence the dispatch of both GFPPs G_3 and G_4. Note that GFPPs G_3 and G_4 produce a total of 71 MW in both *Seq* and *V-B gen* at the day-ahead stage. However, the allocation between the two GFPPs is different and more efficient under *V-B gen*. In particular, the total natural gas consumption by GFPPs in *Seq* is 987 kcf, where 600 kcf are used by GFPP G_3 and the remaining 387 kcf by GFPP G_4. In *V-B gen*, the natural gas volume made available for GFPP G_3 is 420 kcf, while GFPP G_4 consumes 648 kcf. Similarly to *P-B*, the adjustment of natural gas volume availability for each individual GFPP has a direct impact on the day-ahead dispatch which in turn reduces the total expected cost compared to *Seq*. In this case, there is a decrease of the up-regulation cost because the cheaper GFPP G_3 replaces unit G_5. Moreover, a greater portion of the total 40 MW needed for down-regulation is provided by GFPP G_4 that is more cost-effective than GFPP G_3.

Therefore, the benefit from altering the natural gas price or volume availability emerges when the day-ahead dispatch is modified in relation to *Seq* so as more cost-effective capacity for regulation is made available in the balancing stage. It is illustrated that the solutions of *P-B*, *V-B* and *V-B gen* yield an expected system cost in between the two extreme solutions provided by models *Seq* and *Stoch*. In particular, models *Seq* and *Stoch* provide a lower and an upper bound of the expected system cost with respect to scenario set Ω.

The following results are provided for a 24-hour scheduling horizon. Figure 5.8 presents the total expected system cost as a function of the wind power penetration level, where wind power

Table 5.4: Electricity system schedule in MW when total electricity load is 387 MW (variation from *Seq* day-ahead (DA) schedule in bold).

	Seq			*P-B*			*V-B*			*V-B gen*		
Unit	DA	ω_1	ω_2	DA	ω_1	ω_2	DA	ω_1	ω_2	DA	ω_1	ω_2
G_1	80	-10	0	**70**	-10	+10	80	-10	0	80	-10	0
G_2	110	0	0	110	0	0	110	0	0	110	0	0
G_3	50	-9	0	50	-5	0	50	-9	0	**35**	-5	+15
G_4	21	-21	+25	**31**	-25	+25	21	-21	+25	**36**	-25	+25
G_5	0	0	+15	0	0	+5	0	0	+15	0	0	0
WP	126	+40	-40	126	+40	-40	126	+40	-40	126	+40	-40

production is characterized by 20 equiprobable scenarios (available at [82]). The wind power penetration level is defined as the share of installed wind capacity on total system's electricity demand. The upper and lower bounds provided by *Seq* and *Stoch* are depicted in Figure 5.8 with *Stoch* being the more efficient in accommodating high shares of renewables. The inefficiency of *Seq* is more profound for a wind power penetration level above 25%, which results even in an expected cost increase when having a penetration level greater than 40%. The improved dispatch models provide an efficient approximation of the stochastic ideal solution up to a 40% wind power penetration level and only slightly diverge for higher values of penetration. The expected cost of *V-B gen* is lower than *V-B*, confirming its higher flexibility to provide an improved day-ahead dispatch, and *P-B* similarly attains an expected cost close to *Stoch*.

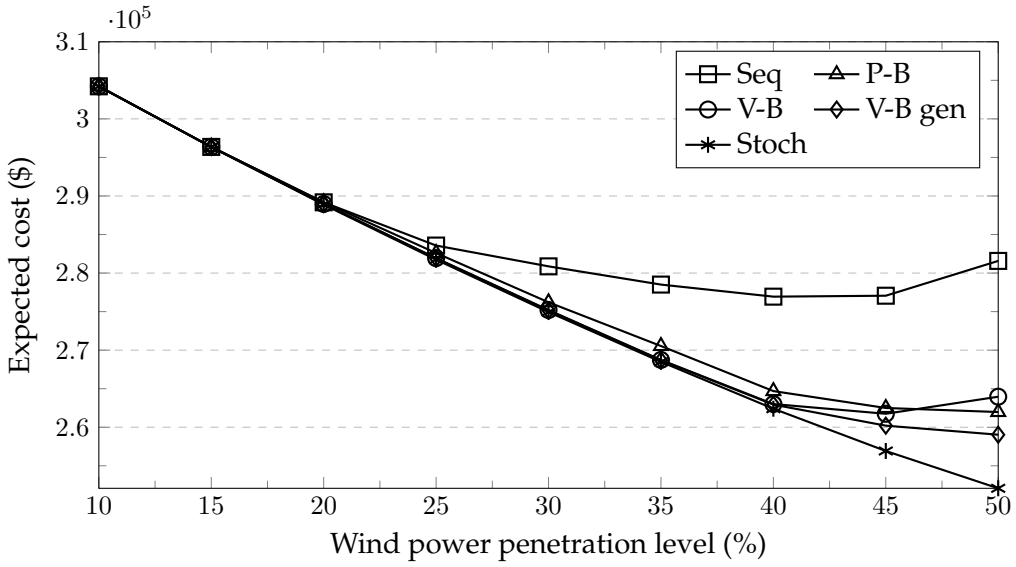

Figure 5.8: Impact of wind power penetration level on the expected system cost (tailored case study).

Additionally, Table 5.5 presents the expected payment/charge to adjust the price of natural gas at the balancing stage and the overall savings in expected cost between *Seq* and *P-B*. We present the results only for wind power penetration levels that models *Seq* and *P-B* provide a different solution. The payment/charge at the day-ahead stage is zero due to constraint (5.5c) but at the balancing stage the system operator could have either a deficit or a surplus under different conditions. However, this financial imbalance is significantly lower than the benefit of reducing the total expected cost

and can be either socialized or utilized for future investments. We observe larger expected savings as wind power penetration increases, while the expected payment/charge remains at the same level that is relatively small. For the case of 50% wind power penetration, *P-B* reduces the expected cost by \$19,601.6 compared to *Seq* and the system operator is expected to receive \$302.3.

Table 5.5: Expected payment/charge at the balancing stage due to flexibility price signal.

Wind power penetration level (%)	25	30	35	40	45	50
Expected savings (\$)	971.5	4,663	8,035.6	12,251.8	14,562.4	19,601.6
Expected payment/charge (\$)	-352.1	-177.1	-21.4	133.5	2.2	302.3

Based on the preceding analysis, the main features of the three proposed dispatch models can be highlighted. First, all three proposed dispatch models bridge the gap between *Seq* and *Stoch*. More importantly, they efficiently approximate the expected cost of *Stoch* and at the same time dispatch the system based on the merit-order principle, which preserves the desired economic principles of the sequential arrangement of trading floors. Another important aspect of the proposed dispatch models is that they are able to alter the system dispatch regardless of the type of the marginal producer, i.e. the last producer scheduled based on the merit-order principle can be a GFPP or a non-GFPP (i.e. power plant consuming another fuel). Regarding the volume-based approaches, at least one GFPP would have to be dispatched in order to attained an improved dispatch solution, while this restriction does not apply to *P-B*. In the case of *V-B*, the natural gas volume availability explicitly affects the scheduling of the GFPP with the greatest power conversion factor. When the control variable χ^v is defined for a specific group of GFPPs, the one with the greatest power conversion factor in this group is affected. Model *V-B gen* is able to change the dispatch of each individual GFPP and thus exhibiting higher adaptability on adjusting the system dispatch in a cost-effective manner. It can be noticed that the allocated power production of GFPPs at the day-ahead stage can be split under different shares to accomplish a decreased balancing cost in real-time operation.

Regarding computational performance, the average solution time for each dispatch model is presented in Table 5.6. Model *P-B* has significantly higher solution time due to the greater number of binary variables required for the linearization of complementarity constraints in the KKT conditions, since the balancing market is also included in the lower-level problem of the bilevel formulation. Moreover, the constraint ensuring cost-neutrality for the system operator at the day-ahead stage comes at a cost of coupling the time periods of the optimization horizon, which also increases the complexity of the problem. Models *V-B* and *V-B gen* are only slightly computationally more expensive than *Seq* and *Stoch* in the tailored case study.

Table 5.6: Average solution time for the tailored case study.

Model	*Seq*	*Stoch*	*V-B*	*V-B gen*	*P-B*
Solution time (sec)	0.3	0.6	1.5	1.5	520

5.4 Performance of the volume-based dispatch model with linepack flexibility and cost recovery of flexible producers

In this section, we focus on the performance of three variants of the volume-based model which permits the incorporation of network constraints in the balancing stage to exploit linepack flexibility.

In addition, cost recovery, which is a favorable economic property preserved by the sequential dispatch model, is discussed via presenting the daily profits of a flexible producer. The analysis is performed on a realistic case study using the IEEE 24-bus Reliability Test System (RTS) [80] and a 12-node natural gas system based on [81]. Wind power production is described via 25 equiprobable scenarios [82]. The data and network topology are provided in the online appendix available in [89]. In addition to *V-B-N* and *V-B-N gen*, a volume-based model that defines the natural gas volume availability for specific areas of the natural gas system is introduced, namely *V-B-N area*. We define two areas which include two GFPPs each. Area I contains GFPP 1 and GFPP 5, while GFPP 7 and GFPP 11 are included in area II. The scheduling horizon is 24 hours.

The total expected cost as a function of the wind power penetration level is illustrated in Figure 5.9. A similar trend to the one in Figure 5.8 is observed. Model *Seq-N* attains the highest expected system cost in all cases. Meanwhile, it can be noticed that allowing more degrees of freedom to define natural gas availability manages to capture more efficiently the benefits of *Stoch-N*.

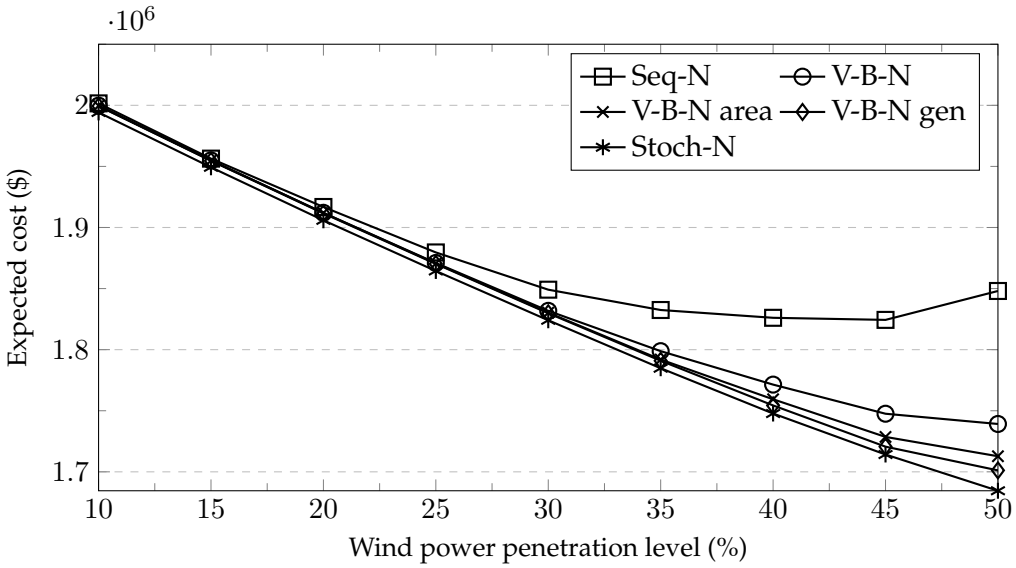

Figure 5.9: Impact of wind power penetration level on the expected system cost (realistic case study).

To quantify the benefit of modeling linepack flexibility, the outcome of dispatch models is calculated also under a purely steady-state operation where natural gas cannot be stored in the pipelines. In this case, the inflow and outflow of each pipeline is equal for each time period ($q^{in}_{m,u,t} = q^{out}_{m,u,t}, \forall (m,u) \in Z, t \in T$). The relative increase in expected cost when neglecting linepack in comparison with the expected cost presented in Figure 5.9 is plotted in Figure 5.10 to compare the two approaches. In the case of not modeling the linepack flexibility, the expected system cost appears to be increasing in all dispatch models. Model *Seq-N* shows the largest increase in expected system cost, having an increase of 3.5% when the wind power penetration level is 50%. Model *Stoch-N*, which is the most efficient, results in a constant decrease of system cost even when the linepack flexibility is not included and is, therefore, affected very little by the increase of the wind power penetration. As far as the three proposed models are concerned, two trends are observed. The first one is that the more the degrees of freedom to define the natural gas volume availability, the smaller is the increase in expected system cost until reaching 30% wind power penetration. When the wind power penetration exceeds 30%, a second trend is observed: model *V-B-N gen*

exhibits the largest increase in expected cost. This difference stems from the fact that *V-B-N gen* can take advantage of the linepack flexibility and achieve a significant decrease in the expected system cost, while performing still adequately when linepack is neglected. Therefore, linepack flexibility turns out to be an important element of the integrated energy system in reducing the total expected system cost and can be efficiently exploited by the proposed volume-based dispatch models.

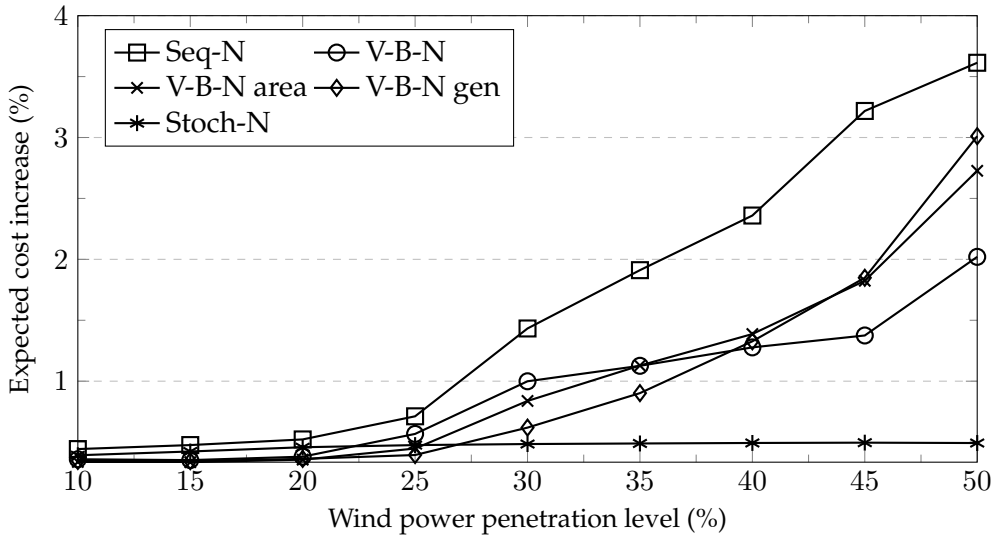

Figure 5.10: Impact of wind power penetration level on the expected system cost increase when neglecting linepack flexibility (realistic case study).

To explore whether flexible producers recover their costs under each dispatch model, Table 5.7 illustrates the daily profits of flexible power plant G_3 when the wind power penetration is 50%. In model *Stoch-N*, the cost recovery for flexible producers is guaranteed only in expectation and not for each wind power scenario. In this case, the flexible producer G_3 exhibits losses in some scenarios, which is shown by the average losses and the probability to have negative profits. On the contrary, models *Seq-N*, *V-B-N*, *V-B-N area* and *V-B-N gen* respect the merit-order principle and thus, the cost recovery is ensured for each wind power scenario. In particular, model *Seq-N* exhibits much larger profits due to the payments to flexible producer G_3 when very costly balancing actions (e.g. load shedding) take place. Such balancing actions are not that frequent in models *V-B-N*, *V-B-N area* and *V-B-N gen*. For this reason, the expected profits of flexible power plant G_3 are lower.

Table 5.7: Daily profits of thermal unit G_3 when the wind power penetration is 50%.

	Seq-N	*Stoch-N*	*V-B-N*	*V-B-N area*	*V-B-N gen*
Expected profit ($)	239,062	4,618	73,895	52,649	47,487
Probability of negative profits*(%)	0	4	0	0	0
Average losses ($)	0	−46.7	0	0	0

* Based on the available scenario set Ω.

The computational performance on the realistic case study is presented in Table 5.8. The deterministic dispatch model *Seq-N* is able to provide a solution in 48 seconds, while models *Stoch-N*, *V-B-N*, *V-B-N area* and *V-B-N gen* that use a probabilistic description of stochastic production are more

computationally expensive. Except for *V-B-N* that has a significantly higher solution time, the *V-B-N area* and *V-B-N gen* models dispatch the energy system in a similar solution time to *Stoch-N*.

Table 5.8: Average solution time for the realistic case study.

Model	*Seq-N*	*Stoch-N*	*V-B-N*	*V-B-N area*	*V-B-N gen*
Solution time (sec)	48	1,100	2,920	1,409	1,034

CHAPTER 6

Data-driven Coordination of Electricity and Natural Gas Systems

Useful information regarding renewable power production can be obtained from the available historical data. To cope with the the uncertainty introduced by renewable energy sources, various approaches have been used such as stochastic programming [21], chance constrained programming [90] and robust optimization [75]. However, such approaches usually make assumptions for the probability distribution of the uncertain parameter or result in overly conservative solutions (see also Section 3.3). In both cases, there is an additional process involved such as scenario or uncertainty set generation. In this chapter, we present two data-driven approaches based on distributionally robust optimization that allow the direct utilization of the available data to exploit underlying temporal and spatial dependencies and provide optimal decisions for the operation of the electricity and natural gas systems under uncertainty.

In distributionally robust optimization, the optimization takes place over a family of probability distributions (i.e. ambiguity set) without having an exact knowledge of the true underlying distribution that characterizes the uncertain parameter. We develop the first data-driven model based on a metric-based ambiguity set to solve the energy and reserve dispatch problem with fuel capacity constraints for Gas-Fired Power Plants (GFPPs). In this model, we make no assumption regarding the existence of the true probability distribution in any parametric family of distributions and handle multiple constraints simultaneously (i.e. joint chance constraints). The ambiguity set is represented as a Wasserstein ball centered at the nominal distribution estimated from the available data. Allowing the definition of a joint violation probability would be of great importance for the system operators, since they can define system-wide risk parameters for the overall system security. The second data-driven model is developed for the independent but coordinated operation of electricity and natural gas systems, where a moment-based ambiguity set is utilized. In this case, only the mean and covariance characterize the family of distributions that is taken into account. This choice of ambiguity set is in line with the desire of having a minimum information exchange between the two system operators when operating the systems independently.

Distributionally robust optimization has been adopted by various works in the field of power systems, such as [50, 51, 91–94], acknowledging the benefits to follow a data-driven approach that utilizes the available renewable power production data. Moreover, distributed approaches to study the coordination of electricity and natural gas systems have been studied in [95–97]. For a more detailed literature survey, see the introductions of [Paper E] and [Paper F].

Section 6.1 provides the framework on which the data-driven models are developed. The performance of the data-driven models is evaluated based on the setup presented in Section 6.2. In Section 6.3, the data-driven model for the coupled operation of electricity and natural gas systems is presented, where the fuel capacity constraints for GFPPs are used to describe the natural gas network (see Section 3.2.2). In Section 6.4, the data-driven and distributed operation of electricity and natural gas systems is coordinated via a distributed algorithm based on the Alternating Direction Method of Multipliers (ADMM). In the second data-driven model, the natural gas system is incorporated with the controllable flow model (see Section 3.2.2).

6.1 Modeling framework

An uncertainty-aware dispatch of electricity and natural gas systems is considered in this chapter to deal with the stochasticity introduced by renewables. The power output of the wind farms is modeled as $\overline{W}(\widehat{W}+\xi)$, where $\overline{W} \in \mathbb{R}_+^{W\times W}$ is the diagonal matrix of the wind farm capacities, $\widehat{W} \in \mathbb{R}^W$, $0 \leq \widehat{W} \leq e$, is the relative power output predicted at the first-stage, and $\xi \in \mathbb{R}^W$, $-\widehat{W} \leq \xi \leq e - \widehat{W}$, is the uncertain deviation from $\widehat{W}$, which is revealed at the second-stage. We assume that ξ follows a distribution $\mathbb{P}$. Note that e is a vector of ones with appropriate dimension. We denote with $x \in \mathbb{R}^{\mathcal{Z}}$ the first-stage decisions, while the recourse actions are restricted to linear decision rules of the form $Y\xi$ with $Y \in \mathbb{R}^{\mathcal{Z}\times W}$ a finite-dimensional coefficient matrix. Using this notation, a distributionally robust optimization problem can be represented compactly as

$$\min_{(x,Y)\in\Theta} \quad \max_{\mathbb{P}\in\mathcal{P}} \mathbb{E}^{\mathbb{P}}[\mathcal{C}^{\mathrm{D}}(x,Y,\xi)] \tag{6.1a}$$

$$\text{s.t.} \quad \min_{\mathbb{P}\in\mathcal{P}} \ \mathbb{P}\left[A^j(Y)\xi \leq b^j(x)\right] \geq 1-\epsilon^j \quad \forall j \in \mathcal{J}, \tag{6.1b}$$

which minimizes the worst-case expected cost and requires that the joint chance constraints are satisfied for all distributions in the ambiguity set $\mathcal{P}$. Note that there are different sets of joint chance constraints indexed by $j \in \mathcal{J}$. Each matrix $A(Y)$ and vector $b(x)$ contains a linear expression of Y and x, respectively. Alternatively, a distributionally robust optimization problem with individual chance constraints can be formulated as

$$\min_{(x,Y)\in\Theta} \quad \max_{\mathbb{P}\in\mathcal{P}} \mathbb{E}^{\mathbb{P}}[\mathcal{C}^{\mathrm{D}}(x,Y,\xi)] \tag{6.2a}$$

$$\text{s.t.} \quad \min_{\mathbb{P}\in\mathcal{P}} \ \mathbb{P}\left[a_k(Y)^\top\xi \leq b_k(x)\right] \geq 1-\epsilon_k \quad \forall k \leq K, \tag{6.2b}$$

by decomposing the matrix $A(Y)$ and the vector $b(x)$ as

$$A(Y) = \begin{bmatrix} a_1(Y)^\top \\ \vdots \\ a_K(Y)^\top \end{bmatrix}, \quad b(x) = \begin{bmatrix} b_1(x) \\ \vdots \\ b_K(x) \end{bmatrix}.$$

Depending on the choice of ambiguity set $\mathcal{P}$ and of the objective function $\mathcal{C}^{\mathrm{D}}(x,Y,\xi)$, we can provide different tractable reformulations of problems (6.1) and (6.2) as described in [Paper E] and [Paper F].

In [Paper E], problem (6.1) with a linear objective function is solved. In this case, we assume that distribution $\mathbb{P}$ is concentrated around 0. Moreover, we suppose that the decision maker has a dataset $\widehat{\Xi}_N = \{\widehat{\xi}_\tau\}_{\tau\leq N}$ consisting of N finitely many training samples drawn independently by $\mathbb{P}$. Initially, the discrete empirical distribution $\widehat{\mathbb{P}}_N$, which is the uniform distribution on the (known)

training samples, is defined to approximate $\mathbb{P}$. Then, the distributionally robust optimization problem (6.1) can be formulated to hedge against all distributions in a neighborhood of $\widehat{\mathbb{P}}_N$ with respect to the Wasserstein metric. The type-1 Wasserstein distance between two distributions $\mathbb{P}_1$ and $\mathbb{P}_2$ on $\mathbb{R}^W$ is defined as

$$\mathbb{W}(\mathbb{P}_1, \mathbb{P}_2) \triangleq \left\{ \begin{array}{ll} \min\limits_{\Pi} & \displaystyle\int_{\mathbb{R}^W \times \mathbb{R}^W} \|\xi_1 - \xi_2\| \, \Pi(\mathrm{d}\,\xi_1, \mathrm{d}\,\xi_2) \\ \text{s.t.} & \Pi \text{ is a distribution on } \mathbb{R}^W \times \mathbb{R}^W \\ & \text{with marginals } \mathbb{P}_1 \text{ and } \mathbb{P}_2, \text{ respectively.} \end{array} \right. \tag{6.3}$$

The Wasserstein distance between $\mathbb{P}_1$ and $\mathbb{P}_2$ can be viewed as the cost of an optimal mass transportation plan Π that minimizes the cost of moving $\mathbb{P}_1$ to $\mathbb{P}_2$, where $\|\xi_1 - \xi_2\|$ is the cost of moving a unit mass from ξ_1 to ξ_2. We denote by $\mathcal{M}(\Xi)$ the set of all distributions on the polyhedron $\Xi = \{\xi \in \mathbb{R}^W : H\xi \leq h\}$ for $H \in \mathbb{R}^{\mathcal{L} \times W}$ and $h \in \mathbb{R}^{\mathcal{L}}$, and we define

$$\mathcal{P} \triangleq \left\{ \mathbb{P} \in \mathcal{M}(\Xi) : \mathbb{W}(\mathbb{P}, \widehat{\mathbb{P}}_N) \leq \rho \right\} \tag{6.4}$$

as the family of all distributions on Ξ that have a Wasserstein distance of at most $\rho \geq 0$ from the empirical distribution $\widehat{\mathbb{P}}_N$. The hope is that, for a judiciously chosen radius ρ, the ambiguity set $\mathcal{P}$ contains the unknown true distribution with high confidence. This ambiguity set can be seen as a Wasserstein ball centered at the empirical distribution $\widehat{\mathbb{P}}_N$ with a radius ρ, as illustrated in Figure 6.1. We refer the reader to [19] for a detailed presentation of the reformulations of distributionally robust optimization problems based on the Wasserstein ambiguity set.

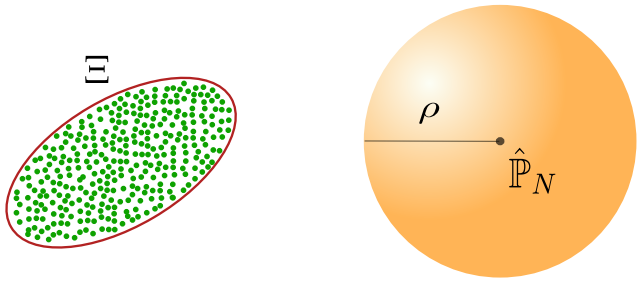

Figure 6.1: Wasserstein ambiguity set.

In [Paper F], we solve problem (6.2) with a quadratic objective function. In this case, the ambiguity set is defined by the first- and second-order moments as follows

$$\mathcal{P} \triangleq \left\{ \mathbb{P} \in \mathcal{M}(\mathbb{R}^W) : \mathbb{E}[\xi] = \widehat{\mu}_0, \mathbb{E}[\xi\xi^\top] = \widehat{\Sigma}_0 \right\}, \tag{6.5}$$

where $\mathcal{M}(\mathbb{R}^W)$ denotes the set of all probability measures on $\mathbb{R}^W$ and $\widehat{\Sigma}_0 \in \mathbb{R}^{W \times W}$ is a positive semi-definite matrix. In this case, we assume that $\widehat{\mu}_0 \in \mathbb{R}^W$ is the mean of ξ. In particular, the empirical mean $\widehat{\mu}_0 = \frac{1}{N}\sum_{\tau=1}^N \widehat{\xi}_\tau$ and covariance matrix $\widehat{\Sigma}_0 = \frac{1}{N}\sum_{\tau=1}^N (\widehat{\xi}_\tau - \widehat{\mu}_0)(\widehat{\xi}_\tau - \widehat{\mu}_0)^\top$ are estimated from the training dataset $\widehat{\Xi}_N$. The reformulation that we follow is presented in [93], while an extensive analysis of moment-based ambiguity sets in distributionally robust optimization problems can be found in [18, 98, 99].

6.2 Performance assessment of data-driven models

To assess the performance of the proposed data-driven models, we use 100 coupled datasets $\{\widehat{\Xi}_N^i, \widehat{\Psi}_{N'}^i\}_{i=1,\ldots,100}$, where $\widehat{\Xi}_N^i$ is a training dataset containing N Independent and Identically

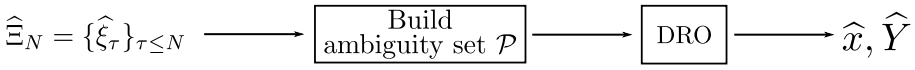

Figure 6.2: Projected operation (DRO: distributionally robust optimization).

Distributed (i.i.d.) sample data, and $\widehat{\Psi}^i_{N'}$ is a testing dataset containing N' i.i.d. realizations. The 100 different coupled datasets are used in order increase the statistical robustness of the empirical out-of-sample estimations calculated in the following. We keep the number of i.i.d. realizations in $\widehat{\Psi}^i_{N'}$ fixed with $N' = 100$. The data consists of wind power forecast errors that is generated with the same method as in [23, Equation (2)] and from the historical data given in [23]. An out-of-sample analysis is carried out on the basis of a *projected* and of a *realistic* operation.

The goal of the projected operation is to assess how the optimal solution of problems (6.1) and (6.2) solved using the (in-sample) training dataset $\widehat{\Xi}_N$ will perform subject to the (out-of-sample) testing dataset $\widehat{\Psi}_{N'}$. As illustrated in Figure 6.2, the respective ambiguity set $\mathcal{P}$ is built and problems (6.1) or (6.2) are solved to obtain the optimal $\widehat{x}^i$ and $\widehat{Y}^i$ solutions for each training dataset $\widehat{\Xi}^i_N$. Then, the out-of-sample cost is calculated for each realization in the testing dataset $\widehat{\Psi}^i_{N'} = \{\widehat{\psi}_\ell\}_{\ell \le N'}$ by

$$\widehat{\mathcal{C}}^i = \mathcal{C}^{\mathrm{D}}(\widehat{x}^i, \widehat{Y}^i, \widehat{\psi}_\ell), \tag{6.6}$$

which is utilized to estimate the expected cost by taking the average over the 100 datasets

$$\widehat{\mathcal{C}} = \frac{1}{100} \sum_{i=1}^{100} \widehat{\mathcal{C}}^i. \tag{6.7}$$

Moreover, we calculate three different metrics for the violation probability, two for individual chance constraints and one for joint chance constraints. The first two metrics provide insights regarding the violation of each individual chance constraint. The following indicator function is used

$$\widetilde{\mathcal{I}}^i_{k\ell} = \begin{cases} 1 & \text{if } a_k(\widehat{Y}^i)^\top \widehat{\psi}^i_\ell \le b_k(\widehat{x}^i), \\ 0 & \text{otherwise} \end{cases}, \tag{6.8}$$

where k indicates each individual chance constraint from (6.2b). Thus, each constraint is evaluated individually and we can calculate the average number of violations for each out-of-sample simulation by

$$\widetilde{\mathcal{V}}^i_\ell = \frac{1}{K} \sum_{k=1}^{K} \left(1 - \widetilde{\mathcal{I}}^i_{k\ell}\right). \tag{6.9}$$

Then, the *empirical violation probability* is calculated by

$$\widetilde{\mathcal{V}}^{\mathrm{emp}} = \frac{1}{N'} \frac{1}{100} \sum_{\ell=1}^{N'} \sum_{i=1}^{100} \widetilde{\mathcal{V}}^i_\ell \tag{6.10}$$

and the *maximum average violation probability* for each chance constraint by

$$\widetilde{\mathcal{V}}^{\max} = \max_{\ell,i} \{\widetilde{\mathcal{V}}^i_\ell\}. \tag{6.11}$$

For each type j of joint chance constraint, we use the following indicator function,

$$\mathcal{I}^i_\ell = \begin{cases} 1 & \text{if } A(\widehat{Y}^i)\widehat{\psi}^i_\ell \le b(\widehat{x}^i), \\ 0 & \text{otherwise} \end{cases}. \tag{6.12}$$

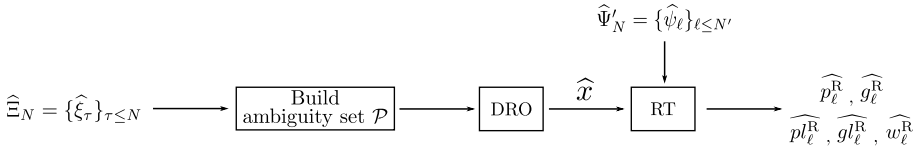

Figure 6.3: Realistic operation (DRO: distributionally robust optimization, RT: real-time dispatch).

Therefore, we can evaluate the violation probability for the testing dataset $\widehat{\Psi}^i_{N'}$ with

$$\widehat{\mathcal{V}}^i = \frac{1}{N'} \sum_{\ell=1}^{N'} \left(1 - \mathcal{I}^i_\ell\right) \tag{6.13}$$

and the *average violation probability* for each type j of joint chance constraint is

$$\widehat{\mathcal{V}} = \frac{1}{100} \sum_{i=1}^{100} \widehat{\mathcal{V}}^i. \tag{6.14}$$

The goal of the realistic operation is to provide a better estimation of the true cost that occurs when removing the assumption of strictly following a linear decision rule $\widehat{Y}$ and allowing the system operator a higher flexibility to adapt the real-time production according to the realization of the stochastic power supply, as depicted in Figure 6.3. In this case, the operator keeps the first-stage decisions $\widehat{x}$ fixed, and after observing the testing dataset, *resolves* an optimal power and natural gas flow problem. In realistic conditions, the system operator will take some actions to ensure that the constraints are not violated and with the proposed procedure we estimate a realistic cost to operate the system. Subsequently, a real-time optimal power and natural gas flow that minimizes the cost of re-dispatch actions is solved for each $\widehat{\psi}^i_\ell \in \widehat{\Psi}^i_{N'}$. The re-dispatch actions may include power adjustments $p^{\mathrm{R}} \in \mathbb{R}^G$ from conventional generators, natural gas adjustments $g^{\mathrm{R}} \in \mathbb{R}^{\mathcal{U}}$ from natural gas producers, electricity load shedding $pl^{\mathrm{R}} \in \mathbb{R}^D_+$, natural gas load shedding $gl^{\mathrm{R}} \in \mathbb{R}^{\mathcal{H}}_+$ and wind spilling $w^{\mathrm{R}} \in \mathbb{R}^W_+$ The chance constraints are replaced by hard constraints, and there is no out-of-sample violation. The analysis focuses on the cost calculated using the optimal solutions $\widehat{x}^i$, $\widehat{p^{\mathrm{R}}_\ell}^i$, $\widehat{g^{\mathrm{R}}_\ell}^i$, $\widehat{pl^{\mathrm{R}}_\ell}^i$, $\widehat{gl^{\mathrm{R}}_\ell}^i$ and $\widehat{w^{\mathrm{R}}_\ell}^i$ of the real-time dispatch problem by

$$\widehat{\mathcal{R}}^i = \frac{1}{N'} \sum_{\ell=1}^{N'} \mathcal{C}^{\mathrm{R}}(\widehat{x}^i, \widehat{p^{\mathrm{R}}_\ell}^i, \widehat{g^{\mathrm{R}}_\ell}^i, \widehat{pl^{\mathrm{R}}_\ell}^i, \widehat{gl^{\mathrm{R}}_\ell}^i), \tag{6.15}$$

where $\mathcal{C}^{\mathrm{R}}$ denotes the function of the real-time cost to operate the system including electricity and natural gas system dispatch costs, as well as load shedding costs. The realistic cost is estimated over the 100 datasets by taking the average

$$\widehat{\mathcal{R}} = \frac{1}{100} \sum_{i=1}^{100} \widehat{\mathcal{R}}^i. \tag{6.16}$$

6.3 Data-driven energy and reserve dispatch with fuel constraints for gas-fired power plants

The energy and reserve dispatch problem with fuel constraints for GFPPs is developed to ensure the safe operation of a power system with high penetration of renewables and a strong interdependence with the natural gas system. The problem is formulated in the form of distributionally robust

joint chance constrained program (6.1) and the Wasserstein ambiguity set $\mathcal{P}$ as defined in (6.4) is utilized. The cost function $\mathcal{C}^{\mathrm{D}}(x, Y, \xi)$ is assumed to be linear. The first-stage decisions x comprise the energy and reserve dispatch of the system and are taken before the realization of uncertainty. The recourse actions $Y\xi$ correspond to the real-time dispatch of the system, where the imbalances due to forecast errors have to be covered. A detailed model formulation is provided in [Paper E].

Leveraging results from [19], an exact reformulation of the objective function (6.1a) and two conservative approximations for the feasible set

$$\Omega_{\mathrm{CC}} \triangleq \left\{ (x, Y) : \min_{\mathbb{P}\in\mathcal{P}} \mathbb{P}\left[A(Y)\xi \leq b(x)\right] \geq 1-\epsilon \right\} \tag{6.17}$$

of a generic joint chance constraint of the form (6.1b) are provided. Both approaches utilize the worst-case Conditional Value-at-Risk (CVaR) [100] to approximate individual worst-case chance constraints, which constitutes the tighter convex inner approximation as described in [90]. The fundamental difference of the two approximation schemes stems from the process of converting the joint chance constraint to a single or multiple individual chance constraints before deploying the CVaR approximation, which can then admit a conic reformulation.

In the first approach, we exploit Bonferroni's inequality to separate each joint chance constraint into a collection of K individual chance constraints with the corresponding $\epsilon_k \geq 0, \forall k = 1, \ldots, K$, and $\sum_k \epsilon_k = \epsilon$. This amounts to approximate Ω_{CC} by the following more conservative set of individual chance constraints

$$\Omega_{\mathrm{B}} \triangleq \left\{ (x, Y) : \min_{\mathbb{P}\in\mathcal{P}} \mathbb{P}\left[a_k(Y)^\top \xi \leq b_k(x)\right] \geq 1-\epsilon_k, \forall k \leq K \right\}. \tag{6.18}$$

that permits the application of CVaR approximation. Therefore, this approach is named *Combined Bonferroni and CVaR Approximation*.

The Bonferroni approximation is inadequate when the violations of different individual chance constraints in (6.18) are significantly correlated [98]. An alternative approach to convert the joint chance constraint to an individual chance constraint can be constructed using the same approach as in [98]. For any vector of scaling parameters $\delta \in \Delta_{++} \triangleq \{\delta \in \mathbb{R}^K_{++} : e^\top \delta = 1\}$ the joint chance constraint (6.1b) is equivalent to

$$\min_{\mathbb{P}\in\mathcal{P}} \mathbb{P}\left[\max_{k\leq K} \left\{ \delta_k \left[a_k(Y)^\top \xi - b_k(x)\right] \right\} \leq 0 \right] \geq 1-\epsilon, \tag{6.19}$$

which constitutes a distributionally robust individual chance constraint and the CVaR approximation can be applied. Note that the overall scale of δ is immaterial, and thus the normalization $e^\top \delta = 1$ does not restrict generality. Optimizing *jointly* over the space of (x, Y) and $\delta \in \Delta_{++}$ results in a non-convex problem. However, for any fixed $\delta \in \Delta_{++}$, optimizing over (x, Y) is a convex problem, and vice versa. Following this observation, we use an iterative approach which *sequentially* optimizes over (x, Y) and δ, which is inspired by [98]. This motivates to name this approach *Optimized CVaR Approximation*.

We highlight that both approaches admit a conic representation, which reduces to simple Linear Programs (LPs) under specific settings of the Wasserstein metric. Note that the choice of ϵ_k highly affects the performance of the combined Bonferroni and CVaR approximation. Nevertheless, choosing the optimal value for ϵ_k is intractable [90, Remark 2.1]. Developing a sequential algorithm in a similar manner to the optimized CVaR unfortunately introduces bilinear terms and is thus

not applicable for large instances. As a consequence, we will fix $\epsilon_k = \epsilon/K$, $\forall k$ as proposed by [90] despite its conservativeness when ϵ is small or when the constraints are positively correlated [98, Example 3.1]. A comprehensive presentation of the tractable reformulations for the combined Bonferroni and CVaR as well as the optimized CVaR approximations, along with a discussion on computational tractability is given in [Paper E].

The two tractable approximations for the distributionally robust joint chance constrained programs are compared using the IEEE 24-bus Reliability Test System (RTS) [80], where the only source of uncertainty is the wind power produced by 6 wind farms. The total wind power capacity is equal to 55% of the whole system demand. In total, there are 12 conventional generators, 6 of which are GFPPs. We introduce 3 natural gas pipelines that serve a pair each. Wind power data consists of wind power forecast errors that is generated with the same method as in [23, Equation (2)] and from the historical data given in [23]. The complete input data and topology of the system is provided in [101]. In all simulations, we use the Wasserstein metric defined by the 1-norm, hence all arising optimization problems are equivalent to tractable LPs. Moreover, we set $\Xi = \mathbb{R}^W$ and thus omit H and h. The same value of ϵ^j is utilized for all joint chance constraints.

The subsequent analysis of the projected and realistic operation is performed for different Wasserstein radius $\rho \in \mathbb{R}_+$ (the specific values used are given in [Paper E]). We note that $\rho = 0$ corresponds to the ambiguity-free attitude that takes into account only the empirical distribution $\widehat{\mathbb{P}}_N$ to approximate the true data generating distribution $\mathbb{P}$. The results related to combined Bonferroni and CVaR and optimized CVaR approaches are denoted with subscript B and O.

6.3.1 Performance assessment based on the projected operation

The procedure of the projected operation is applied for the energy and reserve dispatch problem with fuel constraints for GFPPs, which consists of three joint chance constraints in the form of (6.1b) that are related to the power capacity (gen), line capacity (grid) and pipeline capacity (gas) constraints. For each value of $\rho \in \mathbb{R}_+$, we collect the pairs $\{\widehat{\mathcal{C}}(\rho), \widehat{\mathcal{V}}^j(\rho)\}$ for each one of the joint chance constraints. A Pareto frontier is computed based on the non-dominated points from the collected pairs for the combined Bonferroni and CVaR as well as the optimized CVaR approximations. The Pareto frontier illustrates the trade-off between the expected cost $\widehat{\mathcal{C}}$ and violation probability $\widehat{\mathcal{V}}$ of each constraint, as shown in Figures 6.4 and 6.5. The results are given for $\epsilon^j = 5\%$ and when each training dataset $\widehat{\Xi}^i_N$ contains $N = 50$ or $N = 200$ samples.

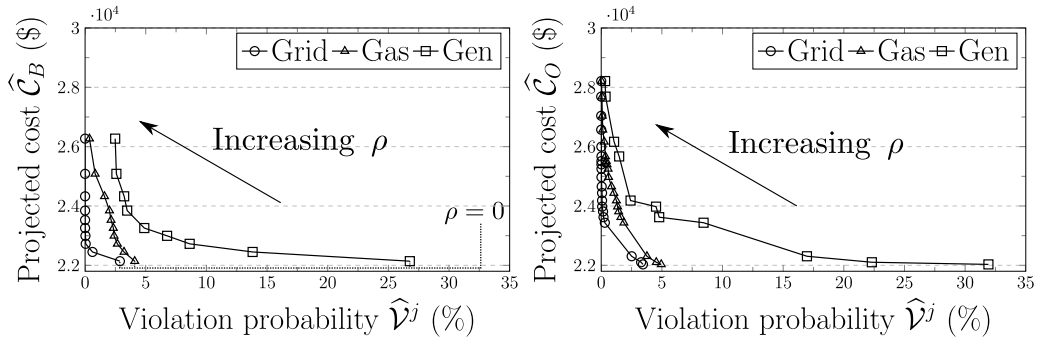

Figure 6.4: Pareto frontier of combined Bonferroni and CVaR (left) and optimized CVaR (right) approximations ($\epsilon^j = 5\%$ and $N = 50$).

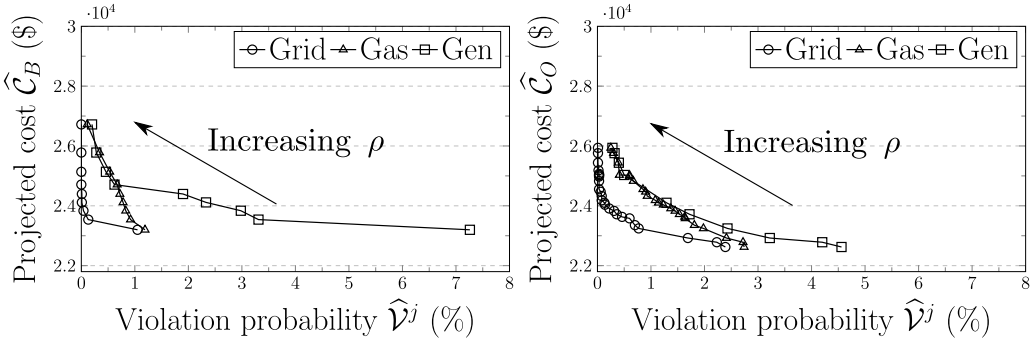

Figure 6.5: Pareto frontier of combined Bonferroni and CVaR (left) and optimized CVaR (right) approximations ($\epsilon^j = 5\%$ and $N = 200$).

In all frontiers, $\rho = 0$ is always a non-dominated point: it has the lowest expected cost but at the downside of the highest violation probability. For a high value of Wasserstein radius ρ, both approaches provide solutions which can satisfy the violation probability of 5% even when $N = 50$. We observe three main experimental trends. First, for a fixed N, increasing ρ results in a decrease of the violation probability $\widehat{\mathcal{V}}$ for each type of joint chance constraint. This fact can be explained by the bigger size of the ambiguity set, which leads to more conservative solutions when the radius is increased. A more conservative solution directly translates to a lower violation probability in the out-of-sample dataset. Second, as N increases, the violation probability tends to decrease when comparing solutions with the same value of ρ. In this case, the empirical distribution $\widehat{\mathbb{P}}_N$ better approximates $\mathbb{P}$, which again makes it more probable that $\mathbb{P}$ belongs to the Wasserstein ball for a fixed value of ρ. In all cases, there is a trade-off between $\widehat{\mathcal{V}}$ and $\widehat{C}$: the decrease in $\widehat{\mathcal{V}}$ is followed by an increase in $\widehat{\mathcal{C}}$ as more costly generators are dispatched. Finally, we can search for a wider range and pick larger values of ρ in the optimized CVaR approximation because it is less conservative than the combined Bonferroni and CVaR approximation.

6.3.2 Performance assessment based on the realistic operation

The realistic operation is utilized to evaluate solutions $(\widehat{x}, \widehat{Y})$ when only the first-stage decision $\widehat{x}$ is implemented and the real-time adjustments are acquired by a deterministic real-time optimal power flow problem with fuel constraints for GFPPs. This procedure is repeated for all $\rho \in \mathbb{R}_+$ for both approximations of joint chance constraints.

For the optimized CVaR approximation, Figure 6.6 illustrates $\widehat{\mathcal{R}}_O(\rho)$ as a function of ρ for $\epsilon^j = 5\%$ and different values of N. It can be noticed that for each level of sample size N, there exists an optimal radius $\widehat{\rho}^\star$ which minimizes the realistic cost $\widehat{\mathcal{R}}_O$. Comparing to the ambiguity-free approach with the Wasserstein radius $\rho = 0$, solving the problem with $\widehat{\rho}^\star$ yields a lower realistic cost. Moreover, this reduction is more significant for the cases of lower sample size N. For instance, $\widehat{\mathcal{R}}_O(\widehat{\rho}^\star)$ is 7.9% lower than the ambiguity-free cost $\widehat{\mathcal{R}}_O(0)$ when $N = 25$, while this reduction is 1.9% at $N = 200$. To examine the effect of ρ on the variability of $\widehat{\mathcal{R}}_O^i$, we plot the interquantile range between the 10^{th}- and 90^{th}-quantile of $\widehat{\mathcal{R}}_O^i$ in Figure 6.7, which demonstrates a similar pattern with the average realistic cost $\widehat{\mathcal{R}}_O$. Similar plots for the combined Bonferroni and CVaR approximation are included in [Paper E]. These results show the advantages of employing the distributionally robust attitude compared to the ambiguity-free one with $\rho = 0$. In all cases, solving the energy and reserve dispatch problem with fuel constraints for GFPPs with $\rho > 0$ reduces both the average and

the variability of the out-of-sample cost in the realistic operation. The results of the distributionally robust attitude with $\rho > 0$ are more profound under the low sample size N.

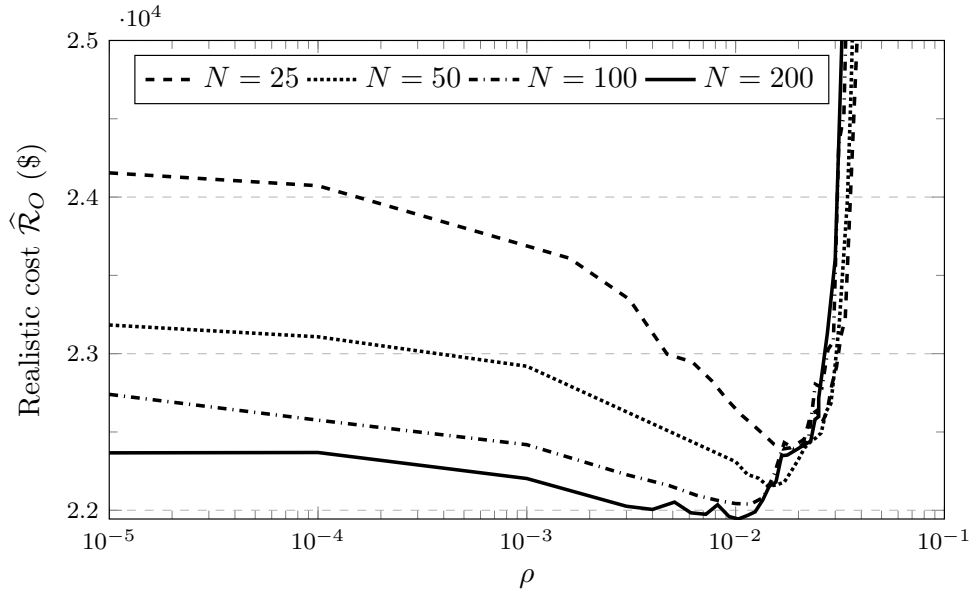

Figure 6.6: Average realistic cost $\widehat{\mathcal{R}}_O$ as a function of Wasserstein radius ρ (logarithmic scale is used in the x-axis to improve readability).

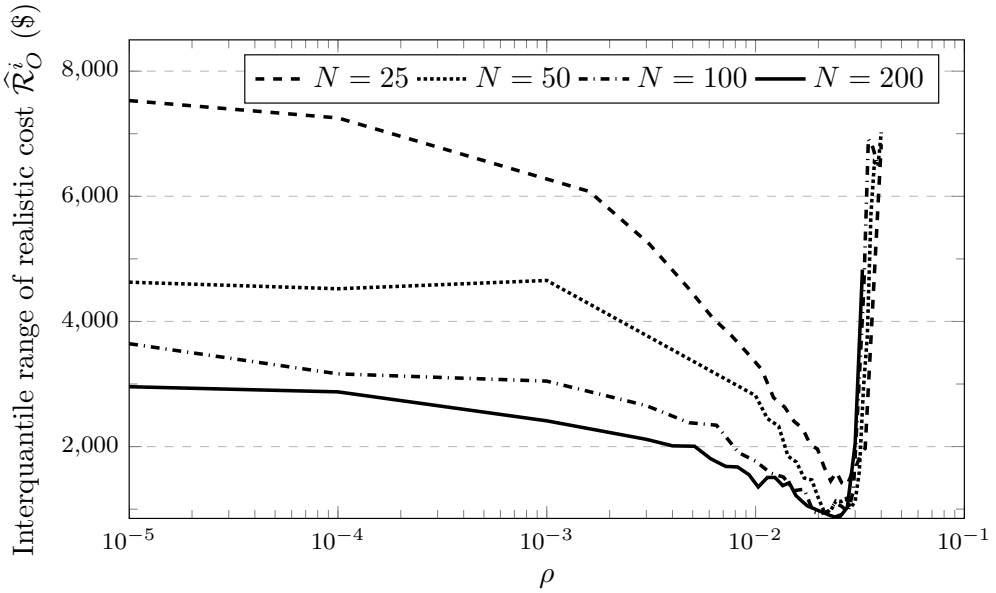

Figure 6.7: Interquantile range of realistic cost $\widehat{\mathcal{R}}_O^i$ between the 10^{th} and 90^{th} quantile as a function of Wasserstein radius ρ (logarithmic scale is used in the x-axis to improve readability).

Table 6.1 presents the optimal radius $\widehat{\rho}^\star$ and the corresponding $\widehat{\mathcal{R}}^\star$ for various ϵ^j and different number of samples N for both approximations. The cost for the combined Bonferroni and CVaR approximation $\widehat{\mathcal{R}}_B^\star$ is reported as the percentage difference from $\widehat{\mathcal{R}}_O^\star$. The realistic cost $\widehat{\mathcal{R}}_O^\star$ is lower than $\widehat{\mathcal{R}}_B^\star$ in all cases with the greatest difference takes place at $\epsilon^j = 1\%$. For a fixed value of ϵ^j, it can be observed that an increase of the number of samples N results in a decrease of the

optimal realistic cost $\widehat{\mathcal{R}}^\star$ and radius $\widehat{\rho}^\star$. More specifically, radius $\widehat{\rho}^\star$ tends to zero with an increase in N, which is coherent with the observations in [19, Section 7]. Moreover, for a fixed number of samples N, decreasing ϵ^j yields a lower optimal radius $\widehat{\rho}^\star$ as the feasible space of probability constraints becomes more stringent. This effect is more profound for the combined Bonferroni and CVaR approximation since it is more conservative than the optimized CVaR approximation due to setting $\epsilon_k = \epsilon^j/K$, $\forall k$. On the upside, decreasing ϵ^j also decreases $\widehat{\mathcal{R}}^\star_O$ since less costly real-time adjustments are activated due to increased robustness.

Table 6.1: Optimal realistic expected cost $\widehat{\mathcal{R}}^\star$ and Wasserstein radius $\widehat{\rho}^\star$ for combined Bonferroni and CVaR and optimized CVaR approximations.

	$N=25$				$N=50$			
ϵ^j	$\widehat{\mathcal{R}}^\star_O$ (\$)	$\widehat{\rho}^\star_O$	$\widehat{\mathcal{R}}^\star_B$	$\widehat{\rho}^\star_B$	$\widehat{\mathcal{R}}^\star_O$ (\$)	$\widehat{\rho}^\star_O$	$\widehat{\mathcal{R}}^\star_B$	$\widehat{\rho}^\star_B$
1%	22,269	0.0030	+4.00%	0.0001	22,105	0.0026	+1.71%	0.0001
5%	22,392	0.0168	+1.43%	0.0008	22,154	0.0143	+1.49%	0.0005
10%	22,414	0.0400	+1.31%	0.0018	22,275	0.0300	+0.94%	0.0009
	$N=100$				$N=200$			
ϵ^j	$\widehat{\mathcal{R}}^\star_O$ (\$)	$\widehat{\rho}^\star_O$	$\widehat{\mathcal{R}}^\star_B$	$\widehat{\rho}^\star_B$	$\widehat{\mathcal{R}}^\star_O$ (\$)	$\widehat{\rho}^\star_O$	$\widehat{\mathcal{R}}^\star_B$	$\widehat{\rho}^\star_B$
1%	22,032	0.0008	+0.53%	0	21,932	0.0005	+0.89%	0
5%	22,039	0.0118	+0.50%	0	21,944	0.0103	+0.48%	0
10%	22,135	0.0250	+0.35%	0.0003	22,042	0.0230	+0.80%	0

Additionally, we compare the performance of the distributionally robust optimization models with a robust optimization approach that minimizes the worst-case cost and risk constraints are satisfied for any realization of the uncertain parameter in the support Ξ [75]. The robust optimization model is presented in [Paper E]. Table 6.2 presents the realistic cost $\widehat{\mathcal{R}}_{RO}$ and the interquantile range of $\widehat{\mathcal{R}}^i_{RO}$ between 10^{th} and 90^{th} quantile for different number of samples N. In all cases, $\widehat{\mathcal{R}}_{RO}$ is significantly higher than $\widehat{\mathcal{R}}^\star_O$ and $\widehat{\mathcal{R}}_O(0)$ acquired by the distributionally robust and ambiguity-free approaches. This result demonstrates the fact that the first-stage decisions $\widehat{x}^i$ obtained from the robust optimization model are overly conservative. The robust solution varies with N as we estimate mean $\widehat{W}$ from the training sample.

Table 6.2: Realistic cost $\widehat{\mathcal{R}}_{RO}$ and interquantile range of realistic cost $\widehat{\mathcal{R}}^i_{RO}$ between 10^{th} and 90^{th} quantile for the robust optimization model.

	$N=25$	$N=50$	$N=100$	$N=200$
$\widehat{\mathcal{R}}_{RO}$ (\$)	29,690	29,644	29,673	29,687
Interquantile range of $\widehat{\mathcal{R}}^i_{RO}$ (\$)	1,466	1,246	895	687

Computational performance is reported for the setting with $\epsilon^j = 5\%$ and $N = 200$. Solving problem (6.1) under the combined Bonferroni and CVaR approach takes on average 20 seconds, while for the optimized CVaR approach the average time is 38 seconds. Note that the reported time for optimized CVaR approximation is until the convergence of the algorithm, where in the experiment we consistently observe convergence in less than 3 iterations. The average time to solve the robust optimization model was 0.75 seconds. The real-time optimal power flow is solved in 0.12 seconds on average.

The proposed optimized CVaR approach outperforms the combined Bonferroni and CVaR approximation in terms of realistic expected system cost for each fixed N and ϵ^j. Moreover, it has a satisfactory computational performance that allows to consider its application in practice

by system operators. Both approximation schemes for the distributionally robust joint chance constraints result in LPs to be solved under specific norms of the Wasserstein metric, which further permits the utilization of parallel computing in case needed to tackle computational issues. Moreover, following the proposed approach based on the Wasserstein ambiguity set does not raise any limitations with respect to the choice of the Wasserstein radius ρ since the radius ρ is calibrated through an estimation practice. Therefore, the choice of ρ depends on the available data and the problem in question, in a sense that the estimation practice will yield the optimal radius ρ for the specific case. The value of ρ would then determine if the decision maker would need to take an ambiguity-free with $\rho = 0$ or a distributionally robust with $\rho > 0$ attitude. It has been observed that the value of ϵ^j has also an impact on the realistic expected system cost, which motivates to consider ϵ^j combined with ρ in the calibration procedure.

6.4 Data-driven distributed operation of electricity and natural gas systems

In many countries, electricity and natural gas systems are operated independently by different entities that prefer to keep their information private and only share the minimum amount of information needed to guarantee the secure operation of the two energy systems. Initially, we present the coupled dispatch model (6.20) for electricity and natural gas systems, where a distributionally robust individual chance constrained program in the form of problem (6.2) is written and the moment-based ambiguity set $\mathcal{P}$ as defined in (6.5) is used. The model writes as

$$\min_{x_{\mathrm{E}}, Y_{\mathrm{E}}, x_{\mathrm{G}}, Y_{\mathrm{G}}} \quad \max_{\mathbb{P}\in\mathcal{P}} \mathbb{E}^{\mathbb{P}}[\mathcal{C}^{\mathrm{D}}_{\mathrm{E}}(x_{\mathrm{E}}, Y_{\mathrm{E}}, \xi) + \mathcal{C}^{\mathrm{D}}_{\mathrm{G}}(x_{\mathrm{G}}, Y_{\mathrm{G}}, \xi)] \tag{6.20a}$$

$$\text{s. t.} \quad x_{\mathrm{E}}, Y_{\mathrm{E}} \in \Theta_{\mathrm{E}} \tag{6.20b}$$

$$x_{\mathrm{G}}, Y_{\mathrm{G}} \in \Theta_{\mathrm{G}} \tag{6.20c}$$

$$h_{\mathrm{C}}(\Phi x_{\mathrm{E}}, \Phi Y_{\mathrm{E}}, x_{\mathrm{G}}, Y_{\mathrm{G}}) = 0, \tag{6.20d}$$

where Θ_{E} and Θ_{G} capture the feasible sets for the electricity and natural gas systems, respectively. The feasible set Θ_{E} in (6.20b) contains the equality and inequality constraints as well as the distributionally robust individual chance constraints for the operation of the electricity system, such as power capacity, power flow and balance constraints. In a similar manner, feasible set Θ_{G} in (6.20c) contains the same set of constraints for the natural gas system operation. The electricity and natural gas cost functions $\mathcal{C}_{\mathrm{E}}(x_{\mathrm{E}}, Y_{\mathrm{E}}, \xi)$ and $\mathcal{C}_{\mathrm{G}}(x_{\mathrm{G}}, Y_{\mathrm{G}}, \xi)$ are assumed to be quadratic. The first-stage decisions $x_{\mathrm{E}} \in \mathbb{R}^{G}_{+}$ and $x_{\mathrm{G}} \in \mathbb{R}^{\mathcal{U}}_{+}$ comprise the day-ahead schedule of the electricity and natural gas systems, respectively. The recourse actions $Y_{\mathrm{E}} \in \mathbb{R}^{G\times W}$ and $Y_{\mathrm{G}} \in \mathbb{R}^{\mathcal{U}\times W}$ correspond to the real-time dispatch actions to cover the imbalances from forecast errors. Equality constraint (6.20d) links the natural gas consumption of GFPPs to their power production. Diagonal matrix $\Phi \in \mathbb{R}^{G\times G}_{+}$ contains the power conversion factor of GFPPs, while the entries for non-GFPPs are zero. Under the moment-based ambiguity set, the objective function (6.20a) results in a convex quadratic function and the distributionally robust individual chance constraints of the form (6.2b) in Θ_{E} and Θ_{G} are reformulated as second-order cone constraints based on [102]. Therefore, we have a Second-Order Cone Program (SOCP) at hand to be solved. A detailed model formulation is provided in [Paper F].

As illustrated in Figure 6.8, a purely data-driven approach is developed where the mean $\widehat{\mu}_0$ and covariance $\widehat{\Sigma}_0$ are estimated from the historical data to build the moment-based ambiguity set. This approach promotes transparency since the historical data are considered common knowledge

and only two values need to be shared between the electricity and natural gas system operators regarding uncertainty characterization. On the contrary, the system operators would need to reach an agreement for the probability distribution of the uncertain parameter, the scenario generation technique and the number of scenarios in the case of using stochastic programming, while the uncertainty sets would also need to be defined and agreed in case robust optimization is applied. Such assumptions and their limitations are also discussed in [103–105].

An independent operation of the electricity and natural gas systems can be achieved by utilizing a distributed algorithm based on the ADMM [25] to decompose problem (6.20) by relaxing the coupling constraint (6.20d). A detailed presentation of the algorithm is presented in [Paper F]. As shown in Figure 6.8, the electricity and natural gas system operators are solving independently the corresponding electricity and natural gas problem. Then, a system coordinator is introduced to facilitate the communication between the two system operators that only need to communicate the fuel consumption of GFPPs between each other. The proposed algorithm converges efficiently to the same solution of the centralized model (6.20) since its reformulation is a convex problem.

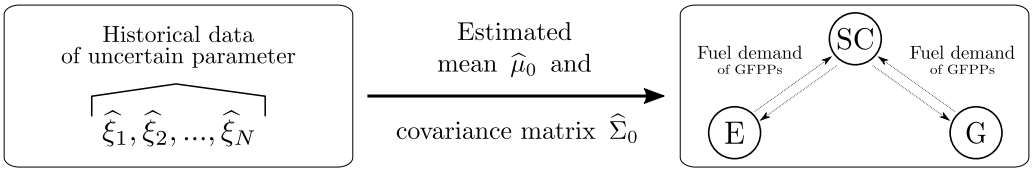

Figure 6.8: Data-driven distributed operation of electricity and natural gas systems via a system coordinator (E: electricity, G: natural gas, SC: system coordinator).

We evaluate the performance of the distributed algorithm and perform the analysis of the projected and realistic operation on an integrated energy system that consists of the IEEE 24-bus Reliability Test System (RTS) [80] and a 12-node natural gas system based on [81]. Wind power is produced by 6 wind farms with an aggregated installed capacity equal to 55% of the peak electricity demand. In all simulations, we schedule wind to the conditional expectation $\widehat{W}$ at the day-ahead stage and thus the mean $\widehat{\mu}_0$ of forecast errors is equal to zero. The wind schedule $\widehat{W}$ and covariance $\widehat{\Sigma}_0$ are inferred from the wind power data, which are generated with the same method as in [23, Equation (2)] and are based on the historical data given in [23]. The complete input data and topology of the system is provided in [106].

6.4.1 Performance of the ADMM-based distributed approach

To assess the performance of the distributed algorithm based on ADMM, a comparison with a fully centralized dispatch model and a sequential dispatch model is performed. The sequential model is built based on [76] that resembles the current operational practice in Great Britain. In [76], an iterative approach is followed that first dispatches the electricity system independently and then the natural gas system is dispatched with the fuel demand of GFPPs as a fixed input. In the event of infeasible fuel schedules of GFPPs in the natural gas dispatch problem, the power production of GFPPs is further constrained in the electricity dispatch problem. This procedure is performed in an iterative manner until the natural gas consumption can be covered by the natural gas system. Note that the residential/industrial natural gas demands have higher priority than the fuel consumption of GFPPs. The cost functions of GFPPs in the sequential dispatch model are calculated based on an estimation of the natural gas price, similarly to Chapter 4. We set the natural gas price estimation

to the mean value of the linear cost coefficient of all natural gas producers. The maximum number of iterations is set to 10^4 for the distributed algorithm and sequential model. For the distributed algorithm, we set the value of penalty parameter in ADMM equal to 0.0001 and the convergence tolerance is set to 10^{-2}.

Table 6.3 presents the value of the objective function for the fully centralized model, distributed algorithm and sequential model when setting $\epsilon_k = 0.1$ for each individual chance constraint in problem (6.20). The information exchange in the distributed algorithm and sequential model is the same, that is the fuel consumption of GFPPs, while the centralized model allows for a full coordination between the electricity and natural gas systems. For this reason, the centralized model attains the solution with the minimum cost. The distributed algorithm returns the same solution as the centralized model, while simulating the two systems independently and allowing only limited information to be shared. The sequential model yields a solution with a 5.2% higher operational cost due to the unsophisticated updates of natural gas consumption of GFPPs over the iterations.

Table 6.3: Value of objective function for centralized model, distributed algorithm and sequential model.

Model	Centralized	Distributed	Sequential
Value of objective function ($)	63,500	63,500	66,821

To gain additional insights into the convergence of the distributed algorithm, we plot the converge of the objective functions and the dispatch of the systems for each iteration η of the algorithm in Figures 6.9 and 6.10. More specifically, Figure 6.9 illustrates the convergence of the objective function (OF) via the ratio:

$$\overline{\gamma}^{\eta} = \frac{\mathrm{OF}^{\eta}_{\text{distributed}} - \mathrm{OF}_{\text{centralized}}}{\mathrm{OF}_{\text{centralized}}} \times 100. \tag{6.21}$$

Similar ratios are calculated for the individual objective functions of the electricity $\overline{\gamma}_{\mathrm{E}}$ and natural gas $\overline{\gamma}_{\mathrm{G}}$ systems. The convergence of dispatch in the electricity (ED) and natural gas (GD) systems is presented in Figure 6.10 by plotting for each iteration the following norms

$$\overline{\chi}^{\eta} = \|\mathrm{ED}^{\eta}_{\text{distributed}} - \mathrm{ED}_{\text{centralized}}\|_2 \tag{6.22a}$$

$$\overline{\upsilon}^{\eta} = \|\mathrm{GD}^{\eta}_{\text{distributed}} - \mathrm{GD}_{\text{centralized}}\|_2. \tag{6.22b}$$

Under this setup, the distributed algorithm converges in 39 iterations and in 65 seconds, i.e. 1.66 seconds per iteration. It can also be observed that the objective function sufficiently approximates the solution of the centralized model already after the 10^{th} iteration. The sequential model converges in 20 seconds but with a lower quality solution in terms of operating cost.

Moreover, Figure 6.10 shows that the distributed algorithm provides a dispatch for both electricity and natural gas producers in a similar manner as the centralized model. The dispatch sufficiently converges already at the 10^{th} iteration. This indicates that the implementation of the distributed algorithm would not have an impact on the profits of the producers and would not alter the market outcomes if the electricity and natural gas systems are dispatched in a distributed manner.

Table 6.4 presents the computational performance of the distributed algorithm in relation to the penalty parameter of ADMM. The penalty parameter has an impact on the number of iterations

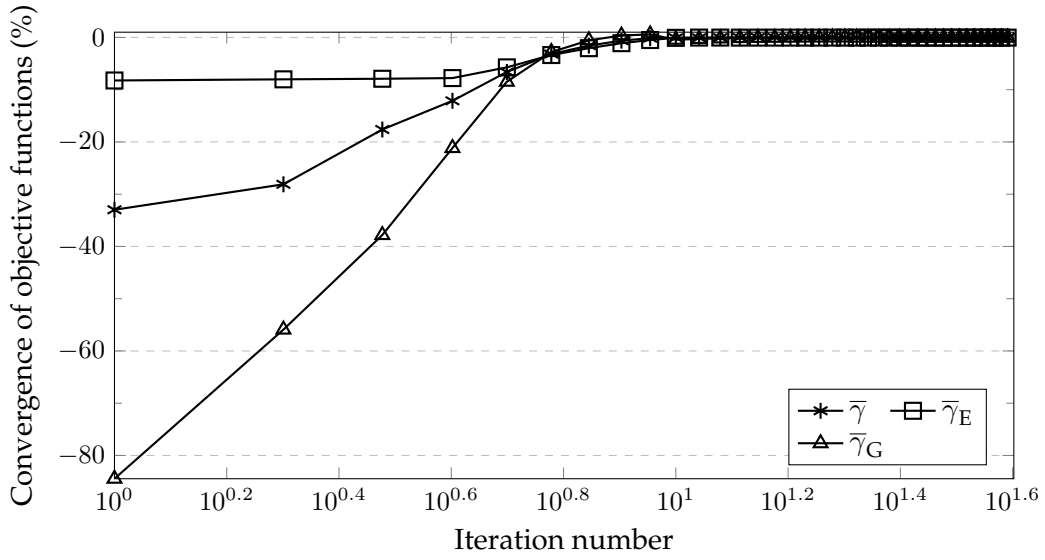

Figure 6.9: Convergence of the objective functions over the iterations (logarithmic scale is used for the x-axis to improve readability).

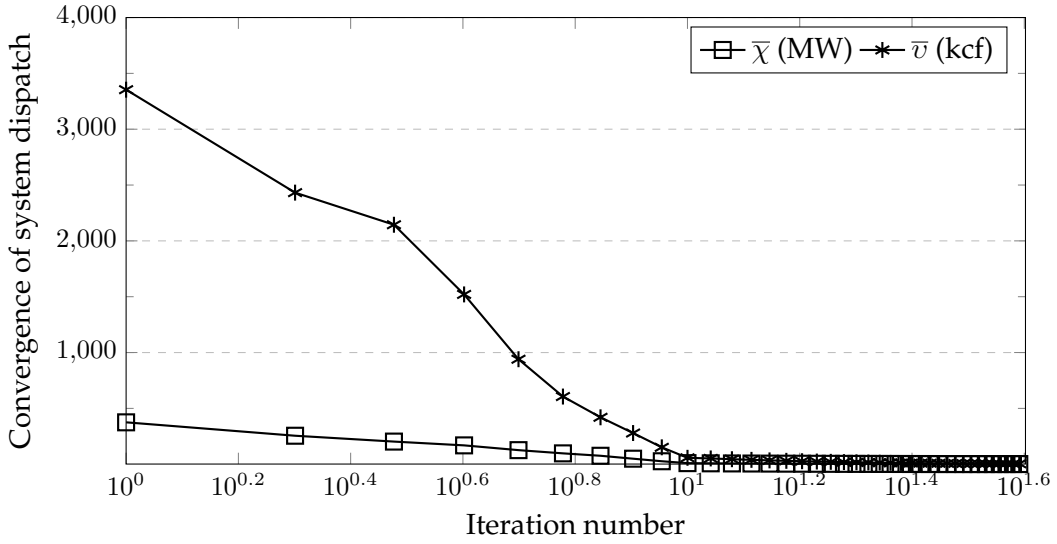

Figure 6.10: Convergence of the system dispatch over the iterations (logarithmic scale is used in the x-axis to improve readability).

and eventually on the solution time, while the time per iteration does not vary much under each case. Therefore, one should carefully choose the value of penalty parameter to achieve an efficient utilization of the distributed algorithm in terms of computational performance.

6.4.2 Performance assessment based on the projected operation

The solution of the distributionally robust chance constrained (*DRCC*) program (6.20) with the moment-based ambiguity set, either solved via the centralized model or the distributed algorithm, is compared with a chance constrained program that assumes a Gaussian distribution of forecast errors (*GCC*) as presented in [48], as well as with a deterministic model that assumes no uncertainty

Table 6.4: Number of iterations and solution time for the distributed algorithm as a function of penalty parameter.

Penalty parameter	Iterations	Time (sec)	Time per iteration (sec)
0.0001	289	475	1.64
0.001	39	65	1.66
0.01	131	223	1.70
0.1	839	1448	1.72

as the one used in [50]. We consider ϵ_k as a design parameter that can be decided by the operators based on the trade-off between the operational cost and the risk of violating the constraints. The same value of ϵ_k is used for all individual chance constraints ranging from 0.05 to 0.5 with a step of 0.05.

Figure 6.11 presents the empirical violation probability $\widetilde{\mathcal{V}}^{\text{emp}}$ for the *DRCC* model and the *GCC* model, while Figure 6.12 the maximum average violation probability $\widetilde{\mathcal{V}}^{\text{max}}$. We report the solutions for different values of ϵ_k. It can be observed that an increase in ϵ_k results in an increase of both $\widetilde{\mathcal{V}}^{\text{emp}}$ and $\widetilde{\mathcal{V}}^{\text{max}}$. Comparing *DRCC* and *GCC* models, model *DRCC* returns always a lower $\widetilde{\mathcal{V}}^{\text{emp}}$ and $\widetilde{\mathcal{V}}^{\text{max}}$ than the *GCC* model. More importantly, *DRCC* model yields a very low $\widetilde{\mathcal{V}}^{\text{emp}}$ for all values of ϵ_k and $\widetilde{\mathcal{V}}^{\text{max}}$ is always below 10%. The increase of ϵ_k results in a greater increase of $\widetilde{\mathcal{V}}^{\text{emp}}$ and $\widetilde{\mathcal{V}}^{\text{max}}$ in model *GCC* and this phenomenon is more profound for values of ϵ_k greater than 0.4. The accepted violation probability imposed by the system operators is satisfied for all values of ϵ_k, except for the instance of $\epsilon_k = 0.05$ in the *GCC* model where $\widetilde{\mathcal{V}}^{\text{max}}$ is greater than 0.05.

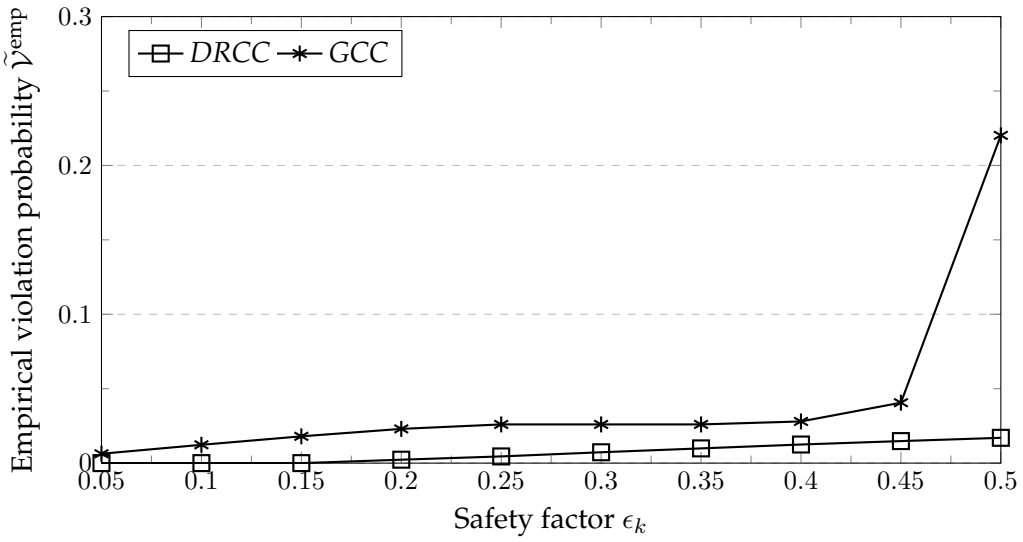

Figure 6.11: Empirical violation probability for *DRCC* and *GCC*.

Figure 6.13 shows the cost difference between the *DRCC* and *GCC* models for the range of ϵ_k values. An increase of ϵ_k results in a reduction of the cost difference between the two models. More specifically, the cost difference is at most 7.11% and it drops close to 0.3% for an ϵ_k greater than 0.35. For small values of ϵ_k, the cost obtained by *DRCC* is higher because it is more conservative compared to *GCC*. Based on these observations for the projected operation, it can be noticed that the system operators are able to choose an appropriate value of ϵ_k to reduce the total cost at the expense of a higher chance of violating the constraints. Model *DRCC* outperforms *GCC* since the

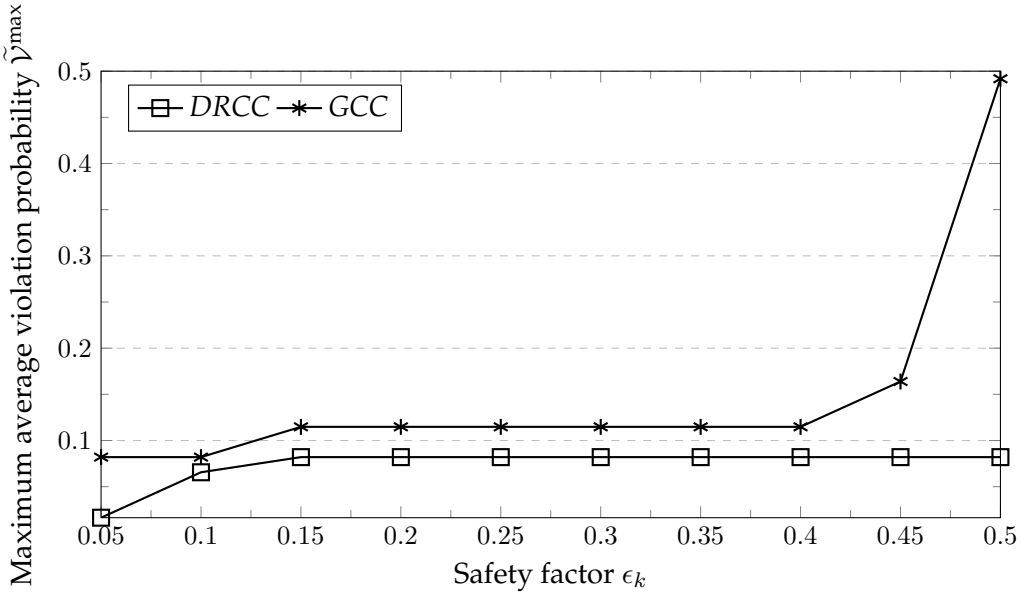

Figure 6.12: Maximum average violation probability for *DRCC* and *GCC*.

system operators are able to pick the value of ϵ_k under *DRCC* in such a way that a system cost very close to the one obtained by *GCC* is achieved but with lower violation probabilities.

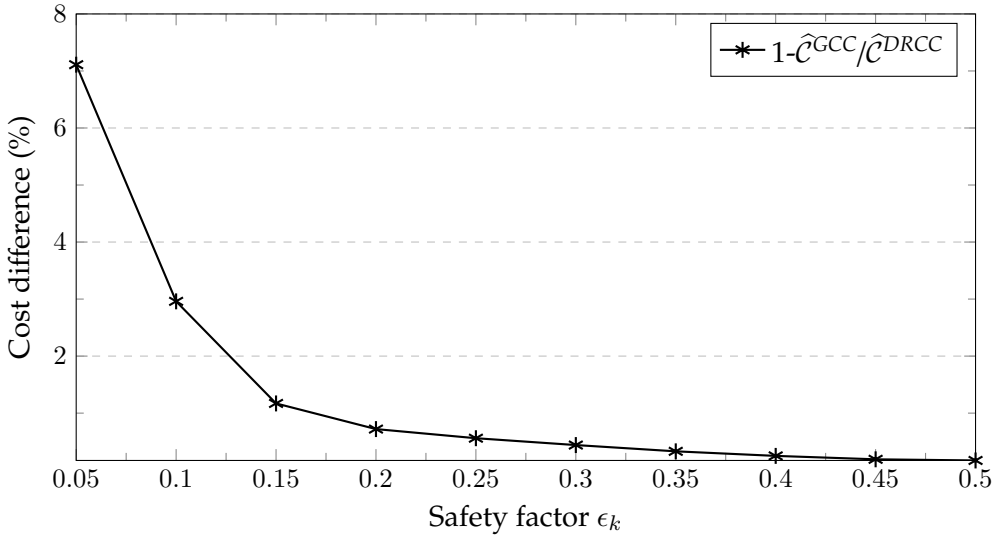

Figure 6.13: Percentage of total cost difference between the *DRCC* and *GCC*.

Table 6.5 presents the projected cost $\widehat{\mathcal{C}}$ as well as the violation probability metrics $\widetilde{\mathcal{V}}^{\text{emp}}$ and $\widetilde{\mathcal{V}}^{\max}$ for all three models. For *DRCC* and *GCC*, the results are reported for $\epsilon_k = 0.35$. It can be noticed that the attained $\widehat{\mathcal{C}}$ is similar for all three models. In particular, the projected cost $\widehat{\mathcal{C}}$ of *DRCC* is 0.3% and 0.46% greater than the cost obtained by the *GCC* and deterministic models, respectively. However, the violation probabilities $\widetilde{\mathcal{V}}^{\text{emp}}$ and $\widetilde{\mathcal{V}}^{\max}$ are lower in the case of *DRCC*. Moreover, the deterministic model attains significantly higher $\widetilde{\mathcal{V}}^{\text{emp}}$ and $\widetilde{\mathcal{V}}^{\max}$ for the majority of the values of ϵ_k both for *DRCC* and *GCC*. Therefore, the need to utilize probabilistic approaches for the operational

limits and account for uncertainty is highlighted.

Table 6.5: Projected cost $\widehat{\mathcal{C}}$ and violation probabilities $\widetilde{\mathcal{V}}^{\text{emp}}$ and $\widetilde{\mathcal{V}}^{\text{max}}$ for $\epsilon_k = 0.35$.

Model	*DRCC*	*GCC*	Deterministic
$\widehat{\mathcal{C}}$ (\$)	61,163	60,957	60,881
$\widetilde{\mathcal{V}}^{\text{emp}}$	0.01	0.03	0.22
$\widetilde{\mathcal{V}}^{\text{max}}$	0.08	0.12	0.49

6.4.3 Performance assessment based on the realistic operation

The realistic operation is utilized to evaluate solutions $(\widehat{x}_{\text{E}}, \widehat{Y}_{\text{E}}, \widehat{x}_{\text{G}}, \widehat{Y}_{\text{G}})$ when only the first-stage decisions $\widehat{x}_{\text{E}}$ and $\widehat{x}_{\text{G}}$ are implemented and the real-time adjustments are acquired by a deterministic real-time optimal electricity and natural gas dispatch problem with network constraints. We compare the solutions obtained by *DRCC*, *GCC* and deterministic models. This procedure is repeated for the different values of $\epsilon_k \in [0.05, 0.5]$.

Figure 6.14 illustrates the realistic cost $\widehat{\mathcal{R}}$ as a function of ϵ_k. It can be observed that *DRCC* outperforms *GCC* for all values of ϵ_k, which indicates that *DRCC* provides more efficient first-stage solutions in terms of realistic cost $\widehat{\mathcal{R}}$. Moreover, the reported $\widehat{\mathcal{R}}$ decreases with a decrease of ϵ_k since there are less costly re-dispatch actions activated when solving the real-time dispatch problem due to increased robustness. The solution obtained from the deterministic model is the same as the one of *GCC* for $\epsilon_k = 0.5$, which is the case with the higher $\widehat{\mathcal{R}}$.

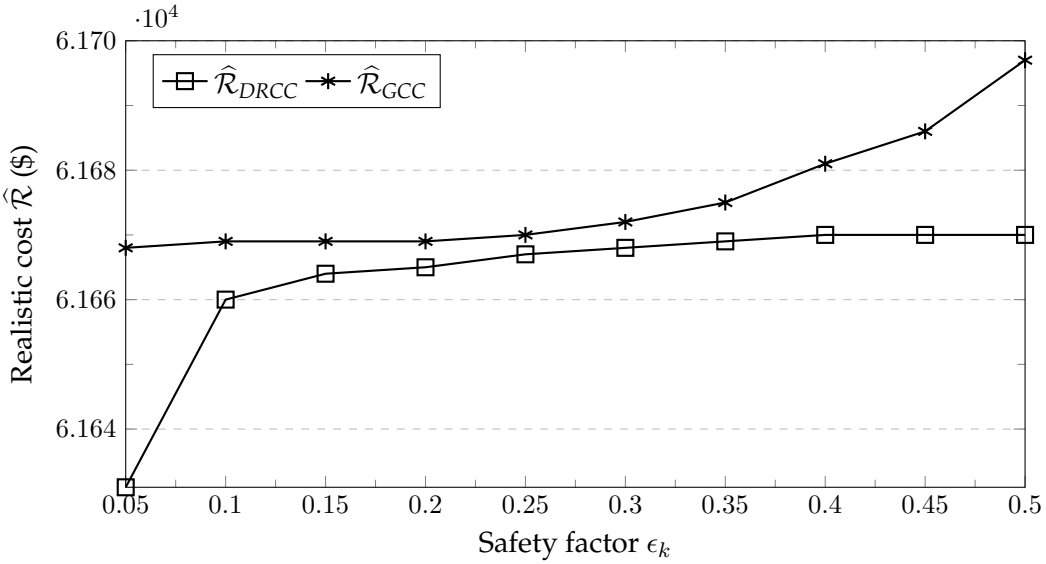

Figure 6.14: Average realistic cost $\widehat{\mathcal{R}}$ as a function of safety factor ϵ_k for *DRCC* and *GCC*.

We report the computational performance for the case with $\epsilon_k = 0.1$, while the solution times obtained for other values of ϵ_k are similar. Model *DRCC* is solved in 35 seconds on average and for *GCC* the average solution time is 1.5 seconds. Finally, the deterministic model is solved in 0.3 seconds on average. Thus, model *DRCC* has a better performance than both *GCC* and deterministic models in terms of realistic cost $\widehat{\mathcal{R}}$ and is solved in a computationally acceptable time.

CHAPTER 7

Conclusions and Perspectives

In this thesis, we addressed the three main research questions regarding the coordination of electricity and natural gas markets under the increased uncertainty introduced by renewables. The first research question pertained to examining various degrees of coordination in terms of coupling the electricity and natural gas systems to identify potential inefficiencies and to propose improvements towards a cost-effective operation. Moreover, electricity and natural gas are commodities traded in markets via complex networks. This motivated us to focus on modeling the energy networks in a market-compatible way that sufficiently describes their underlying physical characteristics in order to address the second research question. Finally, the operational models which were developed in this thesis, considered advanced methods to deal with uncertainty in order to support the operation of energy markets and systems under the unprecedented challenges faced by the transition towards a renewable-based energy system.

7.1 Overview of contributions

A number of novel contributions to the state of the art were presented in this thesis relative to improving the coordination of electricity and natural gas markets as well as revealing available flexibility to accommodate the uncertainty of renewable power production.

A holistic view of the electricity and natural gas systems was adopted in order to take advantage of the different flexible components and utilize them in the most efficient manner for the operation of both energy systems. This was found to be a cost-effective way to reveal existing flexibility from the natural gas system. Apart from operating the Gas-Fired Power Plants (GFPPs) in an economic and secure manner, such an approach provided the opportunity to exploit the inherent flexibility of the natural gas system. The natural gas system provides storage options in the network (i.e. linepack) and in the large storage facilities. To utilize linepack as storage flexibility, the dynamics of the natural gas flows needed to be taken into account. These dynamics would normally be modeled by Partial Differential Equations (PDEs), which are able to fully capture both the temporal and spatial dimensions of natural gas transport. However, such a detailed modeling of natural gas dynamics would highly increase computational complexity and raise market design issues related to pricing electricity and natural gas. To overcome such issues, we proposed a model to efficiently approximate natural gas system dynamics that was formulated as a tractable Mixed-Integer Linear Program (MILP). This model enabled the utilization of the linepack as additional storage flexibility, captured the dynamics of the natural gas transport as well as allowed to derive prices for electricity and natural gas. Security of supply was also increased since the natural gas resources were properly allocated across the network. Such solutions can be readily adopted by system operators to take advantage of the revealed flexibility when operating the systems and by market operators since they are market-compatible is a sense that no limitations regarding the market operations are raised.

The introduction of additional sources of flexibility, such as GFPPs, storage facilities and linepack, requires the proper models to operate them efficiently in a market environment. Studying electricity and natural gas markets under different coordination setups, we were able to identify potential inefficiencies regarding the dispatch of the two systems. More specifically, we examined different levels of coordination between the electricity and natural gas systems and the temporal coordination of the day-ahead and real-time trading floors. These setups range from the current decoupled and deterministic approaches to coupled and uncertainty-aware ones. Initially, the impact of coordination parameters, such as the natural gas consumption of GFPPs and natural gas price, on the operations of both systems and in turn on operational costs was examined. Choosing these parameters in a naive and arbitrary manner when optimizing the two systems independently led to scheduling outcomes with a higher expected cost compared to the cost obtained by a fully coupled approach that utilizes a probabilistic description of uncertainties. The latter model was able to exploit the inherent flexibility of the natural gas system and provide a schedule for the system that accounts for future balancing costs in view of uncertain power supply.

The current market designs are based on a sequential clearing of trading floors with deterministic description of uncertainties. Such designs are highly challenged by the increased uncertainty introduced by renewables and usually lead to solutions that yield a high expected cost. On the other hand, scheduling the systems with a model based on two-stage stochastic programming provides the solution with the least expected system cost. However, this scheduling is not fully compatible with the current sequential market designs. To improve the sequential clearing of trading floors, we followed a coupled model for the electricity and natural gas markets that allowed to define two flexibility signals based on the natural gas volume availability for power production and on the natural gas price perceived by GFPPs. These flexibility signals were optimally set by a volume-based and a price-based model that recast Mathematical Programs with Equilibrium Constraints (MPECs). The advantage of these models is that they can be utilized by market operators as decision-support tools in a sense that their outcomes can be directly incorporated in the existing market structure, where the day-ahead and real-time stages are cleared independently.

The stochastic nature of power production from renewables calls for changes in both system operations due to the immerse uncertainty introduced. Various approaches have been proposed to cope with this challenge including stochastic programming, chance constrained programming and robust optimization. Despite the attractive results of following such approaches, recent developments on data-driven optimization give the possibility to alleviate the barrier of using inaccurate estimates from the uncertain parameters and avoid involving additional processes to characterize uncertainty. In this thesis, we developed two data-driven models based on distributionally robust optimization, where the optimization takes over a family of distributions (i.e. ambiguity set). In these models, the available renewable power production data were directly utilized to build the corresponding ambiguity sets.

In the first data-driven model, we solved the energy and reserve dispatch problem with fuel constraints for GFPPs formulated as a distributionally robust joint chance constrained program. We proposed a convex conservative approximation for distributionally robust joint chance constraints, where the data generating distribution is not assumed to be a member of a parametric family and the ambiguity set is built based on the Wasserstein metric. The obtained approximation is tractable in high dimensional problems and demonstrates superior performance compared to widely used in the literature Bonferroni approximation for joint chance constraints in terms of expected system

cost. Moreover, we provided a systematic way to calibrate the Wasserstein radius (i.e. size of ambiguity set) by an estimation practice depending on the available data. We showed that a distributionally robust attitude is of great significance when few samples are available, while less robustness is needed as more information regarding the distribution of the uncertain parameter becomes available. Utilizing such an approach allows system operators to develop models that incorporate uncertainty from renewable energy sources and additionally give the possibility to properly tune their models in order to attain the required level of robustness that yields the lowest expected costs.

In the second data-driven model, we defined the ambiguity set based on the first- and second-order moments of the uncertain parameter. This distributionally robust optimization model was built with individual chance constraints to obtain an analytical reformulation that results in a tractable Second-Order Cone Program (SOCP). Apart from the appealing benefits of the coupled electricity and natural gas systems operation, distributed approaches can also be efficiently employed to provide practical solutions when the two systems are operated independently. To this end, we proposed a data-driven and distributed approach to dispatch the electricity and natural gas systems with high shares of stochastic power production. The distributed algorithm was developed based on the Alternating Direction Method of Multipliers (ADMM) where only the fuel consumption of GFPPs was shared between the operators. The proposed algorithm is able to systematically update the coordination parameter related to the fuel consumption of GFPPs and converge to the same solution of a centralized approach that co-optimizes the operation of the two energy systems. As far as the uncertainty characterization is concerned, only the mean and covariance matrix needs to be shared between the system operators, which can be inferred from the available historical data. We demonstrated that the proposed model outperforms a classic stochastic approach that assumes normally distributed uncertainty and a deterministic model in terms of expected system cost and violation of constraints. This solution can readily be implemented in practice since it is highly transparent in describing uncertain power supply and returns the solution of the coupled approach with the minimum amount of information shared between the operators. In addition, the proposed algorithm is scalable to large scale problems, since the number of random parameters does not affect the size of the problem, and can be solved for a variety of risk preferences, which can be decided by the decision maker.

7.2 Perspectives for future research

During the course of the research conducted in this thesis, we identified several research questions to be addressed in the future. Future research directions range from dealing with technology-related aspects of the systems to redesigning the energy markets towards accommodating larger shares of renewables in the whole energy system.

A realistic view of the underlying physics of the electricity and natural gas systems can be achieved by the development of mathematical models that involve non-convex constraints. Such a detailed network and component representation would entirely reveal the benefits with regards to exploiting flexibility and increasing security of supply. This becomes highly important especially at the balancing stage, when all the technical constraints need to be satisfied. Taking advantage of the recent developments on convex relaxation techniques for non-convex problems, a more accurate modeling of the electricity and natural gas systems can be achieved which also allows price derivation by preserving convexity of the problems. More specifically, such approaches can

be adopted for the AC optimal power flow problem, as well as the transient natural gas modeling. An interesting future direction would be to develop operational models based on these approaches that overcome limitations with regards to pricing various traded products and reveal opportunities towards defining multi-commodity products for players that participate in both energy markets.

Towards exploiting possibilities to bring operational flexibility in the energy markets, bi-directional energy flows between the electricity and natural gas systems can be considered, as well as the interactions with other energy networks. In particular, the introduction of power-to-gas facilities in the modeling framework can further highlight the benefits of using the natural gas system as an energy storage solution. In a similar direction, the interaction with the heat market and system, via Combined Heat and Power (CHP) plants and heat pumps, can pave the way for optimally operating the three energy systems and revealing additional flexibility. This solution is highly promising in regions where all three energy systems co-exist, as in the case of Denmark, since a proper design of energy markets is considered an inexpensive way to take advantage of the existing infrastructure and have a cost-effective operation of the whole energy system.

The natural gas and heat networks, can be seen as energy storage facilities. The nodes of these networks are connected with pipelines which also offer the possibility to store energy. Therefore, both the temporal and spatial dimensions can be identified in these two networks with regards to storing energy. Mechanisms similar to financial transmission and storage rights that hedge prices in space and time, respectively, can be developed. An interesting future direction would be to propose a mechanism that combines the features of financial transmission and storage rights to hedge both temporal and spatial price variations.

The optimal definition and control of specified coordination parameters results in attaining an improved day-ahead scheduling of the coupled electricity and natural gas system in view of future uncertainties. This proposed mechanism can be generalized in a sense that alternative signals can be generated or different parameters can be tuned in view of other types or combinations of uncertainties. Moreover, different objectives such as addressing reliability risks or setting long term planning goals can be taken into account. To provide more sophisticated decisions, the inclusion of additional market floors, e.g. intra-day market, would be highly relevant.

In a market environment, the proposed dispatch models based on the flexibility signals retain most of the gains of utilizing a stochastic programming approach to dispatch the energy systems and at the same time, are able to keep the current sequential arrangement of trading floors. Therefore, a more cost-effective system dispatch is attained with only slightly altering the current market setup. To accomplish a similar effect, various alternative approaches, such as flexible ramping products, have been considered in practice. In this case, flexible ramping products are defined to address operational challenges of maintaining the system balanced and to increase market efficiency. Using the flexible ramping product as an inspiration, an interesting direction for future research would be to define analogous products on the natural gas side by valuing the flexibility of the natural gas network (i.e. linepack) and ensuring that there is enough linepack to manage the increasingly variable fuel consumption of GFPPs. In a similar context, the introduction of virtual-bidders in the electricity and natural gas markets as well as, allowing the GFPPs to self-schedule by adopting a probabilistic description of uncertainties, are arbitrage-based options that can enhance market efficiency both on the electricity and natural gas side. More specifically, an interesting case to consider would be that each one of these energy arbitragers would have an imperfect view of

uncertainties meaning that their beliefs are different from the actual distribution characterizing uncertain parameters.

Building on the two proposed data-driven models, there are several interesting directions to be further investigated. Extending the findings regarding the reformulation of joint chance constraints with the Wasserstein ambiguity set, alternative ambiguity sets can be considered to provide tractable reformulation of distributionally robust joint chance constrained programs. Tractable reformulations of joint chance constraints are of great interest since they would allow the system operators to define system-wide risk parameters to the constraints, instead of individual ones. Another interesting direction is to solve a distributionally robust chance constrained problems in a distributed manner but for a variety of agents that have a different belief on characterizing uncertainty. That way, the agents would not need to agree on a common description for the ambiguity sets. Moreover, the models utilized by system and market operators are often described via mathematical programs. The continuously increasing deployment of renewable energy sources will require to solve these problems in a high dimensional setting which raises computational issues. To tackle such tractability issues, especially in practical applications, the utilization of machine learning offers a great potential to predict the outcomes of the respective mathematical programs.

Finally, the energy sector is becoming increasingly digitalized with large volumes of energy data (e.g. renewable power production and smart meter data) being collected over the last years. To closely follow this transformation, data-driven approaches in combination with machine learning will be key tools to exploit the acquired information from the collected data towards enabling new opportunities for the efficient operation of future energy systems and markets. Adopting such novel approaches for the development of the operational models will eventually enable the integration of higher shares of renewables, increase coordination among energy sectors, as well as bring additional benefits to the society and end-users by decreasing operational costs.

Bibliography

[1] R. D. Tabors, S. Englander, and R. Stoddard. Who's on first? The coordination of gas and power scheduling. *The Electricity Journal*, 25(5):8–15, 2012.

[2] P. J. Hibbard and T. Schatzki. The interdependence of electricity and natural gas: Current factors and future prospects. *The Electricity Journal*, 25(4):6–17, 2012.

[3] Wind Europe. Wind in power 2017 - Annual combined onshore and offshore wind energy statistics. https://windeurope.org/wp-content/uploads/files/about-wind/statistics/WindEurope-Annual-Statistics-2017.pdf. Online; Accessed: 30.09.2018.

[4] A. Alabdulwahab, A. Abusorrah, X. Zhang, and M. Shahidehpour. Coordination of interdependent natural gas and electricity infrastructures for firming the variability of wind energy in stochastic day-ahead scheduling. *IEEE Transactions on Sustainable Energy*, 6(2):606–615, 2015.

[5] Y. Li, Y. Zou, Y. Tan, Y. Cao, X. Liu, M. Shahidehpour, S. Tian, and F. Bu. Optimal stochastic operation of integrated low-carbon electric power, natural gas, and heat delivery system. *IEEE Transactions on Sustainable Energy*, 9(1):273–283, 2018.

[6] C. He, T. Liu, L. Wu, and M. Shahidehpour. Robust coordination of interdependent electricity and natural gas systems in day-ahead scheduling for facilitating volatile renewable generations via power-to-gas technology. *Journal of Modern Power Systems and Clean Energy*, 5(3):375–388, 2017.

[7] Y. He, M. Shahidehpour, Z. Li, C. Guo, and B. Zhu. Robust constrained operation of integrated electricity-natural gas system considering distributed natural gas storage. *IEEE Transactions on Sustainable Energy*, 9(3):1061–1071, 2018.

[8] A. Zlotnik, L. Roald, S. Backhaus, M. Chertkov, and G. Andersson. Coordinated scheduling for interdependent electric power and natural gas infrastructures. *IEEE Transactions on Power Systems*, 32(1):600–610, 2017.

[9] S. An, Q. L. Li, and T. W. Gedra. Natural gas and electricity optimal power flow. In *2003 IEEE PES Transmission and Distribtion Conference and Exposition*, pages 138–143, 2003.

[10] M. Geidl and G. Andersson. Optimal power flow of multiple energy carriers. *IEEE Transactions on Power Systems*, 22(1):145–155, 2007.

[11] T. Li, M. Eremia, and M. Shahidehpour. Interdependency of natural gas network and power system security. *IEEE Transactions on Power Systems*, 23(4):1817–1824, 2008.

[12] C. Liu, M. Shahidehpour, Y. Fu, and Z. Li. Security-constrained unit commitment with natural gas transmission constraints. *IEEE Transactions on Power Systems*, 24(3):1523–1536, 2009.

[13] C. M. Correa-Posada and P. Sanchez-Martin. Integrated power and natural gas model for energy adequacy in short-term operation. *IEEE Transactions on Power Systems*, 30(6):3347–3355, 2014.

[14] L. Mitridati and J. A. Taylor. Power systems flexibility from district heating networks. In *2018 Power Systems Computation Conference (PSCC)*, 2018.

[15] L. Maurovich-Horvat, P. Rocha, and A. S. Siddiqui. Optimal operation of combined heat and power under uncertainty and risk aversion. *Energy and Buildings*, 110:415 – 425, 2016.

[16] P. Pinson, H. Madsen, H. Aa. Nielsen, G. Papaefthymiou, and B. Klőckl. From probabilistic forecasts to statistical scenarios of short-term wind power production. *Wind Energy*, 12(1):51–62, 2009.

[17] Á. Lorca and X. A. Sun. Adaptive robust optimization with dynamic uncertainty sets for multi-period economic dispatch under significant wind. *IEEE Transactions on Power Systems*, 30(4):1702–1713, 2015.

[18] E. Delage and Y. Ye. Distributionally robust optimization under moment uncertainty with application to data-driven problems. *Operations Research*, 58(3):595–612, 2010.

[19] P. Mohajerin Esfahani and D. Kuhn. Data-driven distributionally robust optimization using the Wasserstein metric: Performance guarantees and tractable reformulations. *Mathematical Programming*, 2017.

[20] International Energy Agency. Energy policies of IEA countries - Denmark 2017 review. http://www.iea.org/publications/freepublications/publication/EnergyPoliciesofIEACountriesDenmark2017Review.pdfl. Online; Accessed: 30.09.2018.

[21] A. Shapiro, D. Dentcheva, and A. Ruszczyński. *Lectures on Stochastic Programming*. Society for Industrial and Applied Mathematics, 2009.

[22] Z.-Q. Luo, J.-S. Pang, and D. Ralph. *Mathematical Programs with Equilibrium Constraints*. Cambridge University Press, 1996.

[23] J. Dowell and P. Pinson. Very-short-term probabilistic wind power forecasts by sparse vector autoregression. *IEEE Transactions on Smart Grid*, 7(2):763–770, 2016.

[24] C. Villani. *Topics in Optimal Transportation*. American Mathematical Society, 2003.

[25] S. Boyd, N. Parikh, E. Chu, B. Peleato, and J. Eckstein. Distributed optimization and statistical learning via the Alternating Direction Method of Multipliers. *Foundations and Trends in Machine Learning*, 3(1):1–122, 2011.

[26] D. Kirschen and G. Strbac. *Fundamentals of Power System Economics*. John Wiley and Sons, 2004.

[27] S. Stoft. *Power System Economics: Designing Markets for Electricity*. Wiley-IEEE Press, 2002.

[28] I.J. Pérez-Arriaga. *Regulation of the Power Sector*. Springer, 2002.

[29] J. Glachant, M. Hallack, and M. Vasquez. *Building Competitve Gas Markets in the EU*. Edward Elgar Publisher, 2013.

[30] T. Koch, B. Hiller, M. Pfetsch, and L. Schewe. *Evaluating Gas Network Capacities*. Society for Industrial and Applied Mathematics, Philadelphia, PA, 2015.

[31] U.S. Energy Information Administration. International energy outlook 2016. Technical report, 2016.

[32] Danish Energy Agency. Overview of the energy sector. https://ens.dk/en/our-services/statistics-data-key-figures-and-energy-maps/overview-energy-sector. Online; Accessed: 30.09.2018.

[33] Energinet.dk. https://en.energinet.dk/. Online; Accessed: 30.09.2018.

[34] Nord Pool Spot. https://www.nordpoolgroup.com/. Online; Accessed: 30.09.2018.

[35] GasPoint Nordic. http://www.gaspointnordic.com/market-data. Online; Accessed: 30.09.2018.

[36] Danish Energy Regulation Authority. National report 2017. http://energitilsynet.dk/fileadmin/Filer/Information/Diverse_publikationer_og_artikler/National_Report_2017_DERA.pdf. Online; Accessed: 30.09.2018.

[37] EEX. https://www.eex.com/en/. Online; Accessed: 30.09.2018.

[38] Powernext. https://www.powernext.com/home. Online; Accessed: 30.09.2018.

[39] PEGAS. https://www.powernext.com/pegas-trading. Online; Accessed: 30.09.2018.

[40] Danish Energy Agency. Biogas in denmark. https://ens.dk/en/our-responsibilities/bioenergy/biogas-denmark. Online; Accessed: 30.09.2018.

[41] M. B. Karan and H. Kazdağli. *The Development of Energy Markets in Europe*, pages 11–32. Springer Berlin Heidelberg, Berlin, Heidelberg, 2011.

[42] C. Weber. Adequate intraday market design to enable the integration of wind energy into the european power systems. *Energy Policy*, 38(7):3155 – 3163, 2010.

[43] Iberian Electricity Market. http://www.mibel.com/. Online; Accessed: 30.09.2018.

[44] G. Pritchard, G. Zakeri, and A. Philpott. A single-settlement, energy-only electric power market for unpredictable and intermittent participants. *Operations Research*, 58:1210–1219, 2010.

[45] J. M. Morales, A. J. Conejo, K. Liu, and J. Zhong. Pricing electricity in pools with wind producers. *IEEE Transactions on Power Systems*, 27(3):1366–1376, 2012.

[46] D. Bertsimas, E. Litvinov, X. A. Sun, J. Zhao, and T. Zheng. Adaptive robust optimization for the security constrained unit commitment problem. *IEEE Transactions on Power Systems*, 28(1):52–63, 2013.

[47] M. Zugno and A. J. Conejo. A robust optimization approach to energy and reserve dispatch in electricity markets. *European Journal of Operational Research*, 247(2):659 – 671, 2015.

[48] D. Bienstock, M. Chertkov, and S. Harnett. Chance-constrained optimal power flow: Risk-aware network control under uncertainty. *SIAM Review*, 56(3):461–495, 2014.

[49] A. Venzke, L. Halilbasic, U. Markovic, G. Hug, and S. Chatzivasileiadis. Convex relaxations of chance constrained AC optimal power flow. *IEEE Transactions on Power Systems*, 33(3):2829–2841, 2018.

[50] W. Xie and S. Ahmed. Distributionally robust chance constrained optimal power flow with renewables: A conic reformulation. *IEEE Transactions on Power Systems*, 33(2):1860–1867, 2018.

[51] W. Wei, J Wang, and S. Mei. Dispatchability maximization for co-optimized energy and reserve dispatch with explicit reliability guarantee. *IEEE Transactions on Power Systems*, 31(4):3276–3288, 2016.

[52] W.W. Hogan and B.J. Ring. On minimum-uplift pricing for electricity markets. http://lmpmarketdesign.com/papers/Hogan_Ring_minuplift_031903.pdf. Online; Accessed: 30.09.2018.

[53] S. Bose and S. H. Low. Some emerging challenges in electricity markets. In *Smart Grid Control: Overview and Research Opportunities*. Springer International Publishing, 2018.

[54] A. Zlotnik, A. M. Rudkevich, E. Goldis, P. A. Ruiz, M. Caramanis, R. Carter, R. Tabors, R. Hornby, and D. Baldwin. Economic optimization of intra-day gas pipeline flow schedules using transient flow models. In *PSIG 2017 Conference*, 2017.

[55] N. Keyaerts. *Gas balancing and line-pack flexibility: Concepts and methodologies for organizing and regulating gas balancing in leberalized and integrated EU gas markets*. PhD thesis, KU Leuven, 2012.

[56] Energinet.dk. Gas market. https://en.energinet.dk/Gas/Gas-Market#Model. Online; Accessed: 30.09.2018.

[57] M. Vazquez and M. Hallack. Interaction between gas and power market designs. *Utilities Policy*, 33:23 – 33, 2015.

[58] G. Gahleitner. Hydrogen from renewable electricity: An international review of power-to-gas pilot plants for stationary applications. *International Journal of Hydrogen Energy*, 38(5):2039 – 2061, 2013.

[59] M Gőtz, J. Lefebvre, F. Mőrs, A. McDaniel Koch, F. Graf, S. Bajohr, R. Reimert, and T. Kolb. Renewable power-to-gas: A technological and economic review. *Renewable Energy*, 85:1371 – 1390, 2016.

[60] B. Zhao, A. J. Conejo, and R. Sioshansi. Coordinated expansion planning of natural gas and electric power systems. *IEEE Transactions on Power Systems*, 33(3):3064–3075, 2018.

[61] R. Bent, S. Blumsack, P. Van Hentenryck, C. Borraz Sanchez, and M. Shahriari. Joint electricity and natural gas transmission planning with endogenous market feedbacks. *IEEE Transactions on Power Systems*, 2018.

[62] R. A. Jabr. A conic quadratic format for the load flow equations of meshed networks. *IEEE Transactions on Power Systems*, 22(4):2285–2286, 2007.

[63] J. Lavaei and S. H. Low. Zero duality gap in optimal power flow problem. *IEEE Transactions on Power Systems*, 27(1):92–107, 2012.

[64] C. Coffrin, H. L. Hijazi, and P. Van Hentenryck. Strengthening the SDP relaxation of AC power flows with convex envelopes, bound tightening, and valid inequalities. *IEEE Transactions on Power Systems*, 32(5):3549–3558, 2017.

[65] R. D. Christie, B. F. Wollenberg, and I. Wangensteen. Transmission management in the deregulated environment. *Proceedings of the IEEE*, 88(2):170–195, 2000.

[66] J.D. Glover, M.S. Sarma, and T.J. Overbye. *Power Systems Analysis and Design*. Cengage Learning, 2012.

[67] J.A. Taylor. *Convex Optimization of Power Systemms*. Cambridge University Press, 2015.

[68] M. Feistauer. *Mathematical Methods in Fluid Dynamics*. Pitman Monographs and Surveys in Pure and Applied Mathematics Series 67, Longman Scientific & Technical, 1993.

[69] M.V. Lurie. *Modeling of Oil Product and Gas Pipeline Transportation*. Wiley VCH, 2009.

[70] F. Rømo, A. Tomasgard, L. Hellemo, M. Fodstad, B. H. Eidesen, and B. Pedersen. Optimizing the Norwegian natural gas production and transport. *Interfaces (Providence)*, 39(1):46–56, 2009.

[71] M. Fodstad, K. T. Midthun, and A. Tomasgard. Adding flexibility in a natural gas transportation network using interruptible transportation services. *European Journal of Operational Research*, 243(2):647–657, 2015.

[72] C. M. Correa-Posada and P. Sanchez-Martin. Integrated power and natural gas model for energy adequacy in short-term operation. *IEEE Transactions on Power Systems*, 30(6):3347–3355, 2014.

[73] C. Borraz-Sanchez, R. Bent, S. Backhaus, H. Hijazi, and P. Van Hentenryck. Convex relaxations for gas expansion planning. *INFORMS Journal on Computing*, 28(4):645–656, 2016.

[74] A. Tomasgard, F. Rømo, M. Fodstad, and K. Midthun. Optimization models for the natural gas value chain. In *Geometric Modelling, Numerical Simulation, Optimization*, pages 521–558. Springer Berlin Heidelberg, 2007.

[75] A. Ben-Tal, L. El Ghaoui, and A. Nemirovski. *Robust Optimization*. Princeton University Press, 2009.

[76] M. Qadrdan, J. Wu, N. Jenkins, and J. Ekanayake. Operating strategies for a GB integrated gas and electricity network considering the uncertainty in wind power forecasts. *IEEE Transactions on Sustainable Energy*, 5(1):128–138, 2014.

[77] P. Dueñas, T. Leung, M. Gil, and J. Reneses. Gas-electricity coordination in competitive markets under renewable energy uncertainty. *IEEE Transactions on Power Systems*, 30(1):123–131, 2015.

[78] M. Babula and K. Petak. The cold truth: Managing gas-electric integration: The ISO New England experience. *IEEE Power Energy Magazine*, 12(6):20–28, 2014.

[79] X. Guo, A. Beskos, and A. Siddiqui. The natural hedge of a gas-fired power plant. *Computational Management Science*, 13(1):63–86, 2016.

[80] C. Grigg, P. Wong, P. Albrecht, R. Allan, M. Bhavaraju, R. Billinton, Q. Chen, C. Fong, S. Haddad, S. Kuruganty, W. Li, R. Mukerji, D. Patton, N. Rau, D. Reppen, A. Schneider, M. Shahidehpour, and C. Singh. The IEEE reliability test system-1996. A report prepared by the reliability test system task force of the application of probability methods subcommittee. *IEEE Transactions on Power Systems*, 14(3):1010–1020, 1999.

[81] C. He, L. Wu, T. Liu, and M. Shahidehpour. Robust co-optimization scheduling of electricity and natural gas systems via ADMM. *IEEE Transactions on Sustainable Energy*, 8(2):658–670, 2017.

[82] W. Bukhsh. Data for stochastic multiperiod optimal power flow problem. https://sites.google.com/site/datasmopf/. Online; Accessed: 30.09.2018.

[83] C. Ordoudis, P. Pinson, and J. M. Morales. Electronic companion - An integrated market for electricity and natural gas systems with stochastic producers. http://doi.org/10.5281/zenodo.546145. Online; Accessed: 30.09.2018.

[84] J. M. Morales, M. Zugno, S. Pineda, and P. Pinson. Electricity market clearing with improved scheduling of stochastic production. *European Journal of Operational Research*, 235(3):765–774, 2014.

[85] Stefanos Delikaraoglou and Pierre Pinson. Optimal allocation of HVDC interconnections for exchange of energy and reserve capacity services. *Energy Systems*, 2018.

[86] V. M. Zavala, K. Kim, M. Anitescu, and J. Birge. A stochastic electricity market clearing formulation with consistent pricing properties. *Operations Research*, 65(3):557–576, 2017.

[87] CAISO. Aliso Canyon gas-electric coordination. http://www.caiso.com/Documents/DraftFinalProposal-AlisoCanyonGas-ElectricCoordinationPhase3.pdf. Online; Accessed: 30.09.2018.

[88] A. Henriot and J.-M. Glachant. Capacity remuneration mechanisms in the European market: now but how? *European University Institute (EUI), Robert Schuman Centre of Advanced Studies (RSCAS)*, 2014.

[89] C. Ordoudis, S. Delikaraoglou, J. Kazempour, and P. Pinson. Electronic companion - Market-based coordination for integrated electricity and natural gas systems under uncertain supply. https://doi.org/10.5281/zenodo.1283327. Online; Accessed: 5.4.2018.

[90] A. Nemirovski and A. Shapiro. Convex approximations of chance constrained programs. *SIAM Journal on Optimization*, 17(4):969–996, 2007.

[91] F. Alismail, P. Xiong, and C. Singh. Optimal wind farm allocation in multi-area power systems using distributionally robust optimization approach. *IEEE Transactions on Power Systems*, 33(1):536–544, 2018.

[92] P. Xiong, P. Jirutitijaroen, and C. Singh. A distributionally robust optimization model for unit commitment considering uncertain wind power generation. *IEEE Transactions on Power Systems*, 32(1):39–49, 2017.

[93] Y. Zhang, S. Shen, and J. L. Mathieu. Distributionally robust chance-constrained optimal power flow with uncertain renewables and uncertain reserves provided by loads. *IEEE Transactions on Power Systems*, 32(2):1378–1388, 2017.

[94] C. Duan, W. Fang, L. Jiang, L. Yao, and J. Liu. Distributionally robust chance-constrained approximate AC-OPF with Wasserstein metric. *IEEE Transactions on Power Systems*, 2018.

[95] Y. Wen, X. Qu, W. Li, X. Liu, and X. Ye. Synergistic operation of electricity and natural gas networks via ADMM. *IEEE Transactions on Smart Grid*, 2017.

[96] C. Wang, W. Wei, J. Wang, L. Bai, Y. Liang, and T. Bi. Convex optimization based distributed optimal gas-power flow calculation. *IEEE Transactions on Sustainable Energy*, 2017.

[97] P. N. Biskas, N. G. Kanelakis, A. Papamatthaiou, and I. Alexandridis. Coupled optimization of electricity and natural gas systems using augmented Lagrangian and an alternating minimization method. *International Journal of Electrical Power and Energy Systems*, 80:202–218, 2016.

[98] S. Zymler, D. Kuhn, and B. Rustem. Distributionally robust joint chance constraints with second-order moment information. *Mathematical Programming*, 137(1):167–198, 2013.

[99] W. Wiesemann, D. Kuhn, and M. Sim. Distributionally robust convex optimization. *Operations Research*, 62(6):1358–1376, 2014.

[100] R. T. Rockafellar and S. Uryasev. Optimization of conditional value-at-risk. *Journal of Risk*, 2(3):21–41, 2000.

[101] C. Ordoudis, V. A. Nguyen, D. Kuhn, and P. Pinson. Electronic companion - Energy and reserves dispatch with distributionally robust joint chance constraints. https://doi.org/10.5281/zenodo.1237026. Online; Accessed: 29.04.2018.

[102] G. C. Calafiore and L. El Ghaoui. On distributionally robust chance-constrained linear programs. *Journal of Optimimization Theory and Applications*, 130(1):1–22, 2006.

[103] A. Ahmadi-Khatir, A. J. Conejo, and R. Cherkaoui. Multi-area energy and reserve dispatch under wind uncertainty and equipment failures. *IEEE Transactions on Power Systems*, 28(4):4373–4383, 2013.

[104] M. Bazrafshan and N. Gatsis. Decentralized stochastic optimal power flow in radial networks with distributed generation. *IEEE Transactions on Smart Grid*, 8(2):787–801, 2017.

[105] Z. Li, W. Wu, M. Shahidehpour, and B. Zhang. Adaptive robust tie-line scheduling considering wind power uncertainty for interconnected power systems. *IEEE Transactions on Power Systems*, 31(4):2701–2713, 2016.

[106] C. Ordoudis and V.A. Nguyen. Electronic companion - Data-driven distributed operation of electricity and natural gas systems. https://doi.org/10.5281/zenodo.1439199. Online; Accessed: 30.09.2018.

Collection of relevant publications

[Paper A] Pierre Pinson, Lesia Mitridati, Christos Ordoudis and Jacob Østergaard (2017). "Towards Fully Renewable Energy Systems: Experience and Trends in Denmark," *CSEE Journal of Power and Energy Systems.*

[Paper B] Christos Ordoudis, Pierre Pinson and Juan Miguel Morales (2018). "An Integrated Market for Electricity and Natural Gas Systems with Stochastic Producers," *European Journal of Operational Research.*

[Paper C] Christos Ordoudis, Stefanos Delikaraoglou, Pierre Pinson and Jalal Kazempour (2017). "Exploiting Flexibility of Coupled Electricity and Natural Gas Systems: A Price-Based Approach," in the *Proceedings of IEEE PowerTech Conference 2017*, Manchester, UK.

[Paper D] Christos Ordoudis, Stefanos Delikaraoglou, Jalal Kazempour and Pierre Pinson (2018). "Market-based Coordination for Integrated Electricity and Natural Gas Systems Under Uncertain Supply," Submitted to *IEEE Transactions on Control of Network Systems.*

[Paper E] Christos Ordoudis, Viet Anh Nguyen, Daniel Kuhn and Pierre Pinson[1] (2018). "Energy and Reserve Dispatch with Distributionally Robust Joint Chance Constraints," working paper to be submitted to *IEEE Transactions on Power Systems.*

[Paper F] Christos Ordoudis and Viet Anh Nguyen[2] (2018). "Data-driven Distributed Operation of Electricity and Natural Gas Systems," *Working paper.*

[1] The list of authors may be subject to changes.
[2] The list of authors may be subject to changes.

[Paper A] Towards Fully Renewable Energy Systems: Experience and Trends in Denmark

Authors:
Pierre Pinson, Lesia Mitridati, Christos Ordoudis and Jacob Østergaard

Published in:
CSEE Journal of Power and Energy Systems, DOI: 10.17775/CSEEJPES.2017.0005.

Towards Fully Renewable Energy Systems: Experience and Trends in Denmark

Pierre Pinson, *Senior Member, IEEE,* Lesia Mitridati, Christos Ordoudis, *Student Member, IEEE,* and Jacob Østergaard, *Senior Member, IEEE*

***Abstract*—Deployment of renewable energy generation capacities and integration of their power production into existing power systems has become a global trend, with a common set of operational challenges stemming from variability and limited predictability of power generation from, e.g., wind and solar. Denmark is a country that invested early in wind energy, rapidly proposing very ambitious goals for the future of its energy system and global energy usage. While the case of Denmark is specific due to its limited size and good interconnections, there may still be a lot to learn from the way operational practice has evolved, also from shifting towards a liberalized electricity market environment, and more generally from going along with other technological and societal evolution. The aim of this paper is to give an overview of recent and current initiatives in Denmark that contributes towards a goal of reaching a fully renewable energy system.**

***Index Terms*—Coordination, energy markets, flexibility, integrated energy systems, renewable energy integration.**

I. Introduction

RENEWABLE energy deployment and integration is a global phenomenon, with numerous countries investing massive efforts to support this trend. Their motivations range from abating climate change's negative effects to ensuring the security of the energy supply. Renewable energy is often seen as a cornerstone in our move towards a more sustainable future [1]. The literature on challenges related to the integration of renewable energy generation is vast, and growing at a rapid pace. It covers a wide range of technical topics—from power system operation and control to economical, environmental, and societal topics in connection with the economics of change, life cycle assessment of renewable energy projects, and social acceptance of distributed energy generation projects. A good starting point to have an overview of challenges related to wind power in power systems is available in [2]. In contrast, it might be more difficult to find literature that tells about how renewable energy integration is seen in practice and supported by a number of initiatives, from adaptation of electricity markets to deployment of new components in the power system, but also of a regulatory nature. A notable exception of an overview of wind power integration studies is in [3] (and follow-up publications), which aims to propose best practice guidelines when designing and reporting on such complex system studies. In this context, we place emphasis here on the case of Denmark, a Scandinavian country with extensive experience in integrating wind power generation into its energy system, and also with very ambitious objectives of having its energy supply (for electricity, industry, transport and heating) fully covered by renewable energy by 2050 [4]. Recently, the IDA Energy Vision 2050 was published to provide an extensive coverage of scenarios and projections for residential electricity, industry, heating and cooling, as well as transport [5].

The Danish situation is often seen as propitious to the integration of renewable energy generation in view of its limited peak load (approximately 6.5 GW), substantial installed generation capacities (nearly 15 GW) and a strong interconnection to neighboring countries (7.2 GW as of 2015), with additional interconnection projects in the pipeline (e.g., with two new links to Germany and the UK, agreed upon in Spring 2016). An overview of such interconnections is given in Fig. 1 as of 2014, with the Skagerrak link to Norway upgraded to 1.7 GW in 2015. A complete description of the current electricity and gas systems in Denmark, as well as plans for their future development, is available in [6]. This situation contrasts with the opposite case of the Iberian peninsula, for instance, with a substantial peak load to be satisfied (up to 49.3 GW) and limited connection to the remainder of the European power system, through the 2.8 GW France-Spain interconnector.

However, reaching a fully renewable energy system is not only a matter of electric infrastructure, but also placing emphasis on other aspects that matter—from market mechanisms that adequately support renewable energy integration to stimulating and operating available flexibility (demand response, electric vehicles and storage, synergies with gas and electricity systems), and finally to having a more holistic view of energy production and consumption in a smart city context. After first giving a brief overview on history and current status with deployment of renewable energy generation capacities in Denmark in Section II, this paper describes in Section III the electricity market and power system operational framework

Manuscript received September 1, 2016; revised October 31, 2016; accepted November 26, 2016. Date of publication March 30, 2017; date of current version January 14, 2017. The authors are partly supported by the Danish Innovation Fund through the projects '5s' – Future Electricity Markets (12-132636/DSF) and CITIES (DSF-1305-00027B), as well as EUDP through the project EnergyLab Nordhavn (EUDP 64015-0055).

P. Pinson (corresponding author, e-mail: ppin@dtu.dk), L. Mitridati, C. Ordoudis, and J. Østergaard are with the Technical University of Denmark, Department of Electrical Engineering, Centre for Electric Power and Energy, Kgs. Lyngby, Denmark.

DOI: 10.17775/CSEEJPES.2017.0005

2096-0042 © 2017 CSEE

allowing the Danish power system to run with high shares of renewable power generation. Current challenges and foreseen changes are discussed. Subsequently in Section IV, emphasis is placed on the idea of getting the demand side to contribute to the integration of renewables by motivating, operating, and rewarding flexibility in consumption, or the so-called demand response. Initiatives to promote demand response were naturally generalized to smart cities considerations since having to look more broadly varied types of electric consumption and their specifics e.g., for transportation, as well as opportunities provided by dense urban environments. Eventually, this leads to the thinking of synergies between energy carriers or energy systems, which we present in Section V. Here, a discussion of the case of gas and heat in the Danish context is presented. Other recent considerations relate to the case of hydrogen and synthetic gas. We present our concluding remarks and perspectives in Section VI.

Source: Energinet.dk

Fig. 1. Interconnection to the Danish power system as of 2014.

II. Brief History and Status of Renewable Energy in Denmark

When thinking of renewable energy in Denmark, one clearly has wind power in mind, particularly, since the country pioneered the use of wind energy to meet its electric power consumption. This originates from a choice in the 1970s to invest in this solution to support abatement of CO_2 emissions. The Danish model is fairly unique, as it has historically been one of the most successful countries in terms of supporting deployment of wind power generation capacities. Starting from 1979, the capacity increased steadily, and only halted for a little period in the early 2000s, see Fig. 2. Looking towards the future, major wind power developments are planned mainly in the form of medium to large offshore wind farms (several hundreds of megawatts each) and through the repowering of older onshore wind farms. As of today, wind power is supplemented by non-negligible solar power capacities, nearly reaching 800 MW at the end of 2015.

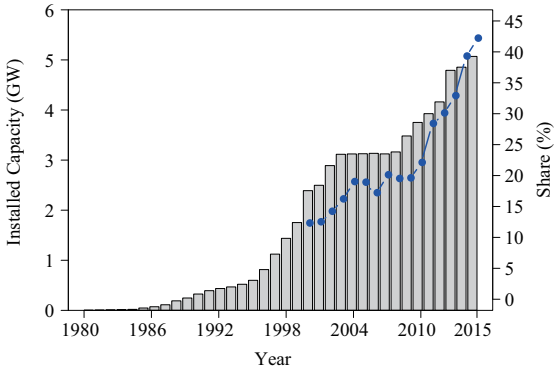

Source: Energinet.dk

Fig. 2. Evolution of installed wind power capacities as well as wind power penetration in Denmark.

The successful deployment of capacities and subsequent integration of renewable energy generation is part of a broader evolution, from a centralized to a decentralized setup for power generation in the country. This decentralization process means that, while Denmark had a limited number of relatively large power plants in the 1980s and 1990s, the power generation landscape rapidly evolved with the deployment of distributed generation capacities, obviously including wind turbines, more recently solar panels, but also combined heat and power (CHP) plants. The latter has the additional advantage of coupling heat and electricity systems which, as will be discussed later in this paper, also brings opportunities to accommodate renewable energy generation, particularly in the context of the fluctuations and limited predictability of CHPs.

For those interested in an exhaustive analysis of the Danish energy system and its evolution over the last two decades, the latest (i.e., for 2014) overall statistics on the Danish energy system are available in [7], giving a broad overview of generation mix, evolution of capacity by type, consumption by sector, etc.

III. From Electricity Markets to Power System Operation

A. Liberalization Process and Current Market Conditions for Renewable Energy Sources

Scandinavia was one of the first regions of the world to liberalize its electricity sector (both generation and retail), after The Energy Act of 1990 which laid the ground for the deregulation process in the region. We mention Scandinavia and not Denmark only because the electricity market is a regional one. With the deregulation of electricity markets also happening in other European countries, all those markets are getting fully integrated, yielding a number of operational and financial benefits, see e.g., [8]. The market operator for Scandinavia, now also covering other countries, e.g., U.K. and the Baltic countries, is Nord Pool[1].

[1]nordpoolspot.com

European electricity markets, such as the Scandinavian one, are primarily composed of a forward allocation mechanism, the day-ahead market, and of a balancing mechanism allowing to settle deviations from day-ahead schedule. Day-ahead markets are organized as zonal markets, hence only considering transmission capacity limitations between market zones. These are to be seen as financial markets anyway, while the link to power system operations is made by communicating energy production and consumption schedules to the various system operators. When reaching the balancing stage eventually, market-based operation is taken over by the system operators over their respective balancing areas. Accommodating renewables in such a deregulated environment is known to yield a number of operational problems (see, e.g., [9]) while support mechanisms and market designs should evolve accordingly [10].

Wind power producers were originally remunerated based on feed-in tariffs in the 1990s, i.e., a fixed price per MWh generated. They eventually got to participate in the electricity market as conventional power producers. This triggered a number of studies on the impact of wind power generation on market prices and market dynamics, see e.g., [11], [12]. Those concluded that, due to very low marginal costs and inherent variability, wind power generation induces a downward pressure on wholesale electricity prices. However, it is not as much the energy actually produced that impact prices than generation forecasts. This is since the day-ahead market is cleared long before operations (12 to 36 hours), hence requiring wind power offers to be based on predictions. An extensive overview of the policy measures, as well as their impact to support wind power in the Danish electricity market can be found in [13]. While wind power is the dominant renewable energy source in Denmark, solar power generation is now becoming non-negligible. Support conditions, as well as impact on electricity markets, are qualitatively similar to the case of wind energy, though with a time delay.

If jointly looking at day-ahead and balancing market mechanisms, these penalize renewable energy producers since day-ahead revenues are eventually decreased due to balancing costs stemming from deviations from day-ahead schedule (in connection with forecasting errors). However, this penalization can also be seen as an incentive for renewable energy producers to improve their forecasts, since intuitively a decrease in forecast error should readily lead to higher revenues. In practice, the situation is quite more complex as originally hinted by [14].

In Denmark a two-price imbalance settlement is used, meaning that only those that contribute to the system imbalance are to be penalized. As an example, a wind power producer who produces more than expected, while the overall system requires extra power to get back to balance, will not be penalized and receive the day-ahead price for each and every MWh in surplus. This asymmetry in balancing penalties may then work as incentives for renewable energy producers to offer in a more strategic manner, even though understanding and predicting system balance and related penalties naturally is a difficult task. In addition, owing to the significant renewable energy penetration in Denmark, offering strategies may definitely affect market outcomes, either since a single producer is a price-maker, or through population effects as actual production, information and its processing, are necessarily dependent for those renewable energy producers. For a discussion on these aspects, the interested reader is referred to [15]. Finally, while these market mechanisms act as an incentive to decrease energy imbalances on a per market unit basis, i.e., hourly, these do not concern the sub-hourly fluctuations in power delivery, which may eventually yield increased needs for ancillary services to accommodate these power fluctuations. Some have recently argued for mechanisms that would allow for a transparent attribution of these ancillary service costs to all actors of the power system, including renewable energy producers, hence laying the ground to support new business cases for flexibility providers, e.g., storage and demand response [16].

B. Links to Operational Aspects and Foreseen Challenges

Electricity markets, both day-ahead and balancing, function based on energy blocks to be delivered or consumed over hourly market time units. Since a constant balance between generation and consumption is needed, schedules obtained through electricity market clearing cannot give a complete overview of power system operational schedules. In practice, the hourly schedules from Nord Pool are translated into 5-minute operational schedule to be transmitted to the TSO [17]. In addition, in order to insure reliable and economic operation, the TSO is to purchase ancillary services, e.g., reserves, which may then be activated to accommodate imbalances. These are purchased before energy is traded through day-ahead market to prevent conflicts between short-term capacity reservation for system services and energy exchanges. With increased renewable energy penetration, this approach to operation is challenged. One may intuitively think of co-clearing reserve and energy, and generalize market mechanisms in a stochastic optimization framework so as to accommodate variability and uncertainty in renewable power generation [9]. Already, the Danish TSO, in concert with other Scandinavian TSOs, has taken a proactive stance when it comes to balancing operation, since power system reserves are deployed preventively and in a regional coordination framework. In practice, provided that transmission capacity is available, the Danish TSO may for instance readily profit from flexible and relatively inexpensive hydro capacities in Norway to balance the power system in Denmark.

Still, as for the case of many system operators worldwide, flexibility and consideration of a finer resolution in operation is a key to accommodating high-frequency fluctuations from both wind and solar power generation. Large Danish offshore wind farms may have power swings in the order of 100 MW within a few minutes, hence requiring availability and adequate operation of flexible balancing units. Flexibility in power system operations is a general concern in relation to renewable energy integration, see e.g., [18], [19].

Both in markets and in operations, forecasting of renewable energy generation is of utmost importance. Denmark was one of the first countries to invest heavily in developing forecasting

methodologies and to integrate forecasts in operational practice since the early 1990s. While renewable energy forecasting attracted little interest worldwide at that time, the literature is expanding steadily, with many new proposals with novel models and usage of new data types (remote sensing, weather forecast information, etc.) being proposed every year. For recent state-of-the-art in wind and solar power forecasting, the reader is referred to [20], [21], and [22]. These developments are generally directly translated to operational solutions made available on a commercial basis by some of the numerous forecast providers that flourish around the globe. Still today, many challenges remain in renewable energy forecasting, stemming from the increasing quantity of data being collected, number of sites to be considered, variety of data to assimilate in forecast methodologies (e.g., from lidars and weather radars for wind energy, and from sky imagers for the case of solar power). An overview of these challenges as well as proposals for better integration of forecasts in power system operation is given in [23]. Maybe the most relevant of these challenges is to optimally estimate forecast uncertainty, in a dynamic and conditional manner, and to then account for such uncertainty information in operational problems.

IV. Flexibility in Electric Power Consumption

Higher shares of wind and solar energy in the energy mix translate to increased needs for backup generation, or storage, for those times with low power generation, as well as increased flexibility to cope with variability in power generation, and re-dispatch in case of forecast errors. Flexibility in power system operation is high in Denmark, thanks to these interconnections, but also thanks to the CHP plants, whose level of flexibility was improved over the years through various technology upgrades. Consequently, in principle, Denmark may not be seen as a country where flexibility in electric power consumption and hence demand response, is the most necessary and most valuable to power system operation. However, flexibility in electric power consumption is seen as a potentially new degree of freedom in power system operation, being also relatively cheap or at least competitive with other flexibility options in terms of operational costs, while requiring limited investment costs. In addition, integration of renewables has supported a move towards electrification of, e.g., transportation (electric vehicles) and heating sectors (heat pumps). Therefore, it might be beneficial to optimize flexible operation of new consumption patterns in a market environment. Deployment of new electric consumption means embracing renewable energy policy is an important component of a future fully-renewable energy system, see e.g., [24], [25].

Demand response presents a large number of opportunities and challenges, which would be too many to discuss here. For an overview, the reader is referred to [26] and references therein. In order to learn about the deployment process, market design, operational aspects, as well as social aspects of demand response, one of the world's largest demand-response research and demonstration experiments was initiated in 2011 on the Danish island of Bornholm, located nearly 40 km off the southern coast of Sweden. The EcoGrid EU[2] project involved nearly 2000 households and small businesses, to take part in a market-based demand response experiment. The hypothesis of the project was that electricity markets could evolve so as to issue prices that would optimally support and control demand response by taking advantage of the dynamic and conditional elasticity of demand. In practice, this conditional dynamic elasticity links to thermal inertia of buildings, flexibility in charging patterns of electric vehicles, etc. An overview of the EcoGrid EU market architecture is given in [27], while it is illustrated in Fig. 3.

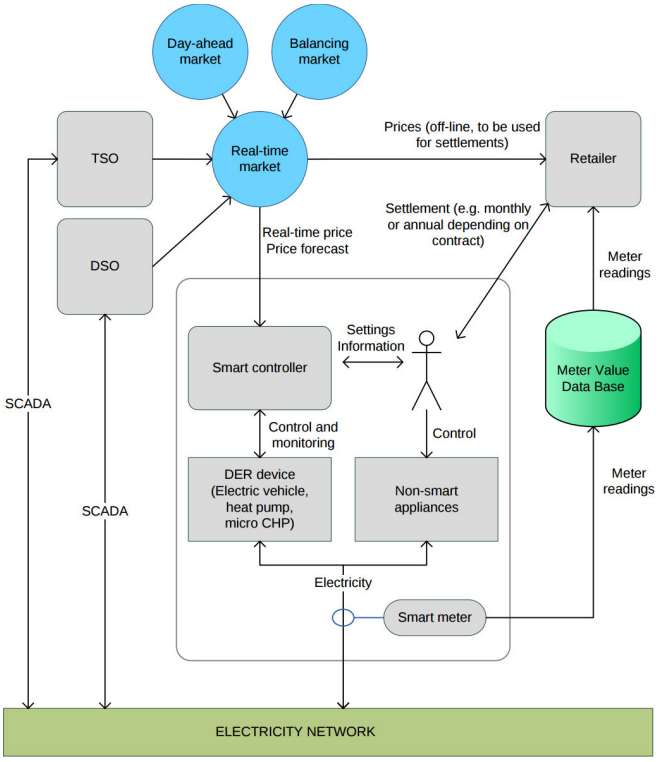

Fig. 3. Complete architecture of the EcoGrid EU experiment, combining control aspects to emulate demand response, market concepts to operate it, as well as metering and settlement aspects (taken from [28]).

The real-world experiment was organized in several phases. The first one was seen as an open-loop experiment to basically assess if and how the control systems deployed (and aggregators) were being responsive to modulation of electricity prices. This revealed to be a difficult task, though allowing to validate the price-responsiveness of most of electric loads involved, while providing a first quantification of the balancing that could be provided by demand response through such a market [29]. Subsequently, the second phase consisted of a closed loop experiment, where the market would be regularly cleared based on forecasts of the conditional elasticity of the electric loads, and then accounted for in the market clearing algorithm. This second phase ran for a period of nearly nine months and permitted to gain practical experience on market-based demand response. An extensive analysis of the market setup and results, also considering remaining challenges in

[2]eu-ecogrid.net

underlying concepts and implementation, is gathered in [30]. Some key figures include achieving a peak flexibility of 21.6%, as well as 8.6% increase in integration of wind power generation. In parallel, the most important conclusions from this analysis related to the need to improve forecasts to be used as input to market clearing, as well as to the thorough consideration of cross- elasticities (i.e., temporal dependence) in demand response. Finally, a third phase of the experiment concentrated on evaluating the possibility to support congestion management with market-based demand response. This part revealed that even though demand response could help, difficulties to predict localized demand response potential for small groups of electric loads, combined with the inherent uncertainty in such response, was potentially tampering the viability of demand response as a practical solution.

V. Smart Energy and Smart Cities

Beyond flexibility in electric power consumption, an approach accommodating further renewable energy relates to a more holistic view of the energy system. This includes interfacing with e.g., heat and gas, and its role in the more general context of smart cities. This approach acknowledges the fact that an increasing share of the population live in cities, and that modern means of data collection, communication and processing will allow for better control, operations, and planning of energy, transportation, etc. in a more integrated manner. For the specific case of Denmark, we first consider synergies between electricity and gas, and then with the heating system, while finally describing and discussing a real-world smart city development in Copenhagen, Denmark's capital city.

A. Potential Synergies with Gas

Gas-fired power plants (GFPPs) comprise one of the main power generation technologies nowadays and they are expected to have an even more prominent role in the future energy system. One of the main reasons for this will be the transition to an environmentally friendly energy system. GFPPs are characterized by fast ramping ability, as well as better efficiency and reduced emissions compared to other thermal power plants. These characteristics make them an ideal choice for the transition to a green energy system, especially if we take into account the potential of using green gases (e.g., biogas and synthetic gas) in the following years. For this reason, the interaction among the energy systems and especially between the electrical and gas networks is expected to increase. On top of that, the utilization of power-to-gas technologies will help this interaction to flourish.

Loose coupling among the electricity, gas and heat systems already exist, as many players (e.g., GFPPs, CHP plants etc.) interact with more than one of them. In countries and regions where these interactions have been noticed, some initial steps towards the coordination of the individual systems have been made, but as the interaction increases, more issues have to be solved. For example, ISO New England, which depends heavily on GFPPs to cover heat and electricity demand, faced significant difficulties in operating the power system in days with high heat and electricity demand [31]. This made it necessary to examine system and market dynamics between natural gas and electricity. Additionally, the need for coordinated operation of natural gas and electricity systems with high shares of renewables, such as in the case of Spain, is discussed in [32]. It is stated that market designs have to be reformulated and that the interdependency of the networks has to be studied under the uncertainty introduced by intermittent renewable energy.

In that vein, Denmark is placing a significant focus on the development and coordination of energy systems with increased shares of renewable energy sources, with the gas system playing an important role. As the shares of wind and solar power are expected to dominate power production, the GFPPs will mainly serve as peak-load generation, ensuring security of supply. For this reason, operation of the gas system has to be optimized and economically adapted under this new setup.

Increasing the interaction among the energy systems will also reveal the potential for energy storage in the gas (and heat, at different temporal and spatial scales) systems. The Danish system operator Energinet.dk owns two gas storage facilities with a capacity of 11 TWh methane gas and an additional capacity of 15–20 GWh in the gas network, which may be seen as large storage capabilities. An important peculiarity of the Danish case is the existence of a common system operator for electricity and natural gas (Energinet.dk) that readily permits a coordinated operation and cost-effective investment decisions for both systems. Such a setup with a common system operator can be also found in other European countries, e.g., Estonia, Luxembourg, and Portugal.

The large-scale integration of renewables in the energy systems can be facilitated by designing a coherent energy system that will be operated optimally under new market structures [33]. Electricity markets are the most mature and already undergoing massive changes due to the increased penetration of renewables in the power system [9]. Substantial changes have also been made in the natural gas market. A gas exchange, Gaspoint Nordic, has been established so that the players have the necessary marketplace to trade natural gas. Historically, the gas market was based on long-term contracts and bilateral agreements. However, a significant shift of the traded volume from the bilateral market to Gaspoint Nordic has been noticed lately. Traded volume in Gaspoint Nordic was 8.3 % of the total traded volume in 2010, while in 2015, this number increased to 58.2 %, showing a transformation of the gas market towards a more liquid and competitive model [34]. These new market models are expected to facilitate the coordination of the energy systems and raise new opportunities for players participating in them.

There are various sources of flexibility that the system operator can utilize to keep the system physically balanced. In Denmark, flexibility services can be procured from the available line pack in the pipeline network, as well as storage facilities that are controlled by the system operator and that can be operated by varying the production from the North Sea. However, the combination of line pack and storage facilities are the most commonly used ones due to their abundance. The

interaction between electricity and gas systems has increased dramatically in real-time operation, which strengthens the need for changes in the design of the gas balancing model. The limited speed with which gas travels when compared to electricity makes the flexibility in the gas system to be location and time dependent [35]. The usual balancing period used for the gas system is one day, and it is common that imbalances within predefined limits are not charged. In recent years, though, the optimal definition of these limits is of high importance as imbalance charges need to reflect the actual balancing costs [36]. Denmark, like most European countries, is putting a lot of focus on building an efficient balancing model, described in [37], that will optimally adjust the trade-off among exploiting the available flexibility of the gas system, ensuring security of supply and reflecting the imbalance costs.

Denmark is also vigorously investing in transforming the gas system to become greener. This can be accomplished by producing biogas from renewable energy sources, such as from biomass by thermal gasification or wind power by electrolysis. Biogas production was 7 PJ in 2015 and is expected to increase up to 14 PJ in 2020 [34]. Additionally, upgrading biogas and injecting it into the natural gas network will set biogas producers in a better and more competitive marketplace that will help the development of this technology in the future. It is foreseen that 10 % of the expected Danish gas consumption will be covered by upgraded biogas in 2020 [34].

The focus placed by various countries, including Denmark, on the coordination between electricity and natural gas systems is highlighted in a number of research studies. The impact of natural gas infrastructures on power systems is examined in [38]. Although the study focuses on the inter- dependency of the two networks in the U.S. setup, it demonstrates the impact of natural gas infrastructure contingencies and natural gas prices on electric power generation scheduling. In order to accomplish an efficient operation of an integrated system, new operational models have to be developed. Within this scope, the coupling model presented in [39] indicates a strong interdependence between the two networks pointing to a high potential in using a global model for operating the two systems. The study was performed in a realistic test case of the Greek electricity and gas systems showing that applying such models in reality is feasible. Additionally, different coordination scenarios between the two networks are studied in [40] quantifying the economic and technical benefits of coupling the electric power and natural gas infrastructures. The increased integration of renewables in the energy system has reinforced the link between the two systems close to real-time operation. For this reason, the proposal of short-term operational models is vital. For instance, a model of simulating the integrated electricity and natural gas systems in short-term operation is presented in [41]. In this work, the systems are coupled by taking into account the dynamics of gas. It is shown that gas travel velocity and the capacity of gas storage in the network play an important role in short-term operation and need to be modeled in order to get the maximum benefit from the system coordination.

As previously mentioned, the gas balancing problem has both a temporal and a spatial dimension making the development of short-term models important. In the same direction, an integrated model with wind power variability is proposed and studied in [42], showing that GFPPs would facilitate the integration of wind energy into power systems. Finally, the effects of utilizing power-to-gas in Denmark are examined in [43]. Test case results show a reduction in total system cost and wind power curtailment highlighting the benefits of investing in this new technology that will allow the bi-directional interaction of the systems to prosper.

These innovative insights will enable and facilitate the coordination of electricity and natural gas systems. Models applied to realistic case studies show a great potential to capture the existing synergies and build up new ones that will assist the progress towards a sustainable energy system in the future.

B. The Case of Heating in Denmark

The development of district heating in urban areas has been identified by the Heat Roadmap Europe as a key recommendation for a low-carbon heating sector in Europe [44]. DH has a central role in Denmark's energy strategy to meet the ambitious target of reaching a fully renewable energy system by 2050 [45], [46]. Indeed, 46% of Danish net heat demand is currently covered by district heating, mainly produced by combined heat and power (CHP) plants.

Interactions with the district heating system can provide additional flexibility in electric power system operation by generating heat from CHP plants during high electricity price periods, or from heat pumps and electric boilers during low electricity price periods. In addition, heat storage in the form of water tanks, combined with relocation technologies, can provide cost-effective energy storage capacity [33]. Exploiting the existing synergies between these systems can improve the efficiency and flexibility of the overall system, as well as facilitate the penetration of renewable energy sources in the power system.

Denmark has long been a leading country in the development of DH and has developed many initiatives to introduce competition and increase the efficiency of the DH system. In the Greater Copenhagen area, the day-ahead heat dispatch is prepared by Varmelast.dk, an independent market operator owned by the three major heat distribution companies. Although supply and retail heat prices are fixed, heat producers compete on their heat production costs and are dispatched based on a merit-order and a least cost principle. Fig. 4 shows the sequence of decisions for heat and electricity dispatch.

For CHPs, heat production costs are calculated as total production costs minus expected revenues from electricity sales. This approach ensures that the most efficient units are dispatched at each hour, and implicitly accounts for the interactions with the power sector. However, research is still needed to increase the flexibility in the heat system and model interactions and uncertainties from other energy systems. Indeed, as the heat dispatch is determined before the opening of the electricity market, and due to the constraints on their joint feasible operating regions, CHPs have a limited flexibility when participating in the day-ahead electricity market. Hence,

they are exposed to the risk of low prices and financial losses when participating in the electricity market eventually. In addition, the work in [48] showed that the inflexible heat-driven dispatch of CHP plants can have a negative impact on the power system and increase wind curtailment.

Additionally, over the last decades, due to the large penetration of wind power and the increasing number of hours with low electricity prices, CHP plants have become less profitable in the power market [49]. This has led to an increase in the use of oil boilers. In that context, large-scale heat pumps, electric boilers and heat storage have been investigated as sustainable alternatives to CHPs. In particular, HOFOR (utility in Copenhagen area) is currently installing in Copenhagen its first large-scale heat pump that will participate in the heat and electricity markets.

The literature on the integration and management of flexible heat sources is profuse. Reference [50] showed that exploiting existing heat storage capability of heat networks could provide operational flexibility and allow higher wind penetration in systems with insufficient ramping capacity. In parallel, Reference [51] showed the benefits of integrating electric boilers, heat pumps, and heat storage in the Danish energy system. By producing heat when electricity prices are low and decoupling the strong linkage between heat and power outputs of CHPs, these technologies can increase the flexibility of the overall system, and again reduce wind curtailment. Additionally, by lowering balancing costs and the number of hours with low electricity prices, these technologies increase the value of wind production. Fig. 5 (inspired by [48]) illustrates the virtually relaxed feasible operating region of an extraction CHP coupled with flexible heat sources. In addition, power-to-heat technologies, such as residential heat pumps and electric boilers, can provide additional flexibility to the system. In order to harness this flexibility from end-users, novel retail approaches are needed and are integrated in the scope of the Energylab Nordhavn project.

However, major challenges remain for the large-scale development of these technologies. Reference [52] showed that current taxes on electricity-based heat producers in Denmark reduced the profitability of electric boilers and heat pumps. In Copenhagen and Odense (third largest city in Denmark), flat heat tariffs for producers and consumers have also been challenged as they do not reflect actual heat production costs. In addition, the introduction of dynamic heat prices could be an additional argument for the development of large-scale heat pumps. In Aarhus (second largest city in Denmark), the heat market operator, Varmeplan Aarhus, has already implemented dynamic heat wholesale prices. Based on the experience in Aarhus, the CITIES project is investigating alternative heat supply tariffs [53].

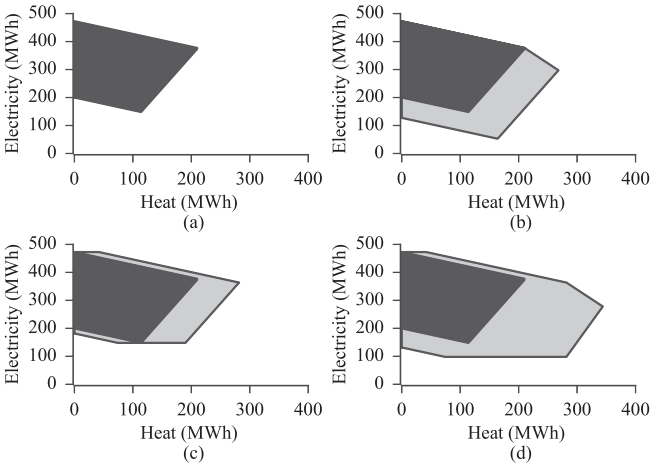

Fig. 5. Joint feasible operating region of an extraction CHP (inspired by [48]). (a) CHP only. (b) CHP and electric boiler. (c) CHP and heat storage. (d) CHP, electric boiler and heat storage.

Additionally, due to the large penetration of stochastic renewable energy sources, it is essential to model the growing uncertainty from the power sector for optimal heat dispatch. Reference [54] introduced uncertainties on heat demand and electricity prices and recast the joint heat and electricity dispatch of CHPs and heat storage in the Copenhagen area using piece-wise linear decision rules. This approach showed improvement in terms of robustness of the solution with minimum financial losses. In [52] the heat and electricity dispatch of CHPs is formulated as a two-stage stochastic optimization problem. This approach showed that traditional deterministic models tend to overestimate the benefits of installing heat pumps and electric boilers.

The aforementioned studies propose a co-optimization approach for heat and electricity dispatch. These approaches show improvements in terms of flexibility of the overall system and wind penetration. However they are difficult to implement

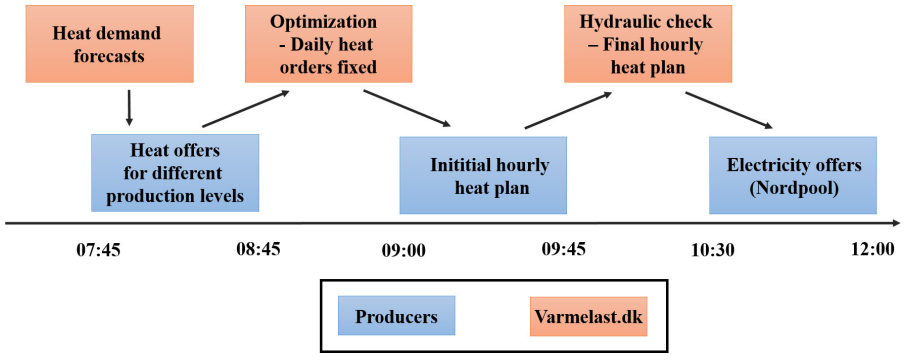

Fig. 4. Procedure for preparing heat plans in the Copenhagen area (inspired by [47]).

in the current Danish market framework. In [55], a novel approach is proposed for heat dispatch that is constrained by electricity dispatch. The day-ahead heat dispatch problem is modeled as a hierarchical stochastic optimization problem, where the lower-level problems represent electricity market clearing scenarios. This method allows independent heat market operators, such as Varmelast.dk, to dispatch optimal heat sources while anticipating the impact of the participation of CHPs in the day-ahead electricity market.

These studies hint at the fact that the development of flexible heat sources and a better modeling of the interactions with the power sector could increase the flexibility of the overall system. While stochastic and robust optimization models have shown improvements in flexibility, heat market operators in Denmark seem reluctant to adopt such methods. In order to better dispatch this potential flexibility in a deterministic market framework, new trading mechanisms incorporating flexible products for heat and electricity should be investigated.

C. EnergyLab Nordhavn Smart Living Lab

As for many other countries, there still remains a gap between all the studies cited here in the literature and actual deployment of operational and transparent solutions of practical value. These should also be supported by viable business models for existing and new actors in the energy system to engage in the proposed new operational practices. With that objective in mind, many initiatives for large demonstration projects have been started throughout Europe. These are most often deployed in a smart city context, hence taking part in a general momentum for improving infrastructures and their usage in urban environments.

In Denmark, Copenhagen aims to be a frontrunner sustainable city, an objective that was formulated in connection with the 2009 United Nations Climate Change Conference. It consists in becoming a carbon-neutral city by 2050. In practice, a relevant initiative is the development of the Nordhavn neighborhood in Copenhagen, to extend with housing and office space for 40,000 inhabitants and 40,000 office spaces in the long term. This extension of the neighborhood is to become a smart living lab for energy and its connection with other infrastructures. The EnergyLab Nordhavn[3] project started in 2015, placing emphasis on energy system integration, interaction with the transportation system, development of ICT- and storage-based management solutions for increased flexibility in power system operation, active distribution network planning etc. It comprises an interesting and ambitious large-scale public-private partnership to support relevant research and transfer of relevant technologies to an urban environment. A strong focus is also on new business models that help to rethink the relationship of customers to energy usage and its utility, e.g., by pricing indoor temperature and comfort instead of the usage of primary energy carriers like electricity and district heating. Such an initiative illustrates the strong commitment of Denmark to new models for research and initiative, seen as a cornerstone to the further integration of renewables into the energy system.

[3]energylabnordhavn.dk

VI. Conclusion

Denmark, supported by a strong political will, is a country that aims to fully meet its energy needs with renewable energy, hence with substantial penetration of wind and solar power generation means. While starting from a favorable standpoint, with good interconnections and existing flexibility on the supply side, it still faces a number of challenges to reach these goals. With a strong commitment to research and development, as well as a proactive attitude towards demonstration and real-world implementation, the country has invested in grand projects that will support renewable energy integration, with a particular focus on gaining and steering new flexibility in the system. Besides the role of interconnectors, such flexibility originates from electric demand response and more generally, coupling with transportation (through electric vehicles), heating (through, e.g., heat pumps and CHP plants), and with the gas system (also through generation means). While most of these developments have focused on technology and infrastructure, it is clear that future steps ought to focus on the social and market components of the renewable energy transition problem. The same way this transition has triggered a number of important changes in the system itself, it may also be an opportunity for changing the way people perceive energy production, exchange and consumption.

Acknowledgments

The authors acknowledge Henning Parbo, and more generally Energinet.dk the Transmission System Operator (TSO) in Denmark, for general input to this paper. Three reviewers, as well as an editor, are to be acknowledged for their comments and suggestions, which permitted to improve the version of the manuscript submitted originally.

References

[1] S. Chu, and A. Majumdar, "Opportunities and challenges for a sustainable energy future," *Nature*, vol. 488, no. 7411, pp. 294–303, Aug. 2012.

[2] T. Ackermann (ed.), *Wind Power in Power Systems, 2nd ed.* New York: Wiley, 2012.

[3] H. Holttinen, P. Meibom, A. Orths, B. Lange, M. O'Malley, J. O. Tande, A. Estanqueiro, E. Gomez, L. Söder, G. Strbac, J. C. Smith, and F. V. Hulle, "Impacts of large amounts of wind power on design and operation of power systems, results of IEA collaboration," *Wind Energy*, vol. 14, no. 2, pp. 179–192, Mar. 2011.

[4] Ministry of Climate, Energy and Building. (2012). Energy policy in Denmark. [Online]. Available: https://ens.dk/sites/ens.dk/files/Globalcooperation/energy_policy_in_denmark_eng.pdf

[5] B. V. Mathiesen, H. Lund, K. Hansen, I. Ridjan, S. R. Djørup, S. Nielsen, P. Sorknæs, J. Z. Thellufsen, L. Grundahl, R. S. Lund, D. W. David, D. Connolly, and P. A. Østergaard. IDA's energy vision 2050: A smart energy system strategy for 100% renewable Denmark. Department of Development and Planning, Aalborg University, Aalborg, Denmark. [Online]. Available: http://vbn.aau.dk/files/222230514/Main_Report_ IDAs_Energy_Vision_2050.pdf

[6] Energinet. System plan in Denmark Electricity and gas in Denmark, Energinet public report, Fredericia, Denmark, 2015. [Online]. Available: https://www.energinet.dk/SiteCollectionDocuments/Engelskedokumenter/Omos/SystemPlan2015.pdf

[7] Danish Energy Agency. (2016, Apr.). Energy statistics 2014 – Data, tables, statistics and maps. Danish Energy Agency, Copenhagen, Denmark. [Online]. Available: http://www.ens.dk/sites/ens.dk/files/info/tal-kort/statistik-noegletal/aarlig-energistatistik/energystatistics2014.pdf

[8] D. Newbery, G. Strbac, and I. Viehoff, "The benefits of integrating European electricity markets," *Energy Policy*, vol. 94, pp. 253–263, Jul. 2016.

[9] J. M. Morales, A. J. Conejo, H. Madsen, P. Pinson, and M. Zugno, *Integrating Renewables in Electricity Markets - Operation Problems*, New York: Springer, 2014.

[10] C. Hiroux and M. Saguan, "Large-scale wind power in European electricity markets: Time for revisiting support schemes and market designs?" *Energy Policy*, vol. 38, no. 7, pp. 3135–3145, Jul. 2010.

[11] P.-E. Morthorst, "Wind power and the conditions at a liberalized electricity market," *Wind Energy*, vol. 6, no. 3, pp. 297–308, Jun. 2003.

[12] T. Jönsson, P. Pinson, and H. Madsen, "On the market impact of wind energy forecasts," *Energy Economics*, vol. 32, no. 2, pp. 313–320, Mar. 2010.

[13] J. Munkgaard and P.-E. Morthorst, "Wind power in the Danish liberalised power market – Policy measures, price impact and investor incentives," *Energy Policy*, vol. 36, no. 10, pp. 3940–3947, Oct. 2008.

[14] K. Skytte, "The regulating power market on the Nordic power exchange Nord Pool: An econometric analysis," *Energy Economics*, vol. 21, no. 4, pp. 295–308, Aug. 1999.

[15] A. Papakonstantinou and P. Pinson, "Population dynamics for renewables in electricity markets: A minority game view," presented at *2016 International Conference on Probabilistic Methods Applied to Power Systems (PMAPS),* Beijing, China, 16–20 Oct. 2016.

[16] F. Bona, N. Gast, N. J. Y. L. Boudec, P. Pinson, and D.-C. Tomozei "Attribution mechanisms for ancillary service costs induced by variability in power delivery," *IEEE Transactions on Power Systems*, vol. PP, no. 99, pp. 1–1, Aug. 2016.

[17] Energinet. dk. (2011, Nov.). Regulation C3 – Handling of notifications and schedules - Daily procedures. [Online]. Available: https://www.energinet.dk/SiteCollectionDocuments/Engelske%20dokumenter/El/Regulation%20C3%20Handling%20of%20notifications%20and%20schedules.pdf

[18] E. Lannoye, D. Flynn, and M. O'Malley, "Evaluation of power system flexibility," *IEEE Transactions on Power Systems*, vol. 27, no. 2, pp. 922–931, Jan. 2012.

[19] J. Y. Zhao, T. X. Zheng, and E. Litvinov, "A unified framework for defining and measuring flexibility in power system," *IEEE Transactions on Power Systems*, vol. 31, no. 1, pp. 339–347, Jan. 2016.

[20] G. Giebel, R. Brownsword, G. Kariniotakis, M. Denhard, and C. Draxl. (2011). The state-of-the-art in short-term prediction of wind power: a literature overview, 2nd edition. [Online]. Available: http://orbit.dtu.dk/files/5277161/GiebelEtAl-StateOfTheArtInShortTermPrediction_ANEMOSplus_2011%20(2).pdf

[21] C. Monteiro, H. Keko, R. Bessa, V. Miranda, A. Botterud, J. Wang, and G. Conzelmann, "A quick guide to wind power forecasting: State-of-the-art 2009," Technical Report ANL/DIS-10-2, Argonne National Laboratory USA, 2009.

[22] R. H. Inman, H. T. C. Pedro, and C. F. M. Coimbra, "Solar forecasting methods for renewable energy integration," *Progress in Energy and Combustion Science*, vol. 39, no. 6, pp. 535–576, Dec. 2013.

[23] P. Pinson, "Wind energy: Forecasting challenges for its operational management," *Statistical Science*, vol. 28, no. 4, pp. 564–585, Nov. 2013.

[24] P. H. Anderson, J. A. Mathews, and M. Rask, "Integrating private transport into renewable energy policy: T*he strategy of creating intelligent recharging grids for electric vehicles*," *Energy Policy*, vol. 37, no. 7, pp. 2481–2486, Jul. 2009.

[25] K. Hedegaard, H. Ravn, N. Juul, and P. Meibom, "Effects of electric vehicles on power systems in Northern Europe," *Energy*, vol. 48, no. 1, pp. 356–368, Dec. 2012.

[26] N. O'Connell, P. Pinson, H. Madsen, and M. O'Malley "Benefits and challenges of electric demand response: A critical review," *Renewable & Sustainable Energy Reviews*, vol. 39, no. 6, pp. 686–699, Nov. 2014.

[27] Y. Ding, S. Pineda, P. Nyeng, J. Østergaard, E. M. Larsen, and Q. Wu, "Real-time market concept architecture for EcoGrid EU – A prototype for European smart grids," *IEEE Transactions on Smart Grid*, vol. 4, no. 4, pp. 2006–2016, Dec. 2013.

[28] P. Lund, P. Nyeng, and co-authors. (2016). Deliverable 6.7: Overall evaluation and conclusions. Energinet, Denmark. [Online]. Available: http://www.eu-ecogrid.net/images/Documents/D6.7 160121 Final.pdf

[29] G. L. Ray, E. M. Larsen, and P. Pinson, "Evaluating price-based demand response in practice - with application to the EcoGrid EU experiment," *IEEE Transactions on Smart Grid*, vol. PP, no. 99, pp. 1–1, Sep. 2016.

[30] E. M. Larsen, "Demand response in a market environment," Ph. D. thesis, Technical University of Denmark, 2016.

[31] M. Babula and K. Petak, "The cold truth: Managing gas-electric integration: The ISO New England experience," *IEEE Power and Energy Magazine*, vol. 12, no. 6, pp. 20–28, Nov. 2014.

[32] B. J. Gil, Á. Caballero, and A. J. Conejo, "Power cycling: CCGTs: The critical link between the electricity and natural gas markets," *IEEE Power and Energy Magazine*, vol. 12, no. 6, pp. 40–48, Nov. 2014.

[33] P. Meibom, K. B. Hilger, H. Madsen, and D. Vinther, "Energy comes together in Denmark: The key to a future fossil-free Danish power system," *IEEE Power and Energy Magazine*, vol. 11, no. 5, pp. 46–55, Sep. 2013.

[34] Energinet. dk. (2015, Nov.). System plan 2015: Electricity and gas in Denmark. [Online]. Available: https://www.energinet.dk/SiteCollectionDocuments/Engelske%20dokumenter/Om%20os/System%20Plan%202015.pdf

[35] N. Keyaerts, "Gas balancing and line-pack flexibility," Ph. D. thesis, University of Leuven, 2012.

[36] A. V. Dinther, and M. Mulder, "The allocative efficiency of the Dutch gas-balancing market," *Competition and Regulation in Network Industries*, vol. 14, no. 1, pp. 47– 72, Jan. 2013.

[37] Energinet. dk. (2016, Oct.). Rules for gas transport version 16.0. [Online]. Available: http://www.energinet.dk/SiteCollectionDocuments/Engelske%20dokumenter/Gas/RfG%20version%2016.0%20-%20Final.pdf

[38] M. Shahidehpour, Y. Fu, and T. Wiedman, "Impact of natural gas infrastructure on electric power systems," *Proceedings of the IEEE*, vol. 93, no. 5, pp. 1042–1056, May 2005.

[39] P. N. Biskas, N. G. Kanelakis, A. Papamatthaiou, and I. Alexandridis, "Coupled optimization of electricity and natural gas systems using aug- mented Lagrangian and an alternating minimization method," *International Journal of Electrical Power & Energy Systems*, vol. 80, pp. 202–218, Sep. 2016.

[40] A. Zlotnik, L. Roald, S. Backhaus, M. Chertkov, and G. Andersson, "Coordinated scheduling for interdependent electric power and natural gas infrastructures," *IEEE Transactions on Power Systems*, vol. 32, no. 1, pp. 600–610, Jan. 2016.

[41] C. M. Correa-Posada and P. Sánchez-Martín, "Integrated power and natural gas model for energy adequacy in short-term operation," *IEEE Transactions on Power Systems*, vol. 30, no. 6, pp. 3347–3355, Nov. 2015.

[42] A. Alabdulwahab, A. Abusorrah, X. P. Zhang, and M. Shahidehpour, "Coordination of interdependent natural gas and electricity infrastructures for firming the variability of wind energy in stochastic day-ahead scheduling," *IEEE Transactions on Sustainable Energy*, vol. 6, no. 2, pp. 606–615, Apr. 2015.

[43] V. Heinisch and L. A. Tuan, "Effects of power-to-gas on power systems: A case study of Denmark," presented at *PowerTech, 2015 IEEE Eindhoven*, 2015.

[44] Heat roadmap Europe – A low-carbon heating and cooling strategy for Europe. [Online]. Available: http://www.heatroadmap.eu/

[45] H. Lund, B. Möller, B. V. Mathiesen, and A. Dyrelund, "The role of district heating in future renewable energy systems," *Energy*, vol. 35, no. 3, pp. 1381–1390, Mar. 2010.

[46] M. Mnster, P. E. Morthorst, H. V. Larsen, L. Bregnbæk, J. Werling, H. H. Lindboe, and L. H. Ravn, "The role of district heating in future Danish energy system," *Energy*, vol. 48, no. 1, pp. 47–55, Dec. 2012.

[47] Varmelast. dk. Heating plans. [Online]. Available: http://www.varmelast.dk/en/heat-plans/heating-plans

[48] X. Y. Chen, C. Q. Kang, M. O'Malley, Q. Xia, J. H. Bai, C. Liu, R. F. Sun, W. Z. Wang, and H. Li, "Increasing the flexibility of combined heat and power for wind power integration in China: Modeling and implications," *IEEE Transactions on Power Systems*, vol. 30, no. 4, pp. 1848–1857, Jul. 2015.

[49] R. Lund and U. Persson, "Mapping of potential heat sources for heat pumps for district heating in Denmark," *Energy*, vol. 110, pp. 129–138, Sep. 2016.

[50] Z. G. Li, W. C. Wu, M. Shahidehpour, J. H. Wang, and B. M. Zhang, "Combined heat and power dispatch considering pipeline energy storage of district heating network," *IEEE Transactions on Sustainable Energy*, vol. 7, no. 1, pp. 12–22, Jan. 2016.

[51] P. Meibom, J. Kiviluoma, R. Barth, H. Brand, C. Weber, and H. V. Larsen, "Value of electric heat boilers and heat pumps for wind power integration," *Wind Energy*, vol. 10, no. 4, pp. 321–337, Jul. 2007.

[52] M. G. Nielsen, J. M. Morales, M. Zugno, T. E. Pedersen, and H. Madsen, "Economic valuation of heat pumps and electric boilers in the Danish energy system," *Applied Energy*, vol. 167, pp. 189–200, Apr. 2016.

[53] M. Togeby, B. Bach, and N. Dupont. (2016). Dynamic prices for district heating in Aarhus – Preliminary results. [Online]. Available: http://

smart-cities-centre.org/wp-content/uploads/021-Nina-Dupond-CITIES-Dynamic-prices-for-district-heating.pdf

[54] M. Zugno, J. M. Morales, and H. Madsen, "Commitment and dispatch of heat and power units via affinely adjustable robust optimization," *Computers & Operations Research*, vol. 75, no. 8, pp. 191–201, Nov. 2016.

[55] L. Mitridati and P. Pinson. (2016, Oct.). Optimal coupling of heat and electricity systems: A stochastic hierarchical approach. Presented at 2016 International Conference on Probabilistic Methods Applied to Power Systems (PMAPS). [Online]. Available: http://pierrepinson.com/docs/Mitridati2016.pdf

Pierre Pinson (M'11–SM'13) received the M.Sc. degree in applied mathematics from the National Institute for Applied Sciences (INSA Toulouse, France) and the Ph.D. degree in energetics from Ecole des Mines de Paris (France). He is a Professor at the Technical University of Denmark (DTU), Centre for Electric Power and Energy, Department of Electrical Engineering, also heading a group focusing on Energy Analytics & Markets. His research interests include among others forecasting, uncertainty estimation, optimization under uncertainty, decision sciences, and renewable energies. He is an Editor for the *International Journal of Forecasting,* and for *Wind Energy*.

Lesia Mitridati received the master's degree in science and executive engineering from Mines ParisTech, France, in 2015. She is currently pursuing the Ph.D. degree at the Department of Electrical Engineering of the Technical University of Denmark (DTU). Her research interests include electricity markets, multi-energy systems, stochastic programming and hierarchical optimization.

Christos Ordoudis (S'08) received the Dipl.-Eng. Degree from the Department of Electrical and Computer Engineering, Aristotle University of Thessaloniki, Greece, in 2012 and the M.Sc. degree in sustainable energy from the Technical University of Denmark in 2014. He is currently pursuing the Ph.D. degree at the Department of Electrical Engineering of the Technical University of Denmark. His research interests include energy markets modeling, power and gas systems economics and operations, optimization theory and decision-making under uncertainty.

Jacob Østergaard (M'95–SM'09) received the M.Sc. degree in electrical engineering from the Technical University of Denmark (DTU), Lyngby, Denmark (DTU), in 1995. He is a Professor and Head of the Centre for Electric Power and Energy, Department of Electrical Engineering at DTU. From 1995 to 2005, he worked for the Research Institute for the Danish Electric Utilities.

Prof. Østergaard serves in several professional organizations including the EU SmartGrids advisory council. His research interests include system integration of wind power, control architecture for future power systems, and demand side.

[Paper B] An Integrated Market for Electricity and Natural Gas Systems with Stochastic Power Producers

Authors:
Christos Ordoudis, Pierre Pinson and Juan Miguel Morales

Published in:
European Journal of Operational Research, DOI: https://doi.org/10.1016/j.ejor.2018.06.036.

European Journal of Operational Research 272 (2019) 642–654

Contents lists available at ScienceDirect

European Journal of Operational Research

journal homepage: www.elsevier.com/locate/ejor

Innovative Applications of O.R.

An Integrated Market for Electricity and Natural Gas Systems with Stochastic Power Producers

Christos Ordoudis [a,*], Pierre Pinson [a], Juan M. Morales [b]

[a] Department of Electrical Engineering, Technical University of Denmark, Kgs. Lyngby, Denmark
[b] Department of Applied Mathematics, University of Málaga, Málaga, Spain

ARTICLE INFO

Article history:
Received 1 July 2017
Accepted 20 June 2018
Available online 27 June 2018

Keywords:
OR in energy
Integrated energy systems
Electricity and natural gas markets coordination
Renewable energy
Stochastic programming

ABSTRACT

In energy systems with high shares of weather-driven renewable power sources, gas-fired power plants can serve as a back-up technology to ensure security of supply and provide short-term flexibility. Therefore, a tighter coordination between electricity and natural gas networks is foreseen. In this work, we examine different levels of coordination in terms of system integration and time coupling of trading floors. We propose an integrated operational model for electricity and natural gas systems under uncertain power supply by applying two-stage stochastic programming. This formulation co-optimizes day-ahead and real-time dispatch of both energy systems and aims at minimizing the total expected cost. Additionally, two deterministic models, one of an integrated energy system and one that treats the two systems independently, are presented. We utilize a formulation that considers the linepack of the natural gas system, while it results in a tractable mixed-integer linear programming (MILP) model. Our analysis demonstrates the effectiveness of the proposed model in accommodating high shares of renewables and the importance of proper natural gas system modeling in short-term operations to reveal valuable flexibility of the natural gas system. Moreover, we identify the coordination parameters between the two markets and show their impact on the system's operation and dispatch.

© 2018 Elsevier B.V. All rights reserved.

1. Introduction

Natural gas is considered an efficient and clean fuel that will have a key role in the future energy system. Older coal and nuclear power plants are gradually decommissioned and replaced by gas-fired power plants (GFPPs) and renewable sources of energy. The electric power sector is expected to be the main driver of natural gas consumption increase in the future (U.S. Energy Information Administration, 2016), which will result in a tight coupling of both energy systems. In addition, the large-scale integration of uncertain and variable renewable energy production makes operational flexibility essential in energy systems. GFPPs are a well-suited flexible component for the energy system that can support other flexible sources in the power system (e.g., hydro power) but, most importantly, enhance the link with the natural gas system and the opportunity to exploit its available flexibility. In order to facilitate the operation of the future energy system, the structure of electricity and natural gas markets needs to be reconsidered.

In the existing setup, the main inefficiencies stem from the imperfect coordination between the trading floors, as well as between the markets for those two energy commodities, i.e., electricity and natural gas. Traditionally, the electricity and natural gas markets are cleared independently and their communication is based on the interface provided by GFPPs via predefined coordination parameters, such as their fuel consumption, which depends on their dispatch in the electricity market and the price of natural gas (Duenas, Leung, Gil, & Reneses, 2015). These parameters are defined in a static way due to the imperfect coordination between the two markets. However, a static definition of these parameters does not permit the development of an efficient coordinated setup between the two markets that will allow the interaction of the two systems to flourish. In various regions around the world that highly depend on GFPPs for electricity production, several coordination schemes are considered in practice highlighting the need to further investigate this topic. For instance, ISO New England increased the coordination with the natural gas sector and studies the impact of fuel demand of GFPPs on the operation of both systems (Babula & Petak, 2014). A limited market coordination would result in jeopardizing available flexibility and reliability, which encourages regulators to define setups that support existing synergies. Additionally, current market designs are based on sequential independent

* Corresponding author.
E-mail addresses: chror@elektro.dtu.dk (C. Ordoudis), ppin@elektro.dtu.dk (P. Pinson), juan.morales@uma.es (J.M. Morales).

https://doi.org/10.1016/j.ejor.2018.06.036
0377-2217/© 2018 Elsevier B.V. All rights reserved.

Nomenclature

Parameters

Γ_z	compressor factor located at natural gas network branch z [-].
$\overline{W}_j$	capacity of stochastic power plant j [MW].
ϕ_{i_g}	power conversion factor of natural gas-fired power plant i_g [kcf/MWh].
π_ω	probability of scenario ω [-].
$\tilde{M}$	sufficiently large constant [-].
$\widehat{W}_{j,t}$	expected power production by stochastic power plant j in period t [MW].
$B_{n,\,r}$	absolute value of the susceptance of line (n,r) [per unit].
C_i^+, C_i^-	up/down regulation offer price of dispatchable power plant i [$/MWh].
C_k^+, C_k^-	up/down regulation offer price of natural gas producer k [$/kcf].
C_s^+, C_s^-	up/down regulation offer price of natural gas storage s [$/kcf].
$C^{\text{sh, E}}$	cost of electricity load shedding [$/MWh].
$C^{\text{sh, G}}$	cost of natural gas load shedding [$/kcf].
C_i	day-ahead offer price of dispatchable power plant i [$/MWh].
C_k, C_s	day-ahead offer price of natural gas producer k and storage s [$/kcf].
$D_{n,t}^{\text{E}}$	electricity demand at node n and in period t [MW].
$D_{m,t}^{\text{G}}$	natural gas demand at node m and in period t [kcf/h].
$E_s^{\text{min/max}}$	minimum and maximum level of storage s [kcf].
$F_{n,r}^{\text{max}}$	transmission capacity of line (n,r) [MW].
G_k^+, G_k^-	maximum up/down reserve offered by natural gas producer k [kcf/h].
G_k^{max}	capacity of natural gas producer k [kcf/h].
IR_s, WR_s	injection and withdrawal rates of storage s [kcf/h].
$K_{m,u}^{\text{h/f}}$	linepack (h) and natural gas flow (f) constant of pipeline (m,u) [kcf/psig, kcf/(psig · h)].
P_i^+, P_i^-	maximum up/down reserve offered by dispatchable power plant i [MW].
P_i^{max}	capacity of dispatchable power plant i [MW].
$PR_m^{\text{min/max}}$	minimum and maximum pressure at node m [psig].
$W_{j,\,\omega,\,t}$	power production by stochastic power plant j in scenario ω, period t [MW].

Sets

Ω	set of stochastic power production scenarios ω.
Θ	set of primal optimization variables defined for each optimization model.
$A_m^{I_g}$	set of natural gas-fired power plants i_g located at natural gas network node m.
A_m^K	set of natural gas producers k located at natural gas network node m.
A_m^S	set of natural gas storages s located at natural gas network node m.
A_n^I	set of dispatchable power plants i located at electricity network node n.
A_n^J	set of stochastic power plants j located at electricity network node n.
I	set of dispatchable power plants i.
I_c	set of thermal power plants i_c ($I_c \subset I$).
I_g	set of natural gas-fired power plants i_g ($I_g \subset I$).
J	set of stochastic power plants j.
K	set of natural gas producers k.
L	set of electricity transmission lines l.
M	set of natural gas network nodes m.
N	set of electricity network nodes n.
S	set of natural gas storages s.
T	set of time periods t.
V	set of fixed pressure points v for the linearization of Weymouth equation.
Z	set of natural gas network branches z.

Variables

$\hat{\delta}_{n,t}$	voltage angle at node n and in period t [rad].
$\hat{\lambda}_{n,t}^{\text{E}}$	electricity locational marginal price in day-ahead market at node n and period t [$/MWh].
$\hat{\lambda}_{m,t}^{\text{G}}$	natural gas locational marginal price in day-ahead market at node m and period t [$/kcf].
$\hat{f}_{n,r,t}$	power flow on line (n,r) and in period t [MW].
$\tilde{\delta}_{n,\omega,t}$	voltage angle at node n in scenario ω, period t [rad].
$\tilde{\lambda}_{n,\omega,t}^{\text{E}}$	electricity locational marginal price in balancing market at node n in scenario ω, period t [$/MWh].
$\tilde{\lambda}_{m,\omega,t}^{\text{G}}$	natural gas locational marginal price in balancing market at node m in scenario ω, period t [$/kcf].
$\tilde{f}_{n,r,\omega,t}$	power flow on line (n,r), in scenario ω, period t [MW].
$e_{s,\,t}$	natural gas volume in storage facility s and in period t [kcf].
$g_{k,\omega,t}^{+/-}$	up/down regulation provided by natural gas producer k in scenario ω, period t [kcf/h].
$g_{s,t}^{\text{in/out}}$	in- and outflow natural gas rates of storage s in period t [kcf/h].
$g_{s,\omega,t}^{\text{in/out,r}}$	in- and outflow natural gas rates of storage s in scenario ω, period t [kcf/h].
$g_{k,\,t}$	day-ahead dispatch of natural gas producer k in period t [kcf/h].
$h_{m,\,u,\,t}$	average mass of natural gas (linepack) in pipeline (m,u), period t [kcf].
$h_{m,u,\omega,t}^{\text{r}}$	average mass of natural gas (linepack) in pipeline (m,u), scenario ω, period t [kcf].
$l_{n/m,\omega,t}^{\text{sh,E/G}}$	electric power and natural gas load shedding at node n/m in scenario ω, period t [MW, kcf/h].
$p_{i,\omega,t}^{+/-}$	up/down regulation provided by dispatchable power plant i in scenario ω, period t [MW].
$p_{i,t}$, $w_{j,t}$	day-ahead dispatch of power plants i and j in period t [MW].
$pr_{m,\omega,t}^{\text{r}}$	pressure at node m in scenario ω, period t [psig].
$pr_{m,\,t}$	pressure at node m and in period t [psig].
$q_{m,u,\omega,t}^{\text{in/out,r}}$	in- and outflow natural gas rates of pipeline (m,u) in scenario ω, period t [kcf/h].
$q_{m,\,u}$	natural gas flow in pipeline (m,u) [kcf/h].
$q_{m,u,t}^{\text{in/out}}$	In- and outflow natural gas rates of pipeline (m,u) in period t [kcf/h].
$w_{j,\omega,t}^{\text{sp}}$	power spilled by stochastic power plant j in scenario ω, period t [MW].
$y_{m,u,\omega,t}^{\text{r}}$	binary variable defining the direction of the natural gas flow in pipeline (m,u), scenario ω, period t {0,1}.
$y_{m,\,u,\,t}$	binary variable defining the direction of the natural gas flow in pipeline (m,u), period t {0,1}.

auctions, with the day-ahead and the balancing markets as the main trading floors. This sequential approach prevents an intertemporal coordination between these trading floors that could facilitate the integration of variable and uncertain renewables. On

the other hand, a market design based on stochastic programming, as proposed in Pritchard, Zakeri, and Philpott (2010) and Morales, Conejo, Liu, and Zhong (2012), co-optimizes the day-ahead and balancing stages and is able to provide a dispatch that anticipates future balancing needs.

Over the last years, an increased interest in studying the interaction between the electricity and natural gas systems has been raised. Geidl and Andersson (2007) and An, Li, and Gedra (2003) incorporate natural gas network constraints in the optimal power flow problem, while the unit commitment problem with natural gas security constraints is solved in Liu, Shahidehpour, Fu, and Li (2009) and Li, Eremia, and Shahidehpour (2008). Biskas, Kanelakis, Papamatthaiou, and Alexandridis (2016) use an Augmented Lagrangian method to jointly optimize the electricity and natural gas systems including unit commitment decisions. The aforementioned contributions utilize a steady-state approach to model the natural gas system which may result in suboptimal solutions when considering short-term operations. In contrast to the electricity system, natural gas can be stored in the network and moves with a lower speed than electricity. These characteristics are important as they endow the natural gas system with flexibility that can be exploited to ensure reliability; especially in cases of highly variable withdrawals by the GFPPs. Liu, Shahidehpour, and Wang (2011) and Chaudry, Jenkins, and Strbac (2008) model the natural gas system with linepack (i.e., ability of storing natural gas in the pipelines) by solving a mixed-integer nonlinear and a nonlinear program, respectively. However, these approaches do not guarantee global optimal solutions, involve high computation times and are not suitable to be included in a market mechanism as it is hard to derive prices from them. Additionally, Correa-Posada and Sanchez-Martin (2014) propose a linearization approach based on mixed-integer linear programming to efficiently approximate a dynamic natural gas model that is easier to solve at global optimality. Liu et al. (2009), Li et al. (2008) and Alabdulwahab, Abusorrah, Zhang, and Shahidehpour (2015) consider the natural gas network constraints only to ensure feasibility and do not optimize the operational cost of the natural gas system. Hence, the optimal operation of the integrated energy system is not guaranteed.

Several works have dealt with the presence of uncertain renewable production in coordinated electricity and natural gas systems. Alabdulwahab et al. (2015) present a stochastic programming approach, while Bai et al. (2016) utilize interval optimization. In both cases, a proper representation of the natural gas system with linepack is neglected. Qadrdan, Wu, Jenkins, and Ekanayake (2014) and He, Wu, tianqi Liu, and Shahidehpour (2016) take the linepack into account in a stochastic nonlinear program and a robust co-optimization model that utilizes the alternating direction method of multipliers (ADMM) to separate electricity and natural gas systems, respectively. An alternative approach to improve the coordination between electricity and gas networks is proposed in Clegg and Mancarella (2016), where a flexibility metric is calculated and included in the electricity system operation to impose natural gas related constraints. Moreover, the impact of power-to-gas technology is studied in Clegg and Mancarella (2015) along with its potential to facilitate wind power integration.

Acknowledging the necessity for an improved coordination between electricity and natural gas short-term markets with high penetration of stochastic production, we propose a coupled clearing model that anticipates future balancing needs and optimally dispatches the integrated energy system. The proposed model is formulated as a two-stage stochastic programming problem inspired by Morales et al. (2012). Moreover, we include linepack in the natural gas system modeling, which is taken into account both in the day-ahead and balancing stages. Comparing the proposed approach with a purely steady-state natural gas model, we highlight the significance of taking into account the linepack flexibility in real-time operation. The contributions of the paper are summarized as follows:

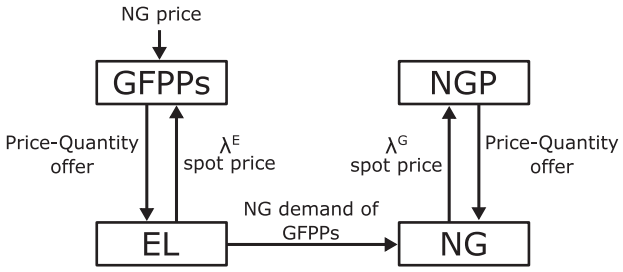

Fig. 1. Electricity and natural gas markets coordination. GFPPs: Gas-fired power plants, NGP: Natural gas producers, EL: Electricity market and NG: Natural gas market.

1. Three market-clearing models are provided, ranging from the current decoupled and deterministic setups to the proposed coupled and stochastic approach. The aim is to identify and address the efficiency improvement by considering a coordinated framework between systems and trading floors.
2. A market design that couples the electricity and natural gas markets in the day-ahead and balancing stages, while considering the uncertainty introduced by stochastic power producers, is proposed. Moreover, an effective pricing scheme is developed and the relation of GFPPs' operating cost with the outcomes of the natural gas market is taken into account.
3. A tractable and linearized natural gas model with linepack is considered, while we show that this approach takes advantage of the flexibility of the natural gas network to facilitate the integration of renewables. Furthermore, we quantify and highlight the increased performance of the model in our analysis.

The remainder of the paper is organized as follows. The coordination framework on which the market-clearing designs are based is introduced in Section 2. Section 3 presents the natural gas system modeling, while the mathematical formulation of the market-clearing models is described in Section 4. Section 5 demonstrates the results in a realistic case study. Finally, Section 6 provides the conclusion with suggestions for future work.

2. Coordination framework

This section presents the coordination framework of electricity and natural gas markets along with the main trading floors in short-term operations. We first discuss the degrees of coordination both system-wise and in time and then formulate the market-clearing models.

2.1. Market designs

Currently, the electricity and natural gas markets are cleared independently and mainly interact through the operation of GFPPs. This interaction is based on the definition of appropriate *coordination parameters* (Sorokin, Rebennack, Pardalos, Iliadis, & Pereira, 2012), such as the price of natural gas and the consumption of GFPPs, as well as the available quantity of natural gas for power production. Fig. 1 illustrates the market setup along with such coordination parameters.

Natural gas markets were historically based on long-term contracts with limited short-term variability. However, recent trends show a transition towards short-term markets, which is further strengthened by the needs of GFPPs, which are expected to have an increased intraday variability due to stochastic renewable production (Zlotnik, Roald, Backhaus, Chertkov, & Andersson,

2017a). In the natural gas market, GFPPs act as buyers to acquire their fuel for power production and mainly purchase natural gas via short-term interruptible contracts or in the gas spot market. The gas supply contracts are signed with natural gas producers at a predefined price, while in the gas spot market the GFPPs buy their fuel at the spot price. The gas spot price may be undefined for a period of the following day at the time of bidding in the electricity market due to the asynchronous setup between the two markets (Hibbard & Schatzki, 2012). Consequently, GFPPs have to use an estimation of the natural gas price and face uncertainty about the price and natural gas availability, when buying from the gas spot market. The fuel price used by GFPPs to bid in the electricity market is considered fixed regardless of the procurement procedure and may not reflect the actual value of natural gas. The price-quantity offers in the electricity market are placed depending on the natural gas price, fuel availability and technical characteristics of GFPPs. Then, the electricity market is cleared and the natural gas demand of GFPPs is given as a fixed input to the natural gas market. Similarly, the natural gas market is cleared based on the price-quantity bids of natural gas producers.

The fuel demand of GFPPs is usually assigned with a lower priority than residential natural gas loads, which may constrain the operation of GFPPs in systems where natural gas is widely used both for power production and heating, e.g., in New England (Babula & Petak, 2014). An additional source of inefficiency on the system operation is introduced by the asynchronous timing of electricity and natural gas markets, which becomes highly essential under an increased system interaction with fluctuating renewables. For this reason, the adoption of a concurrent market timing, as well as the consideration of the physical and economic interplay between the two markets will facilitate their coordination (Hibbard & Schatzki, 2012; Tabors, Englander, & Stoddard, 2012). We capture the interaction between these markets by defining two approaches, namely the *decoupled* and *coupled* electricity and natural gas markets. The decoupled approach mimics the current market setup, while the coupled one addresses the need for having a concurrent and short-term integrated market. A coupled market design will profit from increased operational flexibility and provide the optimal dispatch for the whole energy system, instead of having a static and predefined communication between the two markets. A decoupled setup yields a partial coordination between markets, while a coupled approach optimizes the dispatch of GFPPs by taking into account the conditions in the natural gas market such as the price and availability of natural gas.

In this work, the main focus is placed on two trading floors, namely the day-ahead and balancing markets, in line with the recent trend in the natural gas market where short-term trading is significantly increasing. This way, we consider a design for the natural gas market that is consistent with that of the electricity market. Current market mechanisms clear sequentially these two trading floors. The day-ahead market is initially cleared 12–36 hours in advance of actual delivery, while the balancing market settles the imbalances in relation to the day-ahead schedule to keep the system balanced (Morales, Zugno, Pineda, & Pinson, 2014). In such a sequential arrangement, the dispatch is based on the merit-order principle that maximizes the social welfare of each independent trading floor. However, this approach does not ensure an optimal dispatch in case more than one trading floors are evaluated. In the electricity market, flexible producers may not be scheduled or being fully dispatched, which could lead to scarcity of flexible sources in real-time operation. The aforementioned situation is aggravated with the large-scale integration of uncertain renewables. The power production cost of these sources is close to zero, which makes them the first to be dispatched according to the merit-order principle. Consequently, flexible producers may be left out of the market and higher balancing requirements will arise in real-time. Moreover, the impact of party predictable renewables on the electricity market is transferred to the natural gas market through GFPPs (Keyaerts, Delarue, Rombauts, & William, 2014). In view of an energy system where GFPPs will provide a significant amount of balancing services to support renewable production, the fuel demand of GFPPs will have a more uncertain nature. To that end, a sequential setup can be inadequate also for the natural gas market under a tighter coupling with the electricity one.

The interaction between trading floors is modeled by a *sequential* and a *stochastic* approach. In the sequential setup, the day-ahead and balancing stages are optimized independently under a deterministic description of uncertainties, such as stochastic power production, which results in a lack of temporal coordination. However, a market-clearing model based on stochastic programming is able to co-optimize the dispatch in both trading floors and reduce the operating costs. The utilization of stochastic programming allows for a perfect temporal coordination between the trading floors, provided that the uncertain power production is properly described by a scenario set Ω.

The coupling of electricity and natural gas markets, along with a coordination of the two trading floors would increase the efficiency of operating the whole energy system with high shares of renewables. However, regulatory changes are still needed and market designs have to advance. The use of two-stage stochastic programming for electricity market-clearing is extensively discussed in Morales et al. (2014), highlighting its advantages and potential challenges. On a different front, the electricity and natural gas systems have been essentially operated independently from each other over the years. It has only been recently that some regulatory changes have promoted the coordination between the two energy sectors and markets. For example, the FERC (Federal Energy Regulatory Commission) Order 809 was issued in April 16, 2015 in U.S., which aims at harmonizing the gas market with the needs of the electricity industry (Zlotnik et al., 2017b). In order to accomplish a better coordination, the information exchange needs to be improved, as well as the market structures to become more coherent. Based on this observation, we propose two coupled market-clearing models, while a decoupled one resembles current market designs that have only limited coordination. Such coordination setups have been discussed by various system operators, e.g., in New England (Babula & Petak, 2014) and Denmark (Pinson et al., 2017), showing that it is an approach to be considered also in practice. Currently, the main inefficiencies stem from the uncoordinated operation, while most of the infrastructure already exists in both energy systems. Thus, the coupled operation of energy systems is considered inexpensive compared to solutions that involve further investments. Especially, cases like Denmark, where the two systems are operated by the same entity (i.e., Energinet.dk), would provide an environment that enables cost-efficient and coordinated operations. For these reasons, we focus on studying the three market-clearing models presented in the following section.

2.2. Market-clearing models

Depending on the level of coordination between the electricity and natural gas systems and the temporal coordination of markets, we formulate three models to cover the spectrum of potential outcomes as shown in Fig. 2.

2.2.1. Model Seq-Dec – Sequential decoupled electricity and natural gas model

A decoupled operation of electricity and natural gas systems is considered, while renewable energy production is described in a deterministic manner. The aim of this model is to demonstrate a setup similar to the current one, where the two systems are optimized independently and the day-ahead and balancing trading

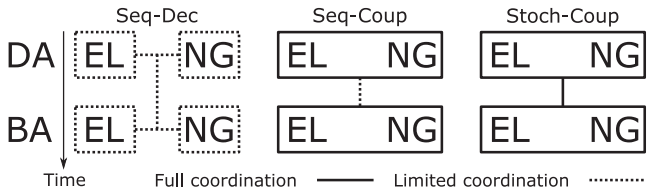

Fig. 2. Market-clearing models. DA: Day-ahead market, BA: Balancing market, EL: Electricity market and NG: Natural gas market.

floors are cleared sequentially. Initially, the electricity system is scheduled and then the fuel consumption of GFPPs is submitted as a fixed demand to the natural gas system. GFPPs have to bid in the electricity market based on an estimation of the natural gas spot price or on the price of the natural gas supply contract. However, this may not be the actual value of natural gas when operating the system. In this work, we define the *actual value* of natural gas at each location of the system as its locational marginal price. Moreover, we give higher priority to residential gas loads than to the demand of GFPPs, which results in GFPPs being one of the first gas consumers to be curtailed in case it is not feasible to cover their demand. We follow an iterative approach that identifies infeasible fuel consumption schedules and constraints the allowed fuel consumption (i.e., equivalent to power production of GFPPs) for the specific time periods of the scheduling horizon (Qadrdan et al., 2014). This approach could lead to suboptimal solutions for the operation of the two systems or even infeasible schedules under cases of highly increased residential electricity and natural gas demands.

2.2.2. Model Seq-Coup – Sequential coupled electricity and natural gas model

A coupled operation of electricity and natural gas systems is taken into account and renewable energy production is again described in a deterministic fashion. In this model, we formulate a single optimization problem for the operation of electricity and natural gas systems, while the day-ahead and balancing markets are still cleared sequentially. In this model, the coordination parameters are not defined in a static manner. The demand of GFPPs is treated as a variable, while the power production cost of GFPPs is defined endogenously and emerges from the cost of natural gas at the specific location. In other words, the power production cost of GFPPs is implicitly calculated through the actual value (i.e., locational marginal price) of natural gas consumed. The goal of this model is to highlight the inefficiencies that arise by having an independent scheduling of the two systems, like in *Seq-Dec*.

2.2.3. Model Stoch-Coup – Stochastic coupled electricity and natural gas model

The operation of electricity and natural gas systems is co-optimized and we consider a probabilistic description of uncertain renewable energy production. The proposed model is formulated as a two-stage stochastic programming problem that resembles a fully integrated system and attains perfect temporal coordination. This approach allows a pre-position of the energy system accounting for the costs of future balancing actions, in contrast to the deterministic models.

In the case that a decoupled operation of the electricity and natural gas systems is considered under uncertain renewable energy production, an additional model can be formulated. Such an approach would simulate the current decoupled setup between electricity and natural gas markets, while each operator utilizes two-stage stochastic programming to achieve a temporal coupling of trading floors. Our focus is on the integrated electricity and natural gas systems, hence the aforementioned approach is not modeled. We compare the coupled approaches with *Seq-Dec*, which reproduces current market setups. The goal is to evaluate the efficiency of each model and show how the level of coordination between the electricity and natural gas systems, as well as the temporal coordination can affect the total expected cost and the dispatch of the units.

3. Natural gas network modeling

In this section, the model of the natural gas system is presented. Natural gas system dynamics are characterized in reality by partial differential equations that are able to describe both the temporal and spatial dimensions of natural gas transport in the network (Borraz-Sanchez, Bent, Backhaus, Hijazi, & Van Hentenryck, 2016). In this work, we make some simplifying assumptions that allow us to capture some dynamics of the natural gas system, such as, the gas flow characteristics, the operation of system branches that contain compressors, the linepack flexibility and the utilization of gas storage facilities. The proposed approach takes into account the aforementioned components and allows their incorporation to the market-clearing models as day-ahead and real-time decisions. An analysis based on transient modeling of the natural gas system dynamics would provide a more realistic view of the natural gas physical behavior in the pipelines but at the same time increase the computational complexity and raise market design issues related to natural gas pricing. We refer the reader to the work of Zlotnik et al. (2017c), who incorporate transient modeling in a market framework and discuss such pricing schemes.

3.1. Nodal and natural gas flow constraints

The pressure at each network node has to be within specified limits in order to guarantee a secure operation of the system,

$$PR_m^{\min} \leq pr_m \leq PR_m^{\max}, \ \forall m \in M. \tag{1}$$

We assume the gas transport being isothermal and in horizontal pipelines (Borraz-Sanchez et al., 2016). Moreover, the flow, pressure and linepack are defined for the middle of each pipeline as average values (Correa-Posada & Sanchez-Martin, 2014). The gas flow depends on the pressure at the adjacent nodes, the physical properties of the pipeline, such as diameter and length, as well as the volumetric characteristics of the gas. We use the Weymouth equation to describe the gas flow from node m to u,

$$q_{m,u} = K_{m,u}^f \sqrt{pr_m^2 - pr_u^2}, \ \forall (m,u) \in Z, \tag{2}$$

where $K_{m,u}^f$ is the Weymouth constant for the specific pipeline. Eq. (2) is nonlinear and non-convex, thus we use an outer approximation approach based on Taylor series expansion around fixed pressure points to linearize it (Rømo et al., 2009; Tomasgard, Rømo, Fodstad, & Midthun, 2007) and provide solutions that are globally optimal. Each equality constraint (2) is then replaced by a set of linear inequalities,

$$q_{m,u} \leq K_{m,u}^f \left(\frac{PR_{m,v}}{\sqrt{PR_{m,v}^2 - PR_{u,v}^2}} pr_m - \frac{PR_{u,v}}{\sqrt{PR_{m,v}^2 - PR_{u,v}^2}} pr_u \right), \quad \forall (m,u) \in Z, \ \forall v \in V, \tag{3}$$

where V is the set of fixed pressure points $(PR_{m,v}, PR_{u,v})$. Using a significant number of fixed points (e.g., around 20 pairs as stated in Fodstad, Midthun, & Tomasgard, 2015) ensures a sufficient approximation of the Weymouth equation. The outer approximation is given by a number of planes, defined as in (3), that are tangent to the cone described by the Weymouth equation (2). Thus, the gas flow through each of the pipelines will be approximated by the only constraint in (3) that is binding (Tomasgard et al., 2007). The linear expressions used in inequalities (3) are formulated based on the fixed pressure points, which in turn depend on

the pressure limits of the two adjacent nodes. We generate these points by choosing multiple pressure values of the adjacent nodes between the pressure limits. The resulting fixed pressure points are used to describe the flow for one direction in the pipeline and may differ from the ones used to describe the opposite direction as the pressure limits of the adjacent nodes are not the same. For this reason, the set of inequalities (3) describing the gas flow from node m to u may be different from the ones describing the gas flow from u to m. We introduce two non-negative variables $q^{+}_{m,u}, q^{-}_{m,u} \geq 0, \forall (m,u) \in Z$ and the binary variable $y_{m,u}$, $\forall (m,u) \in Z$ in order to formulate the following model with bidirectional flows,

$$q_{m,u} = q^{+}_{m,u} - q^{-}_{m,u}, \ \forall (m,u) \in Z, \tag{4a}$$

$$q^{+}_{m,u} \leq \tilde{M} y_{m,u}, \ \forall (m,u) \in Z, \tag{4b}$$

$$q^{-}_{m,u} \leq \tilde{M}(1 - y_{m,u}), \ \forall (m,u) \in Z, \tag{4c}$$

$$y_{m,u} + y_{u,m} = 1, \ \forall (m,u) \in Z, \tag{4d}$$

$$y_{m,u} \in \{0,1\}, \ \forall (m,u) \in Z, \tag{4e}$$

where variable $q^{+}_{m,u}$ denotes the flow in the pipeline from node m to u, while $q^{-}_{m,u}$ from node u to m. Parameter $\tilde{M}$ is a sufficiently large constant. Eq. (4a) defines the unrestricted in sign gas flow in the pipeline, while constraints (4b)-(4e) ensure that only one of the two variables $q^{+}_{m,u}$ and $q^{-}_{m,u}$ will take a value different from zero. In addition, we need to define the following inequalities,

$$\Big\{ q^{+}_{m,u} \leq KI^{+}_{m,u,v} pr_m - KO^{+}_{m,u,v} pr_u + M(1 - y_{m,u}), \tag{5a}$$

$$q^{-}_{m,u} \leq KI^{-}_{m,u,v} pr_u - KO^{-}_{m,u,v} pr_m + M y_{m,u}, \tag{5b}$$

$$q^{-}_{u,m} \leq KI^{+}_{m,u,v} pr_m - KO^{+}_{m,u,v} pr_u + M y_{u,m}, \tag{5c}$$

$$q^{+}_{u,m} \leq KI^{-}_{m,u,v} pr_u - KO^{-}_{m,u,v} pr_m + M(1 - y_{u,m}) \Big\}, \tag{5d}$$

$$\forall \{(m,u) \in Z | m < u\}, \ \forall v \in V,$$

in order to incorporate in the model the physical description of the gas flow derived by the linearization of the Weymouth equation (3). The coefficients of the linear expressions are defined as follows:

$$\left\{ KI^{+}_{m,u,v} = \frac{K^{f}_{m,u} PR_{m,v}}{\sqrt{PR^2_{m,v} - PR^2_{u,v}}}, KO^{+}_{m,u,v} = \frac{K^{f}_{m,u} PR_{u,v}}{\sqrt{PR^2_{m,v} - PR^2_{u,v}}}, \right.$$
$$\left. KI^{-}_{m,u,v} = \frac{K^{f}_{m,u} PR_{u,v}}{\sqrt{PR^2_{u,v} - PR^2_{m,v}}}, KO^{-}_{m,u,v} = \frac{K^{f}_{m,u} PR_{m,v}}{\sqrt{PR^2_{u,v} - PR^2_{m,v}}} \right\}, \tag{6}$$
$$\forall \{(m,u) \in Z | m < u\}, \ \forall v \in V.$$

It can be observed that the direction of the flow will be defined by the binary variable, which in turn will enable the appropriate linearization constraints from the set of (5a)-(5d). For instance, a gas flow from node m to u is described by the linear inequalities that have the same coefficients, i.e., constraints (5a) and (5c). It is ensured that the gas flow in the pipeline will have one direction and that $q_{m,u} = -q_{u,m}, \forall (m,u) \in Z$ will hold. We also introduce two non-negative variables $q^{\text{in}}_{m,u}, q^{\text{out}}_{m,u} \geq 0, \forall (m,u) \in Z$ for the inflow and outflow of each pipeline in order to account for linepack flexibility. The flow in each pipeline is defined as the average of inflow and outflow,

$$q^{+}_{m,u} = \frac{q^{\text{in}}_{m,u} + q^{\text{out}}_{m,u}}{2}, \ \forall (m,u) \in Z, \tag{7a}$$

$$q^{-}_{m,u} = \frac{q^{\text{in}}_{u,m} + q^{\text{out}}_{u,m}}{2}, \ \forall (m,u) \in Z. \tag{7b}$$

The branches of the network with compressors are modeled via a simplified approach that uses a compressor factor Γ_z to define the relation of pressure at the two adjacent nodes as follows,

$$pr_u \leq \Gamma_z \cdot pr_m, \ \forall (m,u) \in Z. \tag{8}$$

The inlet pressure at node m can be lower than the outlet pressure at node u in case the gas flows from node m to u. The definition of gas pressures and flow through Eqs. (1)–(8) is given for each pipeline $(m,u) \in Z$ of the network. However, the variables can be also indexed for each time period t and scenario ω accordingly.

3.2. Natural gas storage constraints

An essential property of the natural gas system is that it can act as a temporary storage and be an economical way of storing energy. Linepack is very important for the short-term operation of the system and denotes the ability of storing a certain amount of natural gas in the pipeline. It is modeled by the following Eqs. (9a) and (9b),

$$h_{m,u,t} = K^{\text{h}}_{m,u} (pr_{m,t} + pr_{u,t})/2, \ \forall (m,u) \in Z, \ \forall t \in T, \tag{9a}$$

$$h_{m,u,t} = h_{m,u,t-1} + q^{\text{in}}_{m,u,t} - q^{\text{out}}_{m,u,t}, \ \forall (m,u) \in Z, \ \forall t \in T. \tag{9b}$$

Eq. (9a) defines the average mass of natural gas in the pipeline that is proportional to the average pressure of the adjacent nodes and a constant $K^{\text{h}}_{m,u}$ describing the pipeline characteristics. The mass conservation of each pipeline is given by (9b), where the inflow and outflow of each pipeline may be different. Eqs. (9a)–(9b) are based on the analysis provided in Correa-Posada and Sanchez-Martin (2014), which describes how the pressure and the velocity of natural gas affect the mass flow. Specific levels of linepack for the initial and last optimization period should be defined to link the current day with the previous and following ones.

Additionally, gas storage facilities are also available and can be utilized as both short- and long-term options. In short-term operation, they ensure security of supply, while they are also efficiently used as seasonal storage. The following equations model the short-term operation of gas storage facilities,

$$E^{\min}_{s} \leq e_{s,t} = e_{s,t-1} + g^{\text{in}}_{s,t} - g^{\text{out}}_{s,t} \leq E^{\max}_{s}, \ \forall s \in S, \ \forall t \in T, \tag{10a}$$

$$0 \leq g^{\text{in}}_{s,t} \leq IR_s, \ \forall s \in S, \ \forall t \in T, \tag{10b}$$

$$0 \leq g^{\text{out}}_{s,t} \leq WR_s, \ \forall s \in S, \ \forall t \in T. \tag{10c}$$

Eq. (10a) defines the temporal balance of the gas storage facility and imposes the upper and lower limits for the volume. These limits are defined by the storage capacity and the cushion gas, which is the minimum amount of gas needed to operate the storage unit (Tomasgard et al., 2007). Constraints (10b)-(10c) enforce the maximum inflow and outflow rates.

4. Market-clearing models

The formulations of market-clearing models *Seq-Dec*, *Seq-Coup* and *Stoch-Coup* are based on the following assumptions. Regarding the stochastic power production, we take into account a single source, namely wind power, while additional uncertainties related to supply or demand side can be similarly modeled and incorporated in the models. Its stochastic nature is described through a finite set of scenarios Ω that is available to the operator, who aims to maximize social welfare, and are properly modeled to account

for temporal and spatial correlations. The uncertainty in the natural gas system stems from the random natural gas demands of GFPPs, which are the result of the stochastic wind power production. Moreover, electricity and natural gas demands are assumed to be inelastic, which allows for an equivalent formulation between the problems of social welfare maximization and cost minimization for the system operation. Thus, in this work, we take the operator's point of view who aims to minimize the total expected cost. The extreme event of load shedding is penalized with a sufficiently large value in both markets. Additionally, we assume that production costs of electricity and natural gas are described via linear functions, while the producers offer their full capacity in the market under perfect competition. More specifically, wind power producers bid in the market with zero marginal cost. The link between the two systems is provided by the GFPPs, being consumers of natural gas and producers of electricity that is sold in the electricity market. The proposed models consider network constraints in both systems. The power transmission network is modeled with DC power flow, while natural gas network modeling is also considered, as described in Section 3. Furthermore, the models are optimized over a multi-period scheduling horizon to account for the inter-temporal constraints of the natural gas network. A concurrent market timing for the electricity and natural gas markets is assumed in the coupled models, as the energy markets are cleared simultaneously. As far as the trading floors are concerned, we consider the day-ahead and balancing stages to clear the markets, while no intraday trading is taken into account. Although this is a common assumption for the electricity market, we extend it also to natural gas market. This way the integration of electricity and natural gas system is facilitated under a consistent market design. Note that trading natural gas in short-terms markets has drawn an increased interest recently and is expected to further evolve in the future.

Following the aforementioned assumptions, the market-clearing models are recast as mixed-integer linear programming (MILP) problems. Fixing the binary variables related to the direction of the gas flow results in a linear programming (LP) problem that can properly provide day-ahead and balancing prices for electricity and natural gas as the dual variables of balancing constraints. The dual variables are indicated after a colon. A detailed mathematical description of the dispatch models is provided in the subsequent subsections.

4.1. Sequential decoupled electricity and natural gas model

The sequential and decoupled model simulates independently the operation of electricity and natural gas systems, as well as clears sequentially the day-ahead and balancing markets. Initially, the optimal day-ahead schedule that minimizes the cost of the power system is determined by model (11) as follows:

$$\underset{\Theta^{\mathrm{ED}}}{\mathrm{Min.}} \sum_{t\in T}\left(\sum_{i_c\in I_c} C_{i_c} p_{i_c,t} + \sum_{i_g\in I_g} C_{i_g} p_{i_g,t}\right) \tag{11a}$$

subject to

$$0 \le p_{i,t} \le P_i^{\max},\ \forall i\in I,\ \forall t\in T, \tag{11b}$$

$$0 \le w_{j,t} \le \widehat{W}_{j,t},\ \forall j\in J,\ \forall t\in T, \tag{11c}$$

$$\sum_{i\in A_n^I} p_{i,t} + \sum_{j\in A_n^J} w_{j,t} - D_{n,t}^{\mathrm{E}} - \sum_{r:(n,r)\in L} \hat{f}_{n,r,t} = 0 : \hat{\lambda}_{n,t}^{\mathrm{E}},\ \forall n\in N,\ \forall t\in T, \tag{11d}$$

$$\hat{f}_{n,r,t} = B_{n,r}(\hat{\delta}_{n,t} - \hat{\delta}_{r,t}) \le F_{n,r}^{\max},\ \forall (n,r)\in L,\ \forall t\in T, \tag{11e}$$

$$\hat{\delta}_{n,t}\ \text{free},\ \forall n/n:\text{ref},\ \hat{\delta}_{n,t}=0,\ n:\text{ref},\ \forall t\in T, \tag{11f}$$

where $\Theta^{\mathrm{ED}} = \{p_{i,t},\ \forall i\in I, t\in T; w_{j,t},\ \forall j\in J, t\in T; \hat{\delta}_{n,t},\ \forall n\in N,\ \forall t\in T\}$ is the set of primal optimization variables. The objective function (11a) to be minimized is the operating cost of the power system, which originates from the energy production cost of the power plants. The GFPPs use an estimation of the natural gas spot price or the price of natural gas contract in order to calculate their price-quantity offers. Constraints (11b) set the bounds of power production for dispatchable power plants, while constraints (11c) limit wind power by the expected wind power production. The power balance at each node of the power system is enforced by (11d). The transmission capacity limits are imposed by (11e) and (11f) defines the voltage angle at each node of the system. Having determined the day-ahead dispatch of the electricity system, we calculate the fuel consumption of GFPPs which in turn translates into a time-varying demand for each node of the natural gas system through $D_{m,t}^{\mathrm{P}} = \sum_{i_g\in A_m^{Ig}} \phi_{i_g} p_{i_g,t},\ \forall m\in M,\ \forall t\in T$. Demand $D_{m,t}^{\mathrm{P}}$ is treated as a parameter in the following model (12) that defines the optimal day-ahead schedule of the natural gas system as follows:

$$\underset{\Theta^{\mathrm{GD}}}{\mathrm{Min.}} \sum_{t\in T}\left(\sum_{k\in K} C_k g_{k,t} + \sum_{s\in S} C_s g_{s,t}^{\mathrm{out}}\right) \tag{12a}$$

subject to

$$0 \le g_{k,t} \le G_k^{\max},\ \forall k\in K,\ \forall t\in T, \tag{12b}$$

$$\sum_{k\in A_m^K} g_{k,t} + \sum_{s\in A_m^S} (g_{s,t}^{\mathrm{out}} - g_{s,t}^{\mathrm{in}}) - D_{m,t}^{\mathrm{G}} - D_{m,t}^{\mathrm{P}} - \sum_{u:(m,u)\in Z} (q_{m,u,t}^{\mathrm{in}} - q_{u,m,t}^{\mathrm{out}}) = 0 : \hat{\lambda}_{m,t}^{\mathrm{G}},\ \forall m\in M,\ \forall t\in T, \tag{12c}$$

$$\text{NG flow constraints (1), (4a)} - \text{(4e), (5a)} - \text{(5d), (7a), (7b), (8)},\ \forall t\in T, \tag{12d}$$

$$\text{NG storage constraints (9a), (9b), (10a)}-\text{(10c)}, \tag{12e}$$

where $\Theta^{\mathrm{GD}} = \{g_{k,t},\ \forall k\in K,\ \forall t\in T; e_{s,t}, g_{s,t}^{\mathrm{in}}, g_{s,t}^{\mathrm{out}},\ \forall s\in S,\ \forall t\in T; h_{m,u,t}, q_{m,u,t}^{\mathrm{in}},\ q_{m,u,t}^{\mathrm{out}}, y_{m,u,t},\ \forall (m,u)\in Z,\ \forall t\in T;\ pr_{m,t}, \forall m\in M, \forall t\in T\}$ is the set of primal optimization variables. The aim is to minimize the operating cost of the natural gas system that is represented in the objective function (12a) as the cost of natural gas production and withdrawal cost from the storage facilities. Constraints (12b) enforce the limits of natural gas production. The gas balance for each node of the system is given by (12c). The operation of the natural gas system is described by the set of constraints (12d) and (12e). In real-time operation, wind power production $W_{j,\omega',t}$ is realized and the balancing markets of electricity and natural gas are cleared independently. The day-ahead schedule of electricity and natural gas systems is treated as fixed parameters (denoted with superscript '*') in the following formulations. The electricity balancing market (13) writes as follows:

$$\underset{\Theta^{\mathrm{ER}}}{\mathrm{Min.}} \sum_{t\in T}\left(\sum_{i_c\in I_c}(C_{i_c}^{+} p_{i_c,\omega',t}^{+} - C_{i_c}^{-} p_{i_c,\omega',t}^{-}) + \sum_{n\in N} C^{\mathrm{sh,E}} l_{n,\omega',t}^{\mathrm{sh,E}} + \sum_{i_g\in I_g}(C_{i_g}^{+} p_{i_g,\omega',t}^{+} - C_{i_g}^{-} p_{i_g,\omega',t}^{-})\right) \tag{13a}$$

subject to

$$\Delta p_{i,\omega',t} = p_{i,\omega',t}^{+} - p_{i,\omega',t}^{-},\ \forall i\in I,\ \forall t\in T, \tag{13b}$$

$$-p^{*}_{i,t} \leq \Delta p_{i,\omega',t} \leq P^{\max}_{i} - p^{*}_{i,t},\ \forall i \in I,\ \forall t \in T, \tag{13c}$$

$$-P^{-}_{i} \leq \Delta p_{i,\omega',t} \leq P^{+}_{i},\ \forall i \in I,\ \forall t \in T, \tag{13d}$$

$$0 \leq l^{\text{sh,E}}_{n,\omega',t} \leq D^{\text{E}}_{n,t},\ \forall n \in N,\ \forall t \in T, \tag{13e}$$

$$0 \leq w^{\text{sp}}_{j,\omega',t} \leq W_{j,\omega',t},\ \forall j \in J,\ \forall t \in T, \tag{13f}$$

$$\sum_{i \in A^{I}_{n}} \Delta p_{i,\omega',t} + l^{\text{sh,E}}_{n,\omega',t} + \sum_{j \in J}(W_{j,\omega',t} - w^{\text{sp}}_{j,\omega',t} - w^{*}_{j,t}) + \sum_{r:(n,r)\in L} \hat{f}^{*}_{n,r,t} - \tilde{f}_{n,r,\omega',t} = 0 : \tilde{\lambda}^{\text{E}}_{n,\omega',t},\ \forall n \in N,\ \forall t \in T, \tag{13g}$$

$$\tilde{f}_{n,r,\omega',t} = B_{n,r}(\tilde{\delta}_{n,\omega',t} - \tilde{\delta}_{r,\omega',t}) \leq F^{\max}_{n,r},\ \forall (n,r) \in L,\ \forall t \in T, \tag{13h}$$

$$\tilde{\delta}_{n,\omega',t}\ \text{free},\ \forall n/n : \text{ref},\ \tilde{\delta}_{n,\omega',t} = 0,\ n : \text{ref},\ \forall t \in T, \tag{13i}$$

where $\Theta^{\text{ER}} = \{p^{+}_{i,\omega',t}, p^{-}_{i,\omega',t},\ \forall i \in I,\ \forall t \in T; w^{\text{sp}}_{j,\omega',t},\ \forall j \in J,\ \forall t \in T; \tilde{\delta}_{n,\omega',t}, l^{\text{sh,E}}_{n,\omega',t},\ \forall n \in N,\ \forall t \in T\}$ is the set of primal optimization variables. The objective function (13a) describes the cost of re-dispatch actions, i.e., up/down regulation and load shedding. The aim is to activate the least-cost re-dispatch actions in order to maintain the system in balance. Power regulation is defined by (13b) and constraints (13c) determine its bounds by taking into account the day-ahead dispatch of power plants. Moreover, constraints (13d) limit power regulation by the reserve capacity offer. These reserve capacity offers are defined via reserve capacity markets and are treated as parameters in the market-clearing models presented in this work. Reserve capacity markets are cleared independently but can be incorporated in the presented market-clearing models as described in (Morales et al., 2012). Electricity load shedding and wind spillage are constrained by the nodal demand and actual wind power realization though (13e) and (13f), respectively. Constraints (13g) guarantee power balance at each node of the electricity network in real-time operation. Constraints (13h) enforce power transmission capacity limits, while (13i) defines the voltage angle of the system nodes. Similarly to the day-ahead stage, the fuel consumption of the GFPPs is converted to a time-varying demand deviation via $D^{\text{PR}}_{m,\omega',t} = \sum_{i_g \in A^{Ig}_{m}} \phi_{i_g} \Delta p_{i_g,\omega',t},\ \forall m \in M,\ \forall t \in T$. The balancing natural gas market is formulated in (14) as follows:

$$\underset{\Theta^{\text{GR}}}{\text{Min.}} \sum_{t \in T}\Big(\sum_{k \in K}(C^{+}_{k} g^{+}_{k,\omega',t} - C^{-}_{k} g^{-}_{k,\omega',t}) + \sum_{m \in M} C^{\text{sh,G}} l^{\text{sh,G}}_{m,\omega',t} + \sum_{s \in S}(C^{+}_{s} g^{\text{out,r}}_{s,\omega',t} - C^{-}_{s} g^{\text{in,r}}_{s,\omega',t})\Big) \tag{14a}$$

subject to

$$0 \leq g^{+}_{k,\omega',t} \leq G^{\max}_{k} - g^{*}_{k,t},\ \forall k \in K,\ \forall t \in T, \tag{14b}$$

$$0 \leq g^{-}_{k,\omega',t} \leq g^{*}_{k,t},\ \forall k \in K,\ \forall t \in T, \tag{14c}$$

$$0 \leq g^{+}_{k,\omega',t} \leq G^{+}_{k},\ \forall k \in K,\ \forall t \in T, \tag{14d}$$

$$0 \leq g^{-}_{k,\omega',t} \leq G^{-}_{k},\ \forall k \in K,\ \forall t \in T, \tag{14e}$$

$$0 \leq l^{\text{sh,G}}_{m,\omega',t} \leq D^{\text{G}}_{m,t},\ \forall m \in M,\ \forall t \in T, \tag{14f}$$

$$\sum_{k \in A^{K}_{m}}(g^{+}_{k,\omega',t} - g^{-}_{k,\omega',t}) + \sum_{s \in A^{S}_{m}}(g^{\text{out,r}}_{s,\omega',t} - g^{\text{in,r}}_{s,\omega',t}) + \sum_{u:(m,u)\in Z}(q^{\text{in},*}_{m,u,t} - q^{\text{out},*}_{u,m,t} - q^{\text{in,r}}_{m,u,\omega',t} + q^{\text{out,r}}_{m,u,\omega',t}) - D^{\text{PR}}_{m,\omega',t} + l^{\text{sh,G}}_{m,\omega',t} = 0 : \tilde{\lambda}^{\text{G}}_{m,\omega',t},\ \forall m \in M,\ \forall t \in T, \tag{14g}$$

NG flow constraints (1), (4a) – (4e), (5a) – (5d), (7a), (7b), (8), $\forall t \in T$, (14h)

NG storage constraints (9a), (9b), (10a) – (10c), (14i)

where $\Theta^{\text{GR}} = \{g^{+}_{k,\omega',t}, g^{-}_{k,\omega',t},\ \forall k \in K,\ \forall t \in T; e^{\text{r}}_{s,\omega',t}, g^{\text{in,r}}_{s,\omega',t}, g^{\text{out,r}}_{s,\omega',t},\ \forall s \in S,\ \forall t \in T;\ h^{\text{r}}_{m,u,\omega',t}, q^{\text{in,r}}_{m,u,\omega',t}, q^{\text{out,r}}_{m,u,\omega',t}, y^{\text{r}}_{m,u,\omega',t}\ \forall (m,u) \in Z,\ \forall t \in T;\ pr^{\text{r}}_{m,\omega',t}, l^{\text{sh,G}}_{m,\omega',t},\ \forall m \in M,\ \forall t \in T\}$ is the set of primal optimization variables. In order to maintain the natural gas system balanced, a set of re-dispatch actions can be activated, namely, up/down regulation from the producers, regulation from the storage facilities and load shedding. The costs of these actions comprise objective function (14a). The upward and downward regulation from natural gas producers is limited by constraints (14b) and (14c) that incorporate also the day-ahead schedules. Additionally, constraints (14d) and (14e) ensure that the regulation from natural gas producers is kept above zero and below the reserve capacity offer. Similarly to the electricity market, reserve capacity offers are defined through the corresponding reserve capacity markets. Natural gas load shedding is limited by the nodal demand through (14f). Observe that an unexpected deviation of wind power production from the day-ahead schedule has to be covered by a re-dispatch action in the power system, which in turn may translate into a deviation for the natural gas system through parameter $D^{\text{PR}}_{m,\omega',t}$ that is also indexed by scenario ω'. Constraint (14g) guarantees the gas balance at each node of the system in real-time operation. The first re-dispatch action that is practically free stems from the linepack flexibility considered in this model through the representation of the natural gas system via constraints (14h) and (14i). This is also a common practice in reality as the natural gas system is mainly balanced via linepack and the costly re-dispatch actions are only activated when flexibility by the temporal coupling of linepack is not available. It should be noted that variables in constraints (14h) and (14i) are to be augmented with superscript r and indexed by scenario ω'. We follow an iterative approach to simulate the operation of electricity and natural gas system in the case of extreme events, such as gas load shedding. If shedding of residential natural gas load takes place, we identify the GFPPs that cause this event and the corresponding nodes of the system. Then, the balancing electricity market is cleared again with additional constraints that enforce bounds on the maximum power production of GFPPs during the necessary time periods. This procedure is repeated until no residential gas load shedding occurs due to the fuel consumption of GFPPs. Solving models (11)–(14) results in calculating the total expected cost of the system under scenario set Ω.

4.2. Sequential coupled electricity and natural gas model

The sequential and coupled dispatch model simulates an energy system where the day-ahead and balancing markets are sequentially cleared, while the operation of electricity and natural gas systems is coordinated. The optimal schedule that minimizes the day-ahead cost of the integrated system is determined by model

(15) as follows:

$$\underset{\Theta^{\mathrm{D}}}{\mathrm{Min.}} \sum_{t\in T}\Big(\sum_{i_c\in I_c} C_{i_c} p_{i_c,t} + \sum_{k\in K} C_k g_{k,t} + \sum_{s\in S} C_s g^{\mathrm{out}}_{s,t}\Big) \tag{15a}$$

subject to

$$\text{DA EL constraints (11b)} - \text{(11f)}, \tag{15b}$$

$$\text{DA NG constraints (12b), (12d), (12e)}, \tag{15c}$$

$$\sum_{k\in A^K_m} g_{k,t} + \sum_{s\in A^S_m}(g^{\mathrm{out}}_{s,t} - g^{\mathrm{in}}_{s,t}) - D^{\mathrm{G}}_{m,t} - \sum_{i_g\in A^{I_g}_m} \phi_{i_g} p_{i_g,t} - \sum_{u:(m,u)\in Z}(q^{\mathrm{in}}_{m,u,t} - q^{\mathrm{out}}_{u,m,t}) = 0 : \hat{\lambda}^{\mathrm{G}}_{m,t},\ \forall m\in M,\ \forall t\in T, \tag{15d}$$

where $\Theta^{\mathrm{D}} = \{\Theta^{\mathrm{ED}}; \Theta^{\mathrm{GD}}\}$ is the set of primal optimization variables. Objective function (15a) determines the day-ahead operating cost of the electricity and natural gas systems. The system operating cost stems from the power production cost of thermal power plants (TPPs, i.e., non-gas) and the natural gas production cost. Note that the power production cost of GFPPs is not included, since it would result in double counting it. The cost of operating GFPPs is explicitly associated with the natural gas system cost through the balancing equation (15d). In this formulation, the fuel consumption is treated as a variable and charged with the locational marginal price ($\hat{\lambda}^{\mathrm{G}}_{m,t}$) since the operation is jointly optimized. Having determined the day-ahead schedule of the integrated energy system, the real-time operation is simulated for each wind power realization $W_{j,\omega',t}$ by model (16) that writes as follows:

$$\underset{\Theta^{\mathrm{R}}}{\mathrm{Min.}} \sum_{t\in T}\Big(\sum_{k\in K}(C^+_k g^+_{k,\omega',t} - C^-_k g^-_{k,\omega',t}) + \sum_{i_c\in I_c}(C^+_{i_c} p^+_{i_c,\omega',t} - C^-_{i_c} p^-_{i_c,\omega',t}) + \sum_{s\in S}(C^+_s g^{\mathrm{out,r}}_{s,\omega',t} - C^-_s g^{\mathrm{in,r}}_{s,\omega',t}) + \sum_{n\in N} C^{\mathrm{sh,E}} l^{\mathrm{sh,E}}_{n,\omega',t} + \sum_{m\in M} C^{\mathrm{sh,G}} l^{\mathrm{sh,G}}_{m,\omega',t}\Big) \tag{16a}$$

subject to

$$\text{BA EL constraints (13b)} - \text{(13i)}, \tag{16b}$$

$$\text{BA NG constraints (14b)} - \text{(14f), (14h), (14i)}, \tag{16c}$$

$$\sum_{k\in A^K_m}(g^+_{k,\omega',t} - g^-_{k,\omega',t}) + \sum_{s\in A^S_m}(g^{\mathrm{out,r}}_{s,\omega',t} - g^{\mathrm{in,r}}_{s,\omega',t}) + \sum_{u:(m,u)\in Z}(q^{\mathrm{in},*}_{m,u,t} - q^{\mathrm{out},*}_{u,m,t} - q^{\mathrm{in,r}}_{m,u,\omega',t} + q^{\mathrm{out,r}}_{m,u,\omega',t}) - \sum_{i_g\in I_g}\phi_{i_g}\Delta p_{i_g,\omega',t} + l^{\mathrm{sh,G}}_{m,\omega',t} = 0 : \tilde{\lambda}^{\mathrm{G}}_{m,\omega',t},\ \forall m\in M,\ \forall t\in T, \tag{16d}$$

where $\Theta^{\mathrm{R}} = \{\Theta^{\mathrm{ER}}; \Theta^{\mathrm{GR}}\}$ is the set of primal optimization variables. The goal is to minimize the cost of re-dispatch actions for the integrated energy system described in (16a). Similarly, the power production costs related to GFPPs are not included since they stem from the natural gas system. Fuel consumption of GFPPs is a variable in the co-optimization model of electricity and natural gas systems. Solving models (15)–(16) results in calculating the total expected cost under scenario set Ω.

4.3. Stochastic coupled electricity and natural gas model

The stochastic and coupled dispatch model optimizes the operation of the integrated energy systems and is formulated in such a way that the day-ahead decisions anticipate future balancing costs over the scenario set Ω. We formulate a two-stage stochastic programming problem (17) that writes as follows:

$$\underset{\Theta^{\mathrm{SC}}}{\mathrm{Min.}} \sum_{t\in T}\Big[\sum_{i_c\in I_c} C_{i_c} p_{i_c,t} + \sum_{k\in K} C_k g_{k,t} + \sum_{s\in S} C_s g^{\mathrm{out}}_{s,t} + \sum_{\omega\in\Omega}\pi_\omega\Big(\sum_{k\in K}(C^+_k g^+_{k,\omega,t} - C^-_k g^-_{k,\omega,t}) + \sum_{i_c\in I_c}(C^+_{i_c} p^+_{i_c,\omega,t} - C^-_{i_c} p^-_{i_c,\omega,t}) + \sum_{s\in S}(C^+_s g^{\mathrm{out},r}_{s,\omega,t} - C^-_s g^{\mathrm{in},r}_{s,\omega,t}) + \sum_{n\in N} C^{\mathrm{sh,E}} l^{\mathrm{sh,E}}_{n,\omega,t} + \sum_{m\in M} C^{\mathrm{sh,G}} l^{\mathrm{sh,G}}_{m,\omega,t}\Big)\Big] \tag{17a}$$

subject to

$$\text{DA coupled EL \& NG constraints (11b), (11d)} - \text{(11f), (15c), (15d)}, \tag{17b}$$

$$0 \le w_{j,t} \le \overline{W}_j,\ \forall j\in J,\ \forall t\in T, \tag{17c}$$

$$\text{BA coupled EL \& NG constraints (16b)} - \text{(16d)},\ \forall\omega\in\Omega, \tag{17d}$$

where $\Theta^{\mathrm{SC}} = \{\Theta^{\mathrm{D}}; \Theta^{\mathrm{R}}_\omega,\ \forall\omega\in\Omega\}$ is the set of primal optimization variables. The expected cost of operating the integrated energy system is given by the objective function (17a) to be minimized. The stochastic and coupled dispatch model permits an implicit temporal coordination of the day-ahead and balancing stages through the expected balancing costs in (17a) and constraints (17d) that are modeled for all scenarios $\omega\in\Omega$. It should be noted that the day-ahead decisions are treated as variables and that the day-ahead wind power production is limited by the installed capacity through (17c). This formulation optimally dispatches the integrated system to account for the uncertain wind power production by anticipating future balancing needs. Flexible producers may be scheduled out of merit-order to make flexibility available at the balancing stage. Moreover, the inclusion of natural gas system constraints in both day-ahead and balancing stages allows for an optimal spatial allocation of linepack flexibility in the system that is significantly important when getting closer to real-time operation.

5. Results

A modified 24-bus IEEE Reliability Test System and a 12-node natural gas system compose the integrated energy system. It consists of 12 power plants, 2 wind farms, 17 electricity loads, 3 natural gas suppliers, 4 natural gas loads and 2 natural gas storage facilities. There are 4 flexible GFPPs that account for 427 MW of the total 3075 MW installed capacity of conventional generation and interconnect the two systems. Wind power uncertainty is modeled by a set of 25 equiprobable scenarios that have proper temporal and spatial correlation, which are available at Bukhsh (2017). The data of the integrated energy system is based on He et al. (2016) and presented along with the network topology in the online appendix available at Ordoudis, Pinson, and Morales (2018). The forecast profile of electricity and residential natural gas demands, as well as the expected wind power production are illustrated in Fig. 3.

5.1. Comparison of market-clearing models and the effect of coordination parameters

In the following analysis, we highlight the inefficiencies arising from fixing the coordination parameters between the two markets

Table 1
Expected cost and share of day-ahead power production. Wind power penetration 40%.

	Total ($)	Day-ahead ($)	Balancing ($)	GFPPs (%)	TPPs (%)
Stoch-Coup	1,747,156	1,755,474	−8,318	10.8	89.2
Seq-Coup	1,817,781	1,731,522	86,259	9.1	90.9
Seq-Dec	1,819,238	1,731,657	87,581	9.2	90.8
Seq-Dec ↑	1,821,399	1,732,185	89,214	6.8	93.2
Seq-Dec ↓	1,866,966	1,741,471	125,495	14.5	85.5

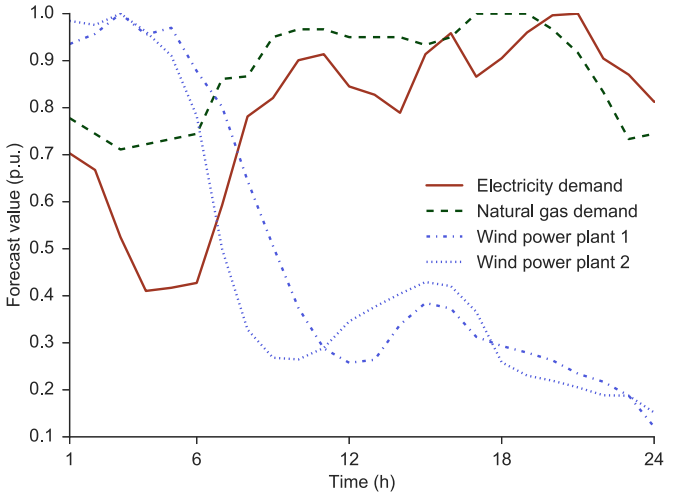

Fig. 3. Forecast profile of electricity and natural gas demands along with expected wind power production of wind power plant 1 and 2.

in the decoupled approach and the benefits of dispatching the energy system in view of future uncertainties along with the linepack flexibility. We consider a 24-hour scheduling horizon, while the level of total system linepack and natural gas in the storage facilities at the end of day is equal to the one at the beginning and accounts for the operation of the following day. For the total system linepack, we set this value equal to 448,000 kcf.

Initially, we examine the effect of utilizing fixed natural gas prices that are usually different from the natural gas marginal prices at each node of the system. Fixed natural gas prices represent the estimation of the natural gas spot price or the price of supply contracts that is used by GFPPs to bid in the electricity market. In our approach, the nodal natural gas prices stemming from the coupled clearing of electricity and natural gas markets are considered an appropriate estimation of the actual natural gas price. The solution of *Seq-Coup* results in day-ahead natural gas prices ($\hat{\lambda}^{G}_{m,t}$) that are used in the *Seq-Dec* model to define the power production cost of GFPPs. Specifically, the day-ahead offer price of GFPPs in *Seq-Dec* is calculated by the multiplication of natural gas price of *Seq-Coup* and the power conversion factor of each plant, i.e., $C_{i_g,t} = \hat{\lambda}^{G}_{m,t}\phi_{i_g}, \forall m \in A^{i_g}_{m}, \forall i_g \in I_g, \forall t \in T$. Upward and downward regulation offer prices are equal to 1.1 and 0.91 of the day-ahead offer price. A mis-estimation of the actual natural gas price by GFPPs is introduced in order to simulate the case that GFPPs bid in the electricity market with a natural gas price different that the actual one. This mis-estimation is simulated by a 10% over- and under-estimation, while such deviation is considered adequate due to the relatively stable natural gas prices in short-term operations. The expected system costs are calculated based on (17a) in order to ensure consistency of the results. Therefore, the offer prices of GFPPs in *Seq-Dec* only affect their position in the merit-order and the unit dispatch, while these prices are not taken into account in the cost calculation.

Tables 1 and 2 show the costs of operating the energy system under the three market-clearing models and the share of day-ahead power production for GFPPs and TPPs for wind power penetration levels, i.e., share of installed wind power capacity on system's demand, of 40% and 50%, respectively. It is observed that *Stoch-Coup* achieves the lowest expected cost in both cases by efficiently accommodating the large shares of renewable power production. This model decides the optimal day-ahead dispatch to account for wind power uncertainty which results in a higher day-ahead cost but lower expected balancing cost, while the share of GFPPs that are efficient balancing producers also increases compared to deterministic models *Seq-Coup* and *Seq-Dec*. The deterministic models schedule the system based on the merit-order principle which may not be appropriate to cope with wind power uncertainty. We would like to note that the characteristics of wind power scenarios (e.g., mean and variance) affect the outcome of the market-clearing models. The *Stoch-Coup* model handles uncertainty more efficiently than the deterministic ones and this can be observed by the greater decrease in expected cost it accomplishes when increasing the wind power penetration level from 40% to 50%. The initial wind power scenarios are normalized and then multiplied by the wind farm capacity; thus a higher penetration level results in scenarios with higher mean and variance. We refer the reader to Ordoudis and Pinson (2016) for further discussion on this issue.

A coupled clearing of electricity and natural gas markets results in lower expected cost compared to the decoupled approaches due to the optimal natural gas price signals, as well as the optimized natural gas flows and linepack. The spatial allocation of natural gas in the system plays an important role for short-term adequacy and available flexibility in view of the ability to store gas in the pipelines. For the cases of natural gas price mis-estimation, it can be noticed that there might be different effects on the total expected cost depending on wind power penetration level. The day-ahead cost increases when the natural gas price is mis-estimated compared to *Seq-Dec* that utilizes the actual natural gas price from *Seq-Coup*. The reason for that is the misplacement of GFPPs in the merit-order because of the over-estimation (↑) or under-estimation (↓) of natural gas price compared to the merit-order built by the actual one. This results in scheduling more expensive units at the day-ahead stage which in turn increases the day-ahead cost. In the under-estimation cases, flexible GFPPs are scheduled more at the day-ahead stage which makes them unavailable to provide up-regulation in real-time operation, thus the expected balancing cost significantly increases as more expensive sources have to be deployed. On the contrary, it is possible to have a reduced total expected cost when the natural gas price is over-estimated. In the case of 50% wind power penetration, flexible GFPPs are scheduled less at the day-ahead stage which makes them available to provide upward regulation services in real-time.

Additionally, the impact of congestion in the natural gas network on the scheduling of GFPPs is illustrated in Table 3 and Fig. 4. The residential natural gas demand is increased by 30% to represent winter conditions, when natural gas is used extensively for heating. The share of GFPPs is reduced from 9.1% to 6.6% and from 9.2% to 6.7% for *Seq-Coup* and *Seq-Dec* respectively. The TPPs have

Table 2
Expected cost and share of day-ahead power production. Wind power penetration 50%.

	Total ($)	Day-ahead ($)	Balancing ($)	GFPPs (%)	TPPs (%)
Stoch-Coup	1,684,075	1,686,504	−2,429	11.7	88.3
Seq-Coup	1,812,790	1,663,477	149,313	7.4	92.6
Seq-Dec	1,814,086	1,663,891	150,195	7.2	92.8
Seq-Dec ↑	1,813,271	1,664,646	148,625	6.1	93.9
Seq-Dec ↓	1,874,907	1,674,110	200,797	14.3	85.7

Table 3
Expected cost and share of day-ahead power production. Wind power penetration 40%. Increased natural gas demand by 30%.

	Total ($)	GFPPs (%)	TPPs (%)
Seq-Coup	1,949,993	6.6	93.4
Seq-Dec	2,018,479	6.7	93.3

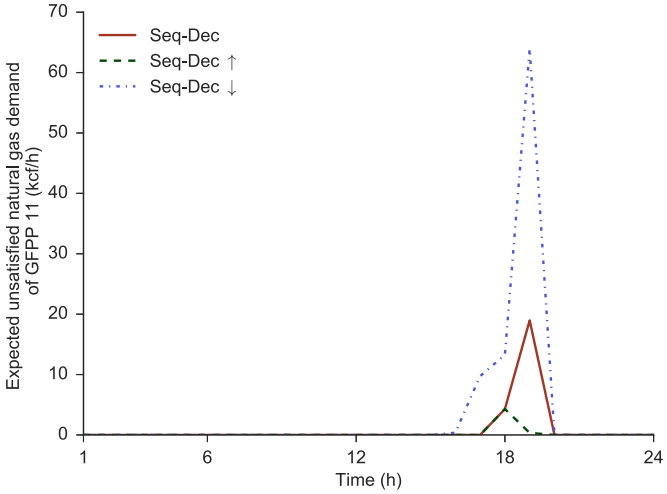

Fig. 4. Expected unsatisfied natural gas demand of GFPP 11 under Seq-Dec.

to cover a higher portion of the electricity demand in this case due to the lower priority assigned to the fuel demand of GFPPs compared to natural gas residential loads. Moreover, it is observed that GFPP 11 is expected to face unsatisfied fuel demand during the hours of peak residential natural gas load under *Seq-Dec*. This phenomenon does not occur when the systems are simultaneously operated in *Seq-Coup*. In this case, the importance of efficiently optimizing the gas flows and the spatial allocation of linepack in the system is more evident. The expected unsatisfied natural gas demand of GFPP 11 is higher when the natural gas price is underestimated as it is scheduled more at the day-ahead stage and lower when the natural gas price is over-estimated.

5.2. The benefits and effects of linepack

The following results aim at exploring the benefits of linepack and the corresponding flexibility revealed. In the following analysis, the wind power penetration level is 50%. Initially, we simulate a purely steady-state operation of the natural gas system, where no linepack is considered and the inflow and outflow of each pipeline is equal ($q^{\text{in}}_{m,u} = q^{\text{out}}_{m,u}, \forall (m,u) \in Z$).

Table 4 presents the expected system cost under *Seq-Coup* and *Seq-Dec* comparing the cases where linepack is considered or neglected (steady-state). The steady-state models result in a higher day-ahead cost for both *Seq-Coup* and *Seq-Dec* because the most expensive natural gas producer is scheduled to meet the demand. In this case, the natural gas demand has to be instantly covered

Table 4
Effect of linepack on expected cost under *Seq-Coup* and *Seq-Dec*. Wind power penetration 50%.

	Total ($)	Day-ahead ($)	Balancing ($)
Seq-Coup	1,812,790	1,663,477	149,313
Steady-state Seq-Coup	1,809,753	1,669,452	140,301
Seq-Dec	1,814,086	1,663,891	150,195
Steady-state Seq-Dec	1,813,271	1,671,109	142,162

Table 5
Effect of linepack on expected cost and share of day-ahead power production under *Stoch-Coup*. Wind power penetration 50%.

	Total ($)	GFPPs (%)	TPPs (%)
Steady-state Stoch-Coup	1,691,728	9.9	90.1
Stoch-Coup	1,684,076	11.7	88.3
Stoch-Coup (+5% initial linepack)	1,631,559	12	88
Stoch-Coup (−5% initial linepack)	1,739,304	10.8	89.2

at each time period by the production units as it is not possible to store natural gas in the network for future utilization. When the linepack is considered, natural gas is only supplied by the two cheaper producers and it is stored in the beginning of the day to be used later during the hours of peak demand. It is observed, though, that the expected balancing costs are lower in the steady-state models. The deployment of the expensive natural gas supplier increases the natural gas price and makes available more cost-effective capacity for down-regulation in the natural gas system. This increased availability of cheaper down-regulation is also reflected in the electricity market through the GFPPs and results in lower expected balancing cost. This observation depends on the structure of scenarios and the type of regulation needed in real-time operation. Nevertheless, it indicates possible inefficiencies that may arise when a flexible component of the system, such as the linepack, is myopically operated.

The subsequent results show that *Stoch-Coup* effectively schedules the system and exploits the available flexibility of linepack under uncertainty of wind power production. The temporal coordination between the two trading floors allows an efficient allocation of natural gas in the system and overcome the aforementioned drawback of the deterministic approaches that are myopic to uncertainties. The steady-state model results in higher expected cost compared to *Stoch-Coup* when linepack is taken into account, as illustrated in Table 5. Moreover, *Stoch-Coup* schedules more the GFPPs by taking advantage of the storage ability in the natural gas system.

The main effect of considering a storage facility in the operation of the energy system is that it flattens the demand profile by filling valleys and shaving peaks, as well as utilizing cheap power production. In order to quantify the flexibility revealed by modeling linepack in the integrated energy system, we simulate a case where an ideal storage facility, i.e., having infinite capacity and charging/discharging rates, is introduced in the electricity network allowing to shift the demand profile in the most cost-effective manner. In this case, the resulting expected cost (*EC*) of *Stoch-Coup* is $1,629,519. The linepack flexibility is quantified by

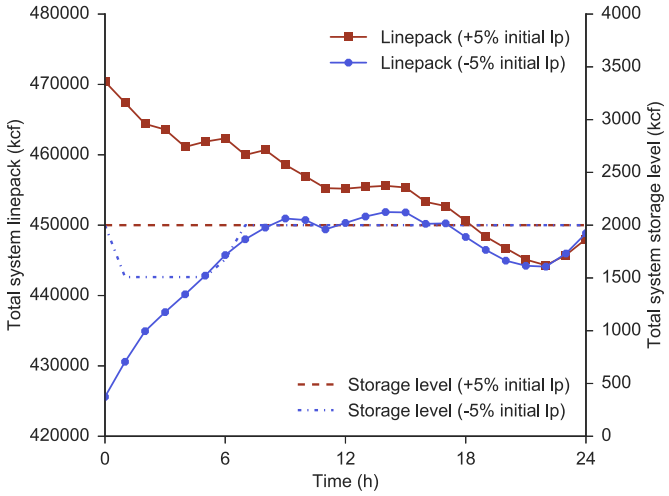

Fig. 5. Total system linepack and storage level (lp: linepack).

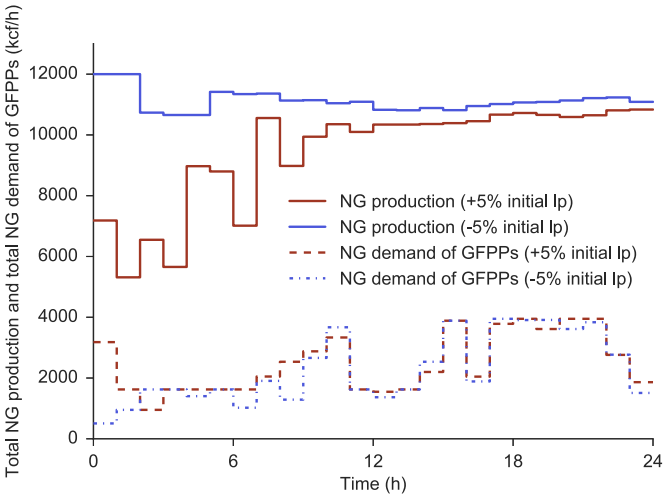

Fig. 6. Total natural gas production and total natural demand of GFPPs (NG: natural gas, lp: linepack).

the following performance ratio,

$$\frac{EC^{ss} - EC}{EC^{ss} - EC^{ideal}} = \frac{1,691,728 - 1,684,016}{1,691,728 - 1,629,519} = 12.4\%.$$

This ratio shows that modeling the natural gas network with linepack flexibility unveils 12.4% of utilizing an ideal storage in the electricity system. This result indicates the need of efficiently modeling the integrated energy market as it provides an economical approach to exploit the available flexibility in the natural gas system.

Furthermore, we examine the effect of the linepack level at the beginning of the day on the system operation by defining two additional cases for the ease of our analysis. These two cases are defined by having a 5% more or less linepack at the beginning of the day in relation to the value at the end of the day. In all cases, the total linepack at the end of the day is equal to 448,000 kcf. The total operating cost is lower when there is higher level of initial linepack in the system. The system is operated by taking advantage of the free energy stored in the natural gas network that also results in scheduling more the GFPPs compared to the base case of *Stoch-Coup*. On the contrary, the expected cost is higher when the gas network has to be filled in order to meet the final condition of the scheduling horizon.

The total linepack of the system is presented in Fig. 5, along with the total storage level. The linepack decreases throughout the scheduling horizon when the initial level is higher than the final condition and the storage is not utilized at the day-ahead stage. It can be noticed that the rate of decrease depends on the residential natural gas demand profile, while there are couple of periods that the linepack is charged when the residential demand is relatively low. On the other hand, the linepack is increased when its initial value is lower at the beginning of the scheduling horizon. The highest rate of increase is observed when the residential natural gas demand is low during the first hours of the day. Moreover, there is a need to discharge the storage facilities to support the secure operation of the system. In both cases, the linepack is decreased below the final hour threshold during the hours of peak residential demand to avoid supplying natural gas by the expensive natural gas producer.

In addition, Fig. 6 illustrates the total natural gas supply and the fuel demand of GFPPs. The natural gas production is significantly higher when the lack of linepack in the system has to be covered. On the contrary, the utilization of linepack to cover natural gas demand during the first half of the scheduling horizon, when the initial value is higher, is demonstrated by the reduced production in the corresponding hours. Moreover, the GFPPs are scheduled more in this case due to the excess of natural gas in the system. This points out another advantage of the coupled approach where the GFPPs will be scheduled according to the gas availability in the system. The GFPPs are serving as a flexible demand component for the natural gas system, by either increasing or decreasing their fuel consumption, in favor of a cost-effective operation.

The optimization problems were solved using CPLEX 12.6.2 under GAMS on a stationary computer with Intel i7 4-core processor clocking at 3.4 GHz and 8 GB of RAM. The average time to solve *Stoch-Coup* was 1540 seconds, while *Seq-Coup* and *Seq-Dec* were solved in less than 90 seconds.

6. Conclusion

This paper proposes a co-optimization model for integrated electricity and natural gas systems that efficiently takes into account uncertain power supply. We follow a linearization approach to approximate the dynamics of the natural gas system that yields a tractable mixed-integer linear programming (MILP) model and considers the possibility to store gas in the pipelines of the natural gas network (i.e., linepack), which is of significant importance in short-term operations. The combination of the aforementioned model properties results in increasing operational flexibility and in improved allocation of gas resources in the network. Moreover, we provide two market-clearing models with a deterministic description of the uncertain power supply and assess the value of coordination between the energy systems and the trading floors.

Initially, the impact of coordination parameters, such as consumption of gas-fired power plants (GFPPs) and natural gas price, is examined in a setup where the electricity and natural gas markets are decoupled. It is shown that both parameters affect the operation of both systems and in turn, the expected cost. A poor definition of these parameters between these markets usually has a negative effect on the expected cost. However, a distorted day-ahead scheduling of GFPPs due to arbitrary definition of these coordination parameters may result in making available reserve capacity that is suitable to cope with the actual imbalances in real-time operation. In contrast, a fully coupled model effectively copes with power supply uncertainty and makes the most of the flexibility inherent to the natural gas system, which is further highlighted by comparing the approaches that linepack is modeled or disregarded. Moreover, our analysis shows that it is not adequate to introduce an additional source of flexibility (e.g., linepack) in the

system without having the proper market design to operate it. Finally, simulation results show that the models efficiently capture the natural gas system behavior.

For future works, the optimal definition of coordination parameters between the two markets needs to be studied. Results in our analysis indicate that a systematic approach to define them is capable of reducing the expected system cost. Moreover, a more detailed description of the natural gas system that models also fuel consumption of compressors could be considered. This would highly increase the computational complexity of the problem. However, tailored decomposition techniques can be applied to overcome this hurdle.

Acknowledgment

The work of Christos Ordoudis and Pierre Pinson is partly funded by the Danish Strategic Research Council (DSF) through projects 5s-Future Electricity Markets, No. 12–132636/DSF and CITIES, No. 1305-00027B/DSF. The work of Juan M. Morales is partly funded by the European Research Council (ERC) under the European Unions Horizon 2020 research and innovation programme (grant agreement No. 755705), by the Spanish Research Agency through project ENE2017-83775-P (AEI/FEDER, UE), and by the Research Funding Program for Young Talented Researchers of the University of Málaga through project PPIT-UMA-B1-2017/18. Finally, we would like to thank the editor and the reviewers for their comments to improve this manuscript.

References

Alabdulwahab, A., Abusorrah, A., Zhang, X., & Shahidehpour, M. (2015). Coordination of interdependent natural gas and electricity infrastructures for firming the variability of wind energy in stochastic day-ahead scheduling. *IEEE Transactions on Sustainable Energy, 6*(2), 606–615. doi:10.1109/TSTE.2015.2399855.

An, S., Li, Q. L. Q., & Gedra, T. W. (2003). Natural gas and electricity optimal power flow. In *2003 IEEE PES Transmission and Distribution Conference and Exposition (IEEE Cat. No.03CH37495): 1* (pp. 138–143). doi:10.1109/TDC.2003.1335171.

Babula, M., & Petak, K. (2014). The cold truth: Managing gas-electric integration: The ISO New England experience. *IEEE Power and Energy Magazine, 12*(6), 20–28. doi:10.1109/MPE.2014.2347611.

Bai, L., Li, F., Cui, H., Jiang, T., Sun, H., & Zhu, J. (2016). Interval optimization based operating strategy for gas-electricity integrated energy systems considering demand response and wind uncertainty. *Applied Energy, 167*, 270–279. doi:10.1016/j.apenergy.2015.10.119.

Biskas, P. N., Kanelakis, N. G., Papamatthaiou, A., & Alexandridis, I. (2016). Coupled optimization of electricity and natural gas systems using augmented lagrangian and an alternating minimization method. *International Journal of Electrical Power and Energy Systems, 80*, 202–218. doi:10.1016/j.ijepes.2016.01.045.

Borraz-Sanchez, C., Bent, R., Backhaus, S., Hijazi, H., & Van Hentenryck, P. (2016). Convex relaxations for gas expansion planning. *INFORMS Journal on Computing, 28*(4), 645–656. doi:10.1287/ijoc.2016.0697.

Bukhsh, W. (2017). Data for stochastic multiperiod optimal power flow problem. https://sites.google.com/site/datasmopf/ Accessed 01.07.17.

Chaudry, M., Jenkins, N., & Strbac, G. (2008). Multi-time period combined gas and electricity network optimisation. *Electric Power Systems Research, 78*(7), 1265–1279. doi:10.1016/j.epsr.2007.11.002.

Clegg, S., & Mancarella, P. (2015). Integrated modeling and assessment of the operational impact of power-to-gas (p2g) on electrical and gas transmission networks. *IEEE Transactions on Sustainable Energy, 6*(4), 1234–1244. doi:10.1109/TSTE.2015.2424885.

Clegg, S., & Mancarella, P. (2016). Integrated electrical and gas network flexibility assessment in low-carbon multi-energy systems. *IEEE Transactions on Sustainable Energy, 7*(2), 718–731. doi:10.1109/TSTE.2015.2497329.

Correa-Posada, C. M., & Sanchez-Martin, P. (2014). Integrated power and natural gas model for energy adequacy in short-term operation. *IEEE Transactions on Power Systems, 30*(6), 3347–3355. doi:10.1109/TPWRS.2014.2372013.

Duenas, P., Leung, T., Gil, M., & Reneses, J. (2015). Gas-electricity coordination in competitive markets under renewable energy uncertainty. *IEEE Transactions on Power Systems, 30*(1), 123–131. doi:10.1109/TPWRS.2014.2319588.

Fodstad, M., Midthun, K. T., & Tomasgard, A. (2015). Adding flexibility in a natural gas transportation network using interruptible transportation services. *European Journal of Operational Research, 243*(2), 647–657. doi:10.1016/j.ejor.2014.12.010.

Geidl, M., & Andersson, G. (2007). Optimal power flow of multiple energy carriers. *IEEE Transactions on Power Systems, 22*(1), 145–155. doi:10.1109/TPWRS.2006.888988.

He, C., Wu, L., Liu, T., & Shahidehpour, M. (2016). Robust co-optimization scheduling of electricity and natural gas systems via ADMM. *IEEE Transactions on Sustainable Energy, 8*, 658–670. doi:10.1109/TSTE.2016.2615104.

Hibbard, P. J., & Schatzki, T. (2012). The interdependence of electricity and natural gas: Current factors and future prospects. *The Electricity Journal, 25*(4), 6–17. doi:10.1016/j.tej.2012.04.012.

Keyaerts, N., Delarue, E., Rombauts, Y., & William, D. (2014). Impact of unpredictable renewables on gas-balancing design in Europe. *Applied Energy, 119*, 266–277. doi:10.1016/j.apenergy.2014.01.011.

Li, T., Eremia, M., & Shahidehpour, M. (2008). Interdependency of natural gas network and power system security. *IEEE Transactions on Power Systems, 23*(4), 1817–1824. doi:10.1109/TPWRS.2008.2004739.

Liu, C., Shahidehpour, M., Fu, Y., & Li, Z. (2009). Security-constrained unit commitment with natural gas transmission constraints. *IEEE Transactions on Power Systems, 24*(3), 1523–1536. doi:10.1109/TPWRS.2009.2023262.

Liu, C., Shahidehpour, M., & Wang, J. (2011). Coordinated scheduling of electricity and natural gas infrastructures with a transient model for natural gas flow. *Chaos An Interdisciplinary Journal of Nonlinear Science, 21*, 1–12. doi:10.1063/1.3600761.

Morales, J. M., Conejo, A. J., Liu, K., & Zhong, J. (2012). Pricing electricity in pools with wind producers. *IEEE Transactions on Power Systems, 27*(3), 1366–1376. doi:10.1109/TPWRS.2011.2182622.

Morales, J. M., Zugno, M., Pineda, S., & Pinson, P. (2014). Electricity market clearing with improved scheduling of stochastic production. *European Journal of Operational Research, 235*(3), 765–774. doi:10.1016/j.ejor.2013.11.013.

Ordoudis, C., & Pinson, P. (2016). Impact of renewable energy forecast imperfections on market-clearing outcomes. In *2016 IEEE International Energy Conference (ENERGYCON)* (pp. 1–6). doi:10.1109/ENERGYCON.2016.7513962.

Ordoudis, C., Pinson, P., & Morales, J. M. (2018). Electronic companion - An integrated market for electricity and natural gas systems with stochastic producers. http://doi.org/10.5281/zenodo.1174979 Accessed 17.02.18. doi:10.5281/zenodo.1174979.

Pinson, P., Mitridati, L., Ordoudis, C., & Østergaard, J. (2017). Towards fully renewable energy systems: Experience and trends in Denmark. *CSEE Journal of Power and Energy Systems, 3*, 26–35. doi:10.17775/CSEEJPES.2017.0005.

Pritchard, G., Zakeri, G., & Philpott, A. (2010). A single-settlement, energy-only electric power market for unpredictable and intermittent participants. *Operations Research, 58*(4-part-2), 1210–1219. doi:10.1287/opre.1090.0800.

Qadrdan, M., Wu, J., Jenkins, N., & Ekanayake, J. (2014). Operating strategies for a GB integrated gas and electricity network considering the uncertainty in wind power forecasts. *IEEE Transactions on Sustainable Energy, 5*(1), 128–138. doi:10.1109/TSTE.2013.2274818.

Rømo, F., Tomasgard, A., Hellemo, L., Fodstad, M., Eidesen, B. H., & Pedersen, B. (2009). Optimizing the norwegian natural gas production and transport. *Interfaces (Providence), 39*(1), 46–56. doi:10.1287/inte.1080.0414.

Sorokin, A., Rebennack, S., Pardalos, P. M., Iliadis, N. A., & Pereira, M. V. F. (2012). Handbook of Networks in Power Systems II. *Energy Systems*. Berlin, Heidelberg: Springer Berlin Heidelberg. doi:10.1007/978-3-642-23406-4.

Tabors, R. D., Englander, S., & Stoddard, R. (2012). Who's on first? The coordination of gas and power scheduling. *The Electricity Journal, 25*(5), 8–15. doi:10.1016/j.tej.2012.05.008.

Tomasgard, A., Rømo, F., Fodstad, M., & Midthun, K. (2007). Optimization models for the natural gas value chain. In *Geometric Modelling, Numerical Simulation, and Optimization* (pp. 521–558). Berlin, Heidelberg: Springer Berlin Heidelberg. doi:10.1007/978-3-540-68783-2_16.

U.S. Energy Information Administration (2016). International Energy Outlook 2016. Technical Report May 2016. www.eia.gov/forecasts/ieo/pdf/0484(2016).pdf Accessed 01.07.17.

Zlotnik, A., Roald, L., Backhaus, S., Chertkov, M., & Andersson, G. (2017a). Coordinated scheduling for interdependent electric power and natural gas infrastructures. *IEEE Trans. Power Syst., 32*(1), 600–610. doi:10.1109/TPWRS.2016.2545522.

Zlotnik, A., Rudkevich, A. M., Carter, R., Ruiz, P. A., Backhaus, S., & Tafl, J. (2017b). Grid architecture at gas-electric interface. Technical Report June 2017. https://gridarchitecture.pnnl.gov/media/advanced/Gas_grid_architecture.pdf Accessed 20.01.18.

Zlotnik, A., Rudkevich, A. M., Goldis, E., Ruiz, P. A., Caramanis, M., Carter, R., et al. (2017c). Economic optimization of intra-day gas pipeline flow schedules using transient flow models. In *PSIG 2017 Conference: PSIG-1715* (pp. 1–25).

[Paper C] Exploiting Flexibility in Coupled Electricity and Natural Gas Markets: A Price-Based Approach

Authors:
Christos Ordoudis, Stefanos Delikaraoglou, Pierre Pinson and Jalal Kazempour

Published in:
Proceedings of IEEE PowerTech Conference 2017, DOI: 10.1109/PTC.2017.7981047.

Note:
The corresponding appendix, which includes some mathematical extensions and additional results, is provided just after the manuscript.

Exploiting Flexibility in Coupled Electricity and Natural Gas Markets: A Price-Based Approach

Christos Ordoudis, Stefanos Delikaraoglou, Pierre Pinson and Jalal Kazempour
Department of Electrical Engineering
Technical University of Denmark
Kgs. Lyngby, Denmark
{chror, stde, ppin, seykaz}@dtu.dk

***Abstract*—Natural gas-fired power plants (NGFPPs) are considered a highly flexible component of the energy system and can facilitate the large-scale integration of intermittent renewable generation. Therefore, it is necessary to improve the coordination between electric power and natural gas systems. Considering a market-based coupling of these systems, we introduce a decision support tool that increases market efficiency in the current setup where day-ahead and balancing markets are cleared sequentially. The proposed approach relies on the optimal adjustment of natural gas price to modify the scheduling of power plants and reveals the necessary flexibility to handle stochastic renewable production. An essential property of this price-based approach is that it guarantees no financial imbalance (deficit or surplus) for the system operator at the day-ahead stage. Our analysis shows that the proposed mechanism reduces the expected system cost and efficiently accommodates high shares of renewables.**

***Index Terms*—Bilevel programming, electricity markets, natural gas markets, stochastic programming.**

NOMENCLATURE

Sets

I	Set of dispatchable power production units i.
I_c	Set of thermal power plants i_c ($I_c \subset I$).
I_g	Set of natural gas-fired power plants i_g ($I_g \subset I$).
J	Set of wind power units j.
K	Set of natural gas production units k.
L	Set of natural gas pipelines l.
$A_l^{i_g}$	Set of natural gas-fired power plants i_g at pipeline l.
Ω	Set of wind power scenarios ω.
T	Set of time periods t.

Variables

$p_{i,t}, w_{j,t}$	Day-ahead dispatch of units i and j in period t [MW].
$p^{+/-}_{i,\omega,t}$	Up/down regulation provided by unit i in scenario ω, period t [MW].
$w^{\text{sp}}_{j,\omega,t}$	Wind power spilled by unit j in scenario ω, period t [MW].
$l^{\text{sh,E}}_{\omega,t}, l^{\text{sh,G}}_{\omega,t}$	Electricity and natural gas load shedding in scenario ω, period t [MW, kNm^3/h].
$g_{k,t}$	Day-ahead dispatch of unit k in period t [kNm^3/h].
$g^{+/-}_{k,\omega,t}$	Up/down regulation provided by unit k in scenario ω, period t [kNm^3/h].
x_t	Natural gas price adjustment [\$/kNm^3].
λ, μ	Dual variables of equality and inequality constraints.

Parameters

D^{E}_t	Electricity demand in period t [MW].
D^{G}_t	Natural gas demand in period t [kNm^3/h].
C_i	Day-ahead offer price of unit i [\$/MWh].
$C^{+/-}_i$	Up/down regulation offer price of unit i [\$/MWh].
$C^{\text{sh,E}}$	Cost of electricity load shedding [\$/MWh].
C^{sp}	Cost of wind power spillage [\$/MWh].
C_k	Day-ahead offer price of unit k [\$/kNm^3].
$C^{+/-}_k$	Up/down regulation offer price of unit k [\$/kNm^3].
$C^{\text{sh,G}}$	Cost of natural gas load shedding [\$/kNm^3].
$P^{\max}_i$	Capacity of dispatchable unit i [MW].
$P^{+/-}_i$	Up/down reserve offer by unit i [MW].
ϕ_{i_g}	Power conversion factor of unit i_g [kNm^3/MWh].
$W_{j,\omega,t}$	Wind power realization in scenario ω, period t [MW].
$\widehat{W}_{j,t}$	Expected wind power by unit j in period t [MW].
$\overline{W}_j$	Capacity of wind power unit j [MW].
$G^{\max}_k$	Capacity of natural gas unit k [kNm^3/h].
$G^{+/-}_k$	Up/down reserve offer by unit k [kNm^3/h].
X	Limit of natural gas price adjustment [\$/kNm^3].
$F^{\text{M}}_{l,t}$	Capacity of natural gas pipeline l in period t [kNm^3/h].
F^{A}_l	Daily contract limit of natural gas pipeline l [kNm^3].

I. INTRODUCTION

In recent years, renewable energy makes up a high share of the total electricity production and is expected to increase further in the future. In view of accomplishing a transition to a green energy system, natural gas-fired power plants (NGFPPs) seem an ideal choice to facilitate this shift due to their operational flexibility and high efficiency, especially if the potential of using green gases (e.g., biogas) is considered.

The tighter coupling of electricity and natural gas markets can promote the integration of renewables in the energy system. Coupling these two markets is a natural way to increase the coordination between the two systems that have existing synergies mainly through the NGFPPs. Authors in [1] and [2] study different coordination setups in short-term operational models and highlight the benefits of such coupling. The effect of natural gas supply uncertainty and price variability on the scheduling of power plants is shown in [3]. Moreover, the case of Spain that builds its energy mix on the basis of combining renewables and NGFPPs is described in [4] indicating the need for a coupled operation of the two systems. Towards that goal, several technical and regulatory challenges need to be addressed, such as the alignment of electricity and natural gas market timing, the establishment of effective mechanisms to couple the operation and the increase of short-term trading in natural gas markets. Authors in [5] extensively discuss the timing between the two markets and how this could be harmonized. In addition, short-term trading of natural gas has increased compared to previous years as spot markets (e.g., Gaspoint Nordic) continuously develop and attract larger volumes for trading [6]. These changes will facilitate the

integration of electricity and natural gas systems to flourish under high shares of renewables. To this end, we develop a market-based coupling where the market timing is concurrent and the quantities are traded in short-term markets.

Current market designs that are based on the sequential clearing of the day-ahead and balancing trading floors may result in significant balancing costs as the penetration of renewables increases. Recent literature, e.g. [7] – [9], discusses the use of stochastic programming to anticipate future balancing needs. We consider this approach as the ideal benchmark in terms of expected cost.

In this paper, we propose a setup that couples electricity and natural gas markets and bridges the efficiency gap between the sequential and stochastic models. From a physical perspective, these two systems interact through the natural gas consumption of NGFPPs, while from an economic viewpoint they are implicitly coordinated through the natural gas price offered to NGFPPs. Exploiting this economic link, we propose a stochastic bilevel model that explicitly captures the temporal coordination between the day-ahead and balancing markets, as well as it respects the existing sequential market structure. This approach is *price-based* and allows the system operator to optimally adjust the natural gas price offered to NGFPPs by providing proper *flexibility price signals*. These price signals aim at modifying the unit dispatch and revealing adequate flexibility to cope with real-time imbalances. This mechanism is designed on a *cost-neutral* basis to ensure that the system operator will be financially balanced at the day-ahead stage. Nevertheless, this action may lead to potential real-time deficit or surplus that can be considered a price-based incentive to promote power system flexibility, akin to the flexible capacity remuneration mechanisms that are currently under discussion in the European electricity market context [10]. Results show a sound increase of market efficiency by the proposed model, as the expected system cost significantly reduces via an improved unit dispatch that effectively handles stochastic production.

This paper is organized as follows. In Sections II-A and II-B, we present the sequential and stochastic dispatch models, respectively. We describe the proposed price-based mechanism in Section II-C. Section III demonstrates the results on a stylized case study, while Section IV concludes the paper.

II. Dispatch models

The models considered in this study assume that electricity and natural gas markets are coupled, i.e., the market clearing is a single optimization problem. This approach is an optimistic view of the current setup, where these markets are actually decoupled and thus loosely coordinated in terms of price, i.e., NGFPPs submit their electricity price-quantity offers based on an estimation and not the true value of the natural gas price.

A. Sequential Coupled Electricity and Natural Gas Model

The sequential dispatch model (*Seq*) clears independently the day-ahead and balancing markets. The optimal schedule that minimizes the day-ahead cost of the integrated system is determined by model (1) as follows,

$$\underset{\Theta^{\mathrm{D}}}{\text{Min.}} \sum_{t\in T}\Big(\sum_{i_c\in I_c} C_{i_c} p_{i_c,t} + \sum_{k\in K} C_k g_{k,t}\Big) \tag{1a}$$

subject to

$$0 \le p_{i,t} \le P_i^{\max} : \underline{\mu}_{i,t}^{\mathrm{P}}, \overline{\mu}_{i,t}^{\mathrm{P}}, \ \ \forall i,t, \tag{1b}$$

$$0 \le w_{j,t} \le \widehat{W}_{j,t} : \underline{\mu}_{j,t}^{\widehat{\mathrm{W}}}, \overline{\mu}_{j,t}^{\widehat{\mathrm{W}}}, \ \ \forall j,t, \tag{1c}$$

$$\sum_{i\in I} p_{i,t} + \sum_{j\in J} w_{j,t} - D_t^{\mathrm{E}} = 0 : \hat{\lambda}_t^{\mathrm{E}}, \ \ \forall t, \tag{1d}$$

$$0 \le \sum_{i_g\in A_l^{I_g}} \phi_{i_g} p_{i_g,t} \le F_{l,t}^{\mathrm{M}} : \underline{\mu}_{l,t}^{\mathrm{M}}, \overline{\mu}_{l,t}^{\mathrm{M}}, \ \ \forall l,t, \tag{1e}$$

$$0 \le \sum_{t\in T}\sum_{i_g\in A_l^{I_g}} \phi_{i_g} p_{i_g,t} \le F_l^{\mathrm{A}} : \underline{\mu}_{l}^{\mathrm{A}}, \overline{\mu}_{l}^{\mathrm{A}}, \ \ \forall l, \tag{1f}$$

$$0 \le g_{k,t} \le G_k^{\max} : \underline{\mu}_{k,t}^{\mathrm{G}}, \overline{\mu}_{k,t}^{\mathrm{G}}, \ \ \forall k,t, \tag{1g}$$

$$\sum_{k\in K} g_{k,t} - D_t^{\mathrm{G}} - \sum_{i_g\in I_g} \phi_{i_g} p_{i_g,t} = 0 : \hat{\lambda}_t^{\mathrm{G}}, \ \ \forall t, \tag{1h}$$

where $\Theta^{\mathrm{D}} = \{p_{i,t}, \forall i,t; w_{j,t}, \forall j,t; g_{k,t}, \forall k,t\}$ is the set of primal optimization variables. The total operating cost in (1a) stems from the power production cost of thermal power plants and the total natural gas production cost. The power production cost of NGFPPs is neglected as this would imply double counting it. Constraints (1b) and (1c) enforce the upper and lower limits of power production of dispatchable and wind power plants. Wind power is constrained by the expected wind generation. Equations (1d) and (1h) represent the power and natural gas balance at the day-ahead stage. The physical pipeline capacity in each hour is imposed by (1e), while (1f) limits the daily natural gas use. The natural gas production limits of each plant are determined through (1g). For the sake of conciseness, we denote the regulation provided by each balancing power plant as $\Delta p_{i,\omega',t} = p_{i,\omega',t}^{+} - p_{i,\omega',t}^{-}$. Having the day-ahead schedule of the integrated system as a fixed parameter (denoted with superscript '*') and for a specific realization of $W_{j,\omega',t}$, the real-time market clearing writes as,

$$\underset{\Theta^{\mathrm{R}}}{\text{Min.}} \sum_{t\in T}\Big(\sum_{k\in K}(C_k^{+} g_{k,\omega',t}^{+} - C_k^{-} g_{k,\omega',t}^{-}) + C^{\mathrm{sh,E}} l_{\omega',t}^{\mathrm{sh,E}} \tag{2a}$$

$$+ \sum_{i_c\in I_c}(C_{i_c}^{+} p_{i_c,\omega',t}^{+} - C_{i_c}^{-} p_{i_c,\omega',t}^{-}) + C^{\mathrm{sh,G}} l_{\omega',t}^{\mathrm{sh,G}} + \sum_{j\in J} C^{\mathrm{sp}} w_{j,\omega',t}^{\mathrm{sp}}\Big)$$

subject to

$$0 \le p_{i,\omega',t}^{+} \le P_i^{\max} - p_{i,t}^{*} : \underline{\mu}_{i,\omega',t}^{\mathrm{PR+}}, \overline{\mu}_{i,\omega',t}^{\mathrm{PR+}}, \ \ \forall i,t, \tag{2b}$$

$$0 \le p_{i,\omega',t}^{-} \le p_{i,t}^{*} : \underline{\mu}_{i,\omega',t}^{\mathrm{PR-}}, \overline{\mu}_{i,\omega',t}^{\mathrm{PR-}}, \ \ \forall i,t, \tag{2c}$$

$$0 \le p_{i,\omega',t}^{+} \le P_i^{+} : \underline{\mu}_{i,\omega',t}^{\mathrm{P+}}, \overline{\mu}_{i,\omega',t}^{\mathrm{P+}}, \ \ \forall i,t, \tag{2d}$$

$$0 \le p_{i,\omega',t}^{-} \le P_i^{-} : \underline{\mu}_{i,\omega',t}^{\mathrm{P-}}, \overline{\mu}_{i,\omega',t}^{\mathrm{P-}}, \ \ \forall i,t, \tag{2e}$$

$$0 \le w_{j,\omega',t}^{\mathrm{sp}} \le W_{j,\omega',t} : \underline{\mu}_{j,\omega',t}^{\mathrm{sp}}, \overline{\mu}_{j,\omega',t}^{\mathrm{sp}}, \ \ \forall j,t, \tag{2f}$$

$$0 \le l_{\omega',t}^{\mathrm{sh,E}} \le D_t^{\mathrm{E}} : \underline{\mu}_{\omega',t}^{\mathrm{sh,E}}, \overline{\mu}_{\omega',t}^{\mathrm{sh,E}}, \ \ \forall t, \tag{2g}$$

$$\sum_{i\in I} \Delta p_{i,\omega',t} + l_{\omega',t}^{\mathrm{sh,E}} + \sum_{j\in J}(W_{j,\omega',t} - w_{j,\omega',t}^{\mathrm{sp}} - w_{j,t}^{*}) = 0 : \tilde{\lambda}_{\omega',t}^{\mathrm{E}}, \ \ \forall t, \tag{2h}$$

$$0 \leq \sum_{i_g \in A_l^{I_g}} \phi_{i_g}(p^*_{i_g,t} + \Delta p_{i_g,\omega',t}) \leq F^{\mathrm{M}}_{l,t} : \underline{\mu}^{\mathrm{MR}}_{l,\omega',t}, \overline{\mu}^{\mathrm{MR}}_{l,\omega',t}, \ \forall l, t, \quad (2i)$$

$$0 \leq \sum_{t \in T} \sum_{i_g \in A_l^{I_g}} \phi_{i_g}(p^*_{i_g,t} + \Delta p_{i_g,\omega',t}) \leq F^{\mathrm{A}}_{l} : \underline{\mu}^{\mathrm{AR}}_{l,\omega'}, \overline{\mu}^{\mathrm{AR}}_{l,\omega'}, \ \forall l, \quad (2j)$$

$$0 \leq g^{+}_{k,\omega',t} \leq G^{\max}_k - g^*_{k,t} : \underline{\mu}^{\text{GR+}}_{k,\omega',t}, \overline{\mu}^{\text{GR+}}_{k,\omega',t}, \ \ \forall k, t, \quad (2k)$$

$$0 \leq g^{-}_{k,\omega',t} \leq g^*_{k,t} : \underline{\mu}^{\text{GR-}}_{k,\omega',t}, \overline{\mu}^{\text{GR-}}_{k,\omega',t}, \ \ \forall k, t, \quad (2l)$$

$$0 \leq g^{+}_{k,\omega',t} \leq G^{+}_k : \underline{\mu}^{\text{G+}}_{k,\omega',t}, \overline{\mu}^{\text{G+}}_{k,\omega',t}, \ \ \forall k, t, \quad (2m)$$

$$0 \leq g^{-}_{k,\omega',t} \leq G^{-}_k : \underline{\mu}^{\text{G-}}_{k,\omega',t}, \overline{\mu}^{\text{G-}}_{k,\omega',t}, \ \ \forall k, t, \quad (2n)$$

$$0 \leq l^{\text{sh,G}}_{\omega',t} \leq D^{\mathrm{G}}_t : \underline{\mu}^{\text{sh,G}}_{\omega',t}, \overline{\mu}^{\text{sh,G}}_{\omega',t}, \ \ \forall t, \quad (2o)$$

$$\sum_{k \in K}(g^{+}_{k,\omega',t} - g^{-}_{k,\omega',t}) + l^{\text{sh,G}}_{\omega',t} - \sum_{i_g \in I_g} \phi_{i_g} \Delta p_{i_g,\omega',t} = 0 : \tilde{\lambda}^{\mathrm{G}}_{\omega',t}, \ \ \forall t, \quad (2p)$$

where $\Theta^{\mathrm{R}} = \{p^{+}_{i,\omega',t}, p^{-}_{i,\omega',t}, \forall i,t; l^{\text{sh,E}}_{\omega',t}, l^{\text{sh,G}}_{\omega',t}, \forall t; w^{\text{sp}}_{j,\omega',t}, \forall j,t; g^{+}_{k,\omega',t}, g^{-}_{k,\omega',t}, \forall k,t\}$ is the set of primal optimization variables. The aim of model (2) is to minimize the balancing cost of re-dispatch actions. Constraints (2b) and (2c) determine the bounds of power regulation taking into account the day-ahead schedule and the capacity of the power plant, while (2d) and (2e) enforce the limits of up- and down-regulation. Wind spillage is restricted by the actual wind power realization and load shedding by electricity demand through (2f) and (2g), respectively. Equation (2h) represents the power balance in real-time operation. The real-time physical pipeline capacity is enforced by (2i), while (2j) imposes the daily natural gas volume limit. Constraints (2k) and (2l) set the bounds of natural gas regulation given the capacity and day-ahead schedule of each plant. Up- and down-regulation levels of natural gas are limited by (2m) and (2n), while load shedding is limited by the natural gas demand in (2o). Constraint (2p) enforces real-time natural gas balancing. In all models, the dual variables of each constraint are indicated after a colon. The dual variables of equality constraints are of particular interest since they reflect the market price for electricity and natural gas. The expected balancing cost over a scenario set Ω is given as the sum of the balancing cost for each scenario ω weighed by its probability of occurrence π_ω.

B. Stochastic Coupled Electricity and Natural Gas Model

The stochastic dispatch model (*Stoch*) optimizes jointly the day-ahead and balancing stages of the integrated electric power and natural gas systems. The problem is formulated as a two-stage stochastic program aiming to minimize the total expected cost and writes as follows,

$$\underset{\Theta^{\mathrm{SC}}}{\text{Min.}} \ \sum_{t \in T}\Big[\sum_{i_c \in I_c} C_{i_c} p_{i_c,t} + \sum_{k \in K} C_k g_{k,t} + \sum_{\omega \in \Omega} \pi_\omega \Big(\sum_{k \in K}(C^{+}_k g^{+}_{k,\omega,t} - C^{-}_k g^{-}_{k,\omega,t}) + \sum_{i_c \in I_c}(C^{+}_{i_c} p^{+}_{i_c,\omega,t} - C^{-}_{i_c} p^{-}_{i_c,\omega,t}) + C^{\text{sh,E}} l^{\text{sh,E}}_{\omega,t} + C^{\text{sh,G}} l^{\text{sh,G}}_{\omega,t} + \sum_{j \in J} C^{\text{sp}} w^{\text{sp}}_{j,\omega,t} \Big) \Big] \quad (3a)$$

subject to

$$\text{constraints (1b), (1d)} - \text{(1h)}, \quad (3b)$$

$$0 \leq w_{j,t} \leq \overline{W}_j : \underline{\mu}^{\overline{\mathrm{W}}}_{j,t}, \overline{\mu}^{\overline{\mathrm{W}}}_{j,t}, \ \ \forall j, t, \quad (3c)$$

$$\text{constraints (2b)} - \text{(2p)}, \ \ \forall \omega, \quad (3d)$$

where $\Theta^{\mathrm{SC}} = \{p_{i,t}, \forall i,t; w_{j,t}, \forall j,t; p^{+}_{i,\omega,t}, p^{-}_{i,\omega,t}, \forall i,\omega,t; g_{k,t}, \forall k,t; w^{\text{sp}}_{j,\omega,t}, \forall j,\omega,t; g^{+}_{k,\omega,t}, g^{-}_{k,\omega,t}, \forall k,\omega,t; l^{\text{sh,E}}_{\omega,t}, l^{\text{sh,G}}_{\omega,t}, \forall \omega,t\}$ is the set of primal optimization variables. In this model, the temporal coordination of the two trading floors is achieved through the real-time constraints (3d) for all scenarios $\omega \in \Omega$. The day-ahead dispatch of wind power is restricted by the installed capacity, instead of the expected wind generation and day-ahead dispatch decisions are treated as variables.

C. Price-Based Coupled Electricity and Natural Gas Model

The proposed dispatch model (*P-B*) that aims at minimizing the expected cost of the integrated energy system and defining the optimal natural gas price adjustment x_t writes as follows,

$$\underset{\Theta^{\mathrm{UL}}}{\text{Min.}} \ \text{(3a)} \quad (4a)$$

subject to

$$-X \leq x_t \leq X, \ \ \forall t, \quad (4b)$$

$$\sum_{t \in T}\sum_{i_g \in I_g} \phi_{i_g} p_{i_g,t} x_t = 0, \quad (4c)$$

$$(p_{i,t}, w_{j,t}) \in \arg\Big\{ \underset{\Theta^{\mathrm{LL}}_1}{\text{Min.}} \ \sum_{t \in T}\Big(\sum_{i_c \in I_c} C_{i_c} p_{i_c,t} + \sum_{i_g \in I_g} C_{i_g,t} p_{i_g,t}\Big) \quad (4d)$$

subject to

$$\text{constraints (1b)} - \text{(1f)}, \quad (4e)$$

$$C_{i_g,t} = (\hat{\lambda}^{\mathrm{G}}_t + x_t)\phi_{i_g}, \ \ \forall i_g, t \Big\}, \quad (4f)$$

$$(p^{+}_{i,\omega,t}, p^{-}_{i,\omega,t}, w^{\text{sp}}_{j,\omega,t}, l^{\text{sh,E}}_{\omega,t}) \in \arg\Big\{ \underset{\Theta^{\mathrm{LL}}_2}{\text{Min.}} \ \sum_{t \in T}\Big(\sum_{i_c \in I_c}(C^{+}_{i_c} p^{+}_{i_c,\omega,t} - C^{-}_{i_c} p^{-}_{i_c,\omega,t}) + \sum_{i_g \in I_g}(C^{+}_{i_g,\omega,t} p^{+}_{i_g,\omega,t} - C^{-}_{i_g,\omega,t} p^{-}_{i_g,\omega,t}) + C^{\text{sh,E}} l^{\text{sh,E}}_{\omega,t} + \sum_{j \in J} C^{\text{sp}} w^{\text{sp}}_{j,\omega,t}\Big) \quad (4g)$$

subject to

$$\text{constraints (2b)} - \text{(2j)}, \quad (4h)$$

$$C^{+}_{i_g,\omega,t} = (\tilde{\lambda}^{\mathrm{G}}_{\omega,t} + x_t)\phi_{i_g}, \ \ \forall i_g, t, \quad (4i)$$

$$C^{-}_{i_g,\omega,t} = (\tilde{\lambda}^{\mathrm{G}}_{\omega,t} + x_t)\phi_{i_g}, \ \ \forall i_g, t \Big\}, \ \ \forall \omega, \quad (4j)$$

$$(g_{k,t}, \hat{\lambda}^{\mathrm{G}}_t) \in \arg\Big\{ \underset{\Theta^{\mathrm{LL}}_3}{\text{Min.}} \ \sum_{t \in T}\sum_{k \in K} C_k g_{k,t} \quad (4k)$$

subject to

$$\text{constraints (1g)} - \text{(1h)}\Big\}, \quad (4l)$$

$$(g^{+}_{k,\omega,t}, g^{-}_{k,\omega,t}, l^{\text{sh,G}}_{\omega,t}, \tilde{\lambda}^{G}_{\omega,t}) \in \arg\Big\{$$

$$\underset{\Theta^{\text{LL}}_4}{\text{Min.}} \sum_{t\in T}\Big(\sum_{k\in K}(C^{+}_{k} g^{+}_{k,\omega,t} - C^{-}_{k} g^{-}_{k,\omega,t})\Big) + C^{\text{sh,G}} l^{\text{sh,G}}_{\omega,t}\Big) \quad \text{(4m)}$$

$$\text{subject to}$$

$$\text{constraints (2k)} - \text{(2p)}\Big\}, \ \forall\omega, \quad \text{(4n)}$$

where $\Theta^{\text{LL}}_1 = \{p_{i,t}, \forall i,t; w_{j,t}, \forall j,t\}$, $\Theta^{\text{LL}}_2 = \{p^{+}_{i,\omega,t}, p^{-}_{i,\omega,t}, \forall i,\omega,t; l^{\text{sh,E}}_{\omega,t}, \forall\omega,t; w^{\text{sp}}_{j,\omega,t}, \forall j,\omega,t\}$, $\Theta^{\text{LL}}_3 = \{g_{k,t}, \forall k,t\}$ and $\Theta^{\text{LL}}_4 = \{g^{+}_{k,\omega,t}, g^{-}_{k,\omega,t}, \forall k,\omega,t; l^{\text{sh,G}}_{\omega,t}, \forall\omega,t\}$ are the sets of primal optimization variables of the lower-level problems. Additionally, $\Theta^{\text{UL}} = \{x_t, \forall t, \Theta^{\text{LL}}_1, \Theta^{\text{LL}}_2, \Theta^{\text{LL}}_3, \Theta^{\text{LL}}_4\}$ is the set of primal optimization variables of the upper-level problem. The upper-level problem minimizes the expected cost of operating the integrated energy system by deciding the optimal value of variable x_t. Additionally, the lower-level problems practically reproduce the sequential coupled electricity and natural gas market. The system operator has the ability to vary the price of natural gas within specified limits, defined by (4b), to achieve a cost-effective system operation. The upper-level variable x_t has an impact on the decisions of the lower-level problems as the day-ahead and up/down regulation offer prices of NGFPPs are affected by this value through (4f), (4i) and (4j). Moreover, the lower-level decision variables affect the total expected cost of the integrated system. Capturing this dependency, the proposed mechanism can reveal the true value of the NGFPPs' flexibility and yield a dispatch that reduces expected system cost while respecting the merit-order principle. Equation (4c) acts as a *cost-neutrality constraint* since it guarantees that this mechanism leaves no financial deficit or surplus to the system operator, i.e., the hourly day-ahead payments or charges are counterbalanced throughout the day. Potential deficit or surplus at the balancing stage is expected to be fairly limited and can be addressed through proper regulation as for instance the capacity payments for power availability in real-time operation.

The bilevel problem (4) can be reformulated as a Mathematical Program with Equilibrium Constraints (MPEC) by replacing the linear, and thus convex, lower level problems by their Karush-Kuhn-Tucker (KKT) conditions. Then, it is transformed into a Mixed-Integer Linear Program (MILP) in order to deal with the bilinear terms that arise from the complementarity conditions. Constraint (4c) is linearized by using the KKT conditions and strong duality theorem. A detailed mathematical description of the aforementioned procedure is presented in the electronic companion of the paper [11].

III. Results

In this section, we illustrate the features of the three dispatch models presented in Section II. We consider a system that comprises three thermal power plants and two NGFPPs which also participate in the natural gas market to acquire their fuel. The unit data are provided in Table I. Up- and down-regulation offer prices are equal to 1.1 and 0.9 of day-ahead offer price. The natural gas price adjustment is limited to \$80/kNm^3. The cost of load shedding is \$1200/MWh and \$1000/kNm^3, while wind spillage is cost free. The peak natural gas and electricity demand are equal to 60 kNm^3/h and to 430 MW, respectively.

TABLE I
Electric Power and Natural Gas System Data

Unit i	1	2	3	4	5	Unit k	1	2
$P^{\max}_i$	80	110	50	100	100	$G^{\max}_k$	150	100
P^{+}_i	10	0	30	25	20	G^{+}_k	50	20
P^{-}_i	10	0	30	25	20	G^{-}_k	50	20
C_i	30	10	-	-	60	C_k	120	160
ϕ_{i_g}	-	-	0.2	0.3	-			

For illustration purposes, we perform a simulation in which wind power uncertainty is characterized by a set of two equiprobable scenarios, namely, ω_1 (166 MW) and ω_2 (86 MW). The marginal cost of wind power is equal to zero and the expected wind power production is 126 MW. We provide results for two time periods to show the effect of adjusted natural gas prices (either increased or reduced) on the schedules of NGFPPs. The results are presented in Tables II, III, IV and V. The lowest expected system cost is obtained by model *Stoch*. Model *Seq* respects the merit-order principle as wind power is dispatched to its expected value due to zero marginal cost and then the power plants are scheduled based on an ascending order of marginal costs. The marginal cost of NGFPPs stems from the multiplication of natural gas price and power conversion factor. In this example, natural gas is only produced by unit K_1, so its price is \$120/kNm^3, which results in a price offer from NGFPP I_4 equal to \$36/MWh. Unit I_5 is the most expensive and thus not scheduled at day-ahead stage.

Table II shows the generation schedule reported by models *Seq* and *P-B*, when the electricity demand is equal to 387 MW. In model *P-B*, variable x_{t_1} is equal to -\$20/kNm^3 that results in a reduced natural gas price of \$100/kNm^3 for all NGFPPs, which in turn affects their marginal cost of power production. The marginal cost of NGFPP I_4 is reduced to \$30/MWh, which is equal to the marginal cost of unit I_1. NGFPP I_4 is now scheduled to 31 MW, while unit I_1 to 70 MW. The day-ahead cost increases compared to *Seq* since in reality the operating cost of the system rises from the actual costs and not the reduced one that NGFPPs buy natural gas. However, this increase is offset by the lower total balancing cost achieved by *P-B*. The up-regulation cost is lower since unit I_1 is able to provide a portion of the total 40 MW needed for up-regulation. This is due to the fact that unit I_1 has a lower real up-regulation cost than unit I_5. Moreover, NGFPP I_4 is more cost-effective for providing down-regulation compared to NGFPP I_3 and thus reduces the down-regulation cost of *P-B*.

Similarly, Table IV shows the schedule of power plants under *Seq* and *P-B*, when the electricity demand is equal to 344 MW. In this case, the value of x_{t_2} is equal to +\$30/kNm^3 which in a similar manner affects the marginal cost of NGFPPs. The marginal cost of NGFPP I_3 is increased to \$30/MWh, which is equal to the marginal cost of unit I_1. This action results in an improved scheduling at the day-ahead stage that will result in a lower expected cost. In both cases, it can

TABLE II
ELECTRIC POWER SYSTEM SCHEDULE IN MW – ($D^{\mathrm{E}} = 387$ MW)

Agent	Seq			P-B		
	Day-ahead	Balancing		Day-ahead	Balancing	
		ω_1	ω_2		ω_1	ω_2
I_1	80	-10	0	70	-10	+10
I_2	110	0	0	110	0	0
I_3	50	-9	0	50	-5	0
I_4	21	-21	+25	31	-25	+25
I_5	0	0	+15	0	0	+5
WP	126	+40	-40	126	+40	-40

TABLE III
EXPECTED SYSTEM OPERATION COST IN \$ – ($D^{\mathrm{E}} = 387$ MW)

	Total	Day-ahead	Balancing	Up regulation	Down regulation
Seq	10 400.4	9 982.8	417.6	990.0	-572.4
Stoch	10 234.8	10 222.8	12.0	660.0	-648.0
P-B	10 273.8	10 042.8	231.0	825.0	-594.0

be observed that x_t affects the natural gas price for power production, which in turn changes the day-ahead dispatch. The dispatch is changed in order to enable more cost-effective power plants to provide the required regulation. These price signals establish a temporal coordination between the two trading floors and thus better exploit the available technical flexibility of the two systems.

TABLE IV
ELECTRIC POWER SYSTEM SCHEDULE IN MW – ($D^{\mathrm{E}} = 344$ MW)

Agent	Seq			P-B		
	Day-ahead	Balancing		Day-ahead	Balancing	
		ω_1	ω_2		ω_1	ω_2
I_1	58	-10	+10	70	-10	+10
I_2	110	0	0	110	0	0
I_3	50	-30	0	38	-30	+12
I_4	0	0	+25	0	0	+18
I_5	0	0	+5	0	0	0
WP	126	+40	-40	126	+40	-40

TABLE V
EXPECTED SYSTEM OPERATION COST IN \$ – ($D^{\mathrm{E}} = 344$ MW)

	Total	Day-ahead	Balancing	Up regulation	Down regulation
Seq	8 932.8	8 566.8	366.0	825.0	-459.0
Stoch	8 859.6	8 206.8	652.8	917.4	-264.6
P-B	8 859.6	8 638.8	220.8	679.8	-459.0

The following results are provided for the whole 24-hour scheduling horizon and 20 wind power scenarios (available at [12]). Fig. 1 shows the expected cost of the coupled electricity and natural gas system for different wind power penetration levels, i.e., share of installed wind power capacity on system's demand. It is observed that *Stoch* results in the lowest expected cost in all cases and efficiently utilizes the increase of wind power production. The expected cost of *Seq* diverges from the corresponding values of the other dispatch models for a wind power penetration level above 25% and shows a significant increase when this share is higher than 40%. On the contrary, the expected cost of the proposed dispatch model *P-B* remains close to *Stoch* over the whole range of wind power penetration. This verifies the ability of *P-B* to bridge the gap between *Seq* and *Stoch* by providing solutions closer to the stochastic ideal, while maintaining the economic properties of the sequential market clearing.

Additionally, Table VI presents the expected payment/charge to adjust the price of natural gas at the balancing stage and the overall savings in expected cost between *Seq*

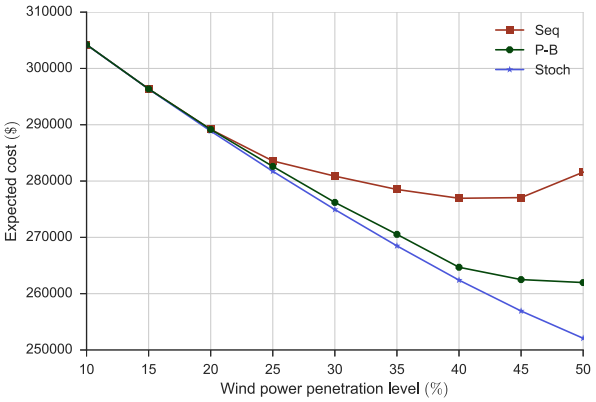

Fig. 1. Impact of wind power penetration level on the expected system cost.

TABLE VI
EXPECTED PAYMENT/CHARGE TO GENERATE FLEXIBILITY PRICE SIGNAL

Wind power penetration level (%)	25	30	35	40	45	50
Exp. savings (\$)	971.5	4 663	8 035.6	12 251.8	14 562.4	19 601.6
Exp. payment/charge (\$)	-352.1	-177.1	-21.4	133.5	2.2	302.3

and *P-B*. Relevant results are only illustrated for wind power penetration levels that models *Seq* and *P-B* provide a different dispatch. The payment/charge at the day-ahead stage is zero due to (4c) but at the balancing stage the system operator could have either a deficit or a surplus under different conditions. However, this financial imbalance is significantly lower than the benefit of reducing the total expected cost and can be either socialized or utilized for future investments. We observe larger expected savings as wind power penetration increases, while the expected payment/charge remains at the same level that is relatively small. For the case of 50% wind power penetration, *P-B* reduces the expected cost by \$19 601.6 compared to *Seq* and the system operator is expected to receive \$302.3.

We now consider a wind power penetration level of 50% to provide useful insights of the proposed dispatch model. Fig. 2 shows the natural gas price adjustment (x_t) and the day-ahead payment/charge in order to generate this signal. It can be observed that the sign of x_t determines whether the system operator has to incur a deficit or a surplus to change the price of natural gas, while the total settlement also depends on the volume of natural gas consumed for power production at the day-ahead stage. The natural gas price is reduced for the majority of time periods, which results in a deficit for the system operator during these hours. However, this deficit is offset by the surplus generated in periods when the natural gas price adjustment is positive, retaining this action as cost-neutral at the day-ahead stage.

Furthermore, we illustrate the natural gas price adjustment (x_t) in relation to the difference in the hourly NGFPPs' share of the total power production between *P-B* and *Seq*. A positive value (green area) shows that NGFPPs are scheduled to produce more at the day-ahead stage under *P-B* than in *Seq*, while a negative value (red area) shows the opposite case. During the first hours of the day, inflexible unit I_2 is mainly dispatched under *Seq*. It can be observed that during the same

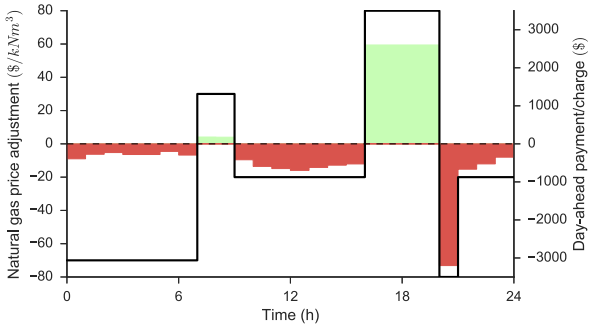

Fig. 2. Hourly natural gas price adjustment (black line: left y-axis) and day-ahead financial settlement of the system operator to adjust the natural gas price (colored areas: right y-axis). Wind power penetration 50%.

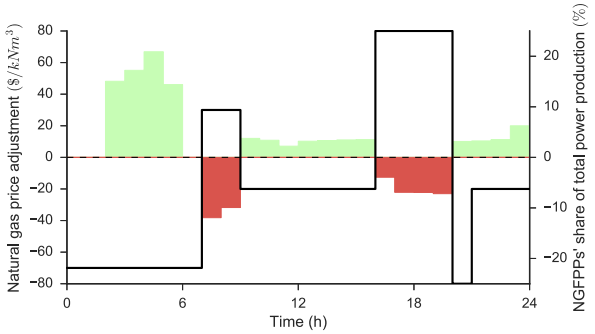

Fig. 3. Hourly natural gas price adjustment (black line: left y-axis) and difference in NGFPPs' share of total power production between *P-B* and *Seq* (colored areas: right y-axis). Wind power penetration 50%.

period, the price of natural gas is reduced under *P-B* in order to schedule NGFPP I_3 and exploit its flexibility. On the contrary, the price of natural gas is increased during hours 17-20, when electricity demand reaches its peak. As a result, a part of the electricity demand covered by NGFPP I_4 is undertaken by unit I_5 and that results in revealing flexibility to handle wind power uncertainty. Moreover, it is noticed that a change in the natural gas price does not always reflect an alternation of the day-ahead dispatch. This decision takes into account the trade-off between improving the dispatch and guaranteeing that this action is cost-neutral at the day-ahead stage.

The pricing scheme of *Stoch* ensures cost recovery for flexible producers only in expectation. However, maintaining a sequential setup to clear the market generates prices that support the dispatch in such a way that the aforementioned property will hold for each scenario of stochastic production. We refer the reader to [8] for further discussion on this topic.

Supplementary results and the code are given in [11] for reader's convenience. The optimization problems were solved using CPLEX 12.6.2 under GAMS on a stationary computer with Inter i7 4-core processor clocking at 3.4 GHz and 8 GB of RAM. The average time to solve *P-B* was 520 seconds.

IV. Conclusion

This paper proposes a price-based coordination between electricity and natural gas markets to bring the expected cost closer to the stochastic ideal solution. Using a natural gas price adjustment component, this mechanism enables an implicit temporal coupling of the day-ahead and balancing markets, while preserving the existing sequential market clearing of those trading floors. We employ a stochastic bilevel model that allows the system operator to anticipate the real-time operation of the integrated system taking into account the economic link between electricity and natural gas markets. The proposed method ensures that the natural gas price adjustment only affects the payment/charge at the balancing stage, where the traded quantities are significantly lower.

For future research, we intend to enrich the current model formulation including electricity network constraints. This will enable us to define more accurately the optimal natural gas price adjustments taking into account potential transmission congestions. The proposed model can be adapted to alternative coordination mechanisms between electricity and natural gas markets, e.g., quantity-based coordination as well as to compare the efficiency of these approaches against direct remuneration mechanisms of flexible producers.

Acknowledgment

The work of the authors is partly funded by the Danish Strategic Research Council (DSF) through projects 5s-Future Electricity Markets, No. 12-132636/DSF and CITIES, No. 1305-00027B/DSF. The authors would like to thank Tue V. Jensen for his help on supplementary material dissemination.

References

[1] A. Zlotnik, L. Roald, S. Backhaus, M. Chertkov and G. Andersson, "Coordinated scheduling for interdependent electric power and natural gas infrastructures," *IEEE Trans. on Power Syst.*, vol. 32, no. 1, pp. 600-610, 2017.

[2] C. M. Correa-Posada and P. Sánchez-Martin, "Integrated power and natural gas model for energy adequacy in short-term operation," *IEEE Trans. on Power Syst.*, vol. 30, no. 6, pp. 3347-3355, 2015.

[3] B. Zhao, A. J. Conejo, and R. Sioshansi, "Unit commitment under gas-supply uncertainty and gas-price variability," *IEEE Trans. on Power Syst.*, doi:10.1109/TPWRS.2016.2602659.

[4] J. Gil, A. Caballero and A. J. Conejo, "Power cycling: CCGTs: The critical link between the electricity and natural gas markets," *IEEE Power and Energy Magazine*, vol. 12, no. 6, pp. 40-48, 2014.

[5] P. J. Hibbard and T. Schatzki, "The interdependence of electricity and natural gas: Current factors and future prospects," *Electricity J.*, vol. 25, no. 4, pp. 6-17, 2012.

[6] P. Pinson, L. Mitridati, C. Ordoudis and J. Østergaard, "Towards fully renewable energy systems - Experiences and trends in Denmark," *CSEE Journal of Power and Energy Systems*, 2016, in press.

[7] G. Pritchard, G. Zakeri and A. Philpott, "A single-settlement, energy-only electric power market for unpredictable and intermittent participants," *Oper. Res.*, vol. 58, no. 4, pp. 1210-1219, 2010.

[8] J. M. Morales, M. Zugno, S. Pineda and P. Pinson, "Electricity market clearing with improved scheduling of stochastic production," *Eur. J. Oper. Res.*, vol. 235, no. 3, pp. 765-774, 2014.

[9] A. Alabdulwahab, A. Abusorrah, X. Zhang and M. Shahidehpour, "Coordination of interdependent natural gas and electricity infrastructures for firming the variability of wind energy in stochastic day-ahead scheduling," *IEEE Trans. Sustain. Energy*, vol. 6, no. 2, pp. 606-615, 2015.

[10] A. Henriot and J. M. Glachant, "Capacity remuneration mechanisms in the European market: now but how?," *European University Institute (EUI), Robert Schuman Centre of Advanced Studies (RSCAS)*, 2014.

[11] C. Ordoudis, S. Delikaraoglou, P. Pinson and J. Kazempour, "Electronic companion for paper: Exploiting flexibility in coupled electricity and natural gas markets: A price-based approach", [Online], http://doi.org/10.5281/zenodo.376307.

[12] W. Bukhsh, "Data for stochastic multiperiod optimal power flow problem," *Website*, Mar. 2017, https://sites.google.com/site/datasmopf/.

Exploiting Flexibility in Coupled Electricity and Natural Gas Markets: A Price-Based Approach

Christos Ordoudis, Stefanos Delikaraoglou, Pierre Pinson and Jalal Kazempour
Department of Electrical Engineering
Technical University of Denmark
Kgs. Lyngby, Denmark
{chror, stde, ppin, seykaz}@dtu.dk

This document serves as an electronic companion for the paper "Exploiting Flexibility in Coupled Electricity and Natural Gas Markets: A Price-Based Approach" to be published in the proceedings of IEEE PES PowerTech 2017. It contains three sections that provide supplemental material relative to the mathematical formulation of the problem and additional results.

1 MPEC formulation of price-based coupled electricity and natural gas model (*P-B*)

In this section the bilevel *P-B* model is reformulated as a Mathematical Program with Equilibrium Constraints (MPEC) by replacing the linear, and thus convex, lower level problems by their Karush-Kuhn-Tucker (KKT) conditions. Then, the resulting MPEC is transformed into a Mixed-Integer Linear Program (MILP) in order to deal with the bilinear terms that arise from the complementarity conditions. We introduce a mapping $M_l^{i_g}$ of the natural gas-fired power plants i_g at pipeline l (entries are equal to 1 if NGFPP is connected to a pipeline and 0 otherwise). The model writes as follows,

$$\underset{\Theta^{\text{MUL}}}{\text{Min.}} \sum_{t\in T}\Big[\sum_{i_c\in I_c} C_{i_c}p_{i_c,t} + \sum_{k\in K} C_k g_{k,t} + \sum_{\omega\in\Omega}\pi_\omega\Big(\sum_{k\in K}(C_k^+ g_{k,\omega,t}^+ - C_k^- g_{k,\omega,t}^-) + \sum_{i_c\in I_c}(C_{i_c}^+ p_{i_c,\omega,t}^+ - C_{i_c}^- p_{i_c,\omega,t}^-)$$
$$+ C^{\text{sh,E}} l_{\omega,t}^{\text{sh,E}} + C^{\text{sh,G}} l_{\omega,t}^{\text{sh,G}} + \sum_{j\in J} C^{\text{sp}} w_{j,\omega,t}^{\text{sp}}\Big)\Big] \tag{1a}$$

subject to

$$-X \le x_t \le X,\ \forall t, \tag{1b}$$
$$\sum_{t\in T}\sum_{i_g\in I_g}\phi_{i_g}p_{i_g,t}x_t = 0, \tag{1c}$$
$$0 \le p_{i,t} \le P_i^{\max} : \underline{\mu}_{i,t}^{\text{P}}, \overline{\mu}_{i,t}^{\text{P}},\ \forall i,t, \tag{1d}$$
$$0 \le w_{j,t} \le \widehat{W}_{j,t} : \underline{\mu}_{j,t}^{\widehat{\text{W}}}, \overline{\mu}_{j,t}^{\widehat{\text{W}}},\ \forall j,t, \tag{1e}$$
$$0 \le \sum_{i_g\in A_l^{I_g}}\phi_{i_g}p_{i_g,t} \le F_{l,t}^{\text{M}} : \underline{\mu}_{l,t}^{\text{M}}, \overline{\mu}_{l,t}^{\text{M}},\ \forall l,t, \tag{1f}$$
$$0 \le \sum_{t\in T}\sum_{i_g\in A_l^{I_g}}\phi_{i_g}p_{i_g,t} \le F_l^{\text{A}} : \underline{\mu}_l^{\text{A}}, \overline{\mu}_l^{\text{A}},\ \forall l, \tag{1g}$$
$$\sum_{i\in I} p_{i,t} + \sum_{j\in J} w_{j,t} - D_t^{\text{E}} = 0 : \hat{\lambda}_t^{\text{E}},\ \forall t, \tag{1h}$$
$$C_{i_c} - \hat{\lambda}_t^{\text{E}} - \underline{\mu}_{i_c,t}^{\text{P}} + \overline{\mu}_{i_c,t}^{\text{P}} = 0,\ \forall i_c,t, \tag{1i}$$
$$\phi_{i_g}(\hat{\lambda}_t^{\text{G}} + x_t) - \hat{\lambda}_t^{\text{E}} - \underline{\mu}_{i_g,t}^{\text{P}} + \overline{\mu}_{i_g,t}^{\text{P}} + \sum_{l\in L} M_l^{i_g}(\phi_{i_g}\overline{\mu}_{l,t}^{\text{M}} + \phi_{i_g}\overline{\mu}_l^{\text{A}} - \phi_{i_g}\underline{\mu}_{l,t}^{\text{M}} - \phi_{i_g}\underline{\mu}_l^{\text{A}}) = 0,\ \forall i_g,t, \tag{1j}$$
$$-\hat{\lambda}_t^{\text{E}} - \underline{\mu}_{j,t}^{\widehat{\text{W}}} + \overline{\mu}_{j,t}^{\widehat{\text{W}}} = 0,\ \forall j,t, \tag{1k}$$
$$0 \le g_{k,t} \le G_k^{\max} : \underline{\mu}_{k,t}^{\text{G}}, \overline{\mu}_{k,t}^{\text{G}},\ \forall k,t, \tag{1l}$$

$$\sum_{k\in K} g_{k,t} - D_t^{\mathrm{G}} - \sum_{i_g\in I_g} \phi_{i_g} p_{i_g,t} = 0 : \hat{\lambda}_t^{\mathrm{G}},\ \ \forall t, \tag{1m}$$

$$C_k - \hat{\lambda}_t^{\mathrm{G}} - \underline{\mu}_{k,t}^{\mathrm{G}} + \overline{\mu}_{k,t}^{\mathrm{G}} = 0,\ \ \forall k,t, \tag{1n}$$

$$0 \le p_{i,\omega,t}^{+} \le P_i^{\max} - p_{i,t} : \underline{\mu}_{i,\omega,t}^{\mathrm{PR+}}, \overline{\mu}_{i,\omega,t}^{\mathrm{PR+}},\ \ \forall i,\omega,t, \tag{1o}$$

$$0 \le p_{i,\omega,t}^{-} \le p_{i,t} : \underline{\mu}_{i,\omega,t}^{\text{PR-}}, \overline{\mu}_{i,\omega,t}^{\text{PR-}},\ \ \forall i,\omega,t, \tag{1p}$$

$$0 \le p_{i,\omega,t}^{+} \le P_i^{+} : \underline{\mu}_{i,\omega,t}^{\mathrm{P+}}, \overline{\mu}_{i,\omega,t}^{\mathrm{P+}},\ \ \forall i,\omega,t, \tag{1q}$$

$$0 \le p_{i,\omega,t}^{-} \le P_i^{-} : \underline{\mu}_{i,\omega,t}^{\text{P-}}, \overline{\mu}_{i,\omega,t}^{\text{P-}},\ \ \forall i,\omega,t, \tag{1r}$$

$$0 \le w_{j,\omega,t}^{\mathrm{sp}} \le W_{j,\omega,t} : \underline{\mu}_{j,\omega,t}^{\mathrm{sp}}, \overline{\mu}_{j,\omega,t}^{\mathrm{sp}},\ \ \forall j,\omega,t, \tag{1s}$$

$$0 \le l_{\omega,t}^{\mathrm{sh,E}} \le D_t^{\mathrm{E}} : \underline{\mu}_{\omega,t}^{\mathrm{sh,E}}, \overline{\mu}_{\omega,t}^{\mathrm{sh,E}},\ \ \forall \omega,t, \tag{1t}$$

$$0 \le \sum_{i_g\in A_l^{I_g}} \phi_{i_g} p_{i_g,\omega,t}^{+} \le F_{l,t}^{\mathrm{M}} - \sum_{i_g\in A_l^{I_g}} \phi_{i_g} p_{i_g,t} : \underline{\mu}_{l,\omega,t}^{\mathrm{MR+}}, \overline{\mu}_{l,\omega,t}^{\mathrm{MR+}},\ \forall l,\omega,t, \tag{1u}$$

$$0 \le \sum_{i_g\in A_l^{I_g}} \phi_{i_g} p_{i_g,\omega,t}^{-} \le \sum_{i_g\in A_l^{I_g}} \phi_{i_g} p_{i_g,t} : \underline{\mu}_{l,\omega,t}^{\text{MR-}}, \overline{\mu}_{l,\omega,t}^{\text{MR-}},\ \forall l,\omega,t, \tag{1v}$$

$$0 \le \sum_{t\in T} \sum_{i_g\in A_l^{I_g}} \phi_{i_g} p_{i_g,\omega,t}^{+} \le F_l^{\mathrm{A}} - \sum_{t\in T} \sum_{i_g\in A_l^{I_g}} \phi_{i_g} p_{i_g,t} : \underline{\mu}_{l,\omega}^{\mathrm{AR+}}, \overline{\mu}_{l,\omega}^{\mathrm{AR+}},\ \forall l,\omega, \tag{1w}$$

$$0 \le \sum_{t\in T} \sum_{i_g\in A_l^{I_g}} \phi_{i_g} p_{i_g,\omega,t}^{-} \le \sum_{t\in T} \sum_{i_g\in A_l^{I_g}} \phi_{i_g} p_{i_g,t} : \underline{\mu}_{l,\omega}^{\text{AR-}}, \overline{\mu}_{l,\omega}^{\text{AR-}},\ \forall l,\omega, \tag{1x}$$

$$\sum_{i\in I}(p_{i,\omega,t}^{+} - p_{i,\omega,t}^{-}) + l_{\omega,t}^{\mathrm{sh,E}} + \sum_{j\in J}(W_{j,\omega,t} - w_{j,\omega,t}^{\mathrm{sp}} - w_{j,t}) = 0 : \tilde{\lambda}_{\omega,t}^{\mathrm{E}},\ \ \forall \omega,t, \tag{1y}$$

$$C_{i_c}^{+} - \tilde{\lambda}_{\omega,t}^{\mathrm{E}} + \overline{\mu}_{i_c,\omega,t}^{\mathrm{PR+}} + \overline{\mu}_{i_c,\omega,t}^{\mathrm{P+}} - \underline{\mu}_{i_c,\omega,t}^{\mathrm{P+}} = 0,\ \ \forall i_c,\omega,t, \tag{1z}$$

$$-C_{i_c}^{-} + \tilde{\lambda}_{\omega,t}^{\mathrm{E}} + \overline{\mu}_{i_c,\omega,t}^{\text{PR-}} + \overline{\mu}_{i_c,\omega,t}^{\text{P-}} - \underline{\mu}_{i_c,\omega,t}^{\text{P-}} = 0,\ \ \forall i_c,\omega,t, \tag{1aa}$$

$$\begin{aligned}&\phi_{i_g}(\tilde{\lambda}_{\omega,t}^{\mathrm{G}} + x_t) - \tilde{\lambda}_{\omega,t}^{\mathrm{E}} + \overline{\mu}_{i_g,\omega,t}^{\mathrm{PR+}} + \overline{\mu}_{i_g,\omega,t}^{\mathrm{P+}} - \underline{\mu}_{i_g,\omega,t}^{\mathrm{P+}}\\ &+ \sum_{l\in L} M_l^{i_g}(\phi_{i_g}\overline{\mu}_{l,\omega,t}^{\mathrm{MR+}} + \phi_{i_g}\overline{\mu}_{l,\omega}^{\mathrm{AR+}} - \phi_{i_g}\underline{\mu}_{l,\omega,t}^{\mathrm{MR+}} - \phi_{i_g}\underline{\mu}_{l,\omega}^{\mathrm{AR+}}) = 0,\ \ \forall i_g,\omega,t,\end{aligned} \tag{1ab}$$

$$\begin{aligned}&-\phi_{i_g}(\tilde{\lambda}_{\omega,t}^{\mathrm{G}} + x_t) + \tilde{\lambda}_{\omega,t}^{\mathrm{E}} + \overline{\mu}_{i_g,\omega,t}^{\text{PR-}} + \overline{\mu}_{i_g,\omega,t}^{\text{P-}} - \underline{\mu}_{i_g,\omega,t}^{\text{P-}}\\ &+ \sum_{l\in L} M_l^{i_g}(\phi_{i_g}\overline{\mu}_{l,\omega,t}^{\text{MR-}} + \phi_{i_g}\overline{\mu}_{l,\omega}^{\text{AR-}} - \phi_{i_g}\underline{\mu}_{l,\omega,t}^{\text{MR-}} - \phi_{i_g}\underline{\mu}_{l,\omega}^{\text{AR-}}) = 0,\ \ \forall i_g,\omega,t,\end{aligned} \tag{1ac}$$

$$C^{\mathrm{sh,E}} - \tilde{\lambda}_{\omega,t}^{\mathrm{E}} + \overline{\mu}_{\omega,t}^{\mathrm{sh,E}} - \underline{\mu}_{\omega,t}^{\mathrm{sh,E}} = 0,\ \ \forall \omega,t, \tag{1ad}$$

$$C^{\mathrm{sp}} + \tilde{\lambda}_{\omega,t}^{\mathrm{E}} + \overline{\mu}_{j,\omega,t}^{\mathrm{sp}} - \underline{\mu}_{j,\omega,t}^{\mathrm{sp}} = 0,\ \ \forall j,\omega,t, \tag{1ae}$$

$$0 \le g_{k,\omega,t}^{+} \le G_k^{\max} - g_{k,t} : \underline{\mu}_{k,\omega,t}^{\mathrm{GR+}}, \overline{\mu}_{k,\omega,t}^{\mathrm{GR+}},\ \ \forall k,\omega,t, \tag{1af}$$

$$0 \le g_{k,\omega,t}^{-} \le g_{k,t} : \underline{\mu}_{k,\omega,t}^{\text{GR-}}, \overline{\mu}_{k,\omega,t}^{\text{GR-}},\ \ \forall k,\omega,t, \tag{1ag}$$

$$0 \le g_{k,\omega,t}^{+} \le G_k^{+} : \underline{\mu}_{k,\omega,t}^{\mathrm{G+}}, \overline{\mu}_{k,\omega,t}^{\mathrm{G+}},\ \ \forall k,\omega,t, \tag{1ah}$$

$$0 \le g_{k,\omega,t}^{-} \le G_k^{-} : \underline{\mu}_{k,\omega,t}^{\text{G-}}, \overline{\mu}_{k,\omega,t}^{\text{G-}},\ \ \forall k,\omega,t, \tag{1ai}$$

$$0 \le l_{\omega,t}^{\mathrm{sh,G}} \le D_t^{\mathrm{G}} : \underline{\mu}_{\omega,t}^{\mathrm{sh,G}}, \overline{\mu}_{\omega,t}^{\mathrm{sh,G}},\ \ \forall \omega,t, \tag{1aj}$$

$$\sum_{k\in K}(g_{k,\omega,t}^{+} - g_{k,\omega,t}^{-}) + l_{\omega,t}^{\mathrm{sh,G}} - \sum_{i_g\in I_g} \phi_{i_g}(p_{i_g,\omega,t}^{+} - p_{i_g,\omega,t}^{-}) = 0 : \tilde{\lambda}_{\omega,t}^{\mathrm{G}},\ \ \forall \omega,t, \tag{1ak}$$

$$C_k^{+} - \tilde{\lambda}_{\omega,t}^{\mathrm{G}} + \overline{\mu}_{k,\omega,t}^{\mathrm{GR+}} + \overline{\mu}_{k,\omega,t}^{\mathrm{G+}} - \underline{\mu}_{k,\omega,t}^{\mathrm{G+}} = 0,\ \ \forall k,\omega,t, \tag{1al}$$

$$-C_k^{-} + \tilde{\lambda}_{\omega,t}^{\mathrm{G}} + \overline{\mu}_{k,\omega,t}^{\text{GR-}} + \overline{\mu}_{k,\omega,t}^{\text{G-}} - \underline{\mu}_{k,\omega,t}^{\text{G-}} = 0,\ \ \forall k,\omega,t, \tag{1am}$$

$$C^{\mathrm{sh,G}} - \tilde{\lambda}_{\omega,t}^{\mathrm{G}} + \overline{\mu}_{\omega,t}^{\mathrm{sh,G}} - \underline{\mu}_{\omega,t}^{\mathrm{sh,G}} = 0,\ \ \forall \omega,t, \tag{1an}$$

$$0 \le \overline{\mu}_{i,t}^{\mathrm{P}} \perp P_i^{\max} - p_{i,t} \ge 0,\ \ \forall i,t, \tag{1ao}$$

$$0 \le \underline{\mu}_{i,t}^{\mathrm{P}} \perp p_{i,t} \ge 0,\ \ \forall i,t, \tag{1ap}$$

$$0 \le \overline{\mu}_{j,t}^{\widehat{\mathrm{W}}} \perp \widehat{W}_j - w_{j,t} \ge 0,\ \ \forall j,t, \tag{1aq}$$

$$0 \le \underline{\mu}_{j,t}^{\widehat{\mathrm{W}}} \perp w_{j,t} \ge 0,\ \ \forall j,t, \tag{1ar}$$

$$0 \le \overline{\mu}^{\mathrm{M}}_{l,t} \perp F^{\mathrm{M}}_{l,t} - \sum_{i_g \in A^{I_g}_l} \phi_{i_g} p_{i_g,t} \ge 0, \ \ \forall l, t, \tag{1as}$$

$$0 \le \overline{\mu}^{\mathrm{A}}_{l} \perp F^{\mathrm{A}}_{l} - \sum_{t \in T} \sum_{i_g \in A^{I_g}_l} \phi_{i_g} p_{i_g,t} \ge 0, \ \ \forall l, \tag{1at}$$

$$0 \le \underline{\mu}^{\mathrm{M}}_{l,t} \perp \sum_{i_g \in A^{I_g}_l} \phi_{i_g} p_{i_g,t} \ge 0, \ \ \forall l, t, \tag{1au}$$

$$0 \le \underline{\mu}^{\mathrm{A}}_{l} \perp \sum_{t \in T} \sum_{i_g \in A^{I_g}_l} \phi_{i_g} p_{i_g,t} \ge 0, \ \ \forall l, \tag{1av}$$

$$0 \le \overline{\mu}^{\mathrm{G}}_{k,t} \perp G^{\max}_{k} - g_{k,t} \ge 0, \ \ \forall k, t, \tag{1aw}$$

$$0 \le \underline{\mu}^{\mathrm{G}}_{k,t} \perp g_{k,t} \ge 0, \ \ \forall k, t, \tag{1ax}$$

$$0 \le \overline{\mu}^{\mathrm{PR+}}_{i,\omega,t} \perp P^{\max}_{i} - p_{i,t} - p^{+}_{i,\omega,t} \ge 0, \ \ \forall i, \omega, t, \tag{1ay}$$

$$0 \le \underline{\mu}^{\mathrm{PR\text{-}}}_{i,\omega,t} \perp p_{i,t} - p^{-}_{i,\omega,t} \ge 0, \ \ \forall i, \omega, t, \tag{1az}$$

$$0 \le \overline{\mu}^{\mathrm{P+}}_{i,\omega,t} \perp P^{+}_{i} - p^{+}_{i,\omega,t} \ge 0, \ \ \forall i, \omega, t, \tag{1ba}$$

$$0 \le \underline{\mu}^{\mathrm{P+}}_{i,\omega,t} \perp p^{+}_{i,\omega,t} \ge 0, \ \ \forall i, \omega, t, \tag{1bb}$$

$$0 \le \overline{\mu}^{\mathrm{P\text{-}}}_{i,\omega,t} \perp P^{-}_{i} - p^{-}_{i,\omega,t} \ge 0, \ \ \forall i, \omega, t, \tag{1bc}$$

$$0 \le \underline{\mu}^{\mathrm{P\text{-}}}_{i,\omega,t} \perp p^{-}_{i,\omega,t} \ge 0, \ \ \forall i, \omega, t, \tag{1bd}$$

$$0 \le \overline{\mu}^{\mathrm{sp}}_{j,\omega,t} \perp W_{j,\omega,t} - w^{\mathrm{sp}}_{j,\omega,t} \ge 0, \ \ \forall j, \omega, t, \tag{1be}$$

$$0 \le \underline{\mu}^{\mathrm{sp}}_{j,\omega,t} \perp w^{\mathrm{sp}}_{j,\omega,t} \ge 0, \ \ \forall j, \omega, t, \tag{1bf}$$

$$0 \le \overline{\mu}^{\mathrm{sh,E}}_{\omega,t} \perp D^{\mathrm{E}}_{t} - l^{\mathrm{sh,E}}_{\omega,t} \ge 0, \ \ \forall \omega, t, \tag{1bg}$$

$$0 \le \underline{\mu}^{\mathrm{sh,E}}_{\omega,t} \perp l^{\mathrm{sh,E}}_{\omega,t} \ge 0, \ \ \forall \omega, t, \tag{1bh}$$

$$0 \le \overline{\mu}^{\mathrm{MR+}}_{l,\omega,t} \perp F^{\mathrm{M}}_{l,t} - \sum_{i_g \in A^{I_g}_l} \phi_{i_g} p_{i_g,t} - \sum_{i_g \in A^{I_g}_l} \phi_{i_g} p^{+}_{i_g,\omega,t} \ge 0, \ \forall l, \omega, t, \tag{1bi}$$

$$0 \le \underline{\mu}^{\mathrm{MR+}}_{l,\omega,t} \perp \sum_{i_g \in A^{I_g}_l} \phi_{i_g} p^{+}_{i_g,\omega,t} \ge 0, \ \forall l, \omega, t, \tag{1bj}$$

$$0 \le \overline{\mu}^{\mathrm{MR\text{-}}}_{l,\omega,t} \perp \sum_{i_g \in A^{I_g}_l} \phi_{i_g} p_{i_g,t} - \sum_{i_g \in A^{I_g}_l} \phi_{i_g} p^{-}_{i_g,\omega,t} \ge 0, \ \forall l, \omega, t, \tag{1bk}$$

$$0 \le \underline{\mu}^{\mathrm{MR\text{-}}}_{l,\omega,t} \perp \sum_{i_g \in A^{I_g}_l} \phi_{i_g} p^{-}_{i_g,\omega,t} \ge 0, \ \forall l, \omega, t, \tag{1bl}$$

$$0 \le \overline{\mu}^{\mathrm{AR+}}_{l,\omega} \perp F^{\mathrm{A}}_{l} - \sum_{t \in T} \sum_{i_g \in A^{I_g}_l} \phi_{i_g} p_{i_g,t} - \sum_{t \in T} \sum_{i_g \in A^{I_g}_l} \phi_{i_g} p^{+}_{i_g,\omega,t} \ge 0, \ \forall l, \omega, \tag{1bm}$$

$$0 \le \underline{\mu}^{\mathrm{AR+}}_{l,\omega} \perp \sum_{t \in T} \sum_{i_g \in A^{I_g}_l} \phi_{i_g} p^{+}_{i_g,\omega,t} \ge 0, \ \forall l, \omega, \tag{1bn}$$

$$0 \le \overline{\mu}^{\mathrm{AR\text{-}}}_{l,\omega} \perp \sum_{t \in T} \sum_{i_g \in A^{I_g}_l} \phi_{i_g} p_{i_g,t} - \sum_{t \in T} \sum_{i_g \in A^{I_g}_l} \phi_{i_g} p^{-}_{i_g,\omega,t} \ge 0, \ \forall l, \omega, \tag{1bo}$$

$$0 \le \underline{\mu}^{\mathrm{AR\text{-}}}_{l,\omega} \perp \sum_{t \in T} \sum_{i_g \in A^{I_g}_l} \phi_{i_g} p^{-}_{i_g,\omega,t} \ge 0, \ \forall l, \omega, \tag{1bp}$$

$$0 \le \overline{\mu}^{\mathrm{GR+}}_{k,\omega,t} \perp G^{\max}_{k} - g_{k,t} - g^{+}_{k,\omega,t} \ge 0, \ \ \forall k, \omega, t, \tag{1bq}$$

$$0 \le \underline{\mu}^{\mathrm{GR\text{-}}}_{k,\omega,t} \perp g_{k,t} - g^{-}_{k,\omega,t} \ge 0, \ \ \forall k, \omega, t, \tag{1br}$$

$$0 \le \overline{\mu}^{\mathrm{G+}}_{k,\omega,t} \perp G^{+}_{k} - g^{+}_{k,\omega,t} \ge 0, \ \ \forall k, \omega, t, \tag{1bs}$$

$$0 \le \underline{\mu}^{\mathrm{G+}}_{k,\omega,t} \perp g^{+}_{k,\omega,t} \ge 0, \ \ \forall k, \omega, t, \tag{1bt}$$

$$0 \le \overline{\mu}^{\mathrm{G\text{-}}}_{k,\omega,t} \perp G^{-}_{k} - g^{-}_{k,\omega,t} \ge 0, \ \ \forall k, \omega, t, \tag{1bu}$$

$$0 \le \underline{\mu}^{\mathrm{G\text{-}}}_{k,\omega,t} \perp g^{-}_{k,\omega,t} \ge 0, \ \ \forall k, \omega, t, \tag{1bv}$$

$$0 \le \overline{\mu}^{\mathrm{sh,G}}_{\omega,t} \perp D^{\mathrm{G}}_{t} - l^{\mathrm{sh,G}}_{\omega,t} \ge 0, \ \ \forall \omega, t, \tag{1bw}$$

$$0 \le \underline{\mu}^{\mathrm{sh,G}}_{\omega,t} \perp l^{\mathrm{sh,G}}_{\omega,t} \ge 0, \ \ \forall \omega, t. \tag{1bx}$$

The nonlinearities that arise from complementarity conditions are linearized via the Fortuny-Amat transformation [1]. We introduce the set of dual variables (λ and μ) Θ^{dual}, thus $\Theta^{\text{MUL}} = \{\Theta^{\text{UL}}, \Theta^{\text{dual}}\}$.

2 Linearization of cost-neutrality constraint

In this section, the aim is to linearize the cost-neutrality constraint (1c). First, we write the strong duality of problem (4d)-(4f) as presented in the original paper,

$$\sum_{t\in T}\Big(\sum_{i_c\in I_c} C_{i_c}p_{i_c,t} + \sum_{i_g\in I_g}(\hat{\lambda}^{\text{G}}_t + x_t)p_{i_g,t}\phi_{i_g}\Big) = \sum_{t\in T}\Big(-\sum_{i\in I}\overline{\mu}^{\text{P}}_{i,t}P^{\max}_i - \sum_{j\in J}\overline{\mu}^{\widehat{\text{W}}}_{j,t}\widehat{W}_{j,t} - \sum_{l\in L}\overline{\mu}^{\text{M}}_{l,t}F^{\text{M}}_{l,t} + \hat{\lambda}^{\text{E}}_t D^{\text{E}}_t\Big) - \sum_{l\in L}\overline{\mu}^{\text{A}}_l F^{\text{A}}_l, \tag{2}$$

We solve for $\sum_{t\in T}\sum_{i_g\in I_g} x_t p_{i_g,t}\phi_{i_g}$,

$$\sum_{t\in T}\sum_{i_g\in I_g} x_t p_{i_g,t}\phi_{i_g} = \sum_{t\in T}\Big(-\sum_{i_c\in I_c} C_{i_c}p_{i_c,t} - \sum_{i\in I}\overline{\mu}^{\text{P}}_{i,t}P^{\max}_i - \sum_{j\in J}\overline{\mu}^{\widehat{\text{W}}}_{j,t}\widehat{W}_{j,t} - \sum_{l\in L}\overline{\mu}^{\text{M}}_{l,t}F^{\text{M}}_{l,t} + \hat{\lambda}^{\text{E}}_t D^{\text{E}}_t - \sum_{i_g\in I_g}\hat{\lambda}^{\text{G}}_t p_{i_g,t}\phi_{i_g}\Big) - \sum_{l\in L}\overline{\mu}^{\text{A}}_l F^{\text{A}}_l. \tag{3}$$

In the case that $\hat{\lambda}^{\text{G}}_t = 0$, the nonlinear term $\sum_{t\in T}\hat{\lambda}^{\text{G}}_t\sum_{i_g\in I_g}\phi_{i_g}p_{i_g,t}$ vanishes. When $\hat{\lambda}^{\text{G}}_t \neq 0$, we multiply equation (1m) with $\hat{\lambda}^{\text{G}}_t$ and we sum over time periods t,

$$\sum_{t\in T}\Big(\hat{\lambda}^{\text{G}}_t\sum_{k\in K} g_{k,t} - \hat{\lambda}^{\text{G}}_t D^{\text{G}}_t - \hat{\lambda}^{\text{G}}_t\sum_{i_g\in I_g}\phi_{i_g}p_{i_g,t}\Big) = 0 \tag{4a}$$

$$\Leftrightarrow \sum_{t\in T}\hat{\lambda}^{\text{G}}_t\sum_{i_g\in I_g}\phi_{i_g}p_{i_g,t} = \sum_{t\in T}\Big(\hat{\lambda}^{\text{G}}_t\sum_{k\in K} g_{k,t} - \hat{\lambda}^{\text{G}}_t D^{\text{G}}_t\Big). \tag{4b}$$

Furthermore, we multiply equality (1n) with $g_{k,t} \neq 0$,

$$C_k g_{k,t} - \hat{\lambda}^{\text{G}}_t g_{k,t} - \underline{\mu}^{\text{G}}_{k,t}g_{k,t} + \overline{\mu}^{\text{G}}_{k,t}g_{k,t} = 0 \ \ \forall k,t. \tag{5}$$

Then, we sum over the natural gas producers k and time periods t,

$$\sum_{t\in T}\Big(\sum_{k\in K} C_k g_{k,t} - \hat{\lambda}^{\text{G}}_t\sum_{k\in K} g_{k,t} - \sum_{k\in K}\underline{\mu}^{\text{G}}_{k,t}g_{k,t} + \sum_{k\in K}\overline{\mu}^{\text{G}}_{k,t}g_{k,t}\Big) = 0 \tag{6a}$$

$$\Leftrightarrow \sum_{t\in T}\hat{\lambda}^{\text{G}}_t\sum_{k\in K} g_{k,t} = \sum_{t\in T}\Big(\sum_{k\in K} C_k g_{k,t} - \sum_{k\in K}\underline{\mu}^{\text{G}}_{k,t}g_{k,t} + \sum_{k\in K}\overline{\mu}^{\text{G}}_{k,t}g_{k,t}\Big). \tag{6b}$$

In equation (4b) the term $\sum_{t\in T}\hat{\lambda}^{\text{G}}_t\sum_{k\in K} g_{k,t}$ is nonlinear and thus substituted by the equivalent expression given in (6b),

$$\sum_{t\in T}\hat{\lambda}^{\text{G}}_t\sum_{i_g\in I_g}\phi_{i_g}p_{i_g,t} = \sum_{t\in T}\Big(\sum_{k\in K} C_k g_{k,t} - \sum_{k\in K}\underline{\mu}^{\text{G}}_{k,t}g_{k,t} + \sum_{k\in K}\overline{\mu}^{\text{G}}_{k,t}g_{k,t} - \hat{\lambda}^{\text{G}}_t D^{\text{G}}_t\Big). \tag{7}$$

Moreover, we substitute the nonlinear term $\sum_{t\in T}\hat{\lambda}^{\text{G}}_t\sum_{i_g\in I_g}\phi_{i_g}p_{i_g,t}$ in the strong duality equation (3) by (7),

$$\sum_{t\in T}\sum_{i_g\in I_g} x_t p_{i_g,t}\phi_{i_g} = \sum_{t\in T}\Big(-\sum_{i_c\in I_c} C_{i_c}p_{i_c,t} - \sum_{i\in I}\overline{\mu}^{\text{P}}_{i,t}P^{\max}_i - \sum_{j\in J}\overline{\mu}^{\widehat{\text{W}}}_{j,t}\widehat{W}_{j,t} - \sum_{l\in L}\overline{\mu}^{\text{M}}_{l,t}F^{\text{M}}_{l,t} + \hat{\lambda}^{\text{E}}_t D^{\text{E}}_t\Big) - \sum_{l\in L}\overline{\mu}^{\text{A}}_l F^{\text{A}}_l - \sum_{t\in T}\Big(\sum_{k\in K} C_k g_{k,t} - \sum_{k\in K}\underline{\mu}^{\text{G}}_{k,t}g_{k,t} + \sum_{k\in K}\overline{\mu}^{\text{G}}_{k,t}g_{k,t} - \hat{\lambda}^{\text{G}}_t D^{\text{G}}_t\Big). \tag{8}$$

From the complementarity condition (1aw) we have,

$$\overline{\mu}^{\text{G}}_{k,t}(G^{\max}_k - g_{k,t}) = 0 \Leftrightarrow \overline{\mu}^{\text{G}}_{k,t}G^{\max}_k = \overline{\mu}^{\text{G}}_{k,t}g_{k,t}, \ \ \forall k,t. \tag{9}$$

Additionally, from the complementarity condition (1ax) we have,

$$\underline{\mu}^{\text{G}}_{k,t}g_{k,t} = 0, \ \ \forall k,t. \tag{10}$$

By substituting (9) and (10) in (8), we have the following linear representation of $\sum_{t\in T}\sum_{i_g\in I_g} xp_{i_g,t}\phi_{i_g}$,

$$\sum_{t\in T}\sum_{i_g\in I_g} x_t p_{i_g,t}\phi_{i_g} = \sum_{t\in T}\Big(-\sum_{i_c\in I_c} C_{i_c}p_{i_c,t} - \sum_{i\in I}\overline{\mu}^{\mathrm{P}}_{i,t}P^{\max}_i - \sum_{j\in J}\overline{\mu}^{\widehat{\mathrm{W}}}_{j,t}\widehat{W}_{j,t} - \sum_{l\in L}\overline{\mu}^{\mathrm{NGA}}_{l,t}F^{\mathrm{NGA}}_{l,t} + \hat{\lambda}^{\mathrm{E}}_t D^{\mathrm{E}}_t\Big) - \sum_{l\in L}\overline{\mu}^{\mathrm{NGA}}_{l}F^{\mathrm{NGA}}_{l} - \sum_{t\in T}\Big(\sum_{k\in K} C_k g_{k,t} + \sum_{k\in K}\overline{\mu}^{\mathrm{G}}_{k,t}G^{\max}_k - \hat{\lambda}^{\mathrm{G}}_t D^{\mathrm{G}}_t\Big). \tag{11}$$

3 Supplementary results

In this section, we provide some additional graphs related to the results of the paper. We illustrate the demand and expected wind power profiles, as well as the day-ahead dispatch of the conventional units under the three different dispatch models for reader's convenience. This way the effect of changing the price of natural gas for power production is demonstrated by comparing the dispatch between *Seq* and *P-B*.

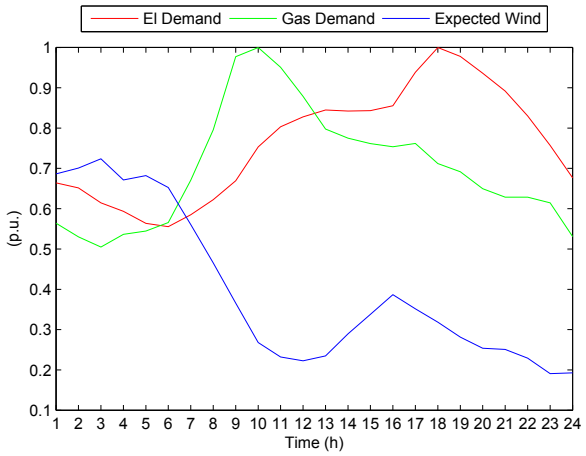

Figure 1: Electricity demand, natural gas demand and expected wind power production profiles.

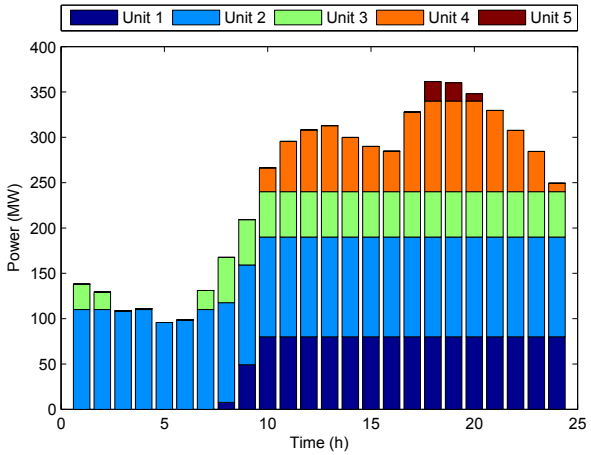

Figure 2: Hourly day-ahead schedule of power plants (Seq).

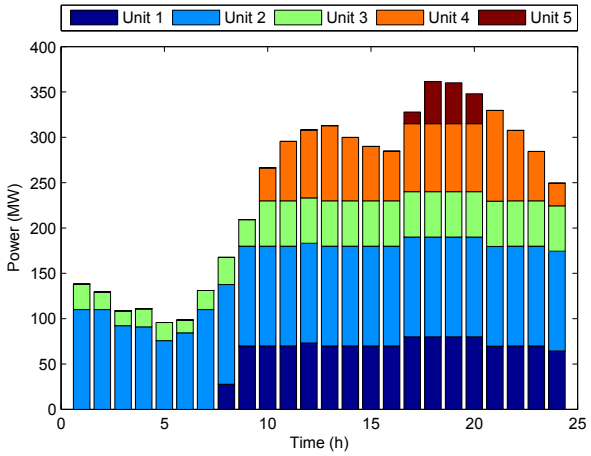

Figure 3: Hourly day-ahead schedule of power plants (P-B).

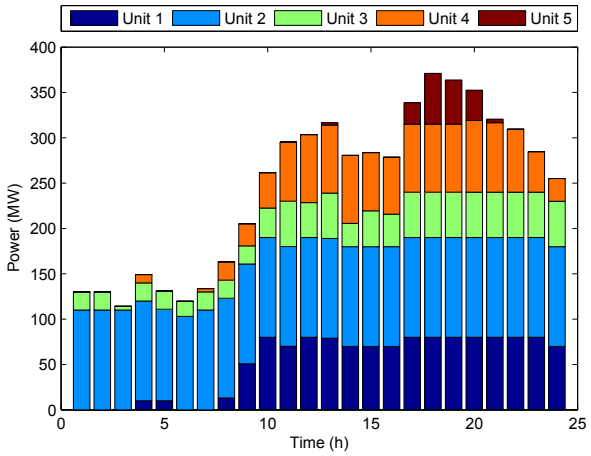

Figure 4: Hourly day-ahead schedule of power plants (Stoch).

Table 1: Profits. Wind power penetration 50%.

		I_1	I_3	I_4	I_5
Seq	Exp. profit ($)	18 725.35	24 634.10	46 411.69	55 360.59
Stoch	Exp. profit ($)	16 989.08	16 376.21	14 532.13	2 805.79
	Aver. losses ($)	-104.57	-106.09	-69.03	-28.37
	Prob. profit<0 (%)	1.2	7.6	9.4	0.3
P-B	Exp. profit ($)	18 452.14	22 044.05	24 001.30	19 771.83

The expected profits of flexible producers are shown in Table 1. The higher expected profits occur under *Seq* due to the high balancing prices that appear when costly balancing actions (e.g., electricity load shedding) take place. In this case, wind power producers have to bear this cost and this may result in negative profits in expectation. Model *P-B* attains to alleviate this effect by significantly reducing the cost of balancing actions. For *Stoch*, the average losses for the time periods and scenarios that a negative profit realizes are provided. Moreover, we calculate the probability of having a negative profit for each time period and scenario. Although the average losses are relatively small, a considerable probability of having a negative profit per time period and scenario emerges. In this example, profits per scenario are positive under *Stoch* but this can not be guaranteed and generalized for every case. Positive profits for each time period and scenario are guaranteed under models *Seq* and *P-B*.

References

[1] J. Fortuny-Amat and B. McCarl, "A representation and economic interpretation of a two-level programming problem," *J. Oper. Res. Soc.*, vol. 32, no. 9, pp. 783-792, 1981.

[Paper D] Market-based Coordination for Integrated Electricity and Natural Gas Systems Under Uncertain Supply

Authors:
Christos Ordoudis, Stefanos Delikaraoglou, Jalal Kazempour and Pierre Pinson

Submitted to:
IEEE Transactions on Control of Network Systems.

Note:
The corresponding appendix, which includes some mathematical extensions, proofs, a detailed nomenclature and additional results, is provided just after the manuscript.

Market-based Coordination for Integrated Electricity and Natural Gas Systems Under Uncertain Supply

Christos Ordoudis, *Student Member, IEEE,* Stefanos Delikaraoglou, *Member, IEEE,*
Jalal Kazempour, *Member, IEEE,* Pierre Pinson, *Senior Member, IEEE*

***Abstract*—The interdependence between electricity and natural gas systems has lately increased due to the wide deployment of gas-fired power plants (GFPPs). Moreover, weather-driven renewables introduce uncertainty in the operation of the integrated energy system, increasing the need for operational flexibility. Recently proposed stochastic dispatch models optimally use the available flexibility and minimize the total expected system cost. However, these models are incompatible with the current sequential market design. We propose a novel method to optimally define the available natural gas volume for power production scheduling, anticipating the real-time flexibility needs. Our model is formulated as a stochastic bilevel program aiming to enhance the inter-temporal coordination of scheduling and balancing operations, while remaining compatible with the sequential clearing of day-ahead and real-time markets. The proposed model accounts for the inherent flexibility of the natural gas system via the proper modeling of linepack properties and reduces the total expected system cost by the optimal definition of natural gas volume availability for GFPPs during the scheduling phase.**

***Index Terms*—Bilevel programming, integrated electricity and natural gas systems, market-based coordination, uncertainty.**

I. Introduction

The coupling between the electricity and natural gas systems has been substantially strengthened due to the increased utilization of gas-fired power plants (GFPPs) over the last decades and this trend is expected to continue in the foreseeable future [1]. In addition, renewable energy sources, such as wind and solar power, already comprise a significant share of the generation mix. The co-existence of these two types of power production plants serves as a promising combination for a smooth transition to a sustainable energy system that is flexible enough to accommodate high shares of renewables. To this end, the interdependence between these two energy systems will increase and the intermittency of renewable energy sources will eventually affect the operation of both systems. Hence, there is a compelling need to introduce mechanisms that treat these systems in an integrated manner.

The coordinated operation of electricity and natural gas systems has been extensively studied lately. The benefits of improved coordination between the two energy systems under high intraday variability of GFPPs' fuel consumption are indicated in [2]. In a similar context, the impact of natural gas supply uncertainty and price variability on the power system dispatch is analyzed in [3], showing that these parameters can considerably alter the market outcomes. Moreover, authors in [4] highlight the benefit in terms of improved flexibility and reliability, when accounting for the ability to store natural gas in the pipelines, known as linepack. Therefore, both physical and economic links between electricity and natural gas systems have an eminent role in short-term operations and are highly essential in the presence of renewables. The effect of uncertain renewable power production to the coupled energy system is analyzed via a robust co-optimization framework in [5], while authors in [6] utilize stochastic programming to dispatch the power system with feasible fuel supply from the natural gas network. Moreover, authors in [7] consider a joint optimization framework that utilizes GFPPs to firm up uncertain power supply from renewables. Taking a market perspective, an equilibrium model for the interdependent electricity and natural gas markets that allows for short-term energy trading based on locational marginal prices is proposed in [8]. Similarly, we study the short-term coupled operation of electricity and natural gas systems in a market framework where the energy commodities are traded based on their marginal prices. Such an approach is highly attractive especially when the two systems are operated by the same entity, e.g. Energinet.dk in Denmark, that is both electricity and natural gas systems' operator [9].

Following the paradigm of the electricity sector, the volume of natural gas traded in the spot markets is continuously increasing [9]. Therefore, the short-term operation of electricity and natural gas systems should be modeled on the basis of a market-based framework. The short-term operation is mainly associated with two trading floors, namely the day-ahead and balancing markets that are cleared in a sequential manner. The day-ahead market is settled 12-36 hours ahead of the actual system operation and the balancing market deals with the necessary adjustments to keep the system balanced. However, this sequential arrangement is inefficient under high shares of stochastic renewable power production due to its deterministic view of the uncertain renewables' production. In the European context, the day-ahead market follows a zonal network representation, while a nodal network representation is considered during the real-time operation. Stochastic programming has been utilized to enhance the temporal coordination between these two trading floors by making use of a probabilistic description of stochastic renewable production [10], [11]. Despite that this approach provides the solution with the minimum expected system cost, it is not compatible with the current market design and in addition it suffers from some design flaws related to the violation of the least-cost merit-order principle [12], [13]. For this reason, several approaches have been proposed that aim at approximating the stochastic ideal solution, while maintaining the current market

C. Ordoudis, J. Kazempour and P. Pinson are with the Department of Electrical Engineering, Technical University of Denmark, Kgs. Lyngby 2800, Denmark e-mail: (chror@elektro.dtu.dk; seykaz@elektro.dtu.dk; ppin@elektro.dtu.dk).

S. Delikaraoglou is with the Power Systems Laboratory, ETH, Zurich, Switzerland e-mail: (delikaraoglou@eeh.ee.ethz.ch).

architecture. An improved dispatch model that minimizes system's expected cost and respects the merit-order principle by scheduling wind power in a value different than its expected production is proposed in [12], while cost recovery[1] of flexible producers is guaranteed for any realization of uncertainty. Additionally, authors in [14] develop a framework to set the available transfer capacity (ATC) in a cost-optimal manner and attain a solution closer to the stochastic one. Finally, a model that efficiently dispatches the power system with an optimal setting of allocation between energy and reserves on the inter-regional HVDC interconnections is proposed in [15]. In the aforementioned works, the system operator is able to properly tune these purely financial parameters, i.e. wind dispatch, ATCs, HVDC allocation, in order to communicate the missing information to the day-ahead stage and achieve a partial temporal coordination between the trading floors.

Following a similar approach, we propose a systematic method to define the optimal natural gas volume that is made available for power production at the day-ahead stage. We consider this natural gas availability as a parameter that can be controlled by the operator and we build a stochastic bilevel model to determine its optimal value, while anticipating the future balancing needs due to forecast errors from uncertain power supply. This mechanism aims to improve the temporal coordination between day-ahead and balancing trading floors and approximate the efficiency of the stochastic solution, while the existing market architecture is preserved. The natural gas availability only affects the day-ahead schedule of the integrated energy system and the real-time balancing takes into account the physical characteristics of the two networks. Regarding the natural gas system, we model the linepack capability to make optimal use of the available network flexibility. Our models achieve optimal operation in terms of total operating cost for the integrated energy system with detailed representation of the technical constraints for both components, i.e. electricity and natural gas networks. Thus, the proposed *volume-based* model optimally determines the natural gas volume offered to GFPPs and in turn provides an appropriate system dispatch to cope with the imbalances in real-time. Finally, we compare the *volume-based* approach with the *price-based* model proposed in [16], which introduces a stochastic bilevel program that generates proper flexibility price signals to adjust the natural gas price perceived by GFPPs in order to provide a more efficient market outcome.

The remaining of the paper is organized as follows. Section II outlines the main properties of each dispatch model for the integrated energy system, while the mathematical formulation is presented in Section III. The results are illustrated in Section IV, and Section V concludes the paper. Finally, additional material including some mathematical extensions, proofs and a detailed nomenclature are given in the online appendix [17].

II. Market-based Coordination

In this paper, we study four dispatch models for scheduling and balancing electricity and natural gas systems. These models achieve different degrees of temporal coordination for the integrated energy system. This section describes their fundamental principles and provides a schematic representation to outline the main properties of each coordination scheme.

A. Sequential Dispatch of Integrated Energy System

The sequential dispatch of the integrated energy system (*Seq*) models a case of perfect inter-systems coordination between electricity and natural gas networks for both day-ahead and balancing markets, as shown in Fig. 1. However, these market floors are cleared in sequential and independent auctions, resulting to imperfect temporal coordination between the scheduling and balancing operations. Having as input a single-valued forecast of the stochastic power production, a common day-ahead market is cleared to obtain the initial operation schedule for both systems. Getting closer to actual operation, when the realization of stochastic production ω' is known, the balancing actions to compensate for potential forecast errors are jointly optimized for both systems through a common balancing market. Even though this sequential approach may be inefficient due to imperfect temporal coordination, it admits an important economic property that ensures cost recovery for flexible producers for any realization of stochastic production, as shown in the electronic companion [17]. Assuming a co-optimization process that minimizes the combined system cost at each market stage, this setup deviates from the current design since it does not respect the asynchronous timing and independent clearing of the respective markets [18]. However, this market model allows us to assess the net value of temporal coordination between the day-ahead and balancing markets of interdependent energy networks.

Fig. 1. Sequential dispatch of integrated energy system. DA: Day-ahead, E: Electricity, G: Natural gas, ΔE: Electricity adjustment, ΔG: Natural gas adjustment.

B. Stochastic Dispatch of Integrated Energy System

To improve the temporal coordination between the scheduling and balancing operations, we construct the stochastic coupled electricity and natural gas dispatch model (*Stoch*) illustrated in Fig. 2. Here, the day-ahead market co-optimizes the electricity and natural gas schedules based on a probabilistic description of uncertain supply, which allows to anticipate the cost of re-dispatch actions in real-time operation. Such probabilistic description is based on the available forecast at the day-ahead stage and may not cover the exact realization in real-time. However, given that the uncertainty modelling adequately captures the true characteristics of the stochastic processes involved, the potential realization will be represented via a set of scenarios Ω. This market setup is mathematically formulated as a two-stage stochastic programming problem that minimizes the total expected cost of the integrated energy system. The definition of this model provides an ideal reference solution that attains perfect inter-systems and temporal coordination, assuming that a realistic range and probability distribution of scenarios are considered. However, its real-life

[1]Revenue of each market participant is greater than or equal to its operating costs.

implementation is restricted because cost recovery for market participants and revenue adequacy[2] for the system operator hold only in expectation [10]. Actually, these fundamental economic properties may be violated for some uncertainty realizations in scenario set Ω since this model does not respect the least-cost merit-order principle in the day-ahead market.

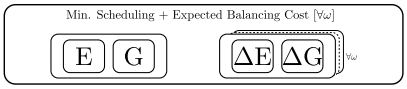

Fig. 2. Stochastic dispatch of integrated energy system.

C. Volume-based Coordination in Sequential Dispatch of Integrated Energy System

Aiming to address the caveat of imperfect temporal coordination of the *Seq* model, while sidestepping the design flaws of the *Stoch* model, we introduce a volume-based (*V-B*) coordination mechanism. This mechanism leverages the physical coupling of electricity and natural gas systems through the GFFPs to implicitly coordinate the day-ahead and balancing markets. The system operator uses as coordination signal an amount χ^v of the natural gas volume that is available to GFFPs at the day-ahead stage, while the full capacity of the natural gas network is released during real-time operation. Note that volume χ^v affects only the fuel demand of GFPPs, while industrial/commercial natural gas loads have higher priority.

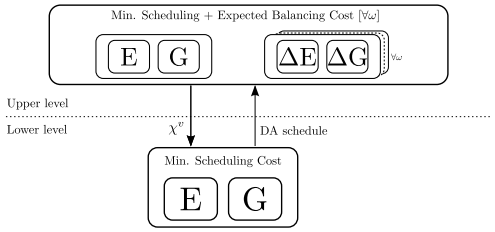

Fig. 3. Volume-based coordination in sequential dispatch of integrated energy system.

A systematic method for the definition of the optimal value of χ^v is mathematically formulated as the stochastic bilevel program presented schematically in Fig. 3. Similar to the *Stoch* model, the upper-level problem minimizes the expected cost of the integrated system, having χ^v as a non-negative decision variable. In turn, the lower-level problem reproduces the day-ahead clearing of the integrated market for a fixed value of χ^v that enters the lower level as a fixed parameter. This structure accounts for the independence of day-ahead and balancing markets, since the day-ahead schedule that is enforced by the lower-level problem has the exact same properties as its counterpart in the *Seq* model. Consequently, the re-dispatch actions are optimized individually for each uncertainty realization in the upper level. Essentially, the optimal value of χ^v is found by anticipating the day-ahead market outcome and the subsequent expected balancing cost.

This coordination mechanism resembles the "maximum gas burn" constraint recently introduced by California Independent System Operator (CAISO) to address reliability risks due to the limited operability of the Aliso Canyon natural gas storage facility. Using this constraint CAISO is able to limit the gas consumption of a group of generators in a defined area [19]. In the same vein, our volume signal χ^v can be applied to a whole control zone or be tailored to specific areas or GFPPs. Nonetheless, the proposed mechanism extends CAISO's approach to consider primarily issues pertaining to forecast errors of stochastic power producers.

[2]Payments made to/received from market participants do not incur financial deficit to the operator.

D. Price-based Coordination in Sequential Dispatch of Integrated Energy System

Apart from the physical interaction of electricity and natural gas networks, there is also an economic link that couples the operation of these systems through the natural gas price offered to GFPPs. Therefore, a coordination mechanism analogous to the volume-based approach outlined above, can be established using instead a price-based (*P-B*) signal χ^p applied to the natural gas prices. To define the optimal value of χ^p we employ the stochastic bilevel optimization model that is depicted schematically in Fig. 4 and presented in [16]. The construction of this model follows the same rationale as the volume-based coordination scheme and thus it also preserves the independent clearing of day-ahead and balancing markets that enforces per-se the merit-order principle.

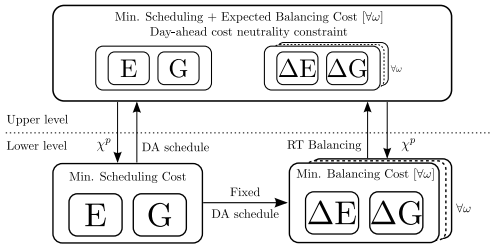

Fig. 4. Price-based coordination in sequential dispatch of integrated energy system. RT: Real-time.

This coordination mechanism allows GFPPs to utilize all available natural gas resources but can instead control (either increase or decrease) the natural gas price that is perceived by the GFPPs via the free in sign χ^p. In turn, this affects their short-term marginal costs and consequently their price offers on the electricity side of the integrated market in both day-ahead and balancing stages. Practically, these price signals reflect the scarcity value of flexible GFPPs for the system operator during real-time balancing. In order to ensure fairness and transparency for all counter-parties, this mechanism is designed on a cost-neutral basis such that the system operator is financially balanced at the day-ahead stage. Potential financial imbalances in the real-time settlements can be compensated using out-of-the-market payments as a supporting mechanism for the flexible producers, similar to the flexible capacity remuneration mechanisms that are currently discussed in the European electricity market context [20].

E. Features of Bilevel Models and Computational Tractability

Since the sequential arrangement between the trading floors is preserved with *V-B* and *P-B* models, cost recovery for flexible producers is guaranteed for each realization of stochastic

production. Moreover, it can be noticed that in *V-B* implementation only the day-ahead stage needs to be included in the lower-level problem since the natural gas volume availability χ^v only affects the natural gas volume that is announced at the day-ahead market stage and then the physical capacity of the natural gas network is made available in real-time. On the contrary, both the day-ahead and balancing markets must be included in the lower-level problem of *P-B*, since the price adjustment χ^p affects the marginal cost of GFPPs in the day-ahead market; however, the real-time price offers have to be altered in a consistent way to preserve the incentive for the provision of balancing services. Since the proposed dispatch models *V-B* and *P-B* are formulated in a bilevel structure, it is necessary to ensure that the lower-level problems are linear and convex in order to allow a single-level reformulation as a tractable mixed-integer linear program (MILP). Therefore, we study two variants of the balancing market in the following section. The first one directly permits the comparison between *V-B* and *P-B* since the balancing market is formulated as a linear program (LP). On the other hand, the second variant can be applied only to *V-B* as it has a detailed formulation for the gas flows in the real-time stage, which requires the introduction of binary variables that make the problem non-convex. Finally, model *V-B* results in a MILP with fewer binary variables than *P-B* as the balancing market is not included in the lower level. Note that since the balancing market is not included in the lower level of *V-B* model, this formulation is less computationally expensive as the number of binary variables is independent of the number of scenarios.

III. Model Formulation

Before presenting the mathematical formulation of the dispatch models, we introduce a set of assumptions utilized in this study. A holistic view of the energy systems is followed, where the electricity and natural gas markets are considered coupled, hence the market clearing is a single optimization problem. Uncertain supply from stochastic producers is modeled via a finite set of scenarios Ω, accounting for temporal and spatial correlations of the forecast errors. We assume that electricity and natural gas demands are inelastic and exactly known, hence we take the operator's perspective that minimizes system's cost. The physical link between the electricity and natural gas systems is provided by GFPPs, where their fuel consumption has a lower priority than industrial/commercial natural gas demands. The cost structure for electricity and natural gas producers is assumed to have the form of linear functions, while stochastic producers bid with zero marginal cost. We focus on the two trading floors of day-ahead and balancing markets, where a pool-based approach, i.e. without network constraints, is used to clear the day-ahead market, while the balancing market is formulated under two different setups. The first setup is formulated as an LP under the assumption that the balancing market is cleared as a pool with additional fuel constraints for the GFPPs based on an *ex-ante* estimation of pipeline capacities, similarly to the approach in [3]. In the second setup, we introduce network constraints for both electricity and natural gas systems. For the power system, we adopt a DC power flow, while a model that approximates gas flow dynamics via linepack consideration is used for the natural gas system [21], which leads to a MILP formulation.

A. Sequential Dispatch of Integrated Energy System

As illustrated in Fig. 1, the day-ahead and balancing markets are cleared independently in the *Seq* model. Initially, the day-ahead market is formulated in (1) as follows,

$$\underset{\Theta^{\mathrm{D}}}{\text{Min.}} \sum_{t\in T}\Big(\sum_{i_c\in I_c} C_{i_c} p_{i_c,t} + \sum_{k\in K} C_k g_{k,t}\Big) \tag{1a}$$

subject to

$$0 \le p_{i,t} \le P_i^{\max},\ \ \forall i,t, \tag{1b}$$

$$0 \le w_{j,t} \le \widehat{W}_{j,t},\ \ \forall j,t, \tag{1c}$$

$$0 \le g_{k,t} \le G_k^{\max},\ \ \forall k,t, \tag{1d}$$

$$\sum_{i\in I} p_{i,t} + \sum_{j\in J} w_{j,t} - \sum_{r_e\in R_e} D^{\mathrm{E}}_{r_e,t} = 0 : \hat{\lambda}^{\mathrm{E}}_t,\ \ \forall t, \tag{1e}$$

$$\sum_{k\in K} g_{k,t} - \sum_{r_g\in R_g} D^{\mathrm{G}}_{r_g,t} - \sum_{i_g\in I_g} \phi_{i_g} p_{i_g,t} = 0 : \hat{\lambda}^{\mathrm{G}}_t,\ \ \forall t, \tag{1f}$$

$$0 \le \sum_{t\in T}\sum_{i_g\in A_\psi^{Ig}} \phi_{i_g} p_{i_g,t} \le |T| \sum_{k\in K} G_k^{\max} - \sum_{t\in T}\sum_{r_g\in R_g} D^{\mathrm{G}}_{r_g,t}, \tag{1g}$$

$$0 \le \sum_{i_g\in A_\psi^{Ig}} \phi_{i_g} p_{i_g,t} \le F_{\psi,t}^{\max} - \sum_{r_g\in A_\psi^{Rg}} D^{\mathrm{G}}_{r_g,t},\ \ \forall \psi,t, \tag{1h}$$

where $\Theta^{\mathrm{D}} = \{p_{i,t},\forall i,t; w_{j,t},\forall j,t; g_{k,t},\forall k,t\}$ is the set of optimization variables. The objective function (1a) to be minimized determines the day-ahead cost of the integrated electricity and natural gas system, including thermal electricity producers i_c, GFPPs i_g and natural gas producers k. Parameters C_i and C_k are production costs, and t is the index for time periods. We have excluded the electricity cost of GFPPs since this is already accounted through the cost of their natural gas consumption. Power production $p_{i,t}$ of power plant i (either thermal or GFPP) is constrained by their generation capacity $P_i^{\max}$ in (1b), while power dispatch $w_{j,t}$ of stochastic (e.g. wind) electricity producer j is bounded by its expected production $\widehat{W}_{j,t}$ in (1c). Moreover, natural gas production $g_{k,t}$ is constrained by capacity $G_k^{\max}$ in (1d) for each producer. The balance in power and natural gas systems is enforced through (1e) and (1f), whose dual variables $\hat{\lambda}^{\mathrm{E}}_t$ and $\hat{\lambda}^{\mathrm{G}}_t$ reflect the market price for electricity and natural gas, respectively. Note that r_e and r_g are indices for electricity and natural gas demands, and their loads are denoted by parameters $D^{\mathrm{E}}_{r_e,t}$ and $D^{\mathrm{G}}_{r_g,t}$. In addition, parameter ϕ_{i_g} refers to the power conversion factor for each GFPP. The marginal cost of each GFPP can be endogenously calculated by the multiplication of the natural gas price and the power conversion factor. Constraints (1g) limit the daily natural gas use of GFPPs up to the available natural gas volume at the day-ahead stage, which is determined by subtracting the commercial/industrial natural gas demand from the total daily available capacity. We introduce a specific set to group GFPPs indexed by ψ, which may comprise GFPPs in a specific area of the natural gas system or even only a particular GFPP. Set A_ψ^{Ig} denotes a subset of GFPPs belonging to the specific area ψ, while similar notation for sets A is used in all formulations. The hourly fuel constraints are imposed in

(1h), where $F^{\max}_{\psi,t}$ denotes the maximum natural gas availability for the specific group of GFPPs. For the sake of conciseness, we denote the power adjustment provided by each power plant as $\Delta p_{i,\omega',t} = p^{+}_{i,\omega',t} - p^{-}_{i,\omega',t}$ with $p^{+}_{i,\omega',t}, p^{-}_{i,\omega',t} \geq 0$ and the natural gas adjustment for each gas producer as $\Delta g_{k,\omega',t} = g^{+}_{k,\omega',t} - g^{-}_{k,\omega',t}$ with $g^{+}_{k,\omega',t}, g^{-}_{k,\omega',t} \geq 0$. The day-ahead schedule is a fixed input (denoted with superscript '*') to the balancing market and model (2) simulates the balancing market to compensate for potential imbalances due to the stochastic power realization $W_{j,\omega',t}$:

$$\underset{\Theta^{\mathrm{R}}}{\text{Min.}} \sum_{t\in T}\Big(\sum_{k\in K}(C^{+}_{k}g^{+}_{k,\omega',t} - C^{-}_{k}g^{-}_{k,\omega',t}) + \sum_{r_e\in R_e} C^{\mathrm{sh,E}} l^{\mathrm{sh,E}}_{r_e,\omega',t} + \sum_{i_c\in I_c}(C^{+}_{i_c}p^{+}_{i_c,\omega',t} - C^{-}_{i_c}p^{-}_{i_c,\omega',t}) + \sum_{r_g\in R_g} C^{\mathrm{sh,G}} l^{\mathrm{sh,G}}_{r_g,\omega',t}\Big) \quad (2a)$$

subject to

$$-p^{*}_{i,t} \leq \Delta p_{i,\omega',t} \leq P^{\max}_{i} - p^{*}_{i,t}, \ \ \forall i,t, \quad (2b)$$

$$-P^{-}_{i} \leq \Delta p_{i,\omega',t} \leq P^{+}_{i}, \ \ \forall i,t, \quad (2c)$$

$$0 \leq w^{\mathrm{sp}}_{j,\omega',t} \leq W_{j,\omega',t}, \ \ \forall j,t, \quad (2d)$$

$$0 \leq l^{\mathrm{sh,E}}_{r_e,\omega',t} \leq D^{\mathrm{E}}_{r_e,t}, \ \ \forall r_e,t, \quad (2e)$$

$$\sum_{i\in I}\Delta p_{i,\omega',t} + \sum_{r_e\in R_e} l^{\mathrm{sh,E}}_{r_e,\omega',t} + \sum_{j\in J}(W_{j,\omega',t} - w^{\mathrm{sp}}_{j,\omega',t} - w^{*}_{j,t}) = 0 : \tilde{\lambda}^{\mathrm{E}}_{\omega',t}, \ \ \forall t, \quad (2f)$$

$$-g^{*}_{k,t} \leq \Delta g_{k,\omega',t} \leq G^{\max}_{k} - g^{*}_{k,t}, \ \ \forall k,t, \quad (2g)$$

$$-G^{-}_{k} \leq \Delta g_{k,\omega',t} \leq G^{+}_{k}, \ \ \forall k,t, \quad (2h)$$

$$0 \leq l^{\mathrm{sh,G}}_{r_g,\omega',t} \leq D^{\mathrm{G}}_{r_g,t}, \ \ \forall r_g,t, \quad (2i)$$

$$\sum_{k\in K}\Delta g_{k,\omega',t} + \sum_{r_g\in R_g} l^{\mathrm{sh,G}}_{r_g,\omega',t} = \sum_{i_g\in I_g}\phi_{i_g}\Delta p_{i_g,\omega',t} : \tilde{\lambda}^{\mathrm{G}}_{\omega',t}, \ \forall t, \quad (2j)$$

$$0 \leq \sum_{t\in T_{i_g}}\sum_{i_g\in A^{I_g}_{z}}\phi_{i_g}(p^{*}_{i_g,t} + \Delta p_{i_g,\omega',t}) \leq F^{\mathrm{A}}_{z}, \ \ \forall z, \quad (2k)$$

$$0 \leq \sum_{i_g\in A^{I_g}_{z}}\phi_{i_g}(p^{*}_{i_g,t} + \Delta p_{i_g,\omega',t}) \leq F^{\mathrm{M}}_{z,t}, \ \ \forall z,t, \quad (2l)$$

where $\Theta^{\mathrm{R}} = \{p^{+/-}_{i,\omega',t}, \forall i,t; l^{\mathrm{sh,E}}_{r_e,\omega',t}, \forall r_e,t; l^{\mathrm{sh,G}}_{r_g,\omega',t}, \forall r_g,t; g^{+/-}_{k,\omega',t}, \forall k,t; \ w^{\mathrm{sp}}_{j,\omega',t}, \ \forall j,t\}$ is the set of optimization variables. The cost of re-dispatch actions is minimized in objective function (2a). Balancing offer prices $C^{+} > C$ and $C^{-} < C$ denote the adjustment costs for thermal power plants i_c and natural gas producers k, while $C^{\mathrm{sh,E}}$ and $C^{\mathrm{sh,G}}$ are costs for load shedding in the two systems. The bounds of power adjustments are defined in (2b) considering the day-ahead dispatch of the power plants. Constraints (2c) limit power adjustments to the maximum capability P^{+}_{i} and P^{-}_{i} of each power plant. Power spillage $w^{\mathrm{sp}}_{j,\omega',t}$ and electricity load shedding $l^{\mathrm{sh,E}}_{r_e,\omega',t}$ are constrained by the realized power production of stochastic producers $W_{j,\omega',t}$ and electricity demand through (2d) and (2e), respectively. Constraint (2f) represents the power balance in real-time operation. The adjustment of natural gas production is limited by (2g), where day-ahead schedules are taken into account. Additionally, constraints (2h) impose the maximum capability G^{+}_{k} and G^{-}_{k} of natural gas adjustments. Natural gas load shedding $l^{\mathrm{sh,G}}_{r_e,\omega',t}$ is limited by the natural gas demand in (2i). Moreover, constraint (2j) imposes real-time natural gas balance. The daily natural gas volume limit F^{A}_{z} for pipeline z is imposed by (2k), while the real-time physical pipeline capacity $F^{\mathrm{M}}_{z,t}$ is enforced by (2l). The upper bounds of (2k) and (2l) are calculated based on an *ex-ante* analysis, where the industrial/commercial natural gas demand is subtracted by the maximum physical capacity of the pipeline and thus no explicit description of natural gas system dynamics is included.

In the remainder of the section, we present a more detailed setup for the balancing market where the network flows in electricity and natural gas systems are taken into account. At the electricity side, a DC power flow is considered with the following set of constraints,

$$\sum_{i\in A^{I}_{n}}(p^{*}_{i,t} + \Delta p_{i,\omega',t}) + \sum_{r_e\in A^{R_e}_{n}} l^{\mathrm{sh,E}}_{r_e,\omega',t} + \sum_{j\in A^{J}_{n}}(W_{j,\omega',t} - w^{\mathrm{sp}}_{j,\omega',t}) - \sum_{r:(n,r)\in L} B_{n,r}(\delta_{n,\omega',t} - \delta_{r,\omega',t}) = \sum_{r_e\in A^{R_e}_{n}} D^{\mathrm{E}}_{r_e,t} : \tilde{\lambda}^{\mathrm{E}}_{n,\omega',t}, \ \forall n,t, \quad (3a)$$

$$B_{n,r}(\delta_{n,\omega',t} - \delta_{r,\omega',t}) \leq F^{\max}_{n,r}, \ \forall (n,r)\in L,t, \quad (3b)$$

$$\delta_{n,\omega',t} \ \text{ free}, \ \ \forall n/n : \text{ref}, \ \ \delta_{n,\omega',t} = 0, \ \ n : \text{ref}, \ \forall t. \quad (3c)$$

More specifically, the real-time balancing is imposed for each node of the power system, hence (3a) replaces (2f). Moreover, constraints (3b) determine the power flow between nodes n and r, where $\delta_{n,\omega',t}$ is the voltage angle defined in (3c). The transmission capacity limits $F^{\max}_{n,r}$ are enforced by (3b).

At the gas side, an isothermal natural gas flow $q_{m,u}$ in horizontal pipelines is assumed [22]. Then, the Weymouth equation is used to describe the natural gas flow from node m to u with the dependency at the pressure pr_m of adjacent nodes,

$$q_{m,u} = K^{f}_{m,u}\sqrt{pr^{2}_{m} - pr^{2}_{u}}, \ \forall (m,u)\in Z, \quad (4)$$

where $K^{f}_{m,u}$ is the Weymouth constant that depends on the physical characteristics of each pipeline Z. Since (4) is non-linear, we use an outer approximation by deriving the Taylor series expansion around fixed pressure points $(PR_{m,v}, PR_{u,v}) \in V$ to obtain a linear expression [23], [24]. Consequently, we replace equality constraints (4) by the following set of linear inequalities,

$$q_{m,u} \leq K^{f}_{m,u}\Big(\frac{PR_{m,v}}{\sqrt{PR^{2}_{m,v} - PR^{2}_{u,v}}}pr_{m} - \frac{PR_{u,v}}{\sqrt{PR^{2}_{m,v} - PR^{2}_{u,v}}}pr_{u}\Big). \quad \forall (m,u)\in Z, \forall v\in V. \quad (5)$$

To ensure an efficient approximation of the non-linear equation (4), we use a large number of fixed pressure points $v \in V$ [25]. Thus, we achieve an outer approximation by the constructed planes in (5) that are tangent to the surface defined by (4) which results in approximating the gas flow by the linear constraint in (5) that is binding [23]. An advanced natural gas system with linepack is modeled using the following constraints:

$$PR^{\min}_{m} \leq pr_{m,\omega',t} \leq PR^{\max}_{m}, \ \ \forall m,t, \quad (6a)$$

$$pr_{u,\omega',t} \leq \Gamma_{z}\cdot pr_{m,\omega',t}, \ \ , \forall (m,u)\in Z,t, \quad (6b)$$

$$q_{m,u,\omega',t} = q^{+}_{m,u,\omega',t} - q^{-}_{m,u,\omega',t}, \ \ \forall (m,u)\in Z,t, \quad (6c)$$

$$0 \le q^{+}_{m,u,\omega',t} \le \tilde{M} y_{m,u,\omega',t}, \ \ \forall (m,u) \in Z, t, \tag{6d}$$

$$0 \le q^{-}_{m,u,\omega',t} \le \tilde{M}(1 - y_{m,u,\omega',t}), \ \ \forall (m,u) \in Z, t, \tag{6e}$$

$$y_{m,u,\omega',t} + y_{u,m,\omega',t} = 1, \ \ \forall (m,u) \in Z, t, \tag{6f}$$

$$y_{m,u,\omega',t} \in \{0,1\}, \ \ \forall (m,u) \in Z, t, \tag{6g}$$

$$q^{+}_{m,u,\omega',t} \le KI^{+}_{m,u,v} pr_{m,\omega',t} - KO^{+}_{m,u,v} pr_{u,\omega',t} + \tilde{M}(1 - y_{m,u,\omega',t}), \forall \{(m,u) \in Z | m < u\}, \forall v, t, \tag{6h}$$

$$q^{-}_{m,u,\omega',t} \le KI^{-}_{m,u,v} pr_{u,\omega',t} - KO^{-}_{m,u,v} pr_{m,\omega',t} + \tilde{M} y_{m,u,\omega',t}, \forall \{(m,u) \in Z | m < u\}, \forall v, t, \tag{6i}$$

$$q^{-}_{u,m,\omega',t} \le KI^{+}_{m,u,v} pr_{m,\omega',t} - KO^{+}_{m,u,v} pr_{u,\omega',t} + \tilde{M} y_{u,m,\omega',t}, \forall \{(m,u) \in Z | m < u\}, \forall v, t, \tag{6j}$$

$$q^{+}_{u,m,\omega',t} \le KI^{-}_{m,u,v} pr_{u,\omega',t} - KO^{-}_{m,u,v} pr_{m,\omega',t} + \tilde{M}(1 - y_{u,m,\omega',t}), \forall \{(m,u) \in Z | m < u\}, \forall v, t, \tag{6k}$$

$$q^{+}_{m,u,\omega',t} = \frac{q^{\text{in}}_{m,u,\omega',t} + q^{\text{out}}_{m,u,\omega',t}}{2}, \ \ \forall (m,u) \in Z, t, \tag{6l}$$

$$q^{-}_{m,u,\omega',t} = \frac{q^{\text{in}}_{u,m,\omega',t} + q^{\text{out}}_{u,m,\omega',t}}{2}, \ \ \forall (m,u) \in Z, t, \tag{6m}$$

$$h_{m,u,\omega',t} = K^{\text{h}}_{m,u} \frac{pr_{m,\omega',t} + pr_{u,\omega',t}}{2}, \ \ \forall (m,u) \in Z, t, \tag{6n}$$

$$h_{m,u,\omega',t} = h_{m,u,\omega',t-1} + q^{\text{in}}_{m,u,\omega',t} - q^{\text{out}}_{m,u,\omega',t}, \forall (m,u) \in Z, t, \tag{6o}$$

$$\sum_{k \in A^K_m} (g^{*}_{k,t} + \Delta g_{k,\omega',t}) + \sum_{r_g \in A^{R_g}_m} l^{\text{sh,G}}_{r_g,\omega',t} - \sum_{i_g \in A^{I_g}_m} \phi_{i_g} (p^{*}_{i,t} + \Delta p_{i_g,\omega',t}) - \sum_{u:(m,u) \in Z} (q^{\text{in}}_{m,u,\omega',t} - q^{\text{out}}_{u,m,\omega',t}) = \sum_{r_g \in A^{R_g}_m} D^{\text{G}}_{r_g,t} : \tilde{\lambda}^{\text{G}}_{m,\omega',t}, \ \forall m, t. \tag{6p}$$

The bounds of pressure at each node of the system $PR^{\min}_m$ and $PR^{\max}_m$ are given by (6a), while the active pipelines are modeled by the relation of pressures between the two adjacent nodes via a compression factor Γ_z in (6b) [4]. More specifically, the outlet pressure at node u is greater than the inlet pressure at node m, when the gas flow is from m to u for the active branches. The natural gas flow $q_{m,u,\omega',t}$ is defined in (6c)-(6g) by two non-negative variables $q^{+}_{m,u,\omega',t}, q^{-}_{m,u,\omega',t} \ge 0$, where the direction of flow is defined by binary variable $y_{u,m,\omega',t}$. Note that parameter $\tilde{M}$ is a sufficient large constant. The physical characteristics of gas flow are introduced in (6h)-(6k) that are derived by (5) with

$$\begin{aligned} \{KI^{+}_{m,u,v} &= \frac{K^f_{m,u} PR_{m,v}}{\sqrt{PR^2_{m,v} - PR^2_{u,v}}}, KO^{+}_{m,u,v} = \frac{K^f_{m,u} PR_{u,v}}{\sqrt{PR^2_{m,v} - PR^2_{u,v}}}, \\ KI^{-}_{m,u,v} &= \frac{K^f_{m,u} PR_{u,v}}{\sqrt{PR^2_{u,v} - PR^2_{m,v}}}, KO^{-}_{m,u,v} = \frac{K^f_{m,u} PR_{m,v}}{\sqrt{PR^2_{u,v} - PR^2_{m,v}}}\}, \\ & \forall \{(m,u) \in Z | m < u\}, \forall v. \end{aligned} \tag{7}$$

Finally, two additional non-negative variables for the inflow and outflow of each pipeline $q^{\text{in}}_{u,m,\omega',t}, q^{\text{out}}_{u,m,\omega',t} \ge 0$ are introduced to model linepack flexibility. Constraints (6l) and (6m) define the flow of each pipeline as the average of inflow and outflow [4]. The average mass $h_{m,u,\omega',t}$ in each pipeline is given by (6n), where $K^{\text{h}}_{m,u}$ is a constant dependent on pipeline characteristics. The mass conservation at each pipeline is enforced by (6o). The natural gas balancing in the real-time is enforced by (6p) that replaces (2j). The presented model approximates the dynamics of the natural gas system and is described in detail in [21]. We refer the reader to [26] for a steady-state modeling of the natural gas system with geometric programming and to [27] for a transient model that closely describes the physical behaviour of the natural gas flow.

The pool-based balancing market is formulated with the set of constraints (2b)-(2l). A different set of constraints is used for the network constrained balancing market that consists of {(2b)-(2e),(2g)-(2i),(3a)-(3c),(6a)-(6p)}. In both cases, the objective function is (2a). We use "*N*" to determine the use of network constrained balancing market, hence models *Seq* and *Seq-N* are formulated. Moreover, the set of primary variables Θ^{R} is extended with $\Theta^{\text{EX}} = \{\delta_{n,\omega',t}, \forall n, t; \ pr_{m,\omega',t} \forall m, t; \ q^{\text{in/out}}_{m,u,\omega',t}, q^{+/-}_{m,u,\omega',t}, h_{m,u,\omega',t}, y_{u,m,\omega',t}, \forall (m,u) \in Z, t\}$ in *Seq-N*. In *Seq-N*, the prices are calculated after having fixed binary variables related to the natural gas flow direction. The expected balancing cost over a scenario set Ω is given as the sum of the balancing cost for each scenario ω weighed by its probability of occurrence π_ω.

B. Stochastic Dispatch of Integrated Energy System

As presented in Fig. 2, the *Stoch* model optimizes jointly the day-ahead and balancing stages of the integrated electric power and natural gas systems. The problem is formulated as a two-stage stochastic program aiming to minimize the total expected cost and writes as follows:

$$\begin{aligned} \underset{\Theta^{\text{SC}}}{\text{Min.}} \ & \sum_{t \in T} \Big[\sum_{i_c \in I_c} C_{i_c} p_{i_c,t} + \sum_{k \in K} C_k g_{k,t} + \sum_{\omega \in \Omega} \pi_\omega \Big(\\ & \sum_{k \in K} (C^{+}_k g^{+}_{k,\omega,t} - C^{-}_k g^{-}_{k,\omega,t}) + \sum_{i_c \in I_c} (C^{+}_{i_c} p^{+}_{i_c,\omega,t} - C^{-}_{i_c} p^{-}_{i_c,\omega,t}) \\ & + \sum_{r_e \in R_e} C^{\text{sh,E}} l^{\text{sh,E}}_{r_e,\omega,t} + \sum_{r_g \in R_g} C^{\text{sh,G}} l^{\text{sh,G}}_{r_g,\omega,t} \Big) \Big] \end{aligned} \tag{8a}$$

subject to

$$\text{constraints } (1b), (1d) - (1h), \tag{8b}$$

$$0 \le w_{j,t} \le \overline{W}_j, \ \ \forall j, t, \tag{8c}$$

$$\text{constraints } (2b) - (2l), \ \ \forall \omega, \tag{8d}$$

where $\Theta^{\text{SC}} = \{\Theta^{\text{D}}; \Theta^{\text{R}}_\omega, \forall \omega\}$ is the set of optimization variables. In this model, the temporal coordination of the two trading floors is achieved through the real-time constraints (8d) for all scenarios $\omega \in \Omega$. When network constrains {(2b)-(2e),(2g)-(2i),(3a)-(3c),(6a)-(6p)} are introduced to replace (8d), the model is named *Stoch-N*. Note that in model (8), the day-ahead dispatch of stochastic producers is restricted by the installed capacity $\overline{W}_j$, according to (8c), instead of the expected power generation and day-ahead dispatch decisions are treated as variables.

C. Volume-based Coordination in Sequential Dispatch of Integrated Energy System

According to Fig. 3, the *V-B* dispatch model that aims at minimizing the expected cost of the integrated energy system and defining the optimal natural gas volume availability writes as follows:

$$\underset{\Theta^{\text{VUL}}}{\text{Min.}} \ (8a) \tag{9a}$$

subject to

$$(2b) - (2l), \ \forall\omega, \tag{9b}$$

$$0 \leq \overline{\chi}^{v}_{\psi} \leq |T| \sum_{k\in K} G^{\max}_{k} - \sum_{t\in T}\sum_{r_g\in R_g} D^{\mathrm{G}}_{r_g,t}, \ \forall\psi, \tag{9c}$$

$$0 \leq \chi^{v}_{\psi,t} \leq F^{\max}_{\psi,t} - \sum_{r_g\in A^{R_g}_{\psi}} D^{\mathrm{G}}_{r_g,t}, \ \forall\psi,t, \tag{9d}$$

$$(p_{i,t}, w_{j,t}, g_{k,t}) \in \arg\Big\{ \underset{\Theta^{\mathrm{VLL}}}{\mathrm{Min.}} \sum_{t\in T}\Big(\sum_{i_c\in I_c} C_{i_c} p_{i_c,t} + \sum_{k\in K} C_k g_{k,t}\Big) \tag{9e}$$

subject to

$$\text{constraints } (1b) - (1f), \tag{9f}$$

$$0 \leq \sum_{t\in T}\sum_{i_g\in A^{I_g}_{\psi}} \phi_{i_g} p_{i_g,t} \leq \overline{\chi}^{v}_{\psi}, \ \forall\psi, \tag{9g}$$

$$0 \leq \sum_{i_g\in A^{I_g}_{\psi}} \phi_{i_g} p_{i_g,t} \leq \chi^{v}_{\psi,t}, \ \forall\psi,t\Big\}, \tag{9h}$$

where $\Theta^{\mathrm{VUL}} = \{\overline{\chi}^{v}_{\psi}, \forall\psi; \chi^{v}_{\psi,t}, \forall\psi,t; \Theta^{\mathrm{R}}_{\omega}, \forall\omega\}$ is the set of optimization variables of the upper-level problem. Additionally, $\Theta^{\mathrm{VLL}} = \Theta^{\mathrm{D}}$ is the set of optimization variables of the lower-level problem. The objective function of model (9) is the same as in (8). Thus, the upper-level problem minimizes the expected cost of operating the integrated energy system by deciding the optimal value of $\overline{\chi}^{v}_{\psi}$ and $\chi^{v}_{\psi,t}$. Variable $\overline{\chi}^{v}_{\psi}$ limits the total daily natural gas consumption of GFPPs according to (9g), while $\chi^{v}_{\psi,t}$ defines their hourly fuel limit in (9h). We define fuel availability $\overline{\chi}^{v}_{\psi}$ and $\chi^{v}_{\psi,t}$ under different setups, ranging from a single value for the whole market to individual values for specific areas or GFPPs. Therefore, these two variables are indexed by $\psi \in \Psi$ that defines the GFPPs that are grouped together in each setup. The lower-level problem reproduces the day-ahead coupled electricity and natural gas market. Under this setup the sequential clearing of day-ahead and balancing markets is practically emulated, since the day-ahead decisions are fixed to the sequential dispatch though (9e)-(9h) and the balancing market is simulated for each independent scenario by imposing constraints (9b) for all $\omega \in \Omega$. The system operator has the ability to decide the natural gas volume that will be made available for power production at the day-ahead stage within specified limits, defined by (9c) and (9d). The upper-level variables $\overline{\chi}^{v}_{\psi}$ and $\chi^{v}_{\psi,t}$ have an impact on the decisions of the lower-level problem as the total fuel availability for GFPPs affects the day-ahead schedule for power production. Moreover, the lower-level decision variables affect the total expected cost of the integrated system. Owning to the this structure, model (9) finds an appropriate dispatch that minimizes expected system cost by revealing flexibility from GFPPs, while ensuring that the least-cost merit-order principle is respected. The different effects of these approaches are illustrated in the numerical study. Similarly, the model is named *V-B-N* with the introduction of network constrains {(2b)-(2e),(2g)-(2i),(3a)-(3c),(6a)-(6p)} to replace (9b). The bilevel problem (9) can be reformulated as a Mathematical Program with Equilibrium Constraints (MPEC) by replacing the linear, and thus convex, lower-level problems by their Karush-Kuhn-Tucker (KKT) conditions as presented in [17].

D. Overview of Dispatch Models

Before proceeding to the numerical results, we provide an overview of the dispatch models and their features in Table I.

TABLE I
DISPATCH MODELS' CHARACTERISTICS

Fuel / Network constraints	*Seq / Seq-N*	*Stoch / Stoch-N*	*V-B / V-B-N*	*P-B / P-B-N*
Temporal coordination	Imperfect	Perfect	Partial	Partial
Coordination mechanism	Non-existing	Explicit	Implicit via χ^{v} *	Implicit via χ^{p}

* The value of χ^{v} can be defined for the whole market, specific areas or GFPPs.

The dispatch models are classified based on the networks' representation in the balancing market, as well as the temporal coordination achieved and the mechanism utilized.

IV. NUMERICAL RESULTS

In this section, we first demonstrate the features of the four dispatch models presented in Section II in a tailored case study. Then, we compare the performance of volume-based variants on a more realistic case study.

A. Tailored Case-Study

1) 1-hour Simulation Results: To allow a fair comparison between *P-B* and *V-B* models, the balancing market in this illustrative example is modeled as a pool with fuel constraints for GFPPs. Moreover, we assume a single type of uncertain supply that is wind power. Here, we consider a system which comprises three thermal power plants (I_1, I_2 and I_5), two GFPPs (I_3 and I_4) that acquire their fuel from the natural gas market, one wind farm (WP) and two natural gas producers (K_1 and K_2). Table II collects the data for the producers in both markets. Wind power is characterized by two equiprobable scenarios ω_1 (166 MW) and ω_2 (86 MW). The offer prices for upward and downward regulation are equal to 1.1 and 0.9 of the day-ahead offer prices. In *P-B*, we limit the natural gas price adjustment to \$1.35/kcf. Moreover, we consider a pipeline capacity of 6,000 kcf. The cost of electricity and natural gas load shedding is \$1,200/MWh and \$600/kcf, while wind spillage is cost-free. The peak electricity and natural gas demand for industrial/commercial loads are equal to 430 MW and 3,600 kcf/h, respectively.

TABLE II
ELECTRIC POWER AND NATURAL GAS SYSTEM DATA

Unit i	I_1	I_2	I_3	I_4	I_5	Unit k	K_1	K_2
$P^{\max}_i$ (MW)	80	110	50	100	100	$G^{\max}_k$ (kcf)	10,000	6,000
P^{+}_i (MW)	10	0	30	25	20	G^{+}_k (kcf)	2,500	1,000
P^{-}_i (MW)	10	0	30	25	20	G^{-}_k (kcf)	2,500	1,000
C_i (\$/MWh)	30	10	-	-	60	C_k (\$/kcf)	2	3
ϕ_{i_g} (kcf/MWh)	-	-	12	18	-			

We solve all dispatch models for 24-hours and provide detailed results for a specific time period. Two variants of (9), where natural gas volume availability is determined for the whole market (*V-B*) and for each individual GFPP (*V-B gen*), are studied. In this instance, natural gas is produced only by unit K_1, hence the natural gas price is \$2/kcf and the marginal costs of GFPPs I_3 and I_4 are \$24/MWh and \$36/MWh.

TABLE III
EXPECTED SYSTEM COST AND ITS BREAKDOWN IN $ WHEN TOTAL POWER LOAD IS 387 MW

	Total	Day-ahead	Balancing	Up regulation	Down regulation
Seq / V-B	10,400	9,982	418	990	-572
Stoch	10,234	10,222	12	660	-648
P-B	10,273	10,042	231	825	-594
V-B gen	10,261	10,162	99	693	-594

The action of adjusting the natural gas price or volume availability becomes beneficial when the day-ahead dispatch is altered with regards to *Seq* to allow more cost-effective power plants to provide the required regulation in the balancing market. This results in an increase of the day-ahead cost and a decrease of expected balancing cost that yields a reduction of total expected cost.

Initially, we demonstrate the performance of all dispatch models in Table III, when the total electricity demand is equal to 387 MW. It can be observed that *Stoch* returns the lowest expected system cost and *Seq* the highest one due to imperfect temporal coordination between day-ahead and balancing markets. Models *P-B*, *V-B* and *V-B gen* attain an expected cost that is in between the ideal solution of *Stoch* and the one of *Seq*. Thus, a reduction of expected system cost can be accomplished, while the system is still dispatched based on the merit-order principle.

The detailed system dispatch is illustrated in Table IV for an electricity demand of 387 MW. Regarding *P-B*, the marginal cost of all GFPPs is affected by adjusting the natural gas price with $\chi^p_{t_1} = -\$0.333$/kcf. The decreased natural gas price of \$1.666/kcf results in a lower marginal cost for GFPP I_4 equal to \$30/MWh, which equals the one of unit I_1. Therefore, unit I_1 is dispatched to 70 MW and GFPP I_4 to 31 MW without breaking the merit order. Model *V-B* returns the same results with *Seq*, as a change of total natural gas volume availability would not decrease the total expected cost. On the contrary, *V-B gen* has a better performance due to its ability to influence the dispatch of both GFPPs I_3 and I_4. Note that GFPPs I_3 and I_4 produce a total of 71 MW in both *Seq* and *V-B gen* at the day-ahead stage. However, the allocation between the two GFPPs is different and more efficient under *V-B gen*. More specifically, the total natural gas volume bought by GFPPs in *Seq* is 987 kcf, where 600 kcf are consumed by GFPP I_3 and the remaining 387 kcf by GFPP I_4. In *V-B gen*, the natural gas volume made available for GFPP I_3 is 420 kcf, while GFPP I_4 consumes 648 kcf. The adjustment of natural gas volume availability has a direct impact on the day-ahead dispatch which in turn reduces the total expected cost compared to *Seq*. The day-ahead cost increases but this increase is counterbalanced by a greater decrease of balancing cost. In particular, the up-regulation cost is decreased because unit I_5 is not activated and the need for up-regulation is covered by the cheaper GFPP I_3. Moreover, a greater portion of the total 40 MW needed for down-regulation is provided by GFPP I_4 that is more cost-effective than GFPP I_3.

The *Stoch* and *Seq* models provide the two extreme solutions in terms of expected cost for all time periods of the scheduling horizon and serve as upper and lower bounds, respectively, for the expected costs of *P-B*, *V-B* and *V-B gen* models. We perform an analogous analysis for the case with a total power load of 344 MW where χ^p gets a positive value and all three improved sequential models achieve the same expected cost with *Stoch*. This fact illustrates that it is possible in specific cases to have an efficient sequential dispatch if the future balancing costs are communicated into the day-ahead market through the operator-defined parameters χ. The additional results are presented in the electronic companion [17].

TABLE IV
POWER SYSTEM SCHEDULE IN MW WHEN TOTAL POWER LOAD IS 387 MW (VARIATION FROM *Seq* DAY-AHEAD (DA) SCHEDULE IN BOLD)

	Seq			*P-B*			*V-B*			*V-B gen*		
Unit	DA	ω_1	ω_2	DA	ω_1	ω_2	DA	ω_1	ω_2	DA	ω_1	ω_2
I_1	80	-10	0	**70**	-10	+10	80	-10	0	80	-10	0
I_2	110	0	0	110	0	0	110	0	0	110	0	0
I_3	50	-9	0	50	-5	0	50	-9	0	**35**	-5	+15
I_4	21	-21	+25	**31**	-25	+25	21	-21	+25	**36**	-25	+25
I_5	0	0	+15	0	0	+5	0	0	+15	0	0	0
WP	126	+40	-40	126	+40	-40	126	+40	-40	126	+40	-40

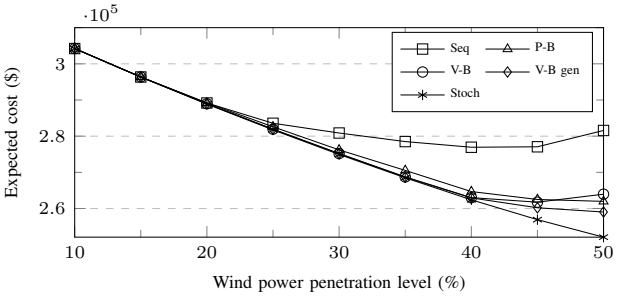

Fig. 5. Impact of wind power penetration level on the expected system cost.

2) 24-hour Simulation Results: Additionally, we provide the following results for the whole 24-hour scheduling horizon, where 20 equiprobable wind power scenarios are utilized (available at [28]). Fig. 5 presents the expected cost of the integrated energy system as a function of wind power penetration level, defined as the share of wind power capacity on total system's electricity demand.

The expected cost of *Stoch* is decreasing with an increase of wind power penetration and achieves the lowest expected cost in all cases. On the other hand, model *Seq* becomes inefficient for a wind power penetration level above 25%, while even an increase of the expected cost is observed when this level is greater than 40%. The *V-B* and *V-B gen* models manage to approximate efficiently the solution of *Stoch* model up to a share of 40%, where they start diverging with an increasing tendency. Note that the expected cost of *V-B gen* is lower than *V-B*, confirming its higher flexibility to provide an improved day-ahead dispatch. Similarly, *P-B* attains an expected cost close to the one obtained by *Stoch*.

We now highlight the main features of the proposed dispatch models. All three *P-B*, *V-B* and *V-B gen* demonstrate a considerable ability to bridge the gap between *Seq* and *Stoch* models. They manage to return an expected system cost closer to the stochastic ideal solution, while still dispatch the system based on the merit-order principle and keep the economic properties of *Seq*. Moreover, they can affect the system dispatch regardless of the type of marginal producer, i.e. GFPP or power plant using another fuel. In models *V-B* and *V-B gen* at least one GFPP would have to be scheduled in order to be able to improve the dispatch of the system, while this restriction does not apply to *P-B*. Additionally,

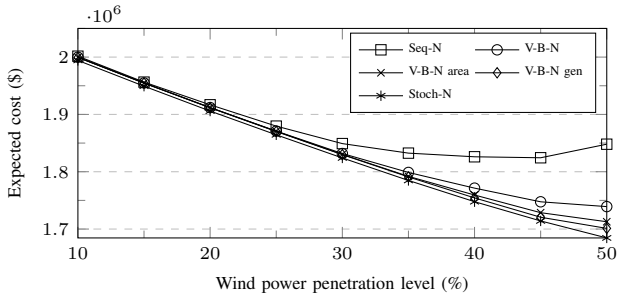

Fig. 6. Impact of wind power penetration level on the expected system cost.

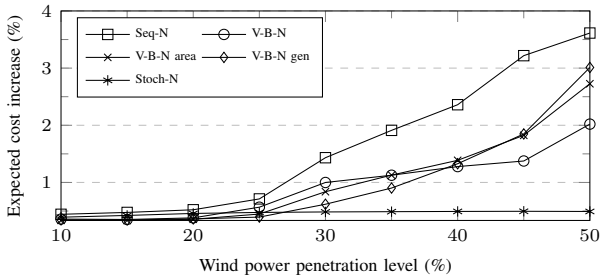

Fig. 7. Impact of wind power penetration level on the expected system cost increase when neglecting linepack modeling.

model *V-B* is able to alter the dispatch of the GFPP with the higher conversion factor. In case the natural gas availability is defined individually for specific areas of the system, the GFPP affected is the one with the greater conversion factor in the specific area. Finally, *V-B gen* is more flexible than *V-B* as it can change the dispatch of each individual GFPP. More specifically, the portion of the day-ahead power to be produced by GFPPs can be split under different shares in order to reveal more cost-effective regulation in the balancing market.

B. Realistic Case-Study

A more realistic case study is considered to assess the performance of the proposed dispatch model *V-B-N* when network constraints are included for the real-time operation of the energy system. The integrated energy system consists of the IEEE 24-bus Reliability Test System (RTS) [29] and a 12-node natural gas system based on [5]. More specifically, there exist 12 conventional power plants, out of which 4 are GFPPs, 2 wind farms and 3 natural gas suppliers. Wind power production is modeled by a set of 25 equiprobable scenarios. The data and network topology are provided in the online appendix available in [17]. Moreover, we introduce a new variant of (9) that defines the natural gas volume availability for specific areas of the integrated energy system, namely *V-B area*. Two areas are determined in this study including two GFPPs in each one of them. More specifically, GFPP 1 and GFPP 5 are included in area I, while GFPP 7 and GFPP 11 in area II. Similarly to Section IV-A, we also examine *V-B-N* and *V-B-N gen*. We optimize over a 24-hour scheduling horizon and we set the level of linepack at the end of the day equal to the one at the beginning of the day that is 448,000 kcf.

The expected system cost for different wind power penetration levels is illustrated in Fig. 6. All models reduce the expected cost compared to *Seq-N* and this reduction is more significant for higher shares of wind power penetration. Moreover, it can be observed that allowing more degrees of freedom to define natural gas availability allows to capture more efficiently the benefits of *Stoch-N*.

Additionally, we quantify the benefits of modeling the linepack in the natural gas system by comparing the outcome of the dispatch models when a purely steady-state operation is followed. In this case, the pipelines are not able to store natural gas, hence the inflow and outflow is equal for each time period. Fig. 7 illustrates the relative increase in expected cost when neglecting linepack in comparison with the expected cost presented in Fig. 6. An increase in expected cost is observed for all dispatch models, when the additional flexibility introduced by linepack is not considered. Model *Stoch-N* is the most advanced one and accomplishes a consistent decrease of expected cost in both cases, which is only slightly affected by wind power penetration level. On the other hand, *Seq-N* is the most inefficient and has the greatest increase when linepack is ignored that results in about 3.5% for a wind power share of 50%. Regarding the proposed volume-based dispatch models, two trends are noticed. Initially, we observe that the more flexible the procedure to define natural gas volume availability, the less the outcome is altered up to a 30% wind power penetration level. Then, the difference in expected cost is higher for *V-B-N gen* at higher penetration levels. This difference though mainly stems from the efficiency of *V-B-N gen* to exploit the linepack flexibility and significantly reduce the expected cost in this case, while still having an adequate performance when linepack is neglected.

TABLE V
DAILY PROFITS OF THERMAL UNIT I_3 IN CASE WIND PENETRATION IS 50%

	Seq-N	*Stoch-N*	*V-B-N*	*V-B-N area*	*V-B-N gen*
Expected profit ($)	239,062	4,618	73,895	52,649	47,487
Probability of negative profits*(%)	0	4	0	0	0
Average losses ($)	0	−46.7	0	0	0

* Based on the available scenario set Ω.

Finally, we illustrate that it is possible for flexible producers to face losses in *Stoch-N* as cost recovery is only guaranteed in expectation and not for each wind power scenario. On the contrary, models *Seq-N*, *V-B-N*, *V-B-N area* and *V-B-N gen* respect the merit-order and thus cost recovery is ensured for each scenario. Table V presents the daily profits for the flexible power plant I_3 for wind power penetration level equal to 50%. For *Stoch-N*, the average losses and the probability of facing a negative profit is shown. Note that the expected profit is significantly higher in *Seq-N* due to the payments to flexible producers under the very costly balancing actions (e.g. load shedding). Such balancing actions are less often under *V-B-N*, *V-B-N area* and *V-B-N gen*; hence, the expected profits are decreased for power plant I_3.

The optimization problems were solved using CPLEX 12.6.2 under GAMS on a stationary computer with Intel i7 4-core processor clocking at 3.4 GHz and 8 GB of RAM. The average solution time is presented in Table VI for both case studies. It can be noticed that *P-B* has significantly higher solution time. This is due to the greater number of binary variables required for the linearization of complementarity constraints in the KKT conditions, since the balancing market is also included in the lower-level problem of the bilevel formulation. Moreover, the time-coupling constraint that ensures

TABLE VI
AVERAGE SOLUTION TIME IN SECONDS

Model	*Seq*	*Stoch*	*V-B*	*V-B gen*	*P-B*
Tailored Case-Study	0.3	0.6	1.5	1.5	520
Model	*Seq-N*	*Stoch-N*	*V-B-N*	*V-B-N area*	*V-B-N gen*
Realistic Case-Study	48	1,100	2,920	1,409	1,034

cost neutrality for the system operator at the day-ahead stage also increases the complexity of the problem.

V. CONCLUSION

This paper proposed a framework to optimally define the natural gas volume availability for power production in an integrated electricity and natural gas system under high shares of stochastic renewables. Releasing in the day-ahead market a proper amount of natural gas to be consumed by the GFPPs allows us to increase the efficiency of the sequential market design via creating an implicit link between the day-ahead and balancing markets. The current sequential market structures are highly challenged from the increased uncertainty and variability introduced by renewables since the description of uncertain parameters is performed in a deterministic way. Using the stochastic dispatch model as an ideal benchmark, the proposed volume-based model is utilized to bridge the efficiency gap between the sequential and stochastic dispatch models. The optimal setting of natural gas availability is achieved through a stochastic bilevel program that anticipates balancing costs, while its outcome can be directly incorporated in the current market structure. In order to fully exploit the flexibility of the integrated energy system and to enhance the overall system efficiency, we approximate the natural gas system dynamics by modeling linepack that plays an important role in short-term operations. Moreover, a comparison with the price-based model that alters the natural gas price perceived by GFPPs to achieve an implicit temporal link is performed.

Our analysis illustrated that the efficiency of the sequential dispatch model through the intelligent adjustment of the natural gas volume or price significantly improves and approximates the stochastic ideal solution. The utilization of such decision-support tools facilitates the integration of renewables and captures the benefits of the stochastic dispatch model, while respecting the least-cost merit-order principle and its economic properties. For future work, more detailed models for the electricity and natural gas systems can be considered, as the utilization of AC power flow and the incorporation of compressors' fuel consumption in the natural gas system. Moreover, potential computational challenges can be tackled by the use of decomposition techniques.

REFERENCES

[1] U.S. Energy Information Administration, "International energy outlook 2016," U.S. Energy Information Administration, Tech. Rep. May 2016.

[2] A. Zlotnik *et al.*, "Coordinated scheduling for interdependent electric power and natural gas infrastructures," *IEEE Trans. Power Syst.*, vol. 32, no. 1, pp. 600–610, Jan. 2017.

[3] B. Zhao, A. J. Conejo, and R. Sioshansi, "Unit commitment under gas-supply uncertainty and gas-price variability," *IEEE Trans. Power Syst.*, vol. 32, no. 3, pp. 2394–2405, 2016.

[4] C. M. Correa-Posada and P. Sanchez-Martin, "Integrated power and natural gas model for energy adequacy in short-term operation," *IEEE Trans. Power Syst.*, vol. 30, no. 6, pp. 3347–3355, 2014.

[5] C. He, L. Wu, T. Liu, and M. Shahidehpour, "Robust co-optimization scheduling of electricity and natural gas systems via ADMM," *IEEE Trans. Sustain. Energy*, vol. 8, no. 2, pp. 658–670, April 2017.

[6] A. Alabdulwahab, A. Abusorrah, X. Zhang, and M. Shahidehpour, "Coordination of interdependent natural gas and electricity infrastructures for firming the variability of wind energy in stochastic day-ahead scheduling," *IEEE Trans. Sustain. Energy*, vol. 6, no. 2, pp. 606–615, 2015.

[7] A. Zeinalzadeh *et al.*, "Using natural gas reserves to mitigate intermittence of renewables in the day ahead market," in *Proc. IEEE 56th Conf. Decision Control*, Dec 2017, pp. 3896–3901.

[8] C. Wang *et al.*, "Equilibrium of interdependent gas and electricity markets with marginal price based bilateral energy trading," *IEEE Trans. Power Syst.*, 2018.

[9] P. Pinson, L. Mitridati, C. Ordoudis, and J. Østergaard, "Towards fully renewable energy systems : Experience and trends in Denmark," *CSEE J. Power Energy Syst.*, vol. 3, no. 1, pp. 26–35, 2017.

[10] J. M. Morales, A. J. Conejo, K. Liu, and J. Zhong, "Pricing electricity in pools with wind producers," *IEEE Trans. Power Syst.*, vol. 27, no. 3, pp. 1366–1376, Aug. 2012.

[11] G. Pritchard, G. Zakeri, and A. Philpott, "A single-settlement, energy-only electric power market for unpredictable and intermittent participants," *Oper. Res.*, vol. 58, no. 4-part-2, pp. 1210–1219, Aug. 2010.

[12] J. M. Morales, M. Zugno, S. Pineda, and P. Pinson, "Electricity market clearing with improved scheduling of stochastic production," *Eur. J. Oper. Res.*, vol. 235, no. 3, pp. 765–774, Jun. 2014.

[13] V. M. Zavala, K. Kim, M. Anitescu, and J. Birge, "A stochastic electricity market clearing formulation with consistent pricing properties," *Oper. Res.*, vol. 65, no. 3, pp. 557–576, 2017.

[14] T. V. Jensen, J. Kazempour, and P. Pinson, "Cost-optimal ATCs in zonal electricity markets," *IEEE Trans. Power Syst.*, 2017.

[15] S. Delikaraoglou and P. Pinson, "Optimal allocation of HVDC interconnections for exchange of energy and reserve capacity services," *Energy Syst.*, Apr 2018. [Online]. Available: https://doi.org/10.1007/s12667-018-0288-6

[16] C. Ordoudis, S. Delikaraoglou, P. Pinson, and J. Kazempour, "Exploiting flexibility in coupled electricity and natural gas markets: A price-based approach," in *2017 IEEE Manchester PowerTech*, June 2017, pp. 1–6.

[17] C. Ordoudis, S. Delikaraoglou, J. Kazempour, and P. Pinson, "Electronic companion - Market-based coordination for integrated electricity and natural gas systems under uncertain supply," https://doi.org/10.5281/zenodo.1283327, 2018, accessed: 5.4.2018.

[18] P. J. Hibbard and T. Schatzki, "The interdependence of electricity and natural gas: Current factors and future prospects," *Electr. J.*, vol. 25, no. 4, pp. 6–17, 2012.

[19] CAISO, "Aliso Canyon gas-electric coordination," 2017, http://www.caiso.com/Documents/DraftFinalProposal-AlisoCanyonGas-ElectricCoordinationPhase3.pdf Accessed 04.04.18.

[20] A. Henriot and J.-M. Glachant, "Capacity remuneration mechanisms in the European market: now but how?" *European University Institute (EUI), Robert Schuman Centre of Advanced Studies (RSCAS)*, 2014.

[21] C. Ordoudis, P. Pinson, and J. M. Morales, "An integrated market for electricity and natural gas systems with stochastic power producers," *under review in Eur. J. Oper. Res. arXiv:1805.04414*.

[22] C. Borraz-Sanchez *et al.*, "Convex relaxations for gas expansion planning," *INFORMS J. Comput.*, vol. 28, no. 4, pp. 645–656, 2016.

[23] A. Tomasgard, F. Rømo, M. Fodstad, and K. Midthun, "Optimization models for the natural gas value chain," in *Geom. Model. Numer. Simulation, Optim.* Berlin, Heidelberg: Springer Berlin Heidelberg, 2007, pp. 521–558.

[24] F. Rømo *et al.*, "Optimizing the Norwegian natural gas production and transport," *Interfaces (Providence).*, vol. 39, no. 1, pp. 46–56, 2009.

[25] M. Fodstad, K. T. Midthun, and A. Tomasgard, "Adding flexibility in a natural gas transportation network using interruptible transportation services," *Eur. J. Oper. Res.*, vol. 243, no. 2, pp. 647–657, 2015.

[26] S. Misra *et al.*, "Optimal compression in natural gas networks: A geometric programming approach," *IEEE Trans. Control Netw. Syst.*, vol. 2, no. 1, pp. 47–56, March 2015.

[27] A. Zlotnik, M. Chertkov, and S. Backhaus, "Optimal control of transient flow in natural gas networks," in *Proc. IEEE 54th Conf. Decision Control*, Dec 2015, pp. 4563–4570.

[28] W. Bukhsh, "Data for stochastic multiperiod optimal power flow problem," 2017, https://sites.google.com/site/datasmopf/ Accessed 04.04.18.

[29] C. Grigg *et al.*, "The IEEE reliability test system-1996. A report prepared by the reliability test system task force of the application of probability methods subcommittee," *IEEE Trans. Power Syst.*, vol. 14, no. 3, pp. 1010–1020, 1999.

Market-based Coordination for Integrated Electricity & Natural Gas Systems Under Uncertain Supply

Christos Ordoudis, Stefanos Delikaraoglou, Jalal Kazempour, Pierre Pinson

This document serves as an electronic companion (EC) for the paper "Market-based Coordination for Integrated Electricity and Natural Gas Systems under Uncertain Supply". It contains four sections that present the MPEC formulation of the bilevel model *V-B*, provide proofs regarding the non-negative profits of flexible producers, a nomenclature and additional results.

1. MPEC formulation of volume-based coupled electricity and natural gas model (V-B)

In this section the bilevel *V-B* model is reformulated as a Mathematical Program with Equilibrium Constraints (MPEC) by replacing the linear, and thus convex, lower level problems by their Karush-Kuhn-Tucker (KKT) conditions. Then, the resulting MPEC is transformed into a Mixed-Integer Linear Program (MILP) in order to deal with the bilinear terms that arise from the complementarity conditions. We introduce a mapping $M_a^{i_g}$ of the natural gas-fired power plants i_g at area a (entries are equal to 1 if NGFPP is connected to an area and 0 otherwise). The model writes as follows,

$$\underset{\Theta^{\text{MUL}}}{\text{Min.}} \sum_{t\in T}\Big[\sum_{i_c\in I_c} C_{i_c}p_{i_c,t} + \sum_{k\in K} C_k g_{k,t} + \sum_{\omega\in\Omega}\pi_\omega\Big(\sum_{k\in K}(C_k^+ g^+_{k,\omega,t} - C_k^- g^-_{k,\omega,t}) + \sum_{i_c\in I_c}(C^+_{i_c}p^+_{i_c,\omega,t} - C^-_{i_c}p^-_{i_c,\omega,t}) + \sum_{r_e\in R_e} C^{\text{sh,E}} l^{\text{sh,E}}_{r_e,\omega,t} + \sum_{r_g\in R_g} C^{\text{sh,G}} l^{\text{sh,G}}_{r_g,\omega,t}\Big)\Big] \tag{1a}$$

subject to

$$-p_{i,t} \le \Delta p_{i,\omega',t} \le P_i^{\max} - p_{i,t},\ \ \forall i,t, \tag{1b}$$

$$-P_i^- \le \Delta p_{i,\omega',t} \le P_i^+,\ \ \forall i,t, \tag{1c}$$

$$0 \le w^{\text{sp}}_{j,\omega',t} \le W_{j,\omega',t},\ \ \forall j,t, \tag{1d}$$

$$0 \le l^{\text{sh,E}}_{r_e,\omega',t} \le D^{\text{E}}_{r_e,t},\ \ \forall t, \tag{1e}$$

$$\sum_{i\in I}\Delta p_{i,\omega',t} + \sum_{r_e\in R_e} l^{\text{sh,E}}_{r_e,\omega',t} + \sum_{j\in J}(W_{j,\omega',t} - w^{\text{sp}}_{j,\omega',t} - w_{j,t}) = 0 : \tilde{\lambda}^{\text{E}}_{\omega',t},\ \ \forall t, \tag{1f}$$

$$-g_{k,t} \le \Delta g_{k,\omega',t} \le G_k^{\max} - g_{k,t},\ \ \forall k,t, \tag{1g}$$

$$-G_k^- \le \Delta g_{k,\omega',t} \le G_k^+,\ \ \forall k,t, \tag{1h}$$

$$0 \le l^{\text{sh,G}}_{r_g,\omega',t} \le D^{\text{G}}_{r_g,t},\ \ \forall t, \tag{1i}$$

$$\sum_{k\in K}\Delta g_{k,\omega',t} + \sum_{r_g\in R_g} l^{\text{sh,G}}_{r_g,\omega',t} - \sum_{i_g\in I_g}\phi_{i_g}\Delta p_{i_g,\omega',t} = 0 : \tilde{\lambda}^{\text{G}}_{\omega',t},\ \ \forall t, \tag{1j}$$

$$0 \le \sum_{t\in T}\sum_{i_g\in A_z^{I_g}}\phi_{i_g}(p_{i_g,t} + \Delta p_{i_g,\omega',t}) \le F_z^{\text{A}},\ \ \forall z, \tag{1k}$$

$$0 \le \sum_{i_g\in A_z^{I_g}}\phi_{i_g}(p_{i_g,t} + \Delta p_{i_g,\omega',t}) \le F^{\text{M}}_{z,t},\ \ \forall z,t, \tag{1l}$$

$$0 \leq \chi^v_\psi \leq |T| \sum_{k\in K} G^{\max}_k - \sum_{t\in T}\sum_{r_g\in R_g} D^{\mathrm{G}}_{r_g,t}, \ \ \forall\psi, \tag{1m}$$

$$0 \leq \chi^v_{\psi,t} \leq F^{\max}_{\psi,t} - \sum_{r_g\in A^{R_g}_\psi} D^{\mathrm{G}}_{r_g,t}, \ \ \forall\psi,t, \tag{1n}$$

$$0 \leq p_{i,t} \leq P^{\max}_i : \underline{\mu}^{\mathrm{P}}_{i,t}, \overline{\mu}^{\mathrm{P}}_{i,t}, \ \ \forall i,t, \tag{1o}$$

$$0 \leq w_{j,t} \leq \widehat{W}_{j,t} : \underline{\mu}^{\widehat{\mathrm{W}}}_{j,t}, \overline{\mu}^{\widehat{\mathrm{W}}}_{j,t}, \ \ \forall j,t, \tag{1p}$$

$$\sum_{i\in I} p_{i,t} + \sum_{j\in J} w_{j,t} - \sum_{r_e\in R_e} D^{\mathrm{E}}_{r_e,t} = 0 : \hat{\lambda}^{\mathrm{E}}_t, \ \ \forall t, \tag{1q}$$

$$0 \leq g_{k,t} \leq G^{\max}_k : \underline{\mu}^{\mathrm{G}}_{k,t}, \overline{\mu}^{\mathrm{G}}_{k,t}, \ \ \forall k,t, \tag{1r}$$

$$\sum_{k\in K} g_{k,t} - \sum_{r_g\in R_g} D^{\mathrm{G}}_{r_g,t} - \sum_{i_g\in I_g} \phi_{i_g} p_{i_g,t} = 0 : \hat{\lambda}^{\mathrm{G}}_t, \ \ \forall t, \tag{1s}$$

$$0 \leq \sum_{t\in T}\sum_{i_g\in A^{I_g}_\psi} \phi_{i_g} p_{i_g,t} \leq x^v_\psi : \underline{\nu}^v_\psi, \overline{\nu}^v_\psi, \ \ \forall\psi, \tag{1t}$$

$$0 \leq \sum_{i_g\in A^{I_g}_\psi} \phi_{i_g} p_{i_g,t} \leq x^v_{\psi,t} : \underline{\mu}^v_{\psi,t}, \overline{\mu}^v_{\psi,t}, \ \ \forall\psi,t \tag{1u}$$

$$C_{i_c} - \hat{\lambda}^{\mathrm{E}}_t - \underline{\mu}^{\mathrm{P}}_{i_c,t} + \overline{\mu}^{\mathrm{P}}_{i_c,t} = 0, \ \ \forall i_c,t, \tag{1v}$$

$$\phi_{i_g}\hat{\lambda}^{\mathrm{G}}_t - \hat{\lambda}^{\mathrm{E}}_t - \underline{\mu}^{\mathrm{P}}_{i_g,t} + \overline{\mu}^{\mathrm{P}}_{i_g,t} + \sum_{\psi\in\Psi} M^{i_g}_\psi (\phi_{i_g}\overline{\mu}^v_{\psi,t} + \phi_{i_g}\overline{\nu}^v_\psi - \phi_{i_g}\underline{\mu}^v_{\psi,t} - \phi_{i_g}\underline{\nu}^v_\psi) = 0, \ \ \forall i_g,t, \tag{1w}$$

$$-\hat{\lambda}^{\mathrm{E}}_t - \underline{\mu}^{\widehat{\mathrm{W}}}_{j,t} + \overline{\mu}^{\widehat{\mathrm{W}}}_{j,t} = 0, \ \ \forall j,t, \tag{1x}$$

$$C_k - \hat{\lambda}^{\mathrm{G}}_t - \underline{\mu}^{\mathrm{G}}_{k,t} + \overline{\mu}^{\mathrm{G}}_{k,t} = 0, \ \ \forall k,t, \tag{1y}$$

$$0 \leq \overline{\mu}^{\mathrm{P}}_{i,t} \perp P^{\max}_i - p_{i,t} \geq 0, \ \ \forall i,t, \tag{1z}$$

$$0 \leq \underline{\mu}^{\mathrm{P}}_{i,t} \perp p_{i,t} \geq 0, \ \ \forall i,t, \tag{1aa}$$

$$0 \leq \overline{\mu}^{\widehat{\mathrm{W}}}_{j,t} \perp \widehat{W}_j - w_{j,t} \geq 0, \ \ \forall j,t, \tag{1ab}$$

$$0 \leq \underline{\mu}^{\widehat{\mathrm{W}}}_{j,t} \perp w_{j,t} \geq 0, \ \ \forall j,t, \tag{1ac}$$

$$0 \leq \overline{\mu}^v_{\psi,t} \perp x^v_{\psi,t} - \sum_{i_g\in A^{I_g}_\psi} \phi_{i_g} p_{i_g,t} \geq 0, \ \ \forall\psi,t, \tag{1ad}$$

$$0 \leq \overline{\nu}^v_\psi \perp x^v_\psi - \sum_{t\in T}\sum_{i_g\in A^{I_g}_\psi} \phi_{i_g} p_{i_g,t} \geq 0, \ \ \forall\psi, \tag{1ae}$$

$$0 \leq \underline{\mu}^v_{\psi,t} \perp \sum_{i_g\in A^{I_g}_\psi} \phi_{i_g} p_{i_g,t} \geq 0, \ \ \forall\psi,t, \tag{1af}$$

$$0 \leq \underline{\nu}^v_\psi \perp \sum_{t\in T}\sum_{i_g\in A^{I_g}_\psi} \phi_{i_g} p_{i_g,t} \geq 0, \ \ \forall\psi, \tag{1ag}$$

$$0 \leq \overline{\mu}^{\mathrm{G}}_{k,t} \perp G^{\max}_k - g_{k,t} \geq 0, \ \ \forall k,t, \tag{1ah}$$

$$0 \leq \underline{\mu}^{\mathrm{G}}_{k,t} \perp g_{k,t} \geq 0, \ \ \forall k,t, \tag{1ai}$$

The nonlinearities that arise from complementarity conditions are linearized via the Fortuny-Amat transformation [1]. We introduce the set of dual variables (λ, μ and ν) Θ^{dual}, thus $\Theta^{\mathrm{MUL}} = \{\Theta^{\mathrm{VUL}}, \Theta^{\mathrm{dual}}\}$. For the network constrained balancing market, we use the set of constraints {(2b)-(2e),(2g)-(2i),(3a)-(3c),(6a)-(6p)} (numbered from the original manuscript) instead of (1b)-(1l).

2. Proofs for the non-negative profits of flexible producers

In this section, we provide the proofs for the non-negativity of profits of flexible producers, when considering a sequential clearing of day-ahead and balancing markets. We would initially like to notice that model *Seq* in the original manuscript is an optimization problem. Let us then introduce model *Seq-Eq*, which is a two-settlement equilibrium model. Considering a different optimization problem for each market participant and the market-clearing conditions for each trading floor (i.e. day-ahead and balancing), we can formulate *Seq-Eq* by writing the KKT conditions for each individual optimization model. This set of KKT conditions is identical to those conditions associated with the *Seq* model, which proves that *Seq* and *Seq-Eq* are equivalent. Thus, any solution of one model is a solution of the other model too. The aforementioned statement holds if the problems are convex. We refer the reader to [2] and [3] for an extensive discussion on this topic and presentation of the approach to equivalently formulate the equilibrium and optimization models.

First, we focus on the thermal power plants that are not consuming natural gas. Focusing to the equilibrium model *Seq-Eq*, the profit maximization problem of each power producer for the day-ahead stage writes as follows,

$$\Big\{\underset{p_{i_c,t}}{\text{Max.}} \sum_{t\in T}\Big[p_{i_c,t}(\hat{\lambda}^{\mathrm{E}}_t - C_{i_c})\Big] \tag{2a}$$

subject to

$$0 \le p_{i_c,t} \le P^{\max}_i : \underline{\mu}^{\mathrm{P}}_{i_c,t}, \overline{\mu}^{\mathrm{P}}_{i_c,t}\Big\}, \ \ \forall i_c, t. \tag{2b}$$

Since program (2) is linear and thus convex, the strong duality theorem holds for the optimal solution and,

$$\sum_{t\in T}\Big[p_{i_c,t}(\hat{\lambda}^{\mathrm{E}}_t - C_{i_c})\Big] = \sum_{t\in T}\overline{\mu}^{\mathrm{P}}_{i_c,t}P^{\max}_{i_c}, \tag{3}$$

where $\overline{\mu}^{\mathrm{P}}_{i_c,t} \ge 0$ and $P^{\max}_{i_c} \ge 0$ which shows that the profits in the day-ahead market are positive. Similarly, we can write the profit maximization problem for the balancing market by having the day-ahead decision $p^*_{i_c,t}$ fixed,

$$\Big\{\underset{\Delta p_{i,\omega',t}}{\text{Max.}} \sum_{t\in T}\Big[\Delta p_{i,\omega',t}(\tilde{\lambda}^{\mathrm{E}}_{\omega',t} - C_{i_c})\Big] \tag{4a}$$

subject to

$$-p^*_{i_c,t} \le \Delta p_{i_c,\omega',t} \le P^{\max}_{i_c} - p^*_{i_c,t} : \underline{\mu}^{\mathrm{R}}_{i_c,\omega',t}, \overline{\mu}^{\mathrm{R}}_{i_c,\omega',t}, \tag{4b}$$

$$-P^{-}_i \le \Delta p_{i_g,\omega',t} \le P^{+}_i : \underline{\mu}^{\mathrm{RR}}_{i_c,\omega',t}, \overline{\mu}^{\mathrm{RR}}_{i_c,\omega',t}\Big\}, \ \ \forall i_c, \omega', t. \tag{4c}$$

We can also write the strong duality theorem for the optimal solution for program (4),

$$\sum_{t\in T}\Big[\Delta p_{i_c,\omega',t}(\tilde{\lambda}^{\mathrm{E}}_{\omega',t} - C_{i_c})\Big] = \sum_{t\in T}\Big(\overline{\mu}^{\mathrm{R}}_{i_c,\omega',t}(P^{\max}_{i_c} - p^*_{i_c,t}) + \underline{\mu}^{\mathrm{R}}_{i_c,\omega',t}p^*_{i_c,t} + \overline{\mu}^{\mathrm{RR}}_{i_c,\omega',t}P^{+}_{i_c} + \underline{\mu}^{\mathrm{RR}}_{i_c,\omega',t}P^{-}_{i_c}\Big), \tag{5}$$

where $\overline{\mu}^{\mathrm{R}}_{i_c,\omega',t}, \underline{\mu}^{\mathrm{R}}_{i_c,\omega',t}, \overline{\mu}^{\mathrm{RR}}_{i_c,\omega',t}, \underline{\mu}^{\mathrm{RR}}_{i_c,\omega',t} \ge 0$. Moreover, the quantities $(P^{\max}_{i_c} - p^*_{i_c,t}), p^*_{i_c,t}, P^{+}_{i_c}, P^{-}_{i_c} \ge 0$. Thus, the profits in balancing market are also positive and this completes the proof. Since cost-recovery holds for model *Seq-Eq*, then it means that it is also ensured in optimization model *Seq* due to their equivalence.

The similar proof can be written for the GFPPs, where the marginal cost (C_{i_c}) is replaced by $\phi_{i_g}\hat{\lambda}^{\mathrm{G}}_t$ and $\phi_{i_g}\tilde{\lambda}^{\mathrm{G}}_{\omega',t}$ for the day-ahead and balancing markets, respectively. The relative proof regarding cost recovery for flexible producers in stochastic dispatch model only in expectation and not per scenario realization of

stochastic power production is presented in [4], while authors in [5] provide a detailed discussion on the topic. Finally, a stochastic market-clearing model that ensures cost-recovery and revenue adequacy per scenario is proposed in [6].

3. Nomenclature

In Tables 1-3, we present the symbols used in the original paper and the description for each one of them.

Table 1. Nomenclature for the variables

Symbol	Description
$p_{i,t}$	Day-ahead dispatch of power plants i in period t [MW]
$w_{j,t}$	Day-ahead dispatch of stochastic power producers j in period t [MW]
$p^{+}_{i,\omega,t}$	Up regulation provided by dispatchable power plant i in scenario ω, period t [MW]
$p^{-}_{i,\omega,t}$	Down regulation provided by dispatchable power plant i in scenario ω, period t [MW]
$w^{\mathrm{sp}}_{j,\omega,t}$	Power spilled by stochastic power plant j in scenario ω, period t [MW]
$l^{\mathrm{sh,E}}_{r_e,\omega,t}$	Electric power load shedding at node n in scenario ω, period t [MW]
$l^{\mathrm{sh,G}}_{r_g,\omega,t}$	Natural gas load shedding at node m in scenario ω, period t [kcf/h]
$\delta_{n,\omega,t}$	Voltage angle at node n in scenario ω, period t [rad]
$g_{k,t}$	Day-ahead dispatch of natural gas producer k in period t [kcf/h]
$g^{+}_{k,\omega,t}$	Up regulation provided by natural gas producer k in scenario ω, period t [kcf/h]
$g^{-}_{k,\omega,t}$	Down regulation provided by natural gas producer k in scenario ω, period t [kcf/h]
$pr^{\mathrm{r}}_{m,\omega,t}$	Pressure at node m in scenario ω, period t [psig]
$h^{\mathrm{r}}_{m,u,\omega,t}$	Average mass of natural gas (linepack) in pipeline (m,u), scenario ω, period t [kcf]
$q^{\mathrm{in,r}}_{m,u,\omega,t}$	Inflow natural gas rates of pipeline (m,u) in scenario ω, period t [kcf/h]
$q^{\mathrm{out,r}}_{m,u,\omega,t}$	Outflow natural gas rates of pipeline (m,u) in scenario ω, period t [kcf/h]
$q_{m,u}$	Natural gas flow in pipeline (m,u) [kcf/h]
$y^{\mathrm{r}}_{m,u,\omega,t}$	Binary variable defining the direction of the natural gas flow in pipeline (m,u), scenario ω, period t {0,1}
χ^{p}_{t}	Natural gas price adjustment in period t [$/kcf]
$\overline{\chi}^{v}_{\psi}$	Daily natural gas volume availability for GFPPs' group in specific area ψ [kcf]
$\chi^{v}_{\psi,t}$	Hourly natural gas volume availability for GFPPs' group in specific area ψ in period t [kcf]

TABLE 2. Nomenclature for the parameters

Symbol	Description
$D^{\mathrm{E}}_{r_e,t}$	Electricity demand r_e and in period t [MW]
$D^{\mathrm{G}}_{r_g,t}$	Natural gas demand r_g and in period t [kcf/h]
C_i	Day-ahead offer price of dispatchable power plant i [$/MWh]
C_i^+	Up regulation offer price of dispatchable power plant i [$/MWh]
C_i^-	Down regulation offer price of dispatchable power plant i [$/MWh]
$C^{\mathrm{sh,E}}$	Cost of electricity load shedding [$/MWh]
C_k	Day-ahead offer price of natural gas producer k [$/kcf]
C_k^+	Up regulation offer price of natural gas producer k [$/kcf]
C_k^-	Down regulation offer price of natural gas producer k [$/kcf]
$C^{\mathrm{sh,G}}$	Cost of natural gas load shedding [$/kcf]
$P_i^{\max}$	Capacity of dispatchable power plant i [MW]
P_i^+	Maximum up regulation capability of dispatchable power plant i [MW]
P_i^-	Maximum down regulation capability of dispatchable power plant i [MW]
ϕ_{i_g}	Power conversion factor of natural gas-fired power plant i_g [kcf/MWh]
$W_{j,\omega,t}$	Power production by stochastic power plant j in scenario ω, period t [MW]
$\widehat{W}_{j,t}$	Expected power production by stochastic power plant j in period t [MW]
$\overline{W}_j$	Capacity of stochastic power plant j [MW]
$G_k^{\max}$	Capacity of natural gas producer k [kcf/h]
G_k^+	Maximum up regulation capability of natural gas producer k [kcf/h]
G_k^-	Maximum down regulation capability of natural gas producer k [kcf/h]
$B_{n,r}$	Absolute value of the susceptance of line (n,r) [per unit]
$F_{n,r}^{\max}$	Transmission capacity of line (n,r) [MW]
$K^{\mathrm{h}}_{m,u}$	Natural gas flow constant of pipeline (m,u) [kcf/psig]
$K^{\mathrm{f}}_{m,u}$	Linepack constant of pipeline (m,u) [kcf/(psig $\cdot$ h)]
$PR_m^{\min}$	Minimum pressure at node m [psig]
$PR_m^{\max}$	Maximum pressure at node m [psig]
Γ_z	Compressor factor located at natural gas network branch z [-]
π_ω	Probability of scenario ω [-]
$\tilde{M}$	Sufficiently large constant [-]
$F^{\mathrm{M}}_{z,t}$	Capacity of natural gas pipeline z in period t [kcf/h]
F^{A}_z	Daily contract limit of natural gas pipeline z [kcf]
$F_{\psi,t}^{\max}$	Maximum natural gas availability for a specific area ψ containing the group of GFPPs [kcf/h]

TABLE 3. Nomenclature for the sets

Symbol	Description
I	Set of dispatchable power plants i
I_c	Set of thermal power plants i_c ($I_c \subset I$)
I_g	Set of natural gas-fired power plants i_g ($I_g \subset I$)
J	Set of stochastic power plants j
L	Set of electricity transmission lines l
N	Set of electricity network nodes n
K	Set of natural gas producers k
Z	Set of natural gas network branches z
M	Set of natural gas network nodes m
R_e	Set of electricity demands r_e
R_g	Set of natural gas demands r_g
V	Set of fixed pressure points v for the linearization of Weymouth equation
Ω	Set of stochastic power production scenarios ω
T	Set of time periods t
A_n^I	Set of dispatchable power plants i located at electricity network node n
A_n^J	Set of stochastic power plants j located at electricity network node n
$A_m^{I_g}$	Set of natural gas-fired power plants i_g located at natural gas network node m
$A_\psi^{I_g}$	Set of natural gas-fired power plants i_g located in a specific area ψ
A_m^K	Set of natural gas producers k located at natural gas network node m
$A_n^{R_e}$	Set of electricity demands r_e located at electricity network node n
$A_m^{R_g}$	Set of natural gas demands r_g located at natural gas network node m
Ψ	Set of groups of natural gas-fired power plants located in a specific area ψ
Θ	Set of primal optimization variables defined for each optimization model

4. Additional Results

Fig. 1 shows the natural gas price adjustment (χ_t^p) and the day-ahead payment/charge in order to generate this signal. Moreover, Fig. 2 illustrate the natural gas price adjustment (χ_t^p) in relation to the difference in the hourly GFPPs share of the total power production between *P-B* and *Seq*. A detailed analysis of these results is presented in [7].

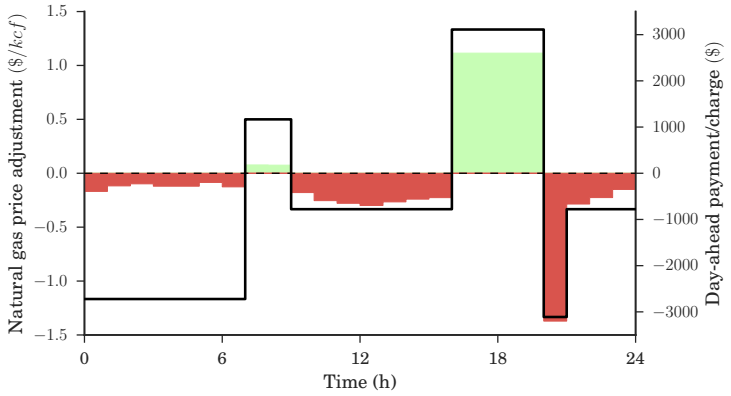

Figure 1. Hourly natural gas price adjustment (black line: left y-axis) and day-ahead financial settlement of the system operator to adjust the natural gas price (colored areas: right y-axis). Wind power penetration 50%.

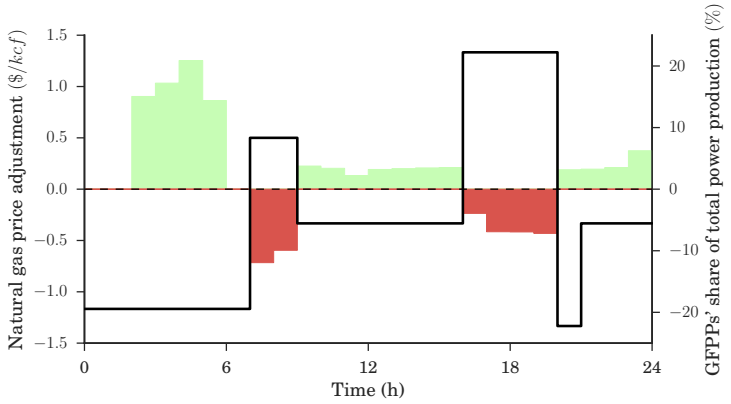

Figure 2. Hourly natural gas price adjustment (black line: left y-axis) and difference in GFPPs share of total power production between P-B and Seq (colored areas: right y-axis). Wind power penetration 50%.

Fig. 3 shows the natural gas volume ($\chi^v_{a,t}$) in relation to the natural gas volume consumed in *Seq* and the the difference in the hourly GFPPs share of the total power production between *V-B* and *Seq*. Moreover, Fig. 4 illustrate the natural gas volume ($\chi^v_{a,t}$) change compared to the natural gas volume consumed in *Seq* in relation to the difference in the hourly GFPPs share of the total power production between *V-B gen* and *Seq*. Thus, the left y-axis illustrates the quantity $\frac{F(V\text{-}B)-F(Seq)}{F(Seq)}$ or $\frac{F(V\text{-}B\ gen)-F(Seq)}{F(Seq)}$, where F is the natural gas volume made available at the day-ahead stage for each dispatch model.

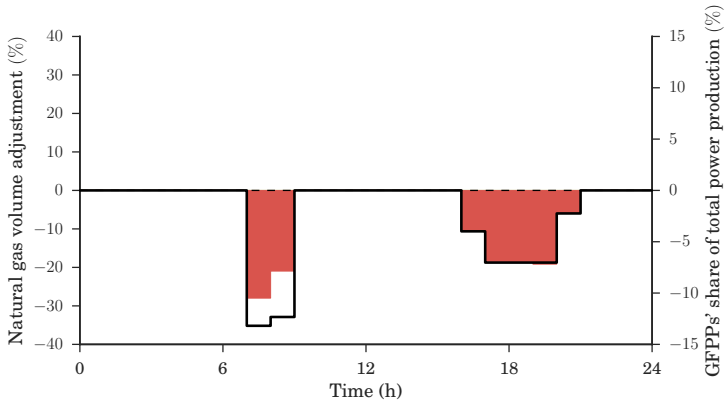

FIGURE 3. Hourly natural gas volume adjustment (black line: left y-axis) and difference in GFPPs share of total power production between *V-B* and *Seq* (colored areas: right y-axis). Wind power penetration 50%.

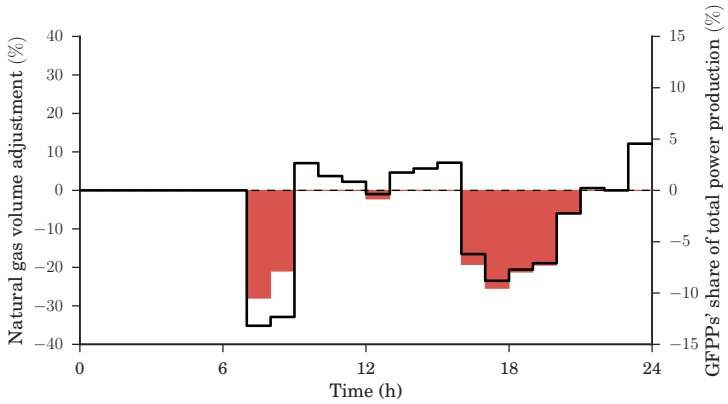

FIGURE 4. Hourly natural gas volume adjustment (black line: left y-axis) and difference in GFPPs share of total power production between *V-B gen* and *Seq* (colored areas: right y-axis). Wind power penetration 50%.

It can be noticed in Fig. 3 that a decrease in the natural gas volume results in a decrease of the power production share of GFPPs compared to the scheduling provided from model *Seq*. A similar effect is also observed in Fig. 4, except for two periods in the middle of the day. During these hours, the total natural gas consumed by GFFPs in *V-B gen* is higher than in *Seq*, while GFPPs' share of total power production is not affected. This happens because there is a sift of "X MW" between the two GFPPs, resulting in the one with the higher power conversion factor to produce more than in *Seq*; hence increase the total gas consumption for power production.

Table 4 illustrates the performance of the dispatch models in terms of expected cost when the electricity demand is equal to 344 MW in order to explore an alternative case of natural gas price adjustment and volume availability. Models *Stoch* and *Seq* provide the two extreme solutions in terms of expected cost. We highlight though that *P-B*, *V-B* and *V-B gen* manage to return the same expected cost as *Stoch*. This fact illustrates that it is possible in specific cases to have an efficient sequential system dispatch if the future balancing costs are communicated into the day-ahead market through the operator-defined parameters χ.

TABLE 4. Expected system cost and its breakdown in $ when total power load is 344 MW

	Total	Day-ahead	Balancing	Up regulation	Down regulation
Seq	8,932.8	8,566.8	366.0	825.0	-459.0
Stoch	8,859.6	8,206.8	652.8	917.4	-264.6
P-B / V-B / V-B gen	8,859.6	8,638.8	220.8	679.8	-459.0

The schedule of power plants is given in Table 5 for D^{E}=344 MW. In *P-B*, the natural gas price adjustment is $\chi^{p}_{t_2}$ = +\$0.5/kcf which increases the marginal cost of GFPP I_3 to \$30/MWh. Thus, an improved day-ahead schedule is achieved by sifting 12 MW from GFPP I_3 to unit I_1, resulting in a lower expected cost. Models *V-B* and *V-B gen* reduce the total natural gas availability from 600 kcf to 456 kcf and return the same improved dispatch as *P-B*.

TABLE 5. Power system schedule in MW when total power load is 344 MW (variation from *Seq* day-ahead (DA) schedule in bold)

	Seq			*P-B*			*V-B*			*V-B gen*		
Unit	DA	ω_1	ω_2	DA	ω_1	ω_2	DA	ω_1	ω_2	DA	ω_1	ω_2
I_1	58	-10	+10	**70**	-10	+10	**70**	-10	+10	**70**	-10	+10
I_2	110	0	0	110	0	0	110	0	0	110	0	0
I_3	50	-30	0	**38**	-30	+12	**38**	-30	+12	**38**	-30	+12
I_4	0	0	+25	0	0	+18	0	0	+18	0	0	+18
I_5	0	0	+5	0	0	0	0	0	0	0	0	0
WP	126	+40	-40	126	+40	-40	126	+40	-40	126	+40	-40

References

[1] J. Fortuny-Amat and B. McCarl, "A representation and economic interpretation of a two-level programming problem," *J. Oper. Res. Soc.*, vol. 32, no. 9, pp. 783–792, 1981.

[2] J. Kazempour and B. F. Hobbs, "Value of flexible resources, virtual bidding, and self-scheduling in two-settlement electricity markets with wind generation - part i: Principles and competitive model," *IEEE Trans. Power Syst.*, vol. 33, pp. 749–759, Jan 2018.

[3] J. Kazempour and B. F. Hobbs, "Value of flexible resources, virtual bidding, and self-scheduling in two-settlement electricity markets with wind generation - part ii: Iso models and application," *IEEE Trans. Power Syst.*, vol. 33, pp. 760–770, Jan 2018.

[4] J. M. Morales, A. J. Conejo, K. Liu, and J. Zhong, "Pricing electricity in pools with wind producers," *IEEE Trans. Power Syst.*, vol. 27, pp. 1366–1376, Aug. 2012.

[5] J. M. Morales, M. Zugno, S. Pineda, and P. Pinson, "Electricity market clearing with improved scheduling of stochastic production," *Eur. J. Oper. Res.*, vol. 235, pp. 765–774, Jun. 2014.

[6] J. Kazempour, P. Pinson, and B. F. Hobbs, "A stochastic market design with revenue adequacy and cost recovery by scenario: Benefits and costs," *IEEE Trans. Power Syst.*, pp. 1–1, 2018.

[7] C. Ordoudis, S. Delikaraoglou, P. Pinson, and J. Kazempour, "Exploiting flexibility in coupled electricity and natural gas markets: A price-based approach," in *2017 IEEE Manchester PowerTech*, pp. 1–6, June 2017.

[Paper E] Energy and Reserve Dispatch with Distributionally Robust Joint Chance Constraints

Authors:
Christos Ordoudis, Viet Anh Nguyen, Daniel Kuhn and Pierre Pinson[3]

Published as:
Working paper to be submitted to IEEE Transactions on Power Systems.

Note:
The corresponding appendix, which includes the mathematical proofs, system data, a detailed nomenclature and additional results, is provided just after the manuscript.

[3]The list of authors may be subject to changes.

Energy and Reserve Dispatch with Distributionally Robust Joint Chance Constraints

Christos Ordoudis, *Student Member, IEEE,* Viet Anh Nguyen, Daniel Kuhn, Pierre Pinson, *Senior Member, IEEE*[*]

***Abstract*—The stochastic nature of power production from renewables calls for changes in system operations due to the immense uncertainty and variability introduced. Various approaches have been proposed to deal with this challenge based on chance constrained programming. However, these problems often assume that the probability distribution of the uncertain parameter is perfectly known and consider chance constraints individually. To address these shortcomings, we consider a data-driven, distributionally robust joint chance constrained program where we use the Wasserstein distance to construct the ambiguity set. We propose a novel approach to safely approximate the feasible set, and the resulting model is a conic program that can be further simplified into a linear program in specific cases. We apply the model to solve the energy and reserve dispatch problem with fuel constraints for gas-fired power plants in view of an increased interdependence between the electricity and the natural gas systems. The numerical study based on an out-of-sample analysis shows the effect of Wasserstein radius on the conservativeness of solutions and demonstrates that a systematic choice of the Wasserstein radius results in attractive solutions in terms of the expected system cost.**

***Index Terms*—Distributionally robust optimization, energy and reserve dispatch, joint chance constraints, Wasserstein metric.**

I. Introduction

The increased deployment of renewable energy sources, including solar, wind and tidal energy, has dramatically shifted the generation mix. Being a key element for the transition towards a more sustainable energy system, renewable energy sources also bring numerous challenges to power system operation because of its highly variable and only partly predictable production [1]. Meanwhile, gas-fired power plants (GFPPs) are able to increase system's flexibility and are widely built to replace older power plants recently. Thus, a tighter coupling of electricity and natural gas systems is foreseeable [2], which behooves us to study both systems in a coordinated manner.

Various approaches have been proposed to deal with the uncertain power production of renewables including robust optimization [3], [4], chance-constrained programming [5]–[7], and stochastic programming [8], [9]. The solutions obtained from robust optimization may be overly conservative because the decisions are optimized for the worst-case realization in the uncertainty set [10]. Alternatively, a chance-constraint approach ensures that stochastic constraints are only satisfied for a predefined probability to alleviate the conservativeness of robust optimization. In the stochastic programming framework, the uncertain parameter is assumed to follow a specific probability distribution [11]. The distribution is chosen to facilitate the reformulation of the problem, for example, Gaussian distribution of forecast errors is assumed in [5] and [7]. Another approach is proposed in [12] that replaces the original set of chance constraints by a finite number of sampled constraints to create an approximate problem. In this case, it is shown that the probability to satisfy the original constraints by the approximate solution essentially increases with an increase of the number of samples used in the approximate problem. However, such an approach would imply that there is a plethora of available samples drawn from the true data generating distribution and would result in large instances of the problem and suffer from computational challenges.

Acknowledging the need to follow a data-driven approach that utilizes the available data at hand, we focus on distributionally robust optimization that fills the gap between stochastic programming and robust optimization by optimizing over a family of distributions (i.e., ambiguity set) that would optimally include the true data generating one. Two types of ambiguity sets are more commonly used in the literature: the moment-based [13] and the metric-based ones [14]. In the first approach, the set is defined by the distributions satisfying moment constraints (e.g., having the same mean and covariance matrix), while in the latter approach the set contains the distributions that are close to the empirical one based on the probability metric selected. Moment-based ambiguity sets have been adopted by various works in the field of power systems, such as [15]–[20]. More specifically, a distributionally robust approach is followed to formulate ambiguous chance constraints in [19] and [20]; however, these constraints are treated as individual chance constraints. There exist only a few papers dealing with distributionally robust joint chance constraints, such as [18], [21], [22], though using moment-based approaches.

There is a recent surge in using the Wasserstein metric in the distributionally robust framework. [23] use the property of the Wasserstein metric to calibrate an uncertainty set from the available data and solve an equivalent robust optimization problem instead of the original chance constrained program. To solve distributionally robust joint chance constraints with the Wasserstein metric, a naive idea is to directly apply the reformulation in [14, Section 5.2]; though, this approach introduces bilinear terms which makes it intractable for high dimensional problems. Recently, mixed-integer conic reformulations of chance constraints with the Wasserstein metric are proposed in [24]–[26]; however, these approaches are prohibitive for problems of high dimensions.

In this paper, we develop a novel approach to solve distributionally robust joint chance constrained programs where the ambiguity set represents a Wasserstein ball centered at a nominal distribution estimated from the available data [14]. Thus, we make no assumption regarding the existence of the true probability distribution in any parametric family of distributions and handle multiple constraints simultaneously. We provide a convex conservative approximation of the feasible set defined by the joint chance constraints and show that

[*]The list of authors may be subject to changes.

our approach outperforms the Bonferroni approximation [27] that is widely used in the literature. Moreover, the effect of adjusting the Wasserstein radius on the performance of the optimal solutions is demonstrated using an intensive out-of-sample analysis. By fine-tuning the radius of the Wasserstein ball, the decision maker attains cost-effective solutions when only limited amount of data is available. Hence, we present a detailed procedure to estimate the optimal Wasserstein radius in order to provide an implementable solution with remarkable out-of-sample performance.

The contributions of this paper are summarized as follows:

1) We propose a new approximation scheme for distributionally robust joint chance constrained programs in which the ambiguity set is defined using the Wasserstein type-1 distance. By associating the joint chance constraint with a positive scaling vector, the feasible set can be safely approximated by a set of conic constraints. Under specific norms of the Wasserstein metric, these conic constraints become linear constraints and the resulting model is tractable in high dimensional problems.
2) We present a simple, yet effective procedure to sequentially optimize over decision variables and scaling factors. This procedure not only improves the quality of the optimal solution but also facilitates the detection of feasible solutions for tightly-constrained systems.
3) We compare the numerical experiments on the problem of energy and reserve dispatch with fuel constraints for GFPPs under uncertain power supply. By comparing the out-of-sample performance, we show that our approach has a substantially better performance compared to existing methods including the ambiguity-free and robust approach, as well as the Bonferroni approximation. A realistic system operation is also modeled by allowing for optimal re-dispatch after the uncertainty realization and provide a systematic method to choose the ambiguity size based on the available data.

The remaining of the paper is organized as follows. Section II provides the problem formulation in the stochastic programming framework, while the distributionally robust approach is presented in Section III. Section IV shows the reformulation of the objective function and two approaches to approximate the ambiguous joint chance constraints under the Wasserstein ambiguity set along with the advantages of the proposed approaches. Numerical results are reported in Section V and Section VI concludes the paper.

II. Model Formulation

We develop a two-stage stochastic program for energy and reserve dispatch with fuel constraints for the GFPPs, which aims to ensure the safe operation of a power system with a high penetration of renewables [8] and a strong interdependence with the natural gas system [28]. Specifically, we consider a combined power system with B buses, L transmission lines, W wind farms, G power plants, D demand centers and P gas pipelines connected to GFPPs. Each transmission line connects a pair of buses, while each wind farm, power plant and demand center is attached to exactly one bus. Each GFPP is served by exactly one gas pipeline. Adopting a DC power flow approximation [29], we denote by $Q^{\mathrm{w}} \in \mathbb{R}^{L\times W}$, $Q^{\mathrm{g}} \in \mathbb{R}^{L\times G}$ and $Q^{\mathrm{d}} \in \mathbb{R}^{L\times D}$ the matrices of power transfer distribution factors. Thus, Q^{w}_{lw} and Q^{g}_{lg} denote the change in the power flow on line l per unit of power generated by wind farm w and power plant g, respectively. Similarly, Q^{d}_{ld} quantifies the change in the power flow on line l per unit of power extracted at demand center d. We denote by $\Phi \in \mathbb{R}_+^{P\times G}$ the matrix of gas transfer distribution factors. Thus, Φ_{pg} stands for the increase in the gas flow through pipeline p per unit of power produced by the corresponding GFPP connected to pipeline p [28]. All information about the topology and physical properties of the two systems is hidden in the transfer distribution factors.

The power output of the wind farms is modeled as $C(\mu+\xi)$, where $C \in \mathbb{R}_+^{W\times W}$ is the diagonal matrix of the wind farm capacities, $\mu \in \mathbb{R}^W$, $0 \leqslant \mu \leqslant e$, is the relative power output predicted at the day-ahead stage, and $\xi \in \mathbb{R}^W$, $-\mu \leqslant \xi \leqslant e-\mu$, is the uncertain deviation from μ, which is revealed in real-time operation. Note that e is a vector of ones with appropriate dimensions. We assume that ξ follows a distribution $\mathbb{P}$ concentrated around 0. Without much loss of generality, we assume that the power consumption $d \in \mathbb{R}_+^D$ at the demand centers is known. The operating decisions for the GFPPs are taken in two stages. At the day-ahead stage, the dispatch $y_0 \in \mathbb{R}_+^G$ as well as the upward and downward reserve capacities $r_+, r_- \in \mathbb{R}_+^G$ are chosen for each power plant. Upon observation of ξ in real-time operation, the real-time adjustments $y_1(\xi) \in \mathbb{R}^G$ to the power production are chosen with the aim to ensure—with high probability—the integrity of the transmission system while respecting the generator capacities. This energy and reserve dispatch problem gives rise to the following two-stage stochastic program.

$$\min_{y_0, y_1(\cdot), r_+, r_-} \quad c^\top y_0 + c_+^\top r_+ + c_-^\top r_- + \mathbb{E}^{\mathbb{P}}[c^\top y_1(\xi)] \tag{1a}$$

$$\text{s.t.} \quad 0 \leqslant r_+ \leqslant \overline{r}, \quad 0 \leqslant r_- \leqslant \overline{r} \tag{1b}$$

$$\underline{y} \leqslant y_0 - r_-, \quad y_0 + r_+ \leqslant \overline{y} \tag{1c}$$

$$e^\top C\,(\mu+\xi) + e^\top\,(y_0 + y_1(\xi)) = e^\top d \quad \mathbb{P}\text{-a.s.} \tag{1d}$$

$$\mathbb{P}[-r_- \leqslant y_1(\xi) \leqslant r_+] \geqslant 1-\epsilon^{\mathrm{gen}} \tag{1e}$$

$$\mathbb{P}[-\overline{f} \leqslant Q^{\mathrm{g}}(y_0 + y_1(\xi)) + Q^{\mathrm{w}}C(\mu+\xi) - Q^{\mathrm{d}}d \leqslant \overline{f}] \geqslant 1-\epsilon^{\mathrm{grid}} \tag{1f}$$

$$\mathbb{P}[0 \leqslant \Phi(y_0 + y_1(\xi)) \leqslant \overline{q}] \geqslant 1-\epsilon^{\mathrm{gas}} \tag{1g}$$

The objective function (1a) reflects the expected operating costs, where $c \in \mathbb{R}^G$ captures the variable costs of the power plants, and $c_+, c_- \in \mathbb{R}^G$ represent the costs of reserving capacity to balance the system in real time [8]. The constraints (1b) limit the (positive and negative) reserve capacity procurements up to the prescribed maximum $\overline{r} \in \mathbb{R}_+^G$, while (1c) ensures that the day-ahead energy and reserve dispatch obey the production limits $\underline{y}, \overline{y} \in \mathbb{R}_+^G$ of the GFPPs. The almost sure constraint (1d) requires that total production matches total demand with probability 1, while the chance constraints (1e)-(1g) ensure that the real-time adjustments to the power output obey the chosen reserve capacities, the power flows respect the capacity limits $\overline{f} \in \mathbb{R}_+^L$ of the transmission lines, and the power outputs of the GFPPs are limited by the maximum delivery rates $\overline{q} \in \mathbb{R}_+^P$ of the natural gas pipelines, respectively. The

prescribed violation probabilities $\epsilon^{\text{gen}}, \epsilon^{\text{grid}}, \epsilon^{\text{gas}} \in (0,1)$ reflect the risk attitude of the decision maker.

The stochastic program (1) is intractable because it constitutes an infinite-dimensional optimization problem. To mitigate its complexity, it has been proposed to approximate the functional recourse decisions $y_1(\xi)$ by linear decision rules of the form $y_1(\xi) = Y\xi$ for some finite-dimensional coefficient matrix $Y \in R^{G\times W}$ [10, § 14]. In the context of chance constrained optimal power flow problems, linear decision rules have been used in [18] and [19]. The stochastic program (1) can thus be approximated by the linear decision rule problem

$$\begin{aligned}
\min_{y_0,Y,r_+,r_-} \quad & c^\top y_0 + c_+^\top r_+ + c_-^\top r_- + \mathbb{E}^{\mathbb{P}}[c^\top Y\xi] && \text{(2a)}\\
\text{s.t.} \quad & \text{Constraints (1b)–(1c)}\\
& e^\top y_0 + e^\top C\mu = e^\top d, \quad e^\top Y + e^\top C = 0 && \text{(2d)}\\
& \mathbb{P}[-r_- \leqslant Y\xi \leqslant r_+] \geqslant 1-\epsilon^{\text{gen}} && \text{(2e)}\\
& \mathbb{P}[-\overline{f} \leqslant (Q^{\text{g}}y_0 + Q^{\text{w}}C\mu - Q^{\text{d}}d)+\\
& \qquad + (Q^{\text{g}}Y + Q^{\text{w}}C)\xi \leqslant \overline{f}] \geqslant 1-\epsilon^{\text{grid}} && \text{(2f)}\\
& \mathbb{P}[0 \leqslant \Phi(y_0 + Y\xi) \leqslant \overline{q}] \geqslant 1-\epsilon^{\text{gas}}, && \text{(2g)}
\end{aligned}$$

where (2d) is obtained by matching the zero- and first-order coefficients of ξ on both sides of (1d), which is allowed because the support of ξ spans $\mathbb{R}^W$ [30, § 2.2]. For ease of exposition, we denote by $x \triangleq (y_0, r_+, r_-) \in \mathbb{R}_+^{3G}$ the collection of all first-stage decisions and by $c_x \triangleq (c, c_+, c_-) \in \mathbb{R}_+^{3G}$ the corresponding aggregate cost vector. Using this notation, problem (2) can be represented more compactly as

$$\begin{aligned}
\min_{(x,Y)\in\Theta} \quad & c_x^\top x + \mathbb{E}^{\mathbb{P}}[c^\top Y\xi] && \text{(3a)}\\
\text{s.t.} \quad & \mathbb{P}\left[A^j(Y)\xi \leqslant b^j(x)\right] \geqslant 1-\epsilon^j \quad \forall j \in \mathcal{J}, && \text{(3b)}
\end{aligned}$$

where Θ stands for the set of all $(x, Y) \in \mathbb{R}_+^{3G} \times R^{G\times W}$ satisfying (1b), (1c) and (2d). The joint chance constraint (3b) is indexed by $j \in \mathcal{J} \triangleq \{\text{gen}, \text{grid}, \text{gas}\}$ and thus encodes the capacity constraints (2e) through

$$A^{\text{gen}}(Y) = \begin{bmatrix} Y \\ -Y \end{bmatrix}, \quad b^{\text{gen}}(x) = \begin{bmatrix} r_+ \\ -r_- \end{bmatrix},$$

the line capacity constraints (2f) through

$$\begin{aligned}
A^{\text{grid}}(Y) &= \begin{bmatrix} Q^{\text{g}}Y + Q^{\text{w}}C \\ -Q^{\text{g}}Y - Q^{\text{w}}C \end{bmatrix},\\
b^{\text{grid}}(x) &= \begin{bmatrix} \overline{f} - Q^{\text{w}}C\mu + Q^{\text{d}}d - Q^{\text{g}}y_0 \\ \overline{f} + Q^{\text{w}}C\mu - Q^{\text{d}}d + Q^{\text{g}}y_0 \end{bmatrix},
\end{aligned}$$

and the pipeline capacity constraints (2g) through

$$A^{\text{gas}}(Y) = \begin{bmatrix} \Phi Y \\ -\Phi Y \end{bmatrix}, \quad b^{\text{gas}}(x) = \begin{bmatrix} \overline{q} - \Phi y_0 \\ \Phi y_0 \end{bmatrix}.$$

In spite of the decision rule approximation, problem (3) remains intractable. In fact, only checking feasibility of the chance constraint (3b) is already #P-hard even if ξ follows a uniform distribution on a box [31]. Moreover, the distribution $\mathbb{P}$, which is needed to evaluate both the expectation in (3a) and the probabilities in (3b), is not even observable in practice but must be inferred from data. Unfortunately, the available data is often scarce, and the procurement of additional samples is either infeasible or expensive. Indeed, any wind power time series is invariably restricted to the service life of the corresponding wind farm. However, if problem (3) is fitted to a small training dataset, and the resulting optimal decisions are evaluated on a (different) test dataset, then the test performance is often disappointing, even if the training and test datasets are governed by the same (unknown) distribution $\mathbb{P}$ [14].

III. Data-driven Distributionally Robust Optimization

Assume now that the decision maker is ignorant of $\mathbb{P}$ but has access to finitely many training samples $\widehat{\xi}_i$, $i \leqslant N$, drawn independently from $\mathbb{P}$ (a wind power time series). As $\mathbb{P}$ is unknown, a fundamental input of problem (3) is thus lacking. A naïve remedy would be to replace the unknown $\mathbb{P}$ with the discrete empirical distribution $\widehat{\mathbb{P}}_N$, that is, the uniform distribution on the (known) training samples. This amounts to solving the sample average approximation of problem (3), which is prone to yield biased decisions that perform poorly in out-of-sample tests for small sample sizes N. Hence, it makes sense to reformulate (3) as a distributionally robust optimization problem that hedges against all distributions in a neighborhood of $\widehat{\mathbb{P}}_N$ with respect to the Wasserstein metric.

Definition 1 (Wasserstein metric)**.** *The type-1 Wasserstein distance between two distributions $\mathbb{P}_1$ and $\mathbb{P}_2$ on $\mathbb{R}^W$ is defined as*

$$\mathbb{W}(\mathbb{P}_1,\mathbb{P}_2) \triangleq \left\{ \begin{array}{ll} \min\limits_{\Pi} & \int_{\mathbb{R}^W\times\mathbb{R}^W} \|\xi_1 - \xi_2\|\, \Pi(\mathrm{d}\,\xi_1, \mathrm{d}\,\xi_2) \\ \text{s.t.} & \Pi \textit{ is a distribution on } \mathbb{R}^W \times \mathbb{R}^W \\ & \textit{with marginals } \mathbb{P}_1 \textit{ and } \mathbb{P}_2\textit{, respectively.} \end{array} \right.$$

The Wasserstein distance between $\mathbb{P}_1$ and $\mathbb{P}_2$ can be viewed as the cost of an optimal mass transportation plan Π that minimizes the cost of moving $\mathbb{P}_1$ to $\mathbb{P}_2$, where $\|\xi_1 - \xi_2\|$ is the cost of moving a unit mass from ξ_1 to ξ_2. In the following we denote by $\mathcal{M}(\Xi)$ the set of all distributions on the polyhedron $\Xi = \{\xi \in \mathbb{R}^W : H\xi \leqslant h\}$, where $H = [I\ -I]^\top$ and $h = [(e-\mu)^\top\ \mu^\top]^\top$, and we define the ambiguity set

$$\mathcal{P} \triangleq \left\{\mathbb{P} \in \mathcal{M}(\Xi) : \mathbb{W}(\mathbb{P}, \widehat{\mathbb{P}}_N) \leqslant \rho\right\}$$

as the family of all distributions on Ξ that have a Wasserstein distance of at most $\rho \geqslant 0$ from the empirical distribution $\widehat{\mathbb{P}}_N$. The hope is that, for a judiciously chosen radius ρ, the ambiguity set $\mathcal{P}$ contains the unknown true distribution with high confidence. Following [14], we can then recast (3) as a distributionally robust optimization problem of the form

$$\begin{aligned}
\min_{(x,Y)\in\Theta} \quad & c_x^\top x + \max_{\mathbb{P}\in\mathcal{P}} \mathbb{E}^{\mathbb{P}}[c^\top Y\xi] && \text{(4a)}\\
\text{s.t.} \quad & \min_{\mathbb{P}\in\mathcal{P}} \ \mathbb{P}\left[A^j(Y)\xi \leqslant b^j(x)\right] \geqslant 1-\epsilon^j \quad \forall j \in \mathcal{J}, && \text{(4b)}
\end{aligned}$$

which minimizes the worst-case expected operating costs and requires that the joint chance constraints are satisfied for all distributions in the ambiguity set $\mathcal{P}$. If the true distribution belongs to $\mathcal{P}$, then the optimal value of (4) overestimates the true expected cost of the optimal decisions. Moreover, the optimal decisions satisfy the true chance constraints. Modelling the ambiguity set as a Wasserstein ball in the space of distributions has several benefits that may appeal to decision makers, i.e.,

it provides rigorous finite-sample and asymptotic consistency guarantees and offers computational tractability [14, § 2].

It is known that the empirical distribution $\widehat{\mathbb{P}}_N$ converges in Wasserstein metric (and thus also weakly) to the unknown true distribution as N tends to infinity. One can thus show that for any given significance level $\beta \in (0,1)$ there is a sequence $\rho_N(\beta) \geqslant 0$, $N \in \mathbb{N}$, that converges to 0 such that the Wasserstein ball of radius $\rho_N(\beta)$ around $\widehat{\mathbb{P}}_N$ contains the unknown true distribution with confidence $1-\beta$ for every N [14, Theorem 3.4]. In practice, the best Wasserstein radius for a given sample size is determined in a data-driven manner, e.g., via cross validation; see Section V. Moreover, the distributionally robust chance constrained program (4) admits several tractable conservative approximations.

IV. Tractable Approximations

The distributionally robust chance constrained program (4) is still hard. Indeed, for $\rho = 0$ it reduces to a classical chance constrained program under the discrete empirical distribution. Such problems are known to be NP-hard even in the simplest settings [32, Theorem 1]. Leveraging results from [14], we now derive tractable conservative approximations for (4). In Section IV-A we first discuss an exact reformulation for the objective function (4a). In Sections IV-B and IV-C we then provide two conservative approximations for the feasible set

$$\Omega_{\mathrm{CC}} \triangleq \left\{ (x,Y) : \min_{\mathbb{P}\in\mathcal{P}} \mathbb{P}\left[A(Y)\xi \leqslant b(x)\right] \geqslant 1-\epsilon \right\}$$

of a generic joint chance constraint of the form (4b), where the superscript j is omitted to avoid clutter. In Section IV-D we finally assess the computational tractability of the two approaches. All proofs are relegated to the e-companion [33].

A. Reformulation of the Objective Function

Evaluating the objective function (4a) for a fixed $Y \in \mathbb{R}^{G\times W}$ necessitates the solution of a worst-case expectation problem of a linear function in ξ over the Wasserstein ball $\mathcal{P}$. By [14, Corollary 5.1] this problem is equivalent to the conic program

$$\begin{aligned}
&\max_{\mathbb{P}\in\mathcal{P}} \mathbb{E}^{\mathbb{P}}[c^\top Y \xi] \\
&= \left\{ \begin{array}{lll}
\min\limits_{\lambda^o, s^o, \gamma^o} & \lambda^o \rho + \frac{1}{N}\sum_{i=1}^N s_i^o & \\
\text{s.t.} & c^\top Y \widehat{\xi}_i + \gamma_i^{o\top}(h - H\widehat{\xi}_i) \leqslant s_i^o & \forall i \leqslant N \\
& \|H^\top \gamma_i^o - Y^\top c\|_* \leqslant \lambda^o & \forall i \leqslant N \\
& \gamma_i^o \in \mathbb{R}_+^M & \forall i \leqslant N \\
& \lambda^o \in \mathbb{R}_+,\ s^o \in \mathbb{R}^N, &
\end{array} \right.
\end{aligned}$$

where $\|\cdot\|_*$ stands for the dual norm of $\|\cdot\|$.

B. Combined Bonferroni and CVaR Approximation

If the joint chance constraint involves K linear inequalities, we can decompose the matrix $A(Y)$ and the vector $b(x)$ as

$$A(Y) = \begin{bmatrix} a_1(Y)^\top \\ \vdots \\ a_K(Y)^\top \end{bmatrix}, \quad b(x) = \begin{bmatrix} b_1(x) \\ \vdots \\ b_K(x) \end{bmatrix}.$$

The joint chance constraint is thus equivalent to

$$\min_{\mathbb{P}\in\mathcal{P}} \mathbb{P}\left[a_k(Y)^\top \xi \leqslant b_k(x)\ \forall k \leqslant K\right] \geqslant 1-\epsilon. \tag{5}$$

Given a set of individual violation tolerances $\epsilon_k \geqslant 0$, $k \leqslant K$, with $\sum_{k=1}^K \epsilon_k = \epsilon$, one can exploit Bonferroni's inequality to split the original joint chance constraint up into a family of K simpler but more conservative individual chance constraints. This amounts to approximating the feasible set Ω_{CC} by

$$\Omega_{\mathrm{B}} \triangleq \left\{ (x,Y) : \min_{\mathbb{P}\in\mathcal{P}} \mathbb{P}\left[a_k(Y)^\top \xi \leqslant b_k(x)\right] \geqslant 1-\epsilon_k, \forall k \leqslant K \right\}.$$

Bonferroni's inequality implies that $\Omega_{\mathrm{B}} \subseteq \Omega_{\mathrm{CC}}$, see [11, § 6.1]. Optimizing over Ω_{B} remains hard even for $\rho = 0$, which prompts us to approximate the individual worst-case chance constraints by worst-case Conditional Value-at-Risk (CVaR) constraints [34]. Thus, Ω_{B} is conservatively approximated by

$$\begin{aligned}
\Omega_{\mathrm{BC}} \triangleq \Big\{ (x,Y) :\ & \\
& \max_{\mathbb{P}\in\mathcal{P}} \mathbb{P}\text{-}\operatorname{CVaR}_{\epsilon_k}\left[a_k(Y)^\top \xi - b_k(x)\right] \leqslant 0\ \forall k \leqslant K \Big\}.
\end{aligned}$$

One can show that Ω_{BC} constitutes the best convex inner approximation of Ω_{B} in a sense made precise in [27], and thus $\Omega_{\mathrm{BC}} \subseteq \Omega_{\mathrm{B}}$. Moreover, we have $\Omega_{\mathrm{BC}} = \Omega_{\mathrm{B}}$ if $\epsilon_k \leqslant N^{-1}$ for all $k \leqslant K$ [24, Corollary 2]. The following proposition further guarantees that optimizing over Ω_{BC} is easy.

Proposition 1. *The set Ω_{BC} admits the conic reformulation*

$$\Omega_{\mathrm{BC}} = \left\{ \begin{array}{ll}
(x,Y) \in \mathbb{R}^{3G} \times \mathbb{R}^{G\times W} : & \\
\lambda_k \rho + N^{-1}\sum_{i=1}^N s_{ik} \leqslant 0 & \forall k \leqslant K \\
\tau_k \leqslant s_{ik} & \forall i \leqslant N, k \leqslant K \\
a_k(Y)^\top \widehat{\xi}_i - b_k(x) + (\epsilon_k - 1)\tau_k & \\
\qquad + \epsilon_k \gamma_{ik}^\top (h - H\widehat{\xi}_i) \leqslant \epsilon_k s_{ik} & \forall i \leqslant N, k \leqslant K \\
\|\epsilon_k H^\top \gamma_{ik} - a_k(Y)\|_* \leqslant \epsilon_k \lambda_k & \forall i \leqslant N, k \leqslant K \\
\gamma_{ik} \in \mathbb{R}_+^{2W} & \forall i \leqslant N, k \leqslant K \\
\tau \in \mathbb{R}^K,\ \lambda \in \mathbb{R}^K,\ s \in \mathbb{R}^{N\times K} &
\end{array} \right\}.$$

C. Optimized CVaR Approximation

The Bonferroni approximation is inadequate when the sets of violating wind power scenarios for different individual chance constraints in Ω_{B} have significant overlap [35]. In this case, one may convert the original (linear) joint chance constraint to an equivalent (nonlinear) individual chance constraint before deploying the CVaR approximation [21], [35]. To do so, denote by $\Delta_{++} \triangleq \{\delta \in \mathbb{R}_{++}^K : e^\top \delta = 1\}$ the relative interior of the probability simplex, and note that (5) is equivalent to

$$\min_{\mathbb{P}\in\mathcal{P}} \mathbb{P}\left[\max_{k\leqslant K}\left\{\delta_k\left[a_k(Y)^\top \xi - b_k(x)\right]\right\} \leqslant 0\right] \geqslant 1-\epsilon \tag{6}$$

for any fixed $\delta \in \Delta_{++}$. Note that the overall scale of δ is immaterial, and thus the normalization $e^\top\delta = 1$ does not restrict generality. Note also that (6) constitutes a distributionally robust individual chance constraint, which is immediately susceptible to the CVaR approximation. To see this, denote by

$$\mathcal{J}_\delta(x,Y) \triangleq \max_{\mathbb{P}\in\mathcal{P}} \mathbb{P}\text{-}\operatorname{CVaR}_\epsilon\left[\max_{k\leqslant K}\left\{\delta_k\left[a_k(Y)^\top \xi - b_k(x)\right]\right\}\right]$$

the worst-case CVaR function, and define

$$\Omega_{\mathrm{C}}(\delta) \triangleq \left\{(x,Y) : \mathcal{J}_\delta(x,Y) \leqslant 0\right\}.$$

As in Section IV-B, one can show that $\Omega_{\mathrm{C}}(\delta) \subseteq \Omega_{\mathrm{CC}}$ for every $\delta \in \Delta_{++}$ [27]. We emphasize that $\Omega_{\mathrm{C}}(\delta)$ depends nontrivially

on δ even though the worst-case probability on the left hand side of (6) is manifestly constant in δ. Hence, δ constitutes a vector of scaling parameters that can be tuned to optimize the quality of the CVaR approximation. The following proposition further guarantees that $\mathcal{J}_\delta(x,Y)$ can be evaluated efficiently, which implies that optimizing over $\Omega_{\rm C}(\delta)$ is easy.

Proposition 2. *For any fixed $(x,Y) \in \mathbb{R}^{3G} \times \mathbb{R}^{G\times W}$ and $\delta \in \Delta_{++}$, the worst-case CVaR $\mathcal{J}_\delta(x,Y)$ coincides with the optimal value of the conic program*

$$\begin{array}{ll} \min & \lambda\rho + \frac{1}{N}\sum_{i=1}^N s_i \\ \text{s.t.} & \tau \in \mathbb{R},\ \lambda \in \mathbb{R},\ s \in \mathbb{R}^N,\ \gamma_{ik} \in \mathbb{R}^{2W}_+ \quad \forall i \leqslant N, k \leqslant K \\ & \tau \leqslant s_i \qquad\qquad \forall i \leqslant N \\ & \delta_k\left[a_k(Y)^\top \widehat{\xi}_i - b_k(x)\right] + (\epsilon-1)\tau \\ & \qquad +\epsilon\gamma_{ik}^\top(h - H\widehat{\xi}_i) \leqslant \epsilon s_i \qquad \forall i \leqslant N, k \leqslant K \\ & \|\epsilon H^\top \gamma_{ik} - \delta_k a_k(Y)\|_* \leqslant \epsilon\lambda \qquad \forall i \leqslant N, k \leqslant K. \end{array}$$

Returning to problem (7), we denote the number of inequalities in the j-th chance constraint by K^j and define Δ^j_{++} as the relative interior of the K^j-dimensional probability simplex. Moreover, for any $\delta^j \in \Delta^j_{++}$, we denote by $\mathcal{J}^j_{\delta^j}(x,Y)$ the worst-case CVaR function corresponding to the j-th chance constraint, $j \in \mathcal{J}$. The previous discussion implies that

$$\min_{(x,Y)\in\Theta} c_x^\top x + \max_{\mathbb{P}\in\mathcal{P}} \mathbb{E}^{\mathbb{P}}[c^\top Y\xi] \tag{7a}$$

$$\text{s.t. } \mathcal{J}^j_{\delta^j}(x,Y) \leqslant 0 \quad \forall j \in \mathcal{J} \tag{7b}$$

constitutes a tractable conic program and provides an upper bound on (7) for every *fixed* set of scaling parameters. In principle, the *best* upper bound can be found by minimizing (7) over all $\delta^j \in \Delta^j_{++}$, $j \in \mathcal{J}$. We emphasize that this best upper bound generally exceeds the optimal value of (7); see [24, § 3]. Moreover, unfortunately, the variant of problem (7) that treats the δ^j as additional decision variables is nonconvex, thus resisting efficient solution. This motivates us to devise an iterative algorithm that optimizes sequentially over (x,Y) and δ^j, $j \in \mathcal{J}$, which is inspired by [21]. In the following we denote by $\eta > 0$ the minimum relative improvement per iteration and by $\bar{t} \in \mathbb{N}$ the maximum iteration count.

0) **Initialization.** Set $g^0 \leftarrow +\infty$, $t \leftarrow 1$, $\delta^j_t \leftarrow e/K^j\ \forall j \in \mathcal{J}$.
1) **Step 1.** Find a solution (x_t, Y_t, v_t) of

$$g_t = \left\{ \begin{array}{ll} \min\limits_{(x,Y)\in\Theta, v\geqslant 0} & c_x^\top x + \max\limits_{\mathbb{P}\in\mathcal{P}} \mathbb{E}^{\mathbb{P}}[c^\top Y\xi] + Me^\top v \\ \text{s.t.} & \mathcal{J}^j_{\delta^j_t}(x,Y) \leqslant v^j \quad \forall j \in \mathcal{J}, \end{array} \right.$$

which is a tractable conic program thanks to the results of Sections IV-A and IV-C. If $|(g_t - g_{t-1})/g_t| < \eta$ or $t \geqslant \bar{t}$, then stop and report (x_t, Y_t, v_t), else go to Step 2.
2) **Step 2.** Find a solution δ_{t+1} of

$$\min_\delta \left\{ \sum_j \mathcal{J}^j_{\delta^j}(x_t, Y_t) : \delta^j \in \Delta^j_{++}\ \forall j \in \mathcal{J} \right\},$$

which is a tractable conic program by virtue of Proposition 2. Set $t \leftarrow t+1$, and return to Step 1.

The sequence $\{g_t\}_{t\in\mathbb{N}}$ of objective values generated by the algorithm is non-increasing and thus guaranteed to converge.

The auxiliary slack variables $v \geqslant 0$ in the optimization problem of Step 1 are penalized with a big-M constant in the objective. They ensure feasibility in case of poor initialization of the scaling parameters. If M is chosen sufficiently large, then the algorithm is guaranteed to terminate with $v = 0$ and thus outputs a decision (x_t, Y_t) that is feasible in (7).

D. Discussion

The results of this section give rise to two tractable conservative approximations for the chance constrained program (4). Under the joint Bonferroni and CVaR approximation, the worst-case expectation in the objective function (4a) is replaced by the conic program derived in Section IV-A, while each joint chance constraint is conservatively approximated by its corresponding Bonferroni feasible set $\Omega_{\rm BC}$, which admits a conic representation by virtue of Proposition 1. This results in a single tractable conic program that can be solved efficiently with off-the-shelf software. Under the optimized CVaR approximation, on the other hand, a feasible (and hopefully near-optimal) solution to (4) is found by the efficient sequential convex optimization algorithm from Section IV-C. We emphasize that all conic programs underlying the two approaches reduce to simple linear programs if the Wasserstein metric is defined in terms of the 1-norm or the ∞-norm.

The sequential convex optimization algorithm underlying the optimized CVaR approximation enjoys several benefits. First, it bypasses the necessity to solve a nonconvex optimization problem with bilinear terms, which emerge in the exact reformulations of joint chance constraints derived in [14, § 5.1]. Moreover, in contrast to the approaches proposed in [18], [24], it remains applicable even when there are $K > 2$ inequalities in the chance constraint and when these inequalities involve products of decision variables and uncertain parameters.

In retrospect, we conclude that the optimized CVaR approximation from Section IV-C is superior to the joint Bonferroni and CVaR approximation from Section IV-B because the feasible set $\Omega_{\rm C}(\delta)$ involves fewer constraints and auxiliary variables than $\Omega_{\rm BC}$. Indeed, $\Omega_{\rm BC}$ introduces $2K + (N \times K) + (N \times K \times 2W)$ auxiliary variables and $K + 4(N \times K)$ constraints, while $\Omega_{\rm C}(\delta)$ creates only $2 + N + (N \times K \times 2W)$ auxiliary variables and $1 + N + 3(N \times K)$ constraints. The relative advantage of $\Omega_{\rm C}(\delta)$ over $\Omega_{\rm BC}$ in terms of complexity of representation becomes increasingly significant for higher dimensions N, K and W. We emphasize that the parsimonious representation of $\Omega_{\rm C}(\delta)$ comes at the expense of solving a sequence of conic programs. However, as we will demonstrate through numerical experiments in Section V, the sequential convex optimization algorithm usually terminates after only a few iterations and outputs superior decisions.

We highlight that the choice of the individual violation tolerances ϵ_k critically affects the performance of the joint Bonferroni and CVaR approximation. Unfortunately, however, finding the optimal values of ϵ_k is hard [27, Remark 2.1], and optimizing separately over the ϵ_k and the decision variables as in the algorithm of Section IV-C is also impractical because of bilinear terms. In the numerical experiments we thus set $\epsilon_k = \epsilon/K$ for all $k \leqslant K$ as recommended in [27] even though this choice is known to be conservative when ϵ is

small or when the inequalities in the joint chance constraint are positively correlated [21, Example 3.1].

V. Numerical Results

We assess the quality of the two approximations described in Section IV on an extended variant of the IEEE 24-bus Reliability Test System [36]. The original system accommodates 24 buses, 34 transmission lines, 12 generators (6 of which are GFPPs) and 17 demand centers. For further details see [36]. We augment this system with 6 wind farms connected to buses 1, 2, 11, 12, 12 and 16, respectively, all of which have a capacity of 250 MW. We also add 3 gas pipelines that serve a pair of GFPPs each. The pipelines serving the pairs $\{1,2\}$, $\{3,4\}$ and $\{5,6\}$ have capacity 10,000 kcf, 5,500 kcf and 7,000 kcf, respectively. Under this parameterization, the total installed wind capacity adds up to 55% of the system demand. We assume that each generator uses at most 40% of its capacity for reserve provision (i.e., $\overline{r} = 0.4\overline{y}$) at a cost equal to 20% of the variable production cost (i.e., $c_+ = c_- = 0.2c$).

All simulations are based on the Wasserstein metric induced by the 1-norm on $\mathbb{R}^W$, and thus all arising optimization problems are equivalent to tractable linear programs. Throughout the experiments, we set $H = 0$ and $h = 0$, which amounts to approximating Ξ by $\mathbb{R}^W$. We have observed that this approximation greatly accelerates the computations but has no significant impact on the results for the Wasserstein radii of interest. Finally, we set ϵ^j to the same $\epsilon \in (0,1)$ for all $j \in \mathcal{J}$.

Recall that the distribution $\mathbb{P}$ of the uncertain deviation ξ from the relative wind power output forecast μ is only indirectly observable through independent and identically distributed (i.i.d.) samples from $\mathbb{P}$. In our experiments we construct μ and synthetic samples from $\mathbb{P}$ as in [37] using relative wind power output data for 6 wind farms in southeastern Australia from 2012 to 2013. We first pass the raw (percentage) data through the inverse logistic function to obtain real-valued data and compute the corresponding sample mean and sample covariance matrix. We then construct i.i.d. samples from $\mathbb{P}$ by applying the componentwise logistic function to random samples from the normal distribution with the estimated mean and covariance matrix.

The complete input data of all numerical experiments is provided in the e-companion [33]. All simulations are run on a 4 core 3.4 GHz desktop computer running Windows 8. All optimization problems are implemented in MATLAB using the YALMIP interface [38] and solved via Gurobi 7.5.

A. Operation without Reoptimization

In the first experiment we assess the candidate solutions of (4) obtained with the methods from Section IV, assuming that the system operator implements the linear decision rules without reoptimizing. From raw data $\widehat{\psi}_i, i = 1,\ldots,N+10^2$, we use the training sample $\widehat{\psi}_i, i = 1,\ldots,N$ to estimate the mean μ. The data $\widehat{\xi}_i, i = 1,\ldots,N+10^2$ is the deviation from μ. To this end, we generate N training samples $\widehat{\xi}_i$, $i \leqslant N$, and 10^2 test samples $\widehat{\xi}_{N+i}$, $i \leqslant 10^2$.

Using the training data, we then solve (4) both with the combined Bonferroni and CVaR approximation as well as the optimized CVaR approximation for $\epsilon = 5\%$ and for different

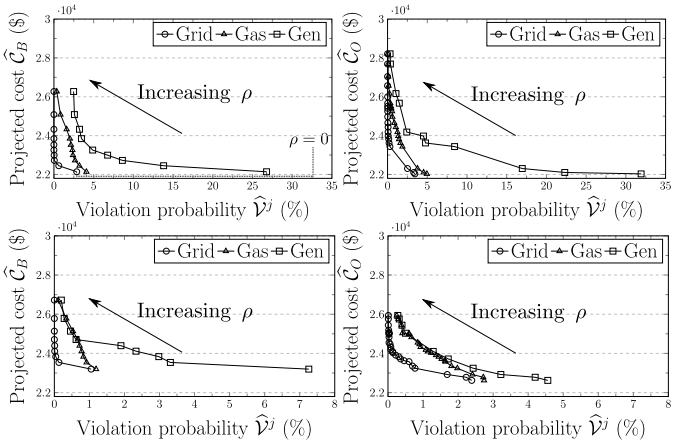

Fig. 1. Pareto frontiers of the out-of-sample costs versus the out-of-sample violation probabilities for the joint Bonferroni and CVaR (left) and optimized CVaR (right) approximations with $N = 50$ (top) and $N = 200$ (bottom).

Wasserstein radii $\rho \in \mathbb{R}_+$. The quality of an optimal solution $\widehat{x}(\rho)$ and $\widehat{Y}(\rho)$ (which constitutes an implicit function of the training samples) is assessed by its empirical out-of-sample cost

$$\widehat{\mathcal{C}}(\rho) = c_x^\top \widehat{x}(\rho) + \tfrac{1}{10^2} \textstyle\sum_{i=N+1}^{N+10^2} c^\top \widehat{Y}(\rho)\widehat{\xi}_i$$

and its empirical out-of-sample violation probabilities

$$\widehat{\mathcal{V}}^j(\rho) = \tfrac{1}{10^2} \textstyle\sum_{i=N+1}^{N+10^2} \mathbb{I}_{A(\widehat{Y}(\rho))\widehat{\xi}_i > b(\widehat{x}(\rho))}, \quad j \in \mathcal{J}.$$

Finally, all results are averaged across 100 independent simulation runs in order increase their statistical robustness.

Figure 1 visualizes the trade-off between the out-of-sample costs and violation probabilities under the two approximations. Note that with increasing Wasserstein radius ρ the costs increase, while all three violation probabilities decrease. This is expected as larger Wasserstein radii result in more conservative solutions that dispatch more expensive generators. The curves in Figure 1 can thus be interpreted as Pareto frontiers. Note that for sufficiently large values of ρ, both approximations can guarantee that all chance constraints are satisfied out of sample (i.e., the empirical violation probabilities are smaller than $\epsilon = 5\%$). We also observe that, as N increases, the violation probabilities for fixed ρ tend to decrease. Finally, for the majority of all Wasserstein radii that result in sufficiently small out-of-sample violation probabilities $\leqslant 5\%$, the optimized CVaR approximation generates lower out-of-sample costs than the combined Bonferroni and CVaR approximation.

B. Operation with Reoptimization

In the second experiment we assess the candidate solutions $(\widehat{x}, \widehat{Y})$ of (4) under the premise that only the first-stage decision $\widehat{x} = (\widehat{y}_0, \widehat{r}_+, \widehat{r}_-)$ is implemented and that the real-time adjustments $y_1(\xi), l(\xi), w(\xi), r(\xi)$ are determined by solving the deterministic optimal power flow problem

$$\begin{array}{ll} \min\limits_{y_1,l,w,r} & c^\top y_1 + c_l e^\top l + c_w e^\top w + c_r e^\top r \\ \text{s.t.} & 0 \leqslant \widehat{y}_0 + y_1 \leqslant \overline{y}, \;\; -(\widehat{r}_- + r) \leqslant y_1 \leqslant \widehat{r}_+ \\ & e^\top y_1 + e^\top (C\xi - w) + e^\top l = 0 \\ & -\overline{f} \leqslant Q^{\mathrm{g}}(\widehat{y}_0 + y_1) \\ & \qquad + Q^{\mathrm{w}}(C\mu + C\xi - w) - Q^{\mathrm{d}}(d - l) \leqslant \overline{f} \\ & 0 \leqslant \Phi(\widehat{y}_0 + y_1) \leqslant \overline{q} \\ & 0 \leqslant l \leqslant d, \quad 0 \leqslant w \leqslant C(\mu + \xi), \quad 0 \leqslant r, \end{array} \tag{8}$$

which optimizes over the power adjustments $y_1 \in \mathbb{R}^G$, the reserve-increase $r \in \mathbb{R}^G_+$, the load shedding quantities $l \in \mathbb{R}^D_+$ at the different demand centers and and the wind spills $w \in \mathbb{R}^W_+$ at the different wind farms. The constraints in the last line of (8) prevent the load shedding and wind spilling quantities from exceeding the actual demands and wind power output realizations, respectively. All other constraints have natural counterparts in (1), and thus their meaning is evident. Note that in contrast to the day-ahead scheduling problem (1), the real-time optimal power flow problem (8) enforces the capacity constraints for the reserves, the transmission lines and the gas pipelines deterministically. Note also that $\widehat{x}$ is a fixed parameter in (8). The real-time power adjustment incurs the same cost as the variable cost of the power plants, while we penalize reserve-increase, load shedding and wind spilling by $c_r > c_l > c_w \geqslant 0$ to preserve their order of activation.

In the above real-time dispatch problem, the joint chance constraints are replaced by hard constraints, and there will be no out-of-sample violation. Empirically, all out-of-sample $r(\xi)$ are zeros, thus the analysis will focus on the empirical cost calculated using the optimal solutions $(y_1(\xi), l(\xi), w(\xi))$ of the real-time dispatch problem by

$$\widehat{\mathcal{R}} = c_x^\top \widehat{x} + \frac{1}{10^2} \sum_{i=N+1}^{N+10^2} c^\top y_1(\widehat{\xi}_i) + c_l e^\top l(\widehat{\xi}_i) + c_w e^\top w(\widehat{\xi}_i),$$

and the results are also averaged over 100 runs. The same process is applied for all possible values of ρ.

For the optimized CVaR approach, Fig. 2 illustrates $\widehat{\mathcal{R}}_{\mathrm{O}}(\rho)$ as a function of ρ for $\epsilon = 5\%$ and different values of N. We observe that at each level of the sample size N, there exists an optimal radius $\widehat{\rho}^\star$ which minimizes the realistic expected cost $\widehat{\mathcal{R}}_{\mathrm{O}}$. Solving the problem with radius $\widehat{\rho}^\star$ leads to a lower empirical average cost compared to the ambiguity-free approach with the radius $\rho = 0$ and this reduction in the expected cost is more substantial under lower sample size N. For example, at $N = 25$, $\widehat{\mathcal{R}}_{\mathrm{O}}(\widehat{\rho}^\star)$ is 7.9% lower than the ambiguity-free cost $\widehat{\mathcal{R}}_{\mathrm{O}}(0)$, and this reduction is 1.9% when $N = 200$. A similar pattern appears in the plot of the interquantile range (IQR) between the 10^{th}- and 90^{th}-quantile of $\widehat{\mathcal{R}}^i_{\mathrm{O}}(\rho)$ in Fig. 3, as well as in the similar plots for the Bonferroni and CVaR approach included in the e-companion [33]. These results show the advantages of employing the distributionally robust optimization approach: in all cases, solving problem (4) with $\rho > 0$ reduces both the empirical average and the variability of the out-of-sample cost in the realistic operation settings. The advantages of distributionally robust optimization are more convincing in the low sample size settings.

Table I presents the optimal radius $\widehat{\rho}^\star$ and the corresponding $\widehat{\mathcal{R}}^\star$ for various ϵ and different number of samples N for both approaches. The cost for the Bonferroni and CVaR approach $\widehat{\mathcal{R}}^\star_{\mathrm{B}}$ is reported as the percentage difference from $\widehat{\mathcal{R}}^\star_{\mathrm{O}}$. In all cases $\widehat{\mathcal{R}}^\star_{\mathrm{O}}$ is lower than $\widehat{\mathcal{R}}^\star_{\mathrm{B}}$, while the greatest difference takes place at $\epsilon = 1\%$. Moreover, we notice that for a fixed ϵ, as the number of samples N increase, the optimal expected cost $\widehat{\mathcal{R}}^\star$ and radius $\widehat{\rho}^\star$ decrease. More specifically, radius $\widehat{\rho}^\star$ tends to zero with an increase in N, which is coherent with the observations in [14, Section 7]. Additionally,

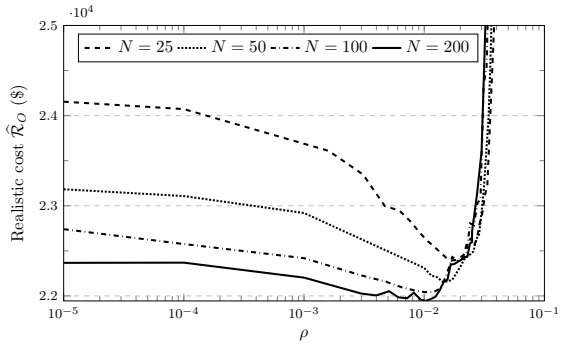

Fig. 2. Average realistic cost $\widehat{\mathcal{R}}_{\mathrm{O}}$ as a function of the Wasserstein radius ρ.

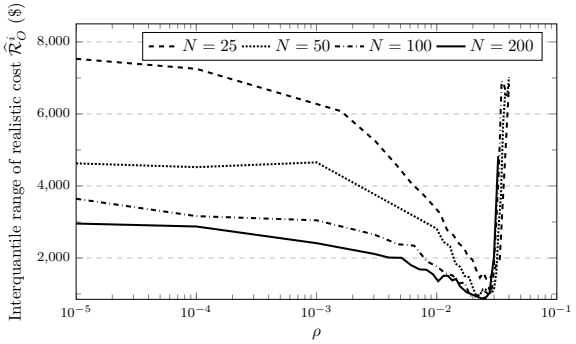

Fig. 3. Interquantile range (between 10^{th} and 90^{th} quantile) of realistic cost as a function of the Wasserstein radius ρ.

for a fixed number of samples N, decreasing ϵ returns a lower optimal radius $\widehat{\rho}^\star$ as the feasible space of probability constraints becomes more stringent. On the upside, decreasing ϵ also decreases $\widehat{\mathcal{R}}^\star_{\mathrm{O}}$ since less costly real-time adjustments are activated due to increased robustness.

A robust optimization model (presented in the e-companion [33]), which minimizes the worst-case cost and risk constraints are satisfied for any realization of uncertain parameter in the support Ξ, is solved and the results are given in Table II for different number of samples N. In all cases, the robust approach yields a significantly higher realistic cost $\widehat{\mathcal{R}}_{RO}$ with respect to the distributionally robust and ambiguity-free approaches, demonstrating the fact that the acquired first-stage decisions $\widehat{x}^i$ are overly conservative. The robust solution varies with N as we estimate mean μ from the training sample.

Computational performance is reported for the setting with $\epsilon = 5\%$ and $N = 200$. Solving program (4) under the Bonferroni and CVaR approximation takes on average 20 seconds, while for the optimized CVaR approximation the average solution time until convergence is 38 seconds. In practice, we consistently observe convergence of the sequential algorithm for optimized CVaR approximation in less than 3 iterations. The average time to solve the robust optimization model and the optimal power flow is 0.75 sec and 0.12 sec, respectively.

VI. Conclusion

In this paper, we proposed a purely data-driven approach to study distributionally robust joint chance constraints based on the Wasserstein metric. Our approach results in a convex conservative approximation of distributionally robust joint chance constraints, where the true data generating distribution is not assumed to be a member of a parametric family and the ambiguity set is nonparametric. We showed that the

TABLE I
OPTIMAL REALISTIC COST $\widehat{\mathcal{R}}^\star$ (\$) AND WASSERSTEIN RADIUS $\widehat{\rho}^\star$ FOR BONFERRONI AND CVaR AND OPTIMIZED CVaR APPROXIMATIONS.

	$N=25$				$N=50$			
ϵ	$\widehat{\mathcal{R}}^\star_{\mathrm{O}}$ (\$)	$\widehat{\rho}^\star_{\mathrm{O}}$	$\widehat{\mathcal{R}}^\star_{\mathrm{B}}$	$\widehat{\rho}^\star_{\mathrm{B}}$	$\widehat{\mathcal{R}}^\star_{\mathrm{O}}$ (\$)	$\widehat{\rho}^\star_{\mathrm{O}}$	$\widehat{\mathcal{R}}^\star_{\mathrm{B}}$	$\widehat{\rho}^\star_{\mathrm{B}}$
1%	22,269	0.0030	+4.00%	0.0001	22,105	0.0026	+1.71%	0.0001
5%	22,392	0.0168	+1.43%	0.0008	22,154	0.0143	+1.49%	0.0005
10%	22,414	0.0400	+1.31%	0.0018	22,275	0.0300	+0.94%	0.0009
	$N=100$				$N=200$			
ϵ	$\widehat{\mathcal{R}}^\star_{\mathrm{O}}$ (\$)	$\widehat{\rho}^\star_{\mathrm{O}}$	$\widehat{\mathcal{R}}^\star_{\mathrm{B}}$	$\widehat{\rho}^\star_{\mathrm{B}}$	$\widehat{\mathcal{R}}^\star_{\mathrm{O}}$ (\$)	$\widehat{\rho}^\star_{\mathrm{O}}$	$\widehat{\mathcal{R}}^\star_{\mathrm{B}}$	$\widehat{\rho}^\star_{\mathrm{B}}$
1%	22,032	0.0008	+0.53%	0	21,932	0.0005	+0.89%	0
5%	22,039	0.0118	+0.50%	0	21,944	0.0103	+0.48%	0
10%	22,135	0.0250	+0.35%	0.0003	22,042	0.0230	+0.80%	0

TABLE II
REALISTIC COST $\widehat{\mathcal{R}}_{RO}$ AND IQR OF REALISTIC COST $\widehat{\mathcal{R}}^i_{RO}$ BETWEEN 10^{TH} AND 90^{TH} QUANTILE FOR ROBUST OPTIMIZATION IN (\$).

	$N=25$	$N=50$	$N=100$	$N=200$
$\widehat{\mathcal{R}}_{RO}$	29,690	29,644	29,673	29,687
IQR $\widehat{\mathcal{R}}^i_{RO}$	1,466	1,246	895	687

approximation is tractable and the optimal solution can be obtained by solving a sequence of conic programming problems. We solved the two-stage problem of energy and reserve dispatch with fuel constraints for GFPPs and demonstrated that the proposed model has superior performance compared to the widely used in the literature Bonferroni and CVaR approximation. A systematic approach to estimate the optimal Wasserstein radius from data is presented. From our numerical study, we note that following a distributionally robust attitude is of great significance when few samples are available, while less robustness is needed as more information for the true data generating distribution becomes available. A future consideration would be to apply decomposition techniques to solve very large instances of such problems.

REFERENCES

[1] L. Söder *et al.*, "Experience and challenges with short-term balancing in European systems with large share of wind power," *IEEE Trans. Sustain. Energy*, vol. 3, no. 4, pp. 853–861, 2012.

[2] U.S. Energy Information Administration, "International energy outlook 2016," Tech. Rep., 2016.

[3] D. Bertsimas, E. Litvinov, X. A. Sun, J. Zhao, and T. Zheng, "Adaptive robust optimization for the security constrained unit commitment problem," *IEEE Trans. Power Syst.*, vol. 28, no. 1, pp. 52–63, 2013.

[4] M. Zugno and A. J. Conejo, "A robust optimization approach to energy and reserve dispatch in electricity markets," *Eur. J. Oper. Res.*, vol. 247, no. 2, pp. 659–671, 2015.

[5] D. Bienstock, M. Chertkov, and S. Harnett, "Chance-constrained optimal power flow: Risk-aware network control under uncertainty," *SIAM Rev.*, vol. 56, no. 3, pp. 461–495, 2014.

[6] M. Lubin, Y. Dvorkin, and S. Backhaus, "A robust approach to chance constrained optimal power flow with renewable generation," *IEEE Trans. Power Syst.*, vol. 31, no. 5, pp. 3840–3849, 2016.

[7] L. Roald, F. Oldewurtel, T. Krause, and G. Andersson, "Analytical reformulation of security constrained optimal power flow with probabilistic constraints," in *2013 IEEE PowerTech Conference*, June 2013, pp. 1–6.

[8] J. M. Morales, A. J. Conejo, K. Liu, and J. Zhong, "Pricing electricity in pools with wind producers," *IEEE Trans. Power Syst.*, vol. 27, no. 3, pp. 1366–1376, 2012.

[9] A. Papavasiliou, S. S. Oren, and R. P. O'Neill, "Reserve requirements for wind power integration: A scenario-based stochastic programming framework," *IEEE Trans. Power Syst.*, vol. 26, no. 4, pp. 2197–2206, 2011.

[10] A. Ben-Tal, L. El Ghaoui, and A. Nemirovski, *Robust Optimization*. Princeton University Press, 2009.

[11] A. Prékopa, *Stochastic Programming*. Springer, 1995.

[12] G. Calafiore and M. Campi, "The scenario approach to robust control design," *IEEE Trans. Automat. Contr.*, vol. 51, no. 5, pp. 742–753, 2006.

[13] E. Delage and Y. Ye, "Distributionally robust optimization under moment uncertainty with application to data-driven problems," *Oper. Res.*, vol. 58, no. 3, pp. 595–612, 2010.

[14] P. Mohajerin Esfahani and D. Kuhn, "Data-driven distributionally robust optimization using the Wasserstein metric: performance guarantees and tractable reformulations," *Math. Program.*, vol. 171, no. 1, pp. 115–166, 2018.

[15] F. Alismail, P. Xiong, and C. Singh, "Optimal wind farm allocation in multi-area power systems using distributionally robust optimization approach," *IEEE Trans. Power Syst.*, vol. 33, no. 1, pp. 536–544, 2018.

[16] W. Wei, J. Wang, and S. Mei, "Dispatchability maximization for co-optimized energy and reserve dispatch with explicit reliability guarantee," *IEEE Trans. Power Syst.*, vol. 31, no. 4, pp. 3276–3288, 2016.

[17] P. Xiong, P. Jirutitijaroen, and C. Singh, "A distributionally robust optimization model for unit commitment considering uncertain wind power generation," *IEEE Trans. Power Syst.*, vol. 32, no. 1, pp. 39–49, 2017.

[18] W. Xie and S. Ahmed, "Distributionally robust chance constrained optimal power flow with renewables: A conic reformulation," *IEEE Trans. Power Syst.*, vol. 33, no. 2, pp. 1860–1867, 2018.

[19] Y. Zhang, S. Shen, and J. L. Mathieu, "Distributionally robust chance-constrained optimal power flow with uncertain renewables and uncertain reserves provided by loads," *IEEE Trans. Power Syst.*, vol. 32, no. 2, pp. 1378–1388, 2017.

[20] K. Baker, E. Dall'Anese, and T. Summers, "Distribution-agnostic stochastic optimal power flow for distribution grids," in *2016 North Am. Power Symp. (NAPS)*, 2016, pp. 1–6.

[21] S. Zymler, D. Kuhn, and B. Rustem, "Distributionally robust joint chance constraints with second-order moment information," *Math. Program.*, vol. 137, no. 1-2, pp. 167–198, 2013.

[22] G. A. Hanasusanto, V. Roitch, D. Kuhn, and W. Wiesemann, "Ambiguous joint chance constraints under mean and dispersion information," *Oper. Res.*, vol. 65, no. 3, pp. 751–767, 2017.

[23] C. Duan, W. Fang, L. Jiang, L. Yao, and J. Liu, "Distributionally robust chance-constrained approximate AC-OPF with Wasserstein metric," *IEEE Trans. Power Syst.*, vol. 33, no. 5, pp. 4924–4936, 2018.

[24] Z. Chen, D. Kuhn, and W. Wiesemann, "Data-driven chance constrained programs over Wasserstein balls," *Optimization Online*, 2018.

[25] W. Xie, "On distributionally robust chance constrained program with Wasserstein distance," *Optimization Online*, 2018.

[26] R. Ji and M. Lejeune, "Data-driven distributionally robust chance-constrained optimization with Wasserstein metric," *Optimization Online*, 2018.

[27] A. Nemirovski and A. Shapiro, "Convex approximations of chance constrained programs," *SIAM J. Optim.*, vol. 17, no. 4, pp. 969–996, 2007.

[28] B. Zhao, A. J. Conejo, and R. Sioshansi, "Unit commitment under gas-supply uncertainty and gas-price variability," *IEEE Trans. Power Syst.*, vol. 32, no. 3, pp. 2394–2405, 2016.

[29] R. D. Christie, B. F. Wollenberg, and I. Wangensteen, "Transmission management in the deregulated environment," *Proc. of the IEEE*, vol. 88, no. 2, pp. 170–195, 2000.

[30] D. Kuhn, W. Wiesemann, and A. Georghiou, "Primal and dual linear decision rules in stochastic and robust optimization," *Math. Program.*, vol. 130, no. 1, pp. 177–209, 2011.

[31] M. Dyer and A. Frieze, "On the complexity of computing the volume of a polyhedron," *SIAM J. Comput.*, vol. 17, no. 5, pp. 967–974, 1988.

[32] J. Luedtke, S. Ahmed, and G. L. Nemhauser, "An integer programming approach for linear programs with probabilistic constraints," *Math. Program.*, vol. 122, no. 2, pp. 247–272, 2010.

[33] C. Ordoudis, V. A. Nguyen, D. Kuhn, and P. Pinson, "Electronic companion - Energy and reserves dispatch with distributionally robust joint chance constraints," https://doi.org/10.5281/zenodo.1237026, 2018, online; Accessed: 29.04.2018.

[34] R. T. Rockafellar and S. Uryasev, "Optimization of conditional value-at-risk," *J. Risk*, vol. 2, no. 3, pp. 21–41, 2000.

[35] W. Chen, M. Sim, J. Sun, and C.-P. Teo, "From CVaR to uncertainty set: Implications in joint chance-constrained optimization," *Oper. Res.*, vol. 58, no. 2, pp. 470–485, 2010.

[36] C. Grigg *et al.*, "The IEEE reliability test system-1996. A report prepared by the reliability test system task force of the application of probability methods subcommittee," *IEEE Trans. Power Syst.*, vol. 14, no. 3, pp. 1010–1020, 1999.

[37] J. Dowell and P. Pinson, "Very-short-term probabilistic wind power forecasts by sparse vector autoregression," *IEEE Trans. Smart Grid*, vol. 7, no. 2, pp. 763–770, 2016.

[38] J. Löfberg, "YALMIP : A toolbox for modeling and optimization in MATLAB," in *2004 IEEE Int. Conf. Robot. Autom.*, 2004, pp. 284–289.

EC - Energy and Reserve Dispatch with Distributionally Robust Joint Chance Constraints

Christos Ordoudis, Viet Anh Nguyen, Daniel Kuhn, Pierre Pinson*

This document serves as an electronic companion (EC) for the paper "Energy and Reserve Dispatch with Distributionally Robust Joint Chance Constraints". It contains seven sections that provide proofs of the prepositions in the original manuscript, a nomenclature, the robust optimization formulation, data for the IEEE 24-bus RTS, the procedure to generate the wind power data, parameters related to the simulations for the numerical results and additional results.

1. Proofs of Proposition 1 and Proposition 2

Proof of Proposition 1. Using standard duality techniques, each worst-case CVaR in

$$\Omega_{\text{BC}} \triangleq \left\{(x,Y) : \max_{\mathbb{P}\in\mathcal{P}} \mathbb{P}\text{-}\,\text{CVaR}_{\epsilon_k}\big[a_k(Y)^\top\xi - b_k(x)\big] \leq 0 \;\; \forall k \leq K\right\}$$

can be rewritten as

$$\begin{aligned}
\max_{\mathbb{P}\in\mathcal{P}} \mathbb{P}\text{-}\,\text{CVaR}_{\epsilon_k}\left[a_k(Y)^\top\xi - b_k(x)\right] &= \max_{\mathbb{P}\in\mathcal{P}}\min_{\tau\in\mathbb{R}}\left\{\tau + \frac{1}{\epsilon_k}\mathbb{E}^{\mathbb{P}}\left[\left(a_k(Y)^\top\xi - b_k(x) - \tau\right)^+\right]\right\} && \text{(1a)}\\
&= \max_{\mathbb{P}\in\mathcal{P}}\min_{\tau\in\mathbb{R}}\left\{\mathbb{E}^{\mathbb{P}}\left[\max\left\{\tau, \frac{1}{\epsilon_k}\left(a_k(Y)^\top\xi - b_k(x)\right) + \left(1-\frac{1}{\epsilon_k}\right)\tau\right\}\right]\right\} && \text{(1b)}\\
&\leq \min_{\tau\in\mathbb{R}}\left\{\max_{\mathbb{P}\in\mathcal{P}}\mathbb{E}^{\mathbb{P}}\left[\max\left\{\tau, \frac{1}{\epsilon_k}\left(a_k(Y)^\top\xi - b_k(x)\right) + \left(1-\frac{1}{\epsilon_k}\right)\tau\right\}\right]\right\}, && \text{(1c)}
\end{aligned}$$

where in (1a) we use the definition of CVaR in [1, Theorem 1], and the inequality in (1c) comes from weak duality. Notice that the objective function of (1b) is convex in τ and linear in $\mathbb{P}$. Furthermore, by the result of [2, Theorem 7.12, part (ii)], one can show that the ambiguity set $\mathcal{P}$ is weakly compact. As a result, [3, Theorem 4.2] implies that sup-inf equals min-max, and (1c) holds with equality. Because the expression inside the expectation is a pointwise maximum of two affine functions in terms of ξ, [4, Corollary 5.1, part (i)] applies and the worst-case expectation over the probability measure $\mathbb{P}$ in (1c) admits a reformulation in the dual form, and we can rewrite each worst-case CVaR value as

$$\max_{\mathbb{P}\in\mathcal{P}} \mathbb{P}\text{-}\,\text{CVaR}_{\epsilon_k}\left[a_k(Y)^\top\xi - b_k(x)\right] = \left\{\begin{array}{lll}
\min\limits_{\tau_k,\lambda_k,s_k,\gamma_k} & \lambda_k\rho + N^{-1}\sum_{i=1}^N s_{ik} & \\
\text{s.t.} & \tau_k \leq s_{ik} & \forall i \leq N\\
& a_k(Y)^\top\widehat{\xi}_i - b_k(x) + (\epsilon_k - 1)\tau_k & \\
& \quad + \epsilon_k\gamma_{ik}^\top(h - H\widehat{\xi}_i) \leq \epsilon_k s_{ik} & \forall i \leq N\\
& \|\epsilon_k H^\top\gamma_{ik} - a_k(Y)\|_* \leq \epsilon_k\lambda_k & \forall i \leq N\\
& \gamma_{ik} \in \mathbb{R}^{2W}_+ & \forall i \leq N\\
& \tau \in \mathbb{R}^K,\ \lambda \in \mathbb{R}^K,\ s \in \mathbb{R}^{N\times K} &
\end{array}\right. \qquad (2)$$

and Ω_{BC} can be reformulated as the intersection of K feasible sets by substituting the value of (2) into (1). This completes the proof. □

*The list of authors may be subject to changes.

Proof of Proposition 2. For an individual chance constraint from the feasible set

$$\Omega_{\mathrm{C}}(\delta) \triangleq \left\{(x,Y) : \max_{\mathbb{P}\in\mathcal{P}} \mathbb{P}\text{-}\,\mathrm{CVaR}_{\epsilon}\left[\max_{k\leq K}\left\{\delta_k\left[a_k(Y)^{\top}\xi - b_k(x)\right]\right\}\right] \leq 0\right\}.$$

the worst case CVaR can be expressed based on definition in [1, Theorem 1] as

$$\max_{\mathbb{P}\in\mathcal{P}} \mathbb{P}\text{-}\,\mathrm{CVaR}_{\epsilon}\left[\max_{k\leq K}\left\{\delta_k\left[a_k(Y)^{\top}\xi - b_k(x)\right]\right\}\right] \tag{3a}$$

$$= \max_{\mathbb{P}\in\mathcal{P}} \min_{\tau\in\mathbb{R}}\left\{\tau + \frac{1}{\epsilon}\mathbb{E}^{\mathbb{P}}\left[\left(\max_{k\leq K}\left\{\delta_k\left[a_k(Y)^{\top}\xi - b_k(x)\right]\right\} - \tau\right)^{+}\right]\right\} \tag{3b}$$

$$= \max_{\mathbb{P}\in\mathcal{P}} \min_{\tau\in\mathbb{R}}\left\{\mathbb{E}^{\mathbb{P}}\left[\max\left\{\tau, \left(\max_{k\leq K}\left\{\frac{\delta_k}{\epsilon_k}\left[a_k(Y)^{\top}\xi - b_k(x)\right]\right\}\right) + \left(1-\frac{1}{\epsilon}\right)\tau\right\}\right]\right\} \tag{3c}$$

$$\leq \min_{\tau\in\mathbb{R}}\left\{\max_{\mathbb{P}\in\mathcal{P}} \mathbb{E}^{\mathbb{P}}\left[\max\left\{\tau, \left(\max_{k\leq K}\left\{\frac{\delta_k}{\epsilon_k}\left[a_k(Y)^{\top}\xi - b_k(x)\right]\right\}\right) + \left(1-\frac{1}{\epsilon}\right)\tau\right\}\right]\right\}. \tag{3d}$$

Using the same reasoning as in the proof of Proposition 1, the inequality in (3d) holds with equality. The expression inside the expectation is the pointwise maximum of $K+1$ affine functions. Thus, we can reformulate the worst-case CVaR based on [4, Corollary 5.1, part (i)] as

$$\max_{\mathbb{P}\in\mathcal{P}} \mathbb{P}\text{-}\,\mathrm{CVaR}_{\epsilon}\left[\max_{k\leq K}\left\{\delta_k\left[a_k(Y)^{\top}\xi - b_k(x)\right]\right\}\right] =$$

$$\begin{cases} \min\limits_{\tau,\lambda,s,\gamma} & \lambda\rho + \frac{1}{N}\sum_{i=1}^{N} s_i & \\ \text{s.t.} & \tau\in\mathbb{R},\ \lambda\in\mathbb{R},\ s\in\mathbb{R}^N,\ \gamma_{ik}\in\mathbb{R}^{2W}_{+} & \forall i\leq N, k\leq K \\ & \tau \leq s_i & \forall i\leq N \\ & \delta_k\left[a_k(Y)^{\top}\widehat{\xi}_i - b_k(x)\right] + (\epsilon-1)\tau & \\ & \quad +\epsilon\gamma_{ik}^{\top}(h - H\widehat{\xi}_i) \leq \epsilon s_i & \forall i\leq N, k\leq K \\ & \|\epsilon H^{\top}\gamma_{ik} - \delta_k a_k(Y)\|_{*} \leq \epsilon\lambda & \forall i\leq N, k\leq K. \end{cases} \tag{4}$$

Replacing (4) into (3) completes the proof. □

2. Nomenclature

In Table 1, we present the main symbols used in the original paper and the description for each one of them.

Table 1. Nomenclature

Symbol	Description
y_0	First-stage power dispatch of conventional power plants
Y	Afine policy to approximate the recourse decisions of conventional power plants
r_-	First-stage downward reserve capacity of conventional power plants
r_+	First-stage upward reserve capacity of conventional power plants
μ	Predicted power production of wind farm
ξ	Random variable with zero mean
C	Diagonal matrix of wind farm capacities
Q	Matrix of power transfer distribution factors
$\overline{r}$	Maximum reserve capacity offered by conventional power plants
$\overline{y}$	Maximum power production of conventional power plants
$\underline{y}$	Minimum power production of conventional power plants
$\overline{\overline{f}}$	Capacity limit of transmission line
$\overline{q}$	Capacity limit of pipeline
Φ	Matrix of gas distribution factors (containing power conversion factor)
d	Electricity demand
c	Variable cost of conventional power plants
c_-	Cost of reserving downward capacity
c_+	Cost of reserving upward capacity
y_1	Power adjustments of conventional power plants in real-time optimal power flow problem
r	Reserve-increase for conventional power plants in real-time optimal power flow problem
l	Load shedding quantities of electricity demand in real-time optimal power flow problem
w	Wind spilling in real-time optimal power flow problem
c_l	Load shedding cost in real-time optimal power flow problem
c_w	Wind spilling cost in real-time optimal power flow problem
c_r	Reserve-increase cost in real-time optimal power flow problem
ϵ	Violation probabilities of joint chance constraints
$\mathbb{P}$	True probability distribution of random variable ξ
$\widehat{\mathbb{P}}_N$	Empirical distribution: uniform distribution on the training samples
Ξ	Support of ξ
N	Number of training samples drawn from $\mathbb{P}$
$\mathcal{P}$	Ambiguity set
ρ	Wasserstein radius
δ	Vector of scaling parameters
η	Minimum relative improvement per iteration in iterative algorithm of Optimized CVaR approximation
v	Auxiliary slack variable in iterative algorithm of Optimized CVaR approximation
M	Big-M constant in iterative algorithm of Optimized CVaR approximation

3. Robust optimization formulation

The robust optimization problem is formulated as follows. Given the raw sample $\widehat{\psi}_i, i = 1, \ldots, N+10^2$, we first estimate the mean using the sample average $\mu = N^{-1}\sum_{i=1}^{N}\widehat{\psi}_i$, and $\widehat{\xi}_i = \widehat{\psi}_i - \mu, i = 1, \ldots, N+10^2$ are the deviation from the estimated mean. In the robust optimization approach, we assume that the uncertain factors ξ varies in the box uncertainty set $\Xi = \{\xi \in \mathbb{R}^W : -\mu \leq \xi \leq e - \mu\}$. The robust program is

$$\begin{aligned} \min_{(x,Y)\in\Theta} \quad & c_x^\top x + c^\top Y\mu \\ \text{s.t.} \quad & A^j(Y)\xi \leq b^j(x) \quad \forall \xi \in \Xi, \forall j \in \{\text{gen}, \text{grid}, \text{gas}\}, \end{aligned}$$

where the worst-case cost is minimized and the constraints are reformulated as robust constraints. The definition of Θ and the mappings $A^j(Y)$ and $b^j(x)$ are analogous to Section II of the main paper. Because the uncertainty set Ξ has 2^W vertices, we replace each robust constraint by 2^W individual constraints for each vertex ξ_v of Ξ, $v = 1, \ldots, 2^W$. The robust problem can be re-expressed as a linear program

$$\begin{aligned} \min_{x,Y,\beta} \quad & c_x^\top x + c^\top Y\mu \\ \text{s.t.} \quad & (x, Y) \in \Theta \\ & A^j(Y)\xi_v \leq b^j(x) \quad \forall v = 1, \ldots, 2^W, \forall j \in \{\text{gen}, \text{grid}, \text{gas}\} \end{aligned}$$

Let $(x^\star, Y^\star, \beta^\star)$ be the optimal solution of the robust program. The out-of-sample performance evaluated on the test sample $\widehat{\xi}_i, i = N+1, \ldots, N+10^2$ is calculated in a similar procedure as in Section V-B of the main paper.

4. Data for the IEEE 24-bus RTS

The 24-bus power system is illustrated in Figure 1. The slack bus of the system is bus 13.

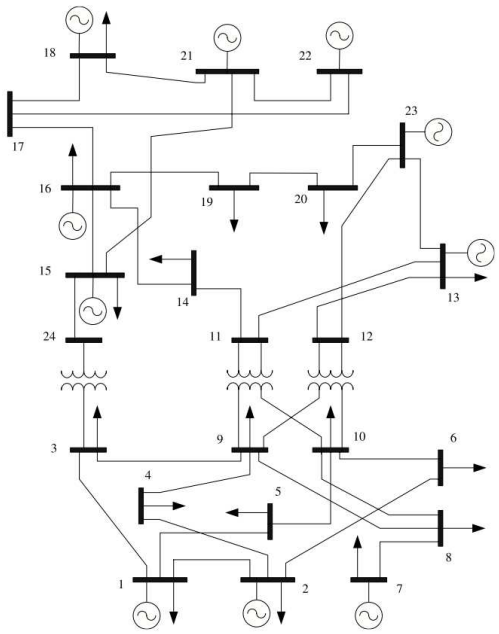

Figure 1. 24-bus power system – Single area RTS-96

Table 2 presents the generating units' data of the power system. The generating units offer a single block of energy, up and down reserve capacity. Table 2 provides the technical data of generating units, the costs, the location on the power system, as well as the conversion factor and the connection with the corresponding pipelines for the gas-fired power plants. There are three pipelines that the gas-fired power plants are connected. Pipeline 1 has a capacity of 10,000 kcf, Pipeline 2 has a capacity of 5,500 kcf and Pipeline 3 has a capacity of 7,000 kcf (kcf: 1,000 cubic feet).

Table 2. Technical Data of Generating Units

Unit #	Bus	$\overline{y}$ (MW)	$\underline{y}$ (MW)	$\overline{r}$ (MW)	c ($/MWh)	c_+ ($/MW)	c_- ($/MW)	Φ (kcf/MWh)	Pipeline
1	1	152	0	60.8	17.5	3.5	3.5	12.65	1
2	2	152	0	60.8	20	4	4	13.45	3
3	7	300	0	120	15	3	3	-	-
4	13	591	0	236.4	27.5	5.5	5.5	-	-
5	15	60	0	24	30	6	6	11.12	2
6	15	155	0	62	22.5	4.5	4.5	-	-
7	16	155	0	62	25	5	5	14.88	1
8	18	400	0	160	5	1	1	-	-
9	21	400	0	160	7.5	1.5	1.5	-	-
10	22	300	0	120	32.5	6.5	6.5	-	-
11	23	310	0	124	10	2	2	16.8	2
12	23	350	0	140	12.5	2.5	2.5	15.6	3

Table 3 presents the bus location of the loads, as well as the load at each bus as a percentage of the total system demand. The total electricity demand is 2,650 MWh and the cost of load shedding is $1,000 /MWh.

TABLE 3. Bus Location and Distribution of the Total System Demand

Load #	\text{Bus}	% of system load	Load #	\text{Bus}	% of system load
1	1	3.8	10	10	6.8
2	2	3.4	11	13	9.3
3	3	6.3	12	14	6.8
4	4	2.6	13	15	11.1
5	5	2.5	14	16	3.5
6	6	4.8	15	18	11.7
7	7	4.4	16	19	6.4
8	8	6	17	20	4.5
9	9	6.1			

The transmission lines data is given in Table 4. The lines are characterized by the bus that are connected, as well as the reactance and the capacity of each line.

TABLE 4. Reactance and Capacity of Transmission Lines

From	To	Reactance (p.u.)	Capacity (MW)	From	To	Reactance (p.u.)	Capacity (MW)
1	2	0.0146	175	11	13	0.0488	500
1	3	0.2253	175	11	14	0.0426	500
1	5	0.0907	400	12	13	0.0488	500
2	4	0.1356	175	12	23	0.0985	500
2	6	0.205	175	13	23	0.0884	500
3	9	0.1271	400	14	16	0.0594	1000
3	24	0.084	200	15	16	0.0172	500
4	9	0.111	175	15	21	0.0249	1000
5	10	0.094	400	15	24	0.0529	500
6	10	0.0642	400	16	17	0.0263	500
7	8	0.0652	600	16	19	0.0234	500
8	9	0.1762	175	17	18	0.0143	500
8	10	0.1762	175	17	22	0.1069	500
9	11	0.084	200	18	21	0.0132	1000
9	12	0.084	200	19	20	0.0203	1000
10	11	0.084	200	20	23	0.0112	1000
10	12	0.084	200	21	22	0.0692	500

There are 6 wind farms of 250 MW with different locations throughout the grid. The wind farms are connected at the 1, 2, 11, 12, 12, 16 bus. The data in Tables 2-4 are based on [5]. We have modified the marginal cost of power production to have different costs for each power plant. The value of power conversion factor and capacity of pipelines are based on the test case used in [6].

5. Wind power data generation for the simulation of numerical results

The data consists of wind power forecast errors that is generated with the same method and the historical data given in [7]. The wind power data are provided by the Australian System Operator [8], which consists of wind power generation recordings from 22 wind farms in the southeastern Australia. The complete dataset can be found in [9]. Data from 2012 and 2013 are normalized by the nominal power of the corresponding wind farm which results in data being in the range of [0,1]. From the csv file that can be found in [9], we have picked the 6 wind farms presented in Table 5.

Table 5. Wind Farm Location and Name tag in csv

WF	Bus	Name tag in csv
1	1	CAPTL_WF
2	2	CATHROCK
3	11	CULLRGWF
4	12	LKBONNY1
5	12	MTMILLAR
6	16	STARHLWF

The wind power data are generated with the following procedure:

(1) The 2 years of data for the 6 wind farms is loaded.
(2) The data range is adjusted to [0.01,0.99] to permit the logit-normal transformation in the next step.
(3) A logit-normal transformation is performed based on [7, Equation (1)].
(4) The mean and covariance are calculated.
(5) We generate the required number of independent and identically distributed random samples by assuming the transformed variable to be normally distributed.
(6) The inverse of logit-normal transformation is applied based on [7, Equation (2)].

We refer the reader to [7] for a detailed presentation of the method and additional insights in very-short-term probabilistic wind power forecasting. Note that the procedure can be found also in the source code provided online.

6. Data for the simulation of numerical results

The positive-valued vector containing the Wasserstein radii for the Combined Bonferroni and CVaR approximation is [0 linspace($10^{-4}, 24 \cdot 10^{-4}, 23$)], while for the Optimized CVaR approximation is given at Table 6.

Table 6. Positive-value Vector containing the Wasserstein radii for Optimized CVaR Approximation

$N = 25$	Vector
$\epsilon = 1\%$	[0 10^{-4} linspace($10^{-3}, 10^{-2}, 23$)]
$\epsilon = 5\%$	[0 linspace($10^{-4}, 3.5 \cdot 10^{-2}, 24$)]
$\epsilon = 10\%$	[0 10^{-4} 10^{-3} 10^{-2} linspace($3.5 \cdot 10^{-2}, 6 \cdot 10^{-2}, 21$)]
$N = 50$	
$\epsilon = 1\%$	[0 10^{-4} linspace($10^{-3}, 6 \cdot 10^{-3}, 23$)]
$\epsilon = 5\%$	[0 10^{-4} 10^{-3} linspace($10^{-2}, 4 \cdot 10^{-2}, 22$)]
$\epsilon = 10\%$	[0 10^{-4} 10^{-3} 10^{-2} $3 \cdot 10^{-2}$ linspace($4 \cdot 10^{-2}, 7 \cdot 10^{-2}, 20$)]
$N = 100$	
$\epsilon = 1\%$	[0 10^{-4} 10^{-3} linspace($3 \cdot 10^{-3}, 4 \cdot 10^{-2}, 22$)]
$\epsilon = 5\%$	[0 10^{-4} 10^{-3} linspace($3 \cdot 10^{-3}, 4 \cdot 10^{-2}, 22$)]
$\epsilon = 10\%$	[0 10^{-4} 10^{-3} $6 \cdot 10^{-3}$ linspace($10^{-2}, 6 \cdot 10^{-2}, 21$)]
$N = 200$	
$\epsilon = 1\%$	[0 10^{-4} 10^{-3} linspace($3 \cdot 10^{-3}, 10^{-2}, 22$)]
$\epsilon = 5\%$	[0 10^{-4} 10^{-3} linspace($3 \cdot 10^{-3}, 2.5 \cdot 10^{-2}, 22$)]
$\epsilon = 10\%$	[0 10^{-4} 10^{-3} linspace($5 \cdot 10^{-3}, 4 \cdot 10^{-2}, 22$)]

Table 7 presents the values of the parameters related to the algorithm utilized in the Optimized CVaR approximation of distributionally robust joint chance constraints.

Table 7. Parameter for the Algorithm in Optimized CVaR Approximation

Parameter	Value
$\overline{t}$	40
η	0.1
$\overline{\delta}$	1000
$\underline{\delta}$	10^{-4}
M	10^6

7. Additional Results

Figs. 2 and 3 illustrate the impact of Wasserstein radius ρ on the expected value and interquantile range between the 10^{th} and 90^{th} quantile of $\widehat{\mathcal{R}}_B^i(\rho)$. For the Combined Bonferroni and CVaR approximation, we have similar observations as the ones for Optimized CVaR approximation presented in the original manuscript.

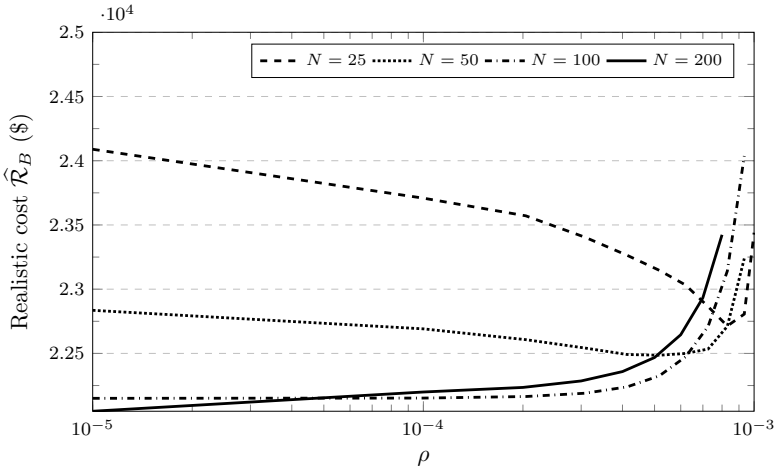

Figure 2. Average realistic cost $\widehat{\mathcal{R}}_B$ as a function of Wasserstein radius ρ.

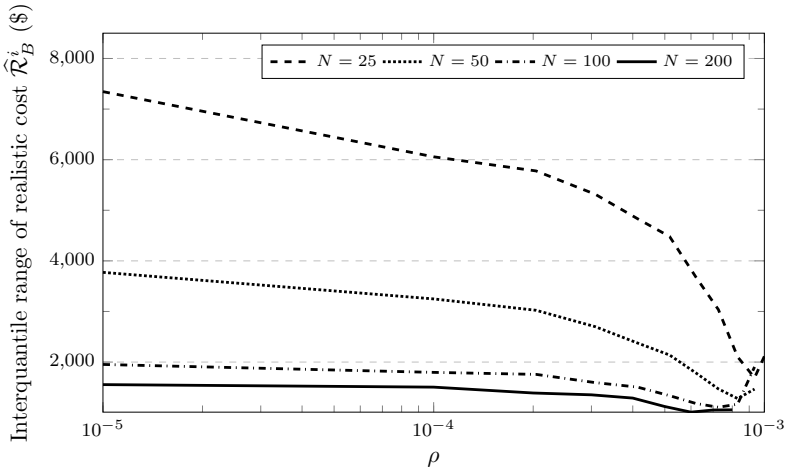

Figure 3. Interquantile range of realistic cost $\widehat{\mathcal{R}}_B^i$ between 10^{th} and 90^{th} quantile as a function of Wasserstein radius ρ.

References

[1] R. T. Rockafellar and S. Uryasev, "Optimization of conditional value-at-risk," *J. Risk*, vol. 2, no. 3, pp. 21–41, 2000.

[2] C. Villani, *Topics in Optimal Transportation*. American Mathematical Society, 2003.

[3] M. Sion, "On general minimax theorems," *Pacific J. Math.*, vol. 8, no. 1, pp. 171–176, 1958.

[4] P. Mohajerin Esfahani and D. Kuhn, "Data-driven distributionally robust optimization using the Wasserstein metric: Performance guarantees and tractable reformulations," *Math. Program.*, Jul 2017.

[5] J. M. Morales, A. J. Conejo, H. Madsen, P. Pinson, and M. Zugno, *Integrating Renewables in Electricity Markets: Operational Problems*. International Series in Operations Research & Management Science, Springer US, 2014.

[6] C. Ordoudis, P. Pinson, and J. M. Morales, "An integrated market for electricity and natural gas systems with stochastic power producers," *Eur. J. Oper. Res.*, 2018.

[7] J. Dowell and P. Pinson, "Very-short-term probabilistic wind power forecasts by sparse vector autoregression," *IEEE Trans. Smart Grid*, vol. 7, no. 2, pp. 763–770, 2016.

[8] Australian Energy Market Operator, "AEMO wind power data." http://www.aemo.com.au/, 2018. Online; Accessed: 06.09.2018.

[9] J. Browell, "AEMO wind power data." http://www.jethrobrowell.com/data-and-code.html, 2018. Online; Accessed: 06.09.2018.

[Paper F] Data-driven Distributed Operation of Electricity and Natural Gas Systems

Authors:
Christos Ordoudis and Viet Anh Nguyen[4]

Published as:
Working paper.

[4]The list of authors may be subject to changes.

Data-driven Distributed Operation of Electricity and Natural Gas Systems

Christos Ordoudis and Viet Anh Nguyen *

Abstract– The simultaneous growth in the installation of renewable energy sources and gas-fired power plants introduces a compelling need to jointly optimize the operation of electricity and natural gas systems under uncertain power supply. However, there exist limitations on the private data that the two system operators are willing to share and this creates challenges in performing a coupled optimization of the electricity and natural gas systems. Moreover, dealing with uncertainty increases the complexity of this problem since efficient and transparent ways would need to be used. Therefore, we propose a distributed algorithm based on the Alternating Direction Method of Multipliers (ADMM) that optimally dispatches electricity and natural gas systems independently, but in a coordinated manner, with the minimum amount of information shared between the two system operators. We utilize a data-driven distributionally robust chance constrained approach, where we optimize over a family of distributions defined by the first and second order moments of the underlying uncertainty that can be estimated from historical data. A second-order cone programming (SOCP) problem reformulation can be developed that guarantees the convergence of the ADMM algorithm and requires only a limited amount of information regarding the underlying distribution to be shared. In the numerical study, we illustrate the performance of the proposed distributed algorithm, which is able to obtain the same solutions as a centralized dispatch of the coupled energy system. We compare the solutions with two benchmark reformulations; one that assumes a normally distributed uncertainty and a deterministic model. That way, we find that the solutions of the proposed model outperform both benchmarks in an out-of-sample

Index terms– ADMM, chance constraints, distributionally robust optimization, distributed operation, electricity and natural gas systems, renewable energy sources.

1. Introduction

Over the last decades, the whole energy system undergoes a transition phase, where the generation mix, the interactions between the various networks and systems' operation are going through unprecedented changes. Two of the main trends in the aforementioned transformation are the transition to a renewable-based power system and the increased interaction between the energy systems. More specifically, natural gas is expected to play an important role in the development of the power system [1], since gas-fired power plants (GFPPs) are the least polluting conventional technology and their high efficiency and flexibility can facilitate the integration of intermittent renewable energy sources, such as wind and solar power. As a consequence, the interaction between the electricity and natural gas systems will be continuously strengthened, as well as the uncertainty and variability of renewables will have an impact on the operation of both energy systems.

Historically, the electricity and natural gas systems have been developed and operated in a decoupled manner, since the interplay between them was fairly limited [2]. The systems have been dispatched individually without taking into account each system's complexities and limitations, which may yield potential challenges nowadays. For instance, fuel supply scarcity from the natural gas network can cause outage of GFPPs that eventually put at risk the security of the power system operation. Moreover, the fuel demand of GFPPs can affect the scheduling of the natural gas system and flows in the pipelines. Therefore, it is essential to set up proper coordination frameworks to ensure the economic and efficient operation of the whole energy system. To accomplish that, the coupled operation of electricity and natural gas systems has been examined in various research studies lately, such as [3, 4, 5, 6, 7, 8]. The power flow problem is solved by taking into account the natural gas flow constraints in [3, 4], while authors in [5, 6] propose the introduction of natural

*The list of authors may be subject to changes.

gas fuel feasibility constraints in the unit commitment problem. The enhanced flexibility and reliability in a coupled operation of the two energy systems is discussed in [7, 8] highlighting the need to incorporate network constraints in the system modeling. In view of high shares of renewables, the effect of uncertain power production to the coupled energy system is examined via a robust optimization framework in [9, 10] and by utilizing stochastic programming in [11, 12, 13].

A common assumption of the aforementioned works is that the electricity and natural gas systems are operated by an integrated utility that is able to control and operate both energy systems with a centralized model. A centralized dispatch model is attractive and can be effectively utilized in practice when the electricity and natural gas systems have the same operator, e.g. Energinet.dk in Denmark [14]. However, the systems are operated by different entities in most of the countries that want to keep their information private, such as network details, system's dispatch and market participants' data, and only share the minimum amount of information needed to guarantee a secure operation of the whole energy system. Along these lines, another issue with regards to the characterization of the uncertainty introduced by renewables and its incorporation in the dispatch models is raised. Following an uncertainty-aware dispatch for the systems would require specific actions by the system operators. More specifically, these actions would include the agreement on the probability distribution of the uncertain parameter, the scenario generation technique and the number of scenarios in the case of stochastic programming, while the uncertainty sets would also need to be defined and agreed in case robust optimization is applied. In this paper, we are interested in answering the following questions. First, how to design a mechanism that allows each operator to dispatch the system independently, while requiring the minimum information sharing? and subsequently: is it possible to attain the solution of a centralized dispatch model with the minimum overall system cost? In terms of dealing with uncertainty, how to develop a model that allows the operators just to share a limited amount of information inferred from historical data?

To address these questions, we develop a *distributed* mechanism in a *data-driven* framework to dispatch electricity and natural gas systems under uncertainty. Regarding the distributed mechanism, various decentralized and distributed approaches have been widely utilized to solve power system operational and market design problems over the years [15, 16, 17, 18, 19] but also to study the coordination between the electricity and natural gas networks lately, as in [20, 21, 22, 23]. More specifically, authors in [20, 21, 22] develop distributed algorithms that solve the electricity and natural gas dispatch problems independently, while in [23] they solve a dispatch problem for a multi-area integrated electricity and natural gas system[1]. Regarding uncertainty modeling, various approaches have been proposed in the literature such as stochastic programming [25, 26, 27, 28], robust optimization [29, 30] and chance constrained programming [31]. In stochastic programming usually a specific distribution is assumed to be followed by the uncertain parameter [32], while robust optimization may yield to overly conservative solutions [33]. Aiming to reduce the conservatiness of solutions, chance constrained programming allows for the violation of uncertain constraints up to a predefined probability. It is common though to assume an underlying distribution for the uncertain parameter in chance constrained programming in order to obtain analytical reformulations, as in [34, 35] that assume Gaussian uncertainty of forecast errors. To overcome these issues, a novel data-driven approach can be adopted, namely distributionally robust optimization. Following this approach, one optimizes over a family of distributions (i.e. ambiguity set) without requiring the exact knowledge of the underlying true distribution. The ambiguity sets are classified based on the approach that is used to characterize the family of distributions. Moment-based ambiguity sets are defined by the distributions that satisfy certain moment constraints [36], while the

[1]The distributed and decentralized algorithms to solve power and natural gas systems' dispatch problems are based on various decomposition coordination algorithms, such as Lagrangian relaxation (LR), alternating direction method of multipliers (ADMM), optimality condition decomposition (OCD), auxiliary problem principle (APP), consensus and innovation (C+I), proximal message passing (PMP) and dual decomposition. Authors in [18] and [24] provide an extensive analysis on the application of such decomposition algorithms to the optimal power flow problems, as well as optimal frequency and voltage control problems, and discuss their key features.

metric-based ones are determined by the distributions that are close to the empirical one with respect to a selected probability metric [37].

In this paper, we propose an algorithm based on ADMM [38] for the distributed operation of electricity and natural gas systems in a distributionally robust framework. Instead of operating the systems in a centralized manner, we introduce a system coordinator that facilitates the communication between the electricity and natural gas system operators. Moreover, we define a moment-based ambiguity set by the mean and covariance matrix that are estimated from the historical data. The proposed setup is illustrated in Figure 1. In contrast to stochastic programming and robust optimization, utilizing a purely data-driven approach with the estimated mean and covariance to be shared between the operators results in a procedure that does not involve any further action like scenario or uncertainty set generation. The mean and covariance can be estimated from the publicly available historical data, which promotes transparency and the operators can be more easily persuaded to treat them as common knowledge. Such assumptions and limitations are also discussed in [26, 28, 30], where information regarding uncertainty characterization has to be shared in the proposed distributed models.

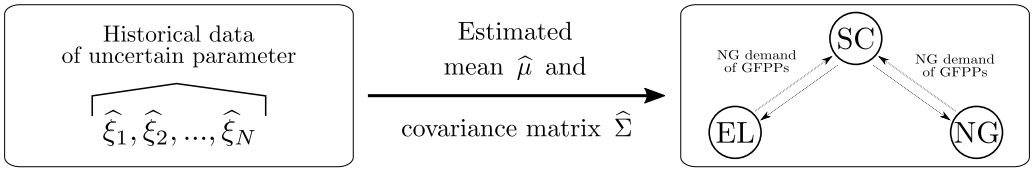

FIGURE 1. Data-driven distributed operation of electricity (EL) and natural gas (NG) systems. SC: system coordinator.

The main contributions of this paper are summarized as follows:

(1) We propose a purely data-driven approach for the dispatch of electricity and natural gas systems that is formulated as a distributionally robust chance constrained (*DRCC*) program where the ambiguity set is defined by the mean and covariance matrix estimated from the historical data. Such an approach results in an analytical reformulation of the problem that is efficiently scalable, since the number of random parameters does not affect the size of the problem as opposed to scenario approaches.
(2) We provide a tractable reformulation of the *DRCC* problem and solve it using ADMM that allows a distributed operation of the electricity and natural gas systems under uncertainty. The two system operators only need to communicate the consumption of GFPPs, while with regards to uncertainty characterization; the estimated mean and covariance are sufficient to describe their ambiguity sets. The proposed algorithm converges efficiently to the same solution of the centralized approach since the reformulation of the original problem results in a convex problem at hand to be solved.
(3) We illustrate the performance of the proposed algorithm in an experimental setup where the electricity and natural gas systems are dispatched centrally, in a distributed manner and with a sequential approach as proposed in [39]. Moreover, we compare the solution of the *DRCC* model with a deterministic approach and an approach where it is assumed that uncertain parameters follow a Gaussian distribution. All the analysis is performed on an out-of-sample basis, meaning that the decisions are tested on unseen realizations of uncertainty. The numerical results show that *DRCC* results in more attractive solutions in terms of violation probability of constraints under various metrics (i.e. empirical violation, maximum average violation and joint violation probability). Finally, a realistic operation that resembles how the system would be dispatched in reality by solving an optimal power and natural gas flow after the realization of uncertainty is introduced, where *DRCC* outperforms the other models in terms of expected cost in a realistic operation.

Compared to [20, 21, 22], the proposed *DRCC* model provides a distributed algorithm to solve the electricity and natural gas systems independently, while incorporating the uncertainty introduced by renewable energy sources. This is considered highly important in view of a tighter coordination between electricity and natural

gas systems where uncertainty and variability impacts the operation of both. Authors in [25, 26, 27, 28, 29, 30, 31], solve power system related problems in a distributed manner under uncertainty by utilizing stochastic programming, robust optimization or chance constraints. On the contrary, we deal with uncertainty in a data-driven framework by utilizing distributionally robust optimization to solve the electricity and natural gas dispatch problem motivated by the foreseen increased availability of data.

The remaining of the paper is organized as follows. Section 2 presents the coupled electricity and natural gas dispatch model in a distributionally robust framework, while the tractable reformulation of the objective function and distributionally robust chance constraints is presented in Section 3. Section 4 presents the reformulation of the problem based on the assumption of Gaussian uncertainty. In Section 5, we provide the distributed algorithm based on ADMM as well as some additional insights. The numerical results are given in Section 6 and Section 7 concludes the paper. Finally, a detailed nomenclature is given in the Appendix A.

Notation: We denote $\mathbb{R}_+$ the non-negative and $\mathbb{R}_{++}$ the positive. Moreover, we use upper case letters for matrices and lower case letters for vectors. Throughout this paper, we use A_i to denote the i-th row vector of matrix $A \in \mathbb{R}^{\mathcal{N}\times\mathcal{K}}$ of arbitrary dimensions. The Frobenius inner product of two matrices $A, B \in \mathbb{R}^{\mathcal{N}\times\mathcal{K}}$ is denoted by $\langle A, B\rangle = \mathrm{Tr}(A^\top B)$. Finally, the Frobenius norm for a real matrix $A \in \mathbb{R}^{\mathcal{N}\times\mathcal{K}}$ is defined as $||A|| = \sqrt{A^\top A}$.

2. Coupled electricity and natural gas model

An integrated setup that optimizes the coupled operation of electricity and natural gas systems under uncertainty is followed in this study. Uncertain power production from Z stochastic producers is modeled by $W(\overline{\mu} + \zeta)$, where $\overline{\mu} \in \mathbb{R}^Z$ is the mean power production and $\zeta \in \mathbb{R}^Z$ a random variable with mean $\mu_0 \in \mathbb{R}^Z$ and covariance matrix $\Sigma_0 \in \mathbb{R}^{Z\times Z}$. The diagonal matrix W contains the installed capacity of stochastic producers. We restrict the recourse actions to linear decision rules[2] and define vector $\xi = [1, \zeta]^\top$ in the following formulation, along the lines with various works in the literature such as [34, 41]. Thus, the power production is formulated as $X\xi$, where $X \in \mathbb{R}^{G\times(Z+1)}$ contains the day-ahead schedule of G conventional power plants in the first column and the real-time adjustments in the remaining columns resulting in a total of $Z + 1$ number of columns. Similarly, the natural gas production from each one of the U producers is described by $Y\xi$ with $Y \in \mathbb{R}^{U\times(Z+1)}$. Note that the day-ahead schedules are the first-stage decisions, while the recourse actions comprise the real-time dispatch of the system to cover the imbalances due to forecast errors. In this work, we assume that the electricity $d \in \mathbb{R}^D$ and natural gas $h \in \mathbb{R}^H$ demands are exactly known[3]. The link between the two systems is defined by GFPPs that consume natural gas in order to produce power. The electricity system is modelled as a network with $\mathcal{E}$ nodes and L transmission lines, while the natural gas network contains M nodes and V pipelines. For the power flow, we use a linearized lossless DC approximation[4] through the utilization of the PTDF matrix $Q \in \mathbb{R}^{L\times\mathcal{E}}$, which defines the power flow as a linear function of nodal injections [43]. More specifically, we define three matrices $Q^{\mathrm{G}} \in \mathbb{R}^{L\times G}$, $Q^{\mathrm{W}} \in \mathbb{R}^{L\times Z}$ and $Q^{\mathrm{D}} \in \mathbb{R}^{L\times D}$ that incorporate already the mapping of conventional power plants, stochastic producers and demands on the network, respectively. For the natural gas flow, we adopt a controllable-flow model[5],

[2]Restricting the functional form of decision rules to be linear yields to an approximation of the original stochastic program; however, it allows for a tractable reformulation of the problem. We refer the interested reader to [40, Section 2.1-2.2] for more information on this topic.

[3]It is possible to introduce uncertain demand profiles by studying a joint probability distribution among the various uncertainties but this refinement is left for future research.

[4]A linearized lossless DC power flow has been widely used in the literature as in [34, 35]. An alternative would be to consider recent advances in the area of convex relaxations for AC power flow (see [42] and references therein), though the tractability of ambiguous chance constraints reformulation would have to be preserved.

[5]A controllable-flow model results in a linear program for the representation of the natural gas system. Including a detailed representation of the natural gas flow dynamics would require the utilization of partial differential equations (PDEs) or under some further assumptions non-linear and non-convex functions such as the Weymouth equation [44]. This would raise significant challenges in the reformulation of distributionally robust chance constraints and is left for future research.

where the nodal gas pressures and linepack are omitted for the sake of computational tractability as in [45]. More specifically, the natural gas flow is fully controllable and is limited by the maximum capacity of each pipeline that can be calculated via an *ex-ante* analysis based on the physical limits of the pressures in the natural gas system. Moreover, the nodal gas balancing is enforced. The *DRCC* coupled dispatch model for electricity and natural gas systems is formulated as

$$\min_{X,Y,C,F} \max_{\mathbb{P}\in\mathcal{P}} \ \mathbb{E}^{\mathbb{P}}[f_x(X,\xi)+f_y(Y,\xi)] \tag{1a}$$

$$\text{s.t.} \ \ \underline{X} \le Xe \le \overline{X} \tag{1b}$$

$$\mathbf{1}^\top Xe + \mathbf{1}^\top W\overline{\mu} = \mathbf{1}^\top d \tag{1c}$$

$$\mathbf{1}^\top XE + \mathbf{1}^\top W = 0 \tag{1d}$$

$$\underline{Y} \le Ye \le \overline{Y} \tag{1e}$$

$$\mathbf{1}^\top Ye = \mathbf{1}^\top Ce + \mathbf{1}^\top h \tag{1f}$$

$$\mathbf{1}^\top YE = \mathbf{1}^\top CE \tag{1g}$$

$$B^{\mathrm{G}}Y + B^{\mathrm{F}}F = B^{\mathrm{D}}h + B^{\mathrm{P}}C \tag{1h}$$

$$\Phi X = C \tag{1i}$$

$$\min_{\mathbb{P}\in\mathcal{P}} \mathbb{P}\left(X_g\xi \le \overline{X}_g\right) \ge 1-\epsilon_g \quad \forall g=1,\dots,G \tag{1j}$$

$$\min_{\mathbb{P}\in\mathcal{P}} \mathbb{P}\left(-X_g\xi \le -\underline{X}_g\right) \ge 1-\epsilon_g \quad \forall g=1,\dots,G \tag{1k}$$

$$\min_{\mathbb{P}\in\mathcal{P}} \mathbb{P}\left(Q_l^{\mathrm{G}}X\xi + (Q_l^{\mathrm{W}}W\overline{\mu} - Q_l^{\mathrm{D}}d) + Q_l^{\mathrm{W}}W\zeta \le \overline{f}_l\right) \ge 1-\epsilon_l \quad \forall l=1,\dots,L \tag{1l}$$

$$\min_{\mathbb{P}\in\mathcal{P}} \mathbb{P}\left(-(Q_l^{\mathrm{G}}X\xi + (Q_l^{\mathrm{W}}W\overline{\mu} - Q_l^{\mathrm{D}}d) + Q_l^{\mathrm{W}}W\zeta) \le \overline{f}_l\right) \ge 1-\epsilon_l \quad \forall l=1,\dots,L \tag{1m}$$

$$\min_{\mathbb{P}\in\mathcal{P}} \mathbb{P}\left(Y_u\xi \le \overline{Y}_u\right) \ge 1-\epsilon_u \quad \forall u=1,\dots,U \tag{1n}$$

$$\min_{\mathbb{P}\in\mathcal{P}} \mathbb{P}\left(-Y_u\xi \le -\underline{Y}_u\right) \ge 1-\epsilon_u \quad \forall u=1,\dots,U \tag{1o}$$

$$\min_{\mathbb{P}\in\mathcal{P}} \mathbb{P}\left(F_v\xi \le \overline{q}_v\right) \ge 1-\epsilon_v \quad \forall v=1,\dots,V \tag{1p}$$

$$\min_{\mathbb{P}\in\mathcal{P}} \mathbb{P}\left(-F_v\xi \le \overline{q}_v\right) \ge 1-\epsilon_v \quad \forall v=1,\dots,V, \tag{1q}$$

where the worst-case expected cost is minimized across all distributions $\mathbb{P}$ in the ambiguity set $\mathcal{P}$ in (1a). We have excluded the cost of GFPPs as this would result in double-counting it. Thus, the cost of GFPPs is calculated from the production cost of natural gas producers instead of incorporating fuel prices for the GFPPs. Inequalities in (1) are formulated as ambiguous individual[6] chance constraints that are defined over ambiguity set $\mathcal{P}$. Therefore, the worst-case probability that each inequality constraint is not violated has to be smaller than $1-\epsilon$. All parameters $\epsilon \in (0,1)$ determine the safety factor for the ambiguous individual chance constraints that is desired. Column vector $e \in \mathbb{R}^{(Z+1)}$ and matrix $E \in \mathbb{R}^{(Z+1)\times Z}$ are utilized to pick the appropriate columns of matrices X and Y in order to define the decisions associated with the day-ahead dispatch and real-time operation. Hence, they have the following form,

$$e = [1;0;\dots;0] \ \text{ and } \ E = \begin{bmatrix} \mathbf{0} \\ I \end{bmatrix}$$

where $\mathbf{0}$ is a zero row vector and $I \in \mathbb{R}^{Z\times Z}$ is the identity matrix. More specifically, constraints (1b) limit the power production at the day-ahead stage between the lower bound $\underline{X} \in \mathbb{R}^G$ and upper bound $\overline{X} \in \mathbb{R}^G$. Enforcing the power balance equality constraint,

$$X\xi + W(\overline{\mu}+\zeta) = d, \ \ \mathbb{P}\text{-a.s.},$$

[6]Utilizing joint chance constraints is possible under specific types of ambiguity sets and type of constraints. In this paper, we focus on individual chance constraints and the interested readers are referred to [46, 47, 48] for additional information on dealing with joint chance constraints.

to hold with probability equal to 1, eventually results in two deterministic constraints by performing the corresponding coefficient matching [40, Section 2.2]. Therefore, the power balance in the nominal case is imposed by (1c), while (1d) ensures that the balancing holds for any realization of the uncertain power production. Similarly, the day-ahead natural gas production is constrained in (1e) for each producer by $\underline{Y} \in \mathbb{R}^U$ and $\overline{Y} \in \mathbb{R}^U$. The natural gas balance in both day-ahead and real-time stages is ensured also with probability equal to 1 by constraints (1f) and (1g), where $C \in \mathbb{R}^{\Gamma \times (Z+1)}$ is the natural gas consumption of GFPPs that constitute a subset of conventional power plants. Equality constraint (1h) ensures the nodal natural gas balancing, where the natural gas flow $F \in \mathbb{R}^{V \times (Z+1)}$ in the pipelines is taken into account. Note that the appropriate mappings in the form of incidence matrices need to be introduced for natural gas producers $B^{\mathrm{G}} \in \mathbb{R}^{M \times U}$, natural gas demands $B^{\mathrm{D}} \in \mathbb{R}^{M \times H}$ and GFPPs $B^{\mathrm{P}} \in \mathbb{R}^{M \times \Gamma}$. The entries of matrix $B^{\mathrm{F}} \in \mathbb{R}^{M \times V}$ are equal to -1 for the pipelines departing from node m and equal to 1 for the pipelines arriving at node m. The coupling constraint (1i) links the natural gas consumption of GFPPs to their power production via the mapping matrix $\Phi \in \mathbb{R}^{\Gamma \times G}$, which contains the power conversion factor of the GFPPs, with a probability equal to 1. Constraints (1j)-(1k) limit the power production in real-time, while the power flow is bounded by the transmission capacity limits $\overline{f} \in \mathbb{R}^L_{++}$ for each transmission line of the power system in (1l)-(1m). The natural gas production in real-time is limited in (1n)-(1o) and the natural gas flow $F \in \mathbb{R}^{V \times (Z+1)}$ needs to satisfy the capacity limits of each pipeline $\overline{q} \in \mathbb{R}^V_{++}$ by (1p)-(1q).

For notational convenience, we provide the following compact form of the optimization problem (1),

$$\min_{X,Y,C,F} \quad \max_{\mathbb{P} \in \mathcal{P}} \quad \mathbb{E}^{\mathbb{P}}[f_x(X,\xi) + f_y(Y,\xi)] \tag{2a}$$

$$\text{s.t.} \quad X \in \mathcal{X} \tag{2b}$$

$$Y, C, F \in \mathcal{Y} \tag{2c}$$

$$\Phi X - C = 0, \tag{2d}$$

where $\mathcal{X}$ captures the feasible set for the electricity system (1b)-(1d) and (1j)-(1m), $\mathcal{Y}$ captures the feasible set of the natural gas system (1e)-(1h) and (1n)-(1q) and (2d) is the coupling constraint.

Following an approach that restricts the recourse actions to linear decision rules, program (1) permits the definition of the integrated energy system's dispatch in view of uncertain power supply. Solving model (1) yields the optimal values of $X^\star$, $Y^\star$, $F^\star$ and $C^\star$ under the specified values of ϵ. Depending on the risk attitude of the decision maker, which is defined by the values of ϵ, a violation of the inequality constraints can be acceptable. In practice, the day-ahead decisions can be defined by model (1) and the real-time production can be decided by solving an economic dispatch model, where the real-time decisions do not need to be linearly dependent on the uncertainty. Therefore, the inclusion of additional variables (i.e. load shedding and wind spilling) is required in this case to guarantee the feasibility of the real-time economic dispatch model.

3. Tractable reformulation of distributionally robust chance constrained program

In this section, we provide a tractable reformulation of *DRCC* problem presented in (1) based on a moment-based ambiguity set. We consider a moment-based ambiguity set that defines the probability distributions taken into account. Having a finite number of samples observed from the true distribution $\mathbb{P}$ at hand, the decision maker collects them in a dataset $\widehat{\mathcal{Z}}_N := \{\widehat{\zeta}_i\}_{i \leq N}$. Thus, we can calculate the empirical mean $\widehat{\mu}_0 = \frac{1}{N}\sum_{i=1}^N \widehat{\zeta}_i$ and covariance matrix $\widehat{\Sigma}_0 = \frac{1}{N}\sum_{i=1}^N (\widehat{\zeta}_i - \widehat{\mu}_0)(\widehat{\zeta}_i - \widehat{\mu}_0)^\top$. The ambiguity set is defined by the first and second order moments [41] as follows

$$\mathcal{P} := \left\{ \mathbb{P} \in \mathcal{M}(\mathbb{R}^Z) : \mathbb{E}[\zeta] = \widehat{\mu}_0, \mathbb{E}[\zeta\zeta^\top] = \widehat{\Sigma}_0 \right\}, \tag{3}$$

where $\mathcal{M}(\mathbb{R}^Z)$ denotes the set of all probability measures on $\mathbb{R}^Z$ and $\widehat{\Sigma}_0$ is a positive semi-definite matrix. Utilizing ambiguity set $\mathcal{P}$, we restrict the true mean and covariance of ζ to be equal to the empirical mean $\widehat{\mu}_0$ and covariance $\widehat{\Sigma}_0$. Uncertainty of the mean and covariance can be included by using the approach proposed in [36]. In our case though we assume that $\widehat{\mu}_0$ and $\widehat{\Sigma}_0$ have been sufficiently approximated from the available

historical data. Conditional mean and covariance estimates can be incorporated in our model if necessary to have more representative estimates (e.g. depending on the hour of the day or season of the year).

3.1. Reformulation of distributionally robust chance constraints

For notational convenience, we use a general form of distributionally robust individual chance constraints to provide the reformulation of (1j)-(1q),

$$\min_{\mathbb{P}\in\mathcal{P}} \mathbb{P}(A_i\xi \leq b_i) \geq 1-\epsilon_i \quad \forall i = 1,\dots,I, \tag{4}$$

where $A \in \mathbb{R}^{\mathcal{N}\times(Z+1)}$ is an arbitrary matrix of proper dimensions. Note that all constraints (1j)-(1q) can be written in the form of (4). Then, we can equivalently reformulate (4) as a second-order cone (SOC) constraint for any $\epsilon \in (0,1)$,

$$\sqrt{\frac{1-\epsilon_i}{\epsilon_i}}\sqrt{A_i\widehat{\Sigma}A_i^\top} \leq (b_i - \widehat{\mu}^\top A_i^\top) \quad \forall i = 1,\dots,I, \tag{5}$$

where

$$\mathbb{E}[\xi] = \widehat{\mu} = \begin{pmatrix} 1 \\ \widehat{\mu}_0 \end{pmatrix}, \quad \mathbb{E}[\xi\xi^\top] = \widehat{\Sigma} = \begin{bmatrix} 1 & \widehat{\mu}_0^\top \\ \widehat{\mu}_0 & \widehat{\Sigma}_0 + \widehat{\mu}_0\widehat{\mu}_0^\top \end{bmatrix} \tag{6}$$

This reformulation is based on [49, Theorem 3.1] for distributionally robust individual chance constraints with given mean and covariance. It can be noticed that taking into account uncertainties leads to tightening each original deterministic constraint $A_i e \leq b_i$ by $\mathcal{T}_i = \sqrt{\frac{1-\epsilon_i}{\epsilon_i}}\sqrt{A_i\widehat{\Sigma}A_i^\top} + \widehat{\mu}_0^\top E^\top A_i^\top$, which increases the system's security by increasing the protection against forecast deviations. We adopt the name of *uncertainty margin*, which is proposed and further discussed in [35, 50], for this reduction.

3.2. Reformulation of objective function

Regarding the objective function in problem (1), we minimize the worst-case expected cost for all distributions in $\mathcal{P}$. The cost functions $f_x(X,\xi)$ and $f_y(Y,\xi)$ are assumed to be quadratic[7] and have the following form,

$$f_x(X,\xi) = (X\xi)^\top \operatorname{diag}(\alpha_x)(X\xi) + \beta_x^\top X\xi + \gamma_x \;\text{ and }\; f_y(Y,\xi) = (Y\xi)^\top \operatorname{diag}(\alpha_y)(Y\xi) + \beta_y^\top Y\xi + \gamma_y,$$

where the vectors α, β and γ contain the cost coefficients. As we assume known mean and covariance of uncertain parameter ζ, the following reformulation can be provided,

$$\mathcal{G}(X,Y) = \max_{\mathbb{P}\in\mathcal{P}} \; \mathbb{E}^{\mathbb{Q}}[f_x(X,\xi)+f_y(Y,\xi)] = \operatorname{Tr}(X^\top \operatorname{diag}(\alpha_x)X\widehat{\Sigma})+\beta_x^\top X\widehat{\mu}+\gamma_x+\operatorname{Tr}(Y^\top \operatorname{diag}(\alpha_y)Y\widehat{\Sigma})+\beta_y^\top Y\widehat{\mu}+\gamma_y$$

which results in a convex quadratic objective function by utilizing the estimated mean and covariance from the available historical data. We define the following functions,

$$\mathcal{G}_x(X) = \operatorname{Tr}(X^\top \operatorname{diag}(\alpha_x)X\widehat{\Sigma}) + \beta_x^\top X\widehat{\mu} + \gamma_x \;\text{ and }\; \mathcal{G}_y(Y) = \operatorname{Tr}(Y^\top \operatorname{diag}(\alpha_y)Y\widehat{\Sigma}) + \beta_y^\top Y\widehat{\mu} + \gamma_y$$

that are used in the subsequent sections.

We are now equipped with all the necessary reformulations for model (1) to replace the distributionally robust individual chance constraints and the objective function as described in Sections 3.1 and 3.2.

[7] It is considered a standard practice to assume quadratic cost functions (similar to [34, 48]), while also linear cost functions can be utilized in our model. Using a higher order polynomial to describe the cost function would require the knowledge of higher order moments (e.g. skewness and kurtosis) for its reformulation.

4. Benchmark model: chance constrained program with Gaussian assumption of uncertainty

In this section, we write problem (1) as a chance constrained program and assume that parameter ζ follows a Gaussian distribution. This assumption allows for an analytical reformulation of chance constraints and serves as a benchmark in order to compare the original *DRCC* problem with. Moreover, a discussion on the tightening of the stochastic constraints by the distributionally robust and benchmark approaches is presented.

4.1. Reformulation of chance constraints and objective function

Assuming a Gaussian distribution, problem (1) can be rewritten as a chance constrained program that can be equivalently reformulated as a convex program [34, 35]. Ambiguous chance constraints (1j)-(1q) are formulated as chance constraints to the following form,

$$\mathbb{P}(A_i\xi \leq b_i) \geq 1-\epsilon_i \quad \forall i = 1,\dots,I, \tag{7}$$

where $A \in \mathbb{R}^{\mathcal{N}\times(Z+1)}$ is an arbitrary matrix of proper dimensions. Since the uncertain parameter ζ follows a multivariate normal distribution with mean $\widehat{\mu}_0$ and known covariance $\widehat{\Sigma}_0$, we provide an analytical reformulation of the individual chance constraint and (7) is equivalent to

$$\mathcal{F}^{-1}(1-\epsilon_i)\sqrt{A_i\widehat{\Sigma}A_i^\top} \leq (b_i - \widehat{\mu}^\top A_i^\top) \quad \forall i = 1,\dots,I, \tag{8}$$

where $\mathcal{F}^{-1}(1-\epsilon_i)$ is the inverse cumulative distribution function. Constraint (8) is an SOC constraint if $\mathcal{F}^{-1}(1-\epsilon_i) \geq 0$, which translates to $1-\epsilon_i \geq 0.5$. In practice, the decision maker would like the individual constraints to hold with a probability higher than 50%, so this is considered a mild assumption. Similarly, a tightening of each original deterministic constraint $A_i e \leq b_i$ by $\mathcal{H}_i = \mathcal{F}^{-1}(1-\epsilon_i)\sqrt{A_i\widehat{\Sigma}A_i^\top} + \widehat{\mu}_0^\top E^\top A_i^\top$ is attained. Finally, the objective function is calculated as the following expectation,

$$\mathbb{E}^{\mathbb{P}}[f_x(X,\xi) + f_y(Y,\xi)] = \mathrm{Tr}(X^\top \mathrm{diag}(\alpha_x)X\widehat{\Sigma}) + \beta_x^\top X\widehat{\mu} + \gamma_x + \mathrm{Tr}(Y^\top \mathrm{diag}(\alpha_y)Y\widehat{\Sigma}) + \beta_y^\top Y\widehat{\mu} + \gamma_y$$

which yields the same expression as $\mathcal{G}(X,Y)$ in Section 3.2.

4.2. Uncertainty margin: A measure for comparing the distributionally robust and benchmark models

It can be noticed that the tractable reformulations of distributionally robust chance constraints (5) and benchmark chance constraints (8) have the same form and the only difference emerges from the multiplication factor of $\sqrt{A_i\widehat{\Sigma}A_i^\top}$. In an attempt to provide additional insights to the tightening of each individual inequality constraints, we plot the multiplication factor with respect to the predefined security level in Figure 2. First, it can be observed that for an increase in the security level $1-\epsilon$ the multiplication factor increases. Therefore, a greater uncertainty margin is required to guarantee the predefined violation probability. The reformulation in (5) is able to provide more robust solutions for higher values of the security level, as well as allows for a wider range of tightening options of the constraints. Note that $\mathcal{F}^{-1}(0.5) = 0$ and that only the domain of $1-\epsilon_i \geq 0.5$ is taken into account to ensure that (8) is an SOCP constraint, while $\sqrt{\frac{1-\epsilon_i}{\epsilon_i}} = 0$ for $\epsilon = 1$.

5. ADMM-based distributed approach

In practice, it may not be desirable to solve the coupled dispatch problem of electricity and natural gas systems centrally since the two systems are operated by different entities in many countries around the world. Moreover, the system operators may not wish to share their private information, such as cost functions, dispatch of the power or natural gas producers and network topology. Therefore, we propose a distributed approach that decomposes the centralized model into an electricity subproblem and a natural gas subproblem that are solved independently.

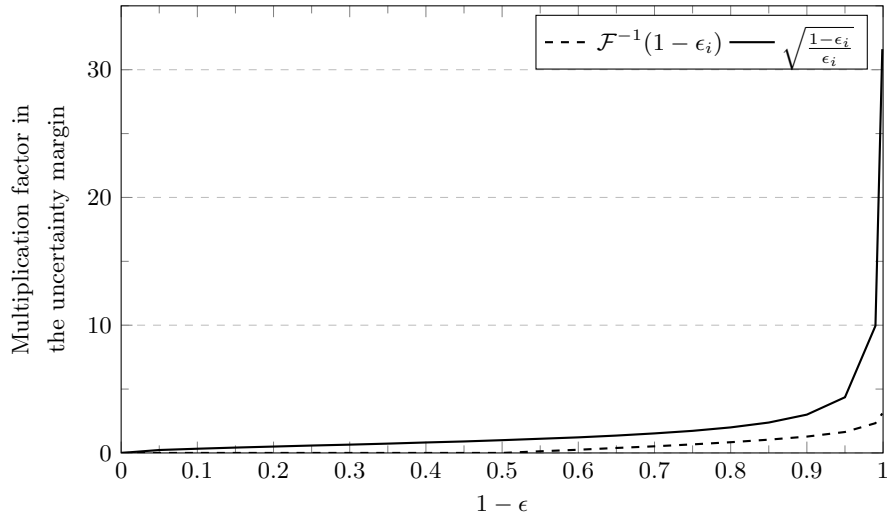

FIGURE 2. Values of the multiplication factor in the uncertainty margin.

Initially, we write the Lagrangian dual problem of (2) by relaxing the coupling constraint (2d),

$$\begin{aligned} \min_{X,Y,C,F} \quad & \max_{\Lambda} \ \mathcal{G}(X,Y) + \big\langle \Lambda, \Phi X - C \big\rangle \\ \text{s.t.} \quad & X \in \mathcal{X} \\ & Y, C, F \in \mathcal{Y} \end{aligned} \tag{9}$$

where $\Lambda \in \mathbb{R}^{\Gamma \times (Z+1)}$ is the dual variable of the coupling constraint. Then, we can equivalently write,

$$\begin{aligned} \max_{\Lambda} \quad & \min_{X,Y,C,F} \quad \mathcal{G}(X,Y) + \big\langle \Lambda, \Phi X - C \big\rangle \\ & \text{s.t.} \quad X \in \mathcal{X} \\ & \qquad Y, C, F \in \mathcal{Y} \end{aligned} \tag{10}$$

since the optimization problem is convex by applying duality. Having relaxed the coupling constraint, we can solve problem (10) in a distributed manner with ADMM [38]. The ADMM algorithm is based on the augmented Lagrangian

$$\mathcal{L}_\rho = \mathcal{G}_x(X) + \mathcal{G}_y(Y) + \big\langle \Lambda, \Phi X - C \big\rangle + \tfrac{\rho}{2} ||\Phi X - C||^2 \tag{11}$$

where $\rho > 0$ is a penalty parameter. The ADMM algorithm iteratively minimizes the augmented Lagrangian with the following steps:

(0) **Initialization.** Set $k \leftarrow 1$, $\Lambda^k \leftarrow \Lambda^{init}$, $X^k \leftarrow X^{init}$ and $C^k \leftarrow C^{init}$

(1) **Step 1.** Solve the electricity subproblem:

$$\begin{aligned} \min_{X} \quad & \mathcal{G}_x(X) + \big\langle \Lambda^k, \Phi X \big\rangle + \tfrac{\rho}{2} ||\Phi X - C^k||^2 \\ \text{s.t.} \quad & X \in \mathcal{X} \end{aligned} \tag{12}$$

in order to obtain the natural gas consumption of GFPPs. Set $X^{k+1} \leftarrow X^\star$, where $X^\star$ is the optimal solution of (12).

(2) **Step 2.** Solve the natural gas subproblem:

$$\begin{aligned} \min_{Y,C,F} \quad & \mathcal{G}_y(Y) - \big\langle \Lambda^k, C \big\rangle + \tfrac{\rho}{2} ||\Phi X^{k+1} - C||^2 \\ \text{s.t.} \quad & Y, C, F \in \mathcal{Y} \end{aligned} \tag{13}$$

in order to obtain the natural gas consumption of GFPPs. Set $C^{k+1} \leftarrow C^\star$, where $C^\star$ is the optimal solution obtained by (13).

(3) **Step 3.** Convergence of the algorithm is monitored by the primal residual $R^{k+1} = \Phi X^{k+1} - C^{k+1}$ and the dual residual $S^{k+1} = \rho(C^{k+1} - C^k)$. If $\|R^{k+1}\| \leq \eta$ and $\|F^{k+1}\| \leq \eta$, where η is small tolerance, then report $(X^{k+1}, Y^{k+1}, C^{k+1}, F^{k+1})$ and stop. Else, Λ is updated:

$$\Lambda^{k+1} = \Lambda^k + \rho(\Phi X^{k+1} - C^{k+1}), \tag{14}$$

by the *system coordinator*, we set $k \leftarrow k+1$ and go back to step 1.

Since the electricity and natural gas subproblems are independent, they can be solved in a distributed fashion where the exchange of information between the two system operators is monitored by the system coordinator as illustrated in Figure 3.

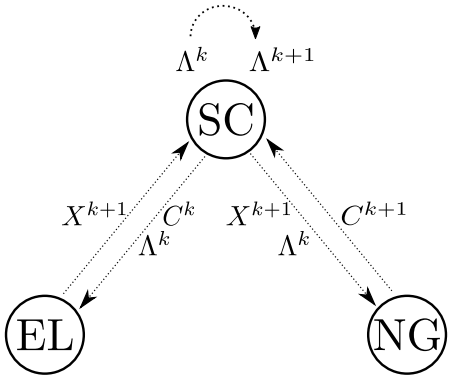

FIGURE 3. ADMM-based distributed algorithm. SC: System coordinator, EL: Electricity system and NG: Natural gas system.

An alternative algorithm to be employed in our study is Lagrangian Relaxation; though, we would need to restrict the objective function to be smooth and differentiable which is not necessary for ADMM. The aforementioned algorithm can be utilized for any problem that the resulting feasible sets $\mathcal{X}$ and $\mathcal{Y}$ are convex, as well as the final form of the objective function is convex with respect to optimization variables. For instance, there are various ambiguity sets that can be utilized to obtain convex feasible sets as in [36, 47, 46, 51, 48] for the case of moment-based ones or as in [37, 52, 53] for the metric-based ones under the respective assumptions mentioned therein. Maintaining the convexity of the original problem guarantees convergence of the algorithm, which highly depends though on the choice of ρ. We refer the reader to [38] for an extensive analysis on the convergence and stopping criterion of the algorithm, as well as some variations and extensions of it. The ADMM algorithm can be applied to non-convex problems as well, but the convergence is not guaranteed.

6. NUMERICAL RESULTS

An integrated energy system that consists of the IEEE 24-bus Reliability Test System (RTS) [54] and a 12-node natural gas system based on [55] is utilized for the case study. We consider a single type of uncertainty that stems from wind power produced by the $Z = 6$ wind farms installed with a total capacity of 55% of the total system's electricity demand. Moreover, wind power is dispatched at the day-ahead stage to the conditional expectation and thus the mean of forecast errors μ_0 is equal to zero. We neglect the constant term γ in the cost functions and set the coefficient of the quadratic term equal to 0.01% of the linear cost coefficient (i.e. $\alpha = 0.0001\beta$). In all simulations, we infer the mean $\overline{\mu}$ and covariance $\widehat{\Sigma}_0$ from the forecast error data that are generated similarly to the procedure presented in [56, Equation (2)] and based on the historical data given in [56]. The forecast errors for the 6 wind farms are illustrated in Figure 4. Moreover, the same value of $\epsilon \in (0, 1)$ for all individual chance constraints is considered in this work. The network topology of the integrated energy system and the corresponding data are provided in detail at the electronic companion [57]. All optimization models that were implemented in Matlab using YALMIP [58] and solved by

Gurobi are available at [57], while the simulations were run on a 4-core 3.4GHz stationary computer under Windows 8.

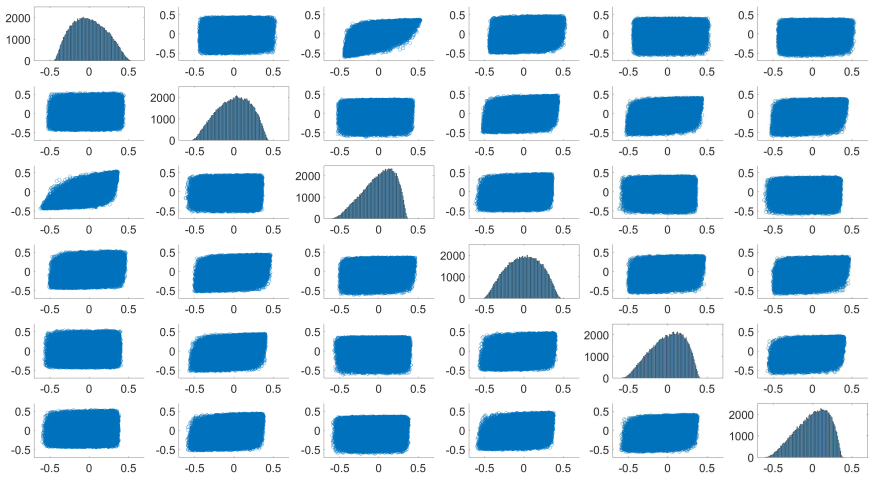

FIGURE 4. Forecast errors for the 6 wind farms. The diagonal plots show the histograms of the forecast errors (x axis: deviation in p.u. and y-axis: number of occurrences), while the off-diagonal plots illustrate the scatter plots between the two corresponding wind farms (x-axis and y-axis: deviation in p.u.).

6.1. **Performance of the ADMM-based distributed approach**

Initially, we compare the performance of the ADMM algorithm presented in Section 5 in terms of system cost and computational needs with a fully centralized model (CM) and the sequential model (SM) presented in [39] that mimics how the electricity and natural gas systems are operated in practice in Great Britain. An iterative approach is described in [39] that first solves the electricity system dispatch disregarding the natural gas system; then, the natural gas system is dispatched with fixed fuel demand from GFPPs; and finally, the power production of GFPPs (i.e. equivalent to fuel consumption) is further constrained in the event of infeasible fuel schedules of GFPPs for the natural gas system. This procedure is carried out until the total natural gas consumption can be met by the natural gas system. Note that the residential and industrial natural gas demands have higher priority than the fuel demand of GFPPs. In this work, we consider a natural gas price estimation that is given as an input in the sequential model to calculate the cost function of GFPPs. This price estimation is equal to the mean value calculated from the linear cost coefficient of all natural gas producers. In this setting, we utilize 1,000 samples of the historical data from [56] for the simulations.

Initially, to evaluate the performance of the proposed distributed algorithm, we pick the value of ρ is equal to 0.001, while the convergence tolerance η is set to 10^{-2}. Moreover, we set a maximum number of iterations equal to 10^4 for the ADMM algorithm and sequential model. Table 1 presents the value of the objective function for the fully centralized model, the ADMM approach and the sequential approach given when setting $\epsilon = 0.1$. The ADMM algorithm achieves the same solution as the centralized model that solves a single optimization problem to dispatch the integrated energy system but by simulating the two systems independently and allowing only limited information to be shared. Moreover, it can be observed that the sequential model yields a solution that has a higher operational cost of around 5.2%, although the information exchange is similar to the proposed ADMM algorithm.

Figures 5-7 provide additional insights into the convergence of the ADMM algorithm. More specifically, Figure 5 illustrates the convergence of the objective function via the ratio $\overline{\gamma}_k = \frac{\mathcal{G}^{\star k}_{\text{ADMM}} - \mathcal{G}^{\star}_{\text{CM}}}{\mathcal{G}^{\star}_{\text{CM}}} \times 100$, while

TABLE 1. Value of the objective function $\mathcal{G}^\star$ in \$ for the centralized model, ADMM algorithm and sequential model.

Model	Centralized	ADMM	Sequential
$\mathcal{G}^\star$ (\$)	63,500	63,500	66,821

similar ratios are calculated for the individual objective functions of the electricity $\overline{\gamma}_k^{\mathrm{EL}}$ and natural gas $\overline{\gamma}_k^{\mathrm{NG}}$ operators for each iteration of the algorithm. Moreover, the norm of the primal residual $\overline{\varrho}_k = \|R^k\|$ is shown in Figure 6 and the convergence of the system dispatch is presented in Figure 7 by plotting the norms $\overline{\chi}_k = \|X^k_{\mathrm{ADMM}} - X_{\mathrm{CM}}\|$ and $\overline{v}_k = \|Y^k_{\mathrm{ADMM}} - Y_{\mathrm{CM}}\|$. The ADMM algorithm converges in 39 iterations and in 65 sec for the predefined threshold (i.e. 1.66 sec per iteration), while it can be observed that the objective function and primal residual approximate the centralized solution very fast and already after the 10^{th} iteration the solution is of high quality. The solution time for the sequential model is 20 sec.

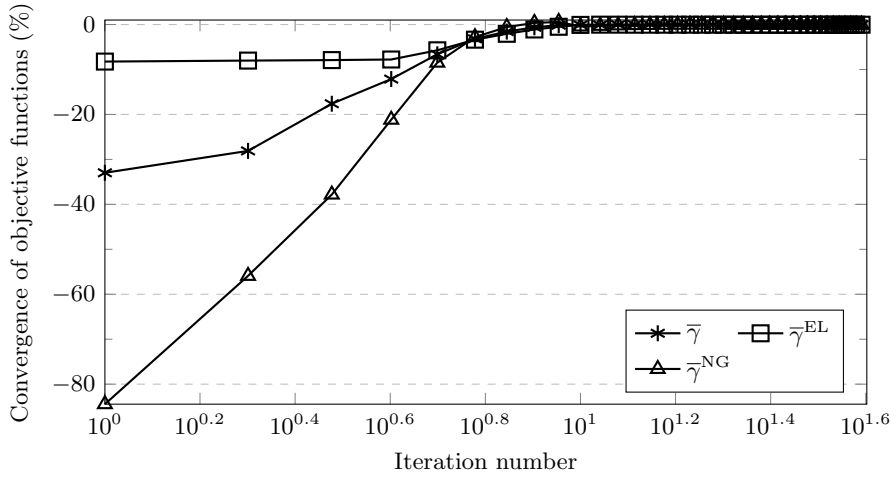

FIGURE 5. Convergence of the objective functions over the iterations.

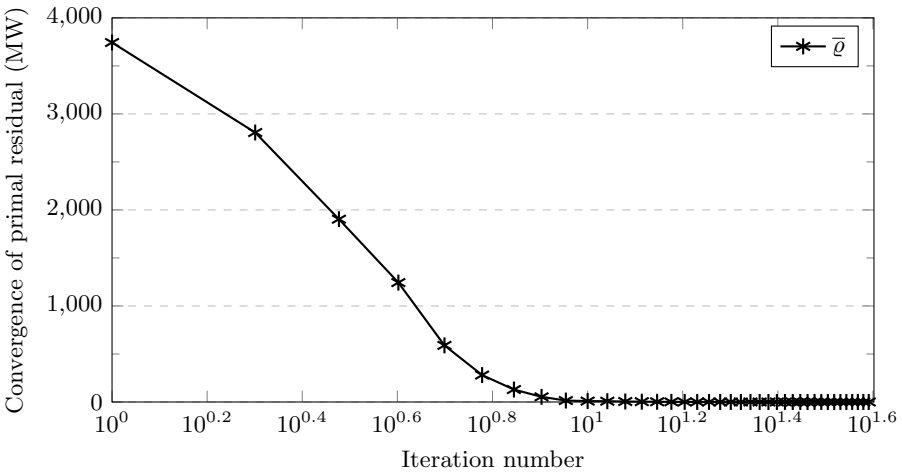

FIGURE 6. Convergence of the primal residual over the iterations.

Additionally, Figure 7 shows the convergence of the integrated system dispatch, where both the power and natural gas producers are dispatched in a similar manner with the centralized model by the distributed algorithm. This verifies that the implementation of the distributed approach would not have an impact on

the profits of the producers and would not alter the market outcomes if the integrated system is scheduled at the day-ahead stage in this distributed fashion.

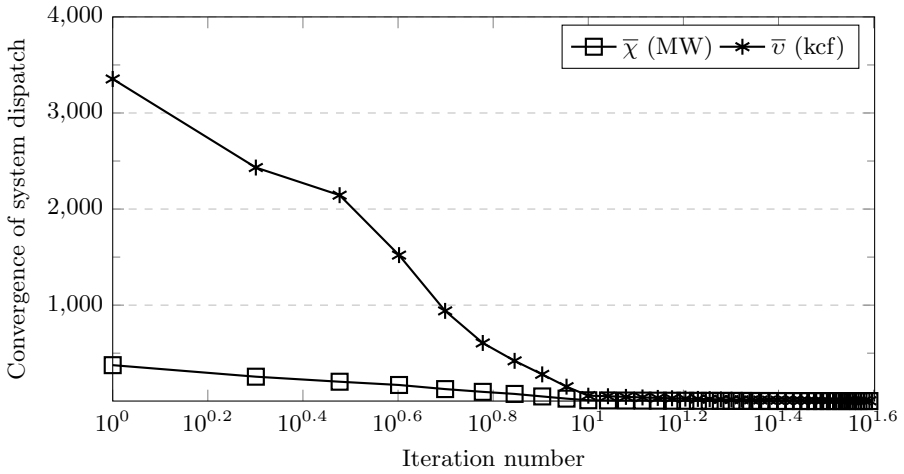

FIGURE 7. Convergence of the system dispatch over the iterations.

As it can be observed in Table 2, the value of ρ has an impact on the number of iterations and eventually on the solution time, while the time per iteration does not vary much under each case. Therefore, one should carefully select the value of ρ in order to achieve an efficient utilization of the algorithm in terms of the convergence time.

TABLE 2. Number of iterations and time for the ADMM algorithm as a function of ρ.

ρ	Iterations	Time (sec)	Time per iteration (sec)
0.0001	289	475	1.64
0.001	39	65	1.66
0.01	131	223	1.70
0.1	839	1448	1.72

6.2. **Out-of-sample evaluation**

The results of the proposed distributionally robust approach are compared with chance constrained program that assumes a Gaussian distribution of forecast errors (GCC) as presented in [34], as well as with a deterministic model (DM) that assumes no uncertainty; hence, with no tightening of each original deterministic constraint $A_i e \leq b_i$. To assess the true operation of the integrated energy system, we evaluate the systems' cost and violation probabilities of chance constraints based on 100 coupled datasets $\{\widehat{\mathcal{Z}}_N^i, \widehat{\Psi}_{N'}^i\}_{i=1,\ldots,100}$, where $\widehat{\mathcal{Z}}_N^i$ is a training dataset containing N independent and identically distributed (i.i.d.) sample data, and $\widehat{\Psi}_{N'}^i$ is a testing dataset containing N' i.i.d. realizations. We keep the number of i.i.d. samples in $\widehat{\mathcal{Z}}_N^i$ and realizations in $\widehat{\Psi}_{N'}^i$ fixed and equal to 100. The coupled datasets $\{\widehat{\mathcal{Z}}_N^i, \widehat{\Psi}_{N'}^i\}_{i=1,\ldots,100}$ are given in the electronic companion [57]. The out-of-sample analysis is carried out on the basis of a *projected* and of a *realistic* operation, as presented in the subsequent subsections. For the projected operation, we consider the safety factor ϵ as a design parameter that is decided by the operator based on the trade-off between the operational cost and the risk of violating the constraints. The analysis is performed to provide indications regarding this trade-off and to compare the three different approaches. In the realistic operation, the system operators re-dispatch the systems after the realization of uncertainty based on an optimal power and natural gas flow problem, where no violation of constraints is allowed. The effect of safety factor ϵ on the realistic systems' cost is presented.

6.2.1. *Projected operation*

The goal of this analysis is to evaluate the performance of the solutions X and Y obtained when solving model (1) with the in-sample dataset $\widehat{\mathcal{Z}}_N$ on the out-of-sample dataset $\widehat{\Psi}_{N'}$. Initially, we solve problem (1) to obtain the optimal $\widehat{X}^i$ and $\widehat{Y}^i$ for each training dataset $\widehat{\mathcal{Z}}_N^i$. Then, the out-of-sample cost is calculated for each realization in the testing dataset $\widehat{\psi}_k^i \in \widehat{\Psi}_{N'}^i$ by

$$\widehat{\mathcal{C}}^i = \mathcal{G}(\widehat{X}^i, \widehat{Y}^i)$$

which is utilized to estimate the expected cost by taking the average over the 100 datasets

$$\widehat{\mathcal{C}} = \frac{1}{100}\sum_{i=1}^{100} \widehat{\mathcal{C}}^i.$$

Moreover, we calculate three different metrics for the violation probability. The first two metrics provide insights regarding the violation of each individual constraint. The following indicator function is used,

$$\widetilde{\mathcal{I}}_{jk}^i = \begin{cases} 1 & \text{if } A_j\widehat{\psi}_k^i \leq b_j, \\ 0 & \text{otherwise} \end{cases}$$

where j indicates each individual chance constraint from (1j)-(1q). Thus, each constraint is evaluated individually and we can calculate the average number of violations for each out-of-sample simulation by

$$\widetilde{\mathcal{V}}_k^i = \frac{1}{J}\sum_{j=1}^{J}\left(1 - \widetilde{\mathcal{I}}_{jk}^i\right),$$

with J the total number of individual inequalities in (1). Then, the *empirical violation probability* is calculated by

$$\widetilde{\mathcal{V}}^{\text{emp}} = \frac{1}{N'}\frac{1}{100}\sum_{k=1}^{N'}\sum_{i=1}^{100}\widetilde{\mathcal{V}}_k^i,$$

and the *maximum average violation probability* for each chance constraint by

$$\widetilde{\mathcal{V}}^{\max} = \max_{k,i}\{\widetilde{\mathcal{V}}_k^i\}.$$

Additionally, the *average violation probability* for each type of chance constraint is calculated jointly with

$$\mathcal{I}_k^i = \begin{cases} 1 & \text{if } A\widehat{\psi}_k^i \leq b, \\ 0 & \text{otherwise} \end{cases}.$$

Therefore, we can evaluate the violation probability for the dataset $\widehat{\Psi}_{N'}^i$ with

$$\widehat{\mathcal{V}}^i = \frac{1}{N'}\sum_{k=1}^{N'}\left(1 - \mathcal{I}_k^i\right),$$

and the average violation probability for each type of chance constraint

$$\widehat{\mathcal{V}} = \frac{1}{100}\sum_{i=1}^{100}\widehat{\mathcal{V}}^i.$$

For the metric of joint chance constraints, we define four different types of chance constraints that are related to the power capacity (pc) constraints (1j)-(1k), the power flow (pf) constraints (1l)-(1m), the natural gas capacity (gc) constraints (1n)-(1o) and the natural gas flow (gf) constraints (1p)-(1q).

Figure 8 presents the empirical and maximum average violation probability for *DRCC* and *GCC*. It can be observed that both $\widetilde{\mathcal{V}}^{\text{emp}}$ and $\widetilde{\mathcal{V}}^{\max}$ increase with an increase of ϵ. Moreover, it is illustrated that *DRCC* returns a lower $\widetilde{\mathcal{V}}^{\text{emp}}$ and $\widetilde{\mathcal{V}}^{\max}$ than *GCC* in all cases. More specifically, *DRCC* yields very low $\widetilde{\mathcal{V}}^{\text{emp}}$, while $\widetilde{\mathcal{V}}^{\max}$ is always below 10%. On the hand, $\widetilde{\mathcal{V}}^{\text{emp}}$ and $\widetilde{\mathcal{V}}^{\max}$ have a higher increase with the increase of ϵ in the case of *GCC*, while this phenomenon is more profound for $\epsilon \geq 0.4$. The accepted violation probability

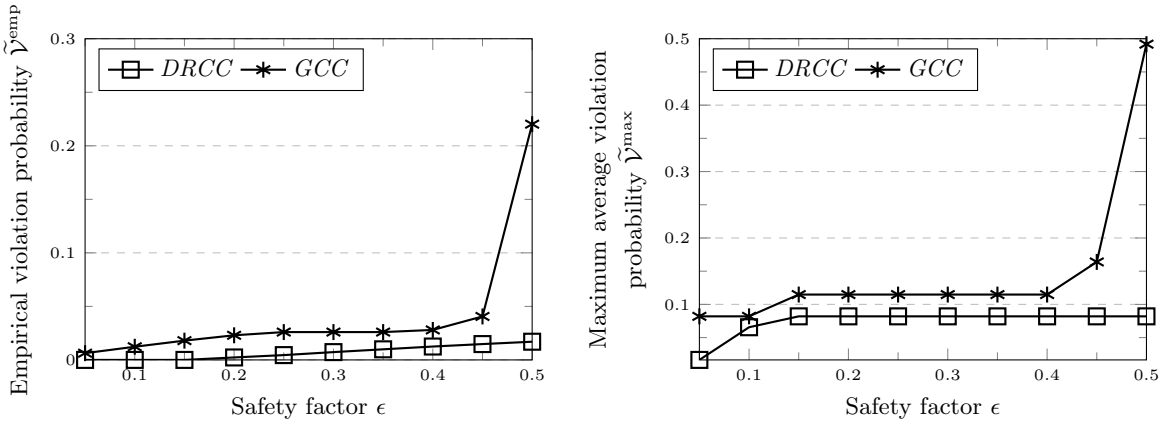

(a) Empirical violation probability. (b) Maximum average violation probability.

FIGURE 8. Empirical and maximum average violation probability for *DRCC* and *GCC*.

that is defined by the operator is satisfied for all cases, except for the instance of $\epsilon = 0.05$ in *GCC* where $\widetilde{\mathcal{V}}^{\max} > 0.05$.

Additionally, Figure 9 presents the joint violation probability for the power capacity and power flow constraints. It can be observed that the solution of *GCC* model does not yield a robust solution since $\widehat{\mathcal{V}}$ is notably high in all cases and especially for large values of ϵ. Note that $\widehat{\mathcal{V}}^{\text{pc}}$ becomes greater than 0.7, when $\epsilon \geq 0.4$, which indicates that is highly probable one of the power capacity constraints to be violated in these cases. On the other contrary, *DRCC* is more efficient since it always returns lower $\widehat{\mathcal{V}}$ than *GCC* and more specifically it obtains a $\widehat{\mathcal{V}}$ very close to 0 for $\epsilon \leq 0.15$. Similarly, Figure 10 illustrates the joint violation probability for the natural gas capacity and flow constraints. Also in this case, *DRCC* outperforms *GCC*; the difference though is less subtle because the operation of the natural gas systems is less stressed.

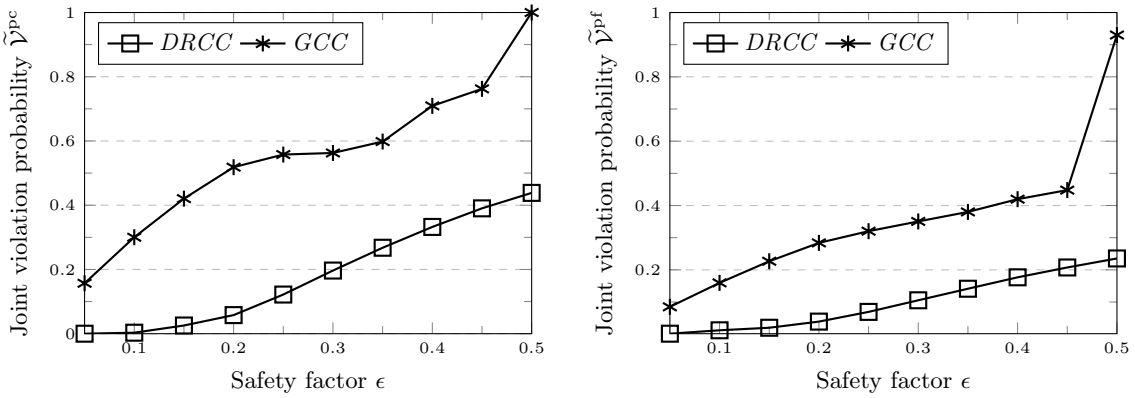

(a) Power capacity constraint. (b) Power flow constraint.

FIGURE 9. Joint violation probability for *DRCC* and *GCC*.

In addition, Table 3 presents the violation probabilities for *DM*. In all cases, the violation probabilities are higher than the corresponding ones of the *DRCC* and *GCC* models. The values are very high, especially for the case of joint violation probabilities. This highlights the need to utilize probabilistic approaches for the operational limits and account for uncertainty.

Figure 11 illustrates the cost difference between the *DRCC* and *GCC* models for different values of safety factors, where it can be observed that the cost difference reduces as the safety factor increases. The cost of *DRCC* is higher since it is more conservative for small ϵ. The cost difference is at most 7.11% and it drops

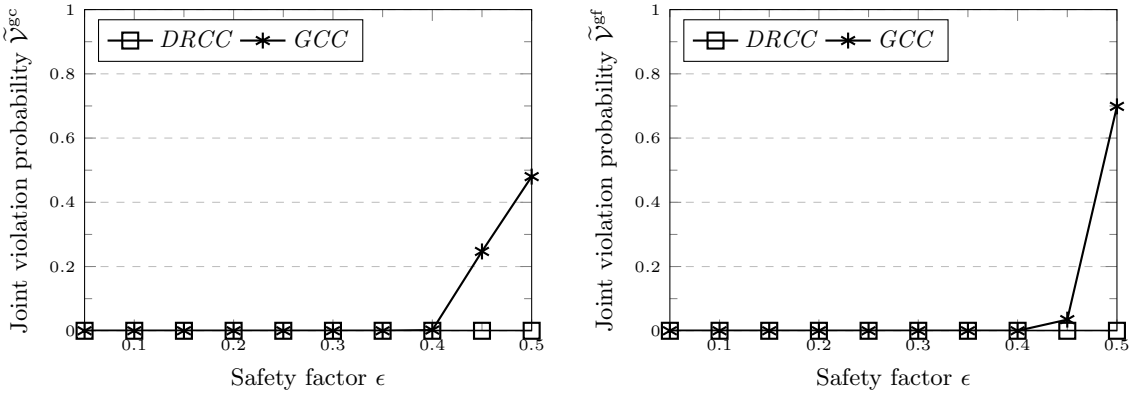

(a) Gas capacity constraint.

(b) Gas flow constraint.

FIGURE 10. Joint violation probability for *DRCC* and *GCC*.

TABLE 3. Violation probabilities for deterministic model

	$\widehat{\mathcal{V}}^{\mathrm{emp}}$	$\widehat{\mathcal{V}}^{\mathrm{max}}$	$\widehat{\mathcal{V}}^{\mathrm{pc}}$	$\widehat{\mathcal{V}}^{\mathrm{pf}}$	$\widehat{\mathcal{V}}^{\mathrm{gc}}$	$\widehat{\mathcal{V}}^{\mathrm{gf}}$
DM	0.22	0.49	1	0.93	0.48	0.69

to almost 0.3% for an $\epsilon \geq 0.35$. Thus, the system operator is able to decide the appropriate ϵ to reduce the total cost at the expense of higher chance of violating the constraints. It can be noticed that *DRCC* is more efficient than *GCC*, since the operator is able to pick the value of ϵ and accomplish a system cost very close to *GCC* but with much lower violation probabilities.

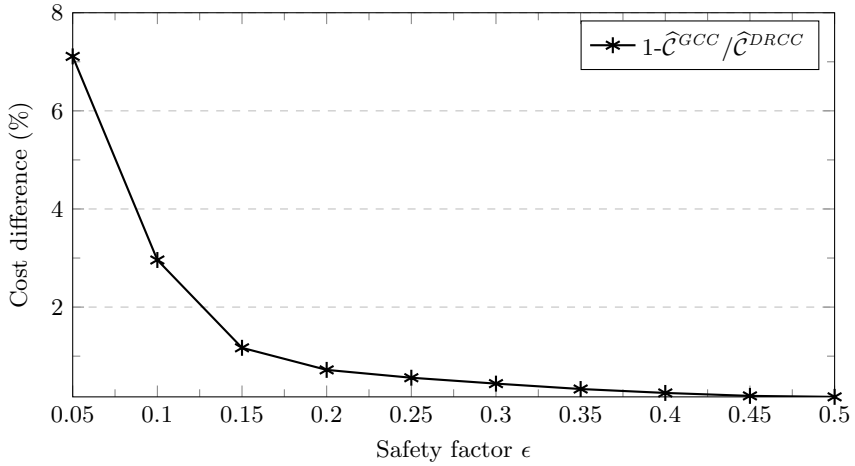

FIGURE 11. Percentage of total cost difference between the *DRCC* and *GCC*.

Table 4 shows the projected cost $\widehat{\mathcal{C}}$ for all three models. For *DRCC* and *GCC*, the value of $\widehat{\mathcal{C}}$ is reported for $\epsilon = 0.35$. It can be noticed that the attained projected cost $\widehat{\mathcal{C}}$ is close for all three models. In particular, the projected cost $\widehat{\mathcal{C}}$ of *DRCC* is 0.3% and 0.46% greater than the one obtained by the *GCC* and deterministic models, respectively. However, all the violation probabilities obtained by *DRCC* are lower compared to *GCC* and *DM*.

TABLE 4. Projected cost $\widehat{\mathcal{C}}$ and violation probabilities $\widehat{\mathcal{V}}^{\mathrm{emp}}$ and $\widehat{\mathcal{V}}^{\mathrm{max}}$ for $\epsilon = 0.35$

Model	DRCC	GCC	DM
$\widehat{\mathcal{C}}$	61,163	60,957	60,881

6.2.2. *Realistic operation*

Aiming to explore how the system would respond in a more realistic setup and estimate its true operational cost, we solve each one of the *DRCC*, *GCC* and *DM* models to obtain the first-stage decisions and then resolve a real-time economic dispatch problem with the first-stage decisions fixed. Following this approach, the system operator is able to adjust the real-time production and provide the necessary actions to keep the system balanced for any realization of stochastic production in a more flexible manner, i.e. without restricting the recourse actions to follow a linear decision rule. Therefore, we solve each model for a given in-sample dataset $\widehat{\mathcal{Z}}_N$ and obtain first-stage decisions $\widehat{X}^i e$ and $\widehat{Y}^i e$. Then, following real-time dispatch problem is solved:

$$
\begin{aligned}
\min_{\Delta p_k, \Delta g_k, l_k^{\mathrm{e}}, l_k^{\mathrm{g}}, w_k} \quad & \mathrm{Tr}(\Delta {p_k}^\top \mathrm{diag}(\alpha_x) \Delta p_k) + \beta_x^\top \Delta p_k + \mathrm{Tr}(\Delta {g_k}^\top \mathrm{diag}(\alpha_y) \Delta g_k) + \beta_y^\top \Delta g_k + \check{c}^\top l_k^{\mathrm{e}} + \check{c}^\top l_k^{\mathrm{g}} \\
\text{s. t.} \quad & 0 \le \widehat{X}^i e + \Delta p_k \le \overline{X} \\
& 0 \le \widehat{Y}^i e + \Delta g_k \le \overline{Y} \\
& \mathbf{1}^\top \Delta p_k + \mathbf{1}^\top (W \widehat{\psi}_k^i - w_k) + \mathbf{1}^\top l_k^{\mathrm{e}} = 0 \\
& B^{\mathrm{G}} (\widehat{Y}^i e + \Delta g_k) + B^{\mathrm{F}} q_k = B^{\mathrm{D}} (h - l_k^{\mathrm{g}}) + B^{\mathrm{P}} (\widehat{X}^i e + \Delta p_k) \\
& -\overline{f} \le Q^{\mathrm{G}} (\widehat{X}^i e + \Delta p_k) + Q^{\mathrm{W}} (W \overline{\mu} + W \widehat{\psi}_k^i - w_k) - Q^{\mathrm{D}} (d - l_k^{\mathrm{e}}) \le \overline{f} \\
& -\overline{q} \le q_k \le \overline{q} \\
& 0 \le l_k^{\mathrm{e}} \le d, \quad 0 \le l_k^{\mathrm{g}} \le h, \quad 0 \le w_k \le W\mu + W\widehat{\psi}_k^i,
\end{aligned}
$$

that minimizes the cost of re-dispatch actions for each realization $\widehat{\psi}_k^i \in \widehat{\Psi}_{N'}^i$ from the out-of-sample dataset. The re-dispatch actions include the adjustments Δp_k and Δg_k for electricity and natural gas, respectively, as well as electricity load shedding $l_k^{\mathrm{e}} \in \mathbb{R}_+^D$, natural gas load shedding $l_k^{\mathrm{g}} \in \mathbb{R}_+^H$ and wind spilling $w_k \in \mathbb{R}_+^Z$ in order to guarantee feasibility of the problem for any realization of the uncertainty. The cost of real-time adjustments stems from the same type of quadratic cost function as described in Section 3.2. Moreover, the constraints are described in model (1), while we have included the last three constraints restricting the load shedding of electricity and natural gas to the nodal demand and wind spilling to the actual wind power realization. The actions of load shedding are penalized by $\check{c} \gg c$ in the objective function, while wind spilling is considered cost-free. Since the chance constraints are replaced with hard constraints, there will be no out-of-sample violation and the analysis is focused on the realistic cost that is calculated by

$$
\widehat{\mathcal{R}}^i = \frac{1}{N'} \sum_{k=1}^{N'} \left(\mathrm{Tr}(\widehat{p_k}^{i\top} \mathrm{diag}(\alpha_x) \widehat{p}_k^i) + \beta_x^\top \widehat{p}_k^i + \mathrm{Tr}(\widehat{g_k}^{i\top} \mathrm{diag}(\alpha_y) \widehat{g}_k^i) + \beta_y^\top \widehat{p}_k^i + \check{c}^\top l_k^{\mathrm{e}} + \check{c}^\top l_k^{\mathrm{g}} \right),
$$

where $\widehat{p}_k^i = \widehat{X}^i e + \Delta p_k$ and $\widehat{g}_k^i = \widehat{Y}^i e + \Delta g_k$ are the actual real-time electricity and natural gas production levels. The realistic cost is estimated over the 100 datasets by taking the average

$$
\widehat{\mathcal{R}} = \frac{1}{100} \sum_{i=1}^{100} \widehat{\mathcal{R}}^i.
$$

Figure 12 presents the realistic cost $\widehat{\mathcal{R}}$ for models *DRCC* and *GCC* as a function of the ϵ. It can be observed that *DRCC* outperforms *GCC* for all values of ϵ illustrating that the *DRCC* provides more efficient first-stage decisions. Moreover, the reported $\widehat{\mathcal{R}}$ decreases with a decrease of ϵ since less costly real-time adjustments are activated due to increased robustness. The solution of *DM* is the same as in the case of *GCC* for $\epsilon = 0.5$, which is the case with the higher $\widehat{\mathcal{R}}$.

We report the computational performance for the case with $\epsilon = 0.1$, while the solution times obtained for other values of ϵ are similar. Model *DRCC* is solved in 35 sec on average and for *GCC* the average solution time is 1.5 sec. Finally, *DM* is solved in 0.3 sec on average.

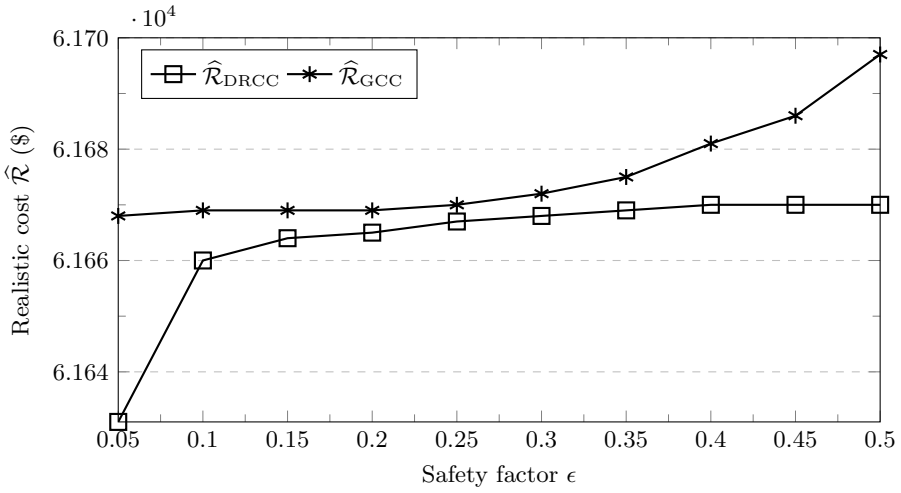

FIGURE 12. Average realistic cost $\widehat{\mathcal{R}}$ as a function of safety factor ϵ for *DRCC* and *GCC*.

7. Conclusion

This paper proposed a distributed and data-driven approach to obtain the electricity and natural gas systems dispatch with high shares of stochastic production from renewable energy sources. More specifically, we formulate the problem in a distributionally robust optimization framework and provide a tractable reformulation by assuming that only the first and second moments of the uncertain parameter are known. The distributed algorithm was developed based on ADMM, which permits to optimally solve the original centralized model in a distributed fashion, and only the natural gas consumption of GFPPs needs to be shared between the two operators. In contrast to other techniques used to deal with uncertainty, such as stochastic programming and robust optimization, the proposed dispatch model can accomodate uncertainty both efficiently and in a transparent manner, since only the mean and covariance matrix need to be shared between the system operators. More importantly, the mean and covariance matrix can be inferred from the available historical data that can be considered publicly available. Our numerical study showed that the ADMM algorithm converges to the global optimum solution after a small number of iterations. Moreover, we demonstrated that the distributionally robust model outperforms a chance constrained approach that assumes Gaussian distribution of forecast errors and a deterministic model. We performed an out-of-sample evaluation on a projected operation and illustrated that the proposed model results in robust solutions even for large safety factors, while it attains a projected cost that is close to the costs obtained by the model that assumes Gaussian uncertainty and the deterministic model. In the realistic operation, the lowest out-of-sample system cost is also obtained by the proposed distributionally robust model.

For future work, a more accurate modeling of the natural gas flow can be considered; however, the convexity of the final problem would need to be preserved to guarantee the convergence of the distributed algorithm. Additionally, a formulation with joint chance constraints can provide additional insights on how the safety factor affects the solutions. Removing the system coordinator by utilizing a decentralized algorithm would allow a direct communication between the system operators and thus is an interesting direction to be examined. Another future direction is to utilize alternative ambiguity sets that permit the reformulation of the distributionally robust problem, such as an ambiguity set based on the Wasserstein metric. Finally, an interesting direction is to examine a similar distributed problem where each one of the agents (e.g. system operators) has a different belief on the ambiguity set.

8. Acknowledgements

The authors would like to thank Jalal Kazempour, Pierre Pinson and Daniel Kuhn for their useful comments and fruitful discussions on the manuscript.

References

[1] U.S. Energy Information Administration, "International energy outlook 2016," tech. rep., 2016.

[2] P. J. Hibbard and T. Schatzki, "The interdependence of electricity and natural gas: Current factors and future prospects," *Electr. J.*, vol. 25, no. 4, pp. 6–17, 2012.

[3] S. An, Q. L. Li, and T. W. Gedra, "Natural gas and electricity optimal power flow," in *2003 IEEE PES Transm. Distrib. Conf. Expo.*, pp. 138–143, 2003.

[4] M. Geidl and G. Andersson, "Optimal power flow of multiple energy carriers," *IEEE Trans. Power Syst.*, vol. 22, pp. 145–155, Feb. 2007.

[5] T. Li, M. Eremia, and M. Shahidehpour, "Interdependency of natural gas network and power system security," *IEEE Trans. Power Syst.*, vol. 23, no. 4, pp. 1817–1824, 2008.

[6] C. Liu, M. Shahidehpour, Y. Fu, and Z. Li, "Security-constrained unit commitment with natural gas transmission constraints," *IEEE Trans. Power Syst.*, vol. 24, pp. 1523–1536, Aug. 2009.

[7] A. Zlotnik, L. Roald, S. Backhaus, M. Chertkov, and G. Andersson, "Coordinated scheduling for interdependent electric power and natural gas infrastructures," *IEEE Trans. Power Syst.*, vol. 32, pp. 600–610, Jan. 2017.

[8] C. M. Correa-Posada and P. Sanchez-Martin, "Integrated power and natural gas model for energy adequacy in short-term operation," *IEEE Trans. Power Syst.*, vol. 30, no. 6, pp. 3347–3355, 2014.

[9] C. He, T. Liu, L. Wu, and M. Shahidehpour, "Robust coordination of interdependent electricity and natural gas systems in day-ahead scheduling for facilitating volatile renewable generations via power-to-gas technology," *Journal of Modern Power Systems and Clean Energy*, vol. 5, pp. 375–388, May 2017.

[10] Y. He, M. Shahidehpour, Z. Li, C. Guo, and B. Zhu, "Robust constrained operation of integrated electricity-natural gas system considering distributed natural gas storage," *IEEE Trans. Sustain. Energy*, vol. 9, pp. 1061–1071, July 2018.

[11] A. Alabdulwahab, A. Abusorrah, X. Zhang, and M. Shahidehpour, "Coordination of interdependent natural gas and electricity infrastructures for firming the variability of wind energy in stochastic day-ahead scheduling," *IEEE Trans. Sustain. Energy*, vol. 6, no. 2, pp. 606–615, 2015.

[12] Y. Li, Y. Zou, Y. Tan, Y. Cao, X. Liu, M. Shahidehpour, S. Tian, and F. Bu, "Optimal stochastic operation of integrated low-carbon electric power, natural gas, and heat delivery system," *IEEE Trans. Sustain. Energy*, vol. 9, pp. 273–283, Jan 2018.

[13] C. Ordoudis, P. Pinson, and J. M. Morales, "An integrated market for electricity and natural gas systems with stochastic power producers," *Eur. J. Oper. Res.*, 2018.

[14] P. Pinson, L. Mitridati, C. Ordoudis, and J. Østergaard, "Towards fully renewable energy systems : Experience and trends in Denmark," *CSEE J. Power Energy Syst.*, vol. 3, no. 1, pp. 26–35, 2017.

[15] A. G. Bakirtzis and P. N. Biskas, "A decentralized solution to the DC-OPF of interconnected power systems," *IEEE Trans. Power Syst.*, vol. 18, pp. 1007–1013, Aug 2003.

[16] G. Hug-Glanzmann and G. Andersson, "Decentralized optimal power flow control for overlapping areas in power systems," *IEEE Trans. Power Syst.*, vol. 24, pp. 327–336, Feb 2009.

[17] B. H. Kim and R. Baldick, "Coarse-grained distributed optimal power flow," *IEEE Trans. Power Syst.*, vol. 12, pp. 932–939, May 1997.

[18] A. Kargarian, J. Mohammadi, J. Guo, S. Chakrabarti, M. Barati, G. Hug, S. Kar, and R. Baldick, "Toward distributed/decentralized dc optimal power flow implementation in future electric power systems," *IEEE Trans. Smart Grid*, pp. 1–1, 2017.

[19] F. Moret and P. Pinson, "Energy collectives: A community and fairness based approach to future electricity markets," *IEEE Trans. Power Syst.*, pp. 1–1, 2018.

[20] Y. Wen, X. Qu, W. Li, X. Liu, and X. Ye, "Synergistic operation of electricity and natural gas networks via ADMM," *IEEE Trans. Smart Grid*, pp. 1–1, 2017.

[21] C. Wang, W. Wei, J. Wang, L. Bai, Y. Liang, and T. Bi, "Convex optimization based distributed optimal gas-power flow calculation," *IEEE Trans. Sustain. Energy*, pp. 1–1, 2017.

[22] P. N. Biskas, N. G. Kanelakis, A. Papamatthaiou, and I. Alexandridis, "Coupled optimization of electricity and natural gas systems using augmented Lagrangian and an alternating minimization method," *Int. J. Electr. Power Energy Syst.*, vol. 80, pp. 202–218, 2016.

[23] Y. He, M. Yan, M. Shahidehpour, Z. Li, C. Guo, L. Wu, and Y. Ding, "Decentralized optimization of multi-area electricity-natural gas flows based on cone reformulation," *IEEE Trans. Power Syst.*, pp. 4531 – 4542, 2018.

[24] D. K. Molzahn, F. Drfler, H. Sandberg, S. H. Low, S. Chakrabarti, R. Baldick, and J. Lavaei, "A survey of distributed optimization and control algorithms for electric power systems," *IEEE Trans. Smart Grid*, vol. 8, pp. 2941–2962, Nov 2017.

[25] L. Halilbašić, S. Chatzivasileiadis, and P. Pinson, "Coordinating flexibility under uncertainty in multi-area AC and DC grids," in *2017 IEEE Manchester PowerTech*, pp. 1–6, June 2017.

[26] A. Ahmadi-Khatir, A. J. Conejo, and R. Cherkaoui, "Multi-area energy and reserve dispatch under wind uncertainty and equipment failures," *IEEE Trans. Power Syst.*, vol. 28, pp. 4373–4383, Nov 2013.

[27] Y. Zhang and G. B. Giannakis, "Distributed stochastic market clearing with high-penetration wind power," *IEEE Trans. Power Syst.*, vol. 31, pp. 895–906, March 2016.

[28] M. Bazrafshan and N. Gatsis, "Decentralized stochastic optimal power flow in radial networks with distributed generation," *IEEE Trans. Smart Grid*, vol. 8, pp. 787–801, March 2017.

[29] Z. Li, W. Wu, B. Zeng, M. Shahidehpour, and B. Zhang, "Decentralized contingency-constrained tie-line scheduling for multi-area power grids," *IEEE Trans. Power Syst.*, vol. 32, pp. 354–367, Jan 2017.

[30] Z. Li, W. Wu, M. Shahidehpour, and B. Zhang, "Adaptive robust tie-line scheduling considering wind power uncertainty for interconnected power systems," *IEEE Trans. Power Syst.*, vol. 31, pp. 2701–2713, July 2016.

[31] A. Hassan, Y. Dvorkin, D. Deka, and M. Chertkov, "Chance-constrained ADMM approach for decentralized control of distributed energy resources," in *2018 IEEE Power System Computation Conference*, pp. 1–7, 2018.

[32] A. Shapiro, D. Dentcheva, and A. Ruszczyński, *Lectures on Stochastic Programming*. Society for Industrial and Applied Mathematics, Jan. 2009.

[33] A. Ben-Tal, L. El Ghaoui, and A. Nemirovski, *Robust Optimization*. Princeton University Press, 2009.

[34] D. Bienstock, M. Chertkov, and S. Harnett, "Chance-constrained optimal power flow: Risk-aware network control under uncertainty," *SIAM Rev.*, vol. 56, no. 3, pp. 461–495, 2014.

[35] L. Roald, F. Oldewurtel, T. Krause, and G. Andersson, "Analytical reformulation of security constrained optimal power flow with probabilistic constraints," in *2013 IEEE PowerTech Conference*, pp. 1–6, June 2013.

[36] E. Delage and Y. Ye, "Distributionally robust optimization under moment uncertainty with application to data-driven problems," *Oper. Res.*, vol. 58, no. 3, pp. 595–612, 2010.

[37] P. Mohajerin Esfahani and D. Kuhn, "Data-driven distributionally robust optimization using the Wasserstein metric: Performance guarantees and tractable reformulations," *Math. Program.*, Jul 2017.

[38] S. Boyd, N. Parikh, E. Chu, B. Peleato, and J. Eckstein, "Distributed optimization and statistical learning via the Alternating Direction Method of Multipliers," *Foundations and Trends in Machine Learning*, vol. 3, no. 1, pp. 1–122, 2011.

[39] M. Qadrdan, J. Wu, N. Jenkins, and J. Ekanayake, "Operating strategies for a GB integrated gas and electricity network considering the uncertainty in wind power forecasts," *IEEE Trans. Sustain. Energy*, vol. 5, pp. 128–138, Jan 2014.

[40] D. Kuhn, W. Wiesemann, and A. Georghiou, "Primal and dual linear decision rules in stochastic and robust optimization," *Mathem. Program.*, vol. 130, pp. 177–209, Nov 2011.

[41] Y. Zhang, S. Shen, and J. L. Mathieu, "Distributionally robust chance-constrained optimal power flow with uncertain renewables and uncertain reserves provided by loads," *IEEE Trans. Power Syst.*, vol. 32, no. 2, pp. 1378–1388, 2017.

[42] A. Venzke, L. Halilbašić, U. Markovic, G. Hug, and S. Chatzivasileiadis, "Convex relaxations of chance constrained ac optimal power flow," *IEEE Trans. Power Syst.*, vol. 33, pp. 2829–2841, May 2018.

[43] R. D. Christie, B. F. Wollenberg, and I. Wangensteen, "Transmission management in the deregulated environment," *Proc. of the IEEE*, vol. 88, pp. 170–195, Feb 2000.

[44] T. Koch, B. Hiller, M. Pfetsch, and L. Schewe, *Evaluating Gas Network Capacities*. Philadelphia, PA: Society for Industrial and Applied Mathematics, 2015.

[45] C. Wang, W. Wei, J. Wang, F. Liu, and S. Mei, "Strategic offering and equilibrium in coupled gas and electricity markets," *IEEE Trans. Power Syst.*, vol. 33, pp. 290–306, Jan 2018.

[46] S. Zymler, D. Kuhn, and B. Rustem, "Distributionally robust joint chance constraints with second-order moment information," *Math. Program.*, vol. 137, no. 1-2, pp. 167–198, 2013.

[47] G. A. Hanasusanto, V. Roitch, D. Kuhn, and W. Wiesemann, "Ambiguous joint chance constraints under mean and dispersion information," *Oper. Res.*, vol. 65, no. 3, pp. 751–767, 2017.

[48] W. Xie and S. Ahmed, "Distributionally robust chance constrained optimal power flow with renewables: A conic reformulation," *IEEE Trans. Power Syst.*, vol. 33, pp. 1860–1867, March 2018.

[49] G. C. Calafiore and L. E. Ghaoui, "On distributionally robust chance-constrained linear programs," *J. Optim. Theory Appl.*, vol. 130, pp. 1–22, Jul 2006.

[50] L. Roald, F. Oldewurtel, B. Van Parys, and G. Andersson, "Security constrained optimal power flow with distributionally robust chance constraints," *arXiv:1508.06061*, 2015.

[51] W. Xie and S. Ahmed, "On deterministic reformulations of distributionally robust joint chance constrained optimization problems," *SIAM J. Optim.*, vol. 28, no. 2, pp. 1151–1182, 2018.

[52] R. Jiang and Y. Guan, "Data-driven chance constrained stochastic program," *Math. Program.*, vol. 158, pp. 291–327, Jul 2016.

[53] A. B. Philpott, V. L. de Matos, and L. Kapelevich, "Distributionally robust SDDP," *Comput. Manag. Sci.*, May 2018.

[54] C. Grigg, P. Wong, P. Albrecht, R. Allan, M. Bhavaraju, R. Billinton, Q. Chen, C. Fong, S. Haddad, S. Kuruganty, W. Li, R. Mukerji, D. Patton, N. Rau, D. Reppen, A. Schneider, M. Shahidehpour, and C. Singh, "The IEEE reliability test system-1996. A report prepared by the reliability test system task force of the application of probability methods subcommittee," *IEEE Trans. Power Syst.*, vol. 14, no. 3, pp. 1010–1020, 1999.

[55] C. He, L. Wu, T. Liu, and M. Shahidehpour, "Robust co-optimization scheduling of electricity and natural gas systems via ADMM," *IEEE Trans. Sustain. Energy*, vol. 8, pp. 658–670, April 2017.

[56] J. Dowell and P. Pinson, "Very-short-term probabilistic wind power forecasts by sparse vector autoregression," *IEEE Trans. Smart Grid*, vol. 7, no. 2, pp. 763–770, 2016.

[57] C. Ordoudis and V. Nguyen, "Electronic companion - Data-driven distributed operation of electricity and natural gas systems." https://doi.org/10.5281/zenodo.1439199, 2018. Online; Accessed: 30.09.2018.

[58] J. Löfberg, "YALMIP : A toolbox for modeling and optimization in MATLAB," in *2004 IEEE Int. Conf. Robot. Autom.*, pp. 284–289, 2004.

Appendices

A. Nomenclature

In Table 5, we present the symbols used in the original paper and the description for each one of them.

Table 5. Nomenclature

Symbol	Description
X	Matrix for conventional power plants dispatch combining the first-stage decisions and affine policy for the second-stage adjustments
Y	Matrix for natural gas producers dispatch combining the first-stage decisions and affine policy for the second-stage adjustments
F	Matrix for natural gas flow combining the first-stage decisions and affine policy for the second-stage adjustments
C	Matrix for fuel consumption of GFPPs combining the first-stage decisions and affine policy for the second-stage adjustments
Λ	Dual variable of coupling constraint
$\overline{\mu}$	Mean power production of stochastic producers
ζ	Random parameter with zero mean
ξ	Vector containing random parameter ζ for the formulation of actual value of decision variables X, Y, C and F
μ_0	Mean value of random parameter ζ
Σ_0	Covariance matrix of random parameter ζ
W	Diagonal matrix containing the capacity of stochastic producers
Q	PDTF matrix
B	Mapping of various components on the natural gas system
$\overline{X}$	Maximum power production of conventional power plants
$\underline{X}$	Minimum power production of conventional power plants
$\overline{Y}$	Maximum production of natural gas producer
$\underline{Y}$	Minimum production of natural gas producer
$\overline{f}$	Capacity limit of transmission line
$\overline{q}$	Capacity limit of pipeline
Φ	Power conversion factor
d	Electricity demand
h	Natural gas demand
ϵ	Safety factor of chance constraint
α, β, γ	Cost coefficients of quadratic objective functions
ρ	Penalty parameter for ADMM algorithm
R	Primal residual for ADMM algorithm
S	Dual residual for ADMM algorithm
N	Number of sample data in the training dataset
N'	Number of realizations in the testing dataset
$\mathbb{P}$	True probability distribution of random variable ζ
$\mathcal{P}$	Ambiguity set
η	Threshold to check the convergence of ADMM algorithm

A sketch of the matrix utilized for the restriction to linear decision rules, which contains both the day-ahead dispatch and the factors for the real-time adjustments. For instance, we provide the form of matrix $X \in \mathbb{R}^{G\times(Z+1)}$ with 3 power plants and 3 stochastic producers, thus the dimension of the matrix is 3×4:

$$X = \begin{bmatrix} x_{11} & x_{12} & x_{13} & x_{14} \\ x_{21} & x_{22} & x_{23} & x_{24} \\ x_{31} & x_{32} & x_{33} & x_{34} \end{bmatrix}$$

More specifically, vector $[x_{11}, x_{21}, x_{31}]$ denotes the day-ahead dispatch of the 3 power plants and the following matrix

$$\begin{bmatrix} x_{12} & x_{13} & x_{14} \\ x_{22} & x_{23} & x_{24} \\ x_{32} & x_{33} & x_{34} \end{bmatrix}$$

contains the affine policies of the corresponding adjustments for each power plant and for each stochastic power producer.

Department of Electrical Engineering
Center for Electric Power and Energy (CEE)
Technical University of Denmark
Elektrovej, Building 325
DK-2800 Kgs. Lyngby
Denmark

www.elektro.dtu.dk/cee
Tel: (+45) 45 25 35 00
Fax: (+45) 45 88 61 11
E-mail: cee@elektro.dtu.dk